DENSITY DEPENDENT EFFECTIVE INTERACTIONS

DENSITY DEPENDENT EFFECTIVE INTERACTIONS AND THE O-p SHELL NUCLEI

By

DAVID JAMES HUGHES, B.Sc.

A Thesis

Submitted to the School of Graduate Studies

in Partial Fulfilment of the Requirements

for the Degree

Doctor of Philosophy

McMaster University

May 1970

DOCTOR OF PHILOSOPHY (1970) McMASTER UNIVERSITY
(Physics) Hamilton, Ontario

TITLE: Density Dependent Effective Interactions and The O-p Shell Nuclei

AUTHOR: David James Hughes, B.Sc.
(University of Wales, Swansea, Wales)

SUPERVISOR: Professor A. B. Volkov

NUMBER OF PAGES: vii, 401

SCOPE AND CONTENTS:

Variational calculations have been performed using various internucleon interactions in an attempt to find an interaction which would reproduce the properties of the O-p shell nuclei. These interactions were derived by fitting procedures to the S-state phase shifts and to the properties of nuclear matter. A satisfactory interaction having been obtained, studies of isobaric nuclei have been undertaken.

ACKNOWLEDGEMENTS

It is a pleasure to thank Dr. A. B. Volkov for supervising this work. Many of the ideas incorporated in the development of the form of the density dependent interaction originate from Dr. Volkov.

I should also like to thank Dr. D. W. L. Sprung and Dr. R. K. Bhaduri for many useful discussions and Mr. R. Leavens for patiently checking the formulae of the Coulomb Matrix Elements. I am particularly indebted to Dr. G. Keech, the Director, and the staff of the Computer Centre at McMaster University.

For financial support during the course of this research, I would like to thank the Physics Department of McMaster University and the National Research Council of Canada.

Finally, my thanks go to Miss C. Wivell for cheerfully typing, correcting and to some extent organizing the final draft of this manuscript into a more presentable form.

TABLE OF CONTENTS

LIST OF TABLES

CHAPTER 1

INTRODUCTION

It is the purpose of this thesis to attempt to develop an "effective" internucleon interaction for use in "Hartree-Fock" and variational calculations of various nuclear systems, in particular, the lighter nuclei. The need for such an interaction originates from the impossibility of performing such calculations using realistic potentials. Typically realistic interactions have either strong repulsive cores and/or velocity dependence or various other forms of non-locality. The repulsive core, which is generally assumed, invalidates the use of the convenient (and often necessary) single particle wave functions which are finite within the range of the core, since perturbative types of calculation of finite nuclei are extremely difficult to perform in an appropriate self consistent manner. Common single particle wave functions used are those of the three dimensional spherical or cylindrical harmonic oscillator well, or, more realistically, some form of the Woods-Saxon well.

Even utilization of the reaction matrix technique, based on the Brueckner-Goldstone theory (Bru 57), for realistic potentials presents great computational difficulty. It has been demonstrated by Moszkowski and Scott (Mos 60)

that the reaction matrix elements can be approximated by using simple "effective" interactions. Kallio and Koltveit (Kal 64, Kal 65) and, more recently, Kuo and Brown (Kuo 65, Kuo 66) have demonstrated that the Moszkowski-Scott separation method is a reasonable one for obtaining matrix elements which can be used to define effective potentials. It was in the spirit of such effective interactions that the potentials, considered in this thesis, were developed (Bro 67).

In performing a variational or shell-model calculation for a finite nucleus, it is necessary to restrict or truncate the basis of the single particle states to just a few relevant states to make the calculation feasible. Even the use of modern fast computers has not altered this situation very dramatically. (It is now possible to rapidly calculate any nucleus with $4<A<16$ if the single particle basis is restricted to the 0-p shell, but it becomes virtually impossible to allow the basis to include single particle states in the s-d shell in such a calculation.)

Thus, in a practical calculation (Mcf 67), the Hilbert space D, of infinite extent, spanned by a complete set of single particle states, is truncated to a model space d, d being a subspace of D.

Thus, if ψ is the trial wave function of a variational calculation in which the complete set of single particle states $|\Phi_i>$ is used as the basis set i.e.

$$|\psi> = \sum_{i\varepsilon D} a_i \, |\Phi_i> \quad ,$$

where the summation is over all single particle states which span the Hilbert space D, then a model trial wave function ψ_d can be considered such that

$$|\psi_d\rangle = P|\Psi\rangle = \sum_{i\epsilon d} a_i |\Phi_i\rangle \quad .$$

The summation is now restricted to the model space d, a sub-space of D, and $|\psi_d\rangle$ is projected out of $|\psi\rangle$ by the projection operator P.

Then, if V is the realistic interaction which would be used in a calculation in the space D, an "effective" interaction V_{eff} used in a calculation in the space d can be constructed to satisfy the requirement

$$V_{eff}|\psi_d\rangle = V|\psi\rangle$$

i.e. the matrix elements of V_{eff} in the truncated basis are equal to the matrix elements of V in the complete basis.

In this work, no attempt is made to derive an "effective" interaction from "first principles". Instead, a phenomenological viewpoint, guided by "first principle" calculations, is taken. It is assumed that an "effective" interaction should satisfy certain empirical data (e.g. the phase-shifts derived from nucleon-nucleon scattering data and the saturation properties of nuclear matter), and also should reproduce various experimentally observed properties of finite nuclei in a calculation using a truncated basis

set of single particle states (e.g. excited state energy levels and binding energies of the A=4 to A=16 nuclei).

The calculation of the properties of the "so-called" O-p shell nuclei has been used to test many theories and ideas (Ing 52; Ing 53; Kur 56; Tal 60; Ami 64; Boy 64; Vol 64; Coh 65; Vol 65; Bar 66; Hal 66; Gol 68). The reason is a practical one. The truncation of the single particle basis to states of the O_s and O_p oscillator wells allows calculation of the nuclei A=4 through A=16 in a reasonable time, while the effect of mixing from higher configurations in the wave function is believed to be minimal for most states under consideration. For these reasons, the excited state spectra of the O-p shell nuclei are chosen, in this thesis, to test the validity of the effective interactions derived by fitting procedures to the scattering data and nuclear matter properties.

The theory of the method employed to calculate these excited state spectra is outlined in Chapter 2. Chapter 3 lists the criteria which the effective interactions are required to satisfy, and presents a selection of effective interactions which have been tested.

Results for the usual local type of Volkov double-gaussian interactions are tabulated in Chapter 4 and the deficiencies of such local interactions are examined. Bhaduri and Tomusiak (Bha 66) have already pointed out that interactions of this type lead to the collapse of

nuclear systems heavier than those considered by Volkov (Vol 65). These authors suggest that effective interactions should be constructed so as to satisfy the saturation properties of infinite nuclear matter.

This procedure has been adopted by many authors (Mut 65; Kri 66; Tab 66; Bri 67; Man 67; Nes 68) with encouraging results. As explained in Chapter 3, the nuclear matter criteria are satisfied, in this thesis, by adding density dependent terms to the basic Volkov-type interaction.

Skyrme (Sky 59) was one of the first authors to suggest that the internucleon interaction should be dependent upon the local density within a nucleus. Many subsequent authors (Squ 58; Bru 59; Bun 65; Bar 66; Lan 68; Spe 68) have found that density dependence is needed in the internucleon force to reproduce experimental results. Manning (Man 67a) has found that in a Hartree-Fock calculation the O-s single particle state is far too low for interactions which do not have any density dependent features. For such interactions Volkov (Vol 70a) finds that particle-hole excitation calculations predict excited states in ^{16}O which are too high, and that adding density dependence to the interaction lowers these states.

Brueckner (Bru 59), in Hartree-Fock studies for finite nuclei, has suggested that a term proportional to the local density squared should be present in the effective internucleon interaction. Bethe (Bet 67; Bet 68; Nem 68)

has suggested that the short range repulsive interaction be replaced by a density dependent interaction and, also that the tensor interaction be likewise treated. Wong (Won 67) proposes that the Pauli operator is dependent on the density to the one third ($\frac{1}{3}$) power.

Kuo and Kuo and Brown (Kuo 65; Kuo 66; Kuo 67) have demonstrated that the 2nd order Born term for the long range tensor interaction (this tensor interaction does not contribute in first order) can be replaced by a central interaction for the $^3S_1$ state in a Moszkowski-Scott separation calculation. This central interaction is density dependent. A similar conclusion has been reached by Bhaduri and Warke (Bha 68), who, by explicit calculation for the O.P.E.P. tensor potential suggest that the density dependence is $\rho^{-1/3}$.

A number of calculations (Gre 62; Gre 67; Lan 67; Ban 69) using density dependent interactions have indicated that it is difficult to distinguish between different density dependencies.

In consideration of the ambiguities associated with the exact nature of the density dependence, the point of view taken in this thesis has been that no form of density dependence should, in principle, be discarded without trial. Kuo (Kuo 65) and Bhaduri (Bha 68) indicate that the range of the density dependent interaction should be one half of that of the non-density dependent interaction. This point

is also examined in this work.

The criteria adopted, and methods used in deriving the effective interactions used in this thesis are explained in Chapter 3 and a number of interactions are tabulated. Density dependence has been attached to both the attractive and repulsive terms of the usual Volkov double-gaussian interaction.

The role of the Majorana exchange strength and the differences in excited state spectra for similar interactions differing only in their predicted values for the binding energy of ^{16}O are discussed in Chapter 5. The importance of a consistent value for the ^{16}O binding energy was not initially recognized and differences in the spectra brought about by different values of this binding energy have to be taken into consideration when other more fundamental modifications of the interaction are compared in later chapters.

The form chosen for the local density and its connection with the actual nuclear density is examined in Chapter 6. It is demonstrated that use of a single gaussian form for the density, designed to fit the mean square radius of the nuclear density, and evaluated at the centre of mass of the interacting nucleons is a suitable approximation for the interactions of prime interest studied in this thesis.

Chapter 7 illustrates the systematic behaviour of the O-p shell excited states for interactions differing

essentially in their attractive and repulsive ranges. An examination of the excited state spectra for different density dependencies is undertaken in Chapter 8 in an attempt to distinguish between different density dependencies. Consideration is also given to choosing the range of the density dependent interaction to differ from that of the non-density interaction.

The role of the repulsive core strength is subjected to examination in Chapter 9 and it is shown that, for reasonable core strengths, no difference in the properties of nuclear matter or the excited state spectra can be distinguished for core strengths differing by 50 Mev. Further consideration is given to the form of the central part of the density dependent interaction in this chapter.

Chapter 10 contains results for all O-p shell nuclei and compares various isobaric nuclei. Results are presented for two interactions whose primary difference is their density dependencies. For both interactions results are given for the excited state spectra, the binding energies, the root-mean-square radii, deformation studies and nuclear density plots for all O-p shell nuclei. Where possible, comparison with experimentally determined properties is attempted.

With the exception of Chapter 10, no detailed comparison is made with experimental results, although such comparisons are utilized extensively in the search for the

"best" effective interactions which are used in Chapter 10.

General conclusions are reported in Chapter 11. Appendix 1 lists the experimentally known binding energies, excited state energy levels and root-mean-square radii for 0-p shell nuclei. Appendix 6 tabulates matrix elements in the j-j coupling scheme up through the 1s-0d shell for the interactions used in Chapter 10. The appropriate matrix elements are compared with those of Kuo and Brown (Kuo 67).

CHAPTER 2

THE VARIATIONAL METHOD

In general, it is desired to obtain stationary solutions for a system of n-particles (nucleons) in motion and interacting with each other. The interaction between the particles is usually considered to be of a local two-body nature i.e. the interaction between the i^{th} and j^{th} nucleons is independent of the positions and velocities of the remaining particles in the system. Consideration of three-body interactions and non-local interactions are usually fairly complex.

Most of the interactions considered in this thesis are non-local, in the sense that they are density dependent and thus, the interaction between the i^{th} and j^{th} particles depends not only on their positions relative to each other, but also on their positions in relation to the rest of the nucleons in the system i.e. their positions in relation to the centre of the nucleus. A further non-locality is introduced by allowing the interactions to be velocity (or state) dependent. It has been noted by Kerman (Ker 69) that there is no real distinction between non-local and velocity dependent interactions. The exact nature of these non-localities and the approximations necessary to enable

computations to be performed for finite nuclei are discussed in Chapter 3.

The Hamiltonian of the A-particle system considered in this work is

$$H = \sum_{i=1}^{A} T_i - T_{C.M.} + \sum_{i<j}^{A} V_{ij}(\underline{r}_i, \underline{r}_j)$$

$$+ c \sum_{i=1}^{A} \underline{\ell}_i \cdot \underline{s}_i + \sum_{i<j}^{A'} \frac{e^2}{|\underline{r}_i - \underline{r}_j|}$$

where T_i is the kinetic energy of the single particle state i,

$T_{C.M.}$ is the energy of the centre-of-mass,

$V_{ij}(\underline{r}_i, \underline{r}_j)$ is the two-body potential which depends on the positions of the interacting nucleus $\underline{r}_i$ and $\underline{r}_j$ (for the local potentials considered in Chapter 4, the dependence is simply on the relative coordinates $\underline{r}_{ij} = \underline{r}_i - \underline{r}_j$),

$\underline{\ell}_i \cdot \underline{s}_i$ is the usual form of the shell model spin-orbit interaction and

$\frac{e^2}{|\underline{r}_i - \underline{r}_j|}$ is the coulomb interaction,

the prime on the summation indicating that the sum is to be taken over proton coordinates only.

No exact solution exists for the n-body problem with n>2 and approximate methods have to be employed. The most useful method used for physical systems is the variational method. The variation principle consists of selecting a completely arbitrary trial function ψ and

varying the functional $\langle\psi|H|\psi\rangle$ (the average energy for the state ψ), in some completely arbitrary fashion to obtain a stationary value for $\langle\psi|H|\psi\rangle$ subject to the normalization condition $\langle\psi|\psi\rangle = 1$.

Such a procedure would lead to the time-independent Schroedinger equation since it is required that (Bet 68)

$$\delta \int \psi^* H \psi \, d\tau = 0$$

and

$$\int \psi^* \psi \, d\tau = 1 \quad .$$

The normalization condition is introduced in the usual Lagrange multiplier way; the real Lagrange multiplier, in this case, being the energy E, i.e.

$$\delta[\int \psi^* H \psi \, d\tau - E \int \psi^* \psi \, d\tau] = 0$$

or

$$\delta \int \psi^*(H-E)\psi \, d\tau = 0 \quad .$$

Since H-E is hermitian this becomes

$$\int \delta \, \psi^*(H-E)\psi \, d\tau + \int [(H-E)\psi]^* \, \delta \, \psi \, d\tau = 0 \quad .$$

If the variation of ψ^* and ψ are considered to be independently arbitrary, then the time-independent Schroedinger equation

$$(H-E)\psi = 0$$

is obtained since it is now required that

$$\int \delta\,\psi^*(H-E)\psi\,d\tau = 0 \quad \text{and} \quad \int \psi^*(H-E)\delta\,\psi = 0 \qquad .(2.1)$$

Approximate solutions to this problem can be obtained by the application of the variation principle where the trial function ψ can be chosen in various fashions and the variation is carried out in some restricted manner.

Thus in most physical applications the Hilbert space spanned by a complete set of orthonormal functions ψ_n is truncated to a N dimensional sub-space and the variational wave function is expressed as

$$\psi = \sum_{n=1}^{N} c_n\,\psi_n \quad .$$

The variation $\delta\,\psi$ is prescribed to be

$$\delta\,\psi = \sum_{n=1}^{N} d_n\,\psi_n$$

so that

$$\psi + \delta\,\psi = \sum_{n=1}^{N} (d_n+c_n)\psi_n \quad .$$

Equation (2.1) now becomes

$$\sum_{m=1}^{N}\sum_{n=1}^{N} d_m\,c_n\,\langle\psi_m|H-E|\psi_n\rangle = 0$$

and, since the d_m's are arbitrary

$$\sum_{n=1}^{N} c_n\,\langle\psi_m|H-E|\psi_n\rangle = 0 \quad .$$

The basis set of functions ψ_n are orthonormal, so that this can be written

$$\sum_{n=1}^{N} c_n (H_{mn} - E\ \delta_{mn}) = 0$$

where

$$H_{mn} = \int \psi_m^* H \psi_n \, d\tau$$

and

$$\delta_{mn} = \begin{cases} 1 & \text{for } n=m \\ 0 & \text{otherwise} \end{cases} .$$

A solution exists for this set of homogeneous equations if and only if

$$\det |H_{mn} - E\ \delta_{mn}| = 0 .$$

The stationary solutions E can thus be obtained by diagonalization of the matrix (H_{mn}) and the appropriate c_n's can be simultaneously determined.

The expectation ground state energy obtained using the Ritz variational method is always greater than the correct solution. Moiseiwitsch (Moi 66) has shown that with increasing N, the Ritz solution converges to the eigenvalue of the Schroedinger (or Sturm-Liouville) equation if the functions ψ_n form a complete set.

In shell model calculations the ψ_n's are chosen to be the product of a number of single particle functions,

the single particle functions being solutions of the Schroedinger equation for the spherically symmetric harmonic oscillator well. In this work, the single particle wave functions are chosen to be solutions of the Schroedinger equation for the cylindrically symmetric harmonic oscillator well.

The single particle wave functions are taken to be the product of a space part, a spin part and an isospin part,

$$\psi_n(r,\sigma,\tau) = \phi_n(r)\ \chi_n(\sigma)\ \phi_n(\tau) \quad .$$

Because of the presence of a Coulomb term and a spin-orbit interaction in the Interaction Hamiltonian, this is an approximation to the true single particle wave function. The contribution of the Coulomb and spin-orbit interactions to the total energy is small so that the separation of the wave function in the above manner should be a good approximation.

The nucleons, being fermions, should obey the Pauli explusion principle and thus have the appropriate symmetry property i.e. their wave functions should be totally antisymmetric with respect to the exchange of any pair of the coordinates.

A wave function which satisfies these symmetry properties and also reduces to zero if two of the identical particles are in the same state is the Slater determinantal

wave function

$$\Psi_{Anti} = \frac{1}{\sqrt{A!}} \sum_{P} (-1)^{P} P \prod_{i=1}^{A} \psi_{n_i}(r_i)$$

where P is the permutation operator and the summation is over all possible permutations. ψ_{n_i} is the single particle wave function and r_i stands for the space, spin and isospin coordinates of the single particle. That this wave function satisfies the requirements outlined above can be seen by rewriting it in the form

$$\Psi_{Anti} = \frac{1}{\sqrt{A!}} \begin{vmatrix} \psi_{n_1}(r_1) & \psi_{n_1}(r_2) & \psi_{n_1}(r_A) \\ \psi_{n_2}(r_1) & \psi_{n_2}(r_2) & \psi_{n_2}(r_A) \\ & & \\ \psi_{n_A}(r_1) & \psi_{n_A}(r_2) & \psi_{n_A}(r_A) \end{vmatrix} .$$

The exchange of any two columns of this determinant results in a change of sign for the wave function and, further, if any $n_i = n_j$, $i \neq j$, then the wave function is zero.

The expectation energy of a Slater determinant is given by the Slater Sum Rule

$$\langle \Psi | H | \Psi \rangle = \sum_{i=1}^{A} \langle \psi_{n_i}(r_i) | T | \psi_{n_i}(r_i) \rangle$$

$$+ \sum_{i<j=1}^{A} \langle \psi_{n_i}(r_i)\ \psi_{n_j}(r_j) | V_{ij} | \psi_{n_i}(r_i)\ \psi_{n_j}(r_j)$$

$$- \psi_{n_j}(r_i)\ \psi_{n_i}(r_j) \rangle$$

+ like terms for the spin-orbit interaction (one-body) and the Coulomb interaction (two-body)

The centre of mass term becomes (Man 67)

$$- \frac{\hbar^2}{2mA} \sum_{i=1}^{A} \langle \psi_{n_i}(\underline{r}_i) | \underline{k}_i^2 | \psi_{n_i}(\underline{r}_i) \rangle - \frac{\hbar^2}{mA} \sum_{i<j=1}^{A} \langle \psi_{n_i}(\underline{r}_i)\ \psi_{n_j}(\underline{r}_j)$$

$$\times\ |\underline{k}_i \cdot \underline{k}_j|\ \psi_{n_i}(\underline{r}_i)\ \psi_{n_j}(\underline{r}_j) \rangle$$

where $\underline{k}_i$ is the conjugate momentum to position $\underline{r}_i$ and m is the average mass of the nucleons.

The usual shell model approximation assumes that it is only necessary to consider the interactions between n of the A nucleons in the system. The A-n other nucleons are assumed to form an inert core. The expectation energy of a Slater determinant in the shell model approximation is then calculated to be

$$\langle \Psi | H | \Psi \rangle = E_0 + \sum_{i=A-n+1}^{A} \varepsilon_j$$

$$+ \sum_{i<j=A-n+1}^{A} \langle \psi_{n_i}(\underline{r}_i)\ \psi_{n_j}(\underline{r}_j) | V_{ij} | \psi_{n_i}(\underline{r}_i)\ \psi_{n_j}(\underline{r}_j)$$

$$- \psi_{n_j}(\underline{r}_i)\ \psi_{n_i}(\underline{r}_j) \rangle$$

where $\sum_{i=A-n+1}^{A} \varepsilon_i$ is formally equivalent to

$$\sum_{i=A-n+1}^{A} \langle \psi_{n_i}(\underline{r}_i) | T_i | \psi_{n_i}(\underline{r}_i) \rangle$$

$$+ \sum_{i=1}^{A-n} \sum_{j=A-n+1}^{A} \langle \psi_{n_i}(\underline{r}_i)\ \psi_{n_j}(\underline{r}_j) | V_{ij} | \psi_{n_i}(\underline{r}_i)\ \psi_{n_j}(\underline{r}_j)$$

$$- \psi_{n_j}(\underline{r}_i)\ \psi_{n_i}(\underline{r}_j) \rangle$$

and E_0 to

$$\sum_{i=1}^{A-n} \langle \psi_{n_i}(\underline{r}_i) | T_i | \psi_{n_i}(\underline{r}_i) \rangle$$

$$+ \sum_{i<j=1}^{A-n} \langle \psi_{n_i}(\underline{r}_i)\ \psi_{n_j}(\underline{r}_j) | V_{ij} | \psi_{n_i}(\underline{r}_i)\ \psi_{n_j}(\underline{r}_j) - \psi_{n_j}(\underline{r}_i)$$

$$\times \psi_{n_i}(\underline{r}_i) \rangle \quad .$$

The core energy, E_0 is normally not calculated and the single particle energies, ε_i are taken from experimental results. The single particle energy can be determined as that energy required to remove a single valence nucleon in state i from the nucleus A+1 leaving the core nucleus A.

The strength of the oscillator well is often used as a parameter in a shell model calculation. In this calculation the oscillator well strengths are determined by requiring that the nucleus saturate i.e. that the ground state binding energy be a minimum.

The basis set of single particle states can be characterized by the quantum numbers $[n,m,n_z]$. In this calculation the single particle states considered (Appendix 2) are

$$[0,0,0] \quad - \quad 0_S \quad \text{state}$$

$$[0,1,0] \quad - \quad 0_{P_{+1}} \text{ state}$$

$$[0,-1,0] \quad - \quad 0_{P_{-1}} \text{ state}$$

$$[0,0,1] \quad - \quad 0_{P_0} \text{ state} \quad .$$

Orthonormality conditions thus allow six independent oscillator parameters (if deformation is also considered)

$$\alpha_S \ , \ \beta_S$$

$$\alpha_{P\pm1} \ , \ \beta_{P\pm1}$$

$$\alpha_{P_0} \ , \ \beta_{P_0} \quad .$$

The total energy E thus is a function of six parameters α_S, β_S, α_{P_0}, β_{P_0}, $\alpha_{P\pm1}$, $\beta_{P\pm1}$

$$E \equiv E(\alpha_S, \beta_S, \alpha_{P_0}, \beta_{P_0}, \alpha_{P\pm1}, \beta_{P\pm1}) \quad .$$

However, since J is not a good quantum number for the basis chosen, meaningful calculations for the excited state spectra can only be performed at zero deformation, $\alpha_i = \beta_i$ and a further necessary requirement that has to be imposed is that $\alpha_{P_0} = \alpha_{P\pm1}$.

It should be noted that, with the restriction $\alpha_{P_0} = \alpha_{P\pm1}$, and at zero deformation, the expressions for ε_j and E_0 of the shell model yield the same contribution for given α_S and α_P for any possible determinantal wave

function. Thus a shell model calculation will give exactly the same excited state spectra for the same values of α_S and α_P as the more complete calculation performed in this work. The shell model, however, is incapable of determining the correct α_S and α_P which would lead to saturation of the system.

The minimum binding energy of most systems studied occurs when the system is deformed, $\alpha_i \neq \beta_i$. The same deformation is assumed for all shells i.e.

$$\alpha_S/\beta_S = \alpha_P/\beta_P = \delta \quad .$$

The deformation parameter quoted in this thesis, ε is that of Volkov (Vol 65). It is related to δ by

$$\delta = \frac{1 - \frac{2}{3}\varepsilon}{1 + \frac{1}{3}\varepsilon} \quad .$$

The direct and exchange potential matrix elements differ in their deformation properties. Their behaviour with deformation has been studied by Volkov (Vol 70). The volume V of the nuclear system remains almost constant during deformation and using this assumption, the dependence of the kinetic energy on the deformation is easily seen.

The volume $V \propto 1/\alpha\sqrt{\beta}$ $(= c/\alpha\sqrt{\beta})$ where α and β are the oscillator parameters for the state considered.

Defining the dimensionless parameters A and B

as

$$A \equiv (V/c)^{2/3}\ \alpha$$

$$B \equiv (V/c)^{2/3}\ \beta$$

and

$$A\sqrt{B} = 1 \quad .$$

A deformation d can be defined as

$$d = \sqrt{A/B}$$

and a state is prolate, spherical or oblate as

$$d \gtreqless 1 \quad .$$

The kinetic energy for a particle in state $[n,m,n_z]$ can be written as

$$T_{nmn_z} = \tfrac{1}{2}[(2n+|m|+1)\alpha + (n_z+\tfrac{1}{2})\beta]\ \frac{\hbar^2}{m}$$

where $\alpha = mw/\hbar$ and $\beta = mw/\hbar$.

Thus

$$T_{nmn_z} = \tfrac{1}{2}\left(\frac{V}{c}\right)^{2/3} \frac{\hbar^2}{m}\ [(2n+|m|+1)A + (n_z+\tfrac{1}{2})\ \frac{1}{A^2}] \quad .$$

Minimization of T with respect to A gives

$$\frac{d\ T_{nmn_z}}{dA} = (2n+|m|+1) - 2(n_z+\tfrac{1}{2})/A^3$$

$$= 0 \text{ for a minimum} \quad .$$

Thus

$$A_{min} = [(2n_z+1)/(2n+|m|+1)]^{1/3}$$

and

$$d_{min} = [(2n_z+1)/(2n+|m|+1)]^{1/3} \quad .$$

Extending this procedure to the minimization of the kinetic energy of a A particle product determinant, the deformations ε shown in Table 2.1 are predicted for the O-p shell nuclei

TABLE 2.1

A	ε	A	ε	A	ε
4	0.00	9	0.48	14	-0.21
5	0.32	10	-0.50	15	-0.09
6	0.46	11	-0.53	16	0.00
7	0.55	12	-0.55		
8	0.60	13	-0.35		

For this calculation α_S equals α_P. For smaller values of σ, where $\sigma = \alpha_P/\alpha_S$, identical results are obtained with regard to the sign of ε but $|\varepsilon|$ is smaller. The predicted ε's are larger generally than those found in actual calculations but, with the exception of ^{9}Be, the correct sign is predicted. The oblate solution for ^{9}Be was very close to the prolate solution. A further extension of the above procedure is examined in Chapter 10.

The interactions considered in this work also have

exchange operators built into their formalism. The basic interaction is modified by the factor

$$[W + M\,P_M + B\,P_\sigma + H\,P_\tau]$$

where P_M is the space exchange operator

$$(P_M = -\,P_\sigma\,P_\tau)$$

P_σ is the spin exchange operator

P_τ is the isospin exchange operator .

The exchange strengths are defined so that

$$W + M = 1 \quad .$$

In the calculation of the potential matrix element, $\langle V_{ij} \rangle$, since the space, spin and isospin wave functions are considered separable, the spin and isospin wave functions can be ignored and the direct matrix elements evaluated in coordinate space are multiplied by the factor

$$[W + B\,\delta_{\sigma_i\sigma_j} + H\,\delta_{\tau_i\tau_j} - M\,\delta_{\sigma_i\sigma_j}\,\delta_{\tau_i\tau_j}] \quad ,$$

the exchange matrix elements, likewise, being multiplied by the factor

$$[-M + W\,\delta_{\sigma_i\sigma_j}\,\delta_{\tau_i\tau_j} + B\,\delta_{\tau_i\tau_j} + H_{\sigma_i\sigma_j}]$$

where $\delta_{\sigma_i\sigma_j} = 1$ if the spins of the i^{th} and j^{th} particles

are the same, zero otherwise and

$$\delta_{\tau_i \tau_j} = 1$$

if the isospins of the i^{th} and j^{th} particles are the same, zero otherwise.

Considering the interaction of one nucleon with the four nucleons of a closed sub-shell, it is easily seen that the direct matrix elements depend on the exchange strengths merely with respect to the factor $\nu_D=(4W-M+2(B+H))$, and that the exchange matrix elements merely depend on

$$\nu_E = (W - 4M + 2(B+H)) \quad .$$

Since $W + M = 1$ ν_D and ν_E can be rearranged to give

$$\nu_D = \frac{1}{4}(6 + 10(W-M) + 8(B+H))$$

$$\nu_E = \frac{1}{4}(-6 + 10(W-M) + 8(B+H)) \quad .$$

Thus, for a determinantal state consisting of a single nucleon (or a single nucleon hole in a sub-shell) outside closed sub-shells, the total energy of the system is invariant to the exchange strengths if

$$\nu = 10(W-M) + 8(B+H)$$

is maintained at a constant value.

This invariance is also true for determinants constructed from only closed sub-shells i.e. those determinants having [4,4,4,-----,4] supermultiplet symmetry.

CHAPTER 3

CHOICE OF AN EFFECTIVE INTERACTION AND CALCULATIONAL ASPECTS

It has already been noted in Chapter 1 that the use of realistic internucleon interactions for the calculation of finite nuclear systems precludes the use of simple single particle basis wave functions, such as the wave functions of the harmonic oscillator well. Goldstone (Gol 57) has indicated that this difficulty can be overcome by using a reaction matrix G instead of the interaction V. Various approximations have been used to derive G from V (Bru 67) but these are all of a complex and time-consuming nature. The main point of interest is that the matrix elements of G can be reasonably well approximated by those of a well behaved potential (Bra 65), thus enabling the properties of finite nuclei to be calculated in a reasonable time.

Moszkowski and Scott (Mos 60) have shown that the repulsive core can be effectively cancelled by part of the attractive tail, the resulting simple potential being zero inside a separation distance d. Bhaduri and Tomusiak (Bha 65) have indicated that this separation distance is energy or velocity dependent; it depends on the relative energy of the interacting nucleons. The separation method results in just the long range part of the realistic potential,

which gives approximately the same matrix elements as does the reaction matrix. Rather than following the formalism to derive this long range velocity dependent interaction, the procedure adopted, in this work, is to obtain the interaction by fitting the S-wave phase shifts at a number of different relative energies.

It has been noted in Chapter 1 that there is considerable evidence that the effective interaction should be density dependent. This density dependence derives from the observation that the G matrix elements depend on the local density (Bha 67; Won 67), and also, that the main contribution of the long range tensor interaction to the G matrix, the second order Born term, can be replaced by a density dependent central interaction (Kuo 66). The exact nature of these density dependencies is unclear at the present time.

Bhaduri and Tomusiak (Bha 66) have shown how important it is to ensure that the effective interaction saturates nuclear matter. The criteria, thus adopted in this thesis to determine the analytic form of the effective interaction are:

1. that the interaction reproduce the experimentally determined S-wave phase shifts for free nucleon-nucleon scattering at various relative energies; in particular those energies which are important for nucleons interacting within a finite nucleus;

2. that the interaction have roughly the same long-range behaviour as "realistic" potentials;
3. that the interaction saturate nuclear matter at the correct saturation density and binding energy per particle;
4. that the interaction have small second order correction terms in nuclear matter;
5. that the matrix elements for the interaction be easily evaluated.

The first two criteria derive from the requirements of the Moszkowski-Scott separation prescription. The third condition ensures that the interaction does not lead to the collapse of nuclear systems heavier than the light nuclei considered in this thesis. The interactions derived in this work are to be used in first order Hartree-Fock and variational calculations. Therefore, to obtain meaningful results for these calculations, the second order correction terms should be small. Sprung (Spr 69a) has indicated that, for the form of the effective interaction used in this work, the fourth requirement limits the size of the repulsive core height to a maximum of approximately 50 Mev.

For a calculation of a finite nucleus, a rapid evaluation of the potential matrix elements is of great practical importance. If the calculation of these matrix elements is too involved there is not much advantage to be

gained by using an effective interaction rather than the more formally correct G reaction matrix technique.

Criterion 5 is well satisfied by forces of the Volkov double-gaussian form:

$$V(r) = (W + M\,P_M + B\,P_\sigma + H\,P_\tau)\ [V_a \exp(-r^2/\lambda_a{}^2) + V_r \exp(-r^2/\lambda_r{}^2)]$$

where P_M, P_σ and P_τ are the usual Majorana (space), spin and isospin exchange operators.

This type of interaction has been used by Volkov (Vol 65) and Hughes and Volkov (Hug 66) in numerous computations. Its radial shape is very similar to that of the Moszkowski-Scott form (Bro 67).

Interactions 1, 2 and 3 of Table 3.1 are of this form. They were derived by crudely fitting the S-wave scattering data at zero relative energy i.e. the scattering length and the effective range. It was also required that they fit the binding energy of either ^{16}O and/or ^{4}He. These interactions do not saturate nuclear matter and thus tend to lead to the collapse of nuclear systems heavier than ^{16}O.

Interactions 4 and 5 represent an improvement over these interactions. They were designed to fit the S-wave scattering data at a number of different relative energies. This was accomplished by making λ_r, k dependent

$$\lambda_r(k) = \lambda_r{}^0[1 + c_1(k-c_2)^2] \qquad .(3.1)$$

k is the relative wave number which is related to the relative energy.

This has the desired effect of changing the attractive tail of the interaction for different relative energies (the analogue of an energy dependent separation distance in the Moszkowski-Scott separation method).

For given V_a, V_r, λ_a and k it is possible to find a λ_r which fits either the triplet or the singlet S-wave phase shift. However, the desired matrix elements are not calculated in the relative coordinate system, and different λ_r's for the singlet and triplet states are not meaningful. Instead an average λ_r is used for which the triplet and singlet values of λ_r are weighted according to their relative strengths, [1 + (B-H)] and [1 - (B-H)] respectively. These average values of λ_r for different k's, k_1, k_2 etc., are well represented by the parabola (3.1).

Thus, for given V_a, V_r and λ_a, the S-wave phase shifts can be used to determine the parameters λ_r^0, c_1, c_2 and (B-H). It should be noted that the possibility of λ_r being greater than λ_a (i.e. the interaction becoming repulsive) for large k now exists. For the interactions used in this thesis and, at the values of k prevelent in the finite nuclei studied, this feature does not appear. It does, however, provide a saturation mechanism in a nuclear matter calculation. In fact, Interactions 4 and 5 do saturate nuclear matter but at an unrealistically high binding

energy per particle and at a saturation density of $k_F = 2.5\ fm^{-1}$ (the accepted saturation density is $k_F = 1.36\ fm^{-1}$).

In order to more realistically saturate nuclear matter, density dependence is introduced into the interaction. The form of the density dependence follows closely that suggested by Bethe (Bet 66), although no restriction is placed on the power of the density dependence. The V_a and V_r of the above form of the interaction are now replaced by

$$V_A(1 + c_3(\frac{3\pi^2}{2}\rho)^{n_1/3})$$

$$(\text{or} \quad V_A(1 + c_3 k_F^{n_1}) \text{ in nuclear matter})$$

and

$$V_R(1 + c_4(\frac{3\pi^2}{2}\rho)^{n_2/3})$$

$$(\text{or} \quad V_R(1 + c_4 k_F^{n_2}) \text{ in nuclear matter}) \quad ,$$

where ρ is the local density and n_1 and n_2 are not necessarily integers. At zero density, the free scattering case, this form of the interaction is identical to the form previously considered and thus the fitting procedure to the S-wave scattering data is unchanged.

For all nuclear systems having [4, 4, ----] supermultiplet symmetry, including nuclear matter and finite nuclei represented by closed sub shells, the total energy is invariant to individual changes in the strengths of the exchange operators, provided the parameter ν is unchanged

(Chapter 2), where

$$\nu = 10(W-M) + 8(B+H) \quad .$$

Thus using the first order formulae quoted in Appendix 5 for nuclear matter properties, c_3 and c_4 can be deduced by fitting the binding energy and saturation density of nuclear matter for any interaction characterized by V_A, V_R, λ_a, λ_r^0, c_1, c_2, n_1, n_2 and ν. The values chosen for the properties of nuclear matter fitted by most interactions presented in Table 3.1 are those suggested by Sprung (Spr 69). They are

B.E./A = - 16 Mev and saturation density, $k_F = 1.36$ fm^{-1}.

The procedure of determining the form of the interaction (for given V_A, V_R, λ_a, λ_r^0, n_1 and n_2) by fits to the scattering data and nuclear matter results in a family of interactions all having identical values for c_1 and c_2 but having different values of ν, c_3 and c_4. This family of interactions will also give different values for K, the compressibility of nuclear matter. At saturation K is defined as

$$K = k_F^2 \frac{d^2(B.E./A)}{d\, k_F^2} \quad .$$

The final interaction chosen, from the family of interactions, to calculate the O-p shell nuclei is obtained by fitting the binding energy of ^{16}O. This determines

unique values for ν, c_3 and c_4.

Table 3.1 lists a number of interactions (Interactions 6 - 37) obtained by following the above procedure. Some of the interactions listed have slightly different forms of the interaction than the form established above and, for some interactions the nuclear matter criteria are different. These exceptions are noted in Table 3.1.

There is complete freedom in the choice of V_A, V_R, λ_a, n_1 and n_2 for the effective interactions. However, the requirement that the second order correction terms in nuclear matter be small imposes the restriction that $|V_A| - |V_R|$, the repulsive core height not be too large. The repulsive core height was fixed at approximately 5 Mev for the interactions first studied during the course of this work. Subsequent investigation of the role of the core height (summarized in Chapter 9) showed that, for reasonable core heights, there were no differences in the properties of nuclear matter or finite nuclei for interactions with the same value of V_A but different values of V_R.

The scattering data fit, taken with the ^{16}O binding energy fit and the normalization condition, W+M = 1, leaves just one degree of freedom in the choice of the exchange operator strengths. This point is examined in Chapter 5.

The local density ρ is generally taken to be that pertaining at the centre of mass of the interacting nucleons. Other interpretations for the local density are considered

in Chapter 6.

Determination of Matrix Elements

For practical reasons the single particle basis chosen for this investigation is that of the cylindrically symmetric harmonic oscillator well. In this basis, some suitable meaning must be given to k in the context of the evaluation of the potential matrix elements $\langle ij|V|k\ell\rangle$. A suitable choice of k is fully discussed by Manning (Man 67) and he has demonstrated that a selection of k satisfying

$$k^2 = \tfrac{1}{4}[(2n_i + |m_i| + 1)\alpha_i + (2n_j + |m_j| + 1)\alpha_j + (2n_k + |m_k| + 1)\alpha_k + (2n_\ell + |m_\ell| + 1)\alpha_\ell + (n_{z_i} + \tfrac{1}{2})\beta_i + (n_{z_j} + \tfrac{1}{2})\beta_j + (n_{z_k} + \tfrac{1}{2})\beta_k + (n_{z_\ell} + \tfrac{1}{2})\beta_\ell]$$

is a satisfactory approximation.

It is of paramount importance to choose the form of the density function ρ so that the required matrix elements can be easily evaluated. Since, in fact, the dependence on the density ρ is such that, generally, ρ appears in the potential matrix elements raised to some non-integer power, a great limitation is placed on the choice of the form of the density function. From this point of view, a satisfactory form of the density function

is the single gaussian form since this form considered to any power is still a gaussian. The necessary gaussian parameters are determined by the requirement that the gaussian distribution have the same mean square expectation values for the cylindrical coordinates ρ and z as does the actual nuclear density or, in practice, as does an approximation to the true nuclear density. The approximation to the actual nuclear density is to consider the 4 S-states to be occupied by a single nucleon and the 12 P-states to be occupied by (A-4)/12 nucleons. This approximation is examined in Chapter 6.

If ρ_0 and z_0 represent root-mean-square dimensions of the approximate nuclear density, then the single gaussian density approximation is of the form

$$\rho_{(i)}(r) = 2^{-1/2}\ \pi^{-3/2}\ \rho_0^{-2}\ z_0^{-1}\ A\ \exp(-\rho^2/\rho_0^{\,2} - z^2/2z_0^{\,2}).$$

Manning (Man 67) has pointed out that this density approximation overestimates the true central density particularly for those nuclei which have a pronounced central dip in their density distributions. He considered a different form of the density approximation (approximation (iv) of Chapter 6). This approximation was designed to give the same central density (the density at the centre of the nucleus) and the same ratio $\langle\rho^2\rangle/\langle z^2\rangle$ as that of the actual nuclear density. In this case, the density approximation is of the form

$$\rho_{(iv)}(r) = D\ \exp(-\rho^2/K\ \rho_0^{\,2} - z^2/2K\ z_0^{\,2})$$

where D is the central density of the true nuclear density and K is defined by

$$K = [2^{-1/2}\ \pi^{-3/2}\ A/D\ \rho_0^{\,2}\ z_0]^{2/3} \quad .$$

For both of these approximations the local density is evaluated at the centre of mass of the interacting particles. In the case where the interacting nucleons are at opposite sides of the nucleus these approximations would consider the local density to be that at the centre of nucleus. This is unrealistic, particularly for light nuclei where the nuclear surface is very important. Thus, in Chapter 6, approximations (ii) and (iii) consider the local density to be evaluated at points other than the centre of mass.

Thus, for approximation (ii), $\rho(R)$ for approximation (i) (where $R = \frac{1}{2}(\underline{r}_1+\underline{r}_2)$) is replaced by

$$\rho\left(\sqrt{\frac{|\underline{r}_1|^2 + |\underline{r}_2|^2}{2}}\right) = \sqrt{\rho(|\underline{r}_1|)\ \rho(|\underline{r}_2|)}$$

for the gaussian form of the density distribution

and for approximation (iii) by

$$(\rho(\underline{r}_1) + \rho(\underline{r}_2))/2$$

Calculational Details

The general variational method employed in the

calculations for finite nuclei has been outlined in Chapter 2. The choice of cylindrically symmetric single particle wave functions means that, for the product determinantal states constructed from this single particle basis J is not a good quantum number. However M, the projection of J onto the symmetry axis, the z-axis, is.

At zero deformation the Hamiltonian is rotationally invariant and the eigenvalues calculated in different M sub-spaces will be degenerate provided the M sub-spaces span the same truncated space, i.e. the single particle basis includes all possible states of the oscillator well characterized by N, where $N = 2n + |m| + n_z$. The different states satisfying this requirement must have the same oscillator strength (i.e. $\alpha_{P_0} = \alpha_{P_{\pm 1}}$). The procedure, thus, followed in assigning the spins, J, of the ground state and excited states is to perform a variational calculation in the M = 0 (or M = ½) sub-space to obtain $\alpha_{S_{min}}$ and $\alpha_{P_{min}}$ such that the ground state binding energy is a minimum. $\alpha_{S_{min}}$ and $\alpha_{P_{min}}$ are used as the oscillator parameters in further diagonalizations of the Hamiltonian in higher M sub-spaces. A simple counting procedure of the number of degeneracies in the different M sub-spaces enables a J to be assigned to a level (e.g. J = 4 can be assigned to an eigenvalue which is degenerate in the M = 4, 3, 2, 1 and 0 sub-spaces).

The ground state binding energy is minimized with

respect to the oscillator parameters of both the S and the P orbitals (α_S and α_P). The procedure adopted was to parameterize the minimization with respect to α_S and σ, where $\sigma = \alpha_S/\alpha_P$. α_S's were found, for three different values of σ, which minimized the ground state binding energy. From this data a σ is evaluated which is considered to be the value of σ which will give the lowest ground state binding energy and a α_S is calculated which gives the minimum ground state binding energy for this value of σ. The basic assumption used in the minimization process was that the nuclear binding energy varies in a parabolic manner with α_S and with σ (Vol 65). This minimization procedure involves sixteen calculations for, and diagonalizations of, the Hamiltonian matrix. The procedure was found to be good for most nuclei studied if the initial choices for α_S and σ were reasonable (i.e. not too different from the final α_S and σ).

The above minimization procedure can be followed at any deformation. By explicit testing, however, it has been found to be sufficient to determine σ at zero deformation and use this value of σ at other deformations, thus merely minimizing the binding energy at these deformations with respect to α_S.

The time required for a full minimization of the ground state binding energy of a nucleus (N,Z) varied considerably, the minimum time (for Z = N = 2) and one

determinantal state) being 3 secs. and the maximum time (for Z = N = 6 and 84 states in the M = 0 sub-space) being 9 minutes. The quoted times are for calculations performed using the CDC 6400 computer at the McMaster University Computational Centre.

TABLE 3.1

Interaction No.	V_A c_1	V_R c_2	λ_a c_3	λ_r^0 c_4	B-H K (Mev)	ν $B.E._{den}$ (Mev)	n_1 ^4He B.E. (Mev)	r.m.s. (fm)	n_2 ^{16}O B.E. (Mev)	r.m.s. (fm)
	-78.03	82.8	1.5	0.8	0.25	-3.0				
1	-	-	-	-	-	-	31.86		112.46	
							1.45		2.08	
	-83.34	144.86	1.6	0.82	0.0	-2.0	-		-	
2	-	-	-	-	-	-	27.17		128.77	
							1.68		2.23	
	-60.0	60.0	1.8	1.01	0.0	-3.0				
3	-	-	-	-	-	-	27.49		104.04	
							1.69		2.40	
	-78.03	82.8	1.5	0.76	0.25	-3.0	-		-	
4	0.496	0.7	-	-	-	-	32.61		113.47	
							1.55		2.28	
	-78.03	82.8	1.5	0.76	0.25	-2.5	-		-	
5	0.496	0.7	-	-	-	-	32.61		127.12	
							1.55		2.22	
	-78.03	82.8	1.5	0.76	0.25	-2.4	1		1	
6	0.496	0.7	+1.21963	5.7207	257	2.18	30.34		128.90	
							2.00		2.87	

TABLE 3.1 - CONTINUED

	-78.03	82.8	1.5	0.76	0.25	-3.0	1	2
7	0.496	0.7	+0.36329	1.1498	236	-0.53	35.47	131.21
							1.83	2.69
*	-78.03	82.8	1.5	0.76	0.25	-2.5	1	2
8	0.496	0.7	-0.72786	2.96976	280	1.74	32.91	125.23
							1.83	2.67
	-250.0	255.0	1.5	1.247	0.4	-1.5	1	1.5
9	0.15	0.836	+0.14987	0.2905	200	19.87	27.87	129.66
							2.07	2.89
	-250.0	255.0	1.5	1.247	0.4	-1.5	1	2
10	0.15	0.836	+0.034498	0.1245	213	19.86	27.28	124.73
							2.04	2.87
	-250.0	255.0	1.5	1.247	0.4	-2.5	1	6
11	0.15	0.836	-0.02853	0.00763	301	12.12	32.79	133.45
							1.90	2.76
	-250.0	255.0	1.5	1.247	0.4	-2.5	1	12
12	0.15	0.836	-0.04196	0.00055	470	12.01	31.48	126.34
							1.89	2.75
*	-250.0	255.0	1.5	1.247	0.4	-2.0	1	2
13	0.15	0.836	+0.08737	0.26774	207	15.99	30.48	133.28
							1.99	2.83
	-250.0	255.0	1.5	1.247	0.4	0.0	1	2
14	0.15	0.836	-0.0169	0.1066	248	31.5	18.68	98.37
							2.19	2.98

TABLE 3.1 - CONTINUED

†	-250.0	255.0	1.5	1.247	0.4	-2.5	1	2
15	0.15	0.836	+0.03105	0.09850	159	14.01	31.34	125.62
							1.95	2.84
†	-250.0	255.0	1.5	1.247	0.4	-2.5	1	2
16	0.15	0.836	+0.0033	0.06291	173	19.57	31.33	126.24
							1.91	2.77
	-250.0	255.0	1.5	1.247	0.4	-1.5	-1	2
17	0.15	0.836	+0.02149	0.09919	196	19.87	28.25	128.45
							2.05	2.88
	-250.0	255.0	1.5	1.247	0.4	-2.0	-1	3
18	0.15	0.836	-0.00687	0.04998	236	15.99	29.76	128.59
							1.97	2.81
	-250.0	255.0	1.5	1.247	0.4	-2.5	-1	4.5
19	0.15	0.836	-0.02127	0.02047	287	12.12	32.32	131.67
							1.90	2.75
	-250.0	255.0	1.5	1.247	0.4	-2.5	-1	6
20	0.15	0.836	-0.03774	0.01015	366	12.12	30.69	123.61
							1.88	2.73
**	-250.0	255.0	1.5	1.247	0.4	-1.5	1	2
21	0.15	0.836	+0.03479	-0.08429	212	-	27.23	122.4
							2.02	2.86
**	-250.0	255.0	1.5	1.247	0.4	-1.5	1	2
22	0.15	0.836	-0.05139	0.12438	213	-	27.25	123.85
							2.03	2.86

TABLE 3.1 - CONTINUED

	-67.50	72.5	1.5	0.602	0.312	-3.6	1	2
23	0.7096	0.5869	+0.38675	1.71262	256	-3.93	37.81	128.77
							1.79	2.68
	-67.50	72.5	1.5	0.602	0.312	-3.5	1	3
24	0.7096	0.5869	+0.27323	0.84495	285	-3.53	-	125.61
								2.65
*	-67.50	72.5	1.5	0.602	0.312	-3.5	1	3
25	0.7096	0.5869	+0.59444	2.20965	320	-3.52	37.91	127.74
							1.75	2.61
	-67.5	72.5	1.5	0.602	0.312	-4.0	2	3
26	0.7096	0.5869	+0.34059	1.38381	332	-5.56	40.73	131.15
							1.75	2.63
*	-67.50	72.5	1.5	0.602	0.312	-4.0	2	3
27	0.7096	0.5869	+0.73526	3.67981	385	-5.56	41.66	133.53
							1.72	2.59
	-73.0	73.0	1.5	0.69818	0.32	-3.25	1	2
28	0.666	0.64238	+0.35872	1.36325	247	-1.68	36.32	128.48
							1.82	2.70
	-73.0	123.0	1.5	0.58538	0.32	-3.25	1	2
29	0.38575	0.65844	+0.35092	1.32535	240	-1.7	35.98	128.11
							1.80	2.67
	-110.0	110.0	1.375	0.85637	0.32	-3.0	1	2
30	0.35633	0.66273	+0.33751	0.69659	238	-0.97	35.99	130.93
							1.82	2.86

TABLE 3.1 - CONTINUED

	-146.77	146.77	1.25	0.86103	0.33	-3.0	1	2
31	0.23516	0.58870	+0.36614	0.57321	251	3.08	35.25	124.55
							1.80	2.67
	-460.0	460.0	1.0	0.88111	0.28	-1.0	1	2
32	0.10327	0.74921	+0.33679	0.30743	330	-5.26	33.13	129.83
							1.77	2.58
	-485.0	485.0	1.0	0.88769	0.28	1.0	1	2
33	0.11616	0.82465	+0.32272	0.31042	371	-1.85	28.24	126.80
							1.82	2.59
	-510.0	510.0	1.0	0.89290	0.28	2.5	1	2
34	0.12674	0.87669	+0.31683	0.31109	407	0.46	25.95	130.19
							1.84	2.58
	-510.0	510.0	1.0	0.89290	0.28	5.0	-1	2
35	0.12674	0.87669	+0.16532	0.11336	301	5.99	23.88	126.81
							1.96	2.66
	-110.0	110.0	1.375	0.85637	0.32	-2.8	1	2
36	0.35633	0.66273	+0.32907	0.70753	242	-0.15	34.4	127.15
							1.84	2.70
	-223.54	223.54	1.375	1.11836	0.35414	-2.7	-1	6
37	0.15961	0.75275	+0.01178	0.01163	316	4.62	34.15	127.19
							1.83	2.70

$$V(r) = [V_A[1 + c_3(\frac{3\pi^2}{2}\rho)^{n_1/3}] \exp(-r^2/\lambda_a{}^2)$$

$$+ V_R[1 + c_4(\frac{3\pi^2}{2}\rho)^{n_2/3}] \exp(-r^2/\lambda_r{}^2(k))]$$

$$[W + M P_M + B P_\sigma + H P_\tau]$$

$$\lambda_r(k) = \lambda_r{}^0(1 + c_1(k - c_2)^2)$$

$$\nu = 10(W-M) + 8(B + H)$$

K - Compressibility of Nuclear Matter

$B.E._{den}$ - Energy of the density dependent part of the interaction in nuclear matter.

---

*For these interactions the range of the basic gaussian for the density dependent parts of the interaction is one half ($\lambda_a/2$ and $\lambda_r/2$) that of the non-density dependent parts of the interaction.

†Interaction 15 has been fitted to a binding energy per particle in nuclear matter of -14 Mev.

Interaction 16 fits nuclear matter at a saturation density of 1.5 fm.

**Interaction 21 is of the basic form

$$(1 + c_3(\frac{3\pi^2}{2}\rho)^{n_1/3} + c_4(\frac{3\pi^2}{2}\rho)^{n_2/3})V_A$$

$$\exp(-r^2/\lambda_a{}^2) + V_R \exp(-r^2/\lambda_r{}^2(b)) \quad .$$

TABLE 3.1 - CONTINUED

Interaction 22 is of the basic form

$$V(r) = V_A \exp(-r^2/\lambda_a{}^2) + (1 + c_3(\frac{3\pi^2}{2}\rho)^{n_1/3} + c_4(\frac{3\pi^2}{2}\rho)^{n_2/3}) V_R \exp(-r^2/\lambda_r{}^2(k)) \quad .$$

CHAPTER 4

LOCAL AND VELOCITY DEPENDENT INTERACTIONS

This chapter is concerned with various non-density dependent interactions. The interactions considered do not fit the criteria established in Chapter 3. Interaction 1 was determined by fitting the zero-energy scattering data of the S-wave i.e. the triplet-even and singlet-even effective ranges and scattering lengths. It was further required that it predict the experimental binding energy of ^{4}He. This interaction has been used in previous calculations (Hug 66) to investigate the 1st excited state of ^{16}O.

Interaction 2 has been used by Volkov (Vol 65) to investigate the deformation of the O-p shell nuclei. It was derived by fitting the zero-energy S-wave scattering data in a very crude manner. Brink (Bri 65) has modified this interaction to the form listed as interaction 3 in Chapter 3.

Since many calculations have been performed using these interactions without the Coulomb interaction being included in the interaction Hamiltonian, it was decided to calculate the O-p shell nuclei with and without the Coulomb term. Thus, not only can the effect of the Coulomb interaction on ground state energies, excitation energies and

root-mean-square radii, be ascertained but also comparisons can be made between results for the type of calculation envisioned in Chapter 2 and those obtained from various projected Hartree-Fock calculations.

A refinement of the basic Volkov interaction, consisting of making the repulsive range velocity (or state dependent) has been suggested (Hug 66a; Man 67). Such an interaction (Interaction 3) is considered in this chapter. This interaction underbinds ^{16}O and a modified version (Interaction 4) is studied which predicts the correct ^{16}O binding energy.

Deformation equilibrium studies are presented for a number of the interactions.

With the exception of the interactions studied in Chapter 10, only one of the isobaric nuclei for a given A was calculated for the interactions. These nuclei were ^{6}Li, ^{7}Be, ^{8}Be, ^{9}B, ^{10}B, ^{11}B, ^{12}C, ^{13}C, ^{14}N. For each nucleus, the strength of the spin-orbit interaction, C, was varied over a given range in discrete steps. The values of C for the different nuclei are summarized in Table 4.1.

It was generally found that these ranges of C variation were adequate either, to produce a "fit" to the spectra of the nucleus being studied, or, to indicate that no "fit" was possible for that interaction. A=15 nuclei were not considered since it is always possible to choose a C such that the correct splitting of the two possible 0-p

TABLE 4.1

A	Initial C (Mev)	Final C (Mev)	Increment in C (Mev)
6	-0.5	-2.5	-0.5
7	-1.0	-3.0	-0.5
8	-1.5	-3.5	-0.5
9	-3.0	-6.0	-1.0
10	-4.0	-6.0	-1.0
11	-3.5	-6.5	-1.0
12	-3.5	-5.5	-0.5
13	-3.5	-5.5	-0.5
14	-4.0	-6.0	-0.5

states is reproduced. Similar considerations apply to the A=5 system. In addition the A=5 nuclei are underbound with respect to ^{4}He and a full variation of the A=5 system with respect to the O-s and O-p oscillator parameters gives a O-p shell oscillator strength of 0 Mev i.e. the minimum energy of the system is for four particles in the O-s shell, ^{4}He.

Interaction 1

Figs. 4.1-4.9 illustrate the results obtained using Interaction 1 following the procedure outlined above. The results are presented for calculations with the Coulomb interaction both present and absent from the interaction Hamiltonian and with a value of the spin-orbit strength, C chosen to give the best fit to the experimentally observed spectra of the nucleus A with the Coulomb interaction included. The excitation energies have a smooth behaviour with the variation in C and better fits to the spectra are possible for values of C intermediary to those considered. Since the purpose of this work is primarily to compare interactions, at this stage, this procedure was not followed. Table 4.2 lists the calculated binding energies and root-mean-square radii for the nuclei considered.

Equilibrium deformation calculations were also performed for this interaction. Table 4.3 summarizes the results of these calculations, which were performed with

TABLE 4.2

A	Coulomb included in Hamiltonian (a)		Coulomb excluded from Hamiltonian (b)		Difference of binding energies between (a) and (b)
	B.E.(MeV)	r.m.s.(fm)	B.E.(Mev)	r.m.s.(fm)	
4	31.86	1.45	32.84	1.44	0.98
6	21.22	2.17	23.12	2.14	1.90
7	21.52	2.22	25.39	2.13	3.87
8	36.30	2.09	40.10	2.06	3.80
9	31.44	2.21	37.23	2.18	5.79
10	41.19	2.23	46.97	2.20	5.78
11	49.74	2.22	55.61	2.19	5.87
12	67.24	2.16	76.16	2.14	8.92
13	69.39	2.19	78.26	2.17	8.87
14	78.02	2.16	90.43	2.13	12.41
16	112.46	2.08	128.72	2.05	16.26

TABLE 4.3

A	Prolate		Oblate	
	Energy gain on deformation	$\varepsilon_{Prolate}$	Energy gain on deformation	ε_{Oblate}
6	0.33	0.27	0.15	-0.1
7	3.70	0.46	0.45	-0.27
8	6.15	0.50	1.45	-0.35
9	1.53	0.43	1.68	-0.38
10	1.68	0.30	2.45	-0.41
11	0.60	0.20	3.85	-0.45
12	0.30	0.15	4.10	-0.45
13	0.20	0.10	1.70	-0.27
14	0.00	0.0	0.10	-0.10

the Coulomb term included. The shapes of the binding energy-deformation plots were similar to those reported by Volkov (Vol 65).

The root-mean-square radii at the equilibrium minima are nearly the same as those at zero deformation for A=9 - A=14 but are substantially less for A=6, 7 and 8. This may be more a reflection on the minimization technique used (since the A=6, A=7 binding energies are calculated to be less than that calculated for ^{4}He) than a realistic result.

Comparisons of Figs. 4.1 - 4.9 with the experimental results indicate that interaction 1 is not capable of reproducing the experimental excitation energies with the exception of ^{6}Li and ^{7}Be. The calculated spectra of A=8 and A=12 could be improved by taking lower values of the spin-orbit interaction but even then the discrepancies between the calculated and experimental excitation energies would be substantial. This interaction was designed to fit the binding energy of ^{16}O without the Coulomb interaction. Thus, no comparison can be made between the experimental binding energies and those quoted in (a) of Table 4.2. The calculated binding energies presented in (b) of Table 4.2 can be compared with the binding energies deduced from experiment, although this procedure is unphysical. This comparison, however, reveals one of the major faults of local interactions of Volkov type; the binding energies

of the open shell nuclei are much too small. This is true even when the energy gained by permitting the nucleus to deform is added to the quoted figures of Table 4.2 (b). For example, the calculated binding energy of ^{14}N is 14 Mev too small. A more alarming feature is that the calculated binding energies of ^{6}Li and ^{7}Be are below the calculated binding energy of ^{4}He. The calculated root-mean-square radii are all too small, indicating the tendency of nuclear systems calculated with this interaction to start collapsing (Bha 66).

Since most calculations of excitation energies are performed with the omission of the Coulomb interaction, it is of some interest to attempt an estimation of the effect of this omission. The Coulomb interaction is repulsive and its inclusion in a calculation would be expected to increase the nuclear size. This is clearly seen in Table 4.2, the greatest change being for the N=3, Z=4 system, ^{7}Be.

The excitation energies are generally only slightly changed (< 0.25 Mev) by switching on the Coulomb interaction. Exceptions are: the $\frac{5}{2}^-$ state of ^{7}Be, lowered by 1.3 Mev, the higher states of ^{8}Be, lowered by 0.6 Mev and the first 0^+ and 1^+ and the higher states of ^{12}C, lowered by less than 0.5 Mev. The most spectacular change is again for ^{7}Be. This is not surprising since ^{7}Be has proportionally more proton bonds than the rest of the nuclei studied.

Interaction 2

For the purposes of deriving an interaction which

reproduces the excited state spectra of O-p shell nuclei, Interaction 2 is not very interesting since spectra calculated using this interaction (Figs. 4.1 - 4.9) have little correspondence with those determined by experiment. However, many authors (Bou 67; Bof 68; Fae 68; Bou 68; Boe 67; Boe 68) have performed Projected Hartree-Fock calculations using this interaction and, thus, a comparison of results can be made. The spin-orbit strengths used in the calculation for Figs. 4.1 - 4.9 are the same as those for Interaction 1. Again calculations are performed both with the Coulomb force included and excluded from the Hamiltonian. The inclusion of the Coulomb interaction has less effect on the excitation energies than for Interaction 1; the $\frac{5}{2}^-$ level of ^{7}Be changes by 0.38 Mev for Interaction 2. The relevent binding energies and root-mean-square radii are recorded in Table 4.4.

The binding energies and root-mean-square radii are again too small; ^{6}Li and ^{7}Be are still not bound with respect to the binding energy of ^{4}He.

Interaction 2 has a longer attractive range than Interaction 1 so that generally the interacting nucleons will be further apart. Thus the root-mean-square radii for Interaction 2 are larger than those for Interaction 1. The Coulomb interaction is inversely proportional to the interaction distance and consequently the Coulomb contribution to the binding at equilibrium is smaller for Interaction

TABLE 4.4

A	Coulomb included in Hamiltonian (a)		Coulomb excluded from Hamiltonian (b)		Difference of binding energy between (a) and (b)
	B.E.(Mev)	r.m.s.(fm)	B.E.(Mev)	r.m.s.(fm)	
4	27.17	1.68	28.01	1.68	0.94
6	20.70	2.38	22.41	2.36	1.71
7	24.33	2.36	27.66	2.33	3.33
8	36.97	2.29	40.44	2.28	3.45
9	36.81	2.39	42.16	2.36	5.35
10	47.82	2.40	53.19	2.37	5.37
11	58.41	2.38	63.88	2.36	5.47
12	76.10	2.35	84.37	2.32	8.27
13	81.60	2.35	89.92	2.32	8.32
14	91.18	2.31	102.84	2.28	11.66
16	128.77	2.23	144.87	2.21	16.10

2 than for Interaction 1.

Although it is the intention of this thesis to attempt to find an "effective" interaction which will "fit" the O-p shell excited state spectra and thus, to some extent, take into account configuration mixing from states outside the O-p shell, it is of interest to compare the results of this calculation with those performed with a single particle basis which includes such configuration mixing. It is known that a Hartree-Fock calculation to first order will not predict much greater binding energies than the variational calculation performed in this thesis. (Boeker (Boe 67), using Interaction 2, obtains a 2.5 Mev gain for the binding energy of ^{8}Be and an 0.5 Mev gain in the binding energy of ^{12}C in a first order Hartree-Fock calculation.) However, a Projected Hartree-Fock (P.H.F.) calculation which includes states of the ls-0d shell can produce much greater binding energy gains. (Bouten et. al. (Bou 67) reports gains of 0.1 Mev for ^{4}He, 4.04 Mev for ^{6}Li, 4.83 Mev for ^{7}Be and 7.83 Mev for ^{8}Be, with substantially smaller root-mean-square radii for all the above nuclei except ^{4}He.) The equilibrium deformations reported by these authors are greater than those found by Volkov (Vol 65).

P.H.F. calculations (in which states of definite orbital angular momentum L are projected out of the usual Slater determinant wave function) also predict greater

L-band separations than are predicted by the variational methods used in this work. Table 4.5 illustrates this point for ^{9}Be. δ_0 is the band separation ($E_{1^-} - E_{L^\pi}$) calculated with no admixture of 1s-0d states and δ is the band separation with 1s-0d states admixed (Bou 68). No spin-orbit term is included in the calculation.

TABLE 4.5

L^π	δ (Mev)	δ_0 (Mev)
2^-	2.0	1.42
3^-	7.1	3.54
4^-	10.1	6.34

The gain in binding energy when the 1s-0d states are admixed is 10.8 Mev. As can be seen from Table 4.5 the projection method has a very great effect on the band separations. It is of some interest to note that for Interaction 2 the rotational energy, $\langle \bar{J}^2 \rangle$ is of the same order as the energy gained by deforming and projecting out of a nuclear system. (Faessler (Fae 68) obtains $\langle \bar{J}^2 \rangle$ = 9.1 Mev in ^{12}C to give a total binding energy of 88 Mev; P.H.F. calculations (Bof 68; Boe 68) predict a ground state binding energy of 87.5 Mev for ^{12}C.)

Interaction 3

Interaction 3 has similar characteristics to Interaction 2. The calculated excited state spectra are

illustrated in Figs. 4.10 - 4.18 and the calculated binding energies and root-mean-square radii in Table 4.6. Again calculations were performed with inclusion and exclusion of the Coulomb interaction in the interaction Hamiltonian.

Interaction 3 has a larger attractive range than Interactions 1 and 2 and thus the calculated r.m.s. radii are larger and the Coulomb energy is smaller. The difference between the calculated excitation energies with and without the Coulomb term is also smaller than for the first two interactions considered.

The excited level spectra are generally very similar to those predicted by Interaction 2 although there are some significant differences. Although Interactions 2 and 3 fit approximately the same scattering data, they have so few parameters in common that no useful guidelines, to designing an interaction to fit the O-p spectra, can be obtained by a comparison of the excitation energies predicted by them.

P.H.F. calculations using Interaction 3 display the same tendencies exhibited by Interaction 2. Thus, for ^{12}C Bouten et. al. (Bou 67) find that the L=0 and L=4 bands, which lie at 2 Mev and 7 Mev excitation in the variational calculation, have excitation energies of 3.15 Mev and 11 Mev for a P.H.F. calculation. Bouten et. al. (Bou 69) have performed a P.H.F. calculation of ^{9}Be with a spin-orbit interaction, which is treated as a perturbation.

The strength of the spin-orbit interaction was -3.0 Mev.

TABLE 4.6

A	Coulomb interaction included (a)		Coulomb interaction excluded (b)		B.E. difference between (a) and (b)
	B.E.(Mev)	r.m.s.(fm)	B.E.(Mev)	r.m.s.(fm)	
4	27.49	1.69	28.33	1.68	0.84
6	19.89	2.59	21.51	2.54	1.62
7	22.55	2.47	25.73	2.43	3.18
8	34.23	2.38	37.57	2.36	3.32
9	32.79	2.53	37.86	2.49	5.07
10	42.21	2.56	47.27	2.53	5.06
11	50.75	2.54	55.87	2.52	5.12
12	66.08	2.50	73.85	2.47	7.77
13	68.72	2.52	76.47	2.49	7.75
14	74.91	2.49	85.74	2.45	10.83
16	104.04	2.40	119.07	2.36	15.03

Table 4.7 tabulates the excitation energies of the levels of ^{9}Be calculated by Bouten et. al. (Bou 69) and compares them with those predicted in the type of calculation performed in this thesis.

The excitation energies of the higher $\frac{5}{2}^-$ and $\frac{7}{2}^-$ levels are much greater for the P.H.F. calculation. The binding energies predicted by P.H.F. calculations, for Interactions 2 and 3 are still much smaller than the

TABLE 4.7

J^{π}	E_x(P.H.F.) (Mev)	E_x(Var.) (Mev)	Expt.(Mev)
$\frac{5}{2}^-$	2.46	2.28	2.43
$\frac{1}{2}^-$	2.59	2.90	
$\frac{3}{2}^-$	5.00	5.10	
$\frac{5}{2}^-$	7.95	5.40	
$\frac{7}{2}^-$	8.72	4.80	6.66

experimental values for the open-shell O-p nuclei. The enhanced separation of levels for P.H.F. calculations is, however, still found for an interaction which overbinds these nuclei. Abragall et. al. (Abr 69) include the Coulomb force in their calculation and use a single gaussian interaction which fits the binding energy of ^{16}O. Table 4.8 lists the results of the P.H.F. calculation with those obtained at zero deformation in a variational calculation.

TABLE 4.8

A	B.E.(Mev)		$E_{x_{2+}}$ (Mev)		$E_{x_{4+}}$ (Mev)	
	Abragall	Present Work	Abragall	Present	Abragall	Present
8	66.2	54.04	3.1	1.87	10.7	6.23
12	93.9	86.20	3.01	1.89	8.01	6.29

A	r.m.s.(fm)	
	Abragall	Present Work
8	2.66	2.38
12	2.68	2.61

Although the results for the excitation energies for all three interactions considered are generally poor when compared with experimental results, it is encouraging that Interaction 1, which fits the zero energy scattering data more closely than do Interactions 2 and 3, predicts excitation energies significantly closer to the experimental

values than do Interactions 2 and 3. Thus, it would seem possible to construct a local interaction of the type considered so far which would "fit" the O-p nuclei excited state spectra. However, there is no significant improvement in the open-shell binding energies for Interaction 1 over Interactions 2 and 3, and it seems likely that no modification of the local Volkov interaction will remove the discrepancy between the calculated and experimental binding energies of the O-p open-shell nuclei.

Since nucleons do not interact with zero relative energy it would be more meaningful to derive the interactions by fitting the scattering data at more realistic relative energies (10 - 100 Mev). Interactions developed with this criterion will now be discussed.

Interaction 4

Interaction 4 differs from Interaction 1 only in respect of the repulsive range. The repulsive range has been made velocity (state) dependent in accordance with the form established in Chapter 2. The binding energies of ^{4}He and ^{16}O are nearly identical for Interactions 1 and 4 but the r.m.s. radii are greater for Interaction 4. The calculated excited state spectra for this interaction are shown in Figs. 4.10 - 4.18, the same spin-orbit strengths being used in the calculations as was used for Interactions 1, 2 and 3. The introduction of velocity dependence into the repulsive range improves the excitation energies with respect

to the experimental values. In particular, the results for ^{12}C are much improved for Interaction 4 compared with the results for Interaction 1. Better fits to the experimental spectra are obtained for Interaction 4 with values of the spin-orbit strength different from those in the calculations illustrated.

Interaction 4, and all subsequent interactions, have only been used in calculations with the Coulomb interaction included in the interaction Hamiltonian.

The binding energies and root-mean-square radii of the O-p nuclei calculated using Interaction 4 are tabulated in Table 4.9.

TABLE 4.9

A	B.E.(Mev)	r.m.s.(fm)
4	32.61	1.55
6	24.13	2.17
7	25.41	2.21
8	38.73	2.18
9	35.99	2.29
10	46.07	2.31
11	54.81	2.32
12	71.76	2.30
13	77.28	2.28
14	85.96	2.27
16	113.47	2.28

The predicted binding energies are closer to the experimental values for this interaction than was so for the previous interactions but the calculated binding energies for the open-shell nuclei are still much too small. ^{6}Li and ^{7}Be are still predicted to be unbound with respect to ^{4}He. With the exception of these two nuclei the r.m.s. radii are very much greater for the velocity dependent interaction when compared with those calculated for the local Interaction 1.

To explain this great difference for the r.m.s. radii between Interactions 1 and 4 it is necessary to examine the repulsive range of Interaction 4 closely. This range is velocity dependent and thus decreases with decreasing kinetic energy provided this energy is less than 40 Mev. In the nuclear systems studied the kinetic energies range from 10 to 30 Mev. Thus, since the potential energy matrix elements increase for a less repulsive interaction (lower repulsive range), Interaction 4 favours regions of low kinetic energy much more strongly than does Interaction 1. The region of low kinetic energy in a nucleus is the surface. For ^{6}Li and ^{7}Be, the relatively few nucleons in the p shell are widely separated in the surface even for Interaction 1 and thus have a minimum kinetic energy already. Interaction 4 thus produces the same r.m.s. radii for these nuclei as Interaction 1. For other nuclei studied this is not so and the r.m.s. radii

are much greater.

The results of equilibrium deformation calculations for Interaction 4 are summarized in Table 4.10. These calculations were performed with a spin-orbit strength of - 2.0 Mev. The equilibrium point is reached in a deformation calculation when the rate at which the potential energy is decreasing is equal to the rate at which the kinetic energy is decreasing. A detailed examination of these factors is extremely complicated. Consider, for example, a system which favours a prolate deformation. The matrix elements favouring the prolate deformation are (Vol 65):

the P_0 kinetic matrix elements

the $P_{\pm 1}$ direct potential matrix elements

the P_0 exchange potential matrix elements.

The prolate deformation is opposed by

the S kinetic matrix elements

the S direct potential matrix elements

the $P_{\pm 1}$ kinetic matrix elements

the P_0 direct potential matrix elements

the $P_{\pm 1}$ exchange potential matrix elements.

Each of these matrix elements vary differently with the deformation parameter.

The situation is even more complex for a velocity dependent interaction since the potential energy matrix elements now depend on the kinetic energies of

the interacting particles. Comparison of matrix elements for Interactions 1 and 4 reveal that, of these matrix elements that favour prolate deformation, the P_0 exchange potential matrix elements are greater and the $P_{\pm 1}$ direct potential matrix elements are lesser for Interaction 4 than for Interaction 1. A similar situation pertains when the matrix elements which oppose a prolate deformation are compared. It is, thus, impossible to predict what the differences for the equilibrium deformation will be between calculations using Interactions 1 and 4.

TABLE 4.10

A	Prolate Energy Gain (Mev) on deformation	ε_p	Oblate Energy Gain (Mev) on deformation	ε_o
6	0.35	0.30	0.10	-0.13
7	3.45	0.45	0.45	-0.26
8	5.15	0.47	1.35	-0.35
9	1.20	0.40	1.65	-0.37
10	1.48	0.27	2.35	-0.43
11	0.45	0.17	3.65	-0.44
12	0.10	0.10	4.10	-0.45
13	0.0	0.0	1.80	-0.30
14	0.0	0.0	0.30	-0.15

Comparing Tables 4.3 and 4.10 it is seen that the equilibrium deformations for Interactions 1 and 4 are

remarkably similar. It would, therefore appear that the kinetic energy plays a dominant role in the equilibrium process for a deformed system (Vol 65).

Interaction 5

Interaction 4 does not predict the correct value for the binding energy of ^{16}O. A slight change in the Mayorana exchange strength enables such a fit. Thus Interaction 5, which predicts a ^{16}O binding of 127 Mev, differs from Interaction 4 only in regard to the value of ν(ν=-2.5 for Interaction 5, ν=-3.0 for Interaction 4). ^{4}He properties are, of course, unchanged, whilst the inter-shell binding energies increase and the root-mean-square radii of the nuclei considered decrease slightly. The increased ν (decreased Mayorana strength) for Interaction 5, gives greater weight to the direct matrix elements than is the case for Interaction 4. These matrix elements increase faster for a decreasing interaction separation than do the exchange matrix elements and thus the nuclear size also decreases. The binding energies and root-mean-square radii calculated for the O-p nuclei using Interaction 5 are listed in Table 4.11.

The binding energies of the open-shell nuclei are still too small and the problem of ^{6}Li and ^{7}Be being underbound with respect to ^{4}He is still unresolved.

The excited state spectra calculated for Interaction

TABLE 4.11

A	B.E.(Mev)	r.m.s.(fm)
4	32.61	1.55
6	25.09	2.13
7	26.09	2.18
8	40.98	2.15
9	39.02	2.25
10	49.89	2.28
11	59.50	2.29
12	76.20	2.25
13	81.17	2.29
14	92.00	2.26
16	127.12	2.22

5 are shown in Figs. 4.9 - 4.18. They are virtually identical with those calculated for Interaction 4. Because the P_0 and $P_{\pm 1}$ states have identical oscillator well parameters the differences $V_{10} - V_{10x}$ and $V_{11} - V_{11x}$ are identical.

$$(V_{10} \equiv \langle P_{\pm 1}\ P_0 | V_{12} | P_{\pm 1}\ P_0 \rangle\ V_{10x} = \langle P_{\pm 1}\ P_0 | V_{12} | P_0\ P_{\pm 1} \rangle).$$

Hence, a change in the weighting factors between direct and exchange matrix elements cannot change the energy difference between different product determinantal states. The slight difference in excitation energies is due to the different sizes of the nuclei for Interactions 4 and 5.

It has been demonstrated in this chapter that, although it is possible to fit the excited state spectra of the O-p nuclei with a local interaction of the Volkov type, such interactions tend to underbind the open-shell nuclei. This remains true for velocity dependent interactions of the kind considered in this thesis. The rest of the thesis is devoted to the study of density-dependent interactions.

FIGURE CAPTIONS

For all figures, excitation energy (in Mev) is plotted to the left of the figure. Full lines designate the calculated levels and dashed lines designate certain experimental levels. For even nuclei the spin J of the level is indicated to the right of the calculated levels and at the left of the figure for the experimental levels, for odd nuclei the value of 2J is likewise indicated.

Figures 4.1 - 4.9 plot the excited state spectra of the O-p shell nuclei calculated for

(a) Interaction 1 with the Coulomb Interaction present in the Interaction Hamiltonian

(b) Interaction 1 with the Coulomb Interaction absent from the Interaction Hamiltonian

(c) Interaction 2 with the Coulomb Interaction present in the Interaction Hamiltonian

(d) Interaction 2 with the Coulomb Interaction absent from the Interaction Hamiltonian.

Figure 4.1 Excited State Spectra of ^{6}Li with spin-orbit strength, C = -1.5 Mev.

Figure 4.2 Excited State Spectra of ^{7}Be with spin-orbit strength, C = -2.0 Mev.

Figure 4.3 Excited State Spectra of ^{8}Be with C = -1.5 Mev.

Figure 4.4 Excited State Spectra of ^{9}B with C = -3.0 Mev.

Figure 4.5 Excited State Spectra of ^{10}B with C = -5.0 Mev.

Figure 4.6 Excited State Spectra of ^{11}B with C = -4.5 Mev.

Figure 4.7 Excited State Spectra of ^{12}C with C = -5.5 Mev.

Figure 4.8 Excited State Spectra of ^{13}C with C = -5.0 Mev.

Figure 4.9 Excited State Spectra of ^{14}N with C = -4.5 Mev.

Figure 4.10 - 4.18 plot the excited state spectra of the O-p shell nuclei calculated for

(a) Interaction 3 with the Coulomb Interaction present in the Interaction Hamiltonian

(b) Interaction 3 with the Coulomb Interaction absent from the Interaction Hamiltonian

(c) Interaction 4

(d) Interaction 5.

Figure 4.10 Excited State Spectra of ^{6}Li with C = -1.5 Mev.

Figure 4.11 Excited State Spectra of ^{7}Be with C = -2.0 Mev.

Figure 4.12 Excited State Spectra of ^{8}Be with C = -1.5 Mev.

Figure 4.13 Excited State Spectra of ^{9}B with C = -3.0 Mev.

Figure 4.14 Excited State Spectra of ^{10}B with C = -5.0 Mev.

Figure 4.15 Excited State Spectra of ^{11}B with C = -4.5 Mev.

Figure 4.16 Excited State Spectra of ^{12}C with C = -5.5 Mev.

Figure 4.17 Excited State Spectra of ^{13}C with C = -5.0 Mev.

Figure 4.18 Excited State Spectra of ^{14}N with C = -4.5 Mev.

Figure 4.1

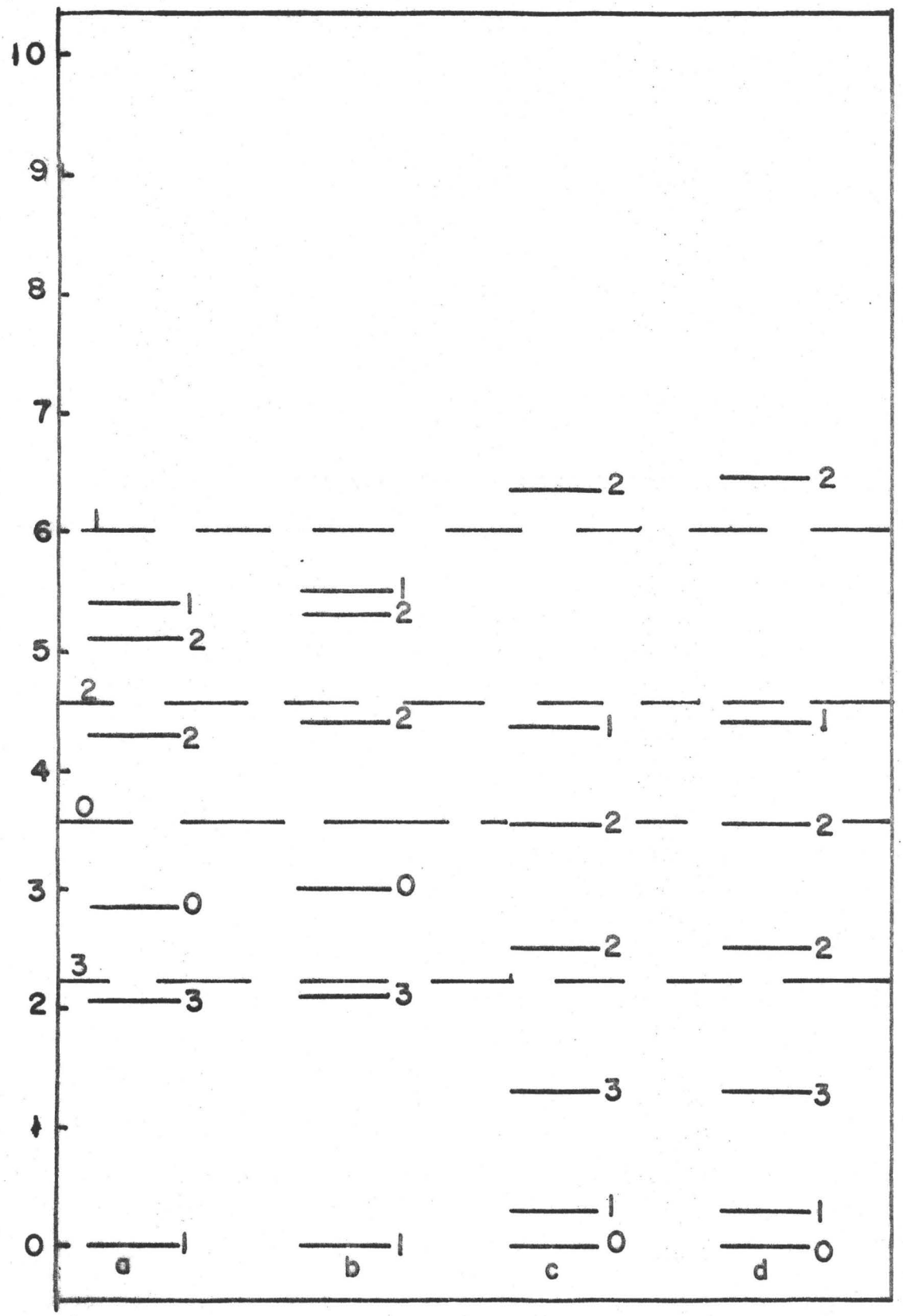

Figure 4.2

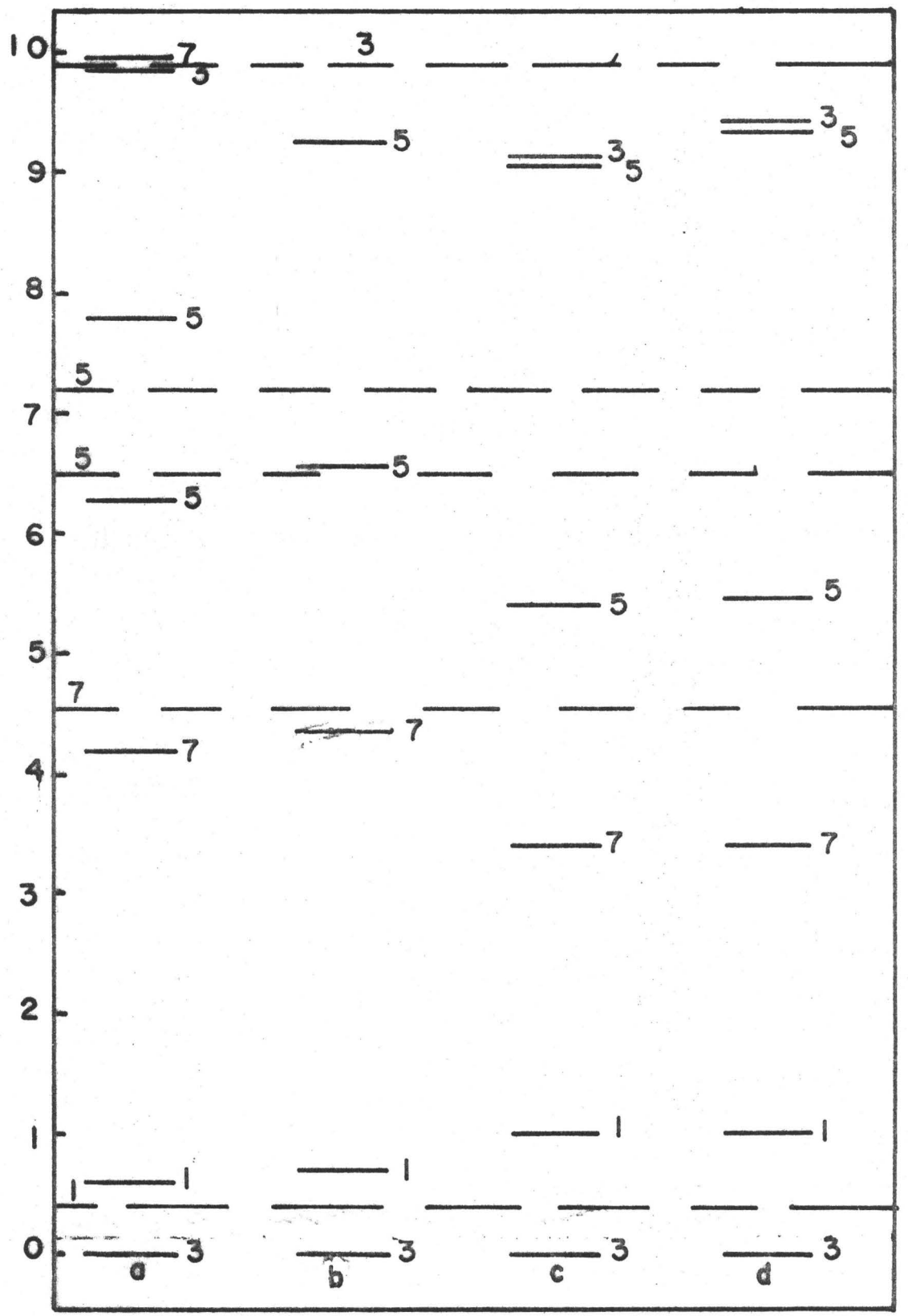

Figure 4.3

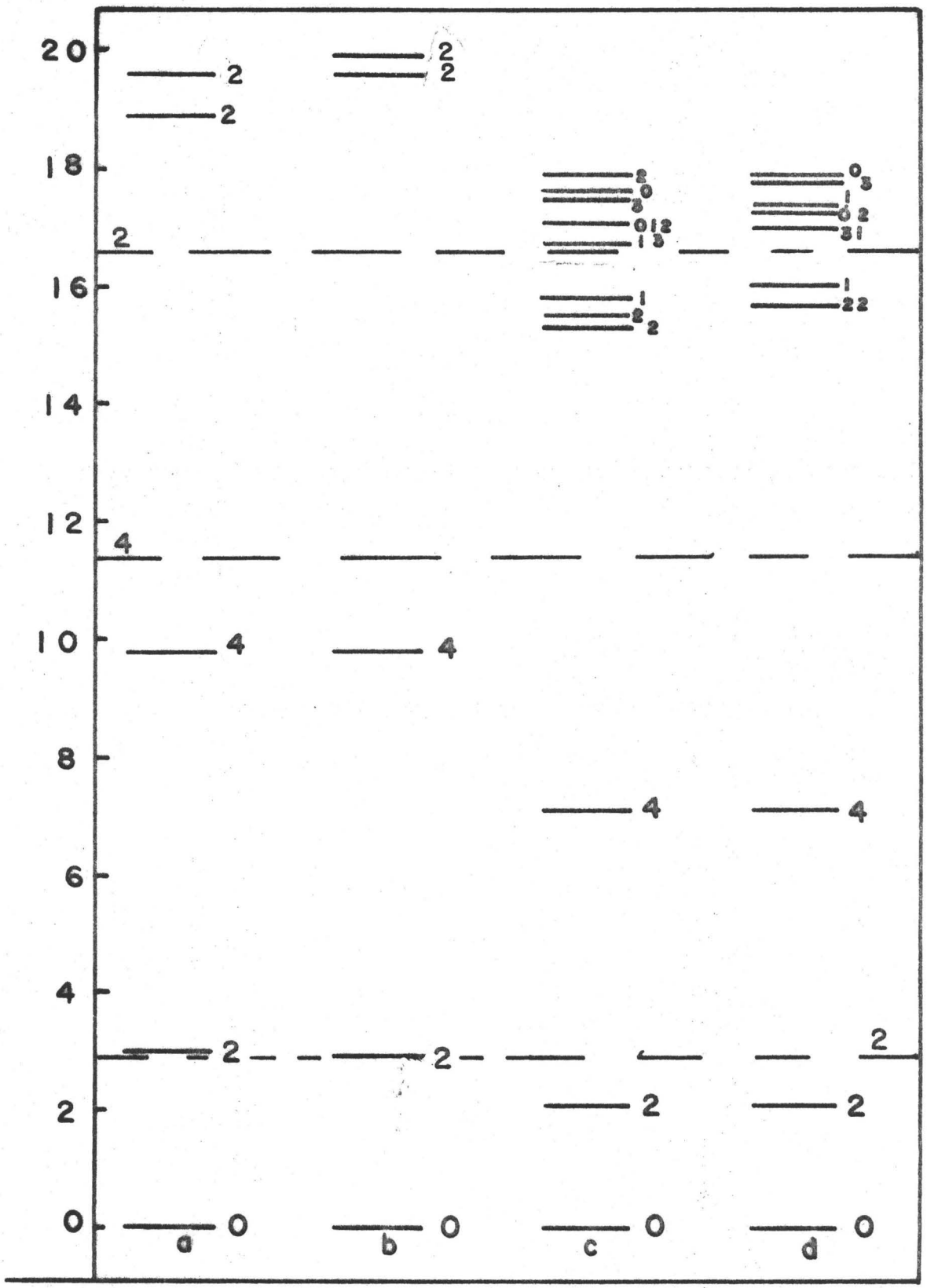

Figure 4.4

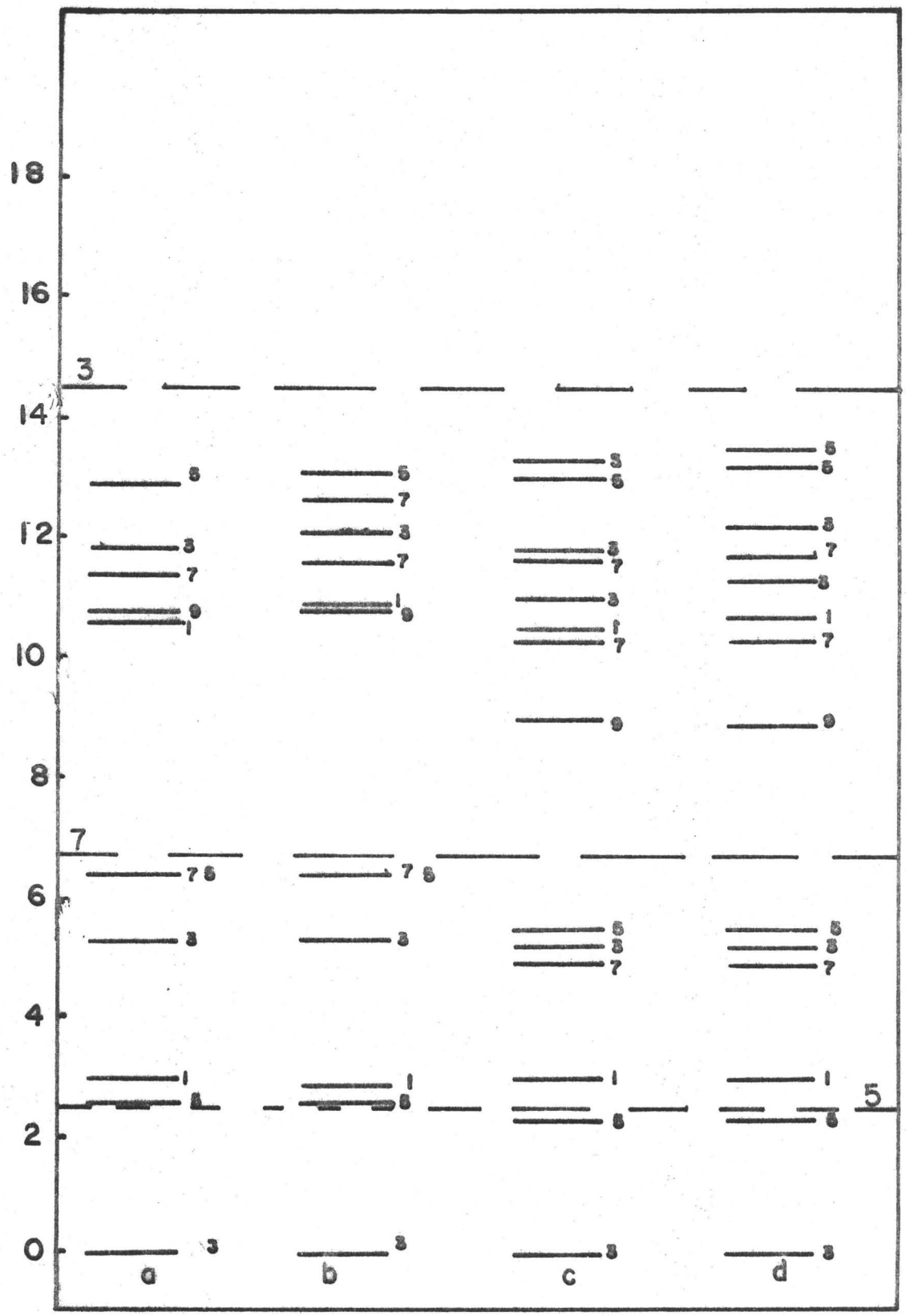

Figure 4.5

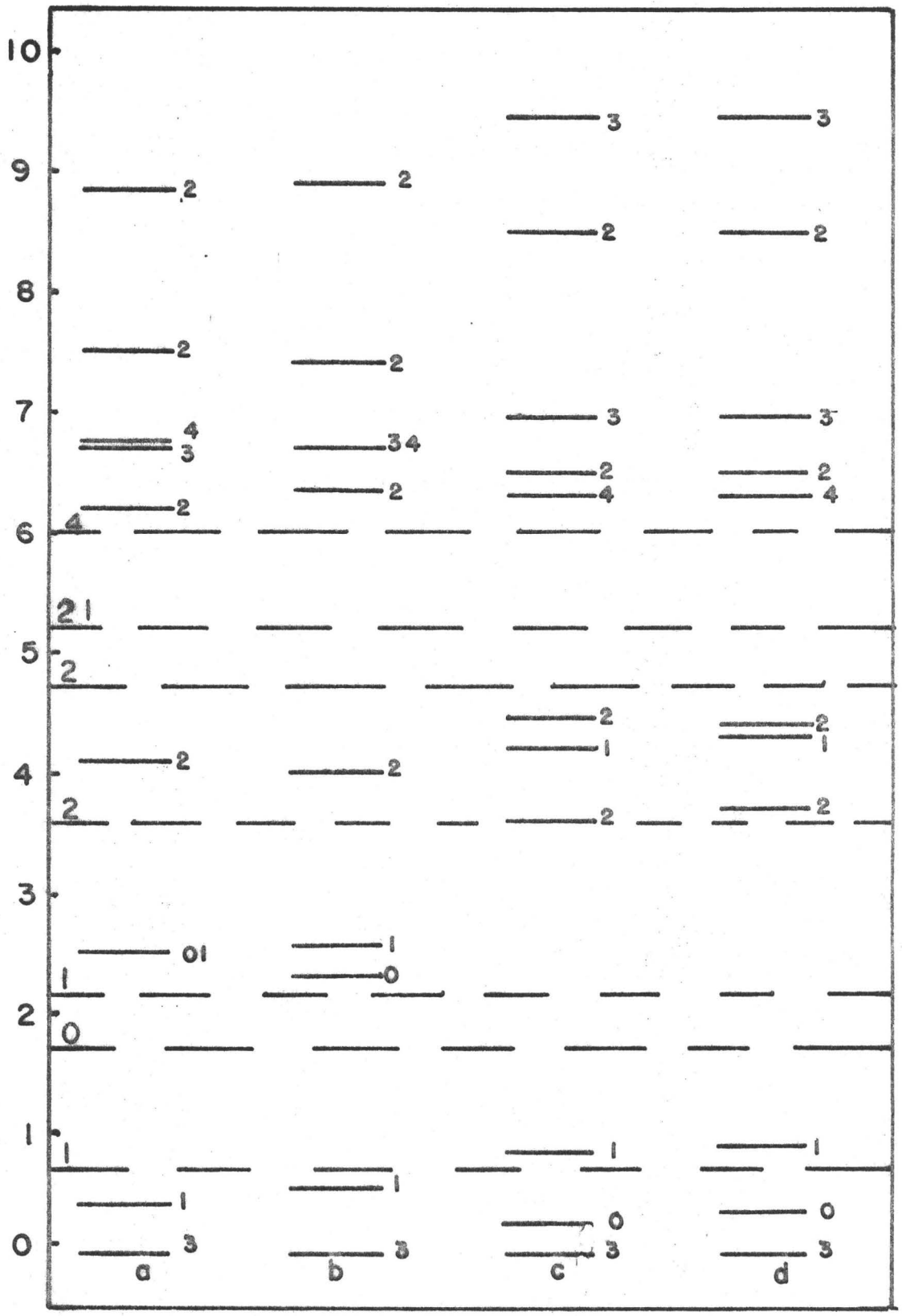

Figure 4.6

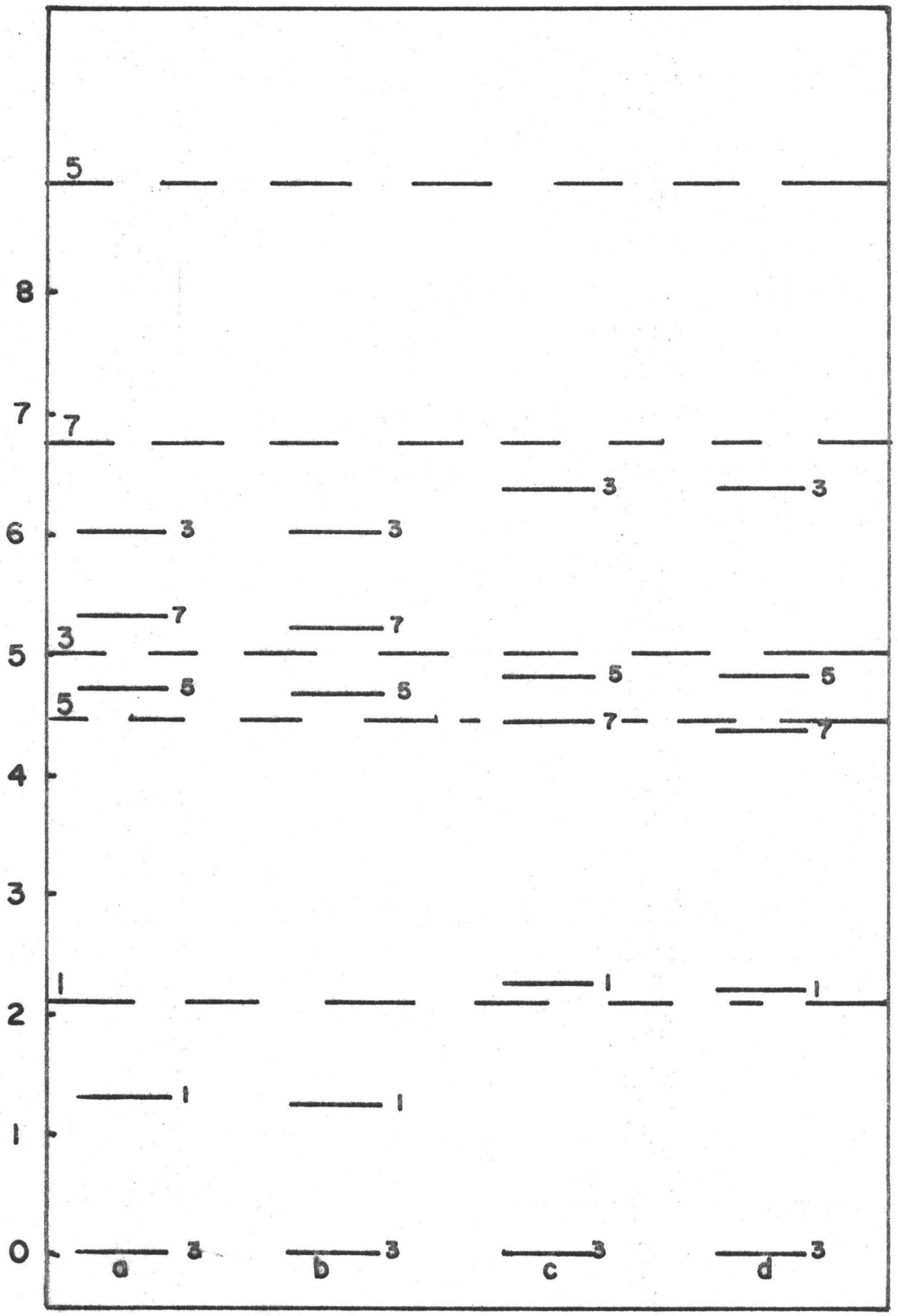

Figure 4.7

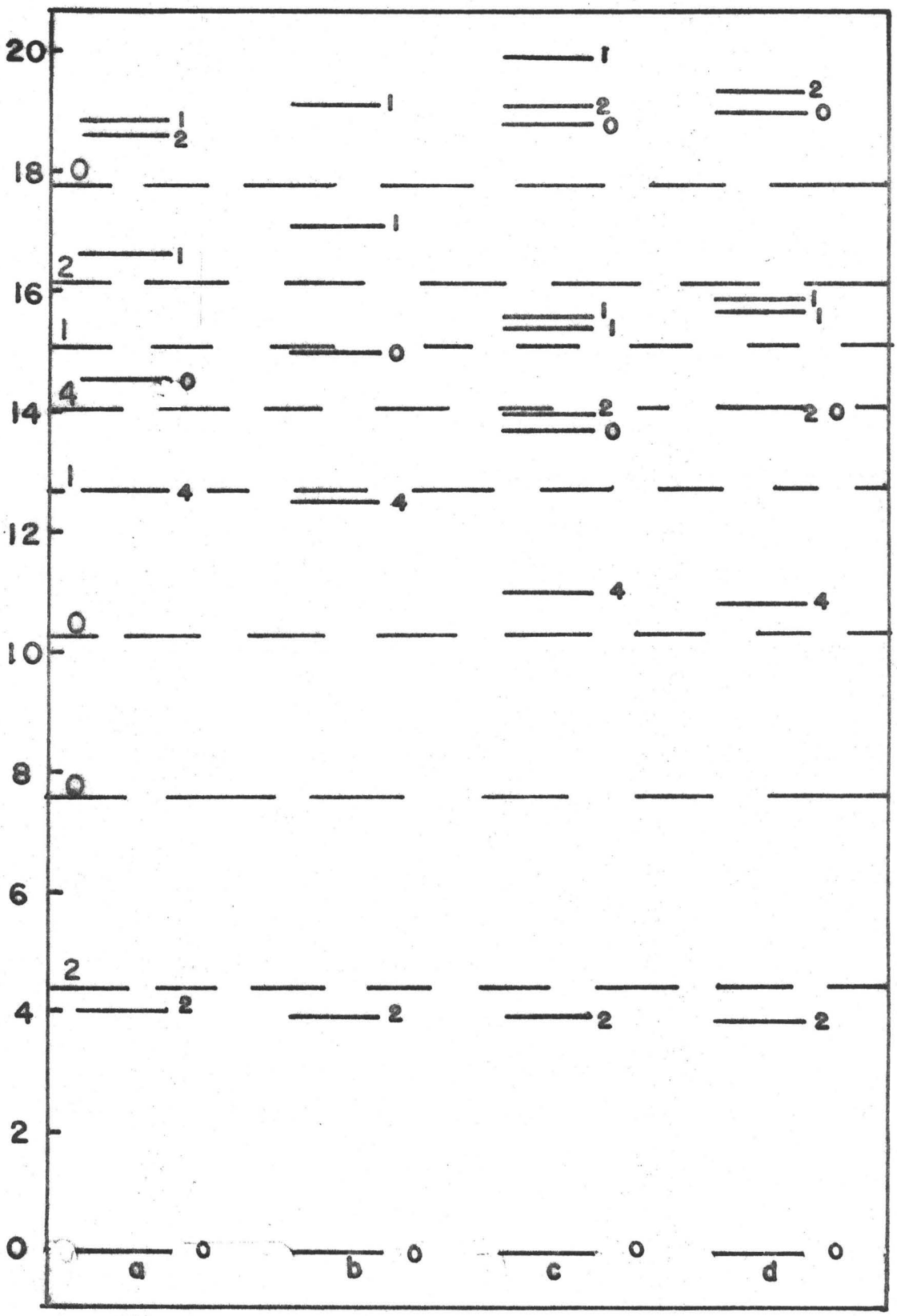

Figure 4.8

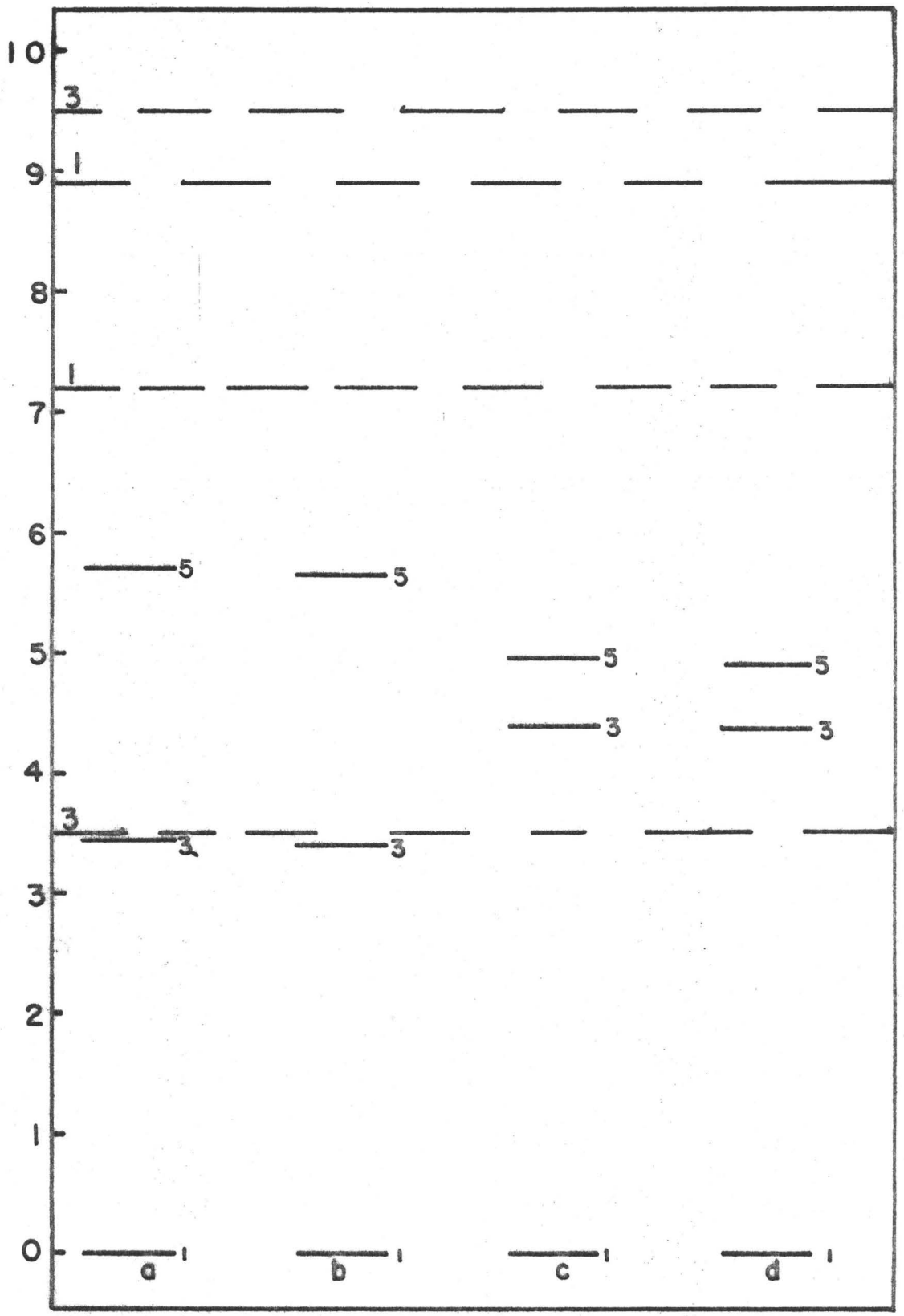

Figure 4.9

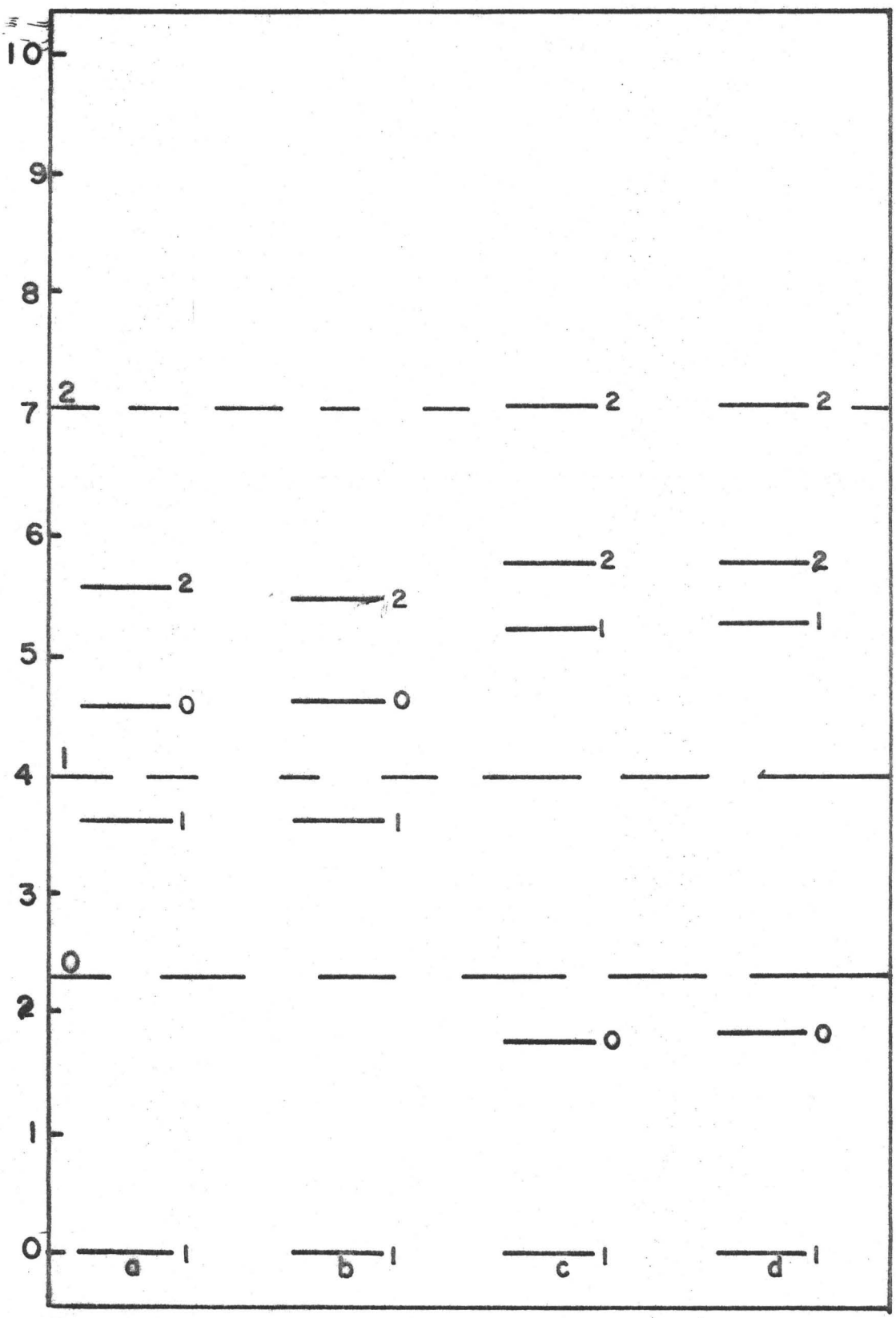

Figure 4.10

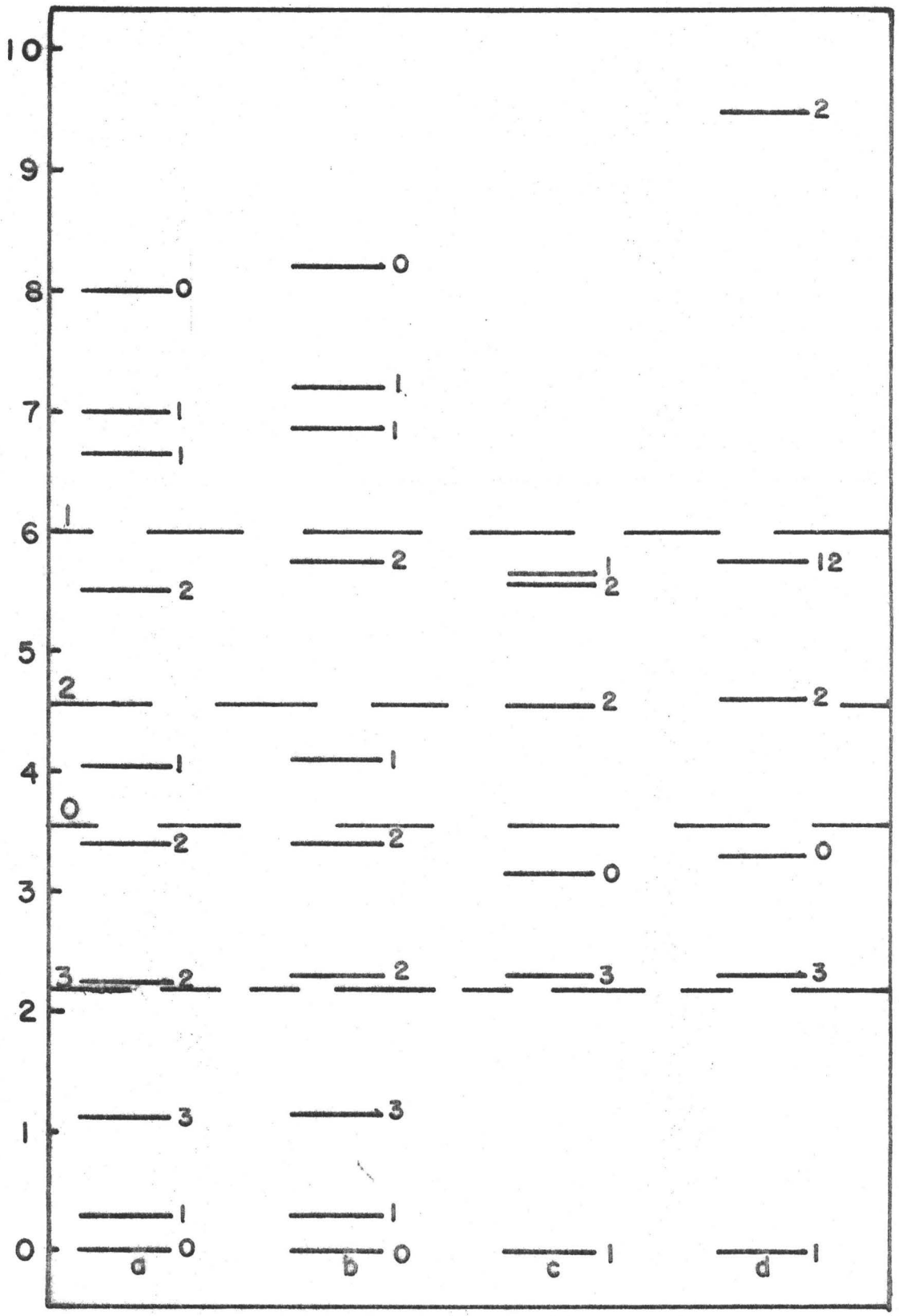

Figure 4.11

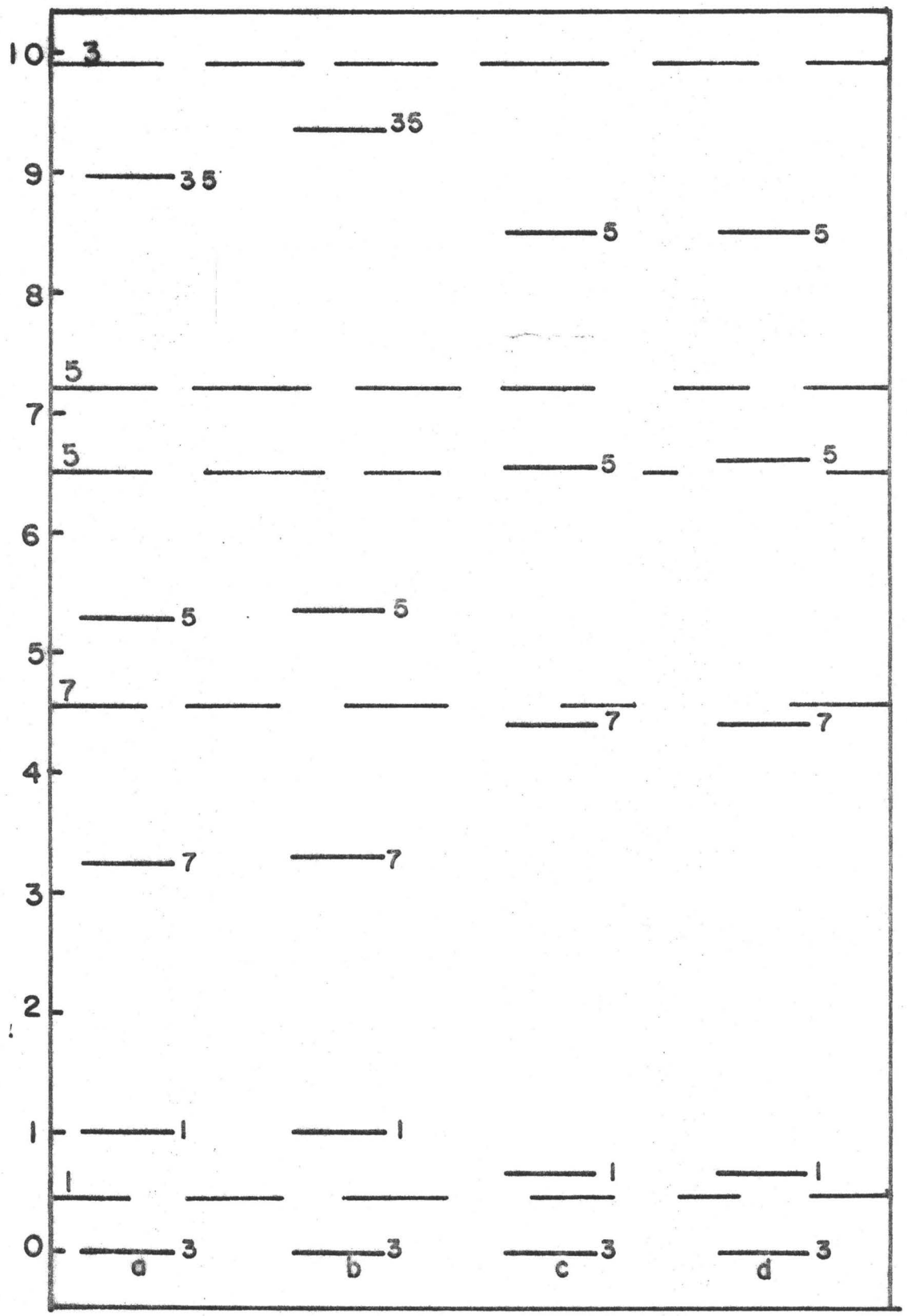

Figure 4.12

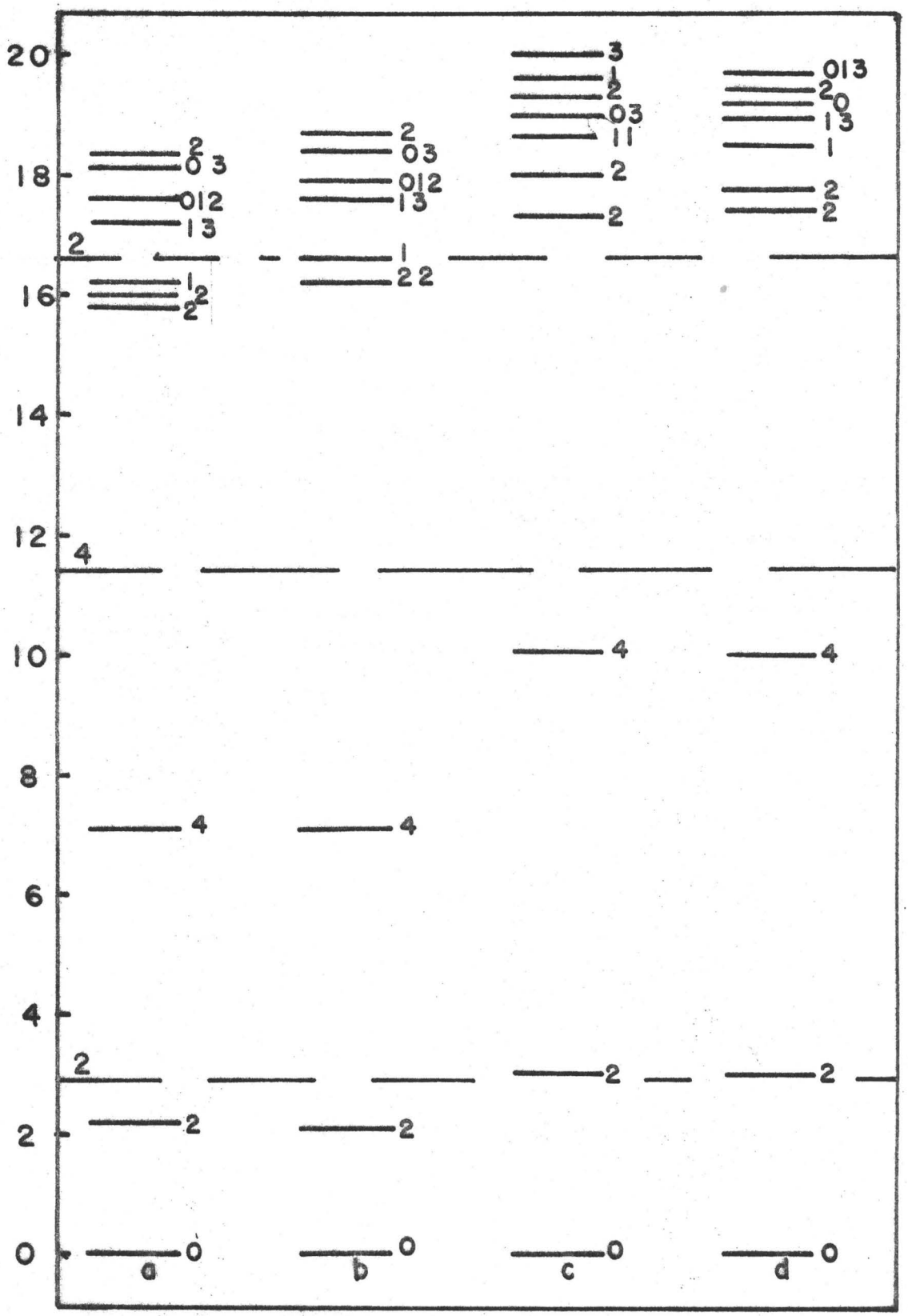

Figure 4.13

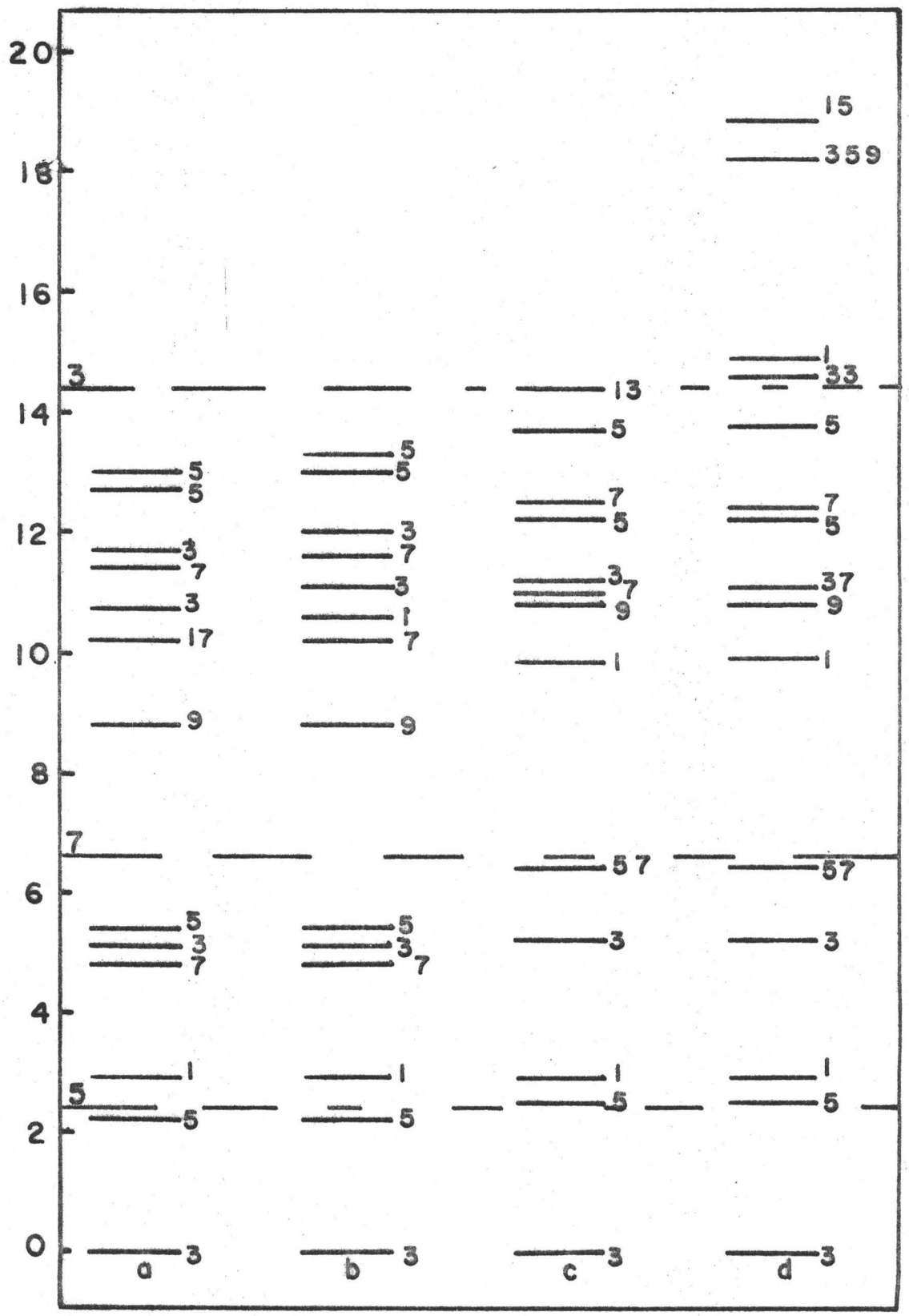

Figure 4.14

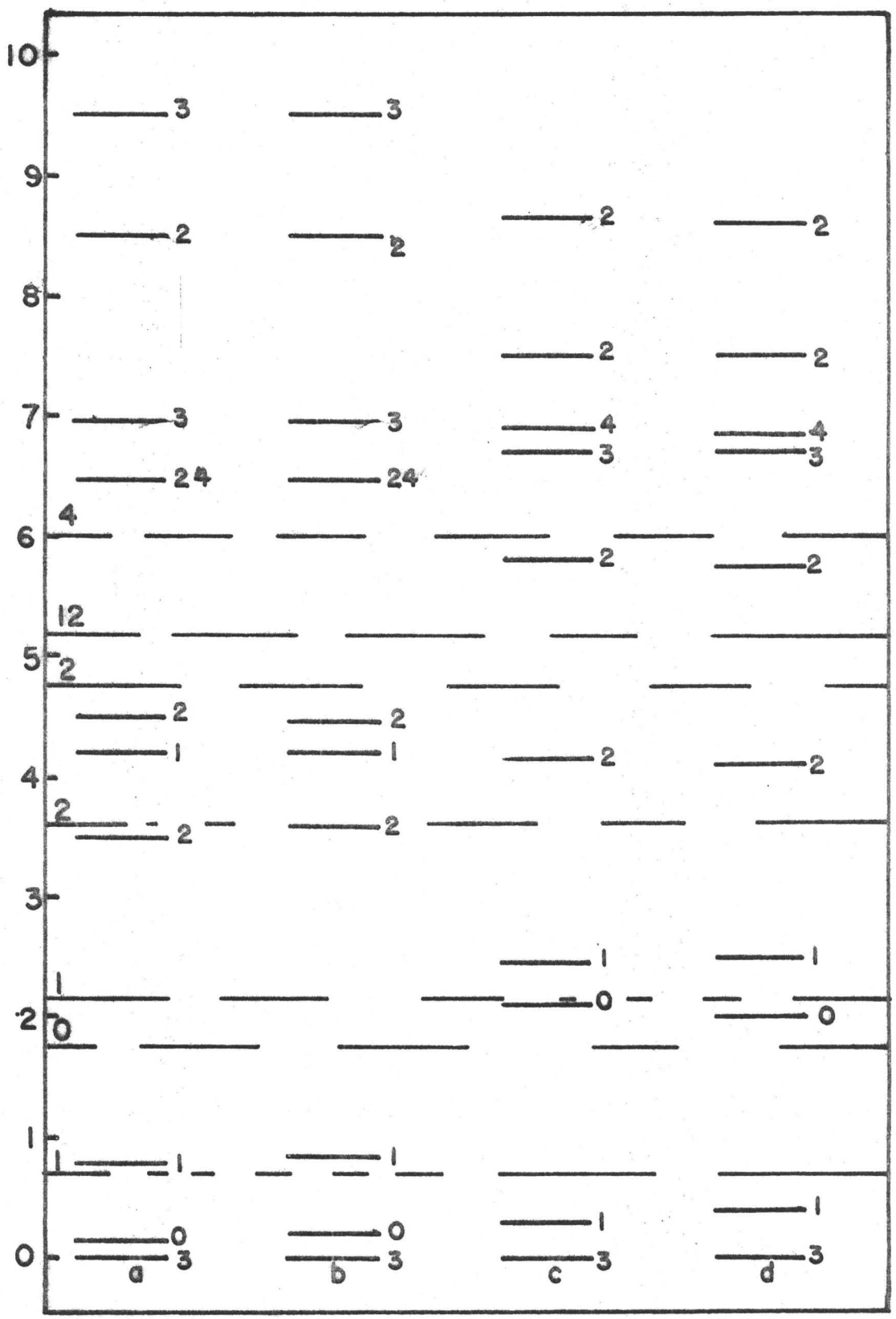

Figure 4.15

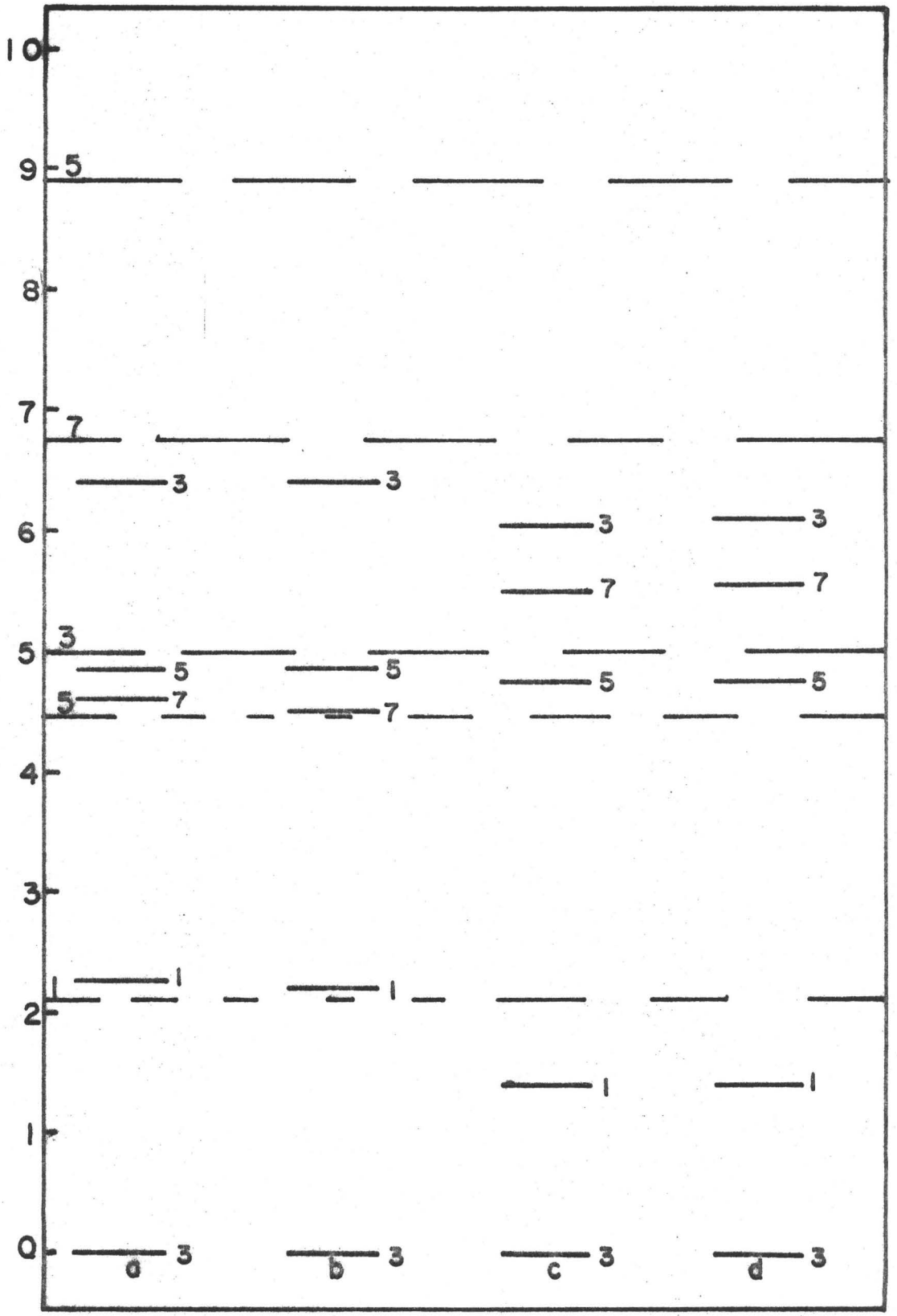

Figure 4.16

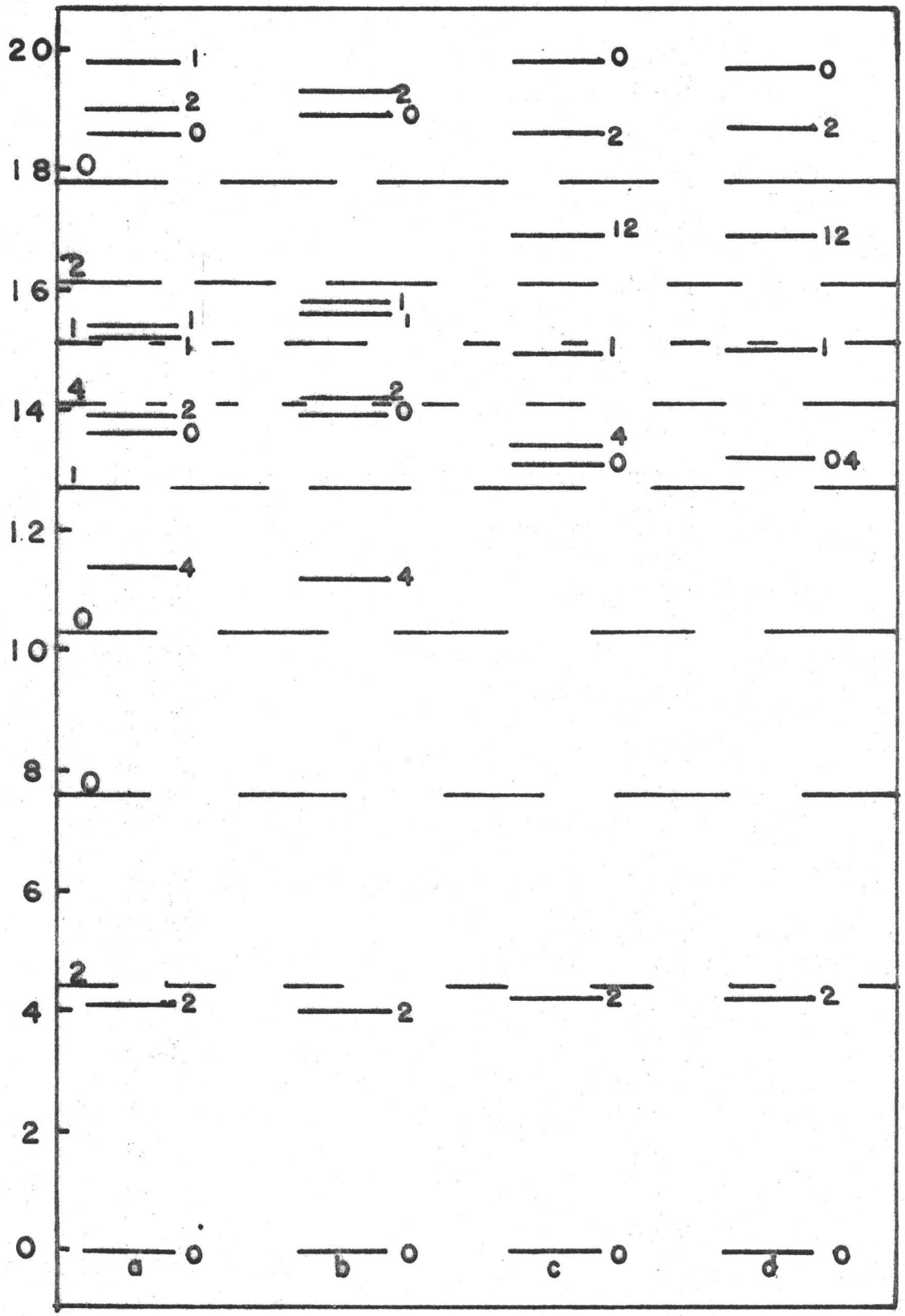

Figure 4.17

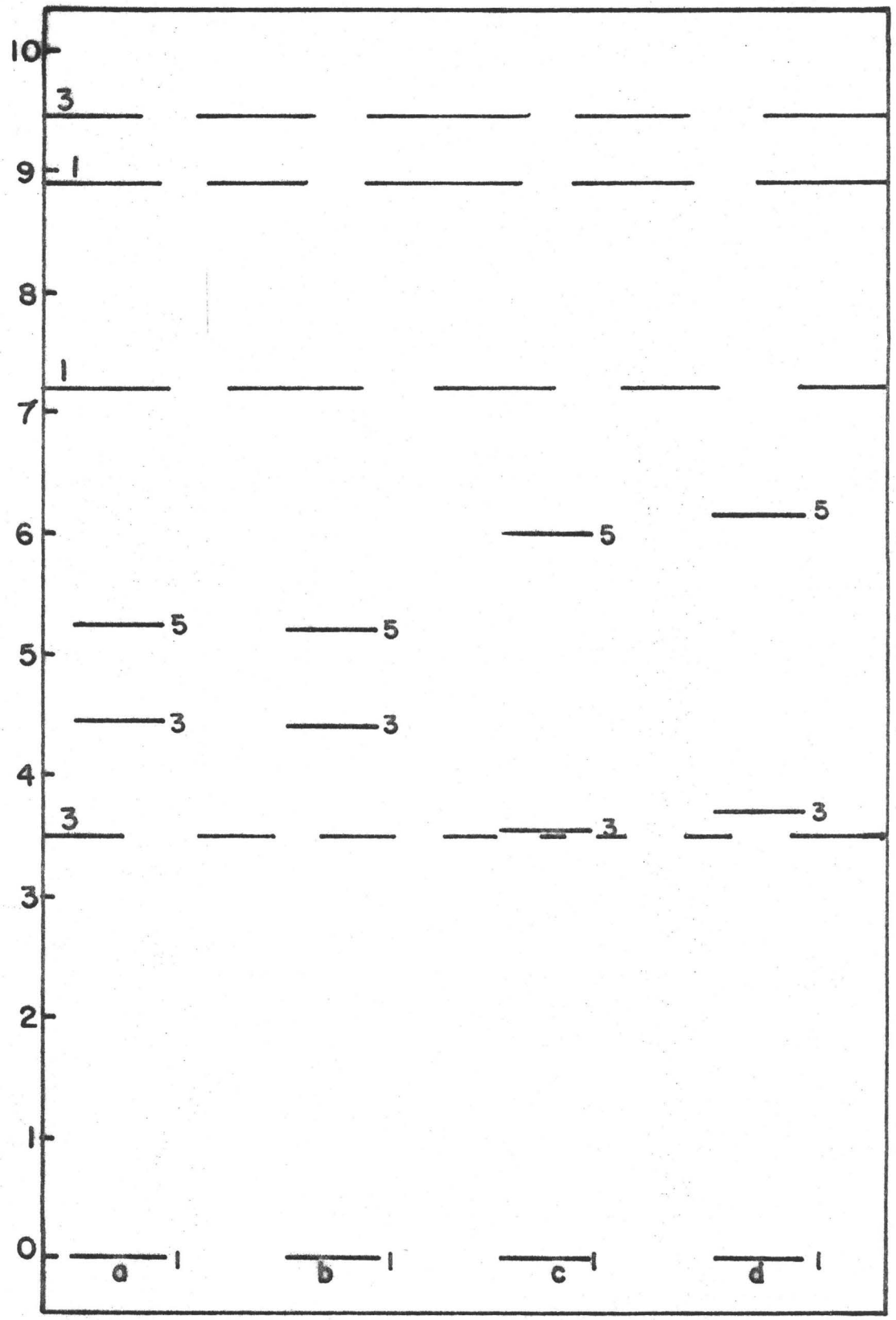

Figure 4.18

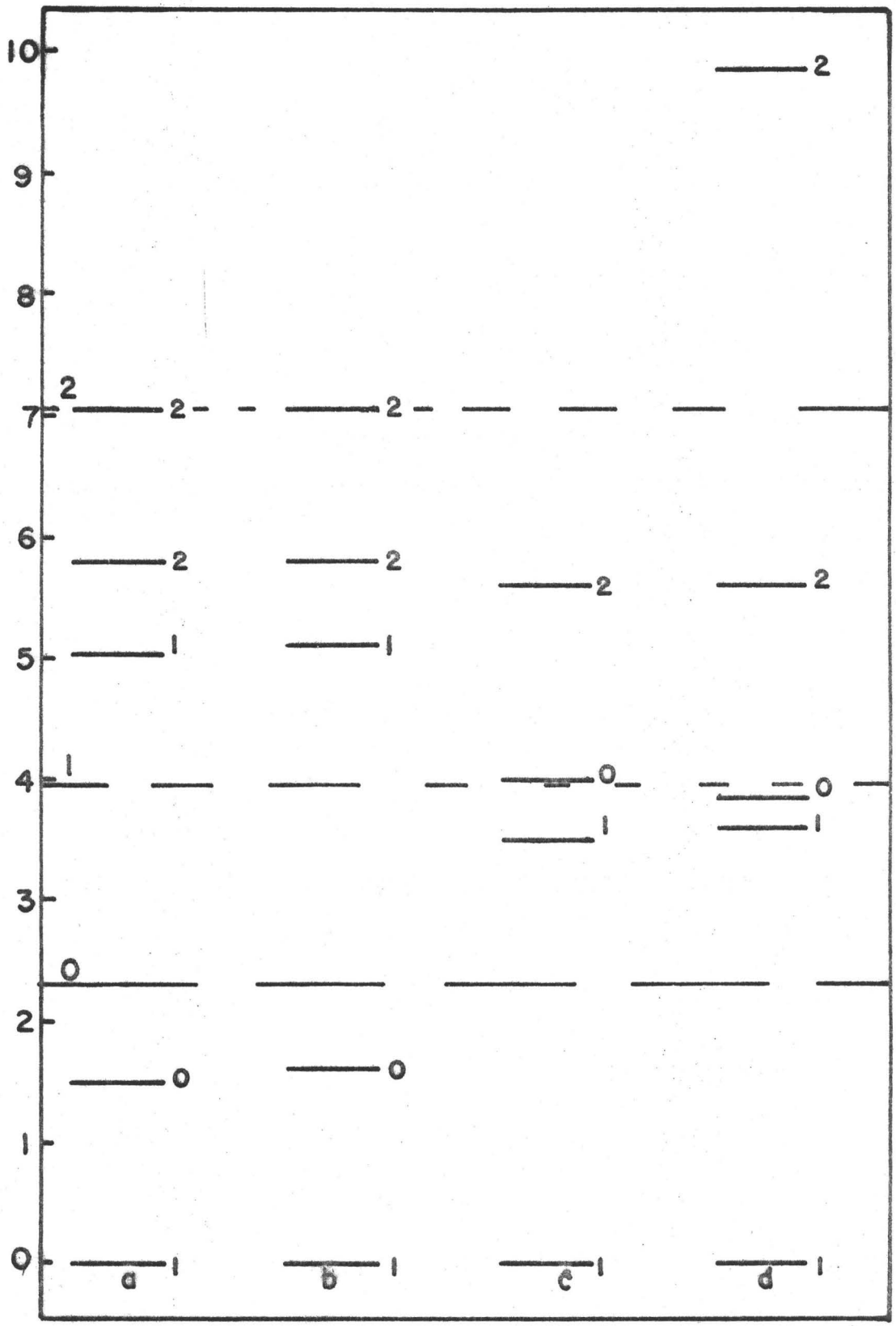

CHAPTER 5

BINDING ENERGY OF ^{16}O AND EXCHANGE STRENGTHS

All interactions considered in this and subsequent chapters are density dependent and of the form discussed in Chapter 3. These interactions are fitted to the properties of nuclear matter and any change in the value of ν also changes the strengths of the density dependence, c_3 and c_4. The ν parameter for any interaction has been established by fitting the ^{16}O binding energy. In Chapter 4 it was demonstrated that the excitation energies of the O-p shell nuclei are essentially unchanged by variation of ν for the local and velocity dependent interactions considered in that chapter. This is not the situation for density dependent interactions. Since the density dependent interactions considered have, in many instances, only been fitted approximately (to within 6 Mev) to the ^{16}O binding energy, it is necessary, when comparing density dependent interactions, to make due allowance for the effect on the excitation energies, for the nuclei calculated, of the different ^{16}O binding energy fits. In this chapter two interactions, 10 and 14, which differ primarily only in the value of ν, are compared.

Comparing the ν values for interactions 10 and 14, it is seen that a decrease in ν increases the ^{16}O binding

energy. The reverse is true for density independent interactions (Chapter 4). For density independent interactions, increased ν weights the direct matrix elements more favourably compared with the exchange matrix elements and thus the binding energies of finite nuclei increase. The requirement that density dependent forces fit nuclear matter criteria complicates this simple situation. For interactions 10 and 14 the energy contribution in nuclear matter of the density dependence is repulsive. Therefore, since the binding energy per particle of nuclear matter fitted by the interactions is the same (-16 Mev per particle) decreasing ν (weighting the exchange matrix elements more strongly than the direct matrix elements) forces the density dependence to become more attractive (from 31.50 Mev/particle for interaction 14 to 19.86 Mev/particle for interaction 10). Because the interactions are further required to saturate nuclear matter both c_3 and c_4 increase with, of course, the attractive density dependent part of the interaction increasing more ($c_3 k_F$ increases by 0.06, $c_4 k_F^2$ by 0.03).

The binding energy situation is more confused for finite nuclei. For ^{4}He, whose binding energy does not depend on the exchange strengths, it is clear that interaction 10 will give a higher binding energy than interaction 14 (by 2.15 Mev per particle). For ^{16}O, the different weighting of the direct and exchange matrix elements will

reduce the binding energy gain due to the less repulsive density dependence of interaction 10. Thus the ^{16}O binding energy is 1.65 Mev higher for interaction 10 than for interaction 14. The compressibility of nuclear matter being, at saturation, essentially the second derivative of the binding energy will be lower for interaction 10 since the attractive density dependence is now relatively stronger than is the case for interaction 14.

Table 5.1 lists the binding energies and root-mean-square radii for the O-p shell nuclei calculated using interactions 10 and 14. The binding energy difficulties experienced for calculations using non-density dependent interactions (Chapter 4) are now resolved. The calculations were performed for the values of the spin-orbit strength extant in Chapter 4.

The root-mean-square radii predicted for the O-p shell nuclei are now generally too large. The radii decrease dramatically for interaction 10 in comparison with interaction 14. It might be argued that the explanation of this is that the compressibility of nuclear matter for interaction 10 is less than that for interaction 14 since the compressibility is a measure of how much energy is needed to reduce the radius of a nuclear system. However, the compressibility of nuclear matter is not a critical parameter in determining the root-mean-square radius. For example, the calculated root-mean-square radii for interaction

TABLE 5.1

A	Interaction 14		Interaction 10	
	B.E.(Mev)	r.m.s.(fm)	B.E.(Mev)	r.m.s.(fm)
4	18.68	2.19	27.28	2.04
6	21.47	2.67	29.85	2.48
7	24.23	2.80	34.45	2.67
8	36.83	2.78	49.81	2.64
9	37.05	2.86	50.26	2.72
10	49.44	2.88	63.24	2.75
11	56.92	2.91	72.13	2.79
12	71.46	2.93	88.75	2.81
13	74.55	2.95	92.98	2.83
14	80.07	2.95	100.67	2.84
16	98.37	2.98	124.73	2.87

12 (compressibility = 470 Mev) are smaller than for interaction 10 (compressibility = 213 Mev). A more critical parameter is the overall contribution of the density dependent part of the interaction ($B.E._{den}$) to the binding energy of nuclear matter. This provides a measure of how repulsive (or attractive) the density dependence is. The interacting nucleons will tend to attempt to move to regions of low density for an interaction which has a repulsive density dependent component and, thus the more repulsive the density dependence the larger the size of the nucleus will be. The contribution to the nuclear matter binding energy of the density dependent part of the interaction is not an exact guide to the root-mean-square radii of the O-p shell nuclei. However, for interactions which differ only in values for ν, c_3 and c_4 it is of critical importance. Table 5.2 lists results for some interactions of this kind.

It can be seen from this table that there is a fairly good correlation between $B.E._{den}$ and root-mean-square radii. However, the above argument is a little too simple. The density dependence, in fact, should be further broken down into an attractive and a repulsive part. The attractive part usually is longer ranged than the repulsive part and thus the mechanism by which the interacting nucleons move further apart and to lower density regions is aided. However, interactions 18, 19 and 20 have no attractive density

TABLE 5.2

Interaction No.	$B.E._{den}$ (Mev)	Compressibility (Mev)	^4He r.m.s. (fm)	^{16}O r.m.s. (fm)
12	12.01	470	1.89	2.75
19	12.12	287	1.90	2.75
11	12.12	301	1.90	2.76
18	15.99	236	1.97	2.81
10	19.86	213	2.04	2.87
9	19.87	200	2.07	2.89
17	19.87	196	2.05	2.88
14	31.50	248	2.19	2.98

dependence. Thus, interaction 20 (omitted from Table 5.2) gives smaller r.m.s. radii than does interactions 19 and 12 although $B.E._{den}$ = 12.12 Mev for this interaction. For similar reasons interaction 17, whose attractive density component depends on the reciprical of the density to the one third power ($\rho^{-1/3}$) gives smaller r.m.s. radii than does interaction 9.

The excited state spectra calculated for interactions 10 and 14 are exhibited in Figs. 5.1 - 5.9. As can be seen substantial differences exist between the results for interactions 10 and 14. These are summarized in Table 5.3 where the difference between the excitation energy for interaction 10 and the excitation energy for interaction 14 (Δ_{exc}) for the excited state J_n^π is shown. The lower index, n, denotes the level order for interaction 10.

The excitation energies for ^{8}Be and ^{12}C, in particular, are very different for interactions 10 and 14. The case of ^{8}Be is of critical importance. Because of the loose fit to the binding energy of ^{16}O, it is possible that, for two interactions, which it is desired to compare (e.g. two identical interactions having different density dependencies), the ^{16}O binding energy might differ by 10 Mev. It would then be meaningless to attribute a difference of 1 Mev in the excitation energy of the second 2^+ state in ^{8}Be to differences between the forms of the interactions.

After the interaction has been derived from fitting

TABLE 5.3

A	Spin-orbit Strength, C (Mev)	J_n^π	Δ_{exc} (Mev)	A	Spin-orbit Strength, C (Mev)	J_n^π	Δ_{exc} (Mev)
6	-1.5	3_1^+	0.30	7	-2.0	$1/2_1^-$	0.00
		2_1^+	0.30			$7/2_1^-$	0.60
		0_1^+	1.60			$5/2_1^-$	1.20
		1_1^+	0.50			$5/2_2^-$	0.55
		2_2^+	1.90			$3/2_1^-$	1.15
8	-3.5	2_1^+	0.35	9	-3.0	$5/2_1^-$	0.10
		4_1^+	1.50			$1/2_1^-$	-0.60
		2_2^+	3.10			$3/2_1^-$	-0.45
		2_3^+	2.25			$7/2_1^-$	1.10
		4_2^+	2.80			$5/2_2^-$	-0.20
		1_1^+	3.40			$1/2_2^-$	1.30
		3_1^+	3.55			$3/2_2^-$	0.80
		3_2^+	3.00			$7/2_2^-$	1.20
						$5/2_3^-$	0.00
						$9/2_1^-$	0.55
10	-5.0	1_1^+	0.00	11	-4.5	$1/2_1^-$	-0.75
		0_1^+	0.90			$5/2_1^-$	-0.20
		1_2^+	-0.65			$7/2_1^-$	-0.25
		2_1^+	-0.40			$3/2_1^-$	-0.15
		2_2^+	1.40			$5/2_2^-$	0.95
		4_1^+	-0.05			$1/2_2^-$	1.00
		3_1^+	-0.10				

TABLE 5.3 - CONTINUED

12	-5.5	2^+_1	-0.00	13	-5.0	$3/2^-_1$	-0.65
		1^+_1	1.30			$5/2^-_1$	-0.40
		0^+_1	-0.30			$1/2^-_1$	0.50
		4^+_1	-0.80			$3/2^-_2$	0.75
		1^+_2	1.80				
		2^+_2	1.75	14	-4.5	0^+_1	1.00
		2^+_3	0.70			1^+_1	-0.45
		0^+_2	1.00			2^+_1	-0.15
						2^+_2	0.75

the scattering data, nuclear matter properties and the ^{16}O binding energy, there is one degree of freedom left in the interaction parameters, namely the choice of one of the exchange strengths. In all calculations quoted in this thesis the isospin exchange was chosen to be a constant, H=0.0. Other possible choices for H are now examined for interaction 23. These choices are tabulated in Table 5.4 where all the exchange strengths are recorded.

Case (a) is the choice normally assigned for an interaction. Case (b) is considered since for this choice of H, the Wigner component of the exchange is zero and choice (c) corresponds to the Rosenfeld choice of the Mayorana exchange strength, M.

The usual excited state spectra for the three cases are plotted in Figs. 5.9 - 5.18. The changes in the excitation energies are tabulated in Table 5.5. The notation is the same as that in Table 5.3, the level ordering being for case (a).

The root-mean-square radii do not differ for the three interactions considered and the binding energies only differ by at the most 0.3 Mev. The excitation energy spectra show some substantial differences. However, they are not large compared with the changes of the excitation energies for interactions which differ in their calculated ^{16}O binding energies. The Bartlett exchange strengths for the interactions considered vary from 0.25 to 0.40 (H=0.0).

TABLE 5.4

	Case (a)	Case (b)	Case (c)
W	0.1952	0.0	-0.22
M	0.8048	1.0	1.22
B	0.3120	0.556	0.831
H	0.0	0.244	0.419

TABLE 5.5

A	J_n^π	$E_x(a) - E_x(b)$ (Mev)	$E_x(a) - E_x(c)$ (Mev)
6	3_1^+	0.00	0.00
	0_1^+	0.00	0.00
	2_1^+	0.00	0.00
	1_1^+	0.00	0.00
	2_1^+	0.05	0.10
7	$1/2_1^-$	-0.05	-0.15
	$7/2_1^-$	0.05	0.05
	$5/2_1^-$	-0.05	-0.05
	$5/2_2^-$	0.30	0.70
	$3/2_1^-$	0.40	0.80
8	2_1^+	0.00	0.00
	4_1^+	0.00	0.00
	2_2^+	-0.30	-0.30
	2_3^+	0.80	1.30
	1_1^+	0.20	0.60
	3_1^+	0.60	1.30
	3_2^+	-0.80	-1.30
	1_2^+	-0.50	-1.00
	0_1^+	-0.80	

TABLE 5.5 - CONTINUED

9	$5/2^-_1$	0.00	0.00
	$1/2^-_1$	0.00	0.00
	$3/2^-_1$	0.00	0.00
	$5/2^-_2$	0.00	0.00
	$7/2^-_1$	0.10	0.10
	$1/2^-_2$	0.20	0.50
	$3/2^-_2$	0.40	0.80
	$7/2^-_2$	0.40	0.80
	$9/2^-_1$	0.10	0.20
	$5/2^-_3$	0.35	0.85
10	1^+_1	-0.30	-0.55
	1^+_2	0.00	-0.10
	0^+_1	0.20	0.40
	2^+_1	0.05	0.10
	2^+_2	0.20	0.45
	3^+_1	-0.10	-0.15
	4^+_1	0.15	0.25
11	$1/2^-_1$	0.00	0.00
	$5/2^-_1$	0.05	0.15
	$7/2^-_1$	0.05	0.15
	$3/2^-_1$	-0.10	-0.10

TABLE 5.5 - CONTINUED

12	2_1^+	0.00	0.00
	0_1^+	0.00	0.20
	1_1^+	0.30	0.70
	4_1^+	0.15	0.35
	1_2^+	0.55	1.25
	2_2^+	0.40	0.90
	2_3^+	0.20	0.60
	0_2^+	0.90	1.80
13	$3/2_1^-$	0.10	0.20
	$5/2_1^-$	0.05	0.60
	$1/2_1^-$	0.40	0.90
	$3/2_2^-$	0.15	0.40
14	1_1^+	0.10	0.20
	0_1^+	0.30	0.60
	2_1^+	0.15	0.30

Thus, if the point of view is adopted that calculations should be performed for constant Majorana exchange strength rather than constant isospin exchange strength the comparitive differences in the spectra will not be very great.

FIGURE CAPTIONS

For all figures, excitation energy (in Mev) is plotted to the left of the figure. Full lines designate the calculated levels and dashed lines designate certain experimental levels. For even nuclei the spin J of the level is indicated to the right of the calculated levels and at the left of the figure for the experimental levels, for odd nuclei the value of 2J is likewise indicated.

Figures 5.1 - 5.9 plot the excited state spectra of the O-p shell nuclei calculated for

(a) Interaction 10

(b) Interaction 14.

Figure 5.1 Excited State Spectra of ^{6}Li with C = -1.5 Mev.

Figure 5.2 Excited State Spectra of ^{7}Be with C = -2.0 Mev.

Figure 5.3 Excited State Spectra of ^{8}Be with C = -3.5 Mev.

Figure 5.4 Excited State Spectra of ^{9}B with C = -3.0 Mev.

Figure 5.5 Excited State Spectra of ^{10}B with C = -5.0 Mev.

Figure 5.6 Excited State Spectra of ^{11}B with C = -4.5 Mev.

Figure 5.7 Excited State Spectra of ^{12}C with C = -5.5 Mev.

Figure 5.8 Excited State Spectra of ^{13}C with C = -5.0 Mev.

Figure 5.9 Excited State Spectra of ^{14}N with C = -4.5 Mev.

Figures 5.10 - 5.18 plot the excited state spectra of the O-p shell nuclei calculated for Interaction 23 with exchange strengths given in

(a) of Table 5.4

(b) of Table 5.4

(c) of Table 5.4.

Figure 5.10 Excited State Spectra of ^{6}Li with C = -1.5 Mev.

Figure 5.11 Excited State Spectra of ^{7}Be with C = -2.0 Mev.

Figure 5.12 Excited State Spectra of ^{8}Be with C = -3.5 Mev.

Figure 5.13 Excited State Spectra of ^{9}B with C = -3.0 Mev.

Figure 5.14 Excited State Spectra of ^{10}B with C = -5.0 Mev.

Figure 5.15 Excited State Spectra of ^{11}B with C = -4.5 Mev.

Figure 5.16 Excited State Spectra of ^{12}C with C = -5.5 Mev.

Figure 5.17 Excited State Spectra of ^{13}C with C = -5.0 Mev.

Figure 5.18 Excited State Spectra of ^{14}N with C = -4.5 Mev.

Figure 5.1

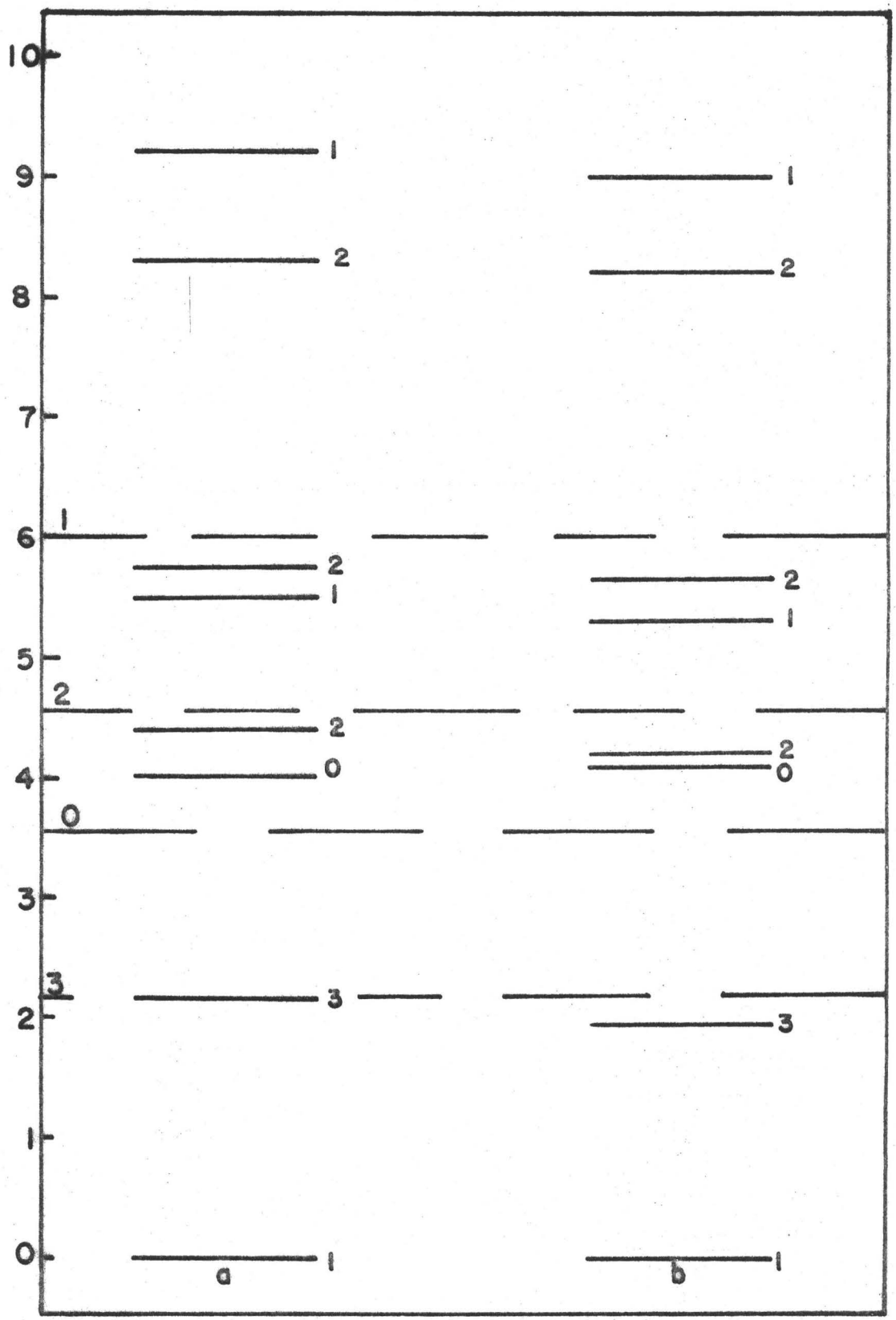

Figure 5.2

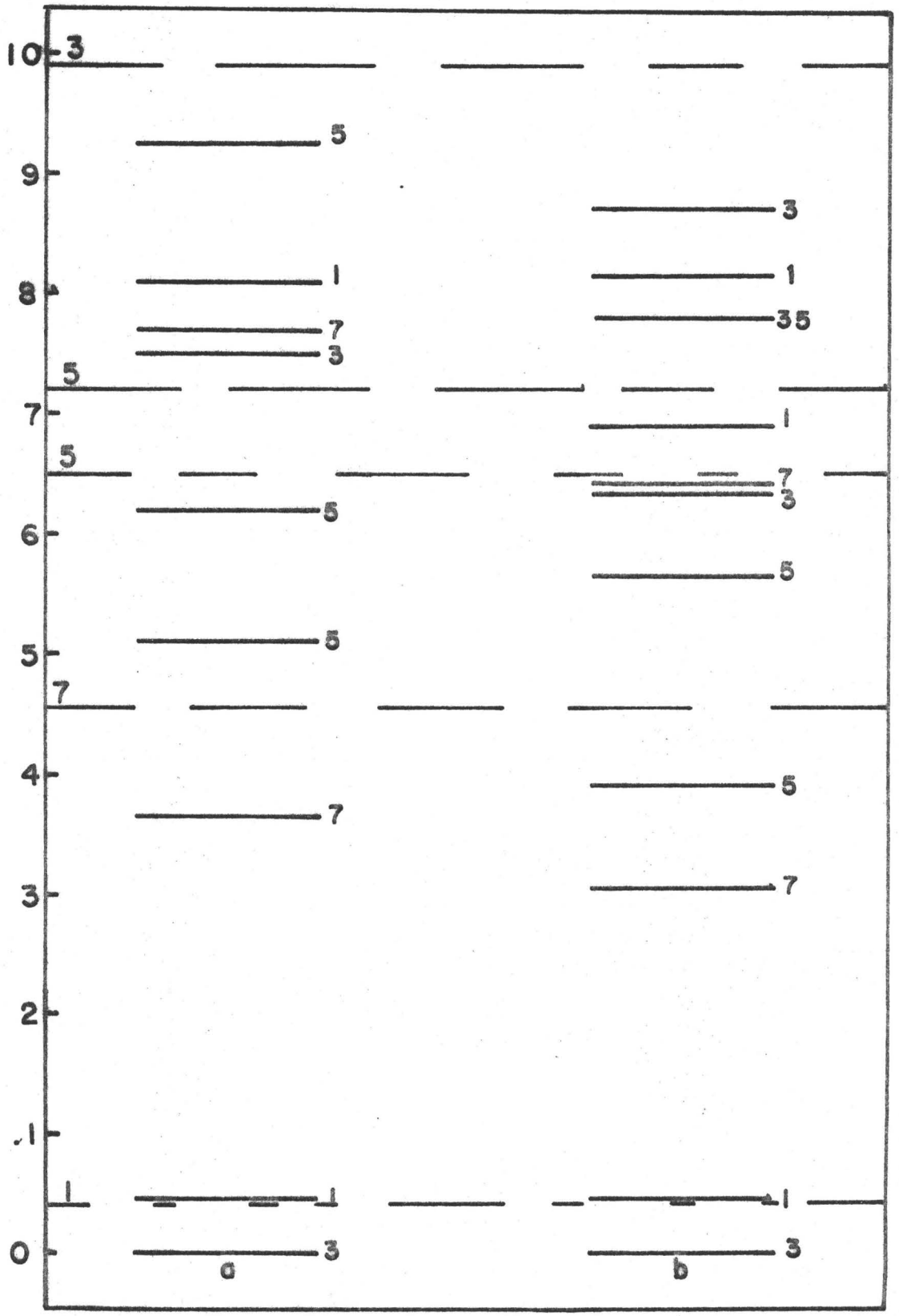

Figure 5.3

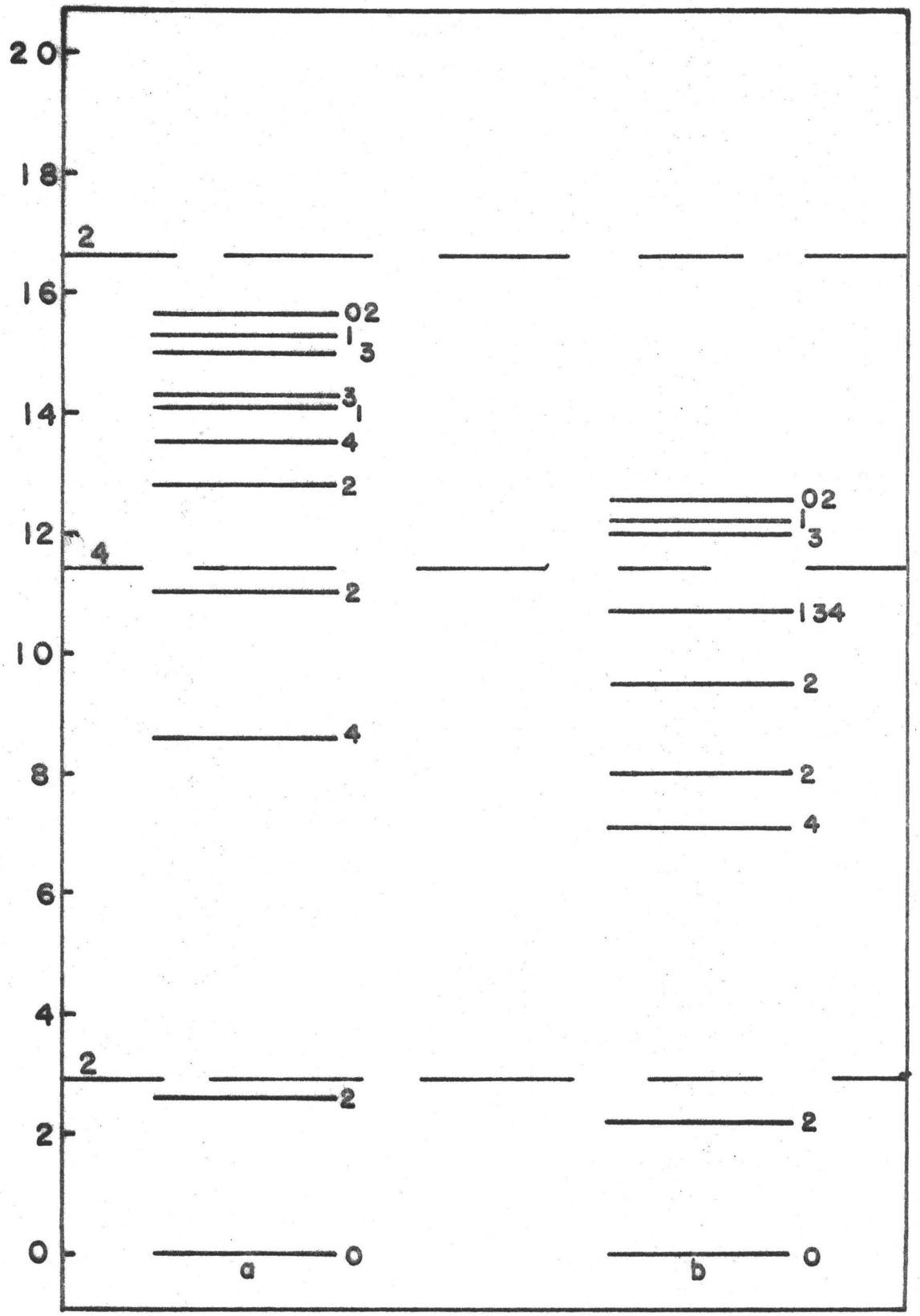

Figure 5.4

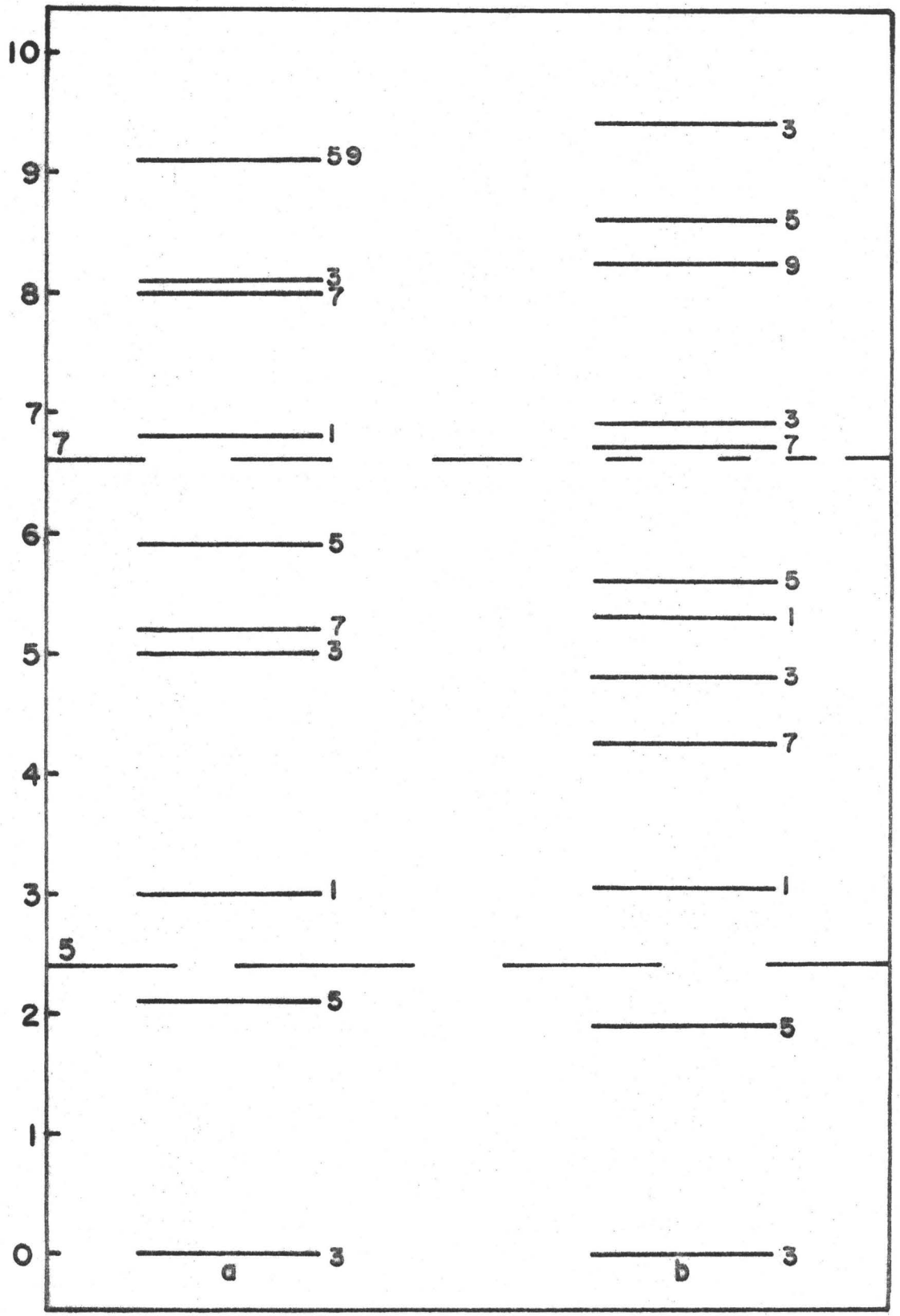

Figure 5.5

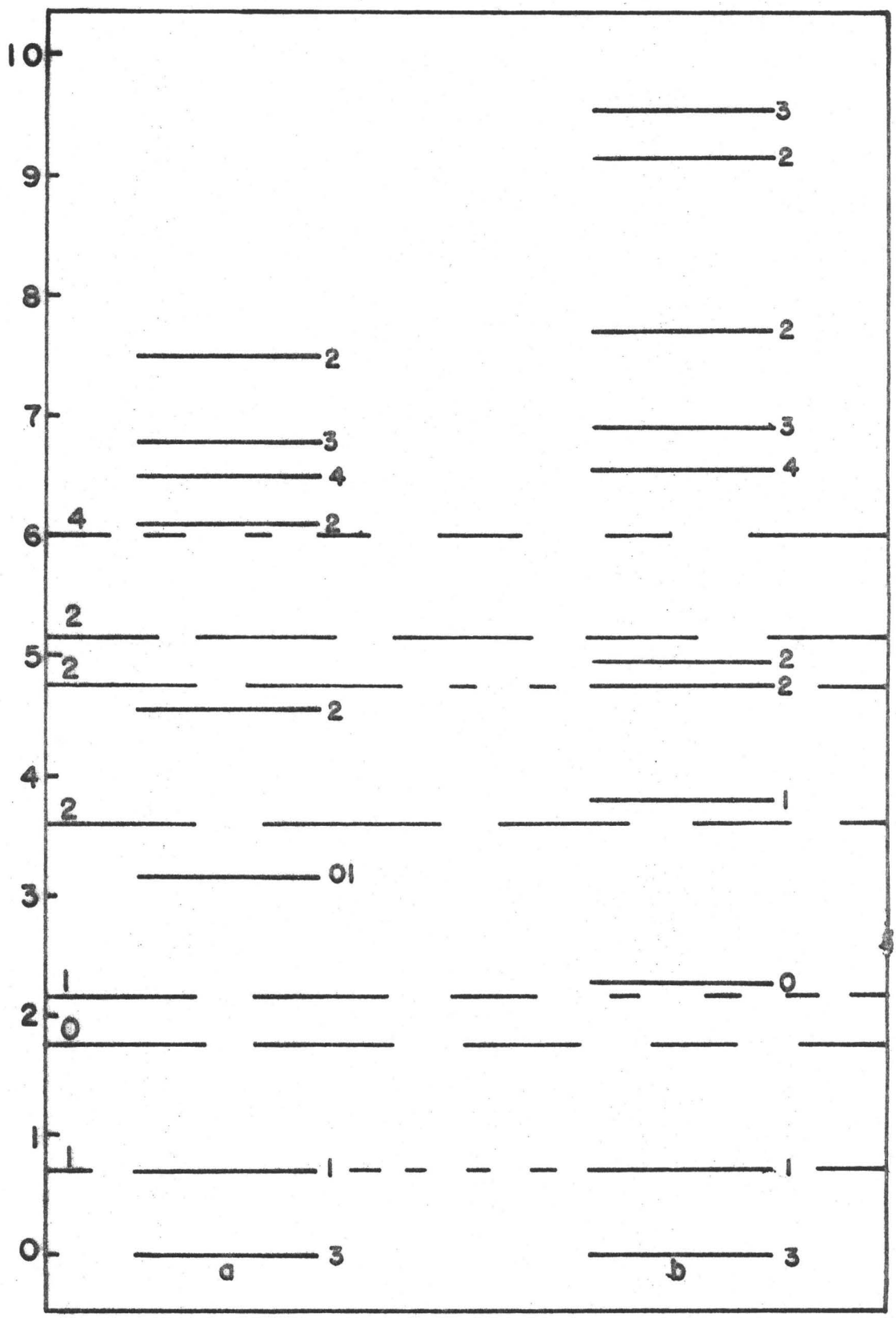

Figure 5.6

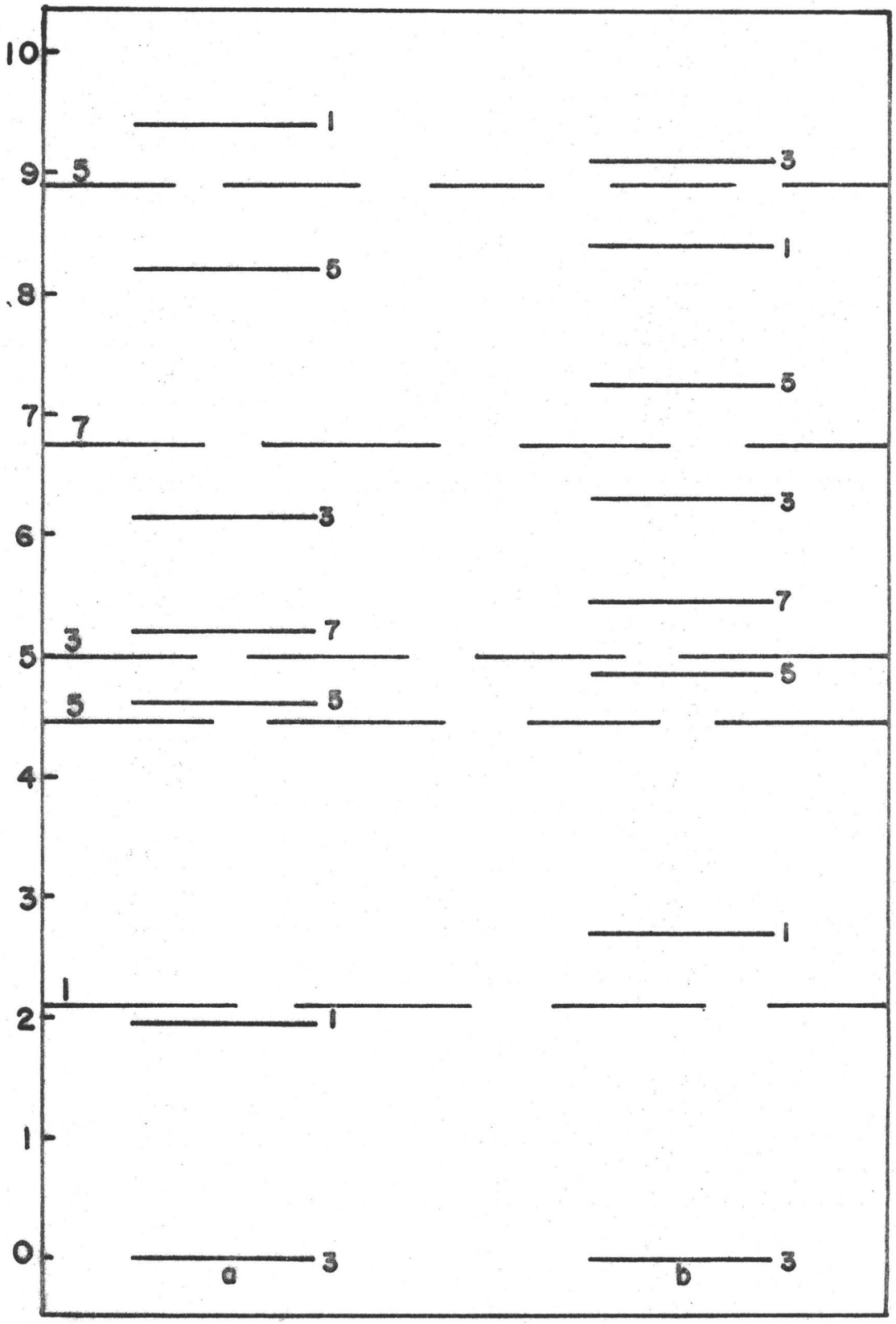

Figure 5.7

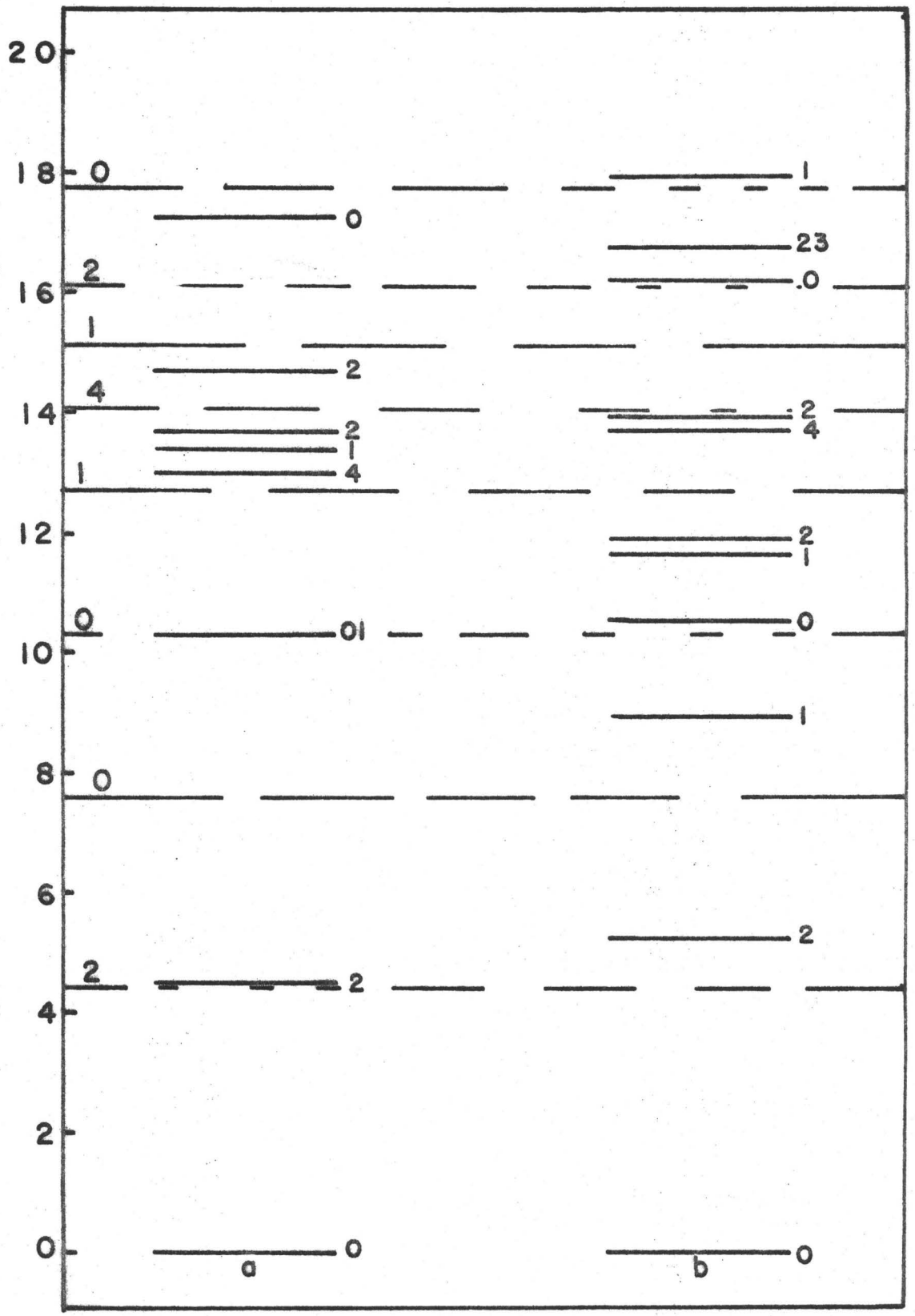

Figure 5.8

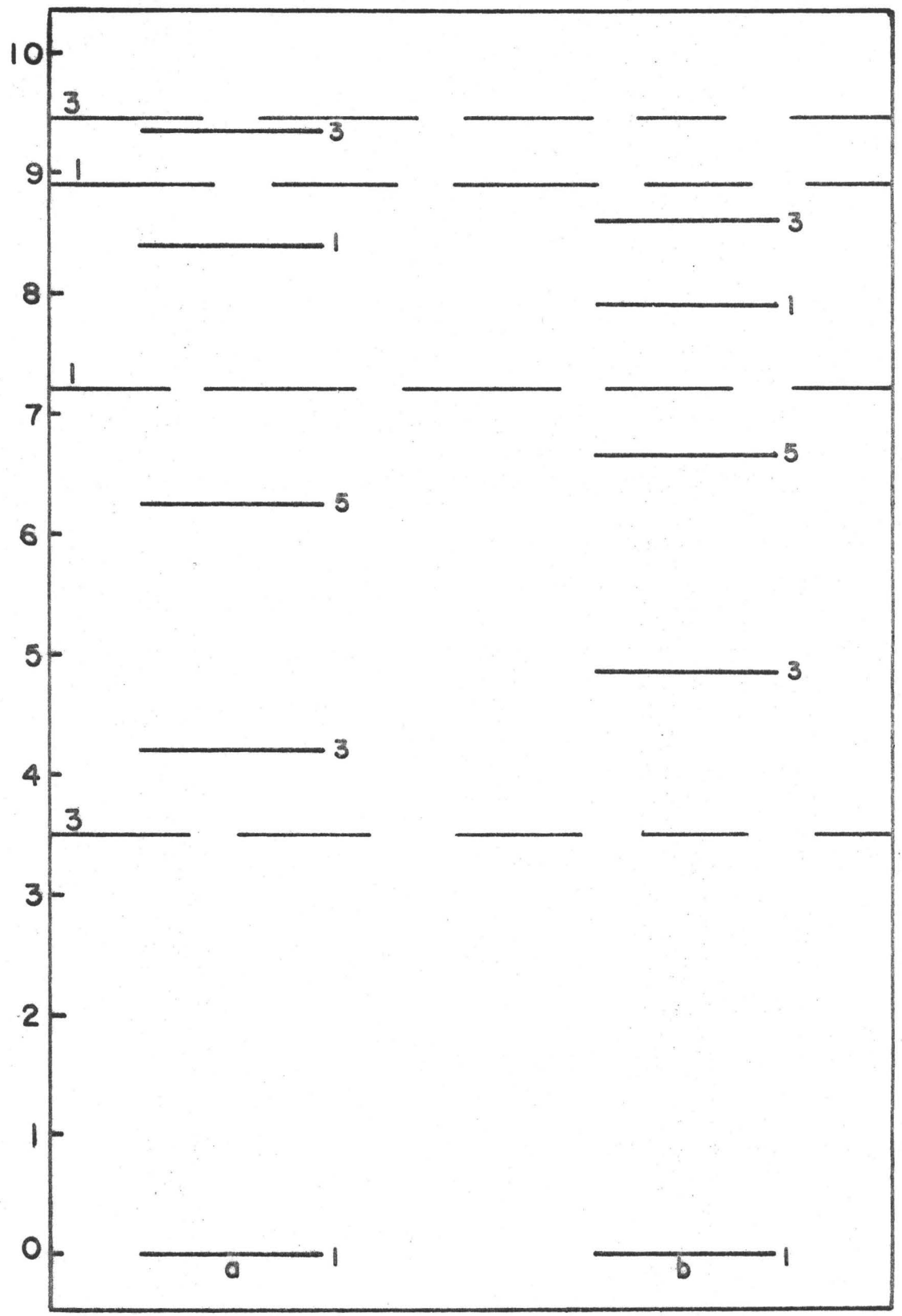

Figure 5.9

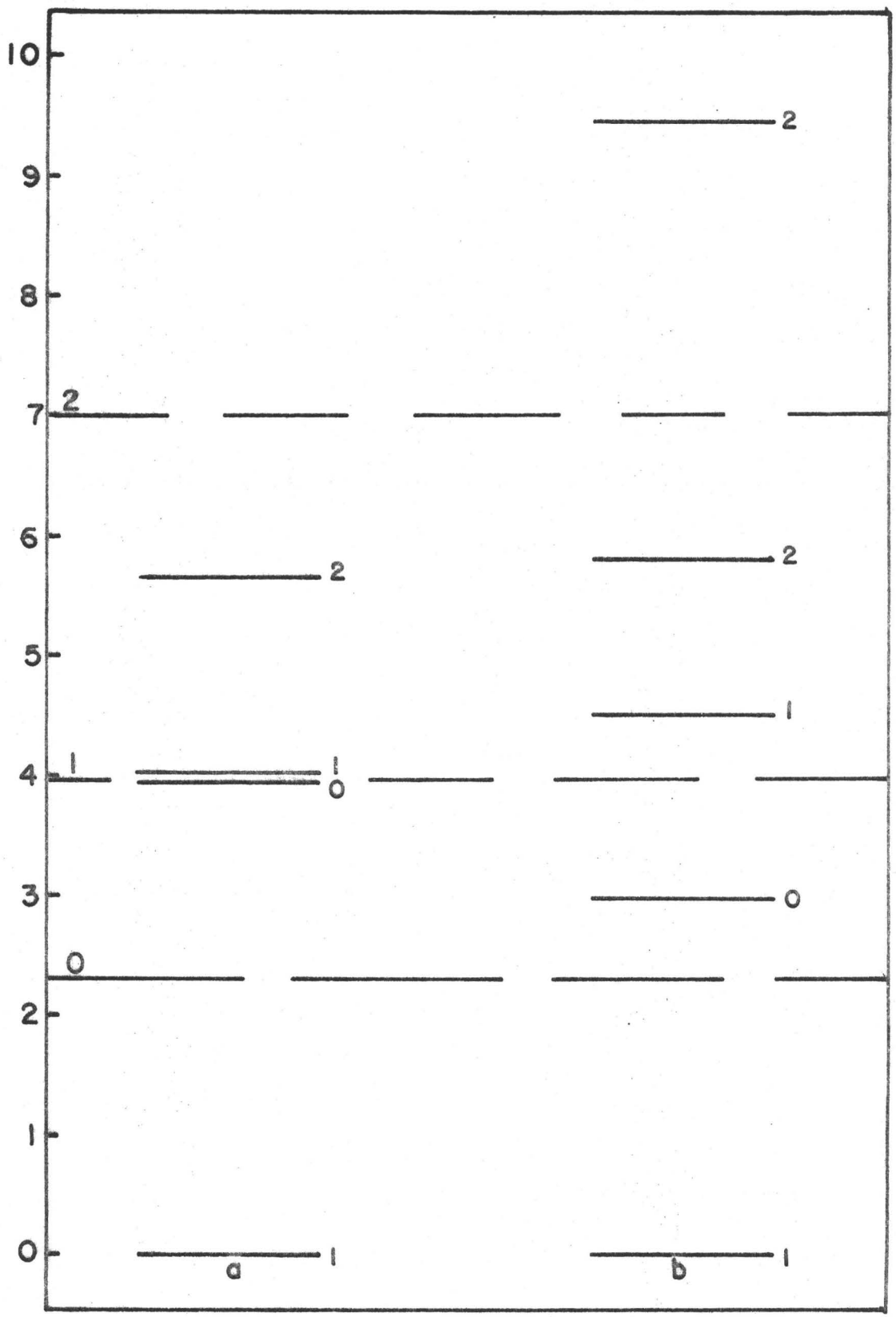

Figure 5.10

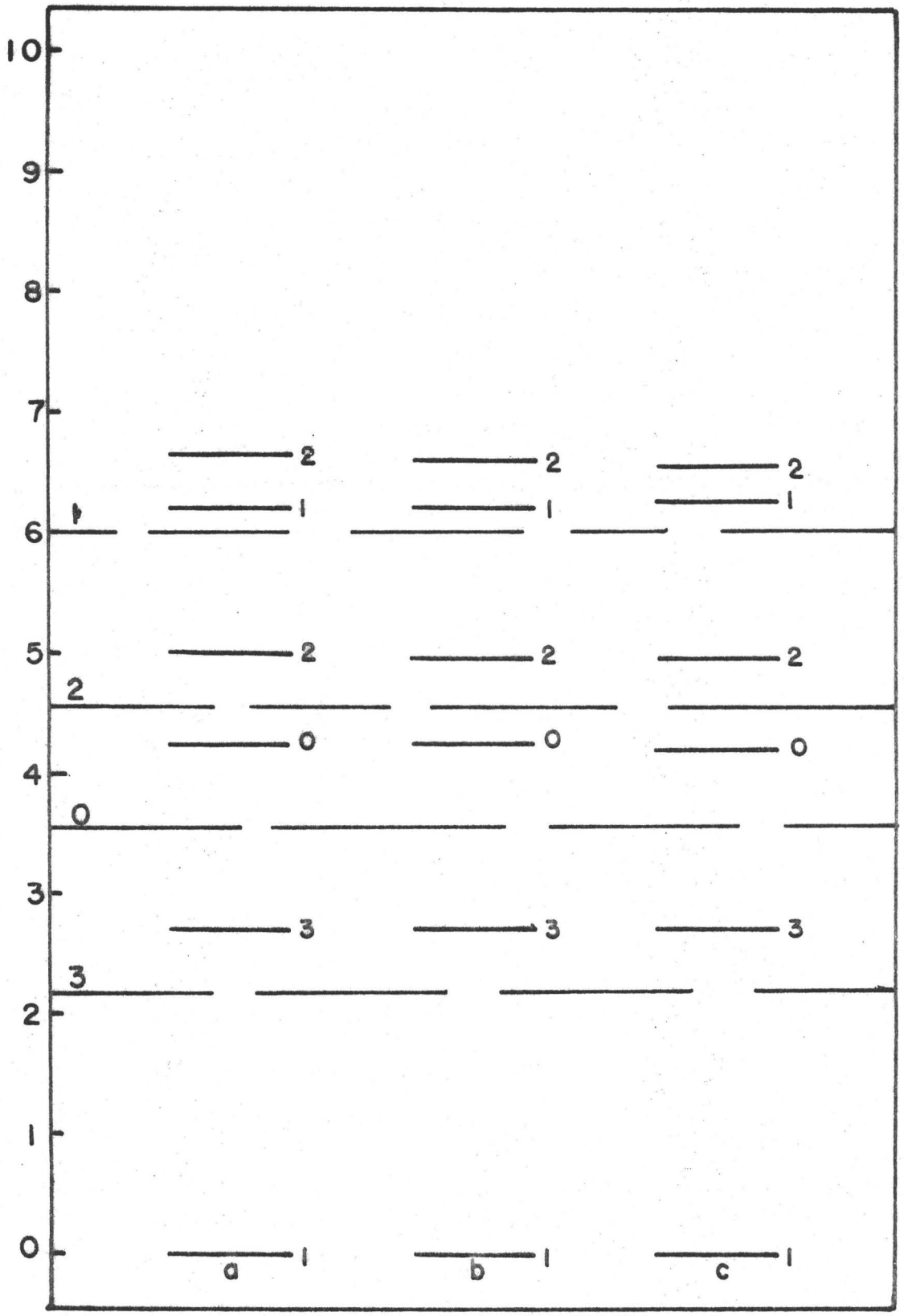

Figure 5.11

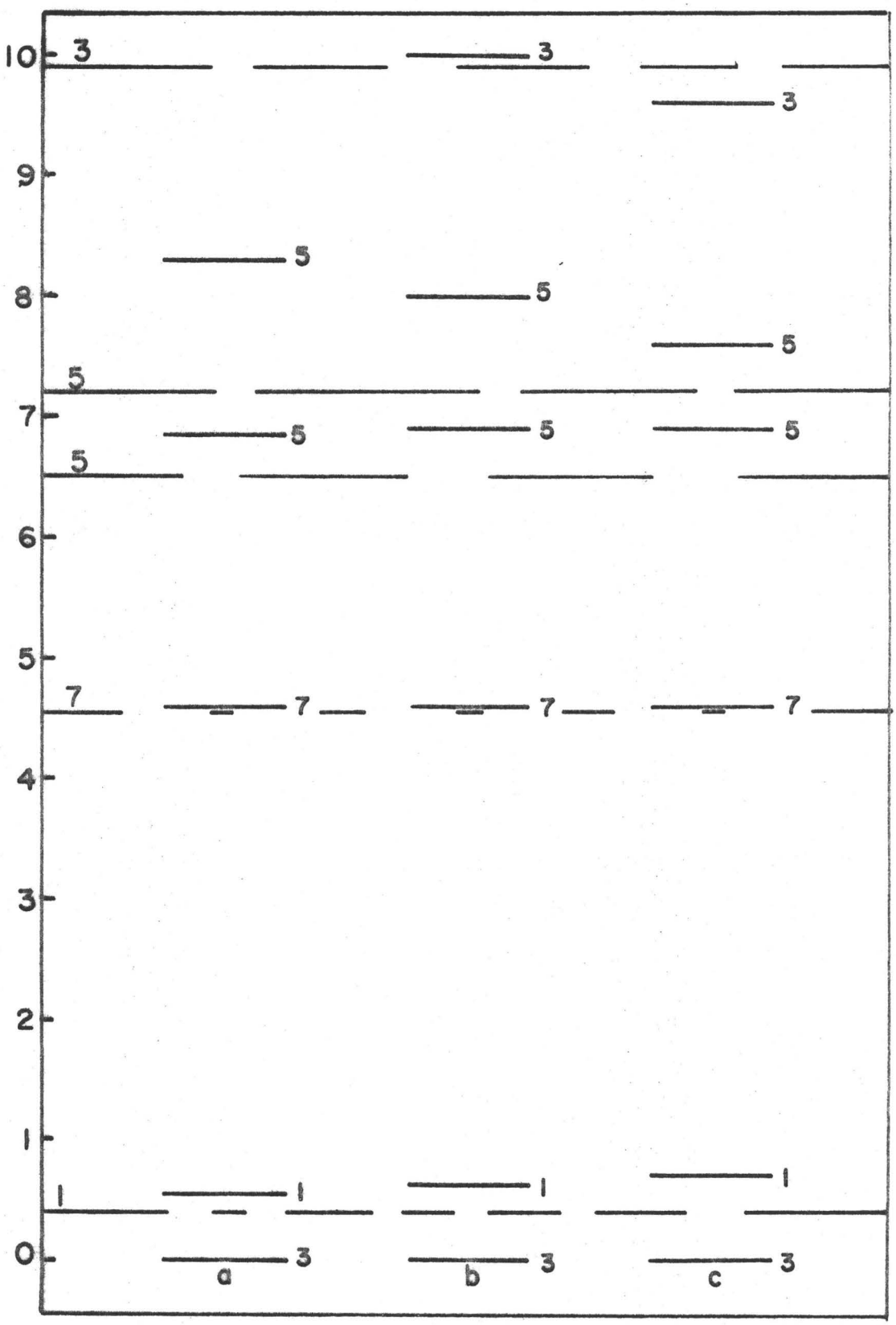

Figure 5.12

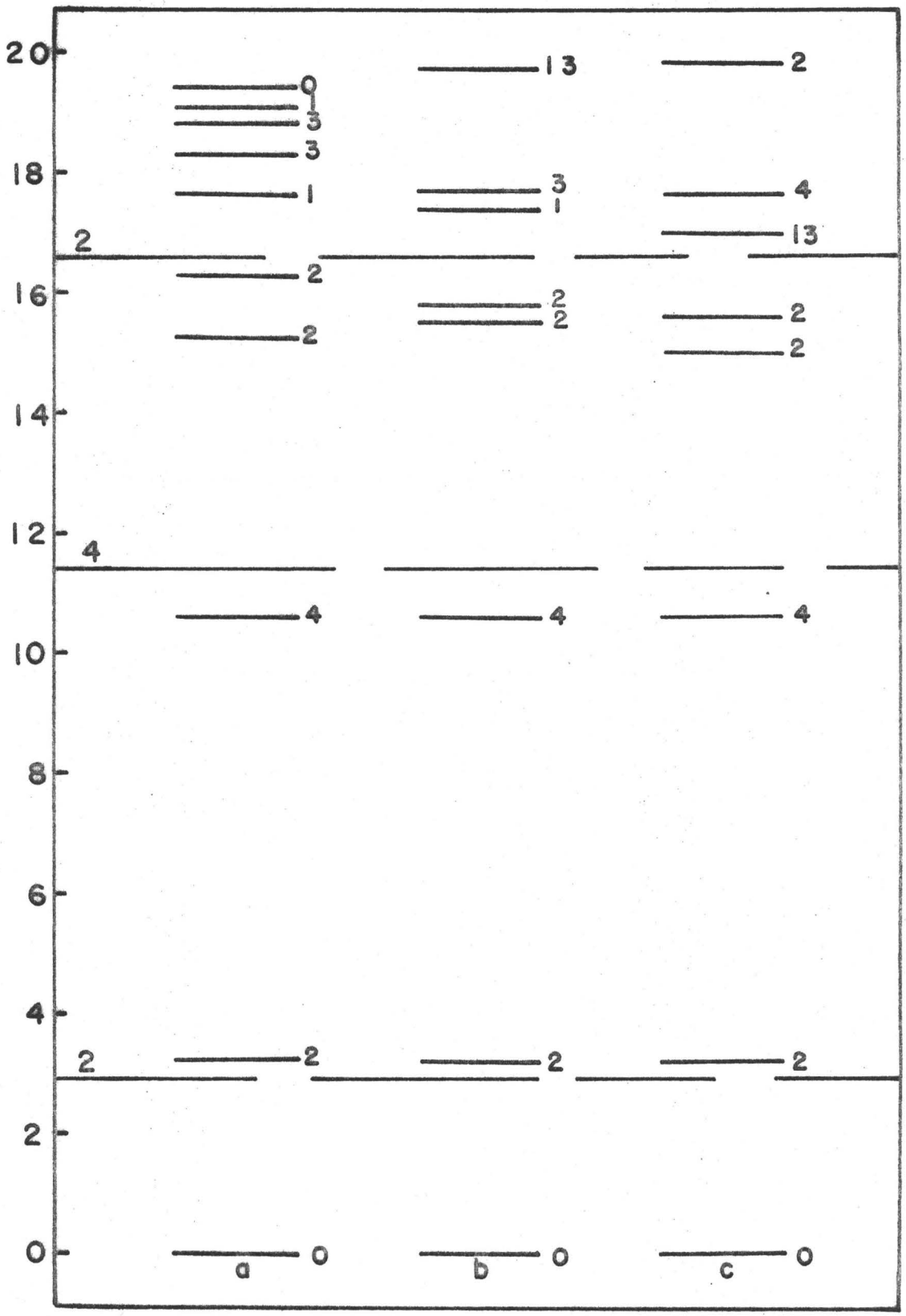
20
18
16
14
12
10
8
6
4
2
0
0
3
1
3
1
2
2
2
13
3
1
2
2
2
4
13
2
2
4
4
4
2
2
2
2
a
0
b
0
c
0

Figure 5.13

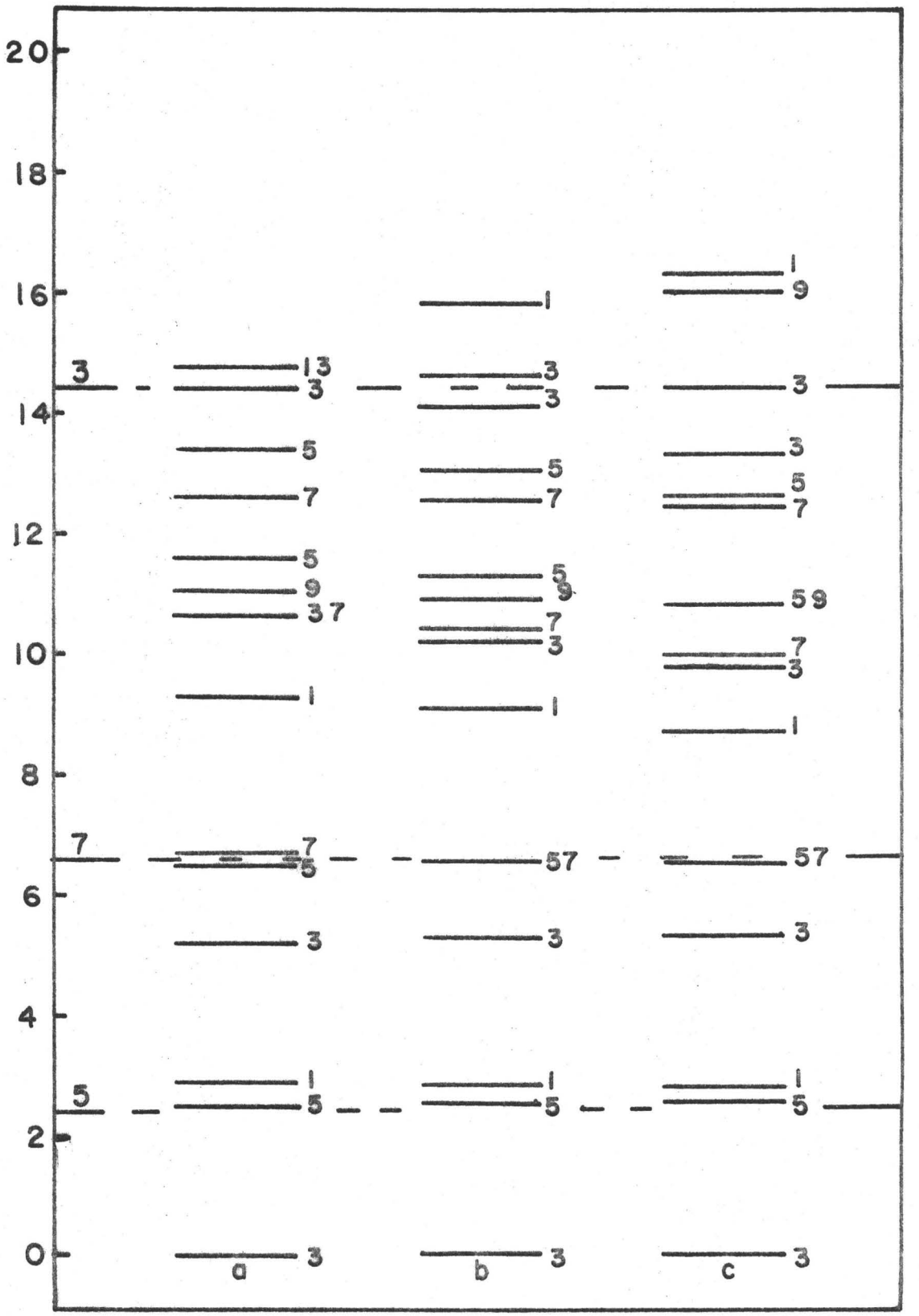
20
18
16
14
12
10
8
6
4
2
0
3
13
3
5
7
5
9
3 7
1
7
7
5
3
1
5
3
3
1
5
3
5
7
5
9
7
3
1
57
3
1
5
3
3
1
9
3
3
5
7
5
9
7
3
1
57
3
1
5
3
a
b
c

Figure 5.14

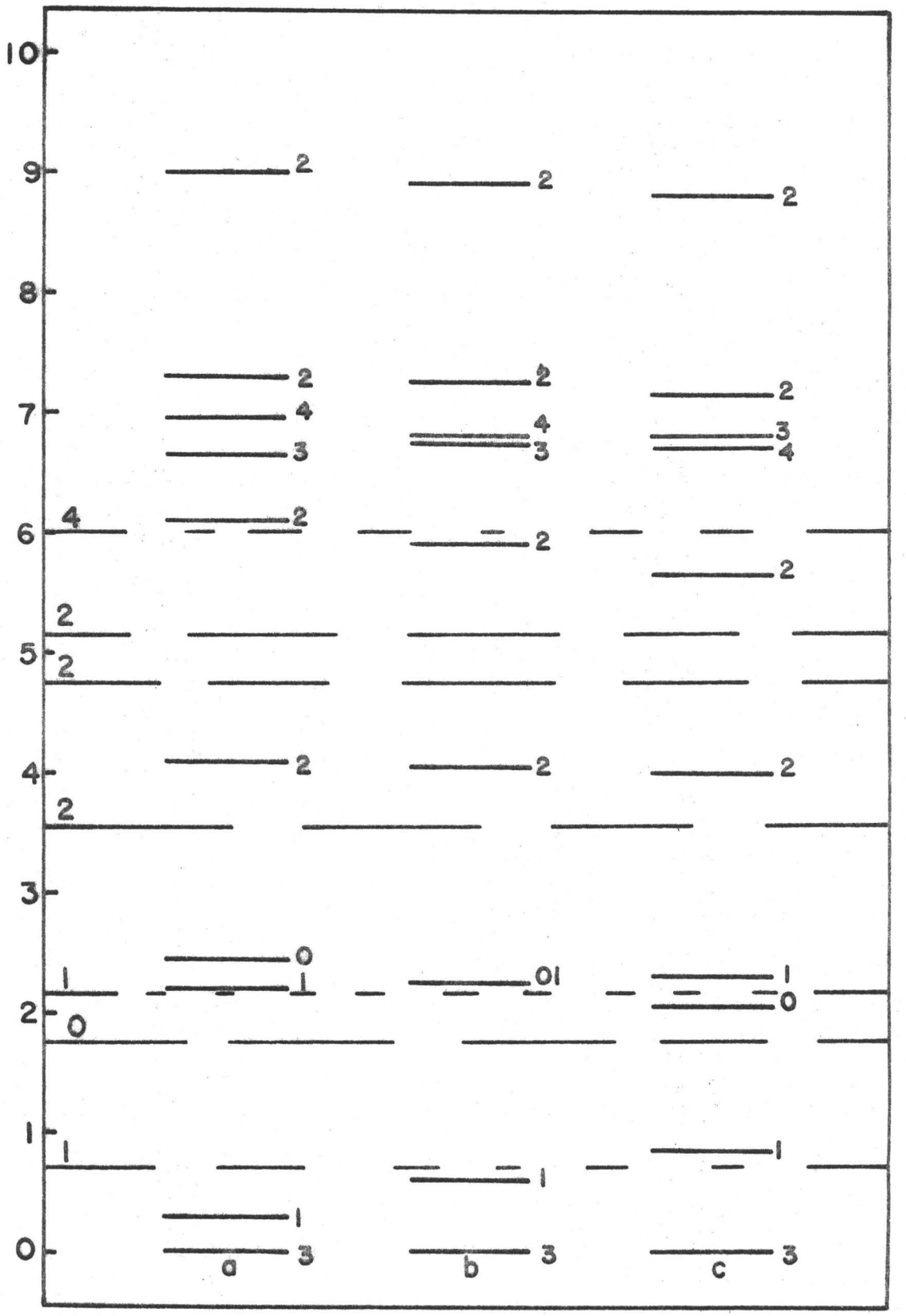

Figure 5.15

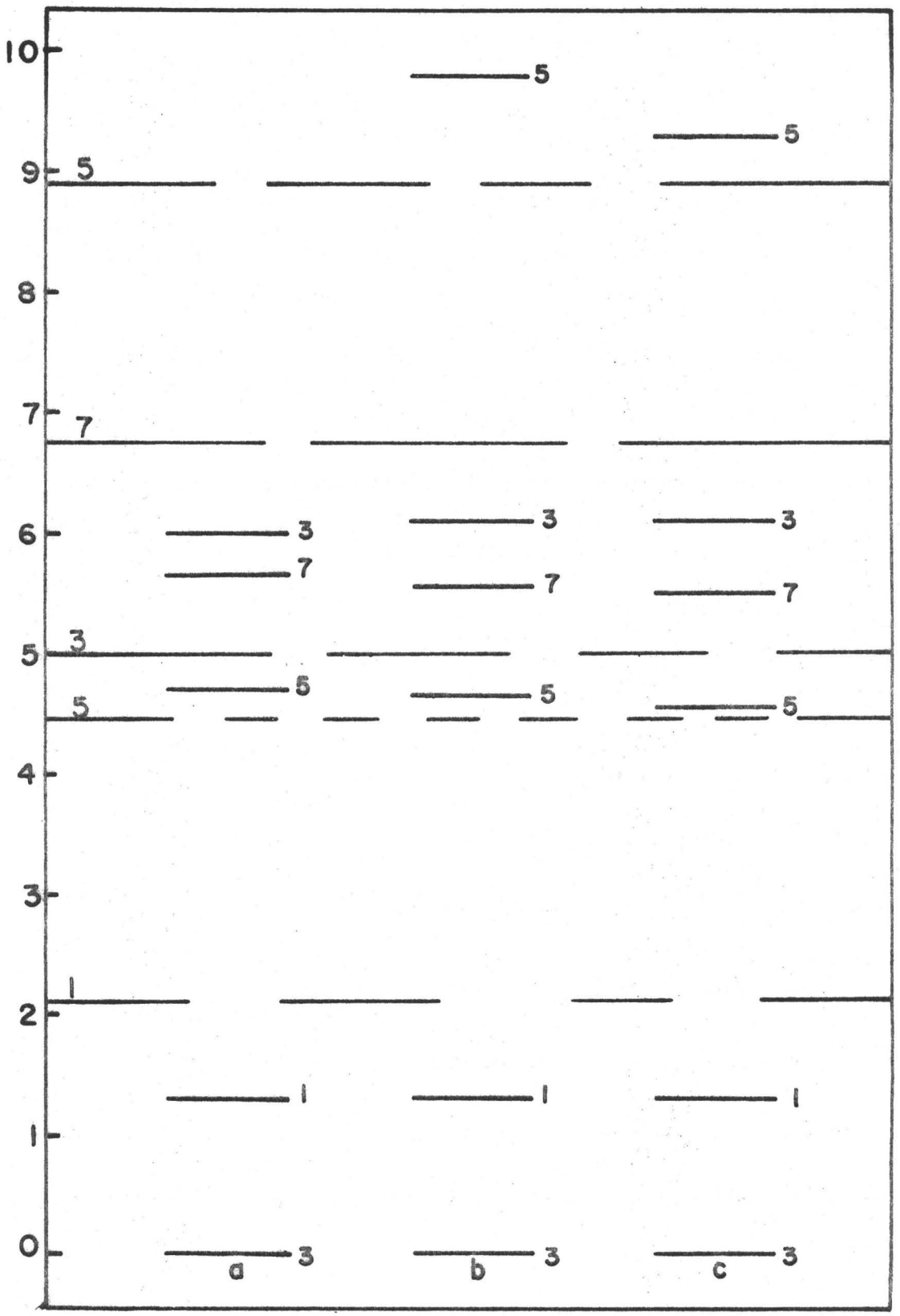

Figure 5.16

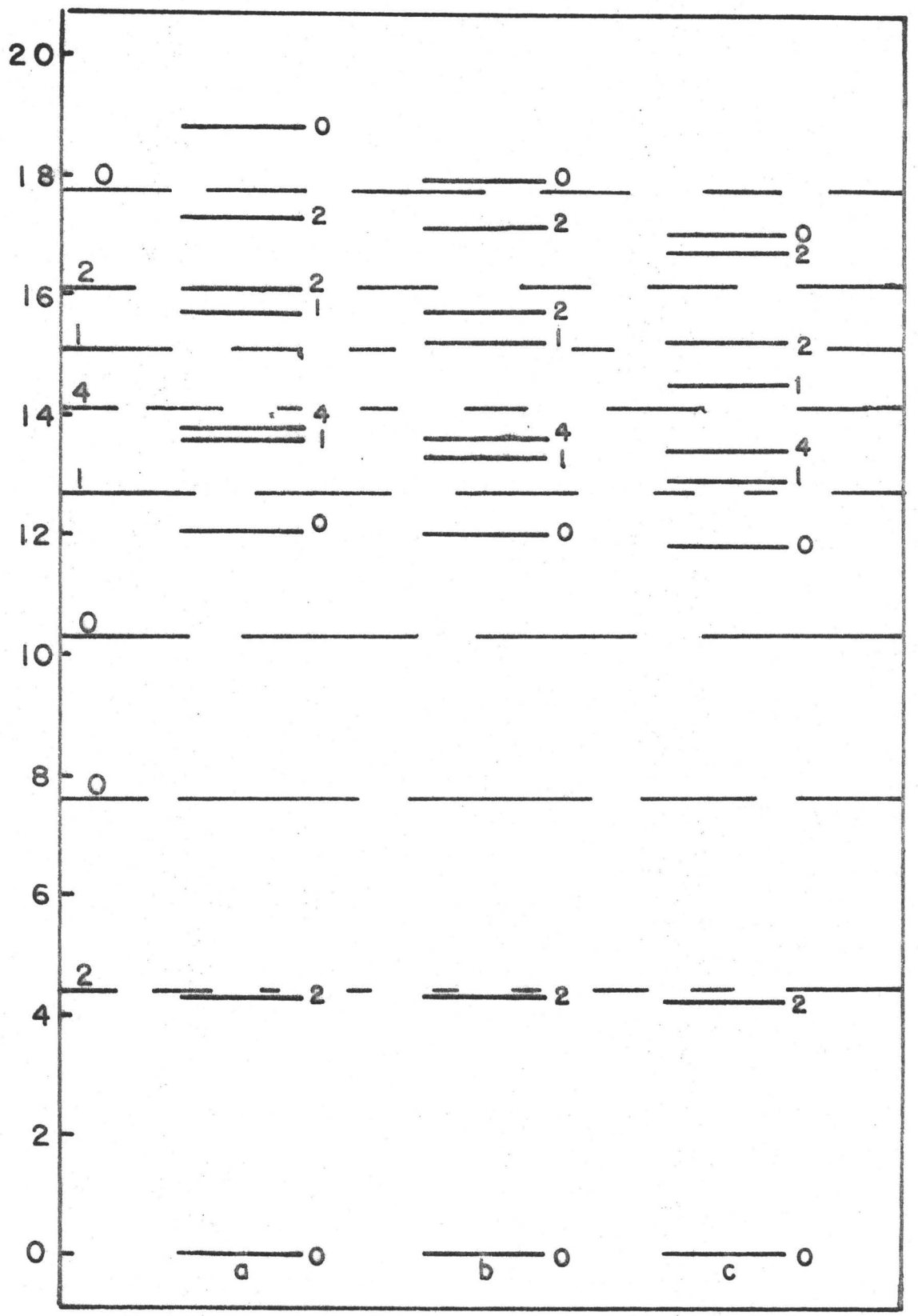

Figure 5.17

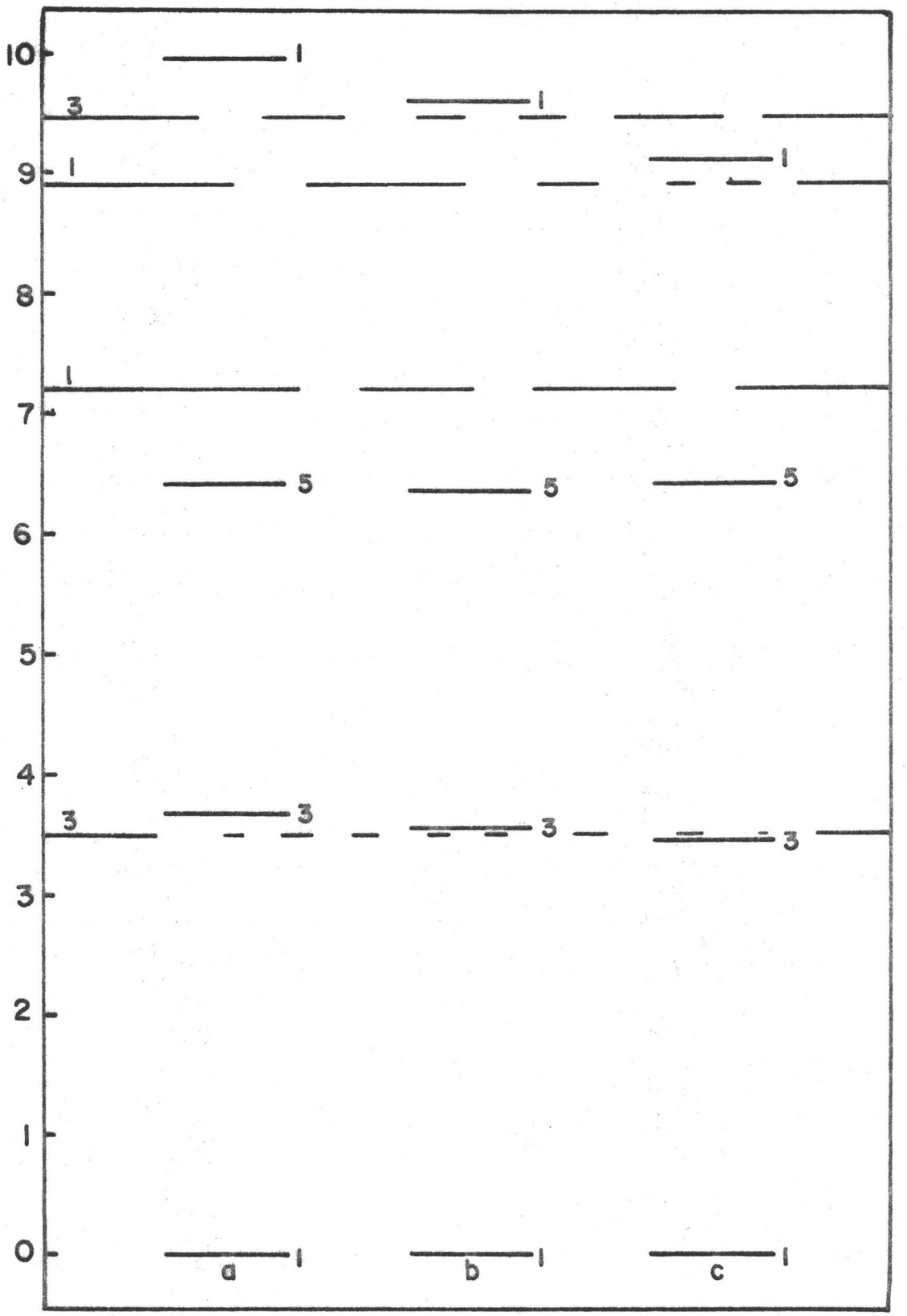

Figure 5.18

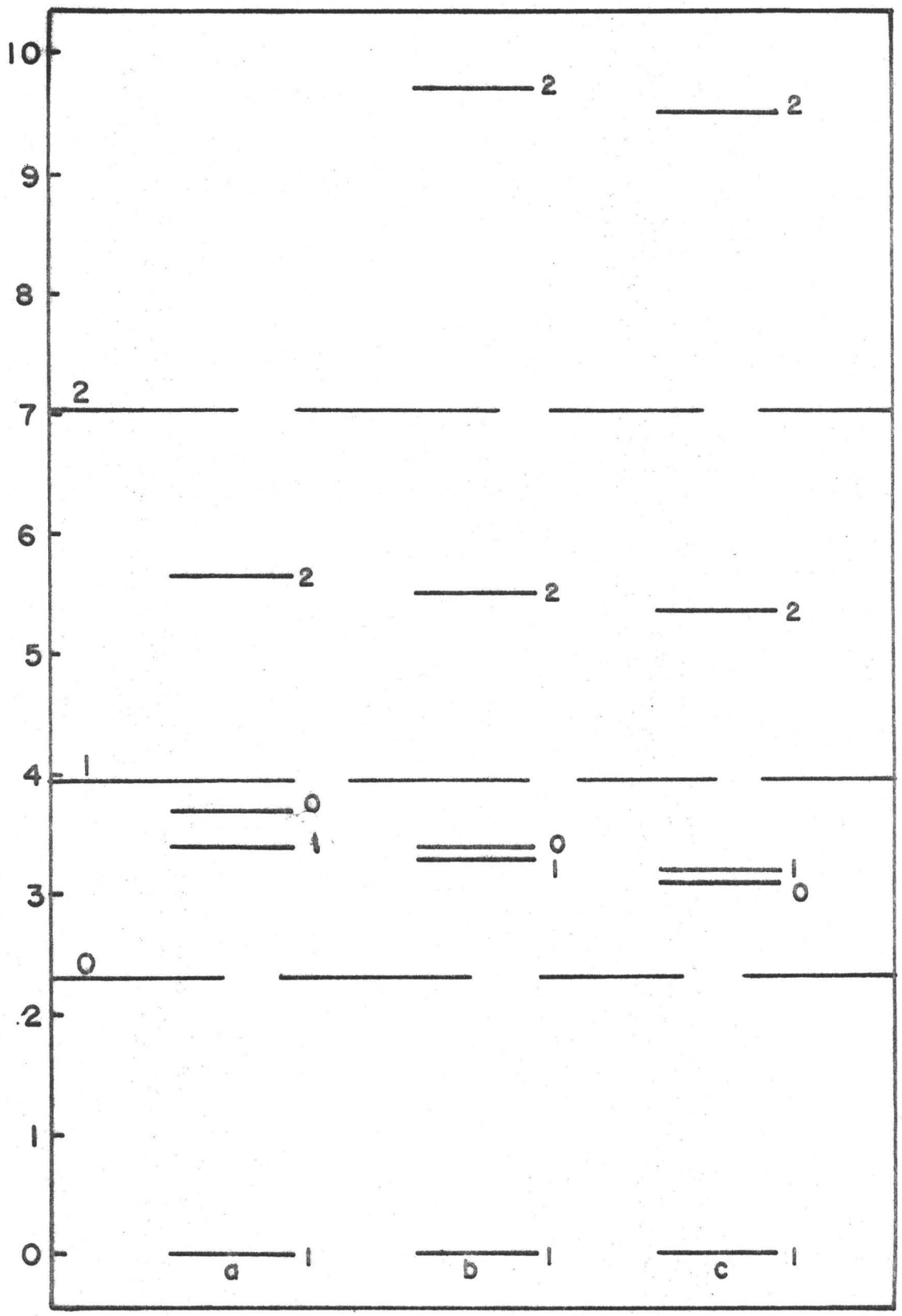

CHAPTER 6

THE DENSITY APPROXIMATION

As explained in Chapter 3 the form used for the nuclear density in the calculation of the required matrix elements is that of a single gaussian evaluated at the centre of mass of the interacting nucleons. The validity of this approximation for the nuclear density is examined in this chapter.

Manning (Man 67) has demonstrated that very different results are obtained if the single gaussian chosen for the density is determined by demanding that it duplicate the central density for the actual nuclear density rather than the root-mean-square radius of the true nuclear density. He suggests that the actual nuclear density should be approximated by more than one gaussian. This presents a great technical difficulty since in the matrix element evaluation the density appears to a non-integer power. For purposes of fast matrix element evaluation, it is required that the density to any power α be of the form

$$\rho^{\alpha}(r) = A_1 \exp(-r^2/a^2) + B_1 \exp(-r^2/b^2)$$

where $\rho(r)$ has the same root-mean-square radius and central density as the actual nuclear density. Thus, in general, there are four unknowns (A_1, B_1, a, b) to be fitted to

three physical quantities (the r.m.s. radius, the central density and the normalization condition $\int \rho(r)dr = A$). As a first approximation b is taken to be a/2 (results with the choice b = a/4 gave identical results to those calculated with b = a/2).

In principle A_1, B_1 and a can now be determined by a numerical computation. This numerical computation is however very time consuming and, to test the validity of the single gaussian density approximation when compared with the double gaussian density approximation, the approach that has been taken is to evaluate the A_1, B_1 and a using a fixed density for the nucleus under consideration rather than the actual nuclear densities generated during the calculation. For comparison purposes, the same procedure has to be adopted to determine the parameters of the single gaussian density approximation. Thus, the parameters of the density approximations were determined by fitting the root-mean-square radii (and the central density for the double gaussian approximation) quoted by Elton (Elt 61) for the A=6, 8, 10, 12, 14 nuclei. These parameters remain constant during the minimization procedure in the calculation. Table 6.1 tabulates the excitation energies calculated for Interaction 23 with Mayorana strength M = 1.0. These are compared with the results obtained for the more self-consistent single gaussian density approximation outlined in Chapter 3.

TABLE 6.1

A	Spin-Orbit strength, C(Mev)	J	E_x(Mev) Single Gaussian	E_x(Mev) Double Gaussian	E_x(Mev) Self-Consistent Single Gaussian
6	-0.5	0	5.04	5.11	4.67
		1	0.0	0.0	0.0
		1	4.93	4.95	4.84
		2	4.45	4.48	4.37
		2	7.29	7.36	6.86
		3	3.70	3.73	3.62
8	-1.5	0	0.0	0.0	0.0
		0	19.05	19.04	18.93
		0	19.67	19.66	19.54
		1	18.47	18.46	18.34
		1	18.76	18.75	18.64
		1	19.43	19.41	19.32
		2	3.11	3.10	3.12
		2	17.15	17.14	17.02

TABLE 6.1 - CONTINUED

		2	17.71	17.70	17.59
		2	19.12	19.10	19.00
		3	18.66	18.65	18.56
		3	19.82	19.81	19.75
		4	10.20	10.19	10.46
10	-4.0	0	2.54	2.53	2.51
		1	0.00	0.00	0.00
		1	0.97	0.97	0.95
		1	8.93	8.93	8.97
		2	3.06	3.06	3.13
		2	5.59	5.60	5.65
		2	5.93	5.91	5.95
		2	7.74	7.73	7.76
		3	0.04	0.04	0.12
		3	5.30	5.30	5.37
		3	9.40	9.39	9.51
		4	6.00	5.99	6.16

TABLE 6.1 - CONTINUED

12	-3.5	0	0.00	0.00	0.00
		0	12.84	12.85	12.75
		0	17.05	17.06	16.96
		1	14.61	14.62	14.54
		1	15.98	15.99	15.87
		1	19.02	19.03	18.93
		1	19.30	19.31	19.21
		2	3.24	3.23	3.30
		2	16.32	16.33	16.22
		2	17.03	17.04	16.99
		2	19.23	19.24	19.13
		2	19.73	19.74	19.67
		3	19.06	19.06	19.00
		4	10.97	10.96	11.21
14	-4.0	0	3.76	3.75	3.67
		1	0.00	0.00	0.00
		1	2.68	2.68	2.61
		2	4.98	4.99	5.00

TABLE 6.1 - CONTINUED

2	9.22	9.21	9.18
3	10.98	10.99	11.0

The binding energies and root-mean-square radii calculated using the different approximations are illustrated in Table 6.2. Also quoted are the central densities and root-mean-square radii for the single and double gaussian density distributions used in the calculation.

C_d is used to denote the value of the central density.

TABLE 6.2

	Single Gaussian			Double Gaussian			Self-Consistent Single Gaussian	
A	B.E. (Mev)	r.m.s. (fm)	C_d	B.E. (Mev)	r.m.s. (fm)	C_d	r.m.s. (fm)	B.E. (Mev)	r.m.s. (fm)
4	36.38	1.79	0.32	36.54	1.79	0.31	1.61	37.81	1.79
6	35.97	2.19	0.15	36.94	2.21	0.14	2.38	35.46	2.30
8	52.14	2.38	0.26	52.51	2.38	0.20	2.17	53.63	2.39
10	59.66	2.54	0.29	59.77	2.53	0.21	2.26	61.71	2.54
12	85.18	2.57	0.28	85.95	2.56	0.16	2.41	86.88	2.59
14	98.62	2.63	0.30	98.86	2.63	0.16	2.48	100.58	2.65
16	128.78	2.64	0.28	129.84	2.63	0.13	2.65	128.77	2.68

As can be seen from Tables 6.1 and 6.2 the results calculated using the fixed single and double gaussian approximations are almost identical. Of particular importance are the results for A=12, 14 and 16 where the central densities for the single gaussian approximation are significantly larger than those for the double gaussian approximation.

The results are also very similar for the more

self-consistent single gaussian approximation. For this interaction it seems appropriate to use the single gaussian density approximation for calculating the excitation energies of the O-p shell nuclei. It should be remembered, however, that this interaction is a weak density dependent interaction in as much that the contribution of the density dependent part of the interaction to the nuclear matter binding energy is comparatively small. For strong density dependent interactions it might be necessary to use a multiple gaussian density approximation.

The single gaussian for the density is obtained by demanding that it have the same values for $<\rho^2>$ and $<z^2>$ as the actual nuclear density (and, of course, the same normalization). The values of $<\rho^2>$ and $<z^2>$ for the true nuclear density are obtained by assuming that each P state is populated by (A-4)/12 particles. If the true density distribution is used these expectation values will, in general, be different ($<r^2> = <\rho^2> + <z^2>$ is, however, identical in the two cases since the oscillator well parameters are identical for the P_0 and $P_{\pm 1}$ states).

A more self-consistent approach to the evaluation of $<\rho^2>$ and $<z^2>$ for the actual nuclear density is to use the wave functions obtained during the calculation. This can be done by an iteration process. The procedure adopted is as outlined below.

At each stage of the minimization (i.e. for each

value of (α_s, α_p), the oscillator well parameters), the following procedure was followed.

(a) The eigenfunctions were obtained with the density zero everywhere.

(b) These wave functions were used to evaluate $\langle\rho^2\rangle$ and $\langle z^2\rangle$ and a single gaussian density distribution was fitted to these values.

(c) Another set of eigenfunctions were obtained using the single gaussian density function obtained at stage (b).

(d) If the ground state binding energy was identical (to within a given tolerence) at stages (b) and (c) the iteration procedure was ended. If not the iteration was repeated at stage (b).

The $\langle\rho^2\rangle$ and $\langle z^2\rangle$ obtained by the above iteration procedure did not, in general, satisfy the condition $2\langle z^2\rangle = \langle\rho^2\rangle$ i.e. the quadrupole moment is not zero and the nuclear system was intrinsically deformed. For ground states with J=0 and J=½, of course, the quadrupole moment was zero. The intrinsic deformation of the system meant that the eigenvalues were not degenerate when calculated in different M sub spaces.

However, the intrinsic quadrupole moments that were obtained were sufficiently small that an identification of the spin of the excited states, J, could be made. The

TABLE 6.3

A	Spin-Orbit Strength, C(Mev)	J	Self-Consistent E_x(Mev)	B.E.(Mev)	r.m.s.(fm)	$Q(fm^2)$	Closed-Shell E_x(Mev)	B.E.(Mev)	r.m.s.(fm)
6	-1.5	1	0.0	31.25	2.80	-0.11	0.0	31.25	2.66
		3	2.17				2.17		
		0	4.07				4.07		
		2	4.42				4.42		
		2	5.76				5.77		
		1	5.51				5.51		
7	-2.0	$\frac{3}{2}$	0.0	34.53	2.64	0.28	0.0	34.45	2.67
		$\frac{1}{2}$	0.48				0.48		
		$\frac{7}{2}$	3.70				3.65		
		$\frac{5}{2}$	5.32				5.10		
		$\frac{5}{2}$	6.27				6.20		
		$\frac{3}{2}$	7.73				7.50		
		$\frac{7}{2}$	7.91				7.70		
		$\frac{1}{2}$	8.39				8.15		

TABLE 6.3 - CONTINUED

8	-2.0	0	0.0	48.86	2.63	0.0	0.0	48.78	2.63
		2	2.63				2.63		
		4	8.64				8.66		
		2	12.22				12.10		
		2	13.80				13.70		
		4	14.56				14.46		
		3	14.67				14.55		
		1	14.74				14.64		
		1	14.98				14.90		
		2	15.17				15.10		
		0	15.25				15.18		
11		$\frac{3}{2}$	0.0	72.03	2.79	-0.51	0.0	72.13	2.79
		$\frac{1}{2}$	1.89				1.96		
		$\frac{5}{2}$	4.57				4.63		
		$\frac{7}{2}$	5.28				5.21		
		$\frac{3}{2}$	6.00				6.15		
		$\frac{5}{2}$	8.17				8.17		

TABLE 6.3 - CONTINUED

		$\frac{1}{2}$				9.42		
		$\frac{3}{2}$				10.21		
12	-3.5	0	0.0	83.92	2.80	0.0	83.92	2.79
		2	2.79			2.79		
		0	8.89			8.91		
		4	9.43			9.41		
		1	10.18			10.19		
		2	12.12			12.14		
		1	12.59			12.62		
		2	13.40			13.42		
		0	14.04			14.06		
		3	14.99			15.01		
		2	15.08			15.09		
		1	15.50			15.52		
		2	15.92			15.95		
13	-4.0	$\frac{1}{2}$	0.0	90.47	2.83	0.0	90.47	2.83
		$\frac{3}{2}$	2.81			2.81		

TABLE 6.3 - CONTINUED

		$\frac{5}{2}$	5.01				5.01		
		$\frac{1}{2}$	7.19				7.20		
		$\frac{3}{2}$	8.28				8.29		
		$\frac{1}{2}$	9.14				9.15		
		$\frac{7}{2}$	9.99				9.98		
		$\frac{3}{2}$	11.11				11.12		
		$\frac{5}{2}$	12.09				12.10		
14	-4.0	1	0.0	99.98	2.84	-0.10	0.0	98.88	2.84
		1	3.25				3.25		
		0	3.94				3.95		
		2	4.99				4.95		
		2	9.51				9.50		
		3	11.00				11.00		
		1	11.83				11.85		

calculations never ran for more than five and less than three iterations. This meant that at least 48 calculations had to be performed for each nucleus. Thus the A=10 and A=9 systems were not calculated in the self-consistent manner outlined above since this would have been extremely time consuming.

Table 6.3 shows the results of the self-consistent approach compared with those obtained by the "closed-shell" approach for Interaction 10. The excitation energies quoted for the self-consistent calculation are those obtained in the M=0 or M=½ sub space and $Q = \langle \rho^2 \rangle - 2\langle z^2 \rangle$.

The results quoted for A=11 are for a calculation in which the iteration procedure had not quite converged. The results for the self-consistent and closed-shell approaches are sufficiently close to indicate that the closed-shell approximation is valid. The greatest discrepancies are for ^{7}Be. Calculations for the weaker density dependent Interaction 23 show that the self-consistent and the closed-shell approach produce results even more identical than is the case for Interaction 10. It is now apparent that the single gaussian "closed-shell" density form is good enough to be used in O-p shell calculations.

The next question that arises is the validity of evaluating the local density at the centre of mass of the interacting particles. For example, if the interacting particles are at opposite sides of the nucleus, and in

particular if they are in the nuclear surface, the above approximation would take the local density to be that at the centre of the nucleus. Thus the local density is greatly overestimated for particles in the nuclear surface.

In this section results for Interaction 23 (with Mayorana strength M=1.0) are presented for three different interpretations of the local density $\rho(\underline{r}_1,\underline{r}_2)$. There are

$$\text{(i)} \quad \rho(\underline{r}_1,\underline{r}_2) = \rho[(\underline{r}_1+\underline{r}_2)/2]$$

$$\text{(ii)} \quad \rho(\underline{r}_1,\underline{r}_2) = \rho[(\frac{\underline{r}_1^{\,2}+\underline{r}_2^{\,2}}{2})^{\frac{1}{2}}]$$

$$\text{(iii)} \quad \rho(\underline{r}_1,\underline{r}_2) = \tfrac{1}{2}[\rho(\underline{r}_1) + \rho(\underline{r}_2)]$$

Figs. 6.1 - 6.8 show the excited state spectra of the O-p shell nuclei obtained with the above three interpretations of the local density. Also shown (iv) are results for Manning's (Man 67) approximation 2 where the single gaussian density function is designed to fit the central density of the actual nuclear density. Table 6.4 list the relevant binding energies and root-mean-square radii. The excitation energies are almost identical for (i), (ii) and (iii) except for ^{6}Li. Even these differences can be explained to a large degree if the differences in ^{16}O binding energies for (i) and (ii) are considered. The calculated excitation energies for interpretation (iv) are quite different than those for the other three interpretations.

TABLE 6.4

	(i)		(ii)		(iii)		(iv)	
A	B.E.(Mev)	r.m.s.(fm)	B.E.(Mev)	r.m.s.(fm)	B.E.(Mev)	r.m.s.(fm)	B.E.(Mev)	r.m.s.(fm)
4	37.81	1.79	35.89	1.81	36.03	1.81	37.81	1.79
6	35.67	2.31	34.14	2.35	34.28	2.34	34.99	2.27
7	38.26	2.37	36.54	2.39	36.71	2.39	38.14	2.34
8	53.80	2.39	51.69	2.40	51.91	2.40	54.47	2.37
9	52.40	2.49	50.28	2.50	50.51	2.50	53.28	2.45
10	63.72	2.53	61.40	2.55	61.65	2.55	65.19	2.49
11	73.09	2.57	70.54	2.59	70.80	2.59	75.38	2.52
12	90.22	2.60	87.32	2.61	87.64	2.61	93.79	2.53
13	93.45	2.64	90.38	2.65	90.73	2.65	97.82	2.56
14	102.26	2.65	98.85	2.67	99.23	2.67	108.12	2.56
16	128.77	2.68	124.58	2.69	125.04	2.69	139.24	2.56

The calculated binding energies are lower for interpretation (ii) than for interpretation (i) (for (iii) the binding energies are slightly higher than for (ii)). Interpretation (ii) was designed to give lower local densities than interpretation (i) and since the density dependent part of the interaction is attractive overall, as can be seen from the nuclear matter data (Chapter 3), the binding energies for (ii) will be lower than for (i). It would also be expected that the root-mean-square radii for (ii) would be smaller than for (i). The reverse is true indicating that interpretation (ii) tends to lower the energy for particles interacting at smaller $|r_1-r_2|$ faster than for larger $|r_1-r_2|$. Interactions whose density dependence is essentially repulsive, such as Interaction 10, predict higher binding energies for (ii) than for (i).

The results for density approximation (iv) underline the danger in taking too simplistic an approach to consideration of the density dependence. Compared with approximation (i), (iv) has much smaller values of the density in the core region and larger values of the density in the surface region. Thus, for Interaction 23 it might be expected that the binding energies for approximation (iv) would be less than for approximation (i) and that the root-mean-square radii would be larger. This is almost the reverse of the true situation. None of the root-mean-square radii conform to this pattern and only the binding energies

of ^{6}Li and ^{7}Be are less for approximation (iv) than for approximation (i).

The actual mechanism for this interaction appears to be that the interacting nucleons can gain more energy by moving closer together and thus reducing the contribution from the repulsive density dependence from that for approximation (i). This is possible because the core (i.e. the region where the density is approximately the same) is of longer range for approximation (iv) than for approximation (i). However, for ^{6}Li and ^{7}Be the P state nucleons are constrained to move nearer the surface by the density independent part of the interaction. Thus, in general, the binding energies increase and the r.m.s. radii decrease. The gain in binding energy for ^{16}O is 11 Mev for Interaction 23. This is much less than for Manning's interaction 4(52 Mev) (Man 67). Interactions whose density dependent contribution to the nuclear matter binding energy is repulsive would be expected to show greater changes than Interaction 23. Interaction 10, for example, exhibits a difference of 44 Mev.

The differences in the excitation energies for approximations (i) and (iv) are slight for most states although there are differences for the more highly excited states. Some of these differences can be explained by the difference in the ^{16}O binding energy for the two approximations (Table 5.3).

Since the excitation energy spectra is of prime interest in this thesis, it is apparent that the closed-shell density approximation (i) can be used in further studies without significant loss in generality.

FIGURE CAPTIONS

For all figures, excitation energy (in Mev) is plotted to the left of the figure. Full lines designate the calculated levels and dashed lines designate certain experimental levels. For even nuclei the spin J of the level is indicated to the right of the calculated levels and at the left of the figure for the experimental levels, for odd nuclei the value of 2J is likewise indicated.

Figures 6.1 - 6.9 plot the excited state spectra of the O-p shell nuclei calculated for Interaction 23 using

(a) density approximation (i)

(b) density approximation (ii)

(c) density approximation (iii)

(d) density approximation (iv)

Figure 6.1 Excited State Spectra of ^{6}Li with C = -2.0 Mev.

Figure 6.2 Excited State Spectra of ^{7}Be with C = -1.5 Mev.

Figure 6.3 Excited State Spectra of ^{8}Be with C = -2.0 Mev.

Figure 6.4 Excited State Spectra of ^{9}B with C = -3.0 Mev.

Figure 6.5 Excited State Spectra of ^{10}B with C = -5.0 Mev.

Figure 6.6 Excited State Spectra of ^{11}B with C = -4.5 Mev.

Figure 6.7 Excited State Spectra of ^{12}C with C = -5.5 Mev.

Figure 6.8 Excited State Spectra of ^{13}C with C = -5.0 Mev.

Figure 6.9 Excited State Spectra of ^{14}N with C = -5.0 Mev.

Figure 6.1

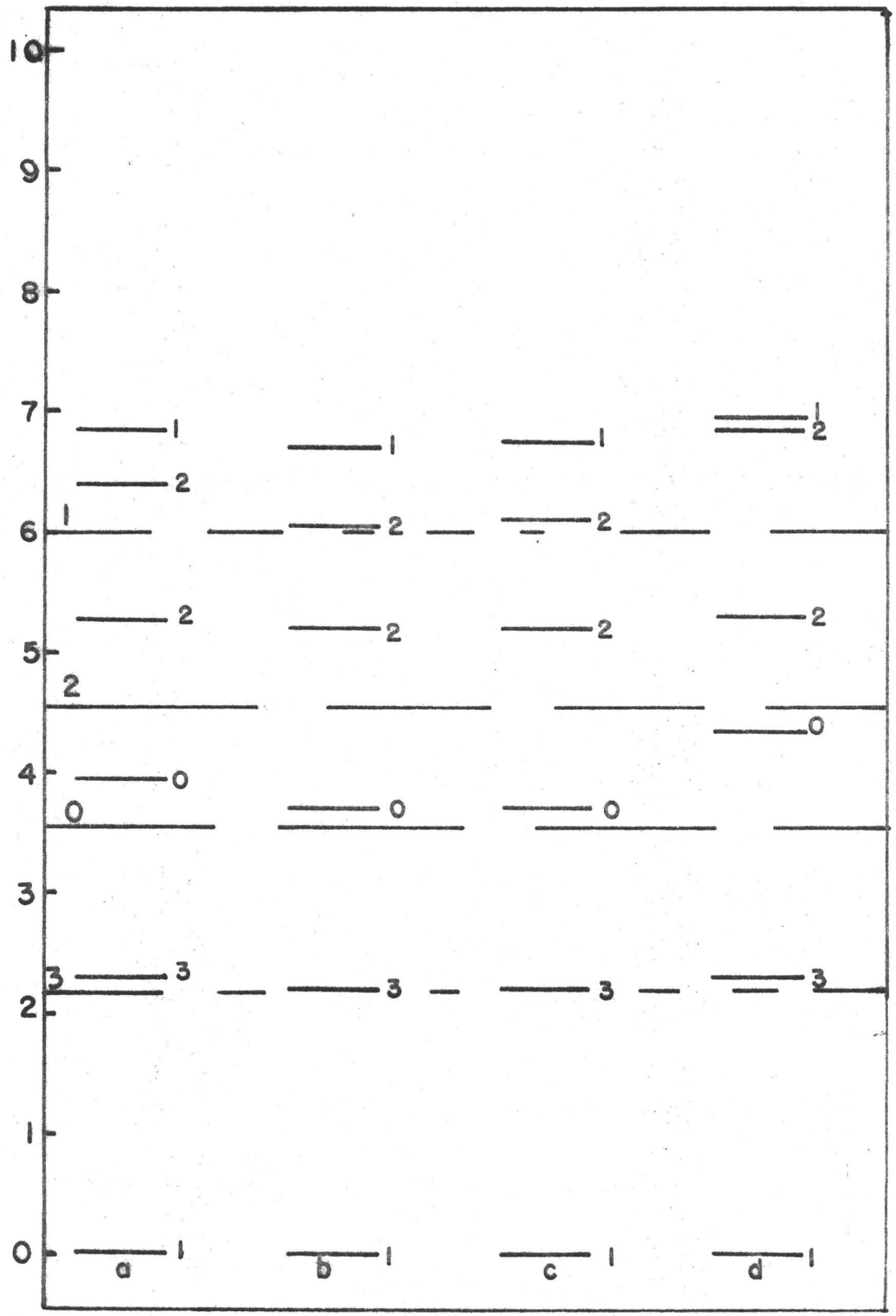

Figure 6.2

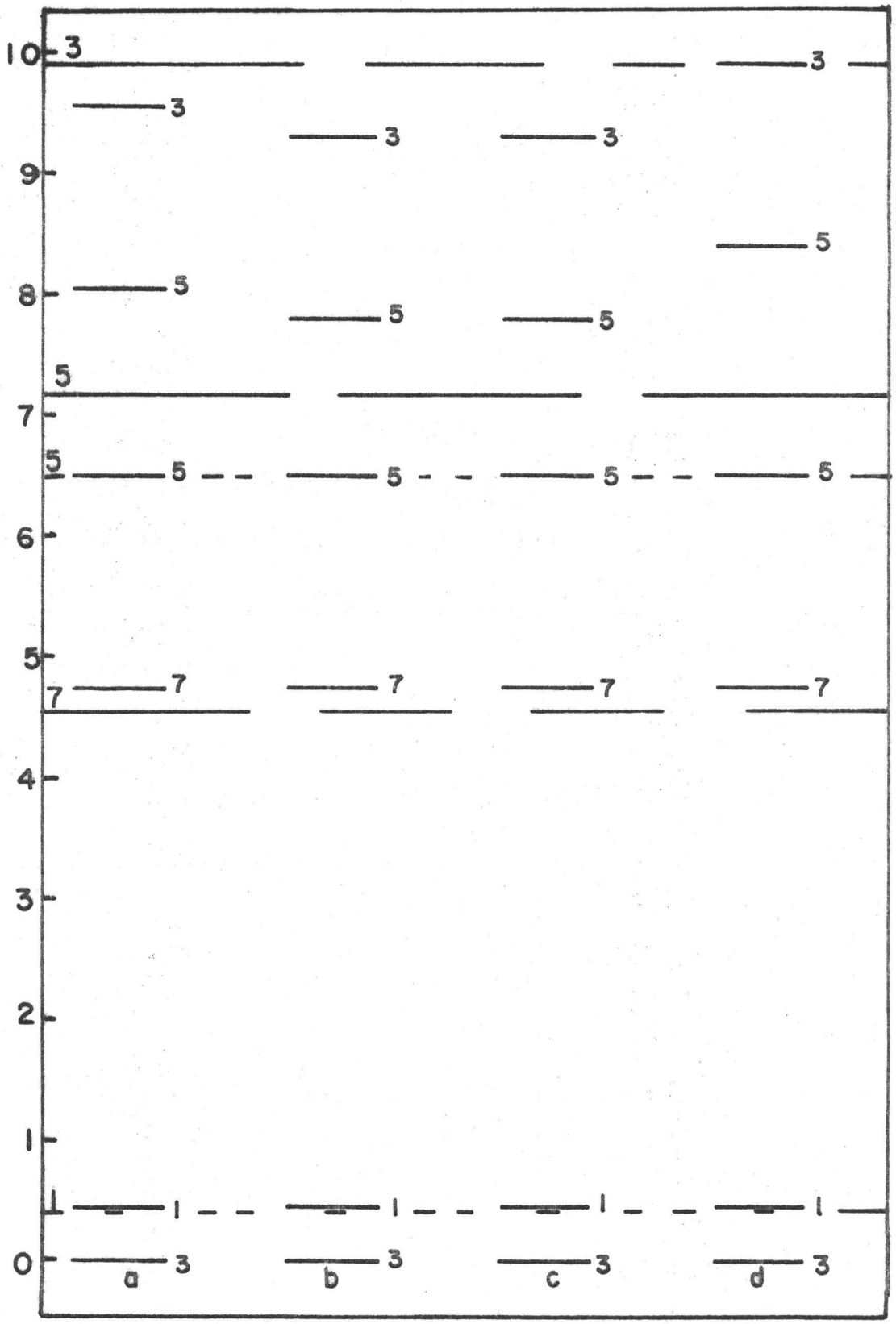

Figure 6.3

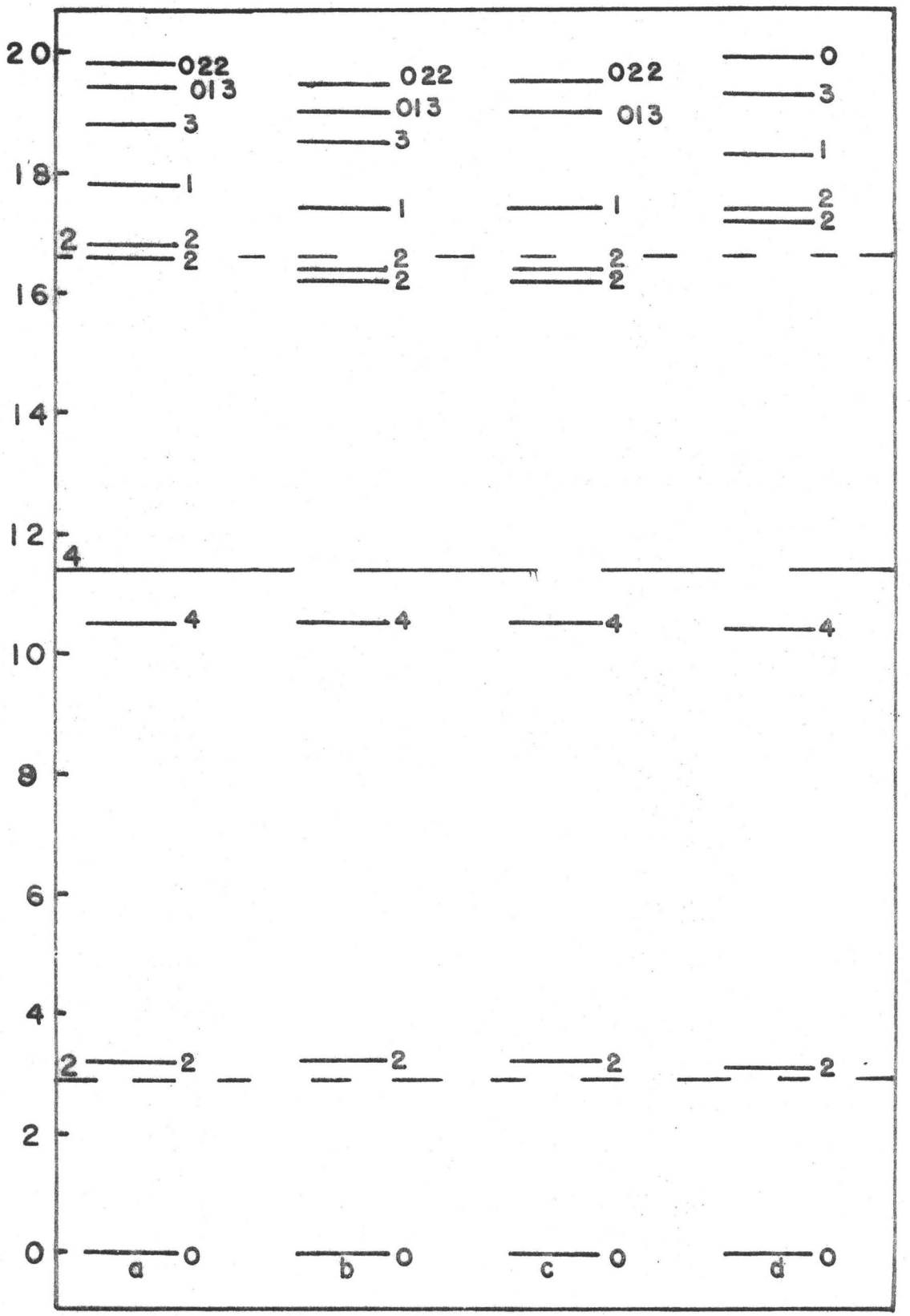

Figure 6.4

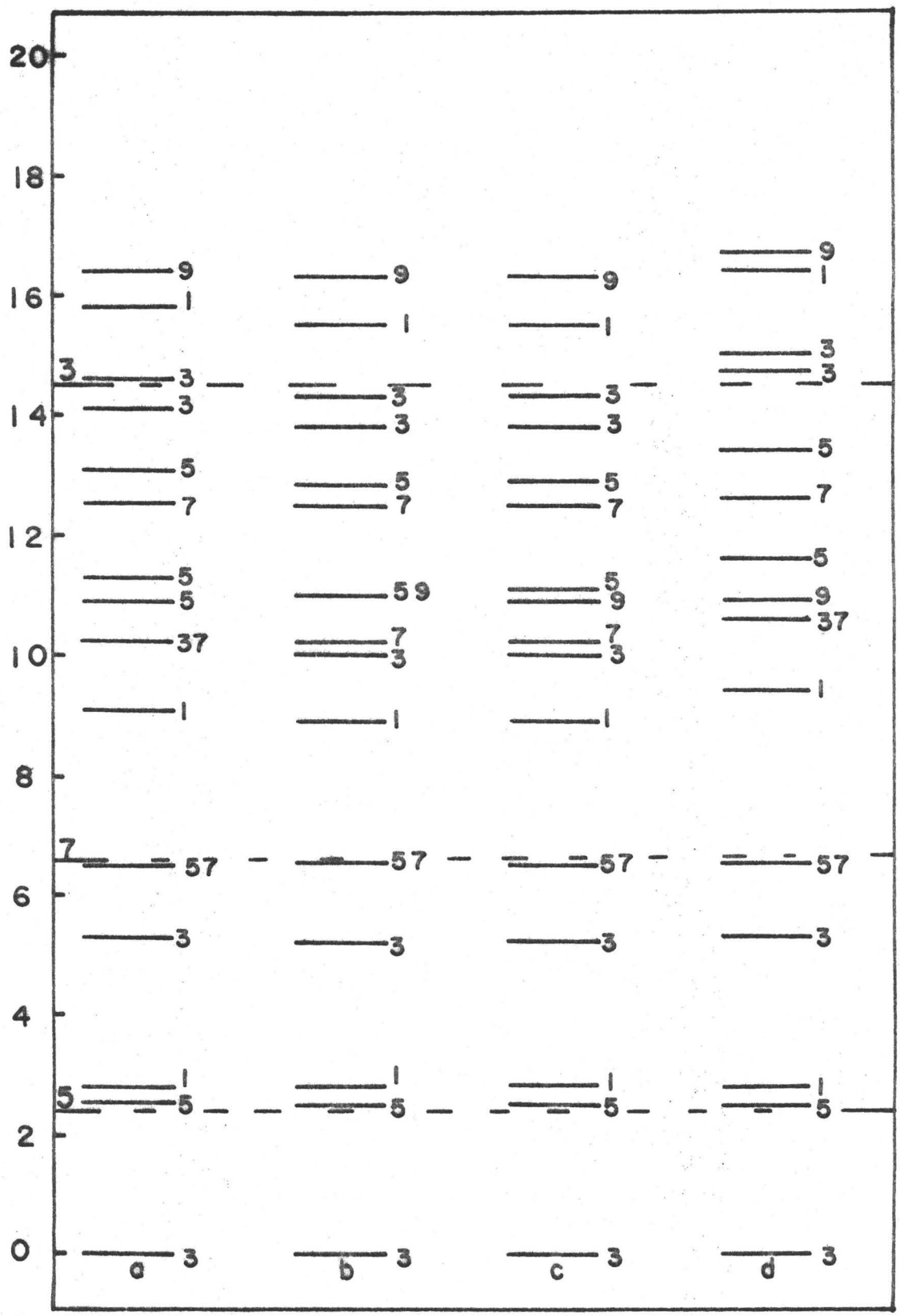

Figure 6.5

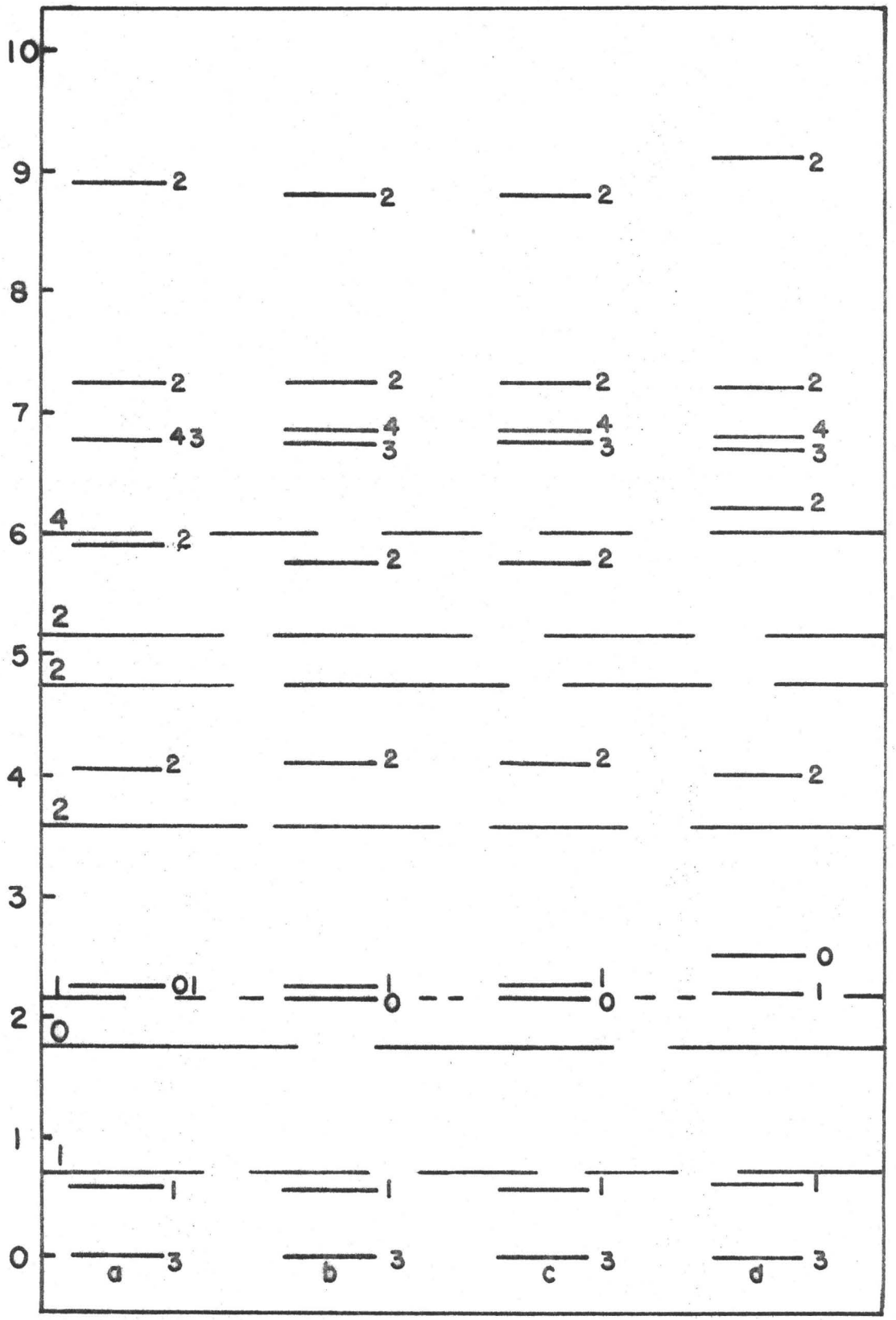

Figure 6.6

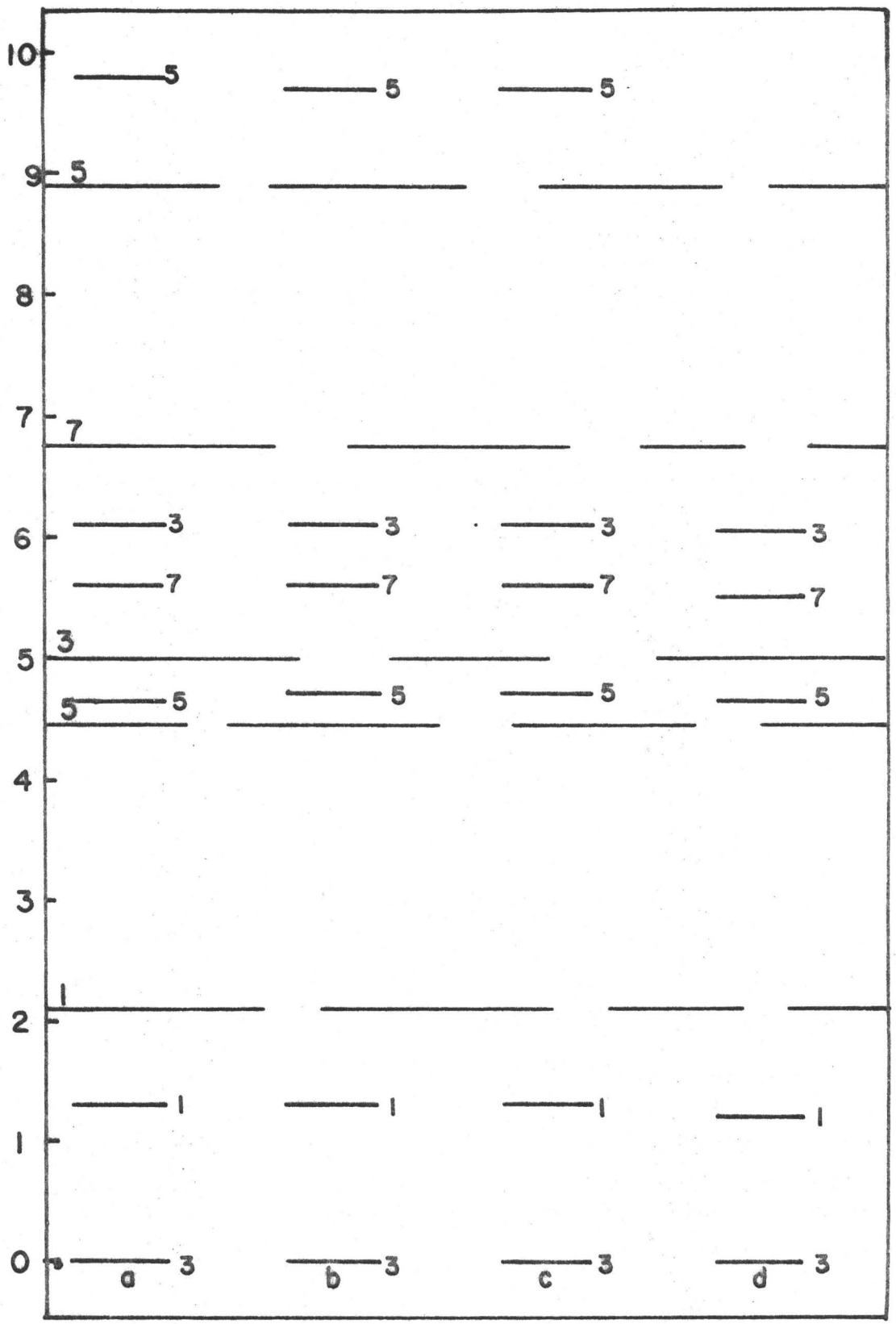

Figure 6.7

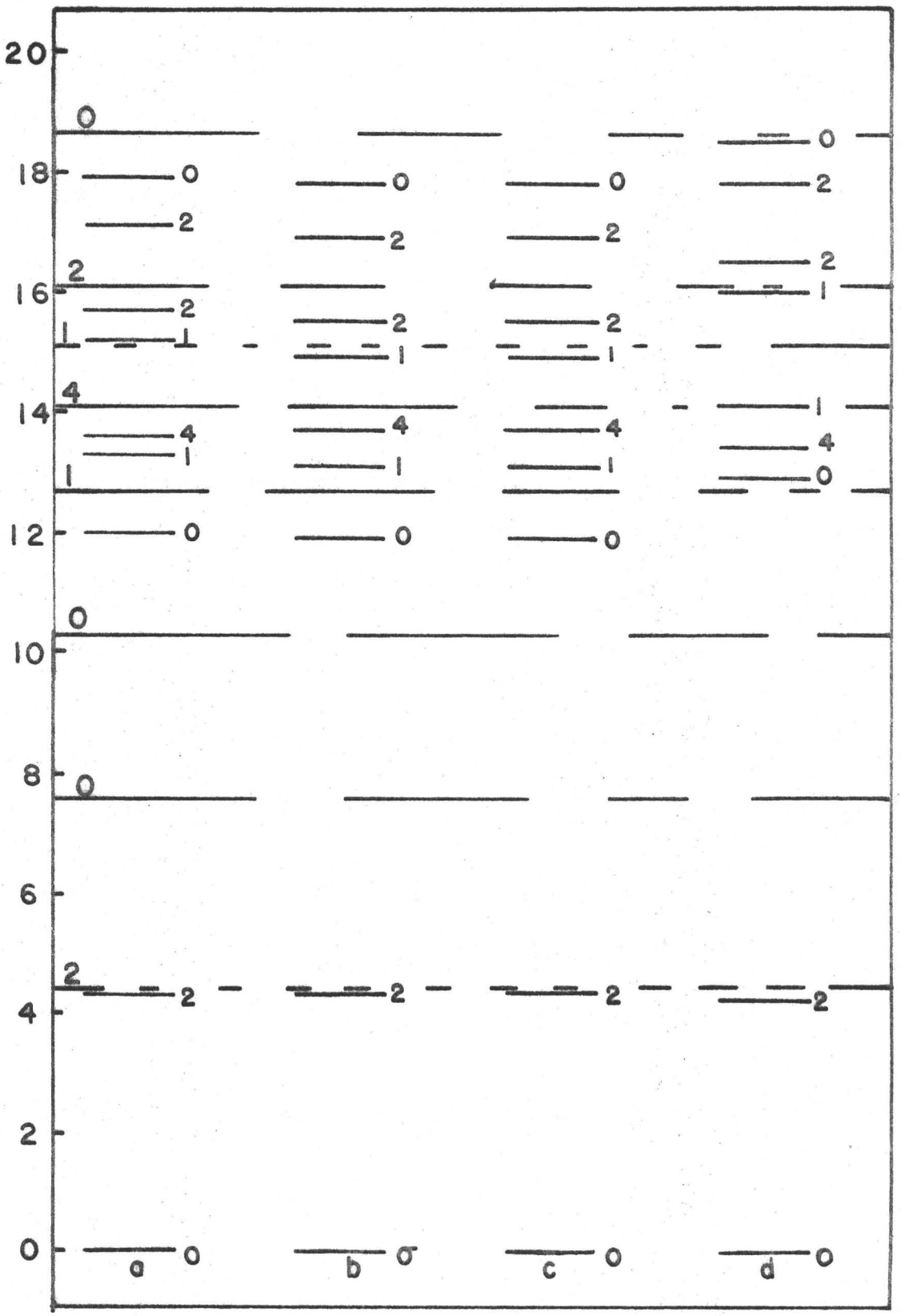

Figure 6.8

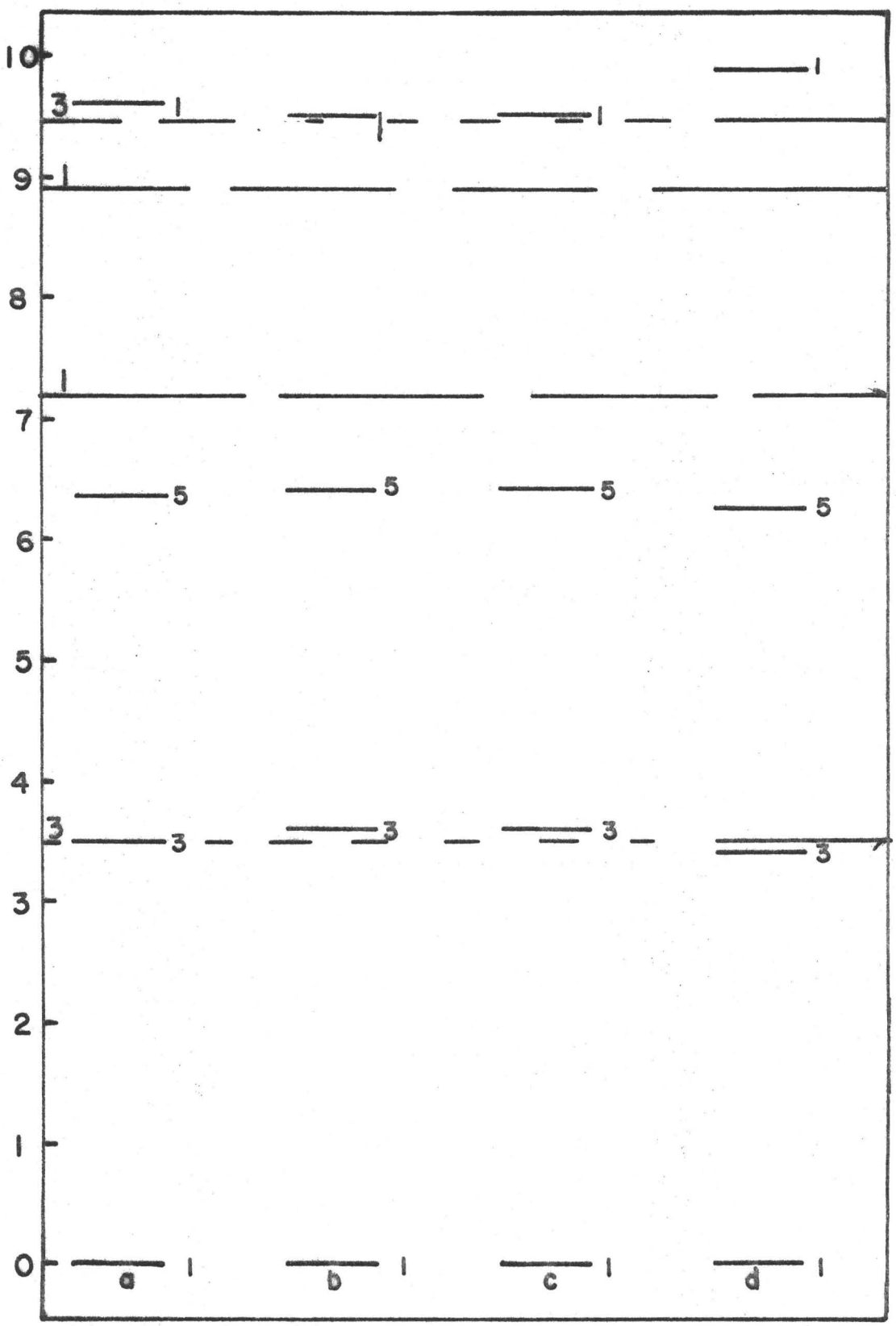

Figure 6.9

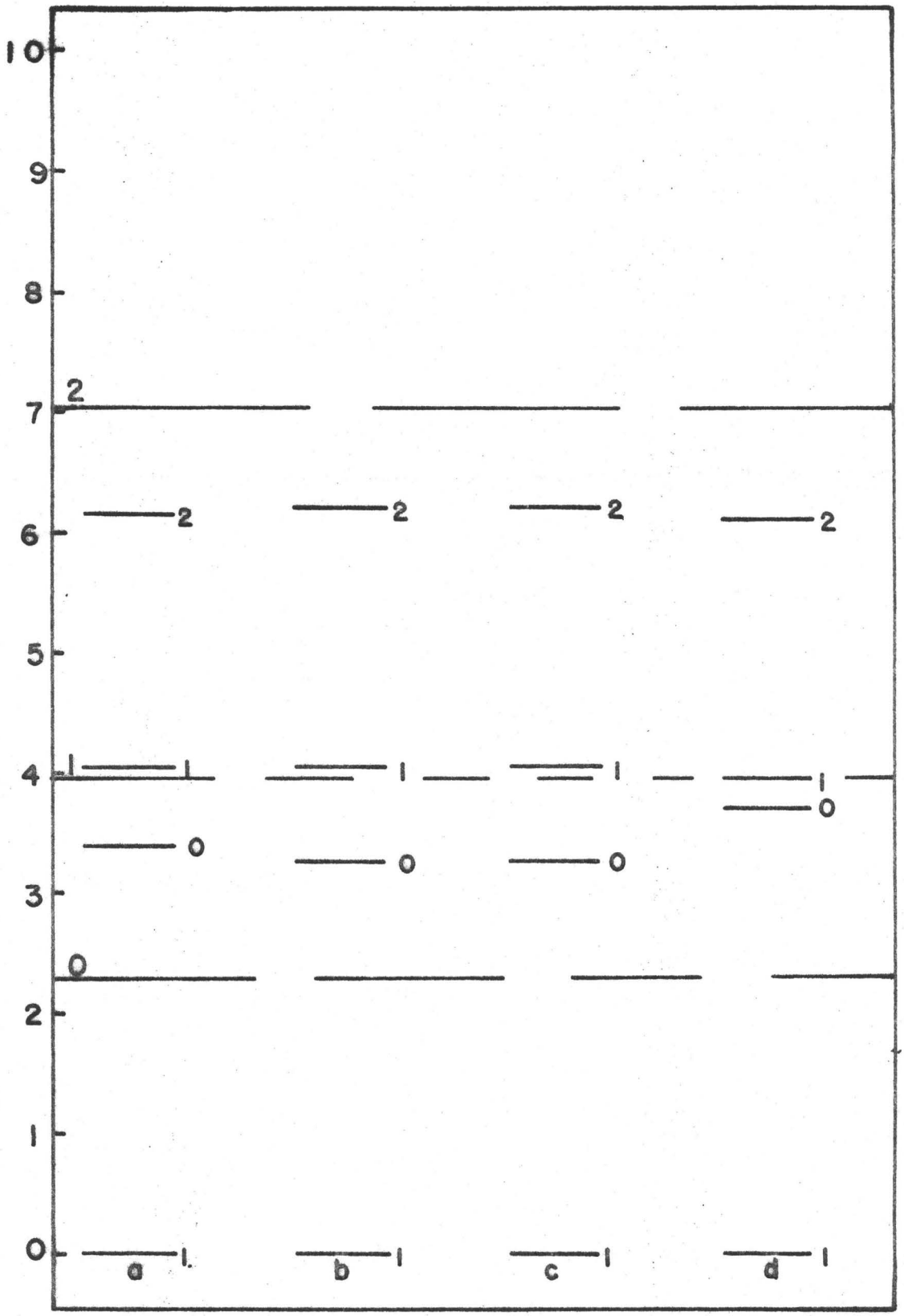

CHAPTER 7

THE ATTRACTIVE AND REPULSIVE RANGE

In this chapter consideration is given to density dependent interactions differing from each other essentially only in regard to their attractive and repulsive ranges. All these interactions fit the same criteria and are of the same basic density dependent form viz. the attractive density dependence is $\rho^{1/3}$ and the repulsive density dependence is $\rho^{2/3}$.

Consideration is first given to Interactions 10 and 23 which have the same attractive range λ_a = 1.5 fm, λ_r^0 being 1.247 fm and 0.602 fm respectively. The repulsive core height is the same for both interactions, 5 Mev. The fit to the scattering data imposes the condition that the attractive strength of the interaction must decrease as the repulsive range decreases. This fit also determines the Bartlett Exchange Strength in relation to the Isospin Exchange Strength (B-H) since it is this parameter which determines the ratio of the singlet and triplet even strengths. It is observed that this parameter also decreases with decreasing repulsive range.

The decreased repulsive range means that the repulsive part of the interaction is weaker and thus to fit the nuclear matter binding energy and the binding energy

of ^{16}O it is necessary that the exchange matrix elements be weighted more strongly i.e. ν decreases and M, the Majorana exchange strength increases. To further satisfy the criteria that nuclear matter saturate at the correct saturation density c_3 and c_4 have to increase and the compressibility of nuclear matter increases. Because of the decreasing repulsive range c_4 increases faster than c_3.

The decreased repulsive range for Interaction 23 means that the root-mean-square radii calculated using this interaction will be smaller. This is seen in Table 7.1 where the binding energies and root-mean-square radii of the O-p shell nuclei calculated using Interactions 10 and 23 are listed. The corresponding excited state spectra are shown in Figs. 7.1 - 7.5.

TABLE 7.1

	Interaction 10		Interaction 23	
A	B.E.(Mev)	r.m.s.(fm)	B.E.(Mev)	r.m.s.(fm)
4	27.28	2.04	37.81	1.79
6	31.37	2.66	35.67	2.31
7	34.14	2.66	38.26	2.37
8	48.78	2.63	54.84	2.39
9	50.00	2.72	52.43	2.49
10	63.24	2.75	63.83	2.53
11	72.13	2.79	73.18	2.57
12	88.75	2.81	90.49	2.60

TABLE 7.1 - CONTINUED

13	92.98	2.83	92.82	2.63
14	101.59	2.84	102.45	2.65
16	124.73	2.87	128.77	2.68

The different values for the ^{16}O binding energies complicate the comparison between the binding energies of the open shell nuclei for the two interactions. For ^{4}He, where the ν parameter plays no part, it is obvious that Interaction 23 will have the higher binding energy since it is the more attractive interaction, its repulsive range being much shorter than is Interaction 10's. As more nucleons are added to the system the ν parameter plays an increasingly more important role and for the nuclei A>10 the binding energies are virtually identical (due regard having been paid to the difference between the ^{16}O binding energies for the interactions). The r.m.s. radii follow the expected trend, decreasing with decreasing repulsive range. They also conform to the argument advanced in Chapter 5 concerning the contribution to the nuclear matter binding energy of the density dependent part of the interaction.

The Majorana exchange strengths and the ^{16}O binding energies are sufficiently close for Interactions 10 and 23 that any differences in the excitation energies of the O-p nuclei for the interactions are brought about by the differences between the interactions themselves. It is seen from

Figs. 7.1 - 7.5 that generally the excitation energies and the spacing between the excited states are much less for Interaction 10. The exceptions to this state of affairs (the lower states of ^{10}B, the $\frac{1}{2}^-$ state of ^{11}B, the $\frac{3}{2}^-$ state of ^{13}C and the 1^+ state of ^{14}N) can partly be explained by the difference in the ^{16}O binding energy for the interactions. This is not the case for the 0^+ states. It should be noted that the interaction whose density dependent part is the more attractive gives the higher excitation energies.

It has been found, during the course of this investigation, that any interaction which predicts approximately the same excitation energy of the second 2^+ state of ^8Be as does Interaction 23 will also give similar results to Interaction 23 for a large number of states in the O-p nuclei. As a consequence some interactions were merely tested by calculating the A=6, 8 and 14 systems. Moreover, for some interactions, the attempt to obtain the minimum binding energy for the A=6 system failed because ^6Li was underbound with respect to the α-particle. Interactions 32, 33 and 34 were treated in this way.

The spectra of ^8Be and ^{14}N calculated using Interactions 32, 33 and 34 are shown in Figs. 7.6 and 7.7. The relevant binding energies and root-mean-square radii are listed in Table 7.2.

These interactions all have the same attractive range λ_a = 1.0 fm. The same trends noted in Table 7.2 in

TABLE 7.2

	Interaction 32		Interaction 33		Interaction 34	
A	B.E.(mev)	r.m.s.(fm)	B.E.(Mev)	r.m.s.(fm)	B.E.(Mev)	r.m.s.(fm)
4	33.13	1.77	28.24	1.82	25.95	1.84
8	56.54	2.27	52.64	2.29	52.40	2.29
14	103.24	2.54	101.37	2.55	104.54	2.53
16	129.83	2.58	126.80	2.59	130.19	2.58

the excitation energies, ^{4}He binding energy and r.m.s. radii are exhibited for decreasing repulsive range. The density dependent contribution to the binding energy of nuclear matter once more decreases with increasing repulsive range. The compressibility, on the other hand shows the opposite trend, it now increases. Thus, although some loose correlation can be established between the calculated excitation energies and the contribution of the density dependence to the nuclear matter energy, no such correlation exists between the excited state spectra and the compressibility of nuclear matter. The small difference between the attractive and repulsive ranges for these interactions means that the ν parameter changes drastically for small changes in the repulsive range.

It has been indicated that the calculated excitation energy of the second 2^+ state in ^{8}Be is a good guide to the separation of many excited states of the other O-p nuclei. Thus in turning to the comparative study of interactions with differing attractive ranges the additional requirement, that the repulsive range be so chosen as to predict the excitation energy of this state, has been added to the criteria required of the interactions listed in Chapter 3. Thus for each λ_a, $\lambda_r{}^0$ is varied so that the second 2^+ state of ^{8}Be is fitted approximately.

This procedure was followed in deriving Interactions 23, 20, 31 and 33 whose attractive ranges are λ_a = 1.5 fm,

TABLE 7.3

	Interaction 23		Interaction 30		Interaction 31		Interaction 33	
A	B.E.(Mev)	r.m.s.(fm)	B.E.(Mev)	r.m.s.(fm)	B.E.(Mev)	r.m.s.(fm)	B.E.(Mev)	r.m.s.(fm)
4	37.81	1.79	35.99	1.82	35.25	1.80	28.24	1.82
6	35.67	2.31	36.06	2.37	-	-	-	-
7	38.26	2.37	38.83	2.38	-	-	36.22	2.33
8	53.84	2.39	54.83	2.40	-	-	52.84	2.29
9	52.43	2.49	53.81	2.49	-	-	51.27	2.41
10	63.83	2.53	65.48	2.54	-	-	64.59	2.42
11	73.18	2.57	75.16	2.58	-	-	73.05	2.50
12	90.49	2.60	92.68	2.60	-	-	92.01	2.48
13	92.82	2.63	95.99	2.64	-	-	95.34	2.52
14	102.45	2.65	104.92	2.65	-	-	103.21	2.55
16	128.77	2.68	130.93	2.68	124.55	2.67	126.80	2.59

1.375 fm, 1.25 fm and 1.0 fm respectively. For Interaction 31 only the spectra of ^{6}Li, ^{8}Be and ^{14}N were calculated. The binding energies and root-mean-square radii calculated for these interactions are listed in Table 7.3, the excited state spectra being shown in Figs. 7.8 - 7.16.

The very different forms of the four interactions considered makes attempts to find smooth variations in the parameters a difficult undertaking. However, some results do show systematic behaviour. The ν parameter increases with decreasing attractive range and following the argument used previously this means that the binding energy of ^{4}He will decrease.

With decreasing attractive range the repulsive range increases and thus it is not clear how the root-mean-square radii will change. In fact, for Interaction 30 they are greater than for Interaction 23 but for Interaction 33 they are smaller. The inter-shell binding energies are almost identical.

Inspecting Figs. 7.8 - 7.16 it is seen that the four interactions do not exactly predict the same excitation energy for the second 2^{+} state of ^{8}Be. In particular for Interactions 23 and 33 this excitation energy differs by 0.7 Mev. In comparing the other excited state spectra for these interactions excitation energies differences of 1 Mev have been ignored. Within these limitations, it is seen that the excitation energies of many of the levels are

identical for all the interactions. The main exceptions to this statement are listed in Table 7.4 where the difference in excitation energy calculated with Interaction 33 to that calculated with Interaction 23 is listed.

The most exceptions are for ^{9}B and ^{12}C although it should be pointed out that more levels are considered in ^{9}B than in other nuclei. The changes tabulated in Table 7.4 are an oversimplification of the situation. The limitation of ignoring changes less than 1 Mev is slightly misleading. The change in excitation energy of the second 2^{+} state of ^{8}Be (0.7 Mev) should cause consistently lesser changes in the excitation energies of most of the other states considered. Also some states will, for example, increase in excitation energy whereas with the difference in the excitation energy of the 2^{+} state of ^{8}Be they would be expected to decrease. In view of the existing complexity of the problem, this point is not emphasized in this discussion. However, in attempting to ascertain the "best" effective interaction it is taken into consideration.

The results for the excitation energies do indicate that the idea of fitting the 2_2^{+} state of ^{8}Be is good as a first test of any interaction. Having satisfied this criteria, however, it is important to examine the other spectra and then possibly relax the ^{8}Be fit. The very different results of Cohen and Kurath (Coh 65) and Amit and Katz (Ami 64) illustrate the dangers of too rigidly

TABLE 7.4

A	J_n^π	$E_x(33) - E_x(23)$ (Mev)
7	$\frac{7}{2}^-_1$	1.45
	$\frac{3}{2}^-_1$	-1.40
8	2^+_1	1.45
	4^+_1	3.75
9	$\frac{5}{2}^-_2$	1.75
	$\frac{7}{2}^-_1$	1.70
	$\frac{1}{2}^-_2$	-1.35
	$\frac{3}{2}^-_2$	1.10
	$\frac{9}{2}^-_1$	3.00
	$\frac{7}{2}^-_3$	2.55
10	4^+_1	2.20
11	$\frac{7}{2}^-_1$	1.30
12	2^+_1	1.05
	1^+_1	-1.60
	4^+_1	2.65
	1^+_2	-1.40
	2^+_3	-1.00

TABLE 7.4 - CONTINUED

13	$\frac{5}{2}^-_1$	1.60
14	0^+_1	-1.35

fitting given levels of the O-p shell nuclei.

Thus, to find the "best" effective interaction for O-p shell nuclei the following procedure was adopted.

(a) Interactions were fitted exactly to the binding energy of ^{16}O.

(b) For such interactions (with different attractive ranges $\lambda_a{}^i$) appropriate repulsive ranges $\lambda_r{}^i$ were found which predicted the correct excitation energy of the 2_2^+ level of ^8Be.

(c) For each interaction characterized by ($\lambda_a{}^i$; $\lambda_r{}^i$) the spectra of all the O-p shell nuclei was calculated.

(d) By comparing these results with those determined from experiment a $\lambda_a{}^b$ is chosen which displays the "best fit" to the spectra.

In general, this $\lambda_a{}^b$ might not be contained in the set of $\lambda_a{}^i$ and it would be necessary to determine a $\lambda_r{}^b$ as outlined above. This $\lambda_r{}^b$ should be readjusted to determine whether a relaxation of the ^8Be criteria produces a better fit to the spectra.

Before this procedure is followed other variations in the particular form of the density dependent interaction are examined. In particular the power of the density dependence and the role of the repulsive core height is examined.

FIGURE CAPTIONS

For all figures, excitation energy (in Mev) is plotted to the left of the figure. Full lines designate the calculated levels and dashed lines designate certain experimental levels. For even nuclei the spin J of the level is indicated to the right of the calculated levels and at the left of the figure for the experimental levels, for odd nuclei the value of 2J is likewise indicated.

Figure 7.1 (a) Excited State Spectra of ^{6}Li calculated for Interaction 23 with C = -2.0 Mev
(b) Excited State Spectra of ^{6}Li calculated for Interaction 10 with C = -2.0 Mev
(c) Excited State Spectra of ^{7}Be calculated for Interaction 23 with C = -1.5 Mev
(d) Excited State Spectra of ^{7}Be calculated for Interaction 10 with C = -1.5 Mev.

Figure 7.2 (a) Excited State Spectra of ^{8}Be calculated for Interaction 23 with C = -2.0 Mev
(b) Excited State Spectra of ^{8}Be calculated for Interaction 10 with C = -2.0 Mev
(c) Excited State Spectra of ^{9}B calculated for Interaction 23 with C = -3.0 Mev
(d) Excited State Spectra of ^{9}B calculated for Interaction 10 with C = -3.0 Mev.

Figure 7.3 (a) Excited State Spectra of ^{10}B calculated for Interaction 23 with C = -5.0 Mev
(b) Excited State Spectra of ^{10}B calculated for Interaction 10 with C = -5.0 Mev
(c) Excited State Spectra of ^{11}B calculated for Interaction 23 with C = -4.5 Mev
(d) Excited State Spectra of ^{11}B calculated for Interaction 10 with C = -4.5 Mev.

Figure 7.4 (a) Excited State Spectra of ^{12}C calculated for Interaction 23 with C = -5.5 Mev
(b) Excited State Spectra of ^{12}C calculated for Interaction 10 with C = -5.5 Mev.

Figure 7.5 (a) Excited State Spectra of ^{13}C calculated for Interaction 23 with C = -5.0 Mev
(b) Excited State Spectra of ^{13}C calculated for Interaction 10 with C = -5.0 Mev
(c) Excited State Spectra of ^{14}N calculated for Interaction 23 with C = -5.0 Mev
(d) Excited State Spectra of ^{14}N calculated for Interaction 10 with C = -5.0 Mev.

Figures 7.6 - 7.7 plot the excited state spectra of ^{8}Be and ^{14}N calculated for

(a) Interaction 32
(b) Interaction 33
(c) Interaction 34

Figure 7.6 Excited State Spectra of ^{8}Be with C = -1.5 Mev.

Figure 7.7 Excited State Spectra of ^{14}N with C = -5.0 Mev.

Figures 7.8 - 7.16 plot the excited state spectra of the O-p shell nuclei calculated for

(a) Interaction 23

(b) Interaction 30

(c) Interaction 33 for Figures 7.8, 7.9, 7.11, 7.12, 7.13, 7.14 and 7.15 but Interaction 31 for Figures 7.10 and 7.16

(d) Interaction 33

Figure 7.8 Excited State Spectra of ^{6}Li with C = -2.0 Mev.

Figure 7.9 Excited State Spectra of ^{7}Be with C = -1.5 Mev.

Figure 7.10 Excited State Spectra of ^{8}Be with C = -2.0 Mev.

Figure 7.11 Excited State Spectra of ^{9}B with C = -3.0 Mev.

Figure 7.12 Excited State Spectra of ^{10}B with C = -5.0 Mev.

Figure 7.13 Excited State Spectra of ^{11}B with C = -4.5 Mev.

Figure 7.14 Excited State Spectra of ^{12}C with C = -5.5 Mev.

Figure 7.15 Excited State Spectra of ^{13}C with C = -5.0 Mev.

Figure 7.16 Excited State Spectra of ^{14}N with C = -5.0 Mev.

Figure 7.1

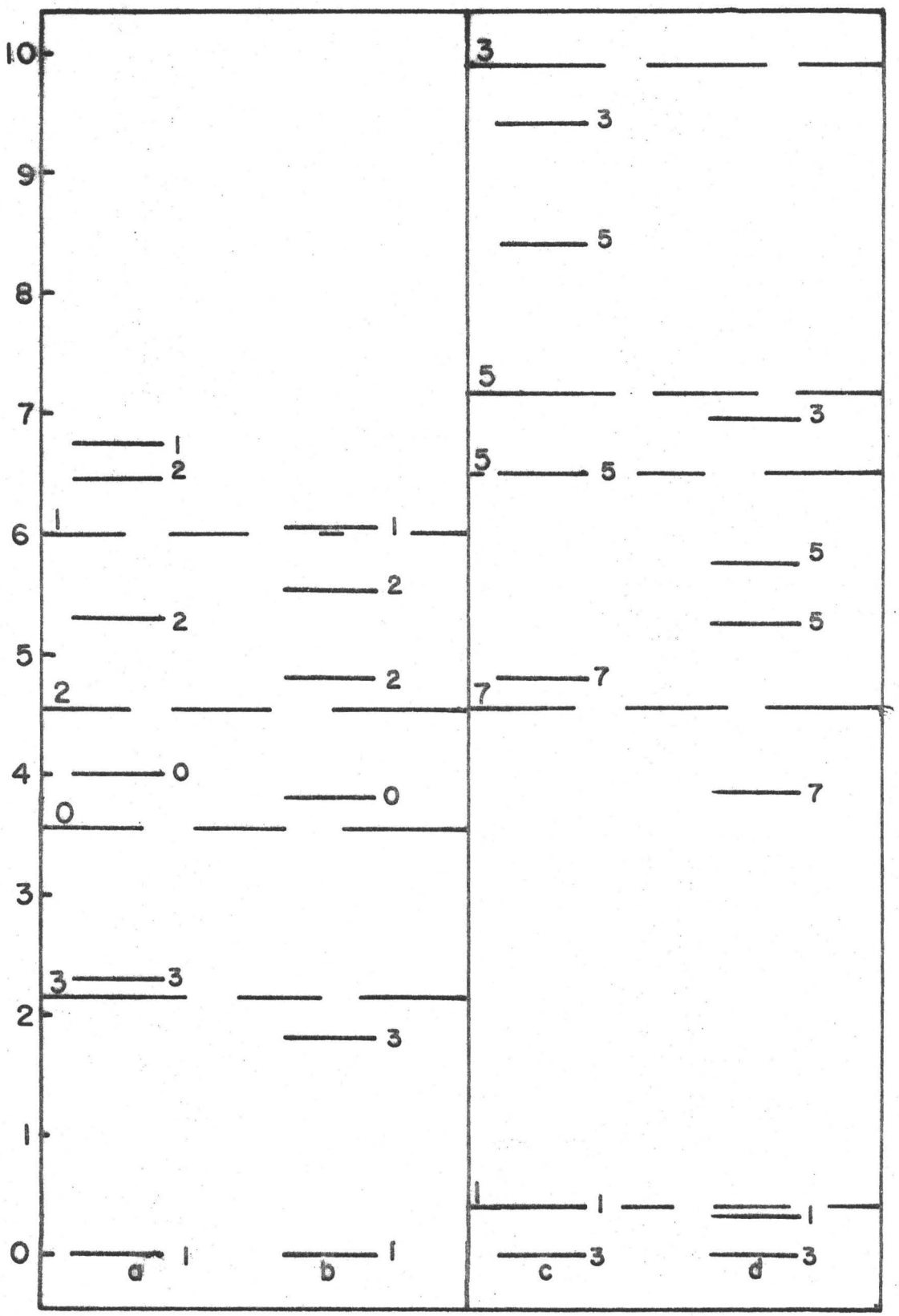

Figure 7.2

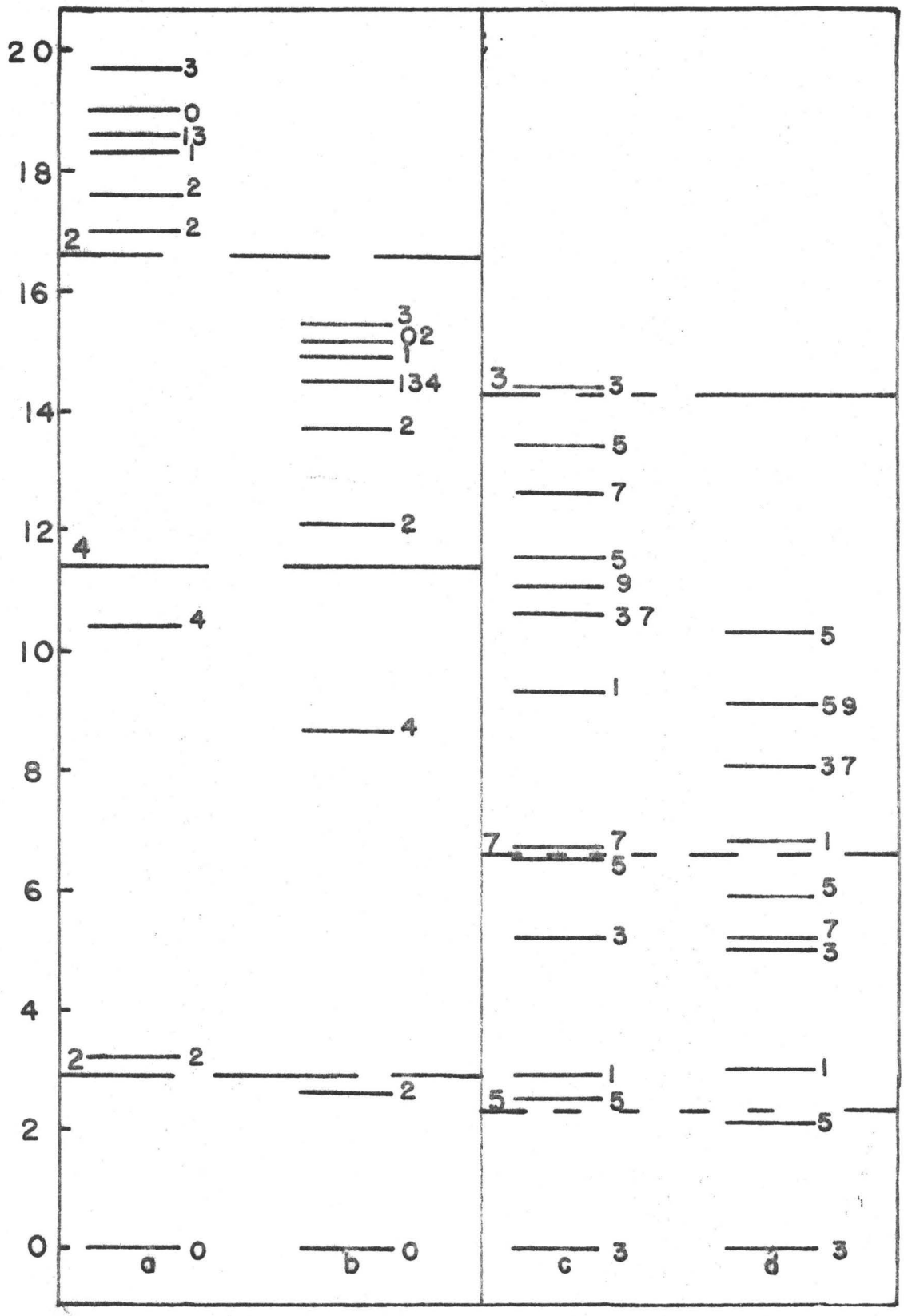

Figure 7.3

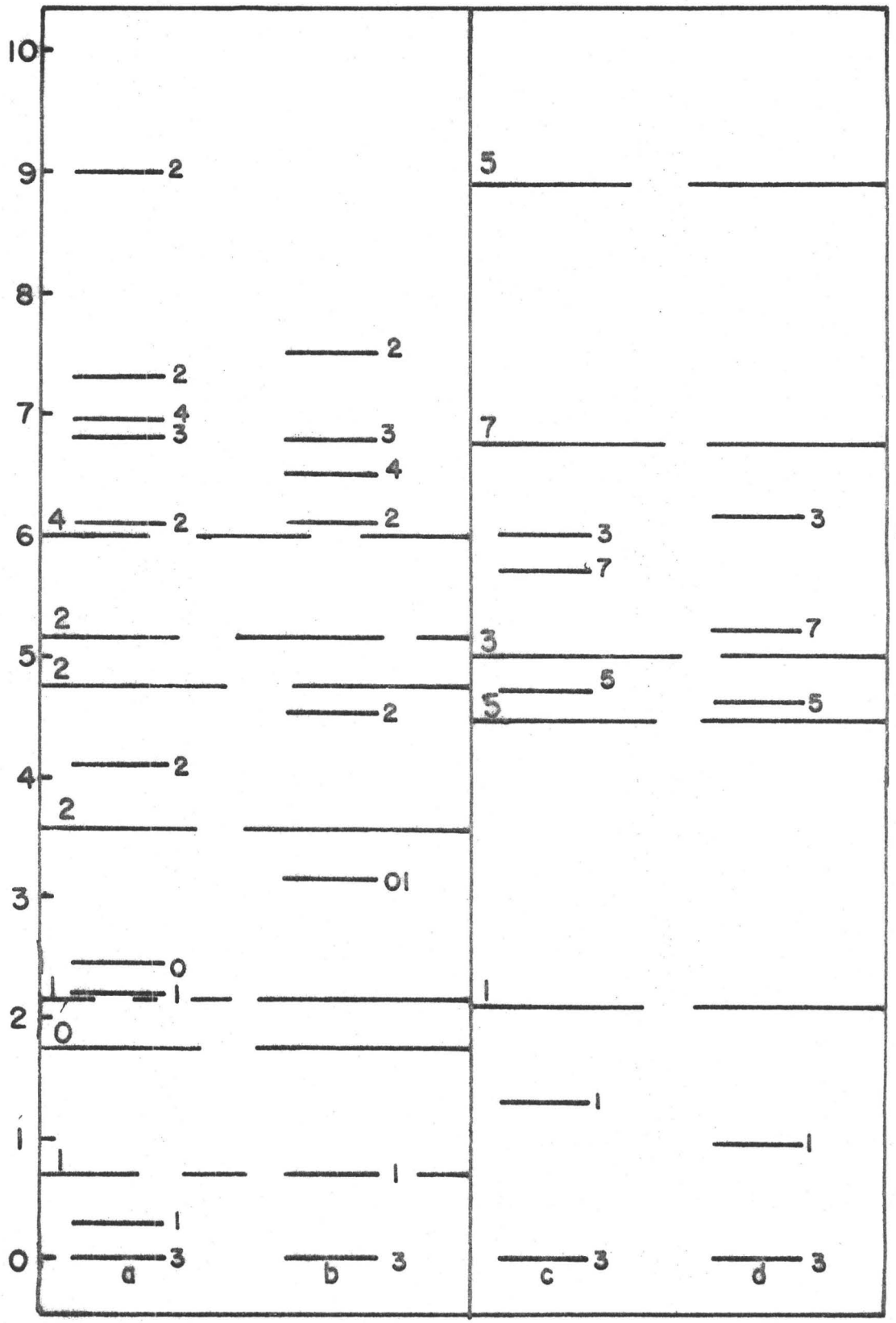

Figure 7.4

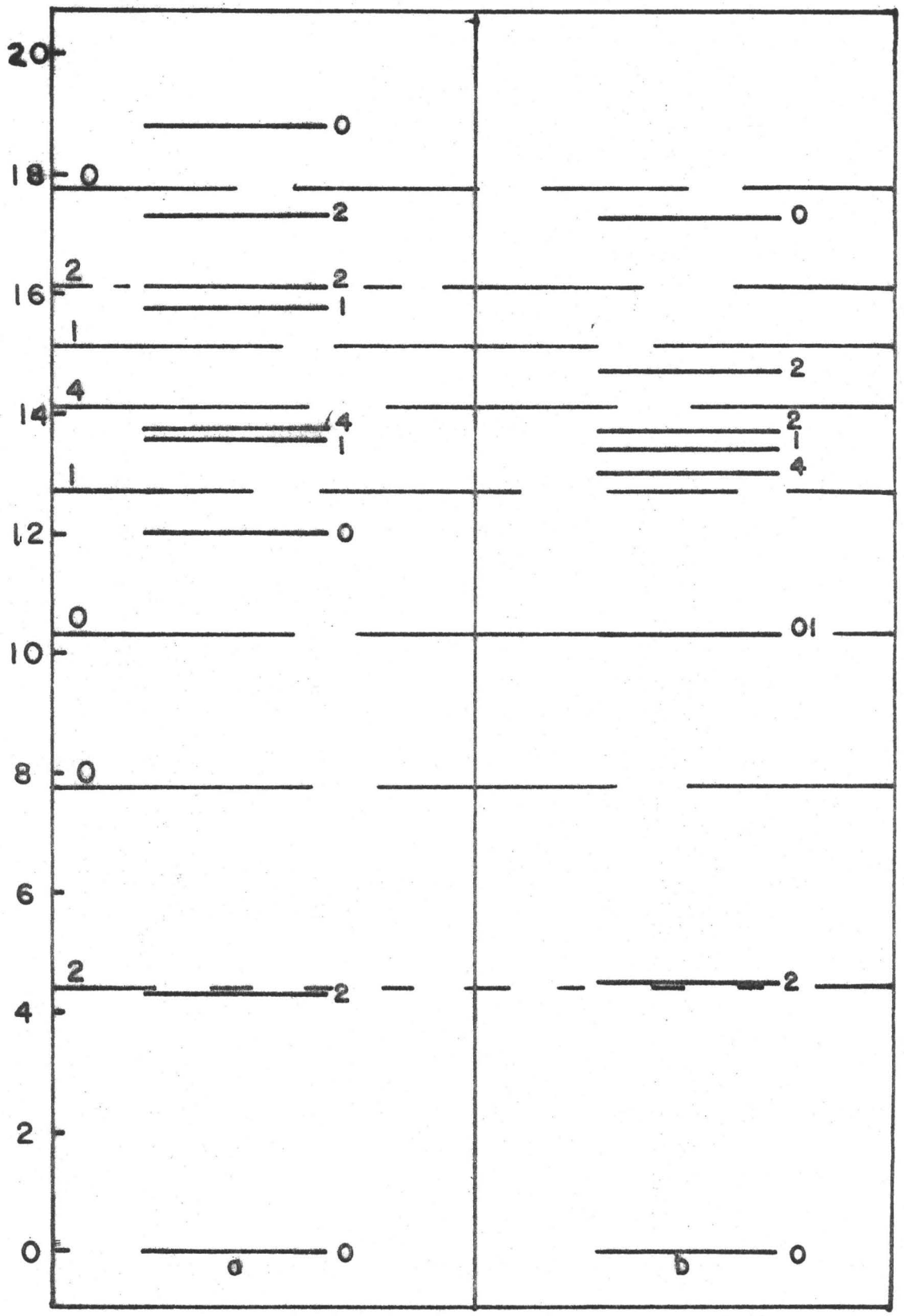

Figure 7.5

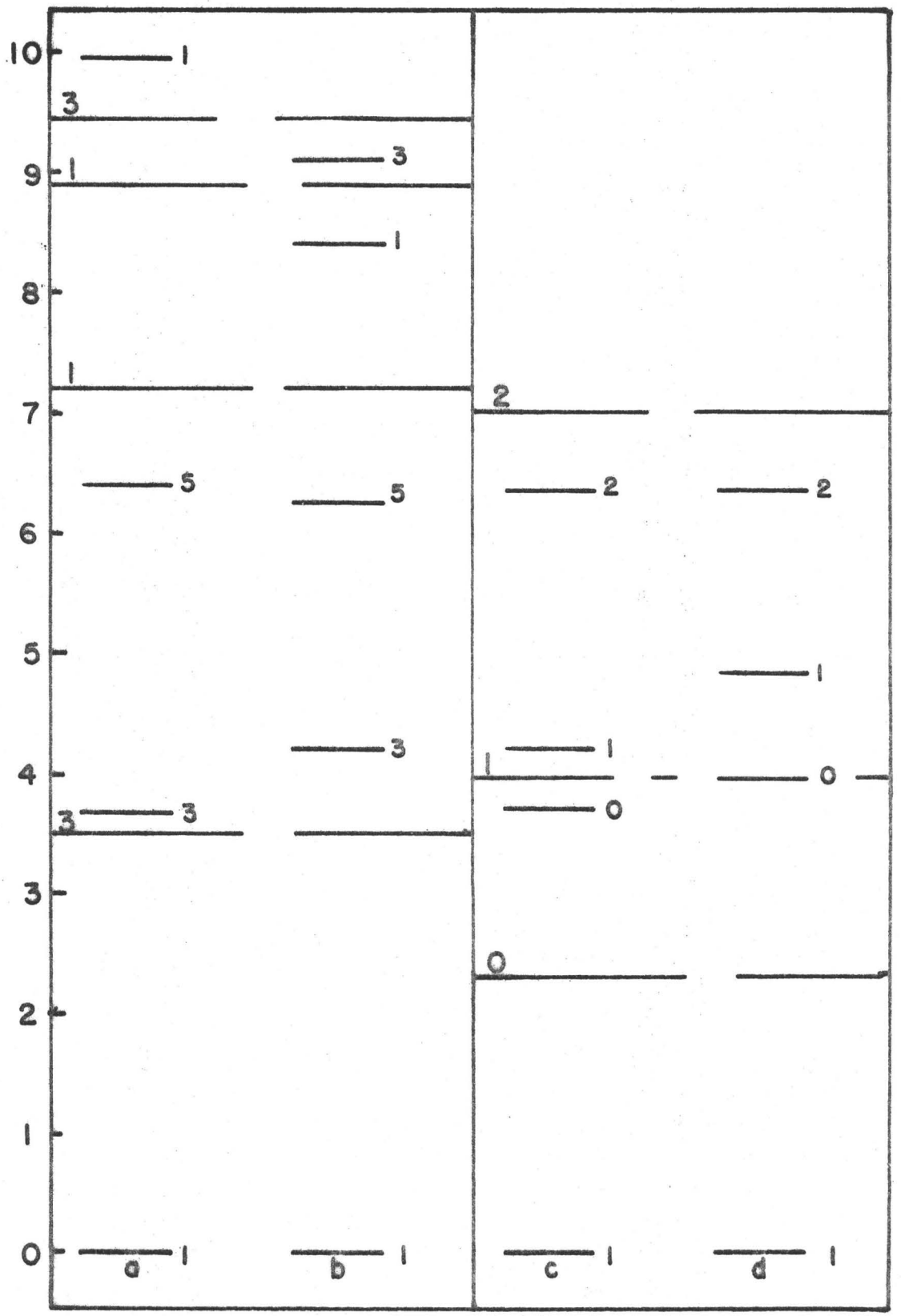

Figure 7.6

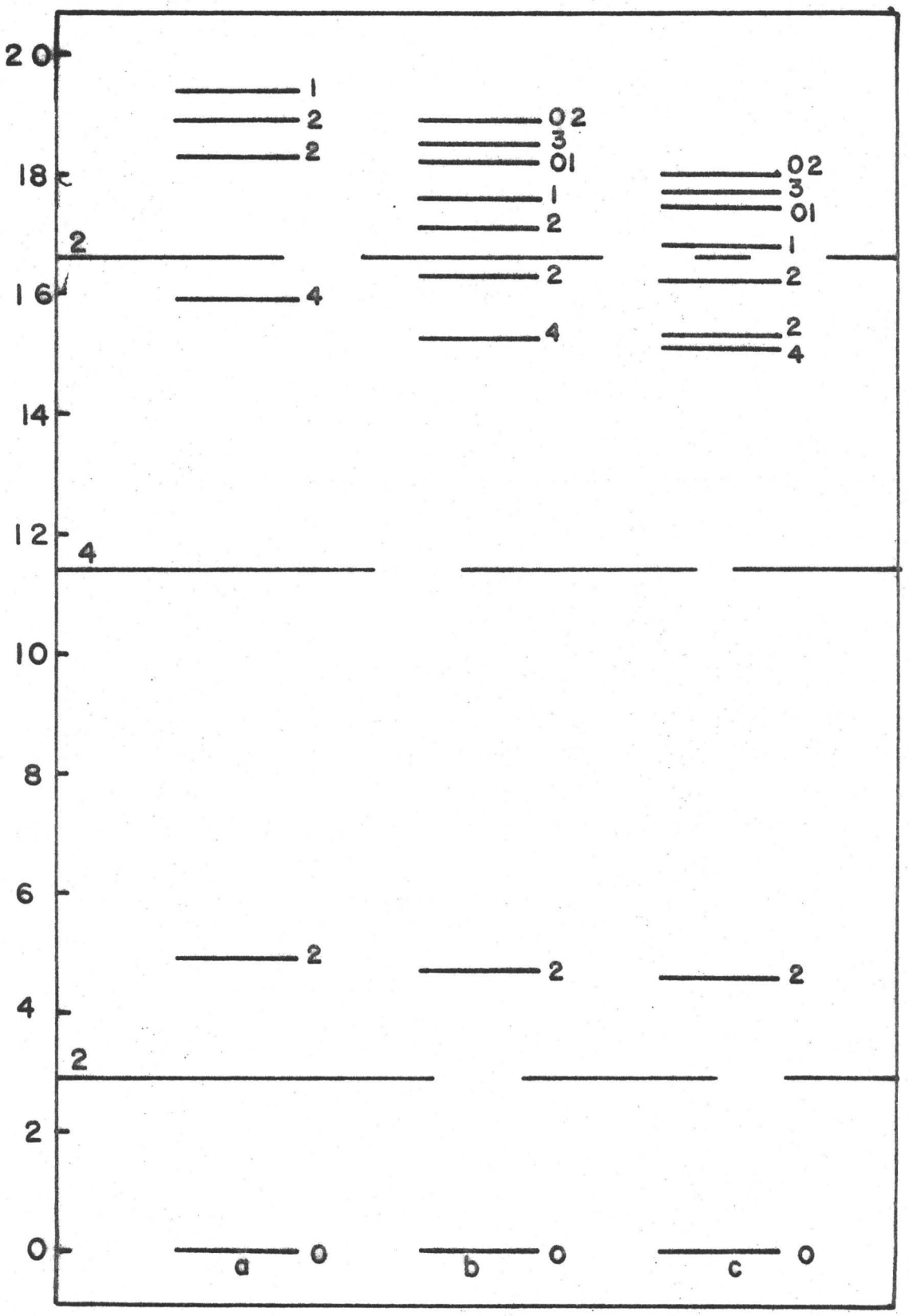
20
18
16
14
12
10
8
6
4
2
0
1
2
2
4
2
02
3
01
1
2
2
4
02
3
01
1
2
2
4
2
2
2
2
0
0
0
a
b
c

Figure 7.7

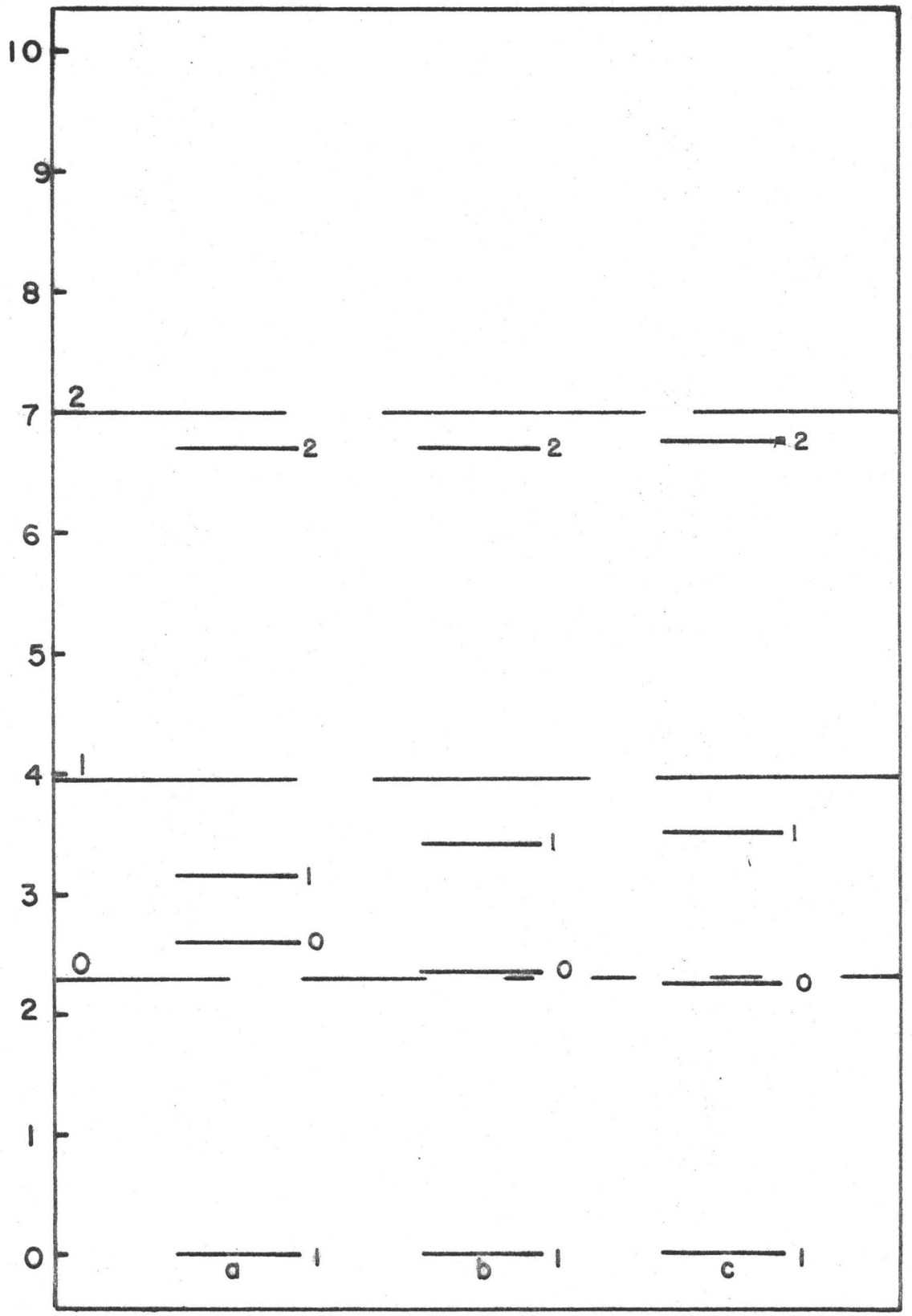

Figure 7.8

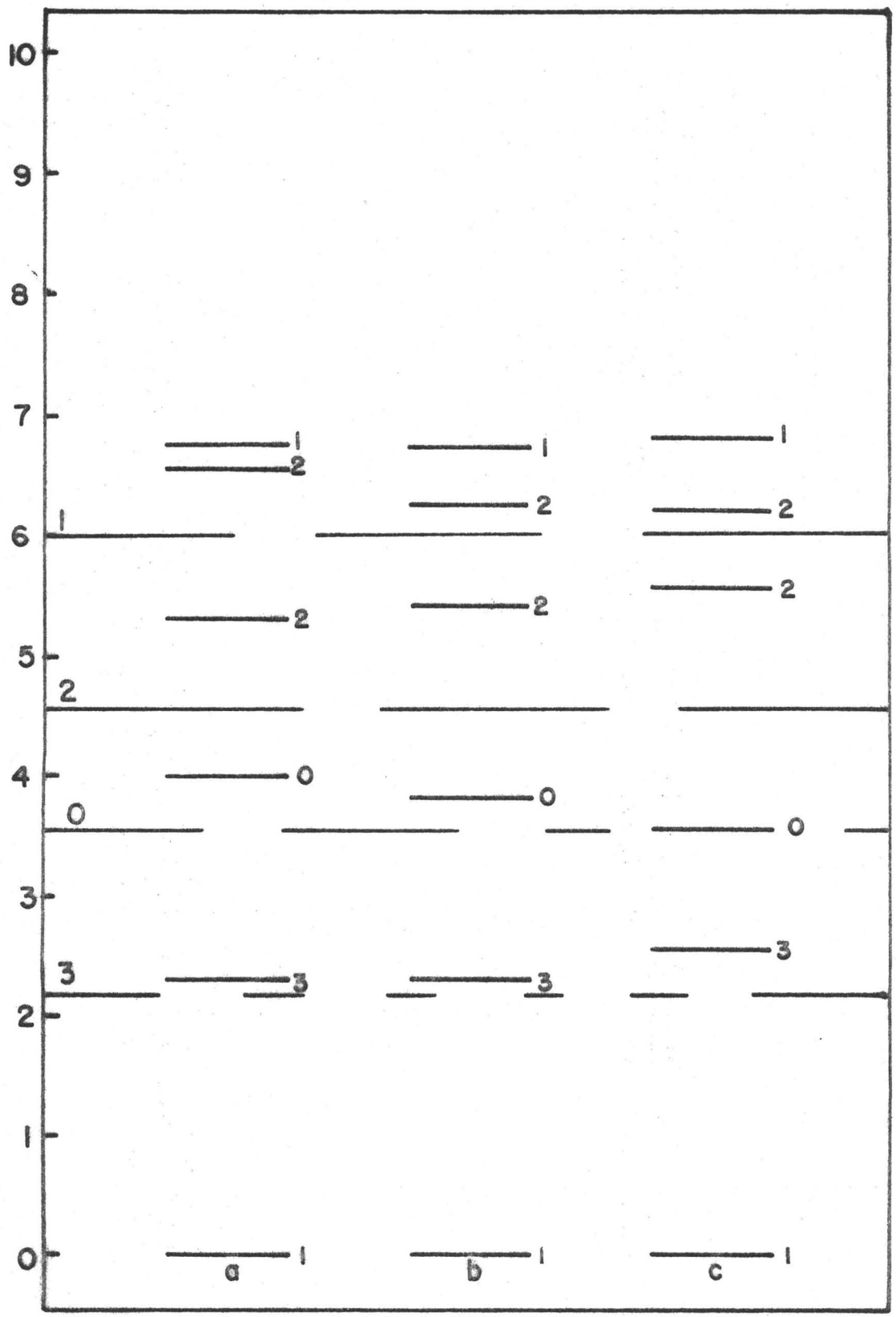

Figure 7.9

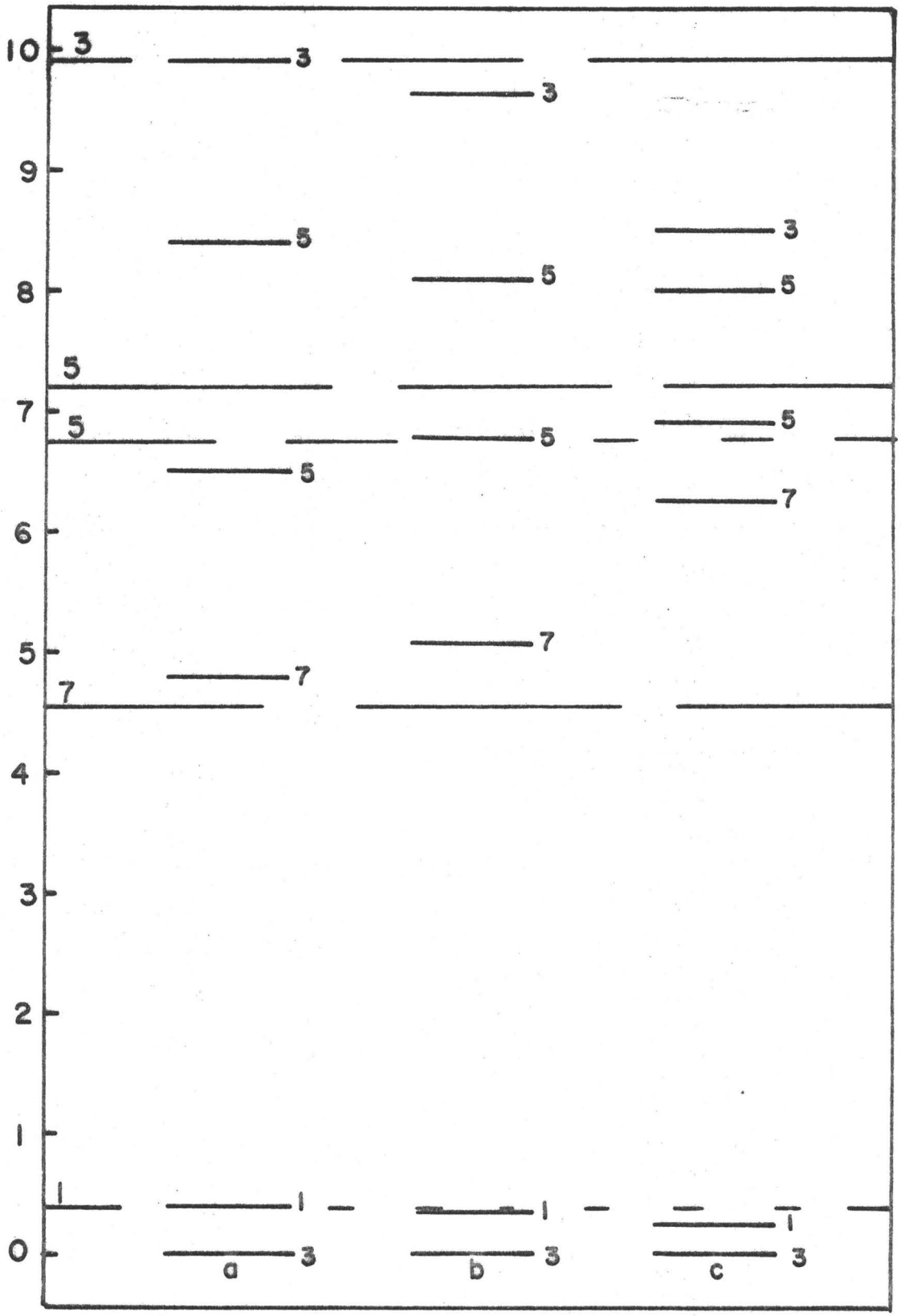

Figure 7.10

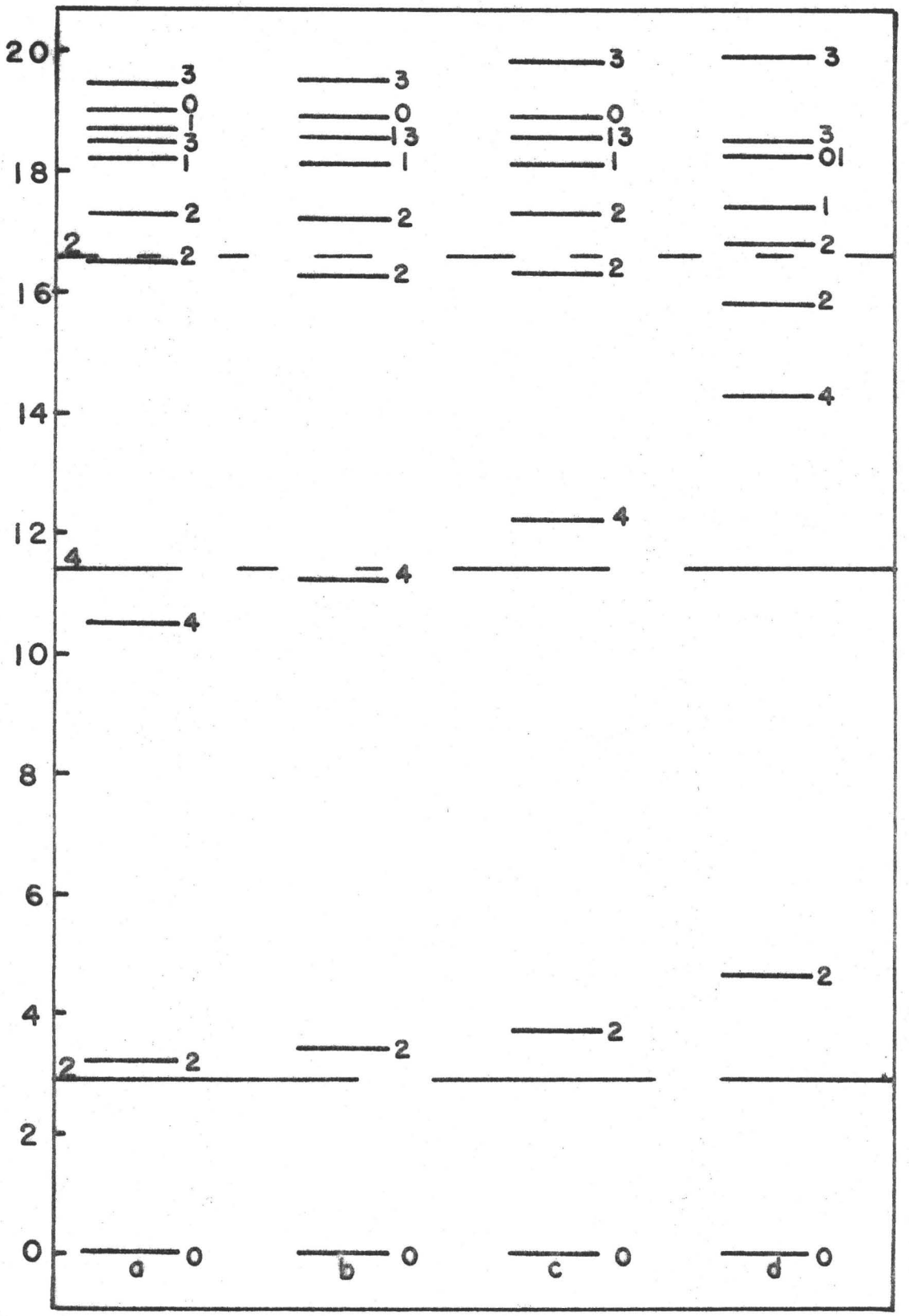

Figure 7.11

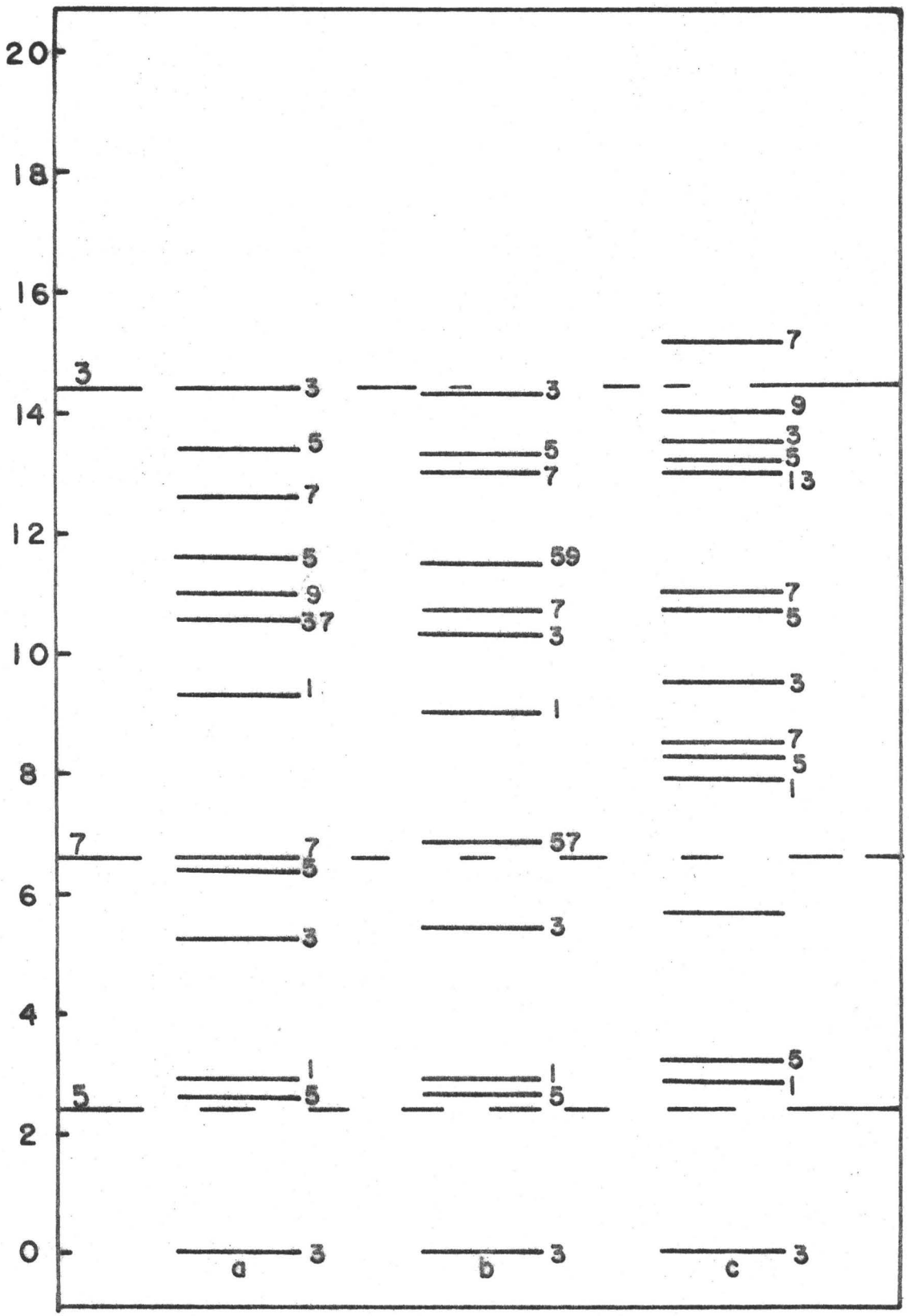

Figure 7.12

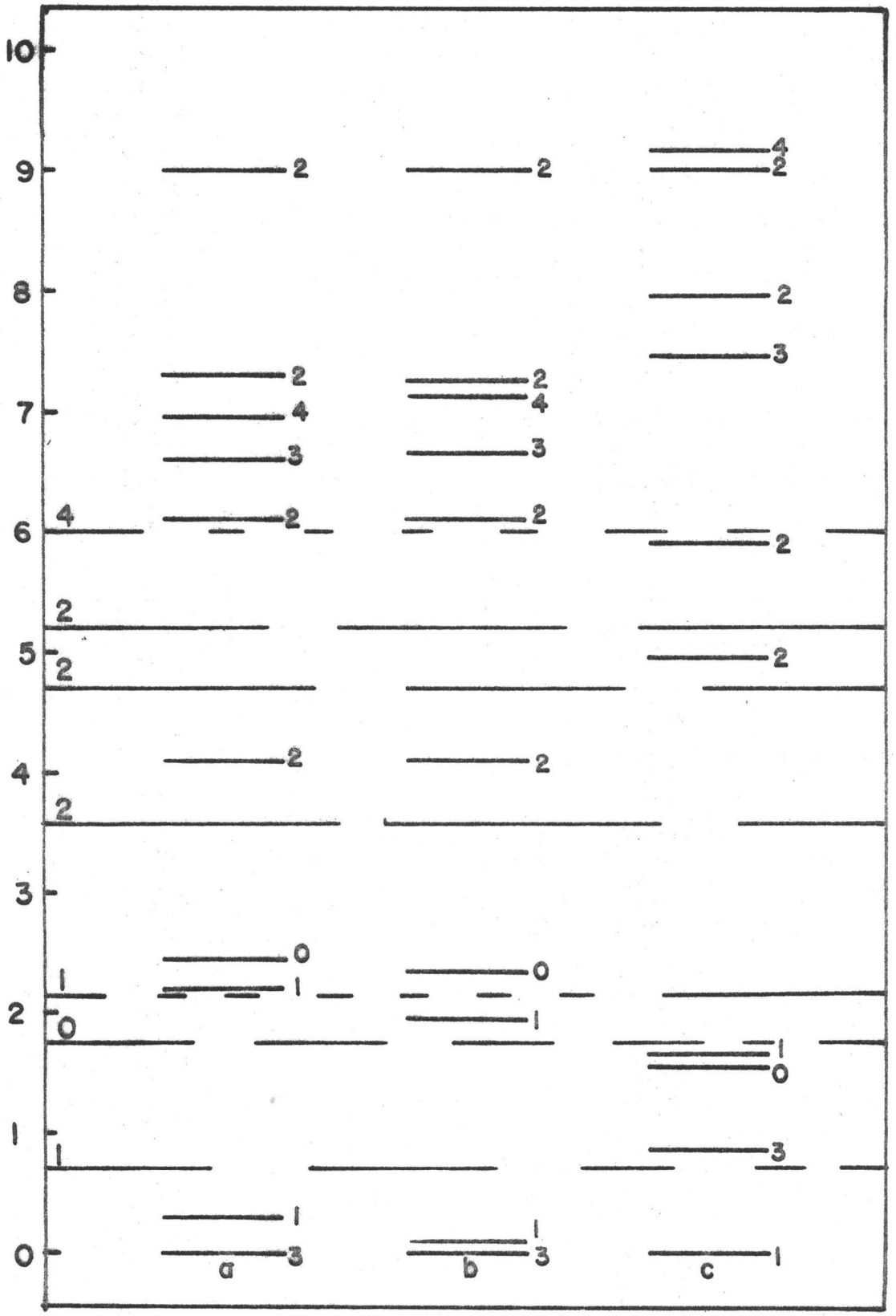

Figure 7.13

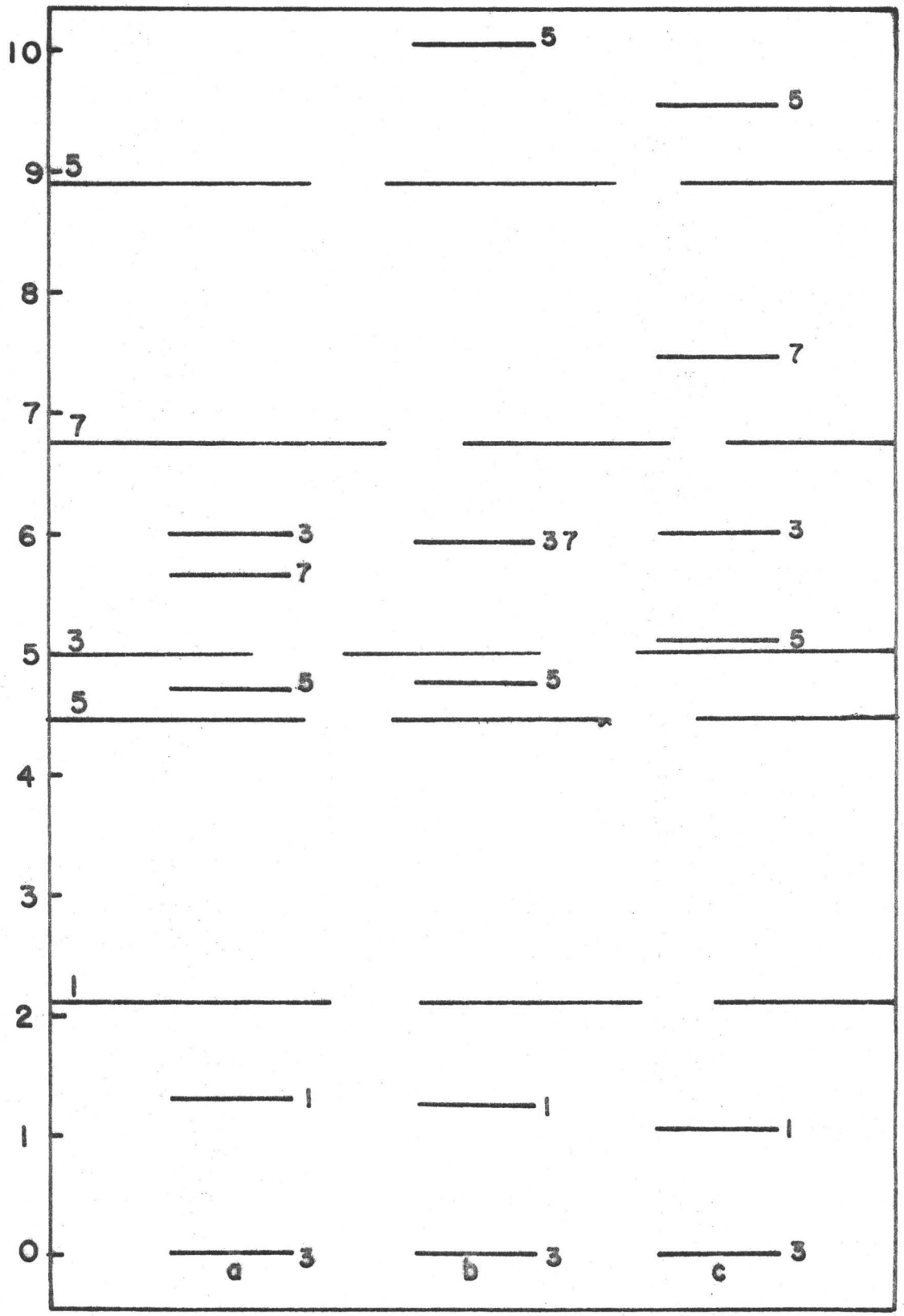

Figure 7.14

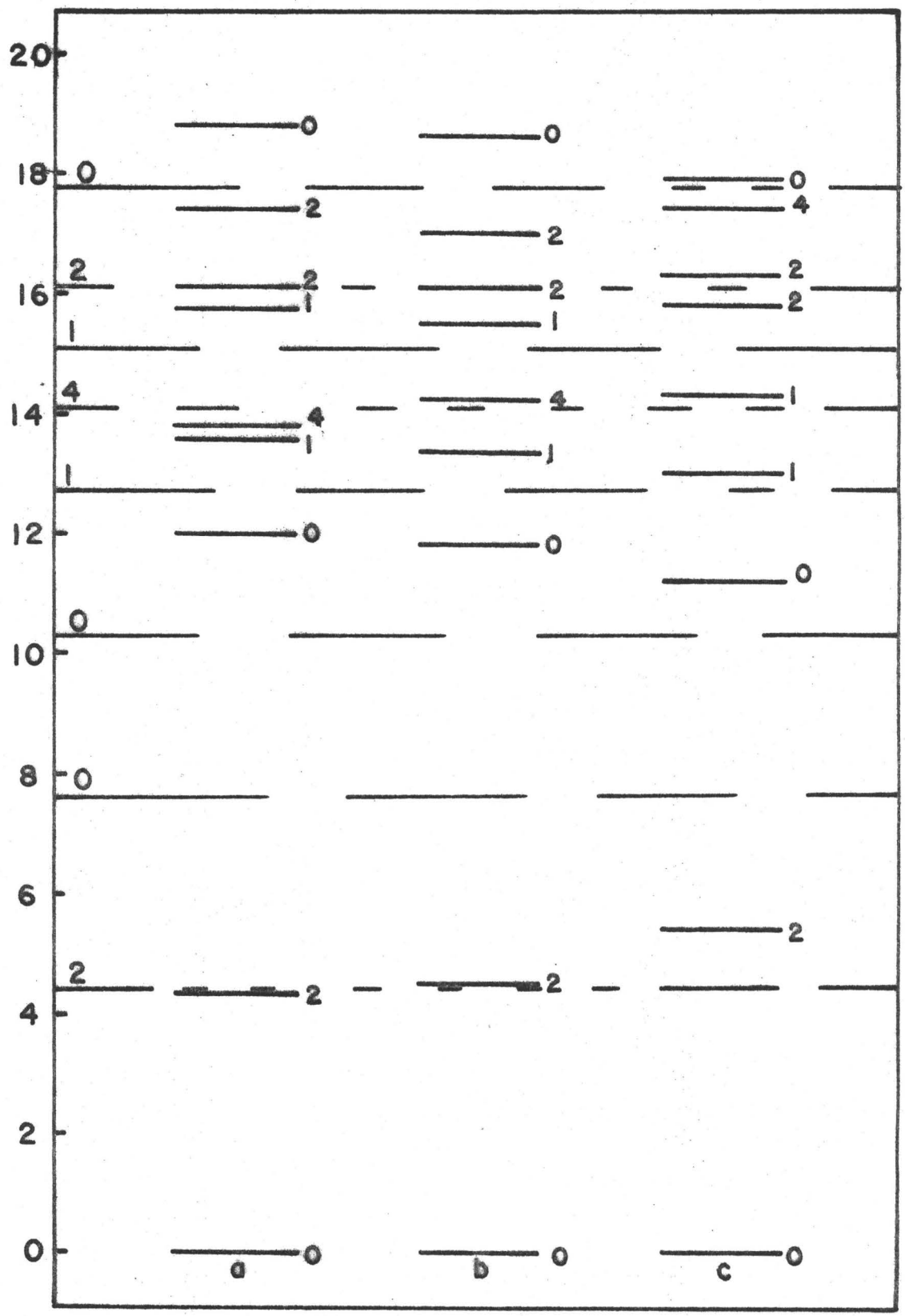

Figure 7.15

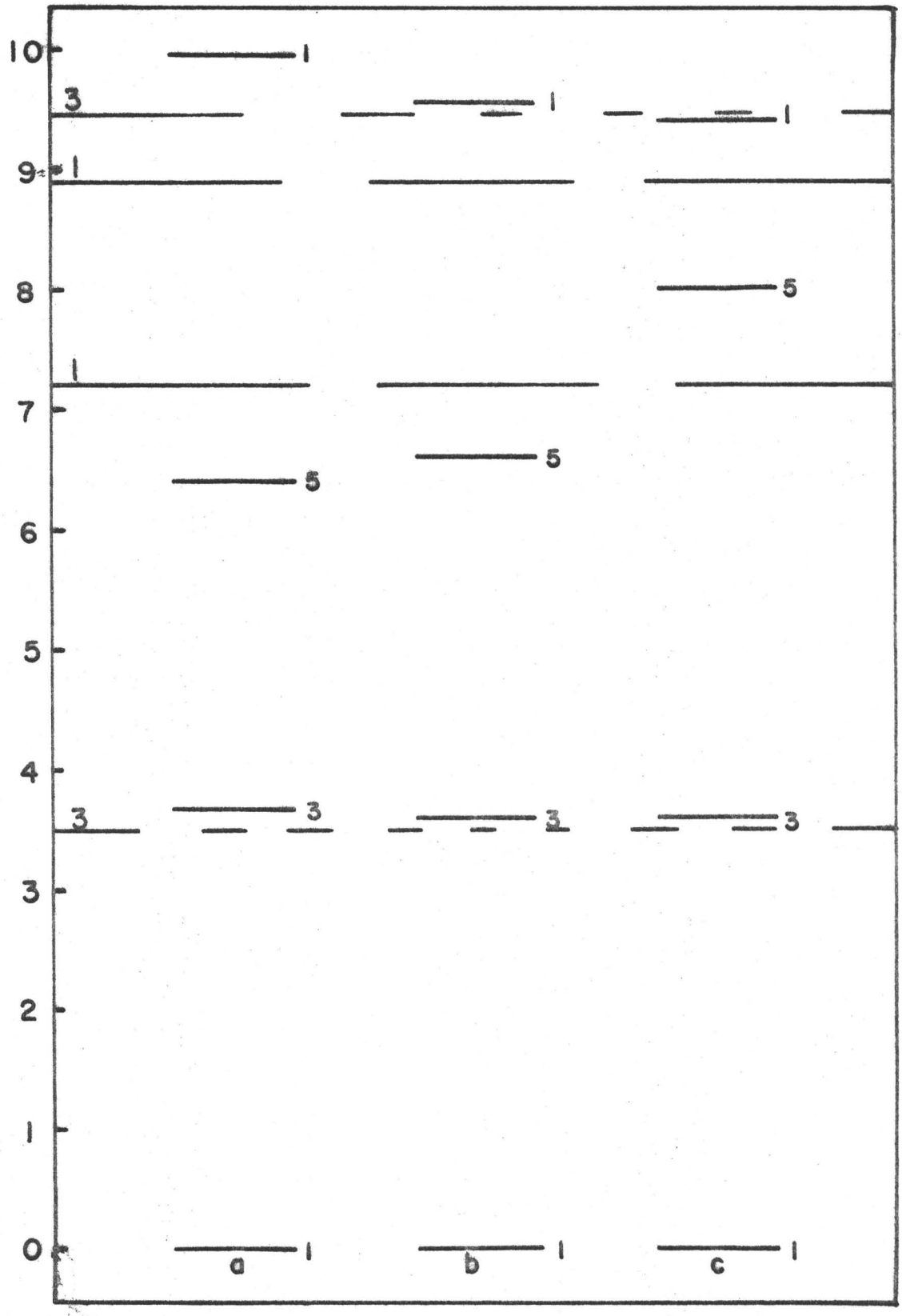

Figure 7.16

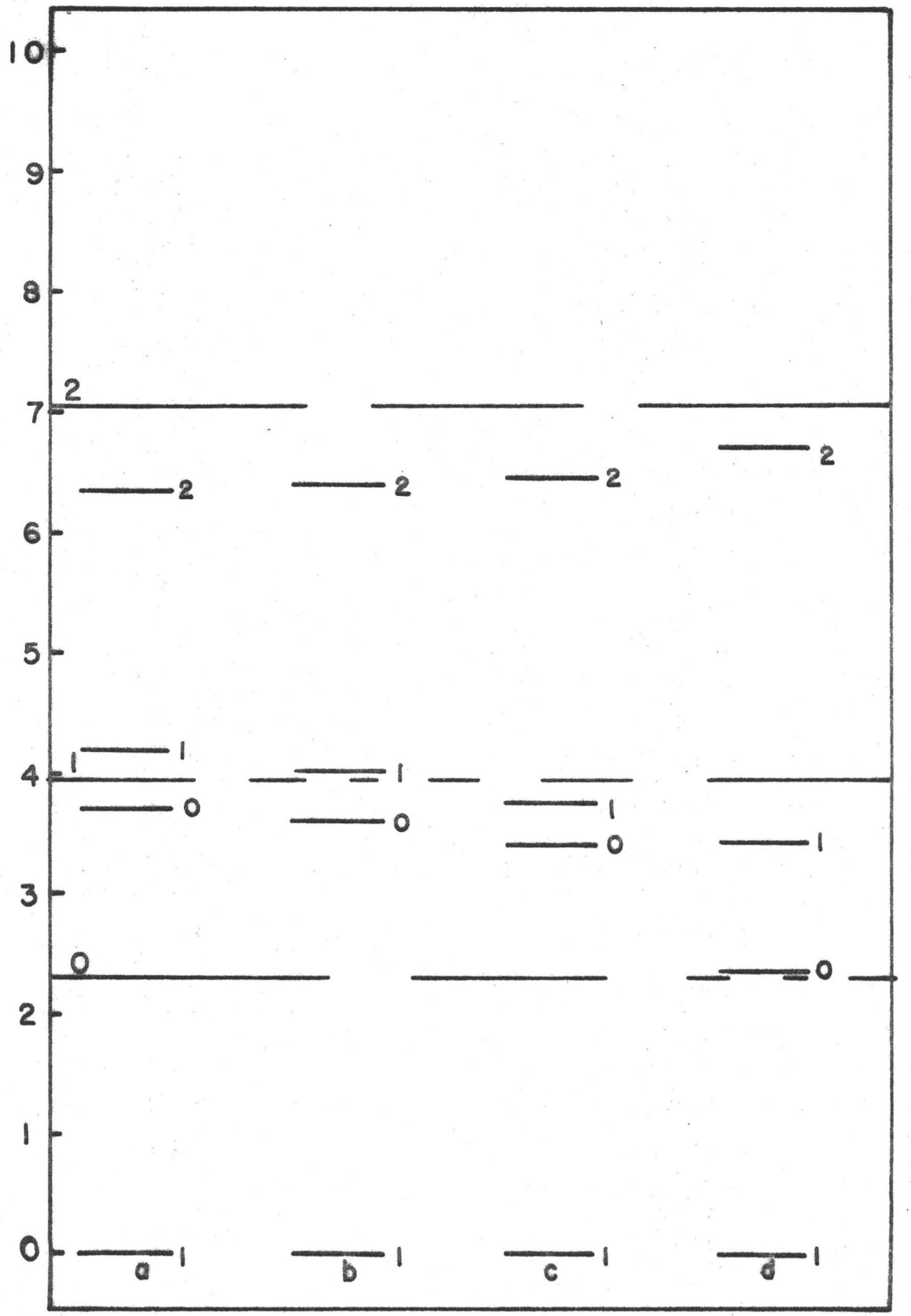

CHAPTER 8

DIFFERENT DENSITY DEPENDENCIES

In previous chapters a number of density dependent interactions have been considered all of which have had the same specific density dependence (a $\rho^{1/3}$ term and a $\rho^{2/3}$ term). In this chapter other density dependencies are considered.

Thus, results are quoted in Table 8.1 for the binding energies and root-mean-square radii of the O-p shell nuclei calculated using Interactions 9, 10 and 11. These interactions differ primarily only in the power of the repulsive density dependence ($\rho^{1/2}$, $\rho^{2/3}$ and ρ^{2} respectively).

The increased power of the density dependence for Interaction 11 compared with Interaction 9 means that to fit the nuclear matter binding energy c_4 has to decrease. In fact, the added condition that nuclear matter saturates causes c_4 to decrease so dramatically (from $c_4 k_F^{3/2} = 0.46$ for Interaction 9 to $c_4 k_F^{3} = 0.05$ for Interaction 11) that the attractive density dependence (c_3) also decreases and the exchange matrix elements are weighted more strongly (ν decreases). Even then the interaction (Interaction 11) with the highest power of the repulsive density dependence is the more attractive interaction (B.E.$_{den}$ (Chapter 3)

is 12.12 Mev for Interaction 11 and is 19.87 Mev for Interaction 9). Although the inter-shell binding energies situation is confused by the differing fits to the ^{16}O binding energy, they do increase for the more attractive interaction. The r.m.s. radii decrease for the more attractive interaction. As might be expected the compressibility of nuclear matter increases with increasing repulsive density dependence.

The excited state spectra of the O-p shell nuclei calculated using Interactions 9 and 10 are illustrated in Figs. 8.1 - 8.9 and for Interaction 11 in Figs. 8.10 - 8.18. Taking into consideration the different ^{16}O binding energies for the three interactions, the excitation energies calculated for the O-p shell nuclei are remarkably similar. Even higher powers of the repulsive density dependence (Interaction 22) have been used without changing the excitation energies significantly. It would thus appear that different density dependencies do not give very different results for the excited state spectra.

However, if Interaction 6 (repulsive density dependence $\rho^{1/3}$) is compared with Interaction 7 (repulsive density dependence $\rho^{2/3}$), the results obtained for the excited state spectra are very different (Figs. 8.1 - 8.9). The binding energies of the nuclei are larger and the r.m.s. radii are smaller for the more attractive interaction (Interaction 7). The excited state spectra calculated for the two interactions are very different, the excitation

energies being generally greater for Interaction 7. The reason for the large differences in excitation energies for Interactions 6 and 7, where no such differences exist for Interactions 9, 10 and 11 would seem to lie in the nature of the repulsive range. The nuclear matter criteria is such that the contributions from the repulsive and attractive density dependent parts of the interaction cancel each other to some extent. In a finite nucleus this cancellation still takes place in the nuclear core but for interactions whose attractive range is much longer than the repulsive range there is no such cancellation in the nuclear surface. Thus for such interactions (Interactions 6 and 7) the precise form of the density dependence becomes important. For interactions whose attractive and repulsive ranges are nearly identical the exact form of the density dependence is not so important because the nuclear matter criteria guarantee the same order of cancellation everywhere within the nucleus whatever the form of the density dependence.

Similar results hold true if interactions which differ in the form of the attractive density dependence are considered. Thus for Interactions 10 and 17, where the attractive and repulsive ranges are nearly equal, the excited state spectra (Figs. 8.1 - 8.18) calculated for the O-p shell nuclei are almost identical whilst for Interactions 24 and 26 (these results are not illustrated) where the attractive range is λ_a = 1.5 fm and the repulsive range is

$\lambda_r^0 = 0.602$ fm, (attractive density dependence is $\rho^{1/3}$ for Interaction 24, and $\rho^{2/3}$ for Interaction 26), the excitation energies are very different.

The nature of the changes in the excitation energies for different density dependencies is the same as that for interactions which differ merely with respect to the repulsive range (or the attractive range). Thus, if the procedure for "fitting" the attractive and repulsive ranges enunciated in Chapter 7 is followed, no unique density dependence can be established.

Kuo and Brown (Kuo 65) suggest that density dependence should to incorporated into the effective interaction to replace the 2nd order Born Term for the tensor interaction. They find that this term can be replaced by a central force of the form

$$\frac{V_{T_\ell}^2}{e_{eff}}$$

where $V_{T_\ell}^2$ is the long range part of the tensor interaction and e_{eff} depends on the local density. This suggests the possibility (for a gaussian interaction) that the density dependent part of the interaction should have half the range of the non-density dependent part of the interaction.

Thus Interactions 8 and 13 are considered and results calculated using these interactions are compared with the results calculated for Interactions 7 and 10. Because of the differing ^{16}O binding energies the comparison of the

excitation energies calculated for the interactions (Figs. 8.1 - 8.18) is very confusing. Careful consideration of the excited spectra does, however, reveal that the excitation energies for Interaction 7 are generally higher than for Interaction 8 whose density dependent part of the interaction has one half the range of the non-density dependent part. This result is to be expected since the region where the attractive density dependence dominates the repulsive density dependence is smaller for Interaction 8 than it is for Interaction 7. Since the attractive and repulsive ranges for Interactions 10 and 13 are almost equal no great differences are found between excitation energies calculated using them. The reduction in range for the density dependent part of the interaction results in reduced r.m.s. radii for the O-p shell nuclei.

TABLE 8.1

Interaction 6			Interaction 7		
A	B.E.(Mev)	r.m.s.(fm)	A	B.E.(Mev)	r.m.s.(fm)
4	30.34	2.00	4	35.47	1.83
6	28.80	2.54	5	34.68	2.40
7	32.28	2.62	6	38.70	2.39
8	45.09	2.67	7	53.74	2.42
9	46.93	2.74	8	52.98	2.51
10	60.35	2.76	9	64.66	2.55
11	69.43	2.80	10	74.55	2.59
12	86.18	2.83	11	92.09	2.61
13	91.67	2.84	12	95.63	2.65
14	101.75	2.85	13	106.50	2.65
16	128.90	2.87	14	131.21	2.69

TABLE 8.1 - CONTINUED

	Interaction 8			Interaction 9	
A	B.E.(Mev)	r.m.s.(fm)	A	B.E.(Mev)	r.m.s.(fm)
4	32.91	1.83	4	27.87	2.07
6	32.32	2.40	6	32.50	2.70
7	35.28	2.39	7	35.76	2.65
8	50.39	2.40	8	50.69	2.66
9	49.68	2.50	9	52.14	2.75
10	60.98	2.53	10	65.83	2.77
11	68.13	2.58	11	74.99	2.81
12	87.24	2.59	12	91.94	2.83
13	90.52	2.63	13	96.60	2.85
14	98.55	2.65	14	105.96	2.86
16	125.23	2.67	16	129.66	2.89

TABLE 8.1 - CONTINUED

A	Interaction 10 B.E.(Mev)	r.m.s.(fm)	A	Interaction 11 B.E.(Mev)	r.m.s.(fm)
4	27.28	2.04	4	32.79	1.90
6	30.13	2.48	6	35.07	2.56
7	34.14	2.66	7	37.87	2.50
8	48.78	2.63	8	53.59	2.49
9	49.25	2.72	9	53.75	2.58
10	63.24	2.75	10	67.03	2.62
11	72.13	2.79	11	76.29	2.66
12	88.75	2.81	12	93.89	2.68
13	92.98	2.83	13	98.04	2.71
14	101.59	2.84	14	107.89	2.73
16	124.73	2.87	16	133.45	2.76

TABLE 8.1 - CONTINUED

	Interaction 13			Interaction 17	
A	B.E.(mev)	r.m.s.(fm)	A	B.E.(Mev)	r.m.s.(fm)
4	30.48	1.99	4	28.25	2.05
6	34.29	2.61	6	37.53	3.48
7	37.49	2.59	7	36.54	2.65
8	52.99	2.59	8	51.80	2.64
9	53.90	2.68	9	52.85	2.74
10	67.48	2.70	10	66.14	2.76
11	76.78	2.75	11	75.28	2.80
12	94.13	2.77	12	92.15	2.82
13	98.66	2.79	13	96.37	2.85
14	108.40	2.80	14	105.35	2.86
16	133.28	2.83	16	128.45	2.88

FIGURE CAPTIONS

For all figures, excitation energy (in Mev) is plotted to the left of the figure. Full lines designate the calculated levels and dashed lines designate certain experimental levels. For even nuclei the spin J of the level is indicated to the right of the calculated levels and at the left of the figure for the experimental levels, for odd nuclei the value of 2J is likewise indicated.

Figures 8.1 - 8.9 plot the excited state spectra of the O-p shell nuclei calculated for

(a) Interaction 6

(b) Interaction 7

(c) Interaction 9

(d) Interaction 10

Figure 8.1 Excited State Spectra of ^{6}Li with C = -2.0 Mev.

Figure 8.2 Excited State Spectra of ^{7}Be with C = -1.5 Mev.

Figure 8.3 Excited State Spectra of ^{8}Be with C = -2.0 Mev.

Figure 8.4 Excited State Spectra of ^{9}B with C = -3.0 Mev.

Figure 8.5 Excited State Spectra of ^{10}B with C = -5.0 Mev.

Figure 8.6 Excited State Spectra of ^{11}B with C = -4.5 Mev.

Figure 8.7 Excited State Spectra of ^{12}C with C = -5.5 Mev.

Figure 8.8 Excited State Spectra of ^{13}C with C = -5.0 Mev.

Figure 8.9 Excited State Spectra of ^{14}N with C = -5.0 Mev.

Figures 8.10 - 8.18 plot the excited state spectra of the O-p shell nuclei calculated for

(a) Interaction 11

(b) Interaction 17

(c) Interaction 8

(d) Interaction 13

Figure 8.10 Excited State Spectra of ^{6}Li with C = -2.0 Mev.

Figure 8.11 Excited State Spectra of ^{7}Be with C = -1.5 Mev.

Figure 8.12 Excited State Spectra of ^{8}Be with C = -2.0 Mev.

Figure 8.13 Excited State Spectra of ^{9}B with C = -3.0 Mev.

Figure 8.14 Excited State Spectra of ^{10}B with C = -5.0 Mev.

Figure 8.15 Excited State Spectra of ^{11}B with C = -4.5 Mev.

Figure 8.16 Excited State Spectra of ^{12}C with C = -5.5 Mev.

Figure 8.17 Excited State Spectra of ^{13}C with C = -5.0 Mev.

Figure 8.18 Excited State Spectra of ^{14}N with C = -5.0 Mev.

Figure 8.1

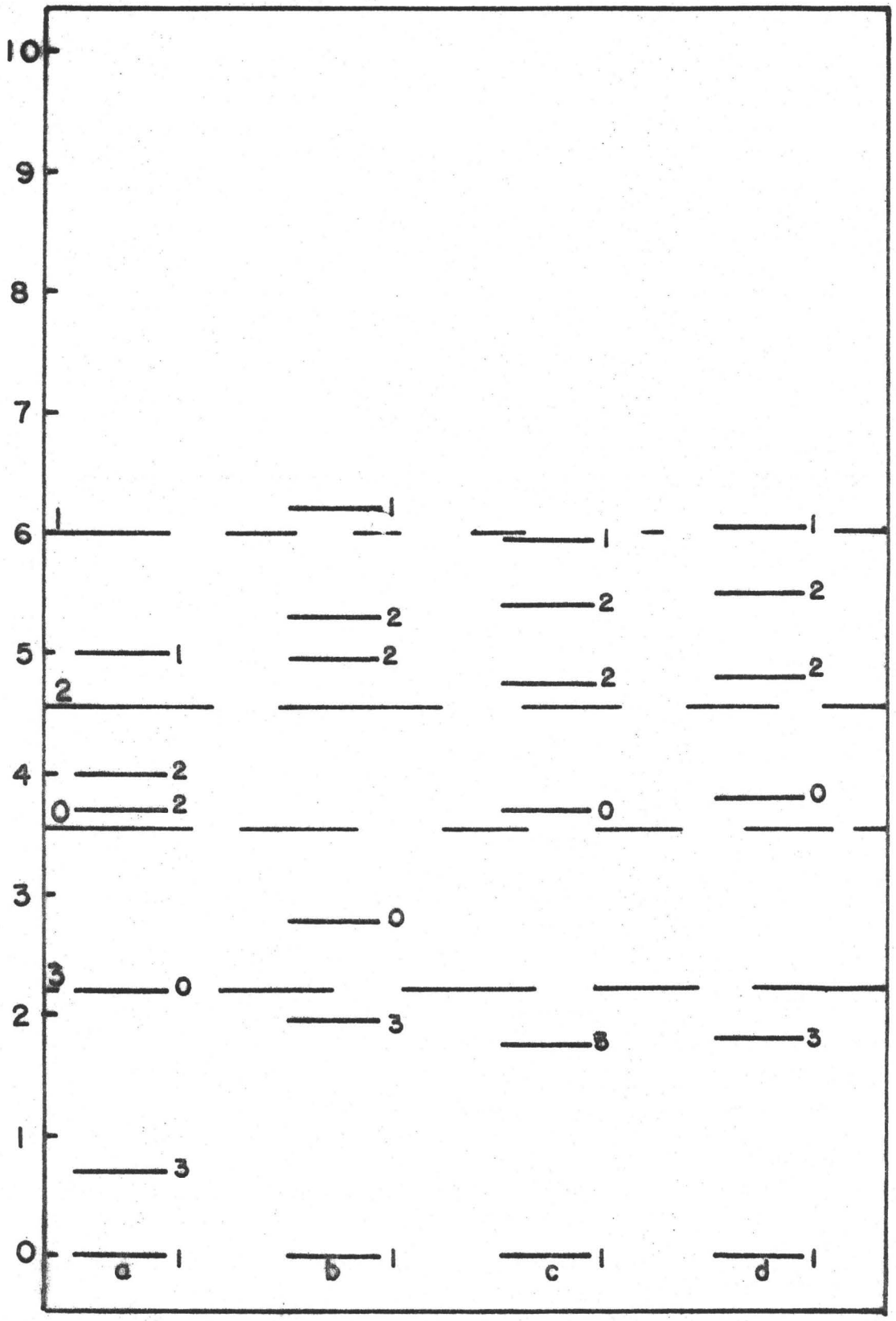

Figure 8.2

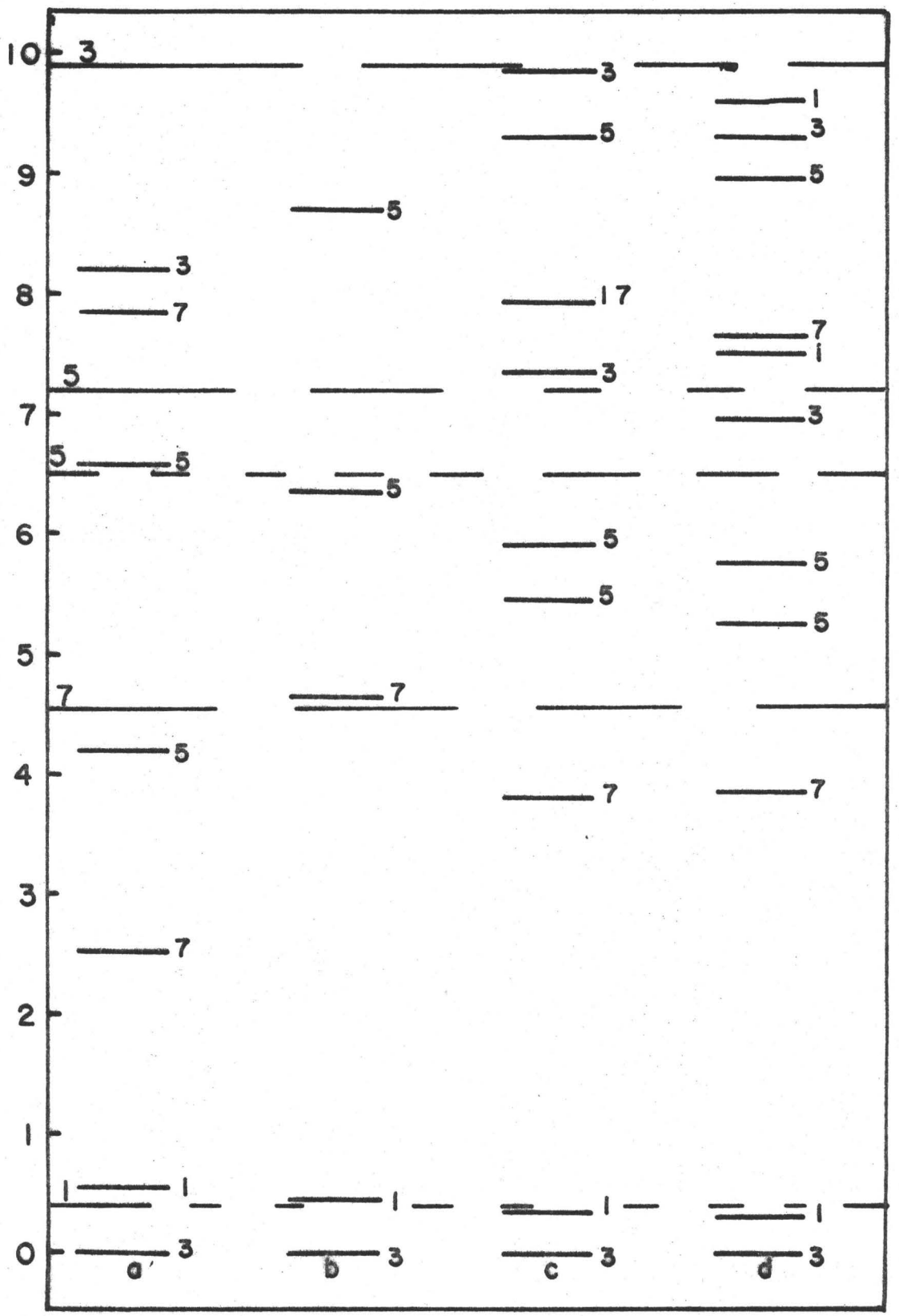

Figure 8.3

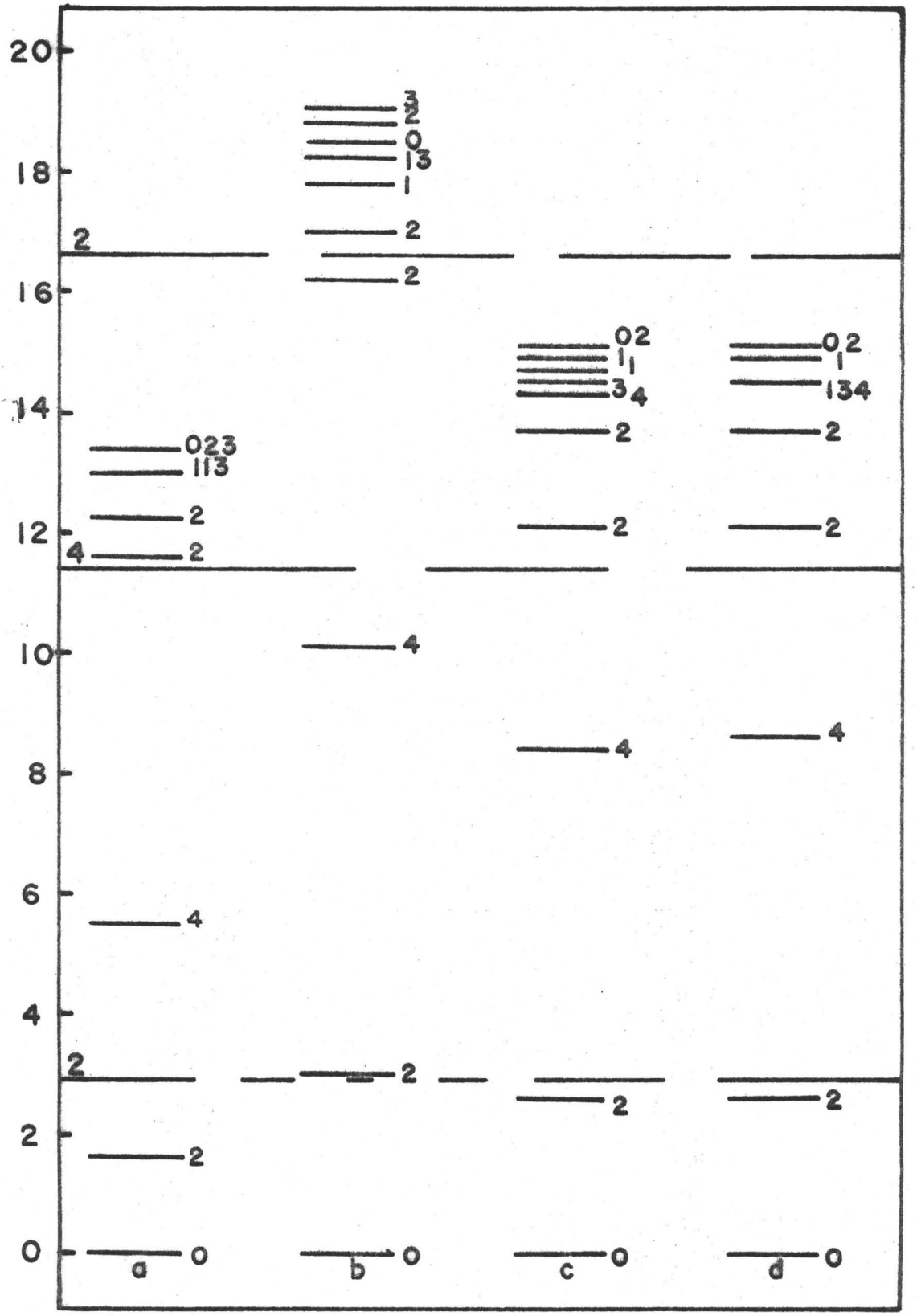
20
18
16
14
12
10
8
6
4
2
0
3
2
0
1
3
1
2
2
2
0
2
1
1
3
4
2
2
0
2
1
1
3
4
4
2
2
0
2
3
1
1
3
2
2
4
2
4
2
4
4
2
2
2
2
2
0
0
0
0
a
b
c
d

Figure 8.4

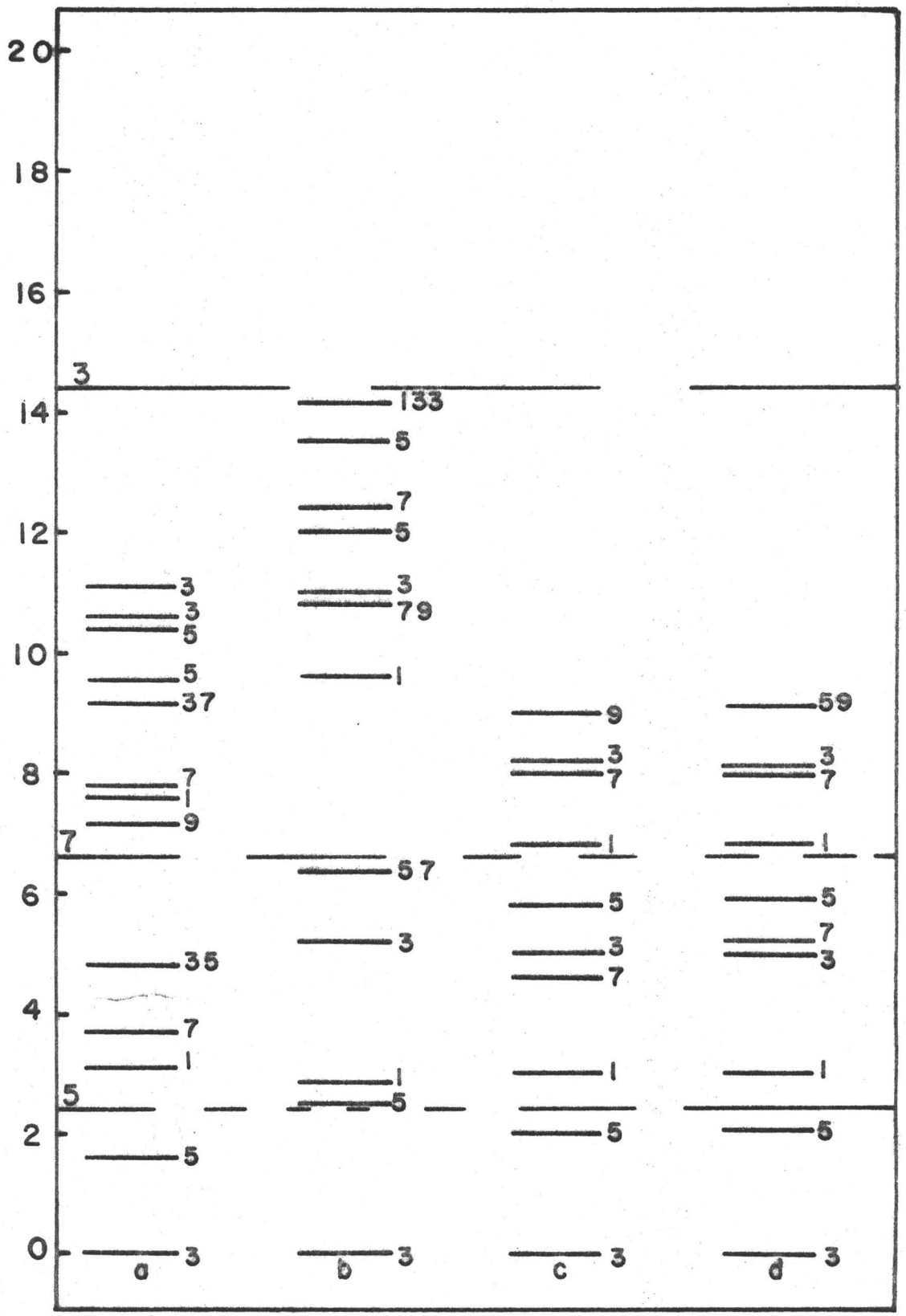
20
18
16
14
12
10
8
7
6
4
5
2
0
3
133
5
7
5
3
79
1
57
3
1
5
3
7
1
5
3
3
5
37
7
1
9
35
7
1
5
3
a
3
b
3
c
3
d
9
3
7
1
5
3
7
1
5
59
3
7
1
5
7
3
1
5

Figure 8.5

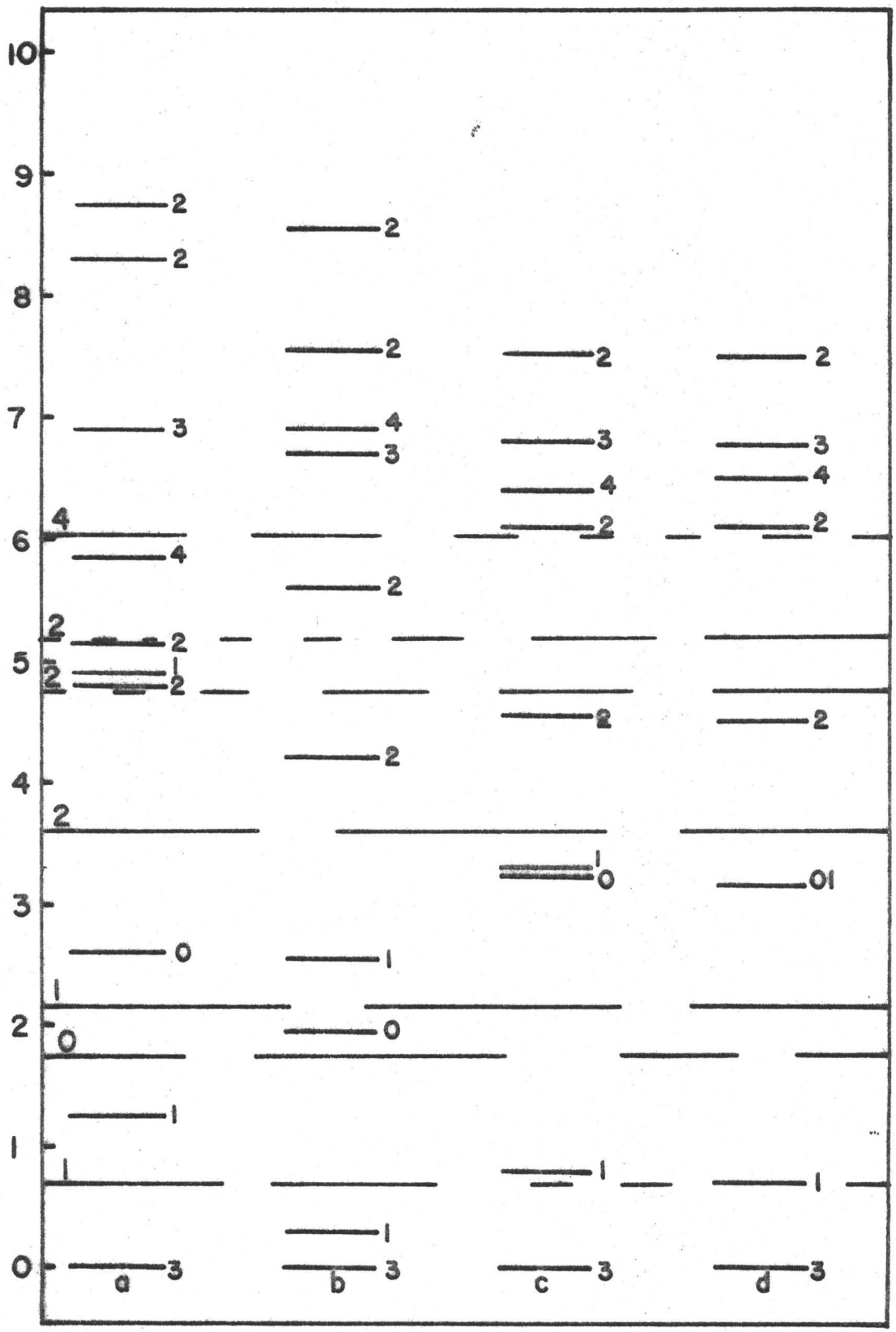

Figure 8.6

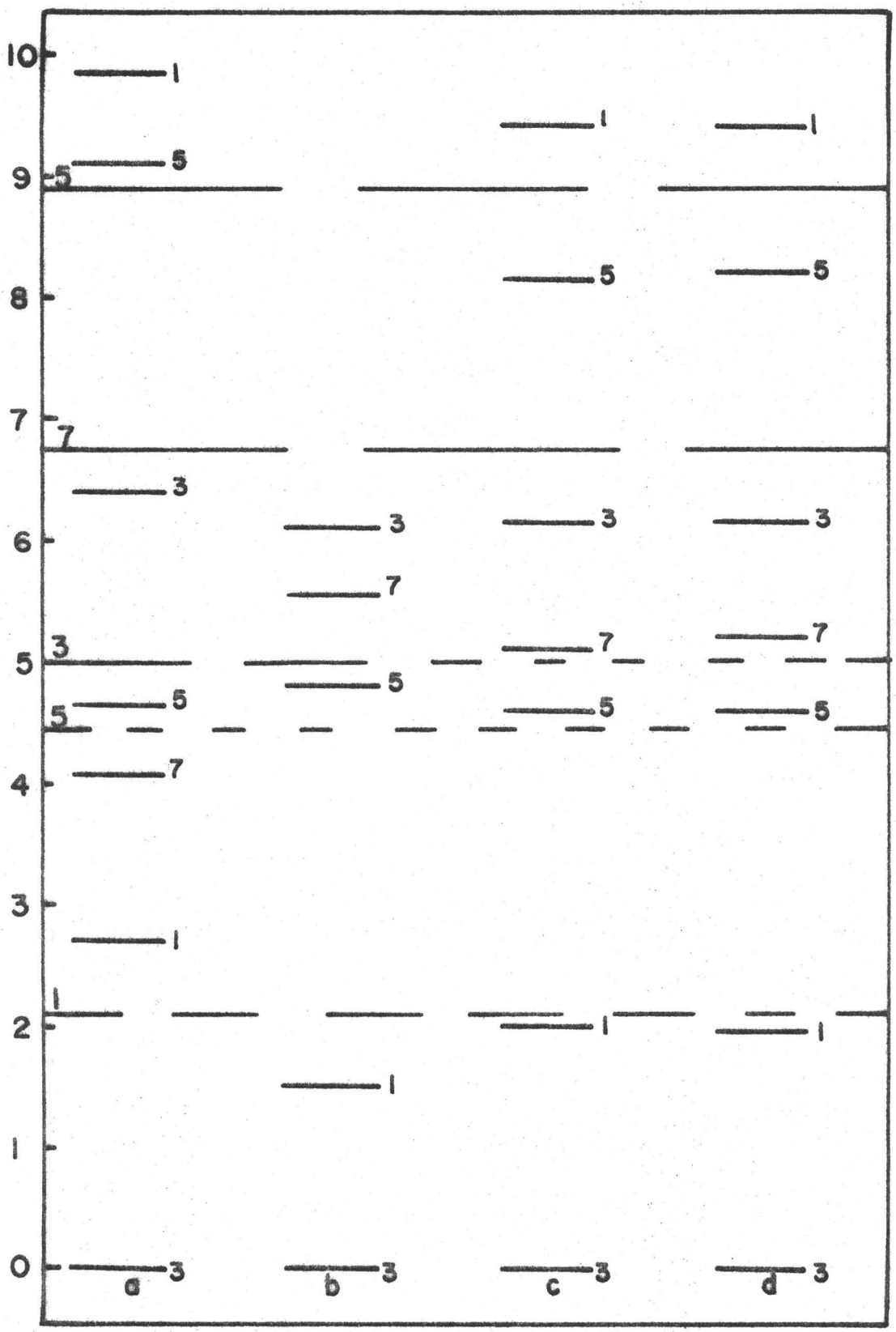

Figure 8.7

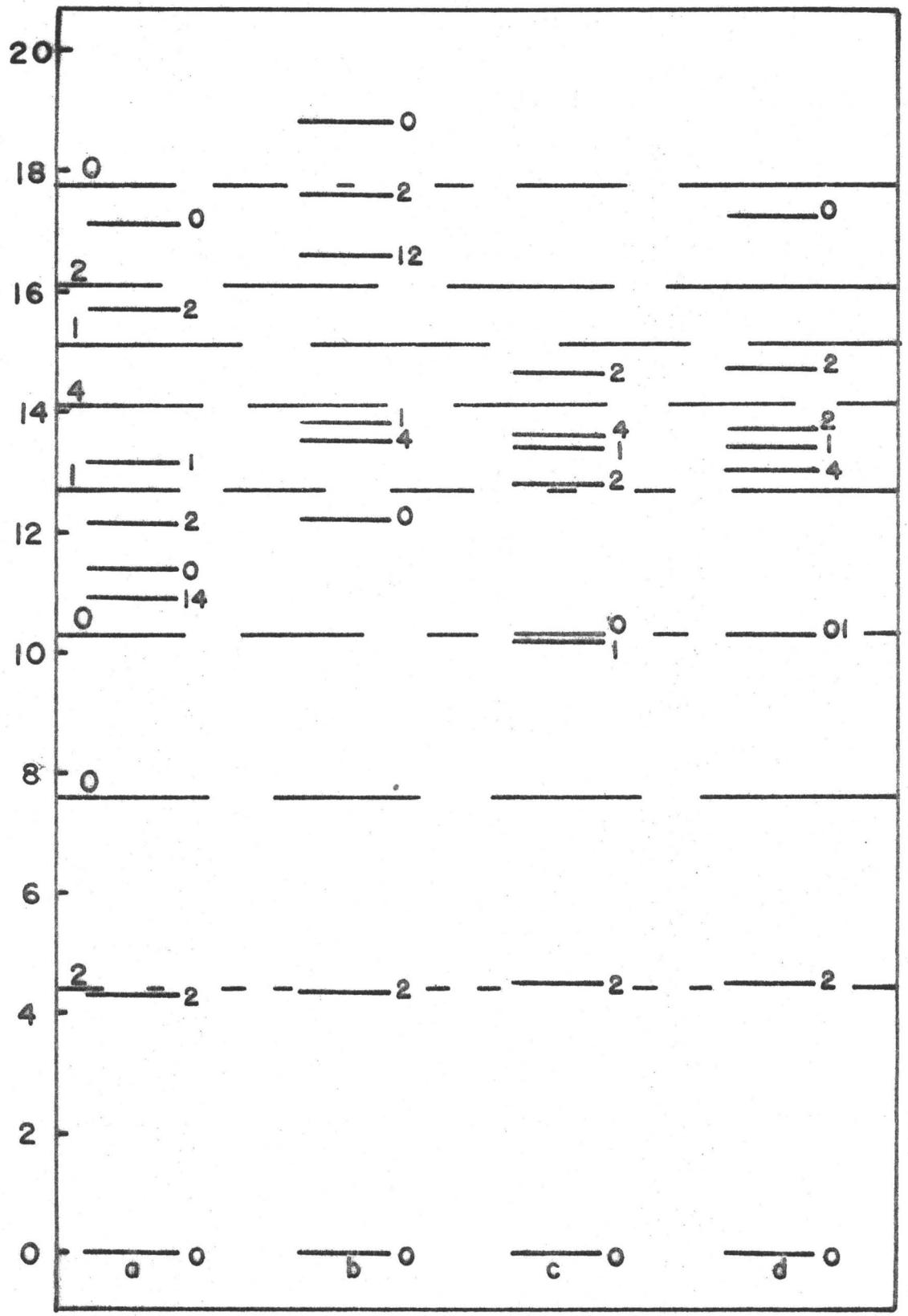

Figure 8.8

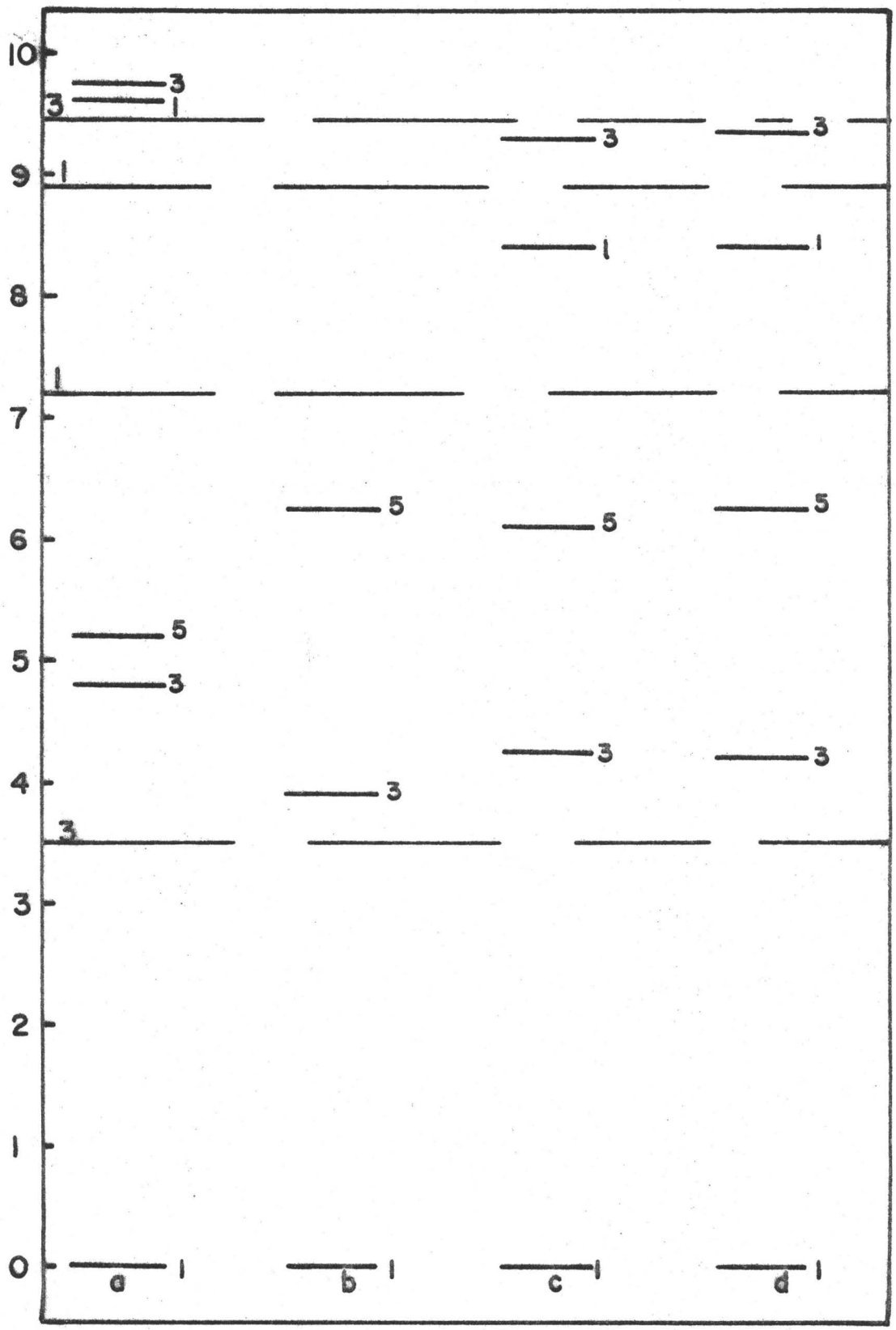

Figure 8.9

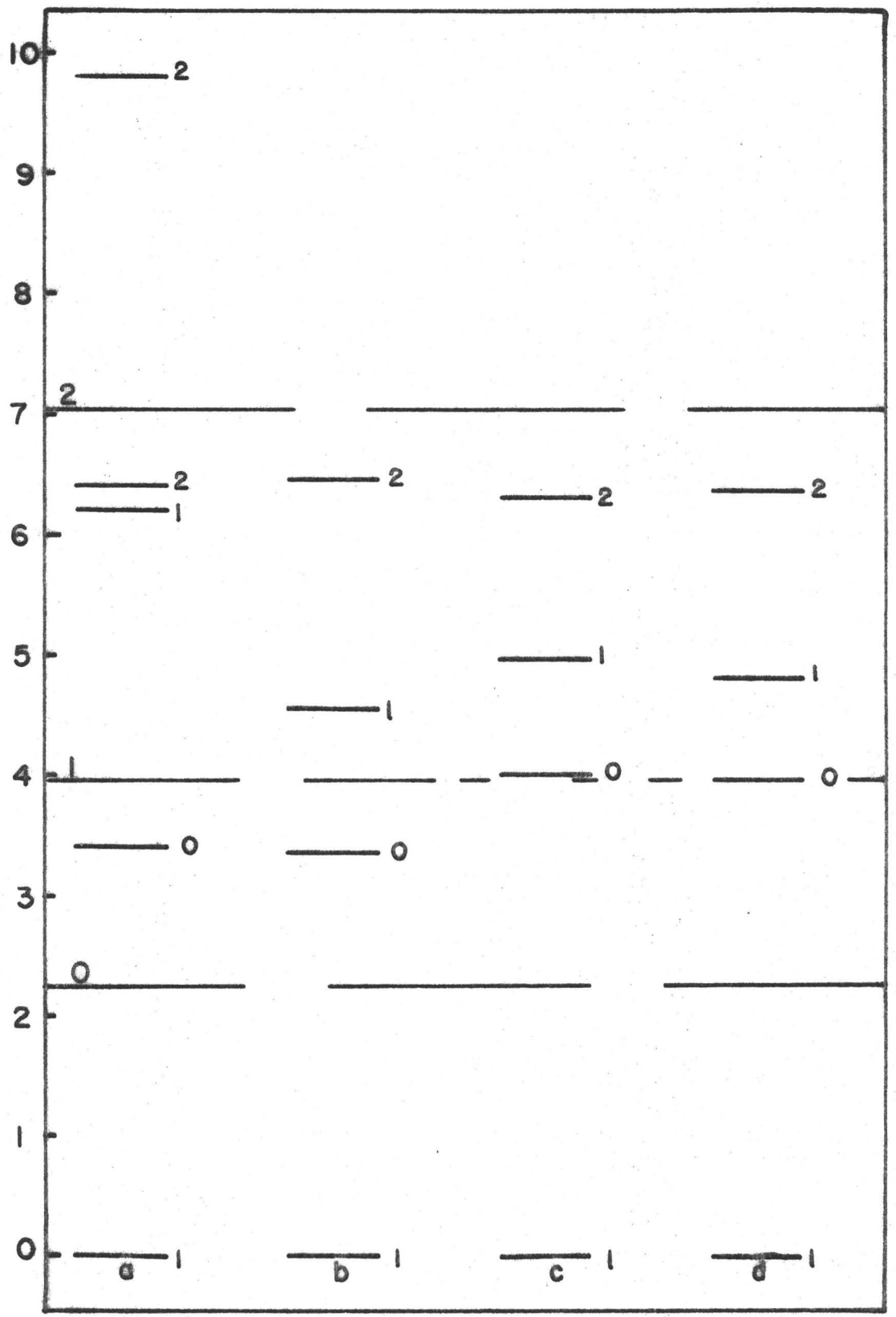

Figure 8.10

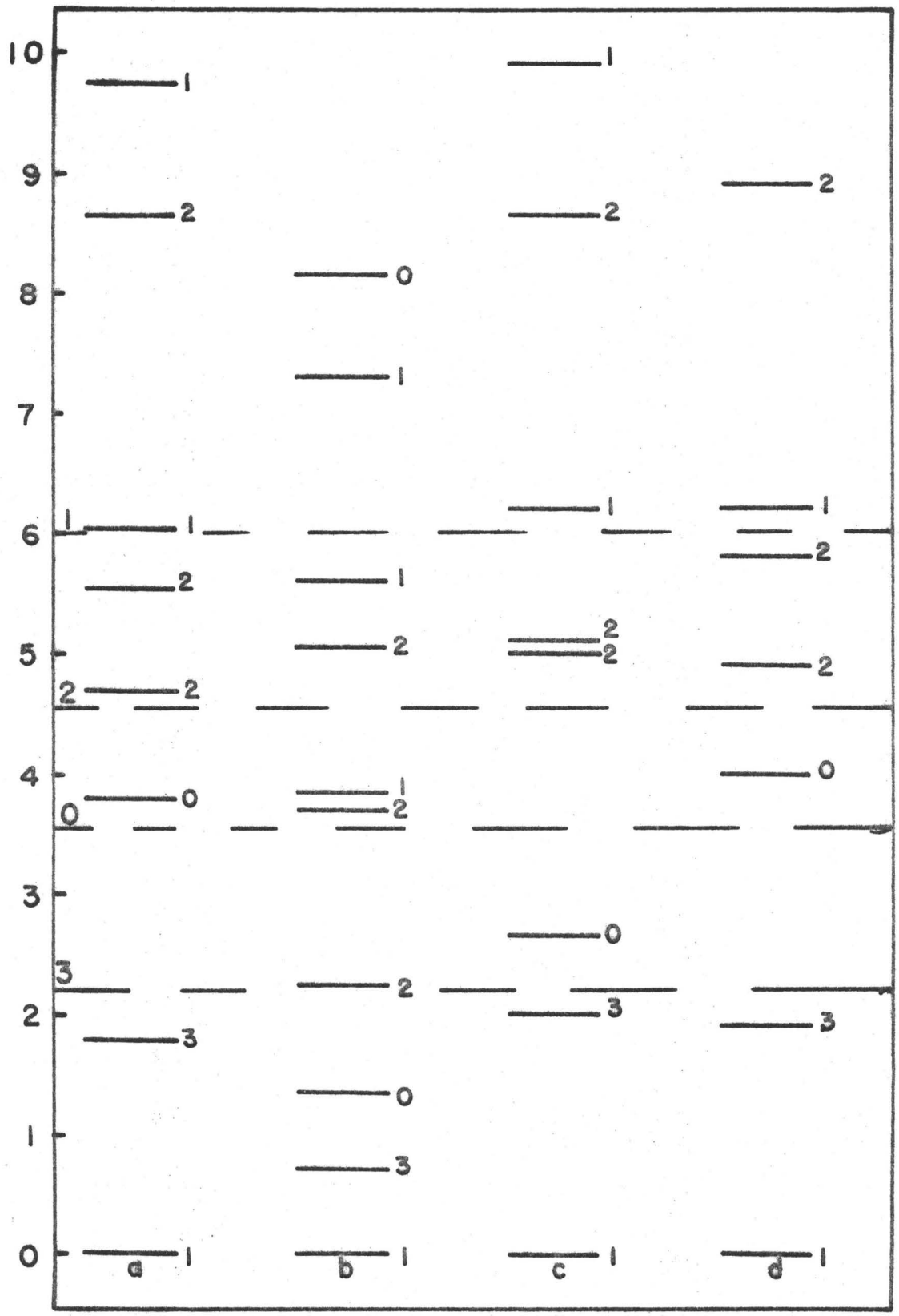

Figure 8.11

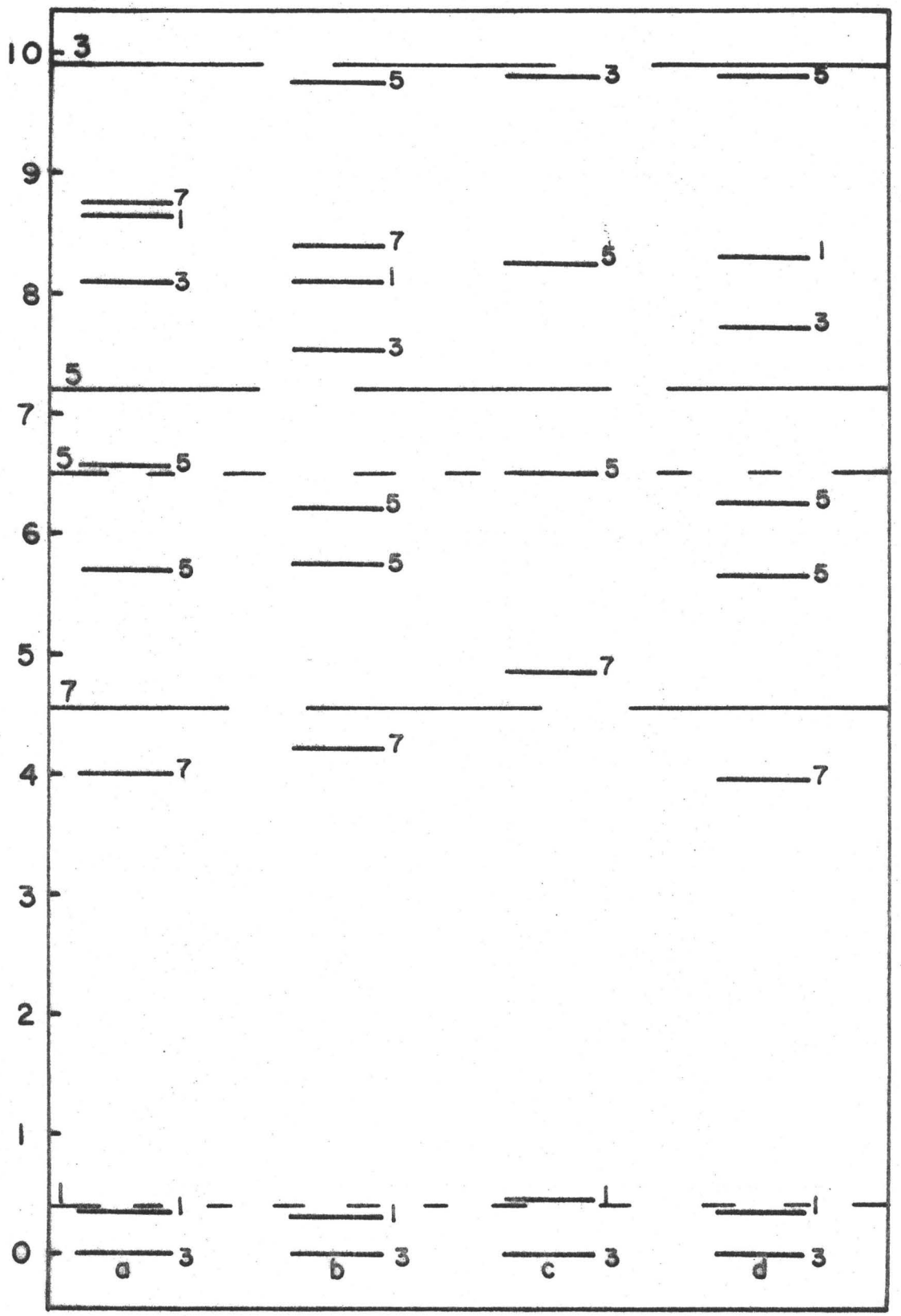
10
9
8
7
6
5
4
3
2
1
0
3
5
3
5
7
1
7
1
3
5
3
1
3
5
5
5
5
5
5
5
5
5
7
7
7
7
7
1
1
1
1
3
3
3
3
a
b
c
d

Figure 8.12

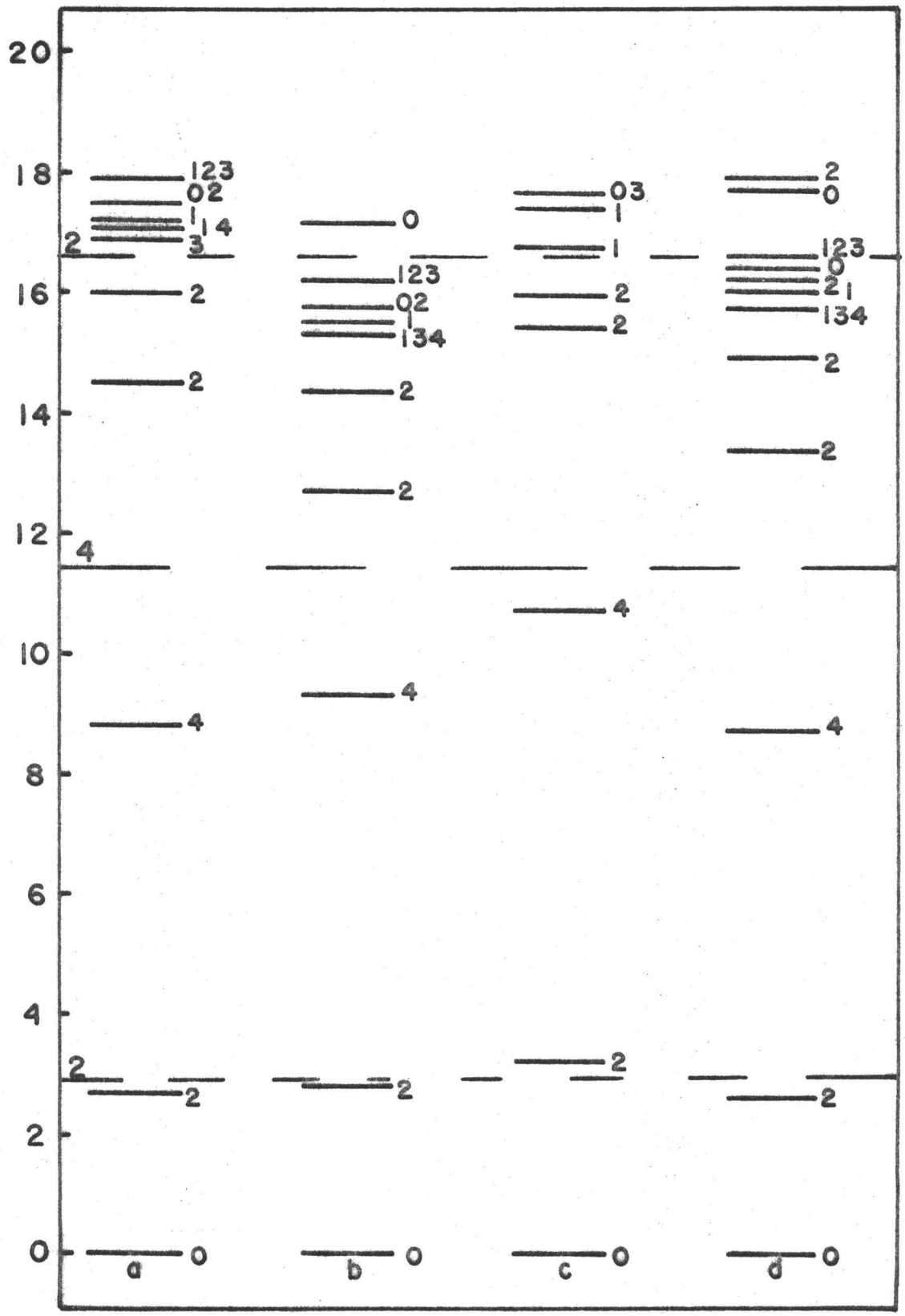
20
18
16
14
12
10
8
6
4
2
0
123
02
1
14
3
2
2
2
4
4
2
0
123
02
1
134
2
2
4
4
03
1
1
2
2
4
2
2
2
0
123
0
21
134
2
2
4
2
2
0
0
0
0
a
b
c
d

Figure 8.13

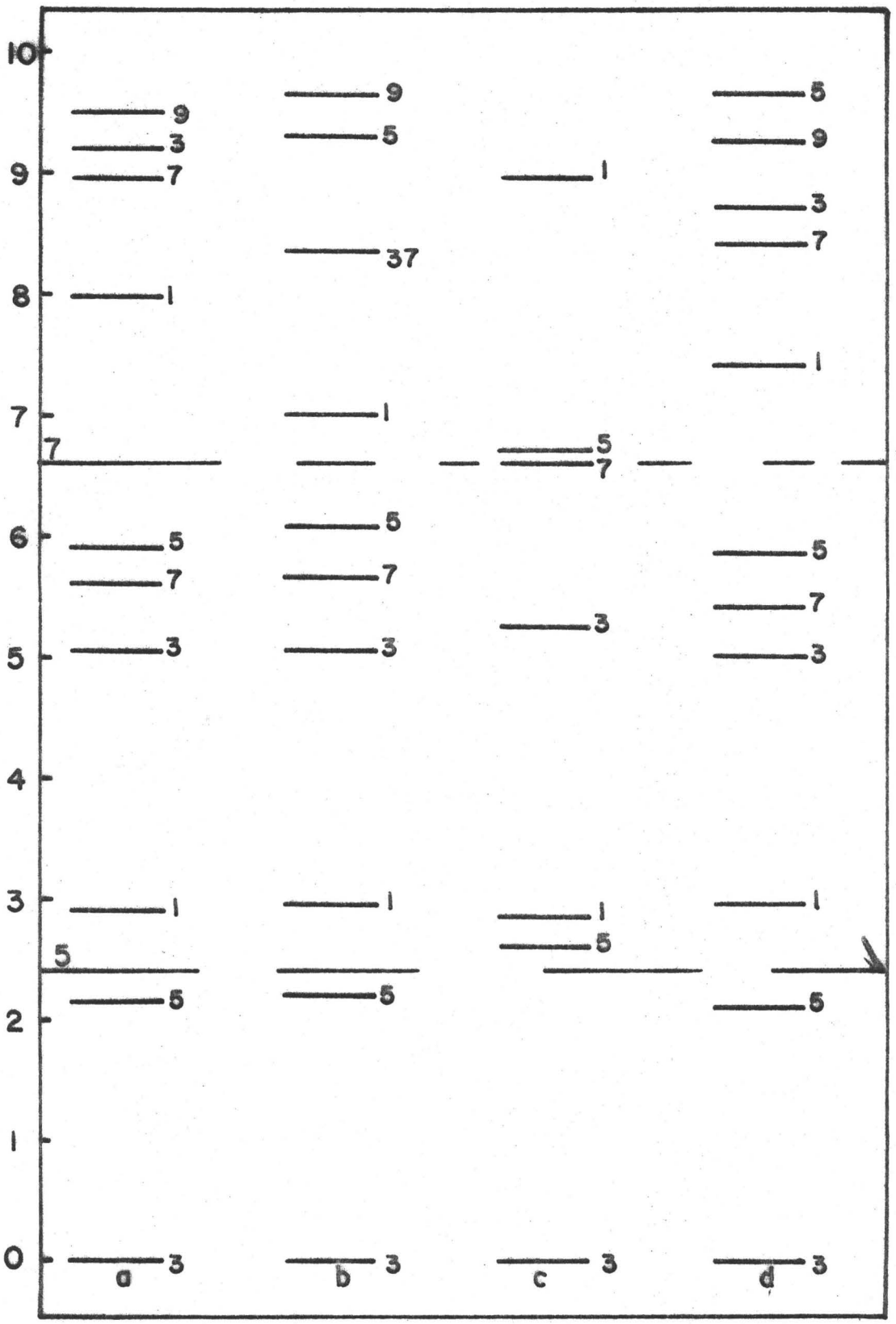

Figure 8.14

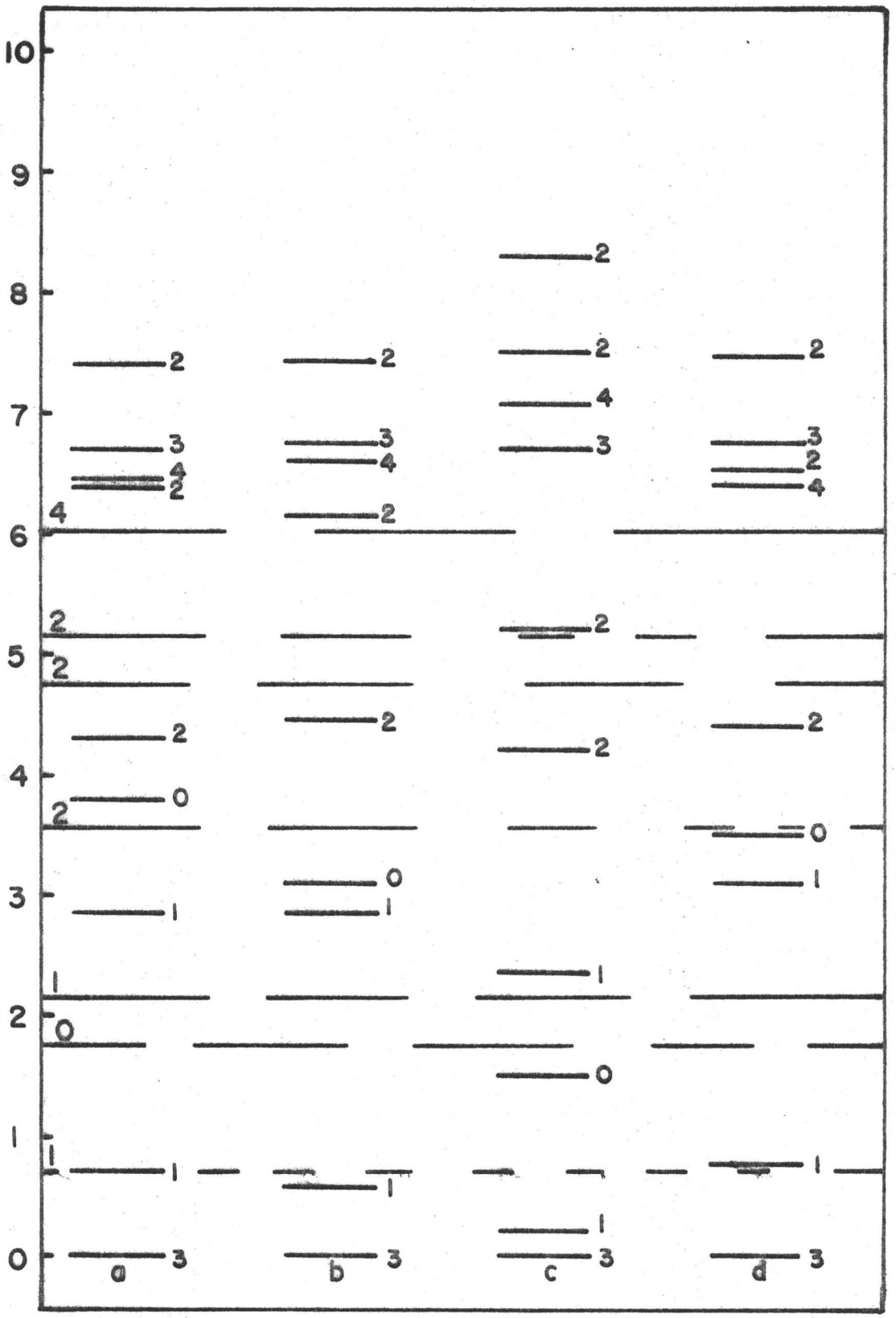

Figure 8.15

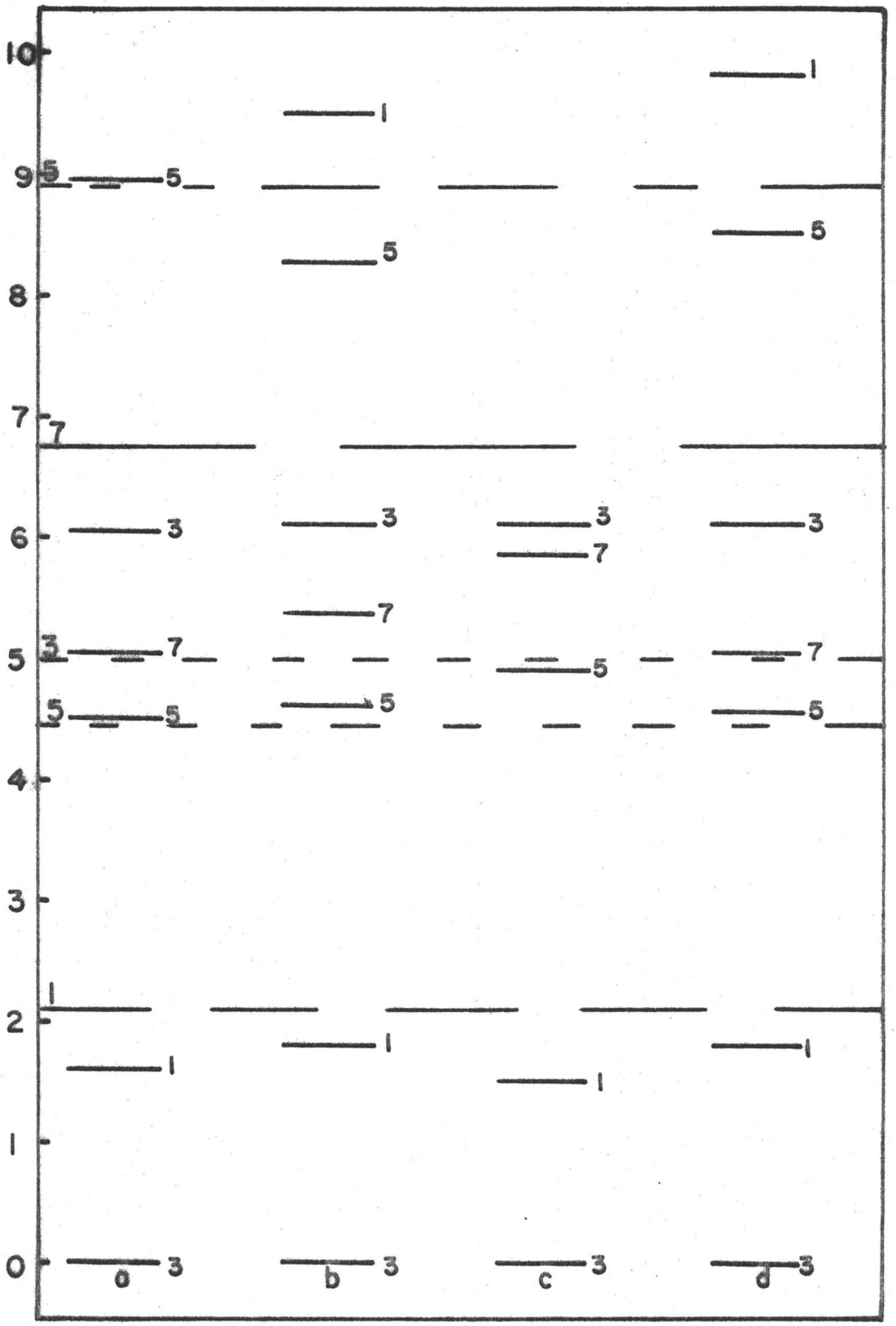

Figure 8.16

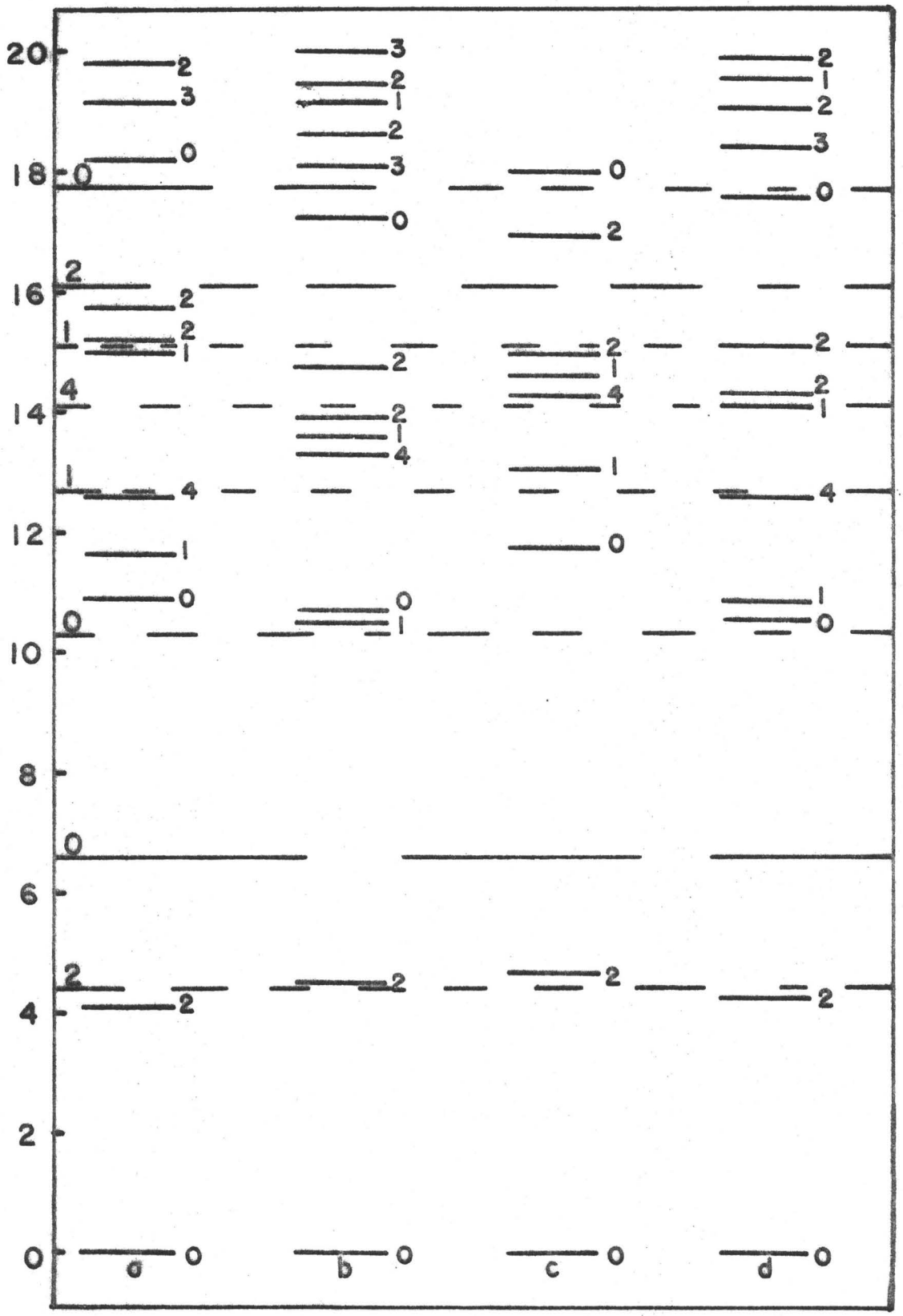

Figure 8.17

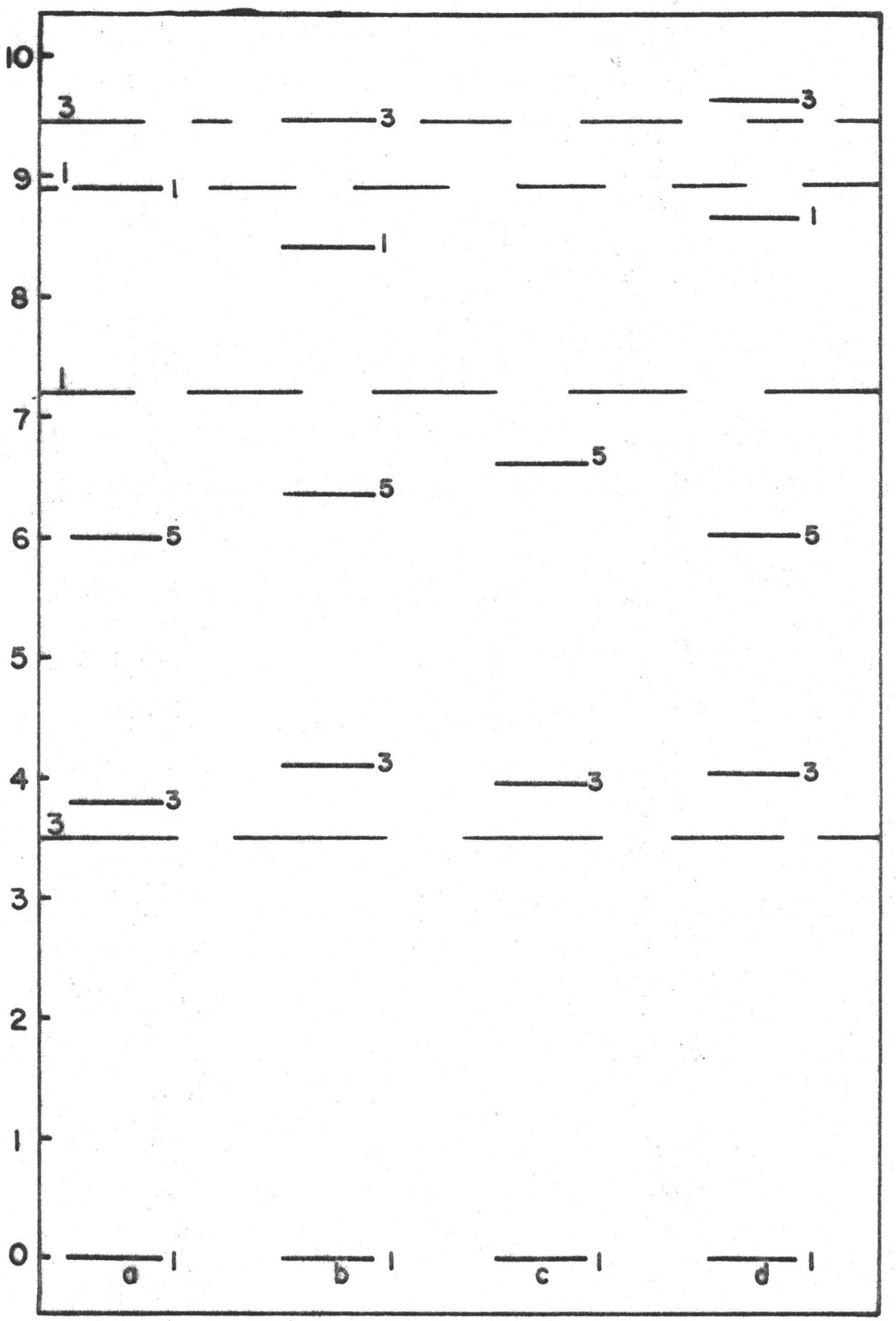

Figure 8.18

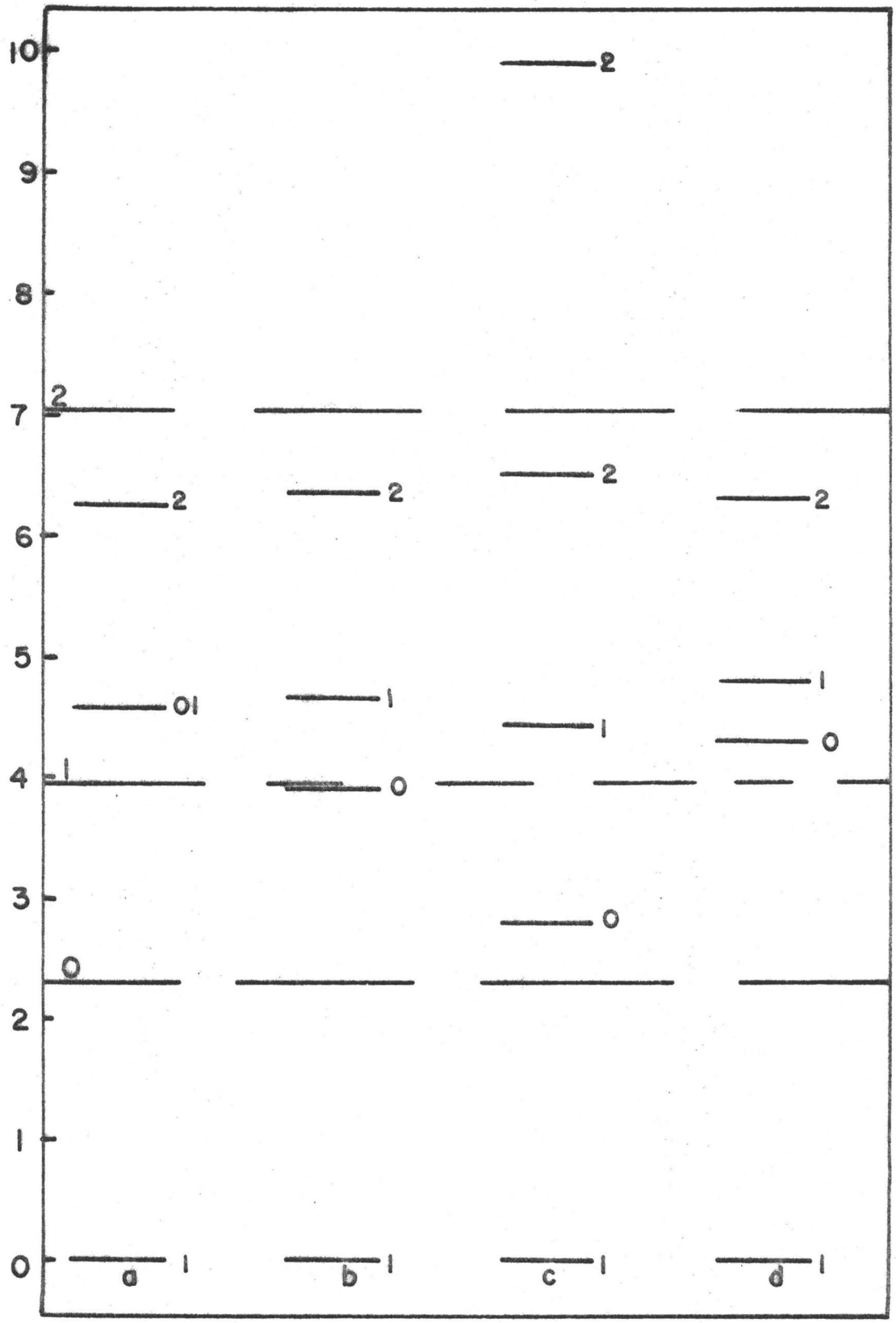

CHAPTER 9

CORE HEIGHT AND RELAXATION OF CRITERIA

In previous chapters many variations of the basic density dependent interaction have been studied. Most of these interactions have a repulsive core height of 5 Mev or less. In this chapter a comparison is made between two interactions, one having a zero core height and one with a core height of 50 Mev.

All density dependent interactions so far considered have consisted of two density dependent parts, one part having the same strength as the attractive non-density dependent interaction, the other part having the strength of the repulsive non-density dependent interaction. Interactions are considered in this chapter for which the strengths (and ranges) of the two density dependent parts of the interaction are identical.

Although the effective interactions used in this thesis are expected to be such that the second order correction terms in nuclear matter are small, it would be extremely fortuitous if these terms were zero. It might, thus, be more meaningful to consider the binding energy of nuclear matter to be different from 16 Mev per particle for a first order calculation. An interaction is constructed

that predicts a binding energy of 14 Mev per particle for the first order nuclear matter calculation. Further, some authors (Spr 69) feel that the saturation density of nuclear matter should be less than $k_F = 1.36$ fm^{-1}. Many previous interactions (Man 67) have been fitted to higher values of k_F and thus in this chapter an interaction which fits nuclear matter to a binding energy of 16 Mev per particle at a saturation density of $k_F = 1.5$ fm^{-1} is considered.

A great restriction, as far as merely fitting the excited state spectra, imposed in the calculations for finite nuclei is that the nucleus is required to saturate i.e. the binding energy is minimized with respect to the parameters of the single particle basis. Such a restriction is not (and generally cannot be) imposed in a typical shell-model calculation. In the calculations of the excited states of the O-p shell undertaken by Halbert et. al. (Hal 66) and used as a basis for comparison in Chapter 10, the oscillator well parameter of the O-p single particle wave functions (α_p) is considered to be a free parameter. A calculation has been performed for Interaction 10 in which α_p is treated as a free parameter, the nucleus being required to saturate only with respect to the O-s oscillator well parameter. The results of this calculation are outlined at the end of this chapter.

Two variations of the basic form of the density dependent interaction outlined in Chapter 3 are considered.

They are

$$\text{(A)}\quad V(r_{ij}) = V_A(1 + c_3(\frac{3\pi^2}{2}\rho(R))^{1/3} + c_4(\frac{3\pi^2}{2}\rho(R))^{2/3})$$

$$\times \exp(-r_{ij}^2/\lambda_a^2) + V_R \exp(-r_{ij}^2/\lambda_r^2(k))$$

and (B)

$$V(r_{ij}) = V_A \exp(-r_{ij}^2/\lambda_a^2)$$

$$+ V_R(1 + c_3(\frac{3\pi^2}{2}\rho(R))^{1/3} + c_4(\frac{3\pi^2}{2}\rho(R))^{2/3})$$

$$\times \exp(-r_{ij}^2/\lambda_r^2(k)) \quad .$$

Specifically, the basic interaction studied is Interaction 10, the (A) variation being Interaction 21 and the (B) variation being Interaction 22. The binding energies and root-mean-square radii for the 0-p shell nuclei are listed in Table 9.1 and the excited state spectra in Figs. 9.1 - 9.9 for the three Interactions 10, 21 and 22. The binding energies, r.m.s. radii and excitation energies (with the exception of ^{6}Li) are almost identical for all three interactions. The differences for ^{6}Li are probably due to minimization difficulties for Interactions 21 and 22. This is reflected in the large r.m.s. radii for ^{6}Li predicted by these interactions. The binding energies predicted for ^{6}Li are in excess of the expected binding energies (binding energy at "true" local minimum) because with such large r.m.s. radii the density approximation

used in the calculation breaks down completely. The compressibilities of nuclear matter and ν's are identical for the three interactions. The only significant differences for the variations are that c_4 has to change for variation (A) and c_3 for variation (B). The fact that the results are virtually identical for the three interactions is not very surprising since the attractive and repulsive ranges of the basic interaction are very nearly equal to each other.

The role of the core height can be seen by comparing the results (Table 9.1, Figs. 9.9 - 9.18) obtained in calculations using Interaction 28 (0 Mev Core Height) and Interaction 29 (50 Mev Core Height). The binding energies and excitation energies for the 0-p shell nuclei are almost identical, as are the parameters derived from the nuclear matter fitting procedure. The phase-fitting procedure would seem to have imposed the condition that interactions having the same V_A and λ_a should be "identically strong"; the interaction with the greater V_R having a shorter repulsive range λ_r^0 and smaller c_1. The minimum of the parabola for $\lambda_r(k)$ is almost the same for the two interactions. The independence of the results for different core heights underlines the restrictive nature of the requirement that the interactions fit the scattering data.

Interactions 15 and 16 are identical to Interaction 10 except that they have been fitted to different nuclear

matter criteria. Interaction 15 predicts a nuclear matter binding energy of 14 Mev per particle at a saturation density $k_F = 1.36$ fm^{-1}; Interaction 16 a nuclear matter binding energy of 16 Mev per particle at saturation density $k_F = 1.5$ fm^{-1}. The excitation energies of the O-p shell nuclei calculated using Interactions 15 and 16 are very similar and generally greater than those calculated for Interaction 10. The root-mean-square radii are smallest for Interaction 16. k_F, the saturation density is related to the r_0 in the formula

$$R = r_0 A^{1/3}$$

for the radius of a finite nucleus by

$$k_F^3 = (9\pi/8)/r_0^3 \quad .$$

It is thus apparent that Interaction 16 should predict smaller radii than interactions which saturate nuclear matter at a lower saturation density. Interaction 15, which is a more attractive interaction (B.E.$_{den}$ = 14.01 Mev) than Interaction 10 (B.E.$_{den}$ = 19.86 Mev), also predicts smaller r.m.s. radii than does Interaction 10.

The excitation energies of the states of the O-p nuclei are generally greater for Interactions 15 and 16 than for Interaction 10. In view of the fact that for Interaction 10 these excitation energies are smaller than the experimental values this is a desirable feature.

However, the changes in the excitation energies are not great enough to justify the abandonment of the nuclear matter criteria established in Chapter 3.

Table 9.2 shows the results of calculations for Interaction 10 in which the binding energy is minimized only with respect to the O-s oscillator well parameter α_s, the ratio of the O-p oscillator well parameter, α_p to the O-s oscillator well parameter, $\sigma = \alpha_p/\alpha_s$, being kept constant. The difficulty of minimizing ^{6}Li with respect to α_p is clearly indicated. The calculation for ^{6}Li quoted in Table 9.1 found a local minimum between $\sigma = 0.9$ and $\sigma = 1.0$. The changes of the excitation energies with σ are substantial and it would be possible to "fit" the experimental excitation energies to a certain extent if σ were a free parameter. For example, the second 2^+ state of ^{8}Be at 16.6 Mev excitation could be fitted by Interaction 10 for $\sigma \simeq 1.3$.

The above results indicate the extreme importance of performing the minimization of the ground state binding with respect to σ very carefully if any confidence is to be placed in the results for the excitation energies. This excludes the possibility of determining α_s and α_p by minimizing the energy of the nuclear system with a reduced basis (i.e. by considering a few of the "lead" determinantal states (Vol 65)).

TABLE 9.1

Interaction 10			Interaction 15			Interaction 16		
A	B.E.(Mev)	r.m.s.(fm)	A	B.E.(Mev)	r.m.s.(fm)	A	B.E.(Mev)	r.m.s.(fm)
4	27.28	2.04	4	31.34	1.95	4	31.33	1.91
6	30.13	2.48	6	34.28	2.68	6	33.16	2.55
7	34.14	2.66	7	36.84	2.57	7	35.77	2.53
8	48.78	2.63	8	52.11	2.57	8	50.88	2.53
9	49.25	2.72	9	52.23	2.67	9	50.93	2.63
10	63.24	2.75	10	65.05	2.71	10	63.80	2.66
11	72.13	2.79	11	71.46	2.75	11	72.48	2.70
12	88.75	2.81	12	90.36	2.77	12	89.28	2.72
13	92.98	2.83	13	93.86	2.80	13	93.00	2.75
14	101.59	2.84	14	102.60	2.81	14	102.12	2.75
16	124.73	2.87	16	125.62	2.84	16	126.24	2.77

TABLE 9.1 - CONTINUED

Interaction 21			Interaction 22			Interaction 28		
A	B.E.(Mev)	r.m.s.(fm)	A	B.E.(Mev)	r.m.s.(fm)	A	B.E.(Mev)	r.m.s.(fm)
4	27.23	2.02	4	27.25	2.03	4	36.32	1.82
6	33.17	3.17	6	31.94	2.91	6	35.25	2.34
7	33.97	2.63	7	34.11	2.63	7	37.98	2.39
8	48.56	2.61	8	48.72	2.62	8	53.55	2.41
9	49.43	2.71	9	49.73	2.72	9	52.55	2.51
10	62.41	2.74	10	62.89	2.74	10	64.25	2.55
11	71.19	2.78	11	71.73	2.78	11	73.66	2.59
12	87.64	2.79	12	88.29	2.80	12	90.97	2.62
13	91.56	2.82	13	92.41	2.73	13	94.34	2.65
14	100.11	2.83	14	101.18	2.84	14	103.35	2.67
16	122.39	2.86	16	123.85	2.86	16	128.48	2.70

TABLE 9.1 - CONTINUED

Interaction 29

A	B.E.(Mev)	r.m.s.(fm)
4	35.98	1.80
6	34.58	2.35
7	37.13	2.38
8	52.74	2.39
9	51.50	2.49
10	63.19	2.53
11	72.47	2.57
12	89.76	2.59
13	92.97	2.63
14	102.00	2.64
16	128.11	2.67

TABLE 9.2

J^{π}	A=6	σ	0.2 E_x(Mev)	0.4 E_x(Mev)	0.6 E_x(Mev)	0.8 E_x(Mev)	1.0 E_x(Mev)
0			1.15	3.04	4.36	5.17	5.65
0			7.82	10.62	12.66	13.94	14.73
1			3.65	5.51	6.31	6.46	6.34
1			5.26	8.36	10.55	11.91	12.74
1			7.09	9.64	12.14	14.04	15.39
2			1.96	4.53	4.92	4.91	4.72
2			3.55	4.56	6.20	7.08	7.53
2			4.80	7.47	9.40	10.62	11.36
3			0.55	1.53	1.92	1.91	1.72
B.E.(Mev)			34.05	31.6	31.21	30.53	29.20
r.m.s.(fm)			3.43	2.59	2.58	2.49	2.47
	A=7	$\sigma\rightarrow$	0.2	0.4	0.6	0.8	1.0
1/2			0.23	0.24	0.31	0.37	0.42
1/2			3.90	5.95	7.31	8.14	8.65
3/2			3.48	5.48	6.78	7.58	8.08
3/2			3.55	6.85	9.01	10.17	10.77
5/2			1.64	3.73	5.06	5.53	5.43
5/2			3.54	5.11	5.70	6.09	6.55
7/2			1.59	3.24	3.81	3.85	3.69
7/2			3.74	6.02	7.44	8.18	8.56
B.E.(Mev)			33.44	33.09	34.08	34.12	33.11
r.m.s.(fm)			3.72	2.96	2.70	2.60	2.57

TABLE 9.2 - CONTINUED

	A=8 σ→	0.2	0.4	0.6	0.8	1.0
1		4.65	9.89	12.85	14.46	15.37
1		5.62	10.40	13.11	14.60	15.48
1		6.13	10.88	13.57	15.03	15.89
2		1.41	2.47	2.72	2.67	2.56
2		3.70	8.25	10.84	12.27	13.11
2		4.44	9.44	12.20	13.72	14.60
2		5.80	10.50	13.15	14.61	15.47
3		5.29	10.15	12.81	14.28	15.13
3		5.49	11.06	14.02	15.52	16.33
4		4.31	7.99	8.82	8.72	8.36
B.E.(Mev)		36.91	42.44	46.75	48.50	48.32
r.m.s.(fm)		3.85	3.01	2.74	2.64	2.61

	A=9 σ→	0.25	0.5	0.75	1.0
1/2		2.36	3.05	3.01	3.00
1/2		3.85	5.37	6.52	7.14
3/2		4.34	4.86	4.99	5.00
3/2		4.76	7.12	7.97	8.44
5/2		1.44	2.04	2.18	2.08
5/2		5.19	5.92	5.93	5.77
5/2		5.83	7.90	8.87	9.36
5/2		6.47	9.09	10.17	10.01
7/2		2.54	4.81	5.30	5.24
7/2		5.74	7.20	7.83	8.10
9/2		6.88	8.90	9.21	9.03

TABLE 9.2 - CONTINUED

B.E.(Mev)		39.03	46.16	49.64	49.60	
r.m.s.(fm)		3.69	2.95	2.75	2.70	
	A=10 σ→	0.2	0.6	1.0	1.4	
0		0.47	2.20	3.35	3.95	
1		0.09	0.42	0.79	1.02	
1		5.34	3.11	3.22	3.46	
2		1.65	3.73	4.50	4.44	
2		6.18	5.01	6.27	6.85	
4		7.07	6.76	6.42	6.19	
B.E.(Mev)		45.72	60.10	63.09	59.37	
r.m.s.(fm)		4.16	2.89	2.73	2.74	
	A=11 σ→	0.25	0.50	0.75	1.0	
1/2		4.00	2.40	2.04	1.95	
3/2		6.31	6.18	6.15	6.15	
5/2		5.40	4.84	4.69	4.61	
5/2		7.01	7.60	7.99	8.21	
7/2		6.28	5.82	5.44	5.14	
B.E.(Mev)		50.66	64.48	70.92	72.05	
r.m.s.(fm)		3.81	3.04	2.83	2.77	
	A=12 σ→	0.2	0.4	0.6	0.8	1.0
0		11.53	9.35	9.27	9.45	9.60
0		14.38	14.67	15.38	15.87	16.19
0		16.00	18.11	19.61	20.46	20.97

TABLE 9.2 - CONTINUED

1		7.74	8.61	9.38	9.83	10.08
1		8.65	10.45	11.80	12.60	13.10
2		6.14	4.83	4.33	4.08	3.92
2		8.99	11.06	12.37	13.05	13.44
2		13.22	12.77	13.21	13.58	13.82
2		15.20	16.06	16.78	17.18	17.42
4		14.39	13.50	12.83	12.29	11.86
B.E.(Mev)		53.72	70.59	81.25	86.11	87.31
r.m.s.(fm)		4.22	3.23	2.94	2.83	2.80
	A=13 $\sigma\rightarrow$	0.2	0.4	0.6	0.8	1.0
1/2		7.66	7.93	8.16	8.32	8.42
3/2		6.04	4.82	4.41	4.27	4.20
3/2		8.02	8.70	9.07	9.25	9.35
3/2		9.65	12.04	13.35	13.61	13.72
5/2		7.38	7.02	6.69	6.43	6.23
7/2		14.46	14.25	13.17	12.82	12.57
B.E.(Mev)		51.94	73.41	85.84	91.45	92.97
r.m.s.(fm)		4.21	3.24	2.97	2.87	2.83
	A=14 $\sigma\rightarrow$	0.2	0.4	0.6	0.8	1.0
0		1.12	2.41	3.15	3.61	3.90
0		15.59	16.64	17.33	17.77	18.06
1		5.93	4.93	4.75	4.77	4.83
1		9.32	11.22	12.24	12.82	13.19
1		15.74	17.71	19.06	19.90	20.47

TABLE 9.2 - CONTINUED

2	7.09	6.31	6.52	6.42	6.36
2	8.65	9.79	10.37	10.70	10.92
2	16.52	18.17	19.06	19.57	19.91
3	14.59	14.21	14.02	13.92	13.86
B.E.(Mev)	50.33	77.76	92.77	99.65	101.82
r.m.s.(fm)	4.17	3.24	2.98	2.88	2.84

FIGURE CAPTIONS

For all figures, excitation energy (in Mev) is plotted to the left of the figure. Full lines designate the calculated levels and dashed lines designate certain experimental levels. For even nuclei the spin J of the level is indicated to the right of the calculated levels and at the left of the figure for the experimental levels, for odd nuclei the value of 2J is likewise indicated.

Figures 9.1 - 9.9 plot the excited state spectra of the 0-p shell nuclei calculated for

(a) Interaction 21

(b) Interaction 22

(c) Interaction 10

Figure 9.1 Excited State Spectra of ^{6}Li with C = -2.0 Mev.

Figure 9.2 Excited State Spectra of ^{7}Be with C = -1.5 Mev.

Figure 9.3 Excited State Spectra of ^{8}Be with C = -2.0 Mev.

Figure 9.4 Excited State Spectra of ^{9}B with C = -3.0 Mev.

Figure 9.5 Excited State Spectra of ^{10}B with C = -5.0 Mev.

Figure 9.6 Excited State Spectra of ^{11}B with C = -4.5 Mev.

Figure 9.7 Excited State Spectra of ^{12}C with C = -5.5 Mev.

Figure 9.8 Excited State Spectra of ^{13}C with C = -5.0 Mev.

Figure 9.9 Excited State Spectra of ^{14}N with C = -5.0 Mev.

Figures 9.10 - 9.18 plot the excited state spectra of the O-p shell nuclei calculated for

(a) Interaction 28

(b) Interaction 29

(c) Interaction 15

(d) Interaction 16

Figure 9.10 Excited State Spectra of ^{6}Li with C = -2.0 Mev.

Figure 9.11 Excited State Spectra of ^{7}Be with C = -1.5 Mev.

Figure 9.12 Excited State Spectra of ^{8}Be with C = -2.0 Mev.

Figure 9.13 Excited State Spectra of ^{9}B with C = -3.0 Mev.

Figure 9.14 Excited State Spectra of ^{10}B with C = -5.0 Mev.

Figure 9.15 Excited State Spectra of ^{11}B with C = -4.5 Mev.

Figure 9.16 Excited State Spectra of ^{12}C with C = -5.5 Mev.

Figure 9.17 Excited State Spectra of ^{13}C with C = -5.0 Mev.

Figure 9.18 Excited State Spectra of ^{14}N with C = -5.0 Mev.

Figure 9.1

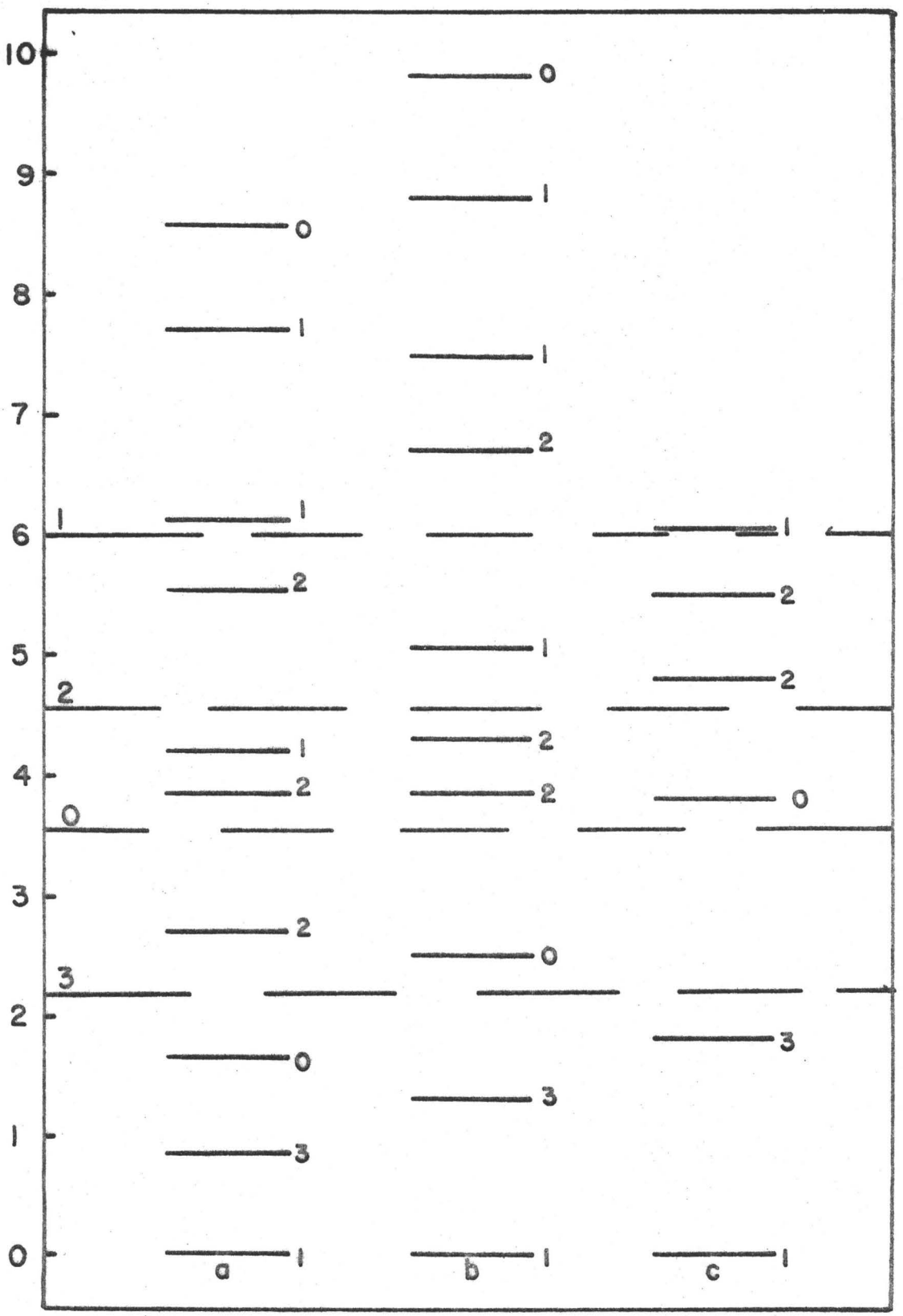

Figure 9.2

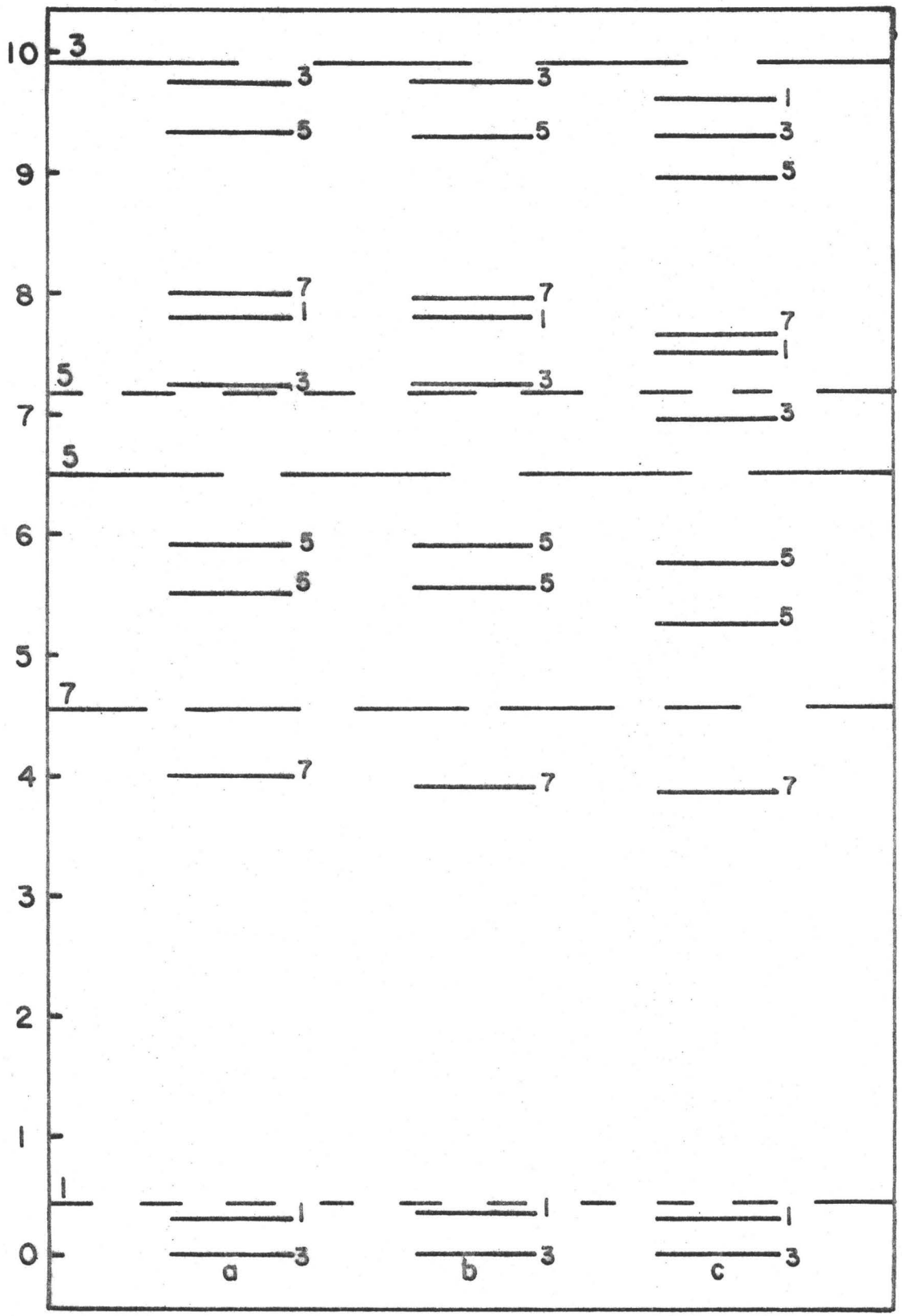

Figure 9.3

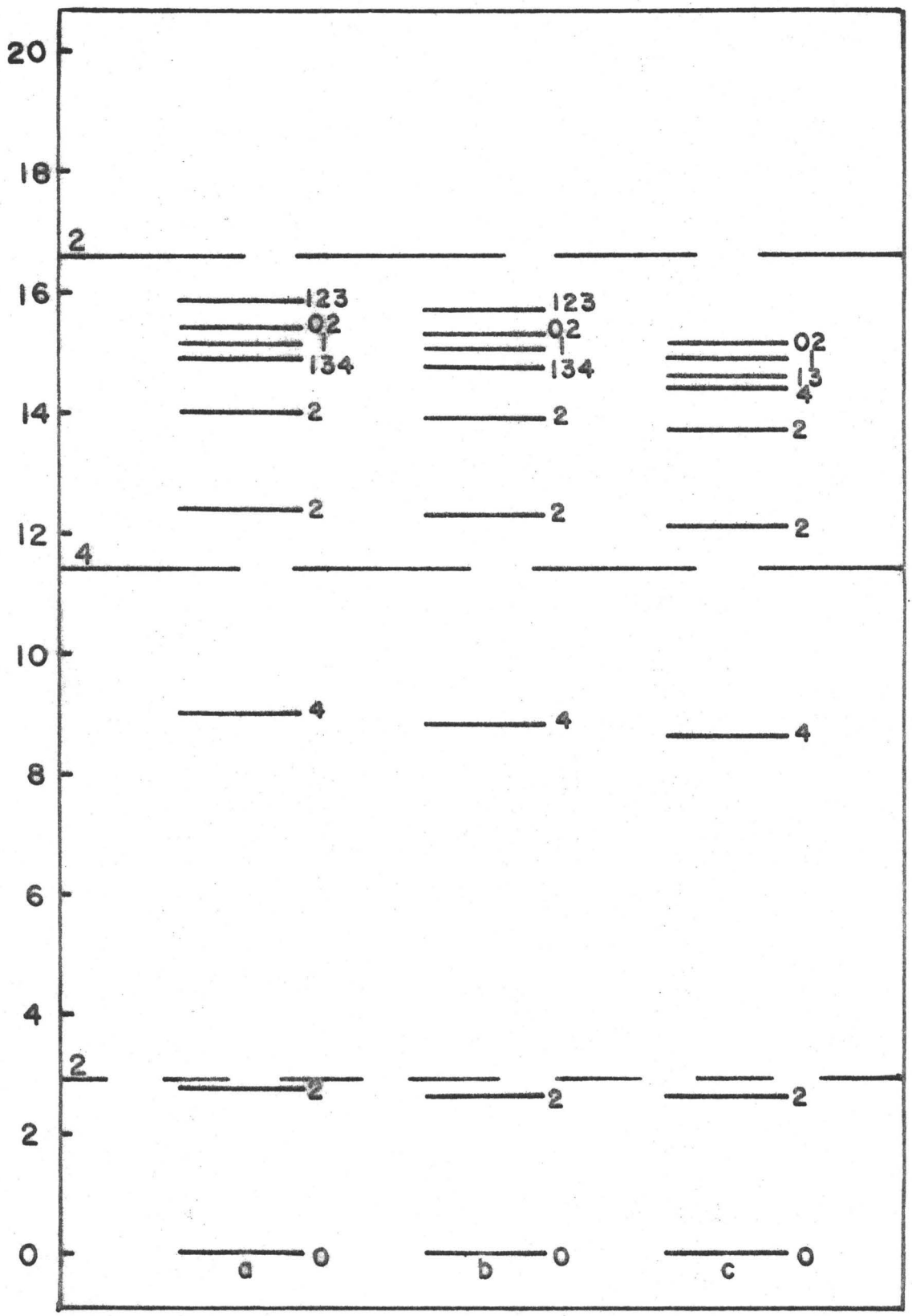
20
18
16
14
12
10
8
6
4
2
0
2
4
2
123
02
134
2
2
123
02
134
2
2
02
13
4
2
2
4
4
4
2
2
2
0
0
0
a
b
c

Figure 9.4

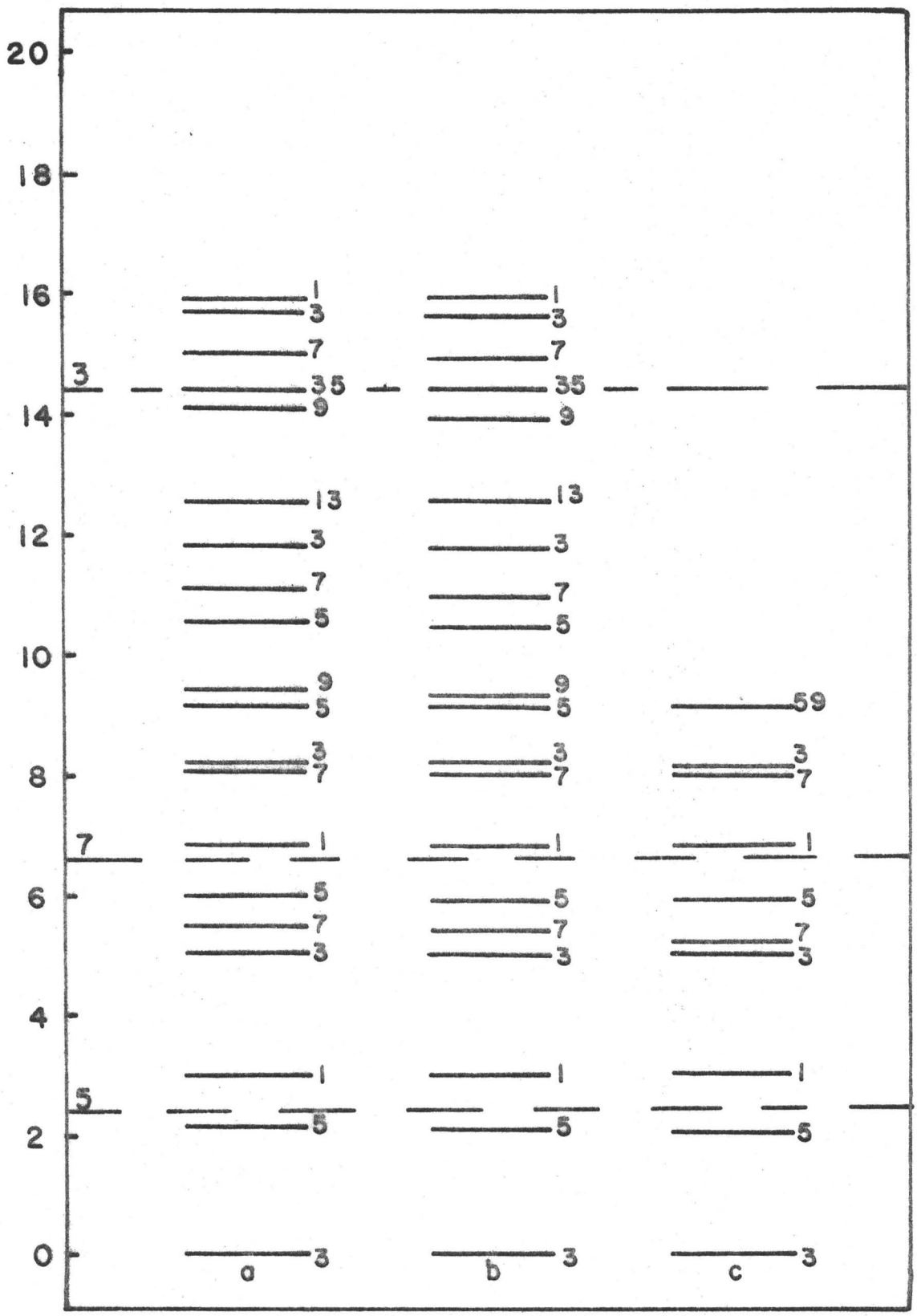
20
18
16
14
12
10
8
6
4
2
0
3
7
5
1
3
7
35
9
13
3
7
5
9
5
3
7
1
5
7
3
1
5
3
a
3
b
3
c
59
3
7
1
5
7
3
1
5
3

Figure 9.5

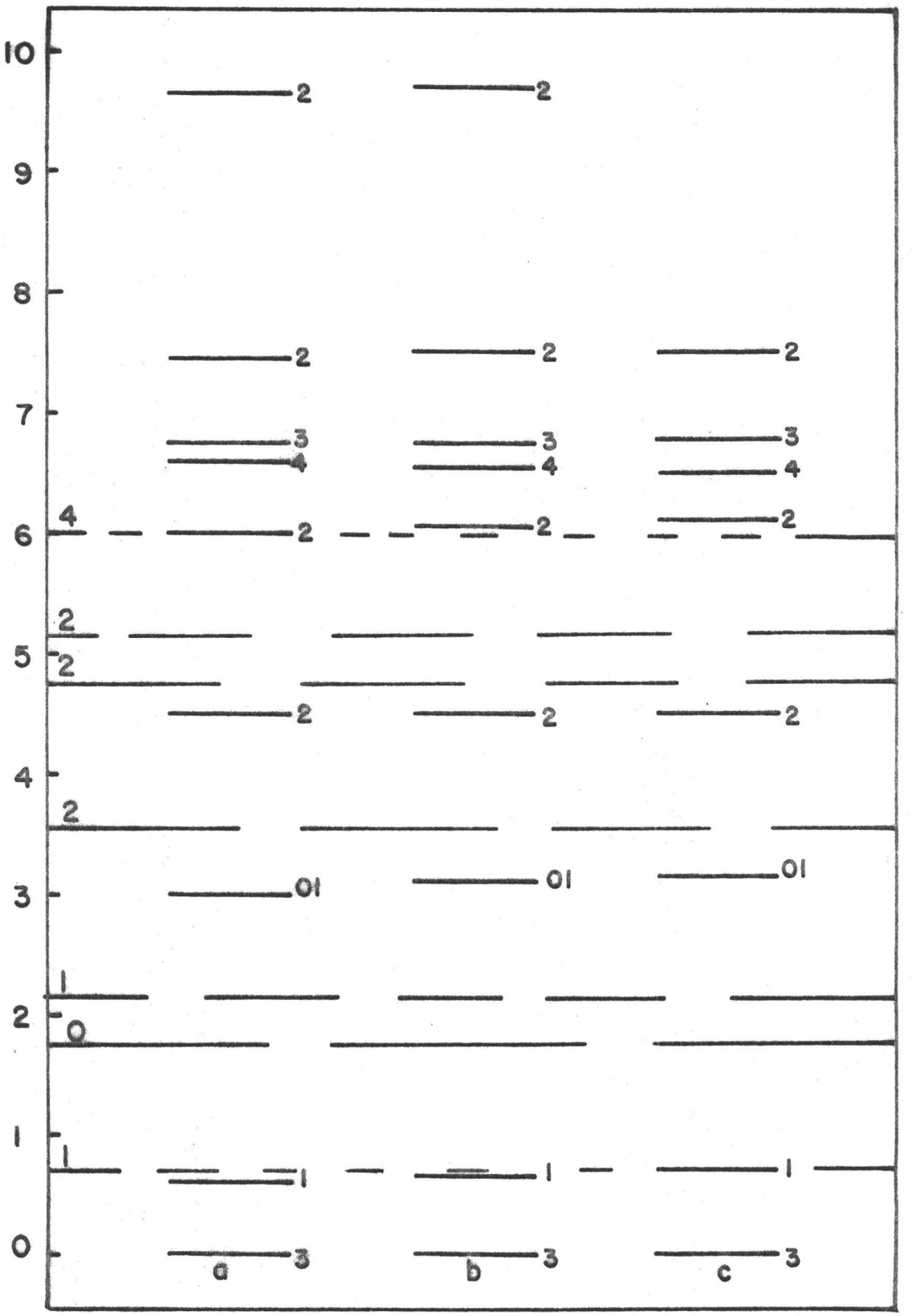
10
9
8
7
6
5
4
3
2
1
0
2
2
2
2
2
3
3
3
4
4
4
4
2
2
2
2
2
2
2
2
2
2
2
01
01
01
1
0
1
1
1
1
3
3
3
a
b
c

Figure 9.6

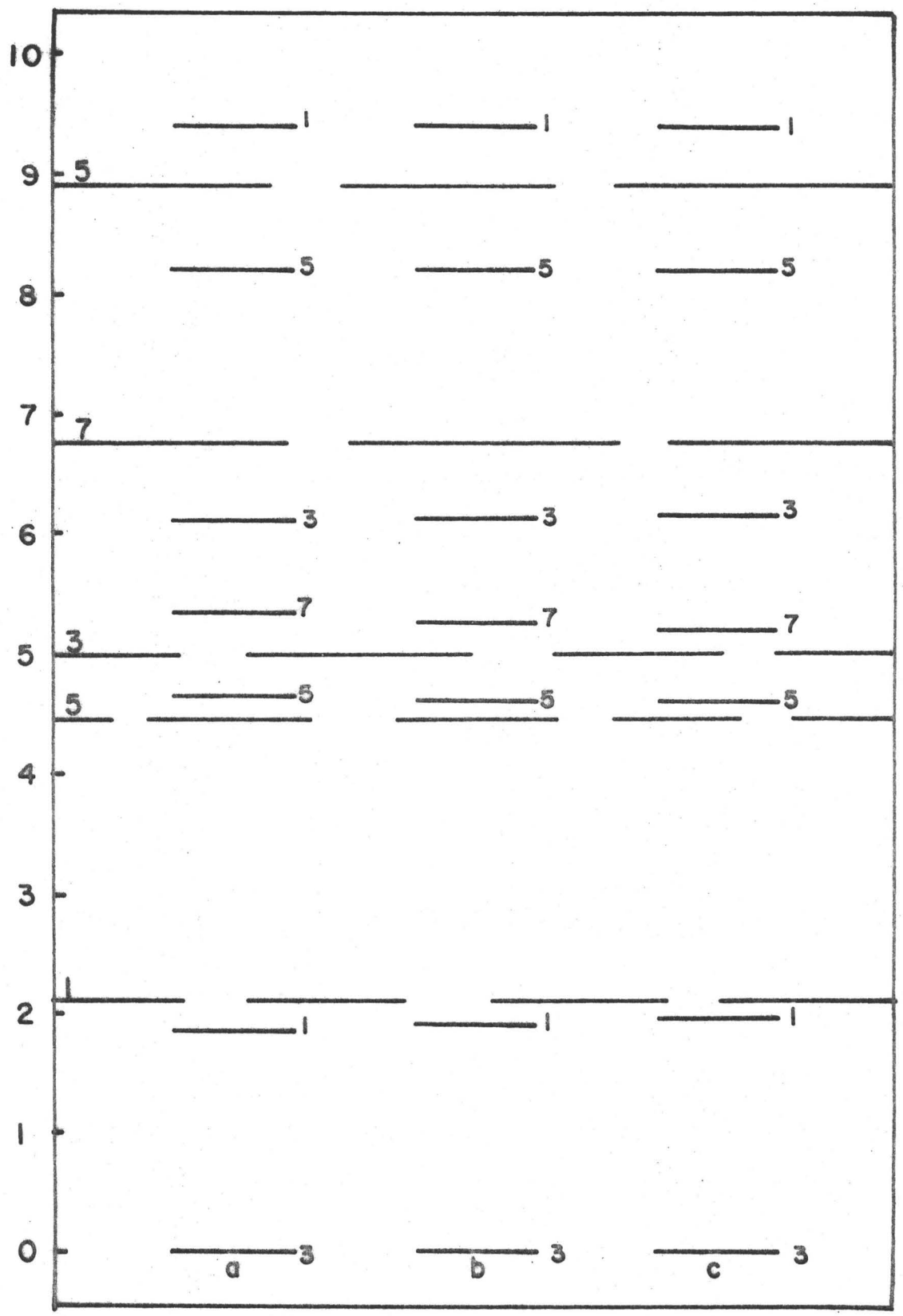

Figure 9.7

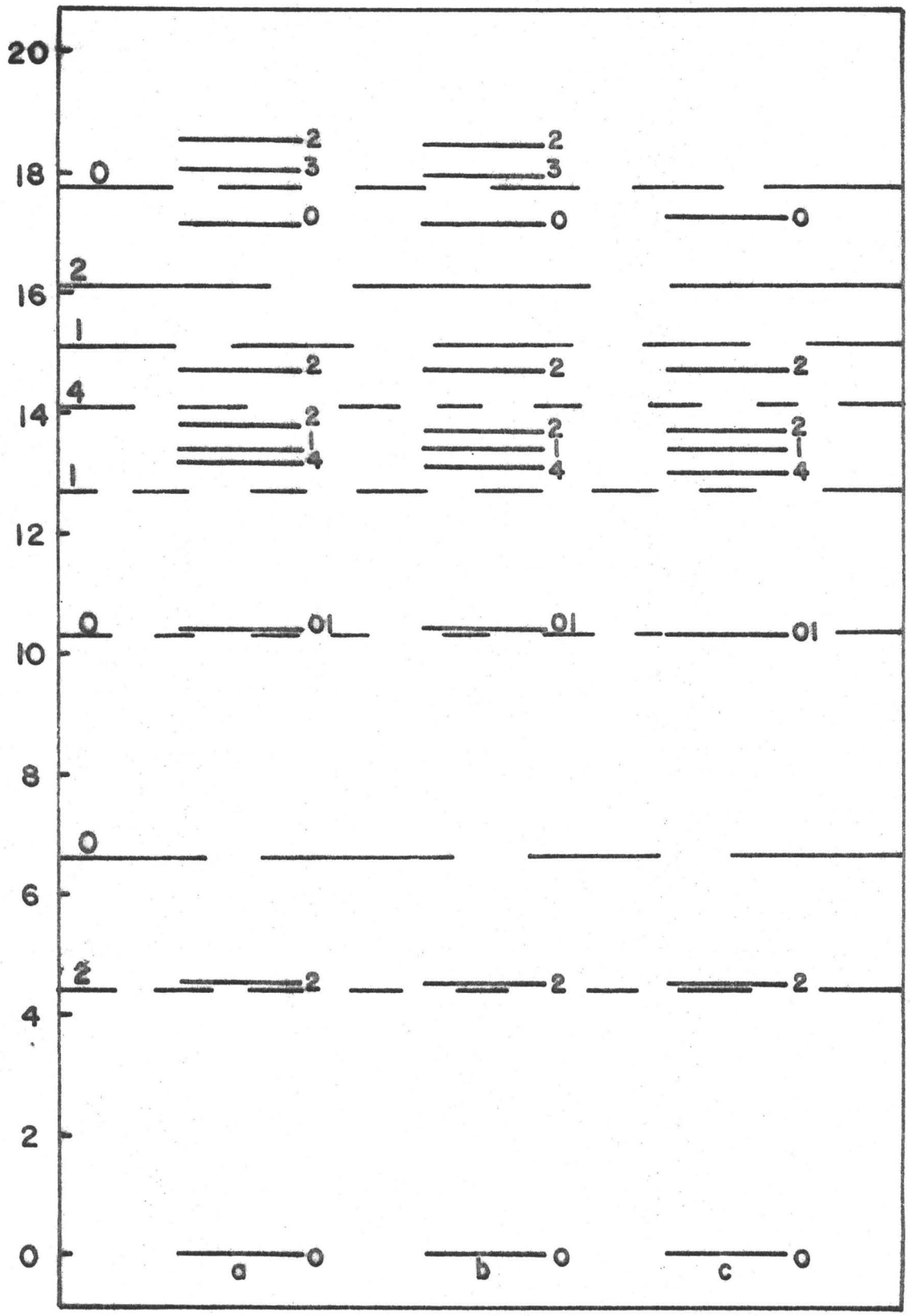

Figure 9.8

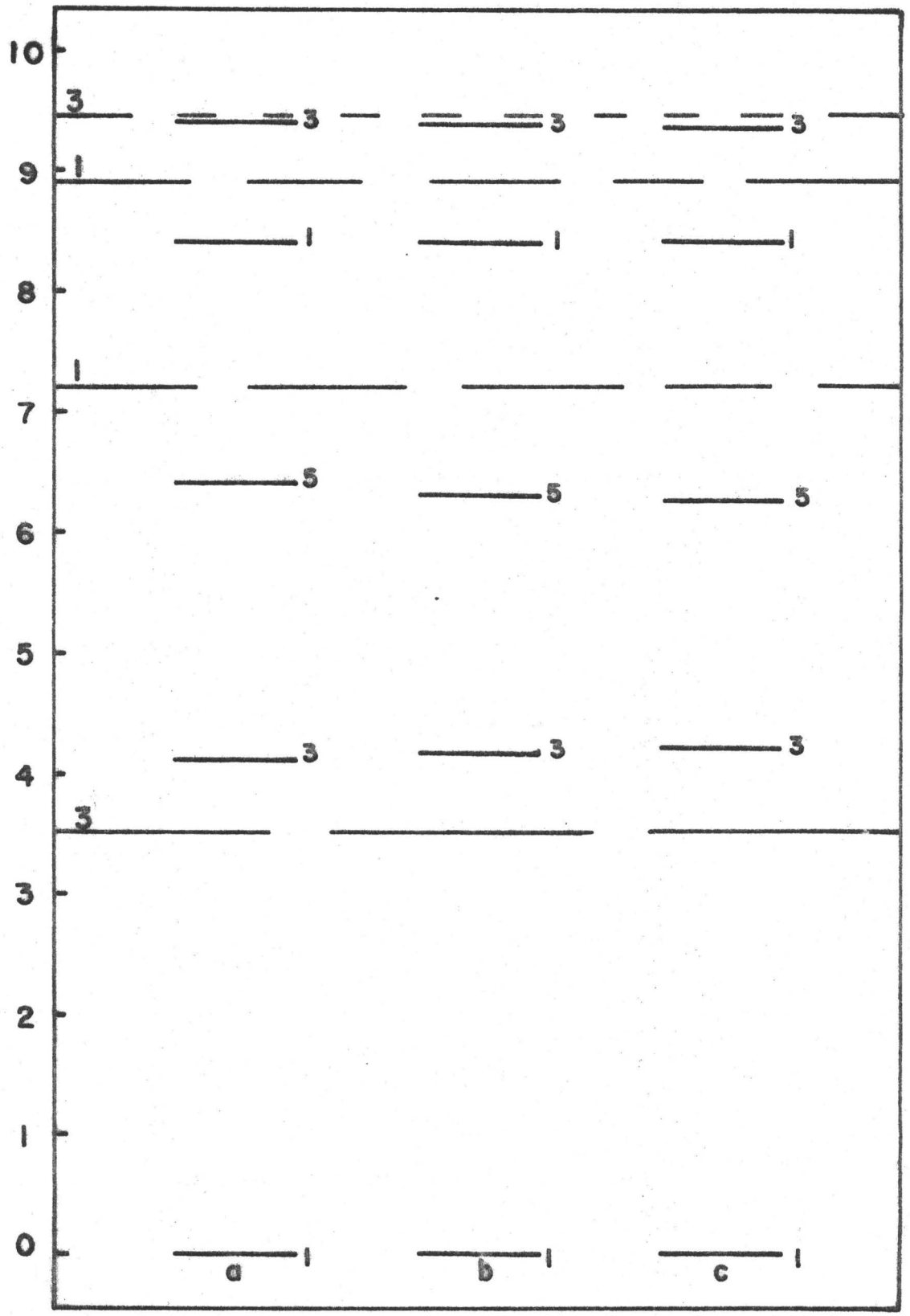

Figure 9.9

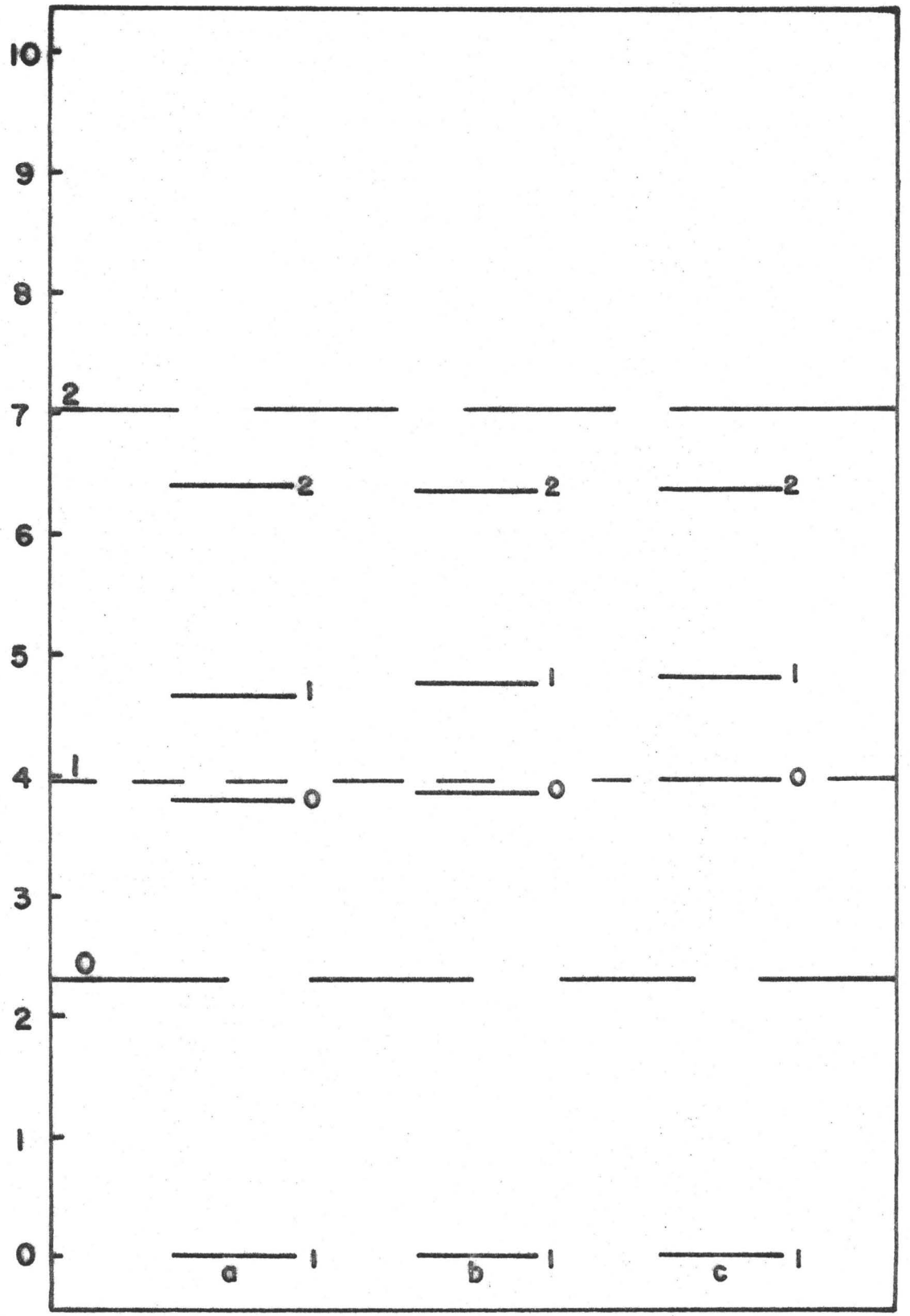

Figure 9.10

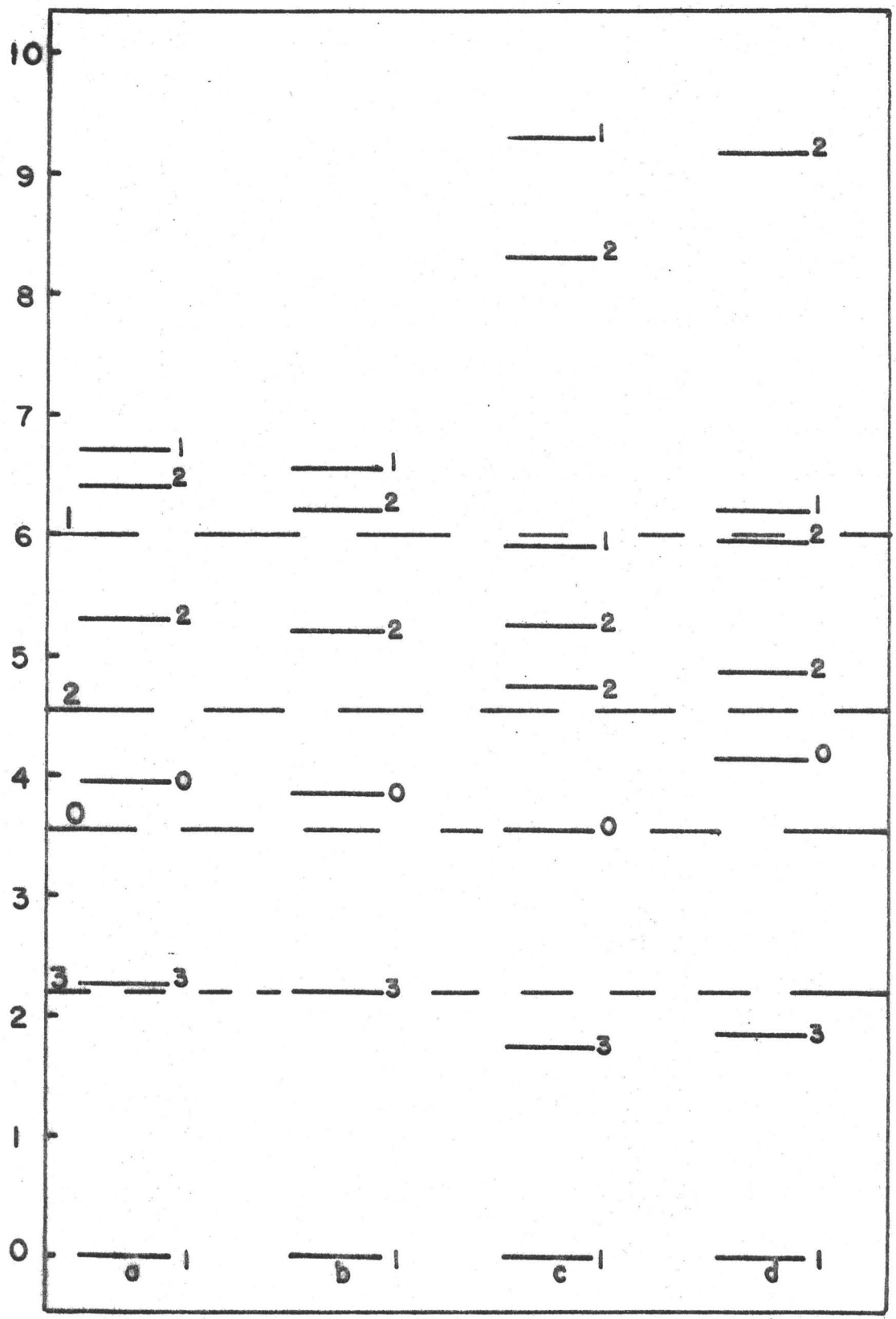

Figure 9.11

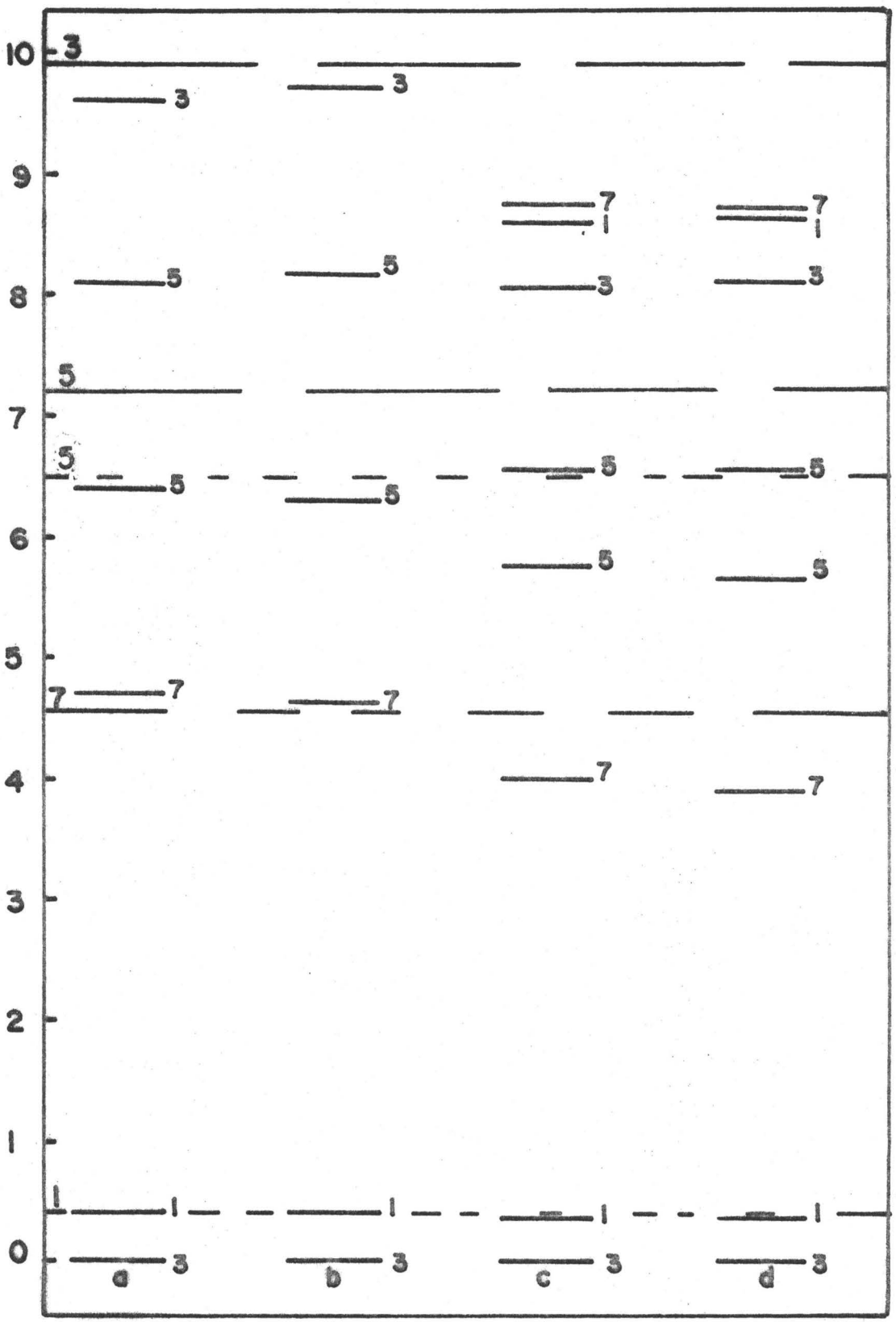

Figure 9.12

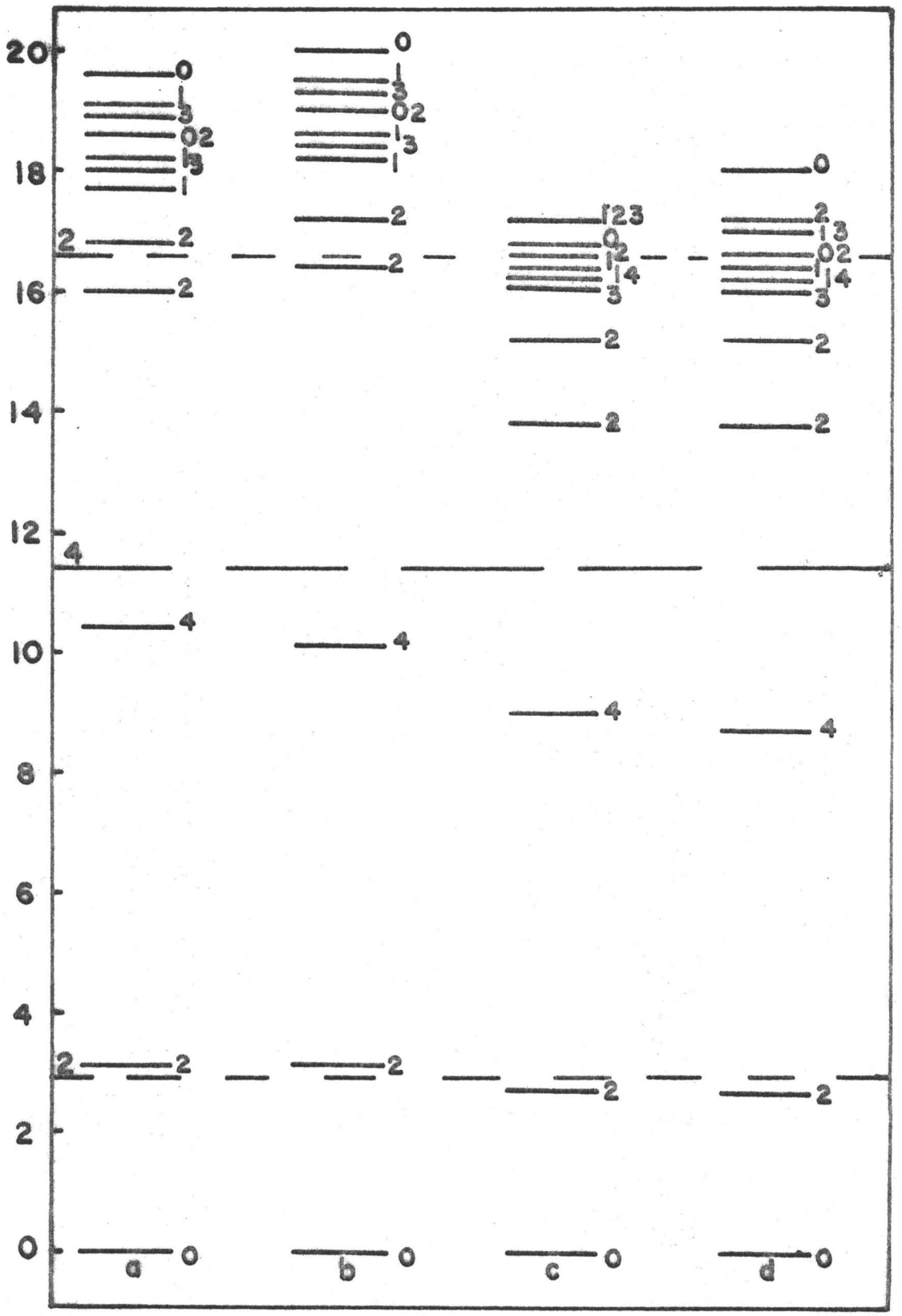

Figure 9.13

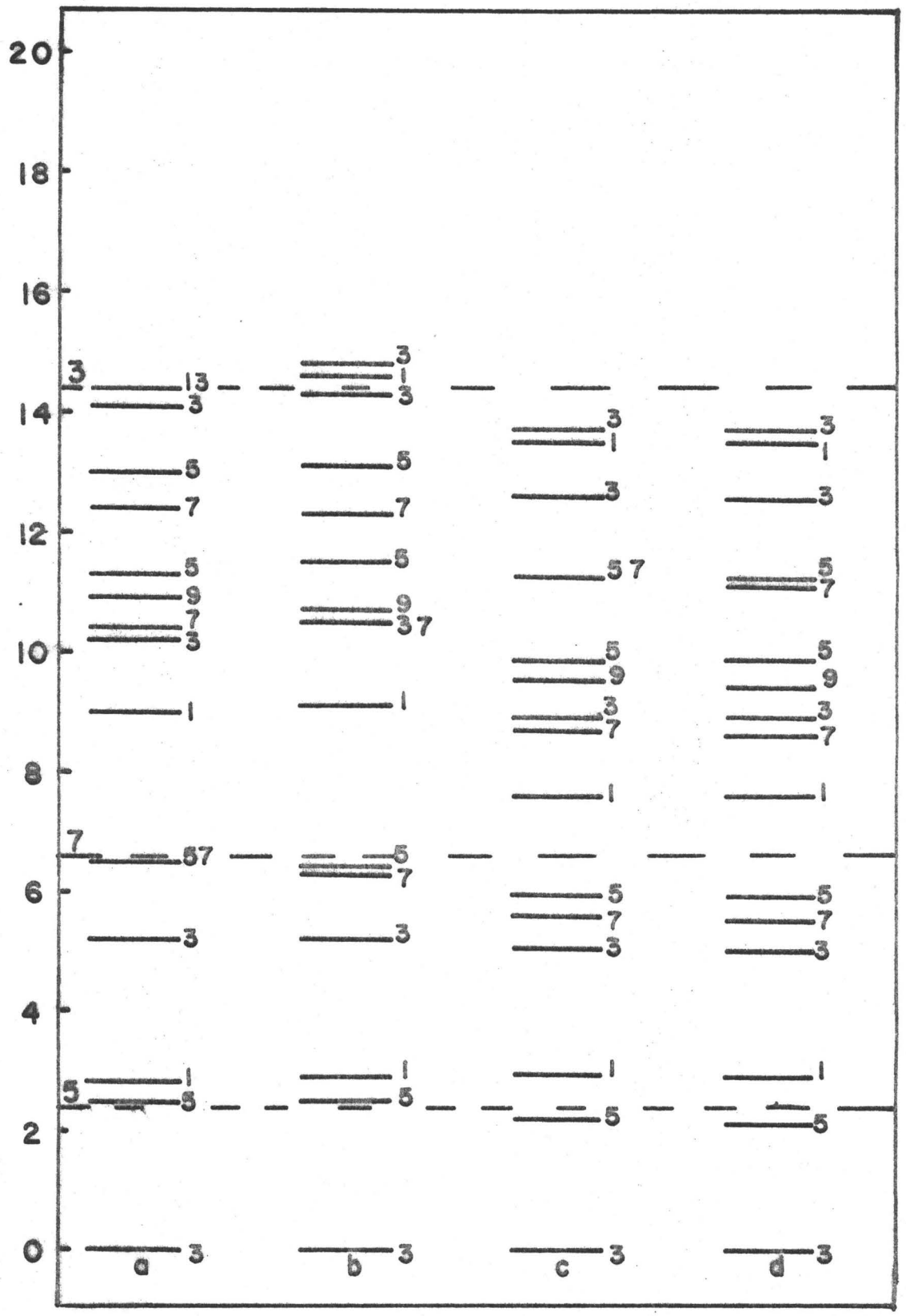

Figure 9.14

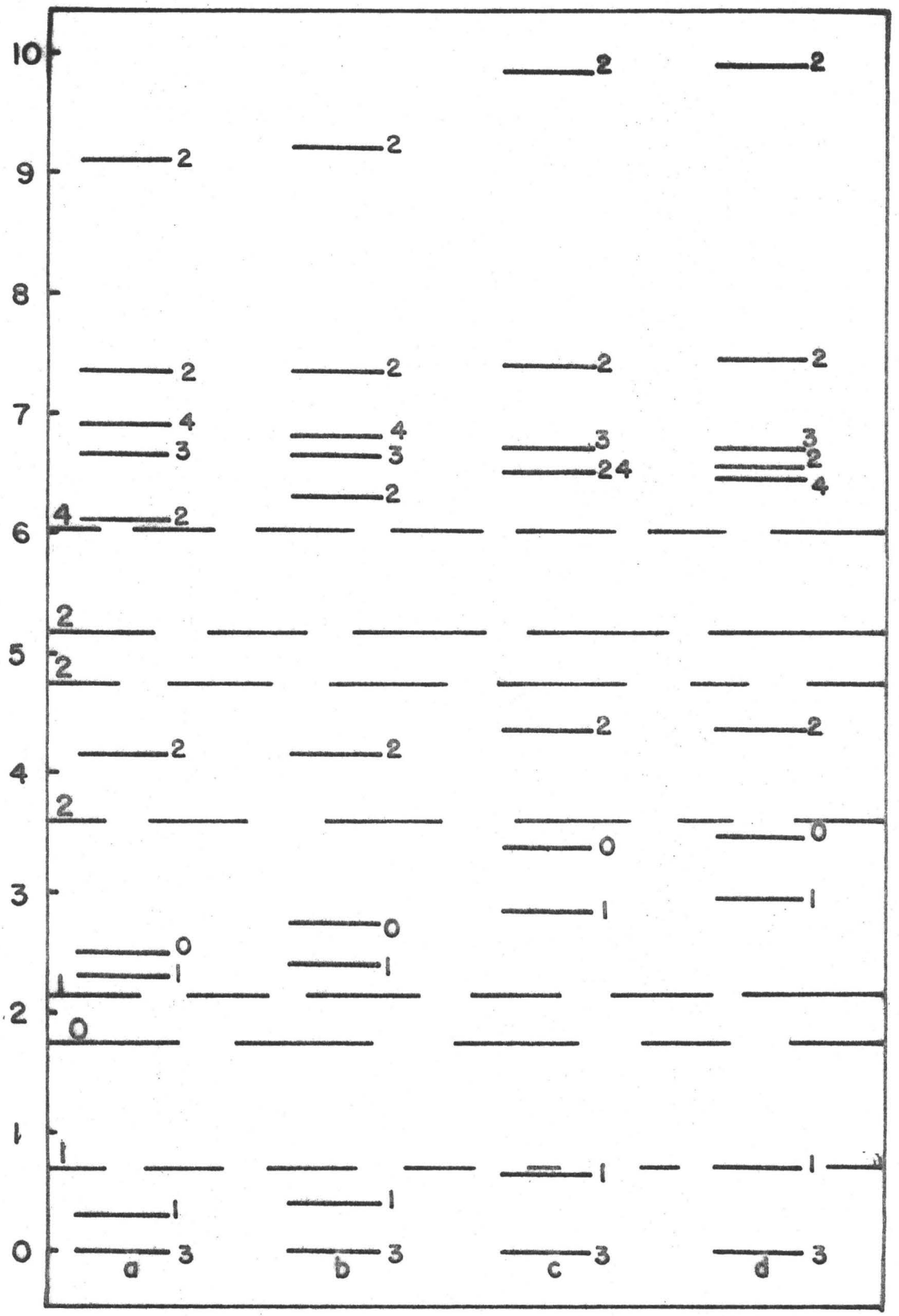

Figure 9.15

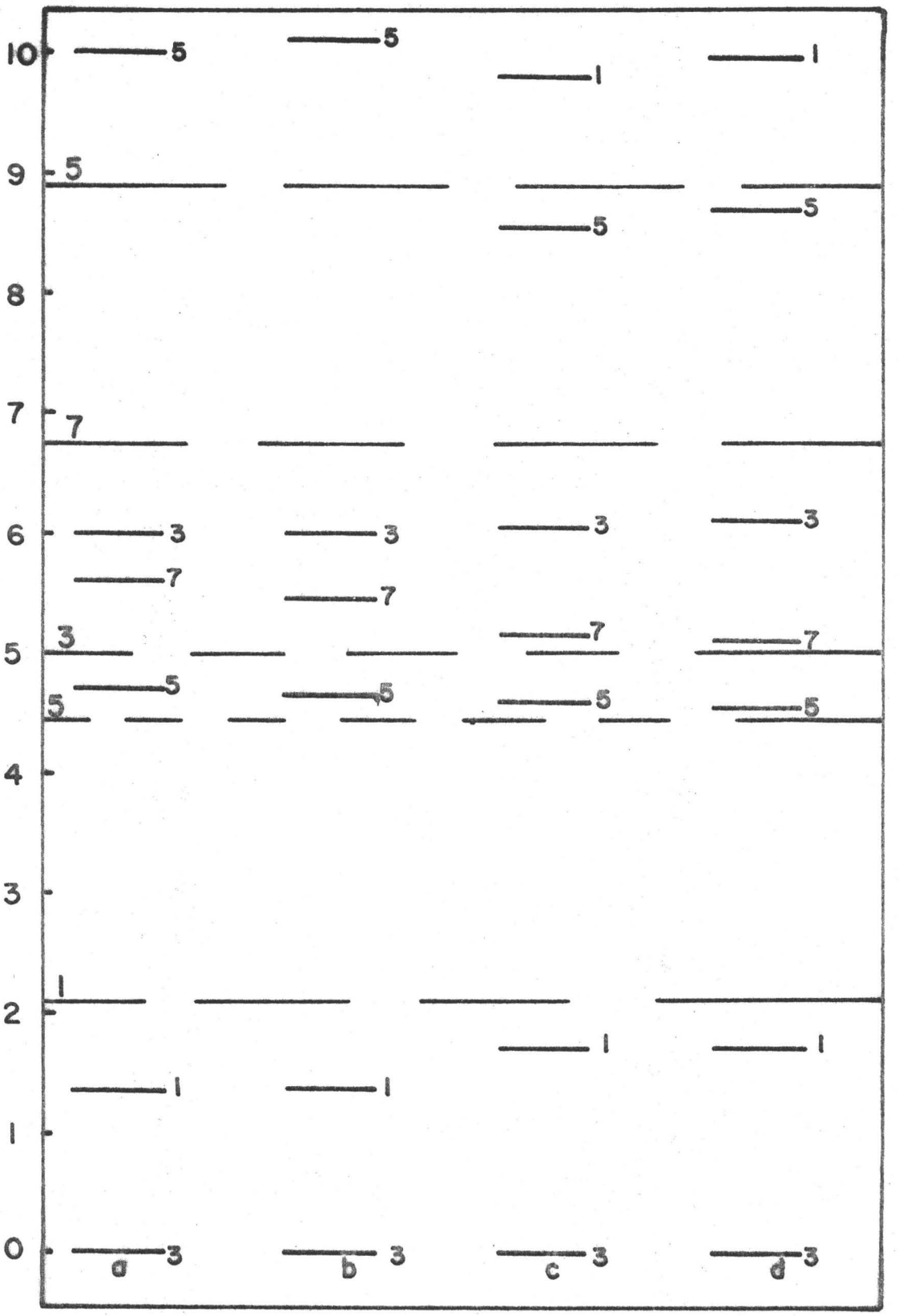

Figure 9.16

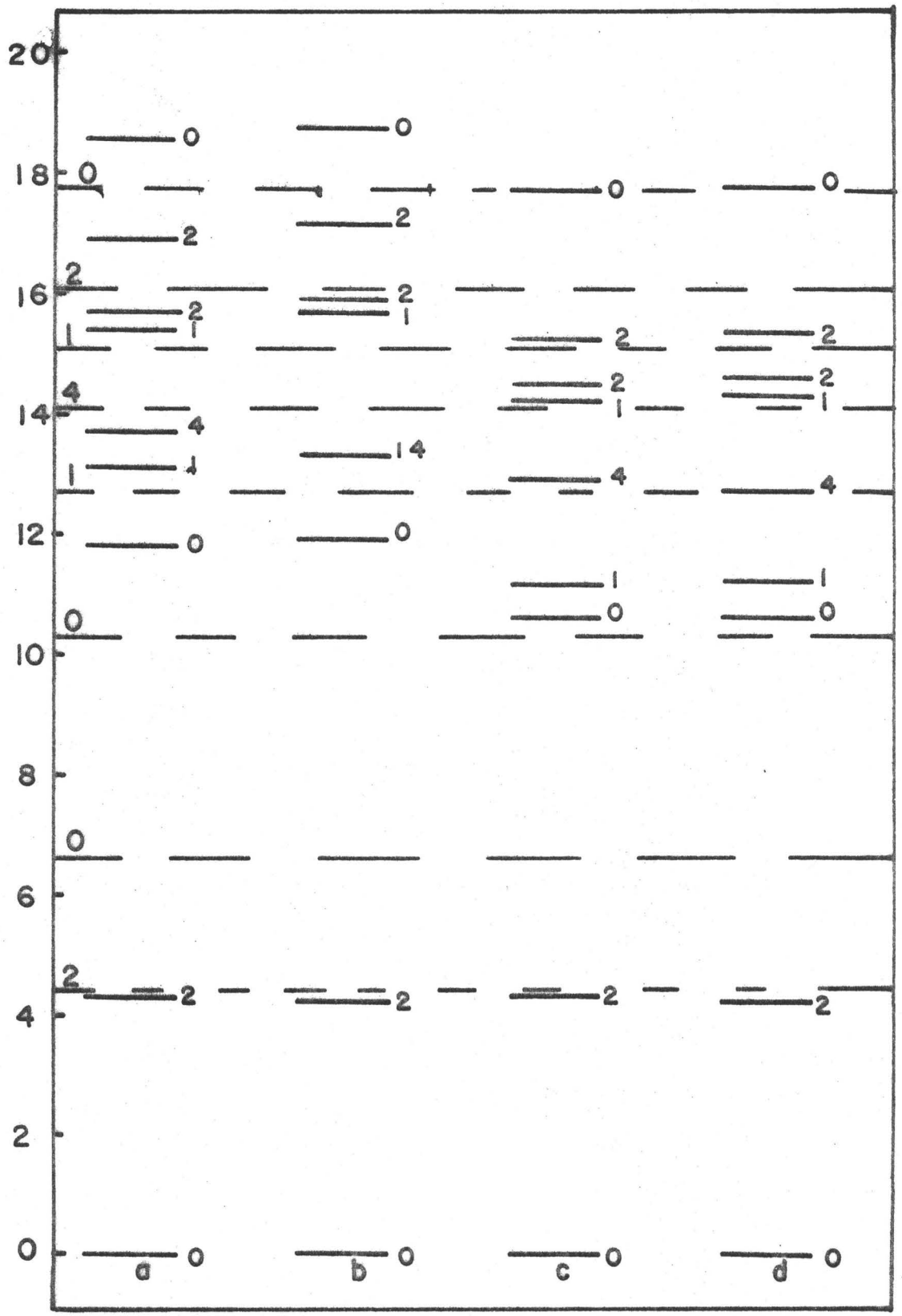

Figure 9.17

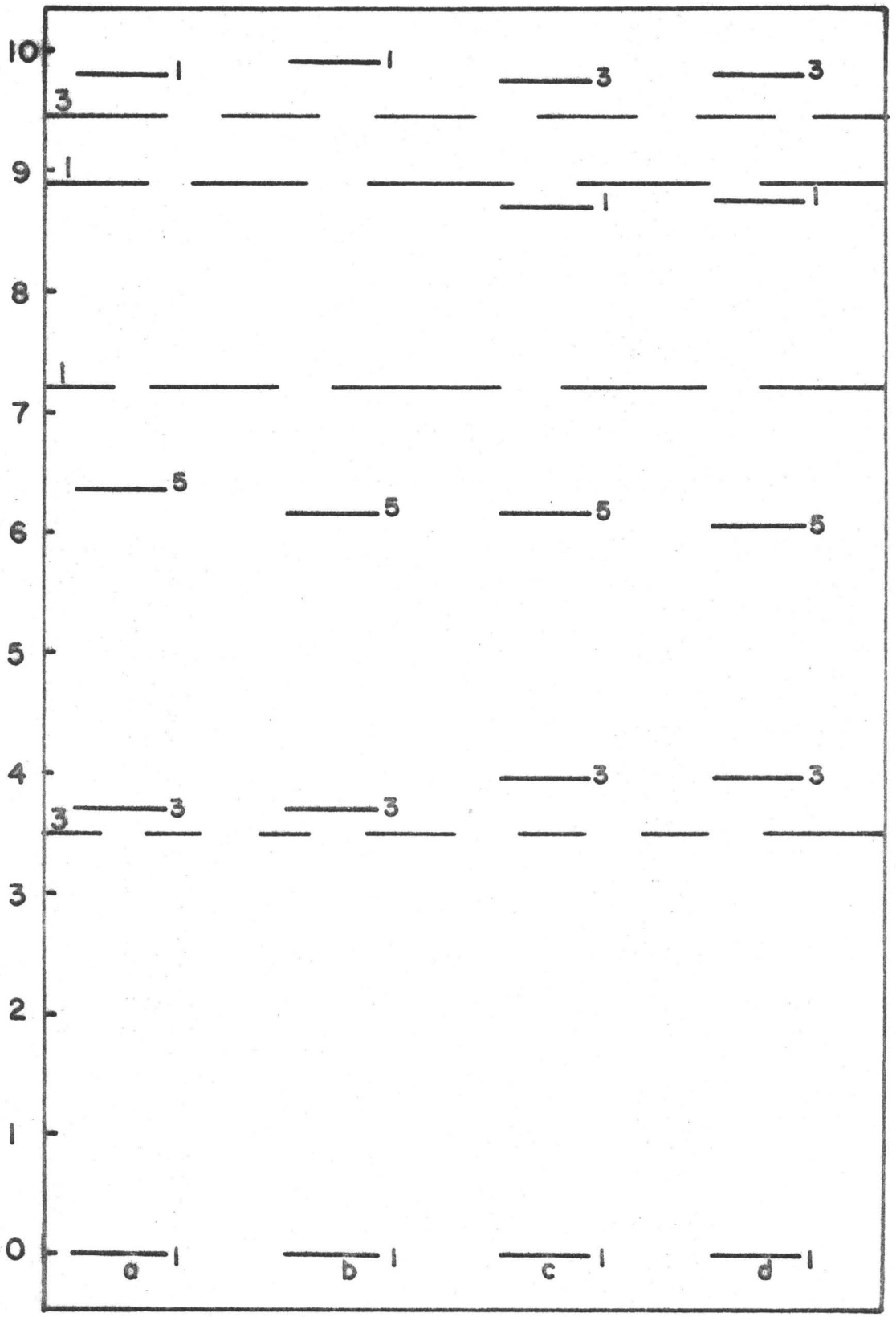

Figure 9.18

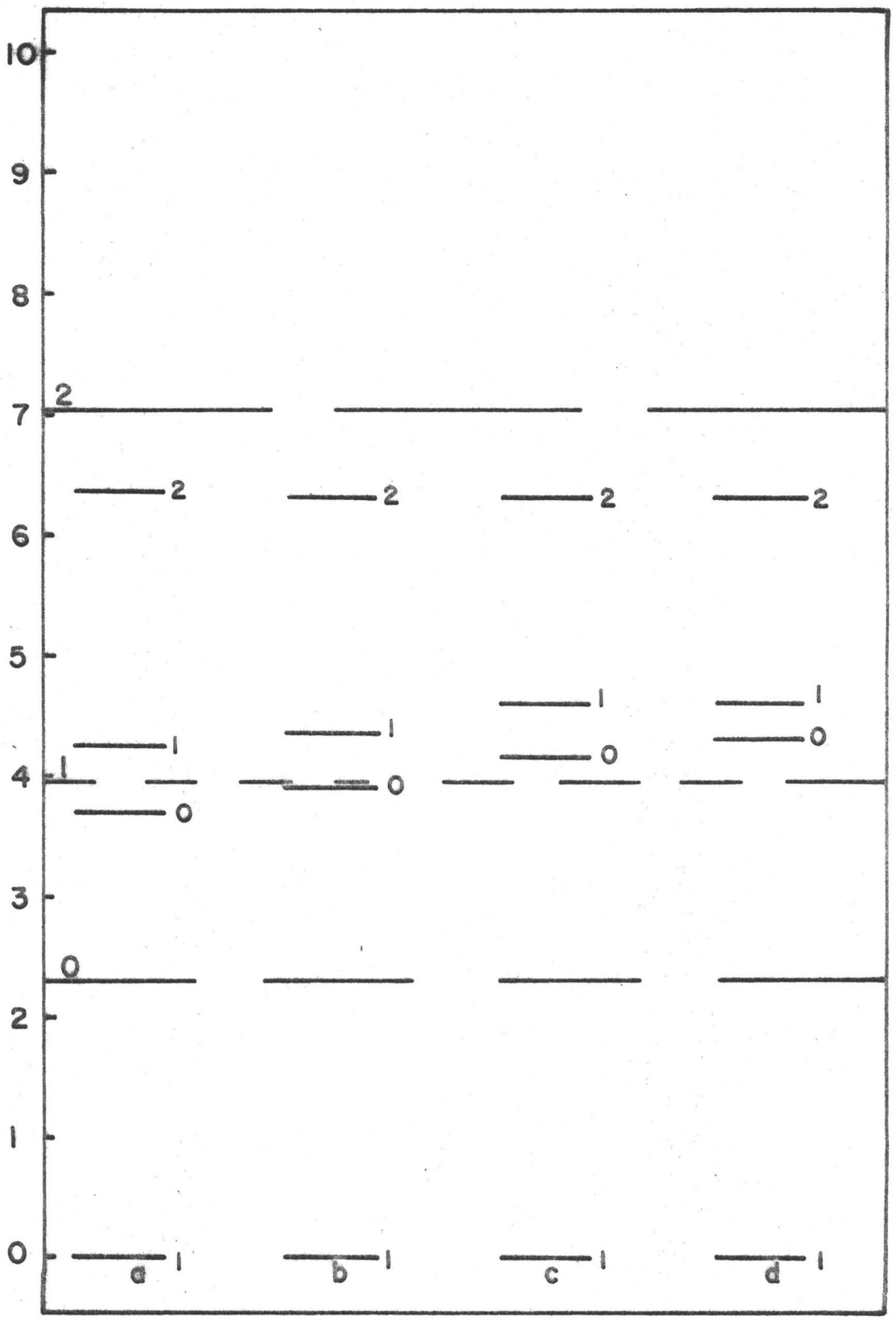

CHAPTER 10

ISOBARIC NUCLEI

In this chapter results are presented for two interactions, Interactions 36 and 37. Calculations have been performed for all possible nuclei that can be constructed from O-p shell single particle states i.e. $2<Z<6$ and $2<N<6$, where Z is the number of protons and N is the number of neutrons.

Interaction 36 was derived using the procedure developed in Chapter 7 and is considered the "best" interaction for the class of interactions having an attractive density dependence of $\rho^{1/3}$ and a repulsive density dependence of $\rho^{2/3}$. Interaction 37 has an attractive density dependence of $\rho^{-1/3}$ and a repulsive density dependence of ρ^{2}. It has the same attractive range as Interaction 36. Slightly better fits to the excited state spectra could be achieved for this form of the density dependent interaction for a different attractive range.

The relevant binding energies, root-mean-square radii and equilibrium deformation properties are listed in Table 10.1 and Table 10.2 for Interactions 36 and 37 respectively. The binding energies and root-mean-square radii are very similar for both interactions, the binding energies for Interaction 37 being slightly larger than for

Interaction 36. ^{4}He and, consequently the A=6 nuclei are overbound for both interactions whilst for the other nuclei the calculated binding energies are in fair agreement with the experimentally deduced values. The worst agreement is for the A=9 nuclear system. Because of the small binding energy for the "last nucleon" in this system, the procedure of considering the P_0 and $P_{\pm 1}$ single particle states to be in the same oscillator well is not valid (Thomas-Ehrman Effect) and thus a calculation performed using this assumption will give less than the true binding energy. The overbinding of the α-particle is a feature common to all density dependent interactions studied which fitted the ^{16}O binding energy. The situation may be that the contribution to the ^{16}O binding energy from excitations out of the O-p shell basis is proportionally greater than is the contribution to the ^{4}He binding energy from excitations out of the O-s shell basis. Crude estimates (Vol 70a) of these contributions indicate that for the form of density dependent interactions being studied, ^{16}O gains 16 Mev and ^{4}He 4 Mev when such excitations are included. As was seen in the comparative study of Interactions 10 and 14 in Chapter 5 a reduction of 16 Mev in the binding energy of ^{16}O would cause a reduction of approximately 6 Mev for the binding energy of ^{4}He.

The r.m.s. radii calculated for the two interactions are generally too large. Inclusion of states from higher

shells has the effect of significantly reducing the r.m.s. radii (Chapter 4). It would, thus, appear that although effective interactions can be found to correctly predict the binding energies of the O-p shell nuclei, other physical properties of these nuclei which are more sensitive to the admixture of states from higher shells will not be reproduced.

The equilibrium deformation results for the two interactions are very similar. Tables 10.3 and 10.4 list the deformations predicted by minimizing the kinetic energies of the ground state of the nuclei (at zero deformation) calculated using Interactions 36 and 37 with respect to the deformation. This approximation, crude as it is, correctly predicts the sign of the deformation for a great number of nuclei. Since the calculation performed is a variational calculation in which the nuclear system is constrained to be undeformed the magnitude of the deformation predicted by the minimization of the kinetic energy should be less than that actually found.

The excited state spectra calculated using Interaction 36 are illustrated in Figs. 10.1 - 10.9 and those calculated using Interaction 37 are illustrated in Figs. 10.10 - 10.18. It should be noted, at this point, that although results are quoted for ^{6}He, ^{6}Be, ^{7}He and ^{7}B, not much reliance can be placed in these results. All these nuclei are underbound with respect to ^{4}He and since, further,

they have just a few nucleons outside the α-particle core, the local minima of the binding energy in the variational space are shallow.

The excitation energies calculated for the two interactions are compared with experiment and with the results of Halbert et. al. (Hal 66) below. In Figs. 10.19 - 10.25 and 10.26 - 10.32 the excited states of the isobaric nuclei are plotted with respect to the ground state of the isobaric nucleus with the greatest binding energy, thus, enabling some tentative value to be assigned for T to some levels. This was not done for the A=6 and A=7 nuclei because of the ambiguities associated with the minimization procedure mentioned above.

A=6

The spectra for Interaction 36 is in general agreement with the experimental results and with those of Halbert et. al. (Hal 66), although the two 2^+ states are a little high. Interaction 37 gives a very poor fit to the spectra. It should be emphasized that this interaction is not the best interaction for the specific density dependencies ($\rho^{-1/3}$ and ρ^2) used. In comparison with Interaction 36 it is seen that the excited states for Interaction 37 are more widely separated, the excitation energies for the 0^+ and second 2^+, in particular, being much greater.

A=7

Again the agreement between the results for Interaction 36 and those of Halbert and experiment are good. In particular, the change in excitation energy of the $\frac{5}{2}^-$ states for the nuclei ^{7}Be and ^{7}Li is of the order of that found experimentally. For this nucleus the results for Interaction 37 are in qualitative agreement with the experimental results.

A=8

The spectra calculated for both interactions are very similar for these nuclei and both agree closely with those of Halbert and with the experimental results. The main difference is that the density dependent interactions predict a number of 0^+ states at about 19 Mev excitation energy in ^{8}Be. The closeness of the higher levels do not allow any assignment of T for any of the states by the methods used in this chapter.

A=9

Interactions 36 and 37 again predict very similar spectra which agree with the experimentally assigned levels. They both predict more low-lying levels than does Halbert's interaction. The experimental spectra of ^{9}B, in fact, does have a number of low-lying levels not seen in ^{9}Be. Once more, the closeness of the excited levels does not allow

any definite T assignments to be made.

A=10

The agreement between experiment and the results calculated for Interaction 36 is not very impressive. The spectra for Interaction 37 differs substantially from that of Interaction 36. The 2^+ state at 9 Mev, the 2^+ at 6 Mev and the 0^+ at 2 Mev in ^{10}B are assigned to be T=1 states.

A=11

Interaction 37 predicts excitation energies greater than those for Interaction 36. Both spectra calculated have the same qualitative features as that of Halbert and both agree to some extent with the experimental results. The first T=3/2 state occurs at 15 Mev excitation in ^{11}B.

A=12

Interactions 36 and 37 predict spectra that are in good agreement with the experimental situation with the exception of the low-lying 0^+ state. They predict results very different, in regard to the second 0^+ state, than does Halbert. The assignment T=1 is made to the 1^+ and 2^+ states at 15 - 16 Mev excitation in ^{12}C.

A=13

The spectral results for Interactions 36 and 37

are similar to each other and to those found by Halbert. A $\frac{7}{2}^-$ state is predicted at about 13 Mev excitation. The excitation energy of this state was found to be very dependent on the strength of the spin-orbit interaction. It is substantially lower for more positive values of C.

A=14

With the exception of the 0^+ state (assigned to be T=1) the results for Interactions 36 and 37 agree with those of Halbert.

Slightly better fits for some of the excited states (e.g. the 0^+ states of ^{10}B and ^{14}N) can be obtained by considering larger values for the Mayorana exchange strength. However, the changes are slight and do not justify fixing the Mayorana strength in this way.

Density plots for some nuclei are shown in Figs. 10.33 - 10.43. These were calculated at zero deformation for Interaction 36. The density plots for Interaction 37 were virtually identical with those for Interaction 36, having slightly higher central regions (the r.m.s. radii are smaller). The even nuclei considered are the T_z=0 nuclei. The odd nuclei have identical density plots for T_z=1 and T_z=-1. The T_z=-1 are the ones illustrated. For the lightest nuclei the densities are too high when compared with those quoted by Elton (Elt 61). However, for A>10 the densities calculated using Interaction 36 do compare well with those of Elton.

TABLE 10.1

A	Spin-Orbit Strength C(Mev)	T_z	Undeformed B.E.(Mev)	Undeformed r.m.s.(fm)	Prolate B.E.(Mev)	Prolate r.m.s.(fm)	Prolate ε	Oblate B.E.(Mev)	Oblate r.m.s.(fm)	Oblate ε
4	0.0	0	34.4	1.84						
		-2	32.30	2.50						
6	-2.0	0	34.37	2.57						
		2	30.64	2.61						
		-3	29.77	2.55				29.95	2.55	-0.15
7	-2.0	-1	38.95	2.40	41.15	2.41	0.37	39.10	2.40	-0.20
		1	37.43	2.87	39.60	2.94	0.40	37.60	2.88	-0.20
		3	26.28	2.87				26.35	2.87	-0.05
		-4	28.70	3.15						
		-2	37.82	2.52				38.50	2.52	-0.25
8	-1.5	0	52.50	2.42	56.20	2.43	0.47	53.00	2.48	-0.25
		2	34.55	2.48				35.13	2.48	-0.23
		4	22.40	2.86						
		-5	26.80	2.99						
		-3	41.63	2.60	42.00	2.61	0.17			

TABLE 10.1 - CONTINUED

9	-3.0	-1	53.70	2.51	53.00	2.52	0.37	54.38	2.51	-0.23
		1	51.83	2.51	51.15	2.51	0.33	52.50	2.51	-0.25
		3	36.10	2.63	36.50	2.63	0.15			
		5	18.15	2.99						
		-6	23.55	2.91						
		-4	42.20	2.69	42.40	2.69	0.10			
		-2	63.10	2.58	63.48	2.58	0.23	63.15	2.58	-0.15
10	-5.0	0	63.43	2.56	64.75	2.57	0.27	64.70	2.57	-0.27
		2	58.93	2.59	59.20	2.59	0.23	59.00	2.60	-0.15
		4	34.20	2.72	34.40	2.72	0.10			
		6	12.63	3.00						
		-5	40.50	2.73	40.70	2.73	0.07			
		-3	61.15	2.64	61.25	2.64	0.15			
11	-4.75	-1	73.45	2.60				74.40	2.60	-0.27
		1	71.60	2.60				72.05	2.61	-0.27
		3	54.34	2.66	54.40	2.66	0.10			
		5	29.50	2.78	29.65	2.78	0.06			

TABLE 10.1 - CONTINUED

		-4	62.86	2.69	62.90	2.69	0.05		
		-2	77.42	2.65				77.55	2.65	-0.07
12	-5.50	0	90.00	2.61	90.15	2.61	0.07	90.15	2.62	-0.25
		2	72.30	2.65				72.40	2.65	-0.07
		4	52.95	2.71	53.00	2.71	0.05			
		-3	80.20	2.69				80.30	2.69	-0.04
13	-5.00	-1	93.30	2.65	93.35	2.65	0.04			
		1	90.56	2.66	90.60	2.66	0.04			
		3	71.64	2.69				71.70	2.69	-0.04
		-2	101.20	2.68	101.30	2.68	0.02			
14	-5.00	0	101.90	2.67						
		2	95.60	2.69	95.63	2.69	0.02			
16	0.00	0	127.15	2.70						

TABLE 10.2

A	Spin-Orbit Strength, C(Mev)	T_z	Undeformed B.E.(Mev)	Undeformed r.m.s.(fm)	Prolate B.E.(Mev)	Prolate r.m.s.(fm)	Prolate ε	Oblate B.E.(Mev)	Oblate r.m.s.(fm)	Oblate ε
4	0.00	0	34.15	1.83						
		-2	33.10	2.33						
6	-1.75	0	35.41	2.42				35.45	2.42	-0.05
		2	28.31	2.57	28.70	2.34	0.3	28.35	2.33	-0.15
		-3	26.90	2.49						
7	-1.50	-1	39.15	2.39	41.18	2.40	0.40	39.40	2.39	-0.20
		1	37.63	2.40	39.65	2.41	0.40	37.90	2.40	-0.20
		3	22.74	2.51						
		-4	31.91	4.36						
		-2	38.30	2.51				38.85	2.51	-0.23
8	-1.50	0	53.20	2.39	57.00	2.40	-0.47	53.80	2.40	-0.28
		2	34.95	2.55				35.45	2.55	-0.23
		4	27.96	4.22						

TABLE 10.2 - CONTINUED

		-5	26.40	3.15						
		-3	41.80	2.60	42.20	2.60	0.16			
9	-3.00	-1	54.38	2.49	53.68	2.49	0.37	55.08	2.50	-0.27
		1	52.48	2.49	51.85	2.49	0.33	53.20	2.50	-0.27
		3	36.25	2.61	36.60	2.61	0.18			
		5	18.30	2.99						
		-6	23.20	2.96						
		-4	41.60	2.69	41.80	2.69	0.10			
		-2	62.41	2.56	62.78	2.56	0.25	62.55	2.56	-0.20
10	-4.50	0	63.28	2.53	63.80	2.55	0.27	63.90	2.54	-0.32
		2	58.18	2.57	58.55	2.57	0.25	58.35	2.57	-0.23
		4	33.55	2.70	33.70	2.70	0.10			
		6	12.43	3.02						
		-5	40.50	2.72	40.60	2.72	0.05			
		-3	62.35	2.62	62.45	2.62	0.12			
11	-5.25	-1	75.60	2.58				76.50	2.58	-0.30
		1	73.20	2.58				74.10	2.59	-0.30

TABLE 10.2 - CONTINUED

		3	55.50	2.64	55.55	2.64	0.05		
		5	28.75	2.78	28.80	2.78	0.05		
		-4	62.97	2.67	63.00	2.67	0.02		
		-2	78.30	2.63				78.45	2.63	-0.06
12	-5.50	0	91.17	2.59	91.20	2.59	0.08	91.55	2.60	-0.30
		2	73.16	2.64				73.30	1.64	-0.07
		4	53.00	2.69						
		-3	80.70	2.68				80.80	2.68	-0.05
13	-5.00	-1	94.40	2.63	94.45	2.63	0.01			
		1	91.65	2.64	91.70	2.64	0.02			
		3	72.40	2.68				72.46	2.68	-0.05
		-2	102.10	2.67						
14	-5.00	0	103.25	2.65						
		2	96.12	2.67						
16	0.00	0	127.90	2.70						

TABLE 10.3

A	T_z	ε	A	T_z	ε
				-6	0.00
				-4	0.08
	-2	0.00		-2	0.00
6	0	-0.02	10	0	-0.21
	2	0.00		2	0.00
				4	0.08
	-3	-0.05		6	0.00
7	-1	0.16			
	1	0.16		-5	0.06
	3	-0.02		-3	0.00
			11	-1	-0.12
	-4	0.00		1	-0.12
	-2	-0.14		3	0.00
8	0	0.00		5	0.06
	2	-0.14			
	4	0.00		-4	0.00
				-2	-0.07
	-5	0.00	12	0	0.00
	-3	0.11		2	-0.07
9	-1	-0.14		4	0.00
	1	-0.14			
	3	0.11		-3	-0.06
	5	0.00	13	-1	0.00
				1	0.00
				3	-0.06

TABLE 10.3 - CONTINUED

A	T_z	ε
	2	0.00
14	0	-0.01
	-2	0.00

TABLE 10.4

A	T_z	ε	A	T_z	ε
	-2	0.00		2	0.00
6	0	-0.01		4	0.08
	2	0.00		6	0.00
	-3	-0.11		-5	0.06
7	-1	0.15		-3	0.00
	1	0.15	11	-1	-0.12
	3	-0.11		1	-0.12
				3	0.00
	-4	0.00		5	0.06
	-2	-0.14			
8	0	0.00		-4	0.00
	2	-0.14		-2	-0.07
	4	0.00	12	0	0.00
				2	-0.07
	-5	0.00		4	0.00
	-3	0.10			
	-1	-0.14		-3	-0.06
	1	-0.14	13	-1	0.00
	3	0.10		1	0.00
	5	0.00		3	-0.06
	-6	0.00		-2	0.00
	-4	0.08	14	0	-0.01
	-2	0.00		2	0.00
10	0	-0.21			

FIGURE CAPTIONS

For all figures, excitation energy (in Mev), is plotted at the left of the figure. The full lines represent the excited levels with the spin J (for even nuclei or 2J (for odd nuclei) appearing to the right of the level.

Figures 10.1 - 10.9 illustrate the excited state spectra for the O-p shell nuclei calculated for Interaction 36.

Figure 10.1 Excited state spectra with C = -2.0 Mev for (a) ^{6}Be, (b) ^{6}Li, (c) ^{6}He.

Figure 10.2 Excited State Spectra with C = -2.0 Mev for (a) ^{7}B, (b) ^{7}Be, (c) ^{7}Li, (d) ^{7}He.

Figure 10.3 Excited State Spectra with C = -1.5 Mev for (a) ^{8}C, (b) ^{8}B, (c) ^{8}Be, (d) ^{8}Li, (e) ^{8}He.

Figure 10.4 Excited State Spectra with C = -3.0 Mev for (a) ^{9}N, (b) ^{9}C, (c) ^{9}B, (d) ^{9}Be, (e) ^{9}Li, (f) ^{9}He.

Figure 10.5 Excited State Spectra with C = -5.0 Mev for (a) ^{10}N, (b) ^{10}C, (c) ^{10}B, (d) ^{10}Be, (e) ^{10}Li.

Figure 10.6 Excited State Spectra with C = -4.75 Mev for (a) ^{11}O, (b) ^{11}N, (c) ^{11}C, (d) ^{11}B, (e) ^{11}Be, (f) ^{11}Li.

Figure 10.7 Excited State Spectra with C = -5.5 Mev for (a) ^{12}O, (b) ^{12}N, (c) ^{12}C, (d) ^{12}B, (e) ^{12}Be.

Figure 10.8 Excited State Spectra with C = -5.0 Mev for (a) ^{13}O, (b) ^{13}N, (c) ^{13}C, (d) ^{13}B.

Figure 10.9 Excited State Spectra with C = -5.0 Mev for (a) ^{14}O, (b) ^{14}N, (c) ^{14}C.

Figures 10.10 - 10.18 plot the excited state spectra of the O-p shell nuclei calculated using Interaction 37.

Figure 10.10 Excited State Spectra with C = -1.75 Mev for (a) ^{6}Be, (b) ^{6}Li, (c) ^{6}He.

Figure 10.11 Excited State Spectra with C = -1.5 Mev for (a) ^{7}B, (b) ^{7}Be, (c) ^{7}Li, (d) ^{7}He.

Figure 10.12 Excited State Spectra with C = -1.5 Mev for (a) ^{8}C, (b) ^{8}B, (c) ^{8}Be, (d) ^{8}Li, (e) ^{8}He.

Figure 10.13 Excited State Spectra with C = -3.0 Mev for (a) ^{9}N, (b) ^{9}C, (c) ^{9}B, (d) ^{9}Be, (e) ^{9}Li, (f) ^{9}He.

Figure 10.14 Excited State Spectra with C = -4.5 Mev for (a) ^{10}N, (b) ^{10}C, (c) ^{10}B, (d) ^{10}Be, (e) ^{10}Li.

Figure 10.15 Excited State Spectra with C = -5.25 Mev for (a) ^{11}O, (b) ^{11}N, (c) ^{11}C, (d) ^{11}B, (e) ^{11}Be, (f) ^{11}Li.

Figure 10.16 Excited State Spectra with C = -5.5 Mev for (a) ^{12}O, (b) ^{12}N, (c) ^{12}C, (d) ^{12}B, (e) ^{12}Be.

Figure 10.17 Excited State Spectra with C = -5.0 Mev for (a) ^{13}O, (b) ^{13}N, (c) ^{13}C, (d) ^{13}B.

Figure 10.18 Excited State Spectra with C = -5.0 Mev for (a) ^{14}O, (b) ^{14}N, (c) ^{14}C.

Figures 10.19 - 10.25 show the relative excitation energies of the levels of the isobaric nuclei calculated for Interaction 36.

Figure 10.19 Relative excitation energies for (a) ^{8}Li, (b) ^{8}Be, (c) ^{8}B.

Figure 10.20 Relative excitation energies for (a) ^{9}Li, (b) ^{9}Be, (c) ^{9}B, (d) ^{9}C.

Figure 10.21 Relative excitation energies for (a) ^{10}Li, (b) ^{10}Be, (c) ^{10}B, (d) ^{10}C.

Figure 10.22 Relative excitation energies for (a) ^{11}Be, (b) ^{11}B, (c) ^{11}C, (d) ^{11}N.

Figure 10.23 Relative excitation energies for (a) ^{12}B, (b) ^{12}C, (c) ^{12}N.

Figure 10.24 Relative excitation energies for (a) ^{13}B, (b) ^{13}C, (c) ^{13}N.

Figure 10.25 Relative excitation energies for (a) ^{14}C, (b) ^{14}N, (c) ^{14}O.

Figures 10.26 - 10.32 show the relative excitation energies of the levels of the isobaric nuclei calculated for Interaction 37.

Figure 10.26 Relative excitation energies for (a) ^{8}Li, (b) ^{8}Be, (c) ^{8}B.

Figure 10.27 Relative excitation energies for (a) ^{9}Li, (b) ^{9}Be, (c) ^{9}B, (d) ^{9}C.

Figure 10.28 Relative excitation energies for (a) ^{10}Li, (b) ^{10}Be, (c) ^{10}B, (d) ^{10}C.

Figure 10.29 Relative excitation energies for (a) ^{11}Be, (b) ^{11}B, (c) ^{11}C, (d) ^{11}N.

Figure 10.30 Relative excitation energies for (a) ^{12}B, (b) ^{12}C, (c) ^{12}N.

Figure 10.31 Relative excitation energies for (a) ^{13}B, (b) ^{13}C, (c) ^{13}N.

Figure 10.32 Relative excitation energies for (a) ^{14}C, (b) ^{14}N, (c) ^{14}O.

Figures 10.33 - 10.43 show plots of the density of various nuclei calculated at zero deformation by Interaction 36.

Figure 10.33 Plot of density for ^{4}He.

Figure 10.34 Plot of density for ^{6}Li.

Figure 10.35 Plot of density for ^{7}Li.

Figure 10.36 Plot of density for ^{8}Be.

Figure 10.37 Plot of density for ^{9}Be.

Figure 10.38 Plot of density for ^{10}B.

Figure 10.39 Plot of density for ^{11}B.

Figure 10.40 Plot of density for ^{12}C.

Figure 10.41 Plot of density for ^{13}C.

Figure 10.42 Plot of density for ^{14}N.

Figure 10.43 Plot of density for ^{16}O.

Figure 10.1

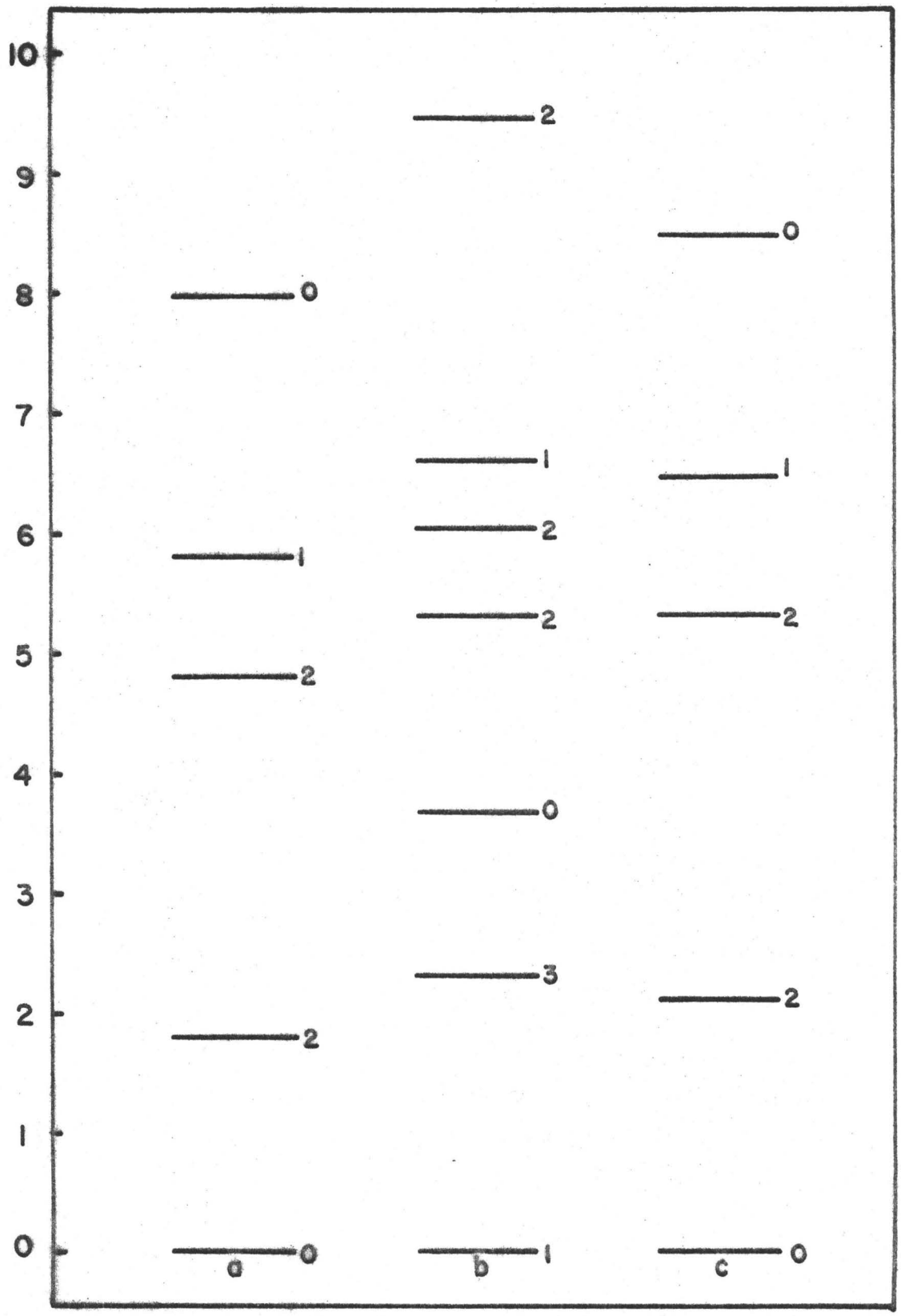

Figure 10.2

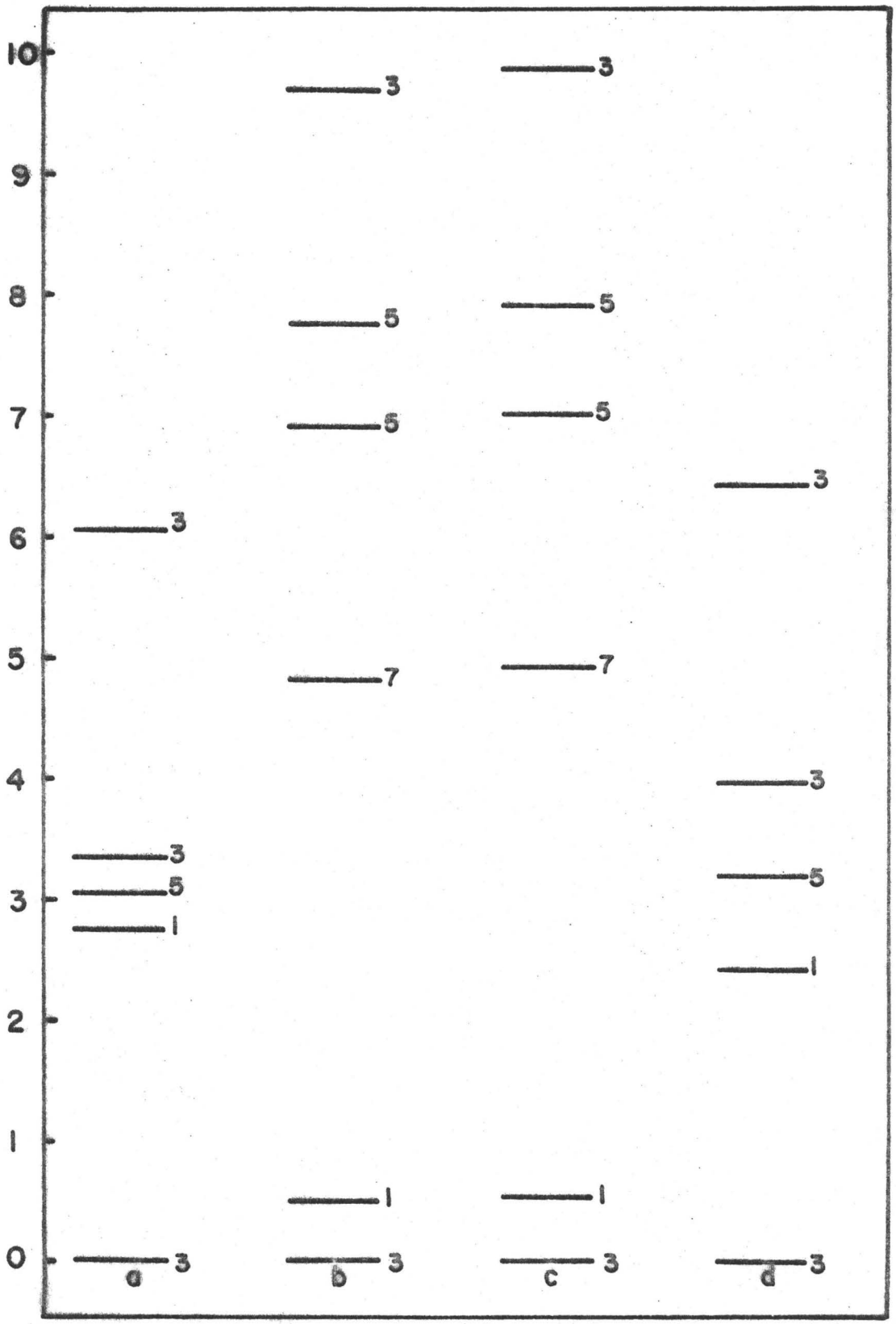

Figure 10.3

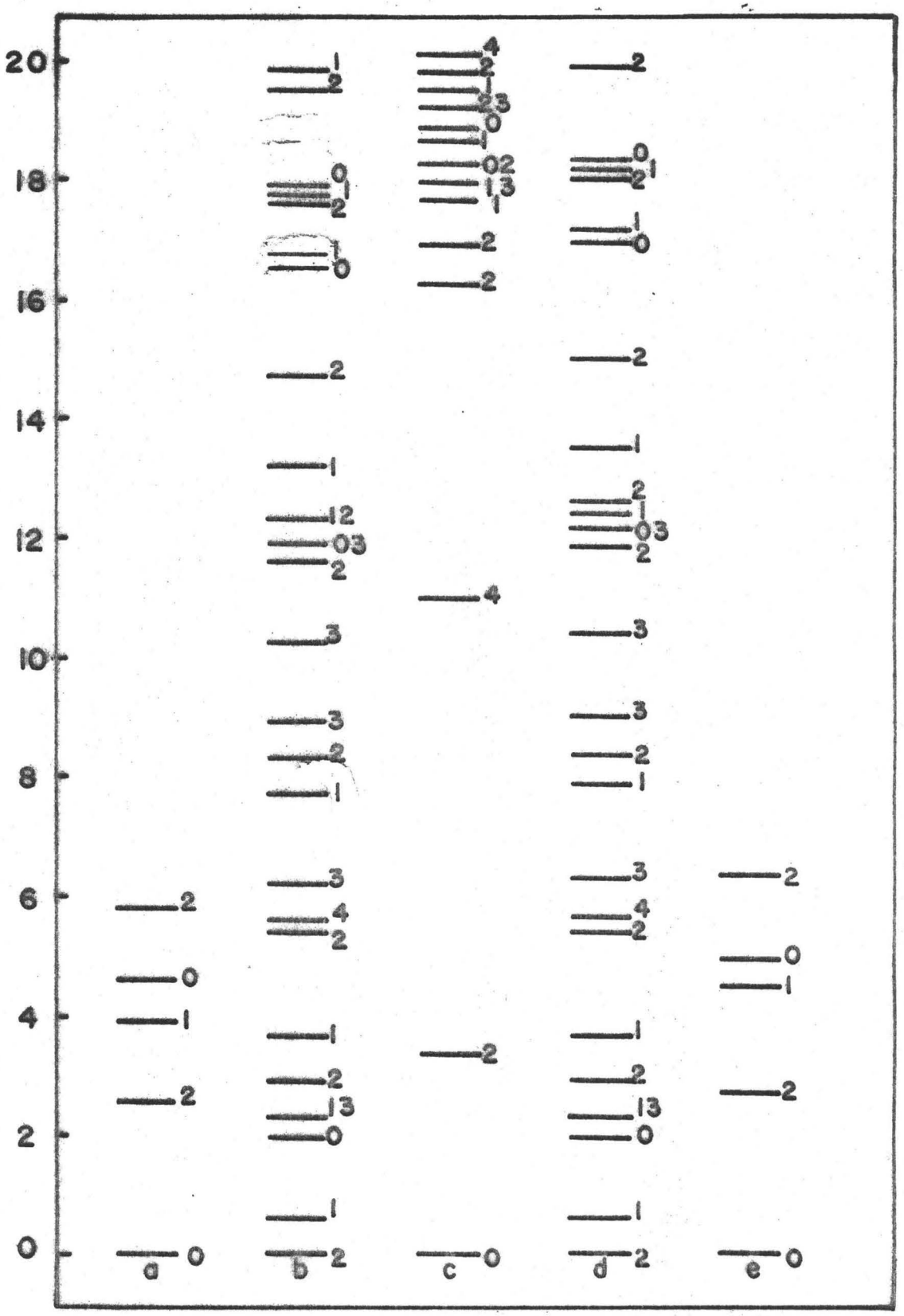

Figure 10.4

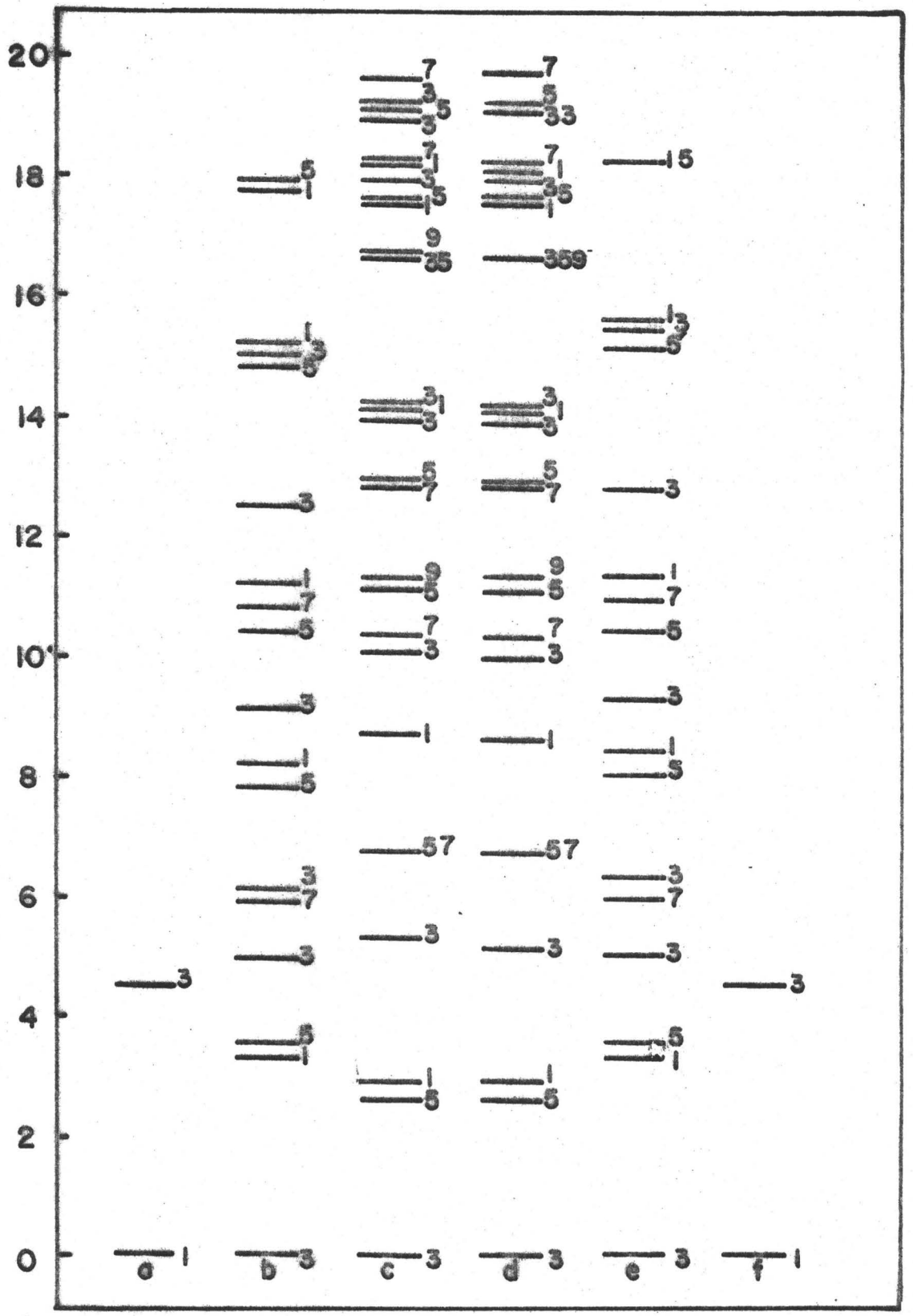

Figure 10.5

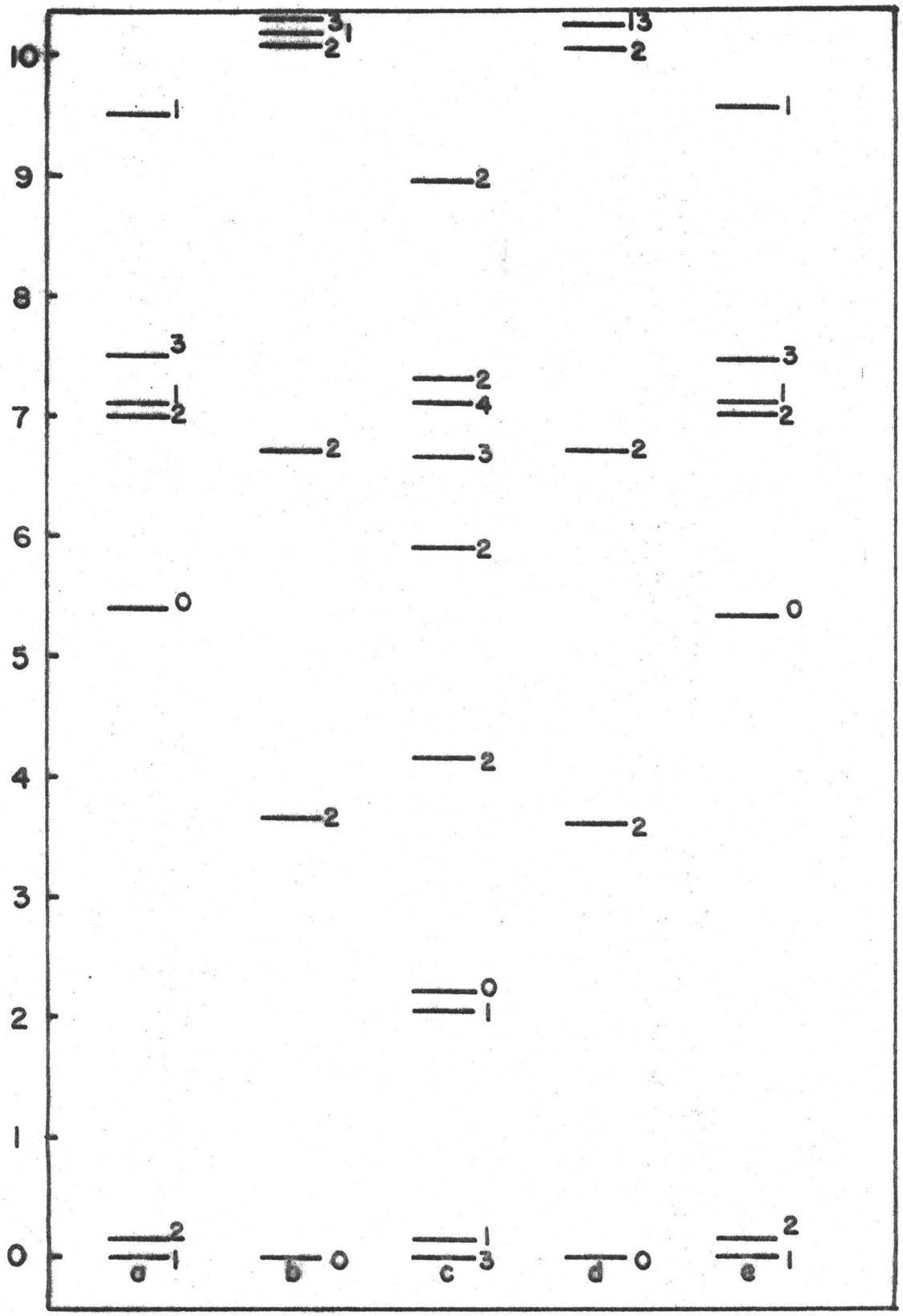

Figure 10.6

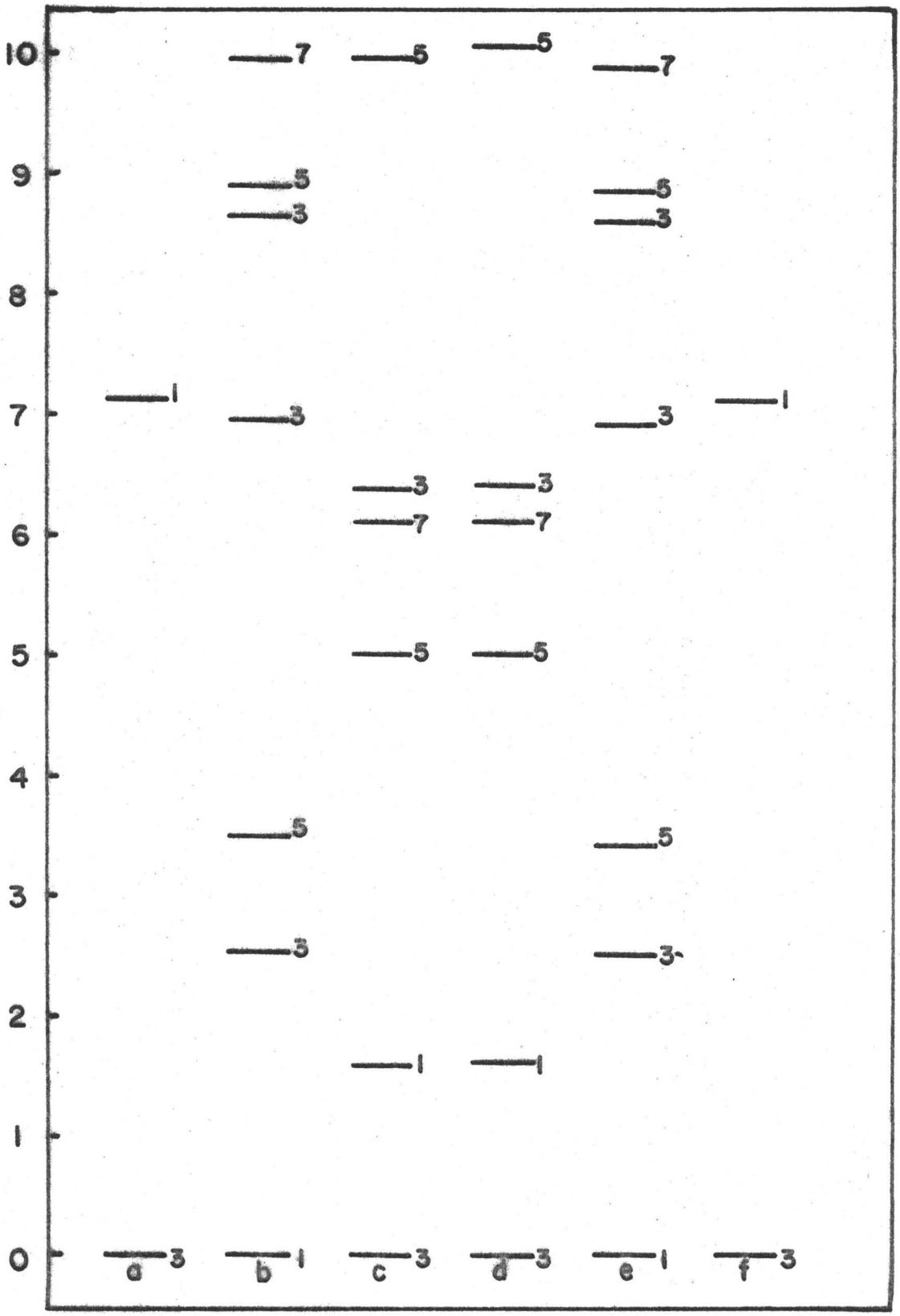

Figure 10.7

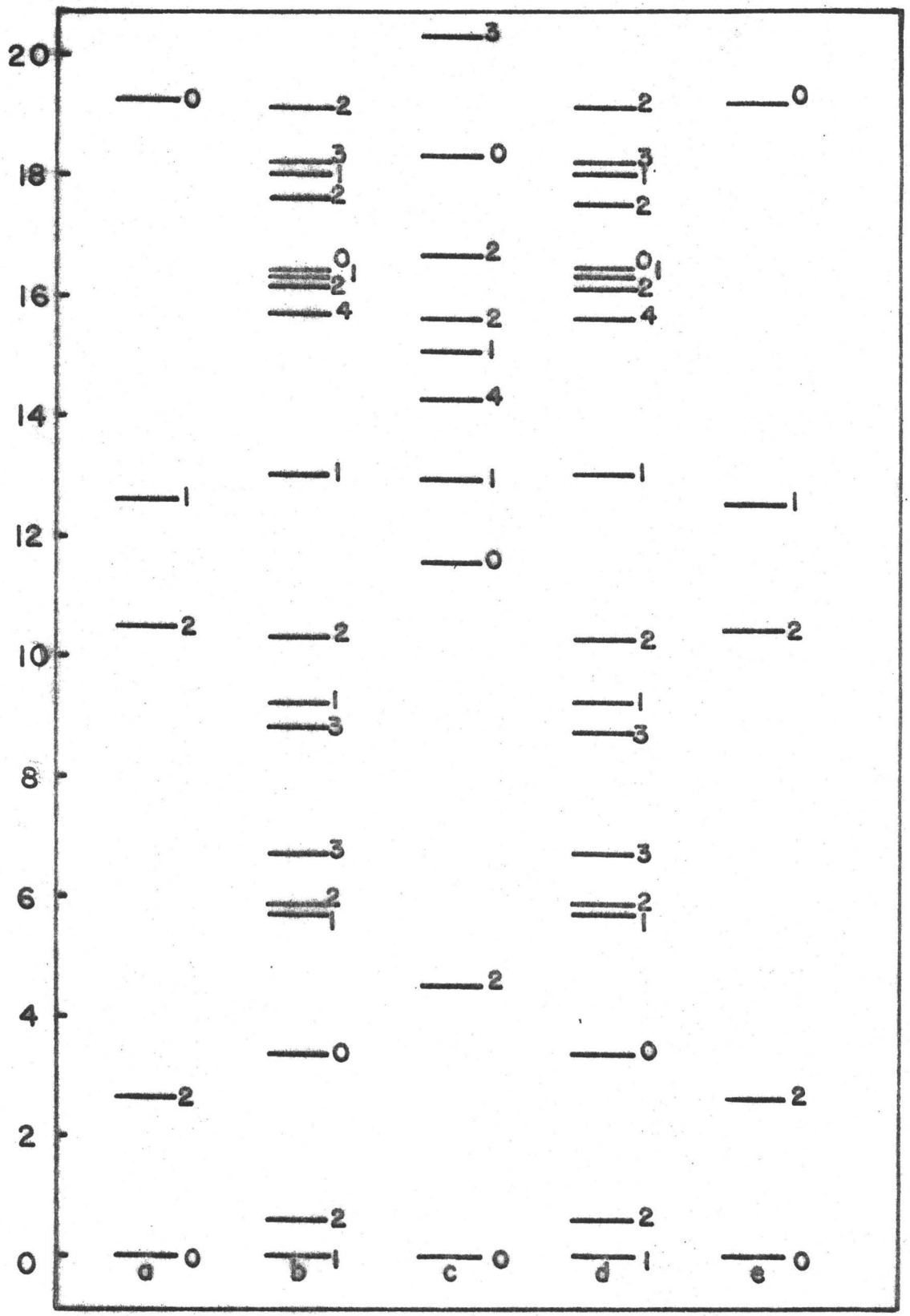

Figure 10.8

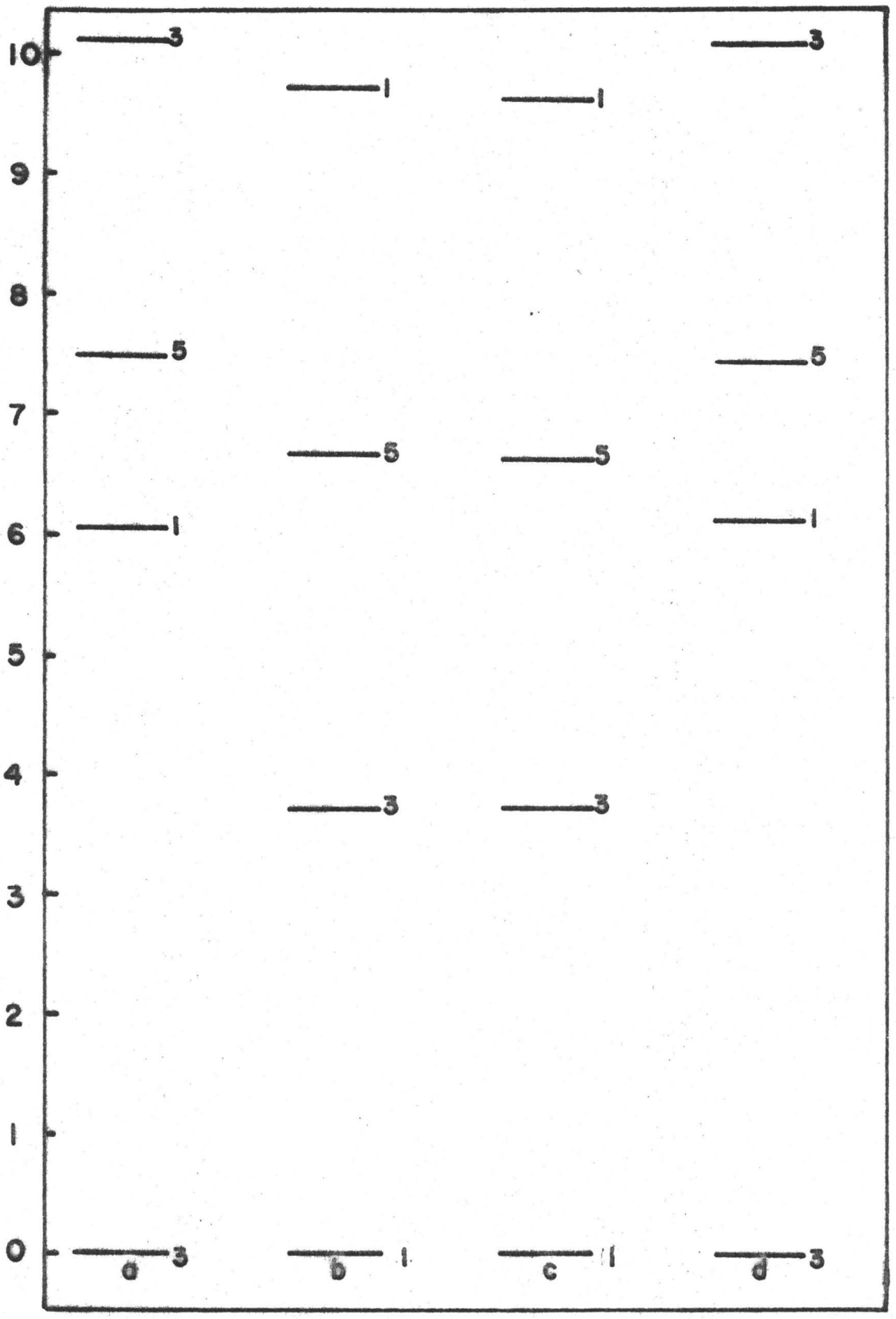

Figure 10.9

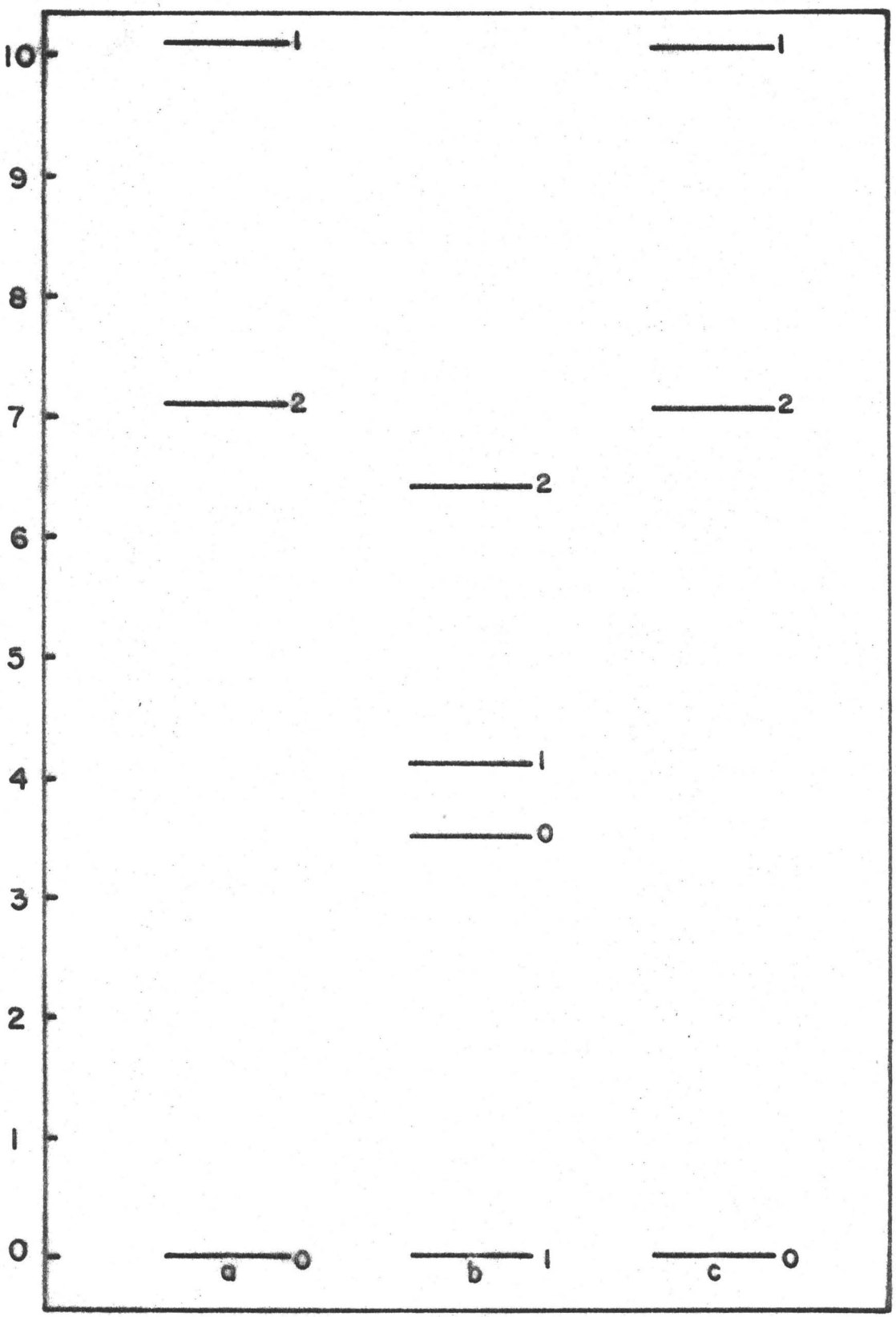

Figure 10.10

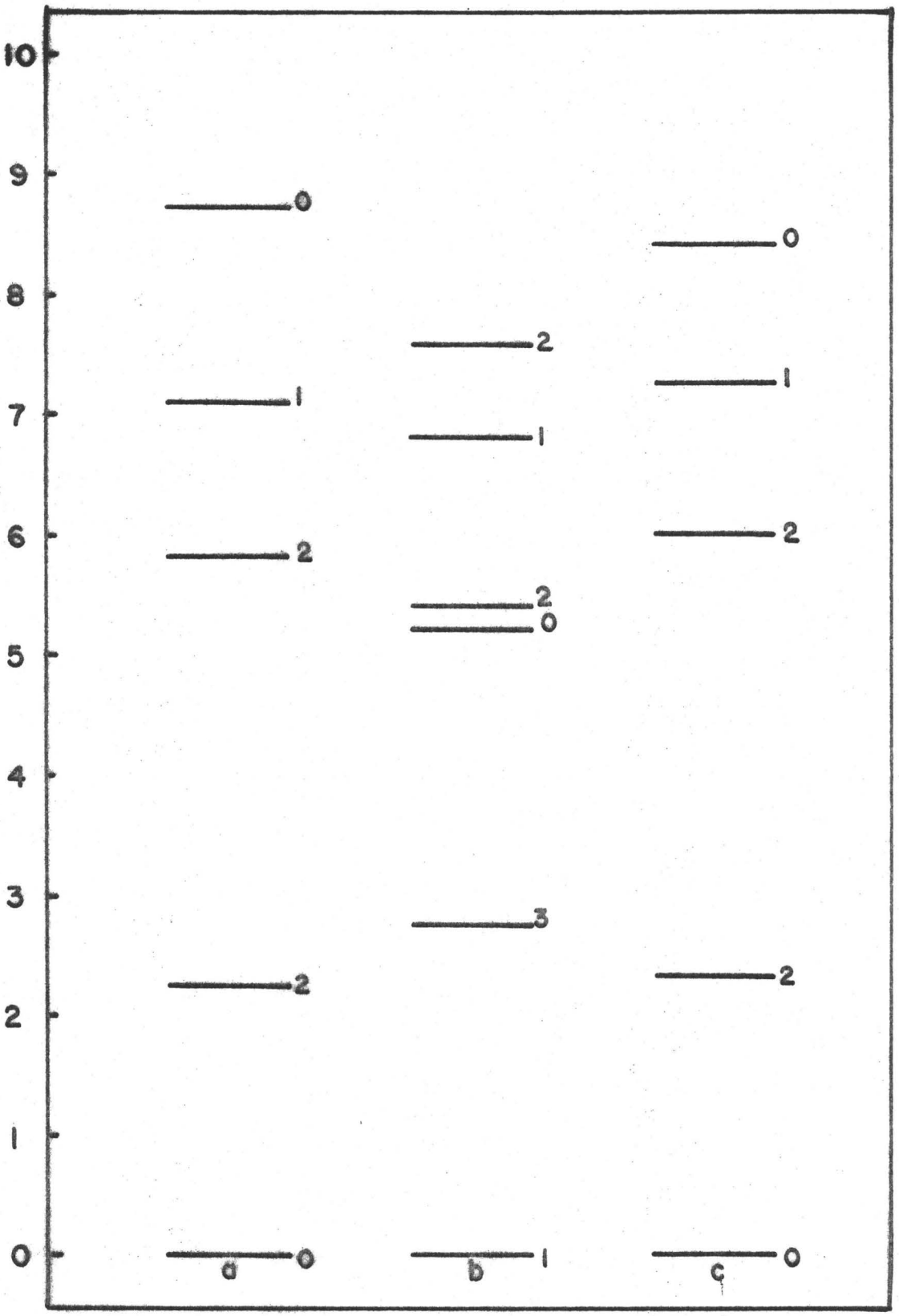

Figure 10.11

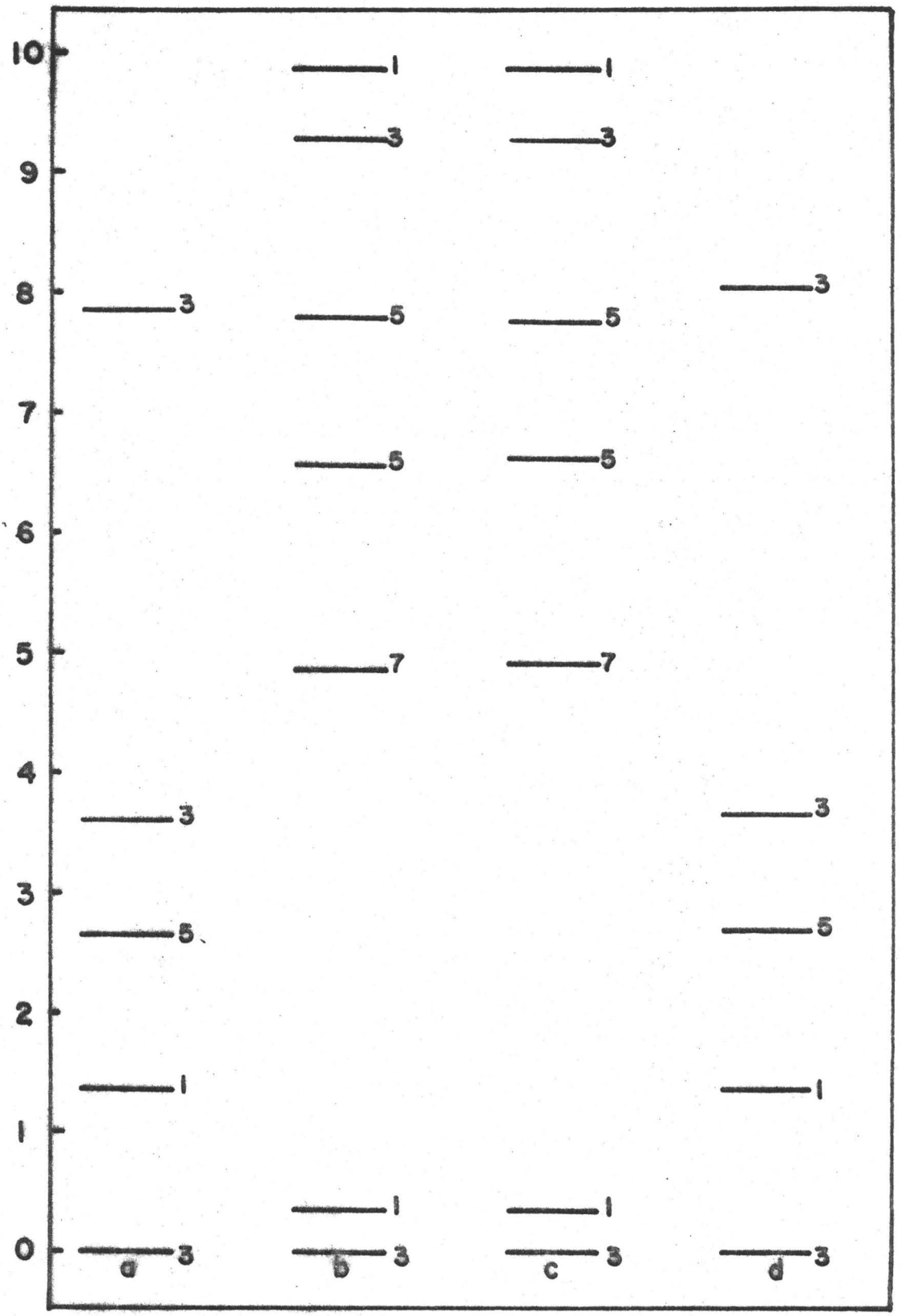

Figure 10.12

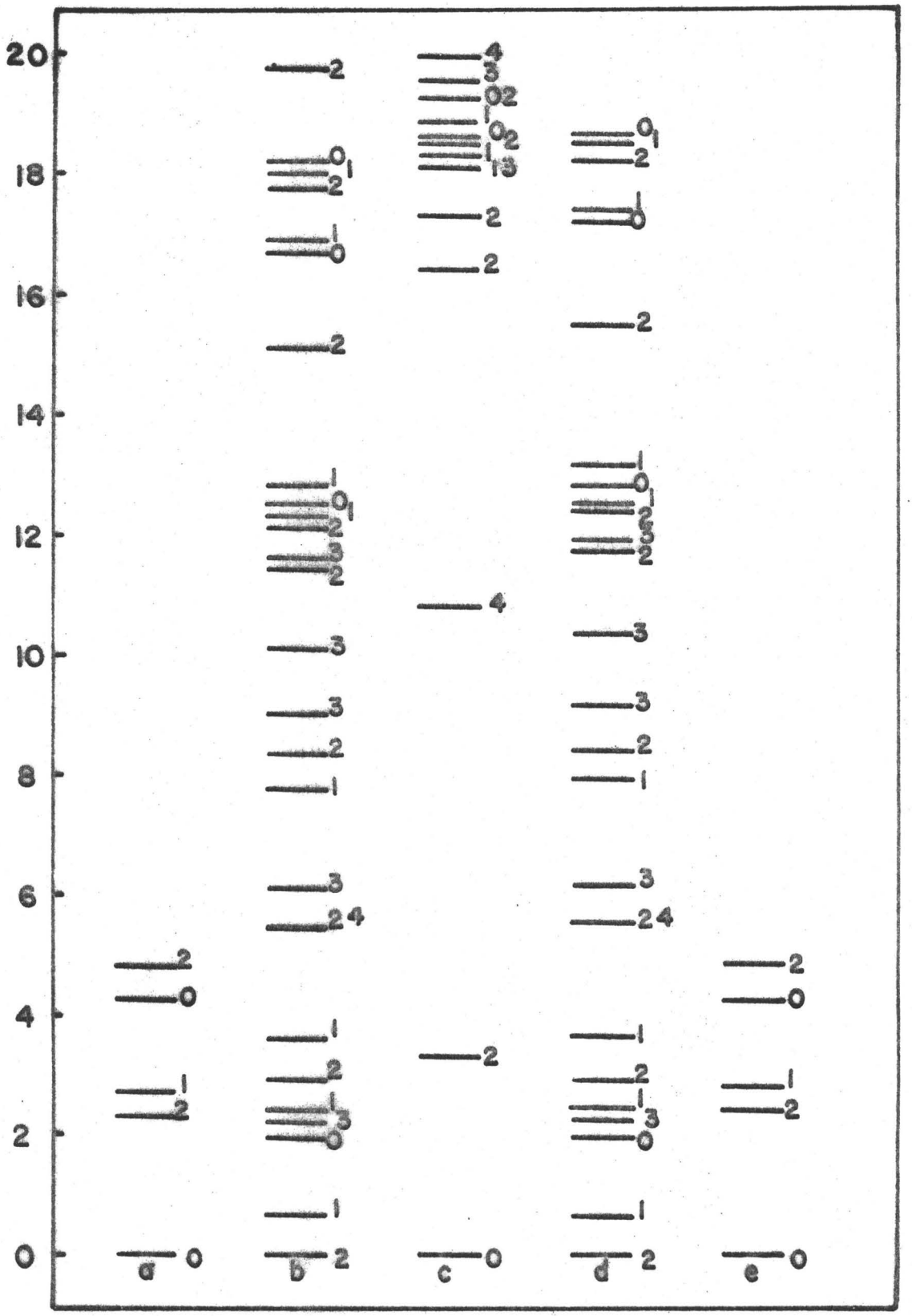

Figure 10.13

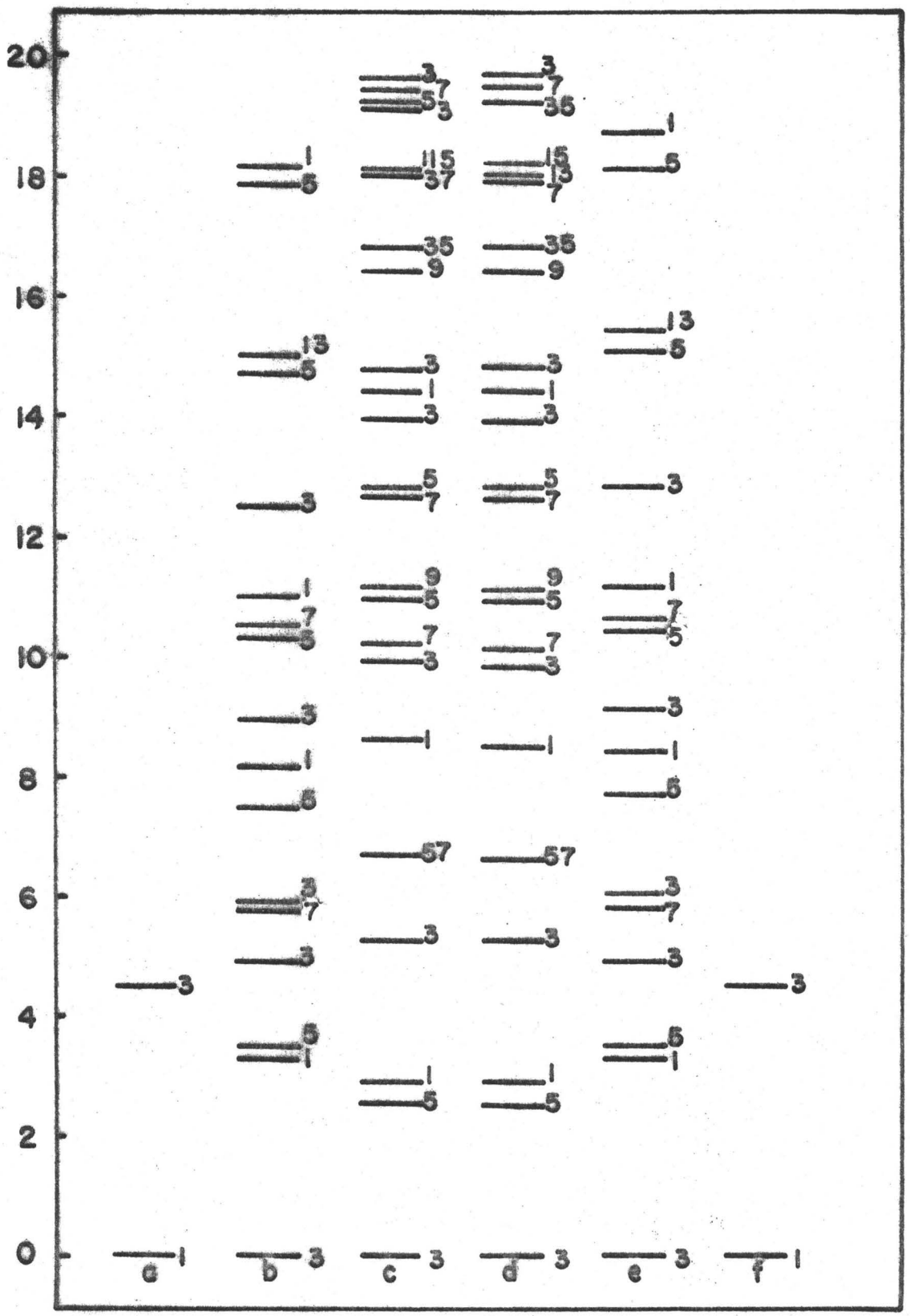

Figure 10.14

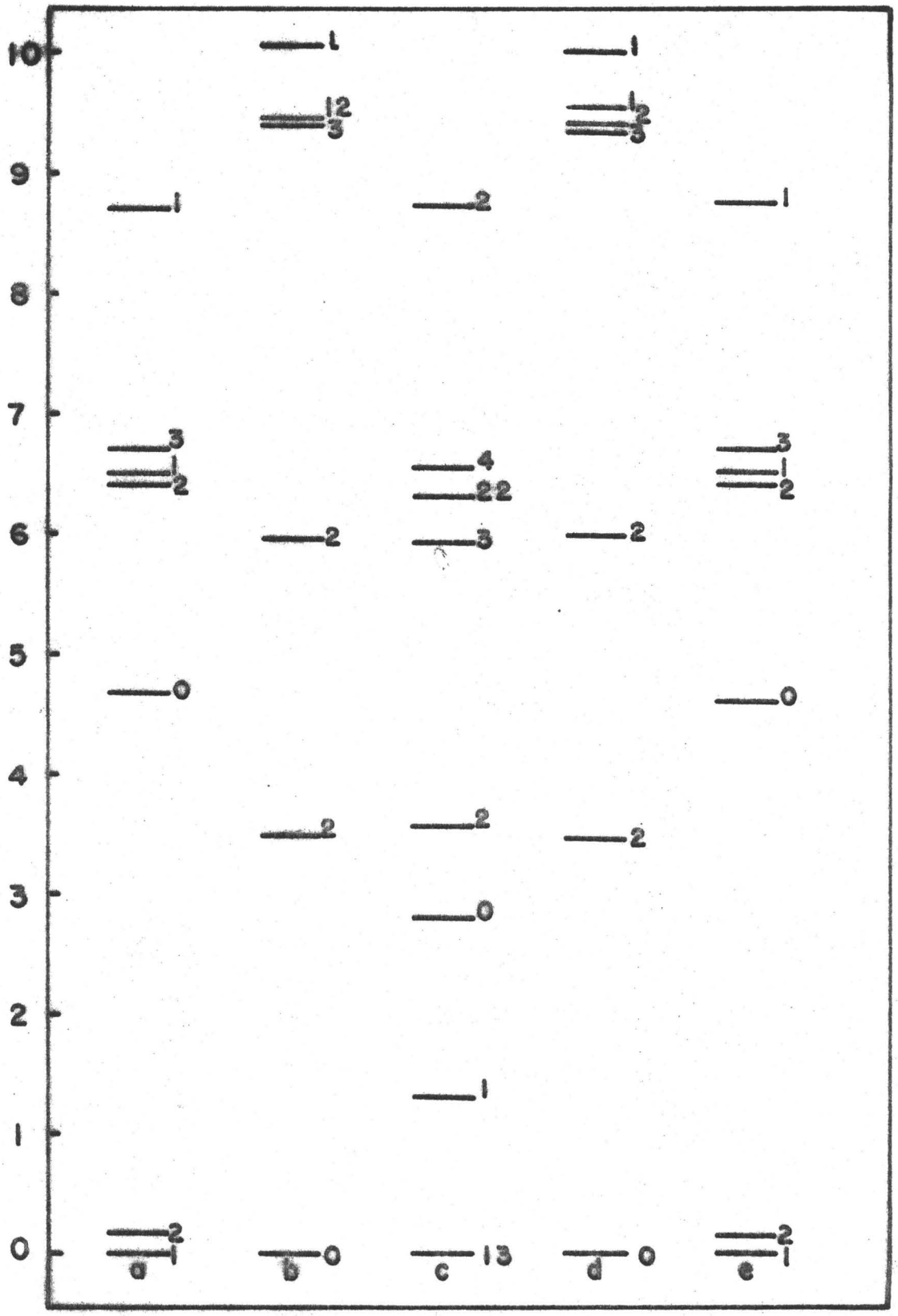

Figure 10.15

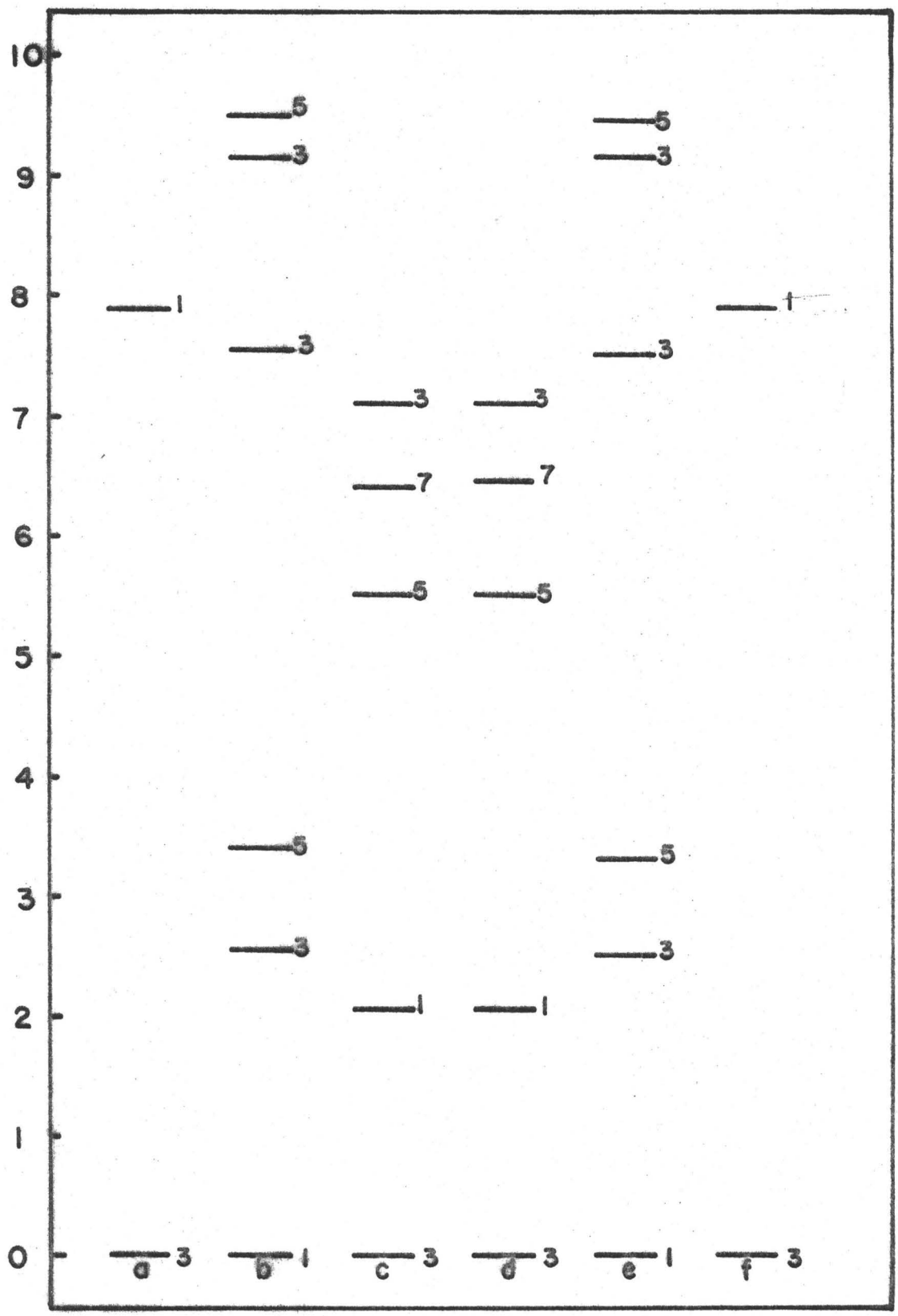

Figure 10.16

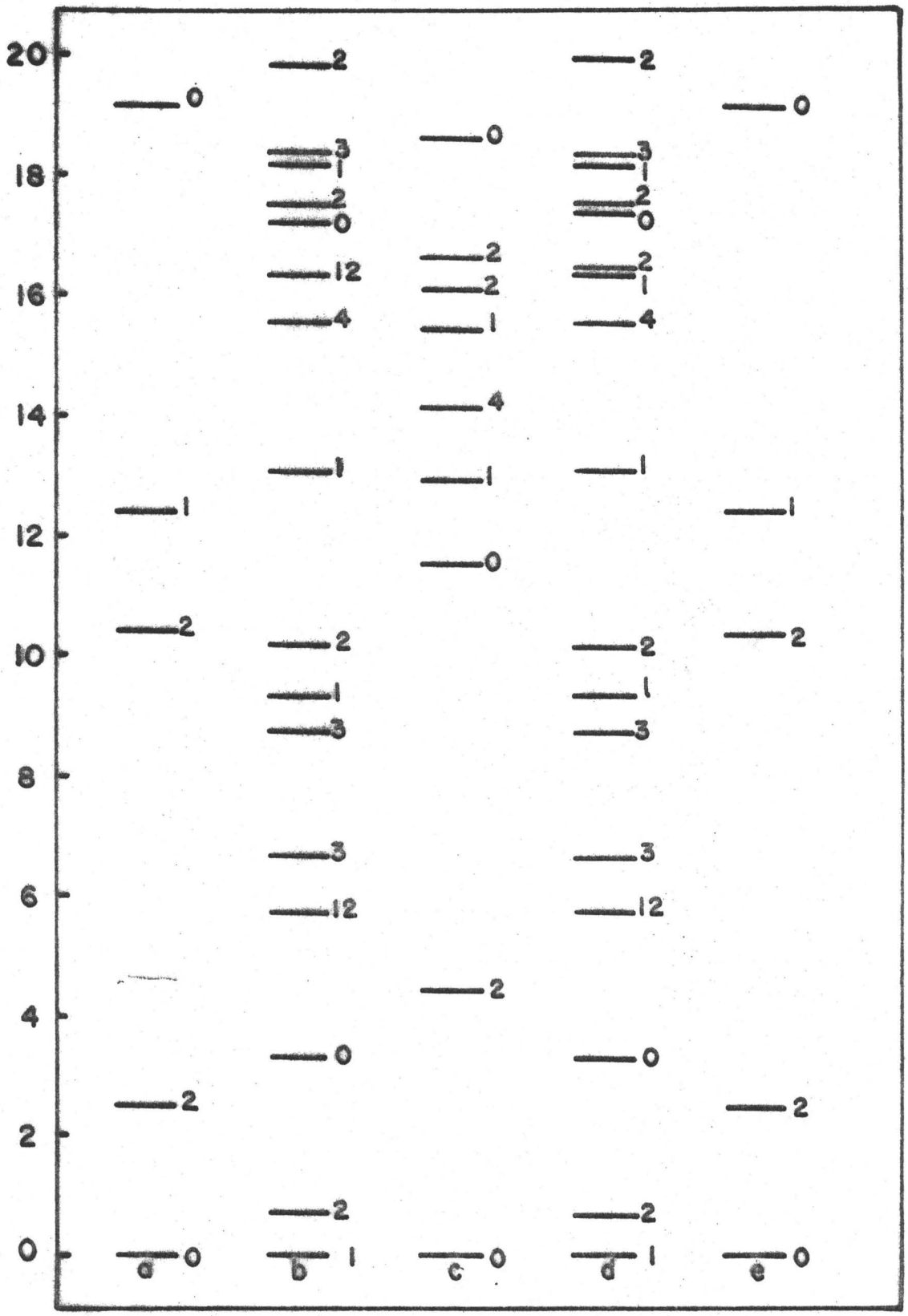

Figure 10.17

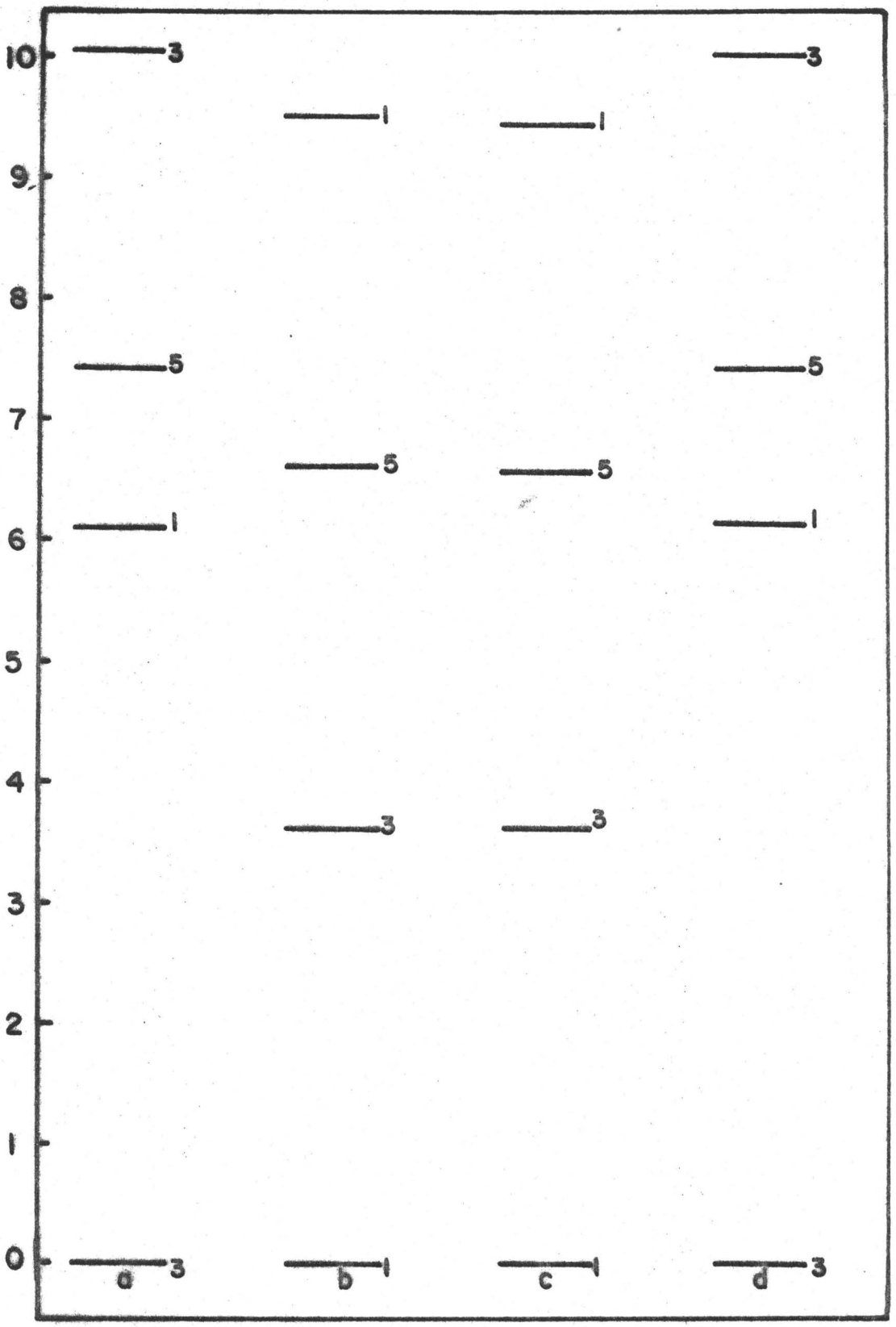

Figure 10.18

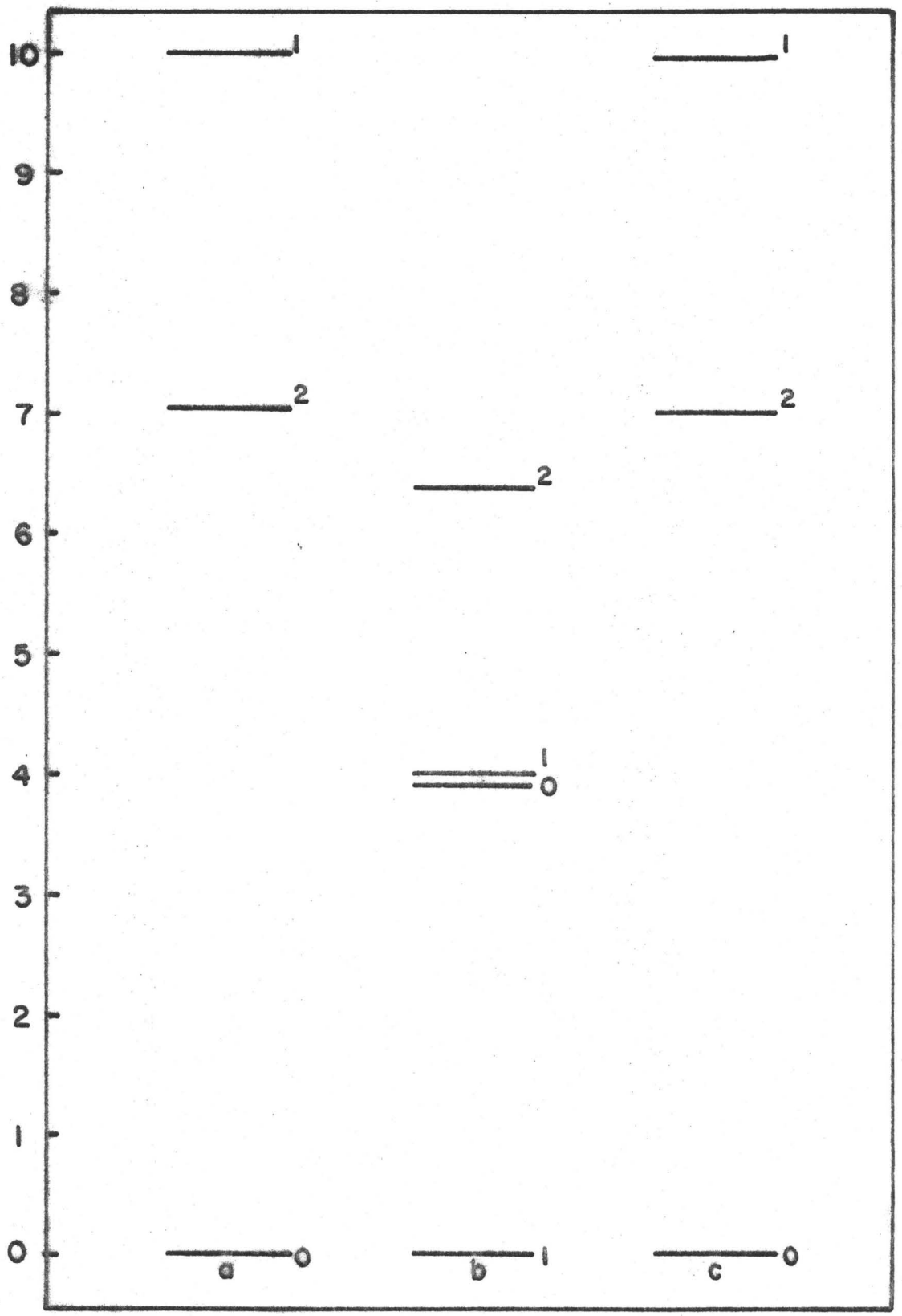

Figure 10.19

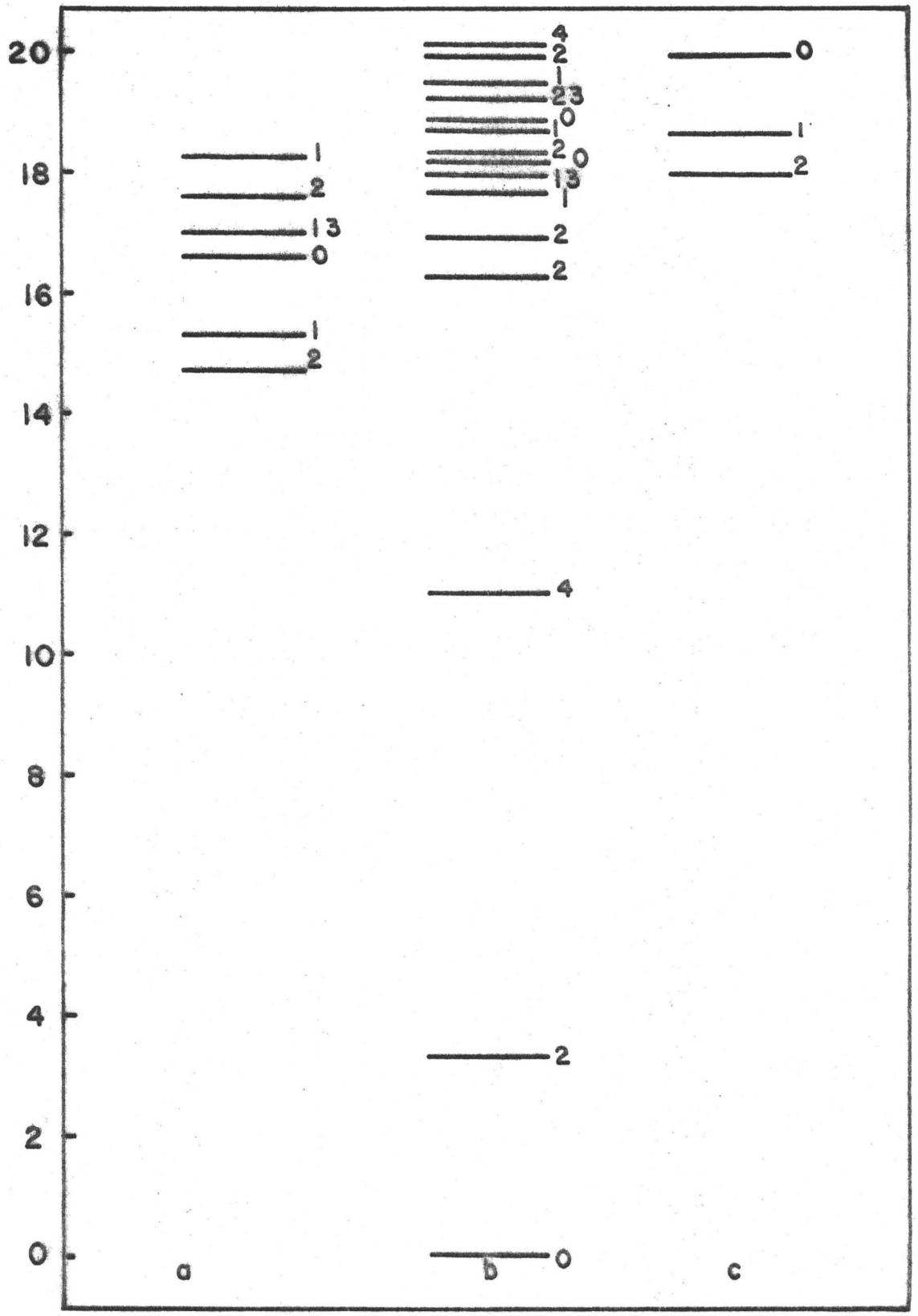

Figure 10.20

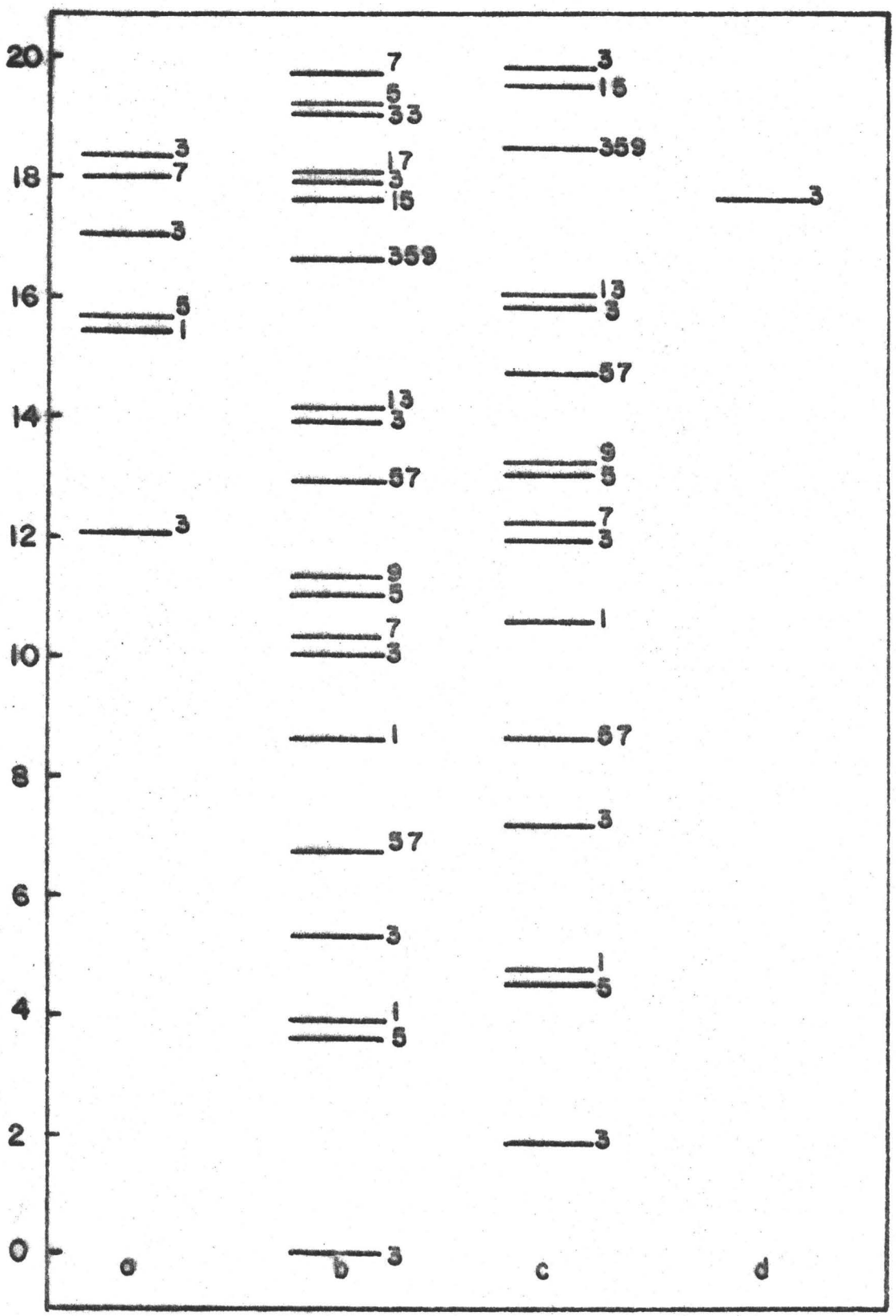
20
18
16
14
12
10
8
6
4
2
0
a
b
c
d
3
7
3
5
1
3
7
5
33
17
3
15
359
13
3
57
9
5
7
3
1
57
3
1
5
3
3
15
359
13
3
57
9
5
7
3
1
57
3
1
5
3
3

Figure 10.21

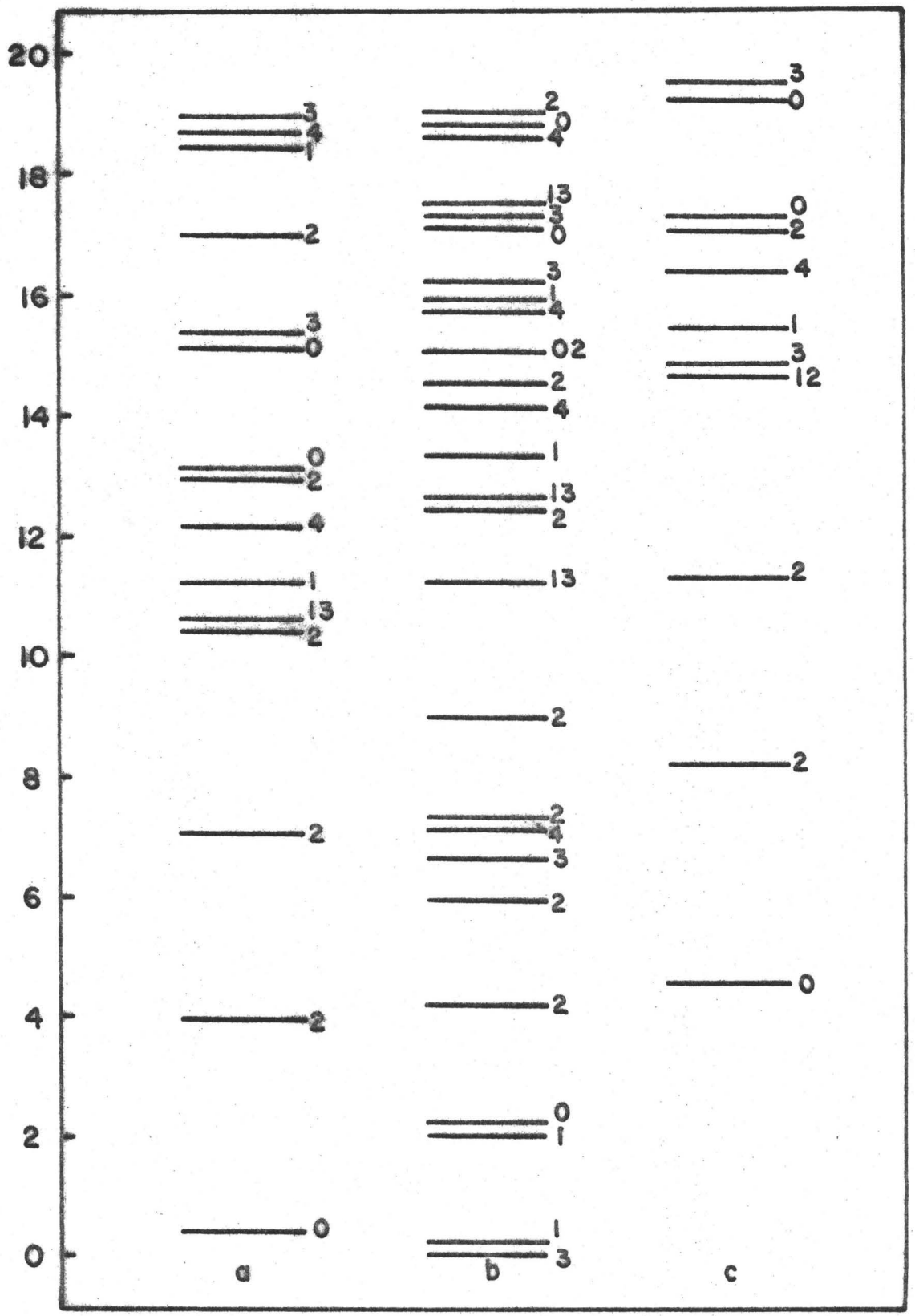

Figure 10.22

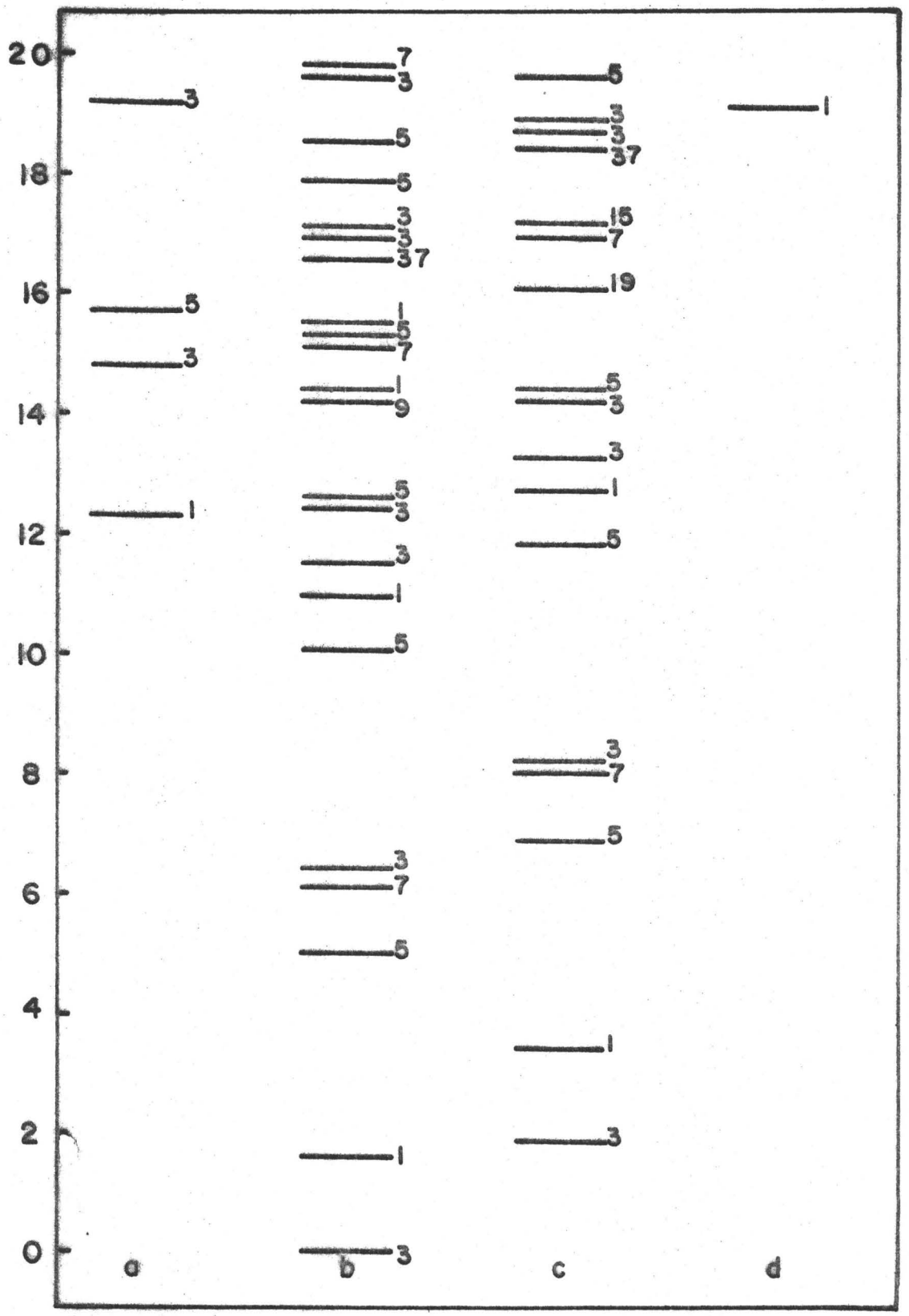

Figure 10.23

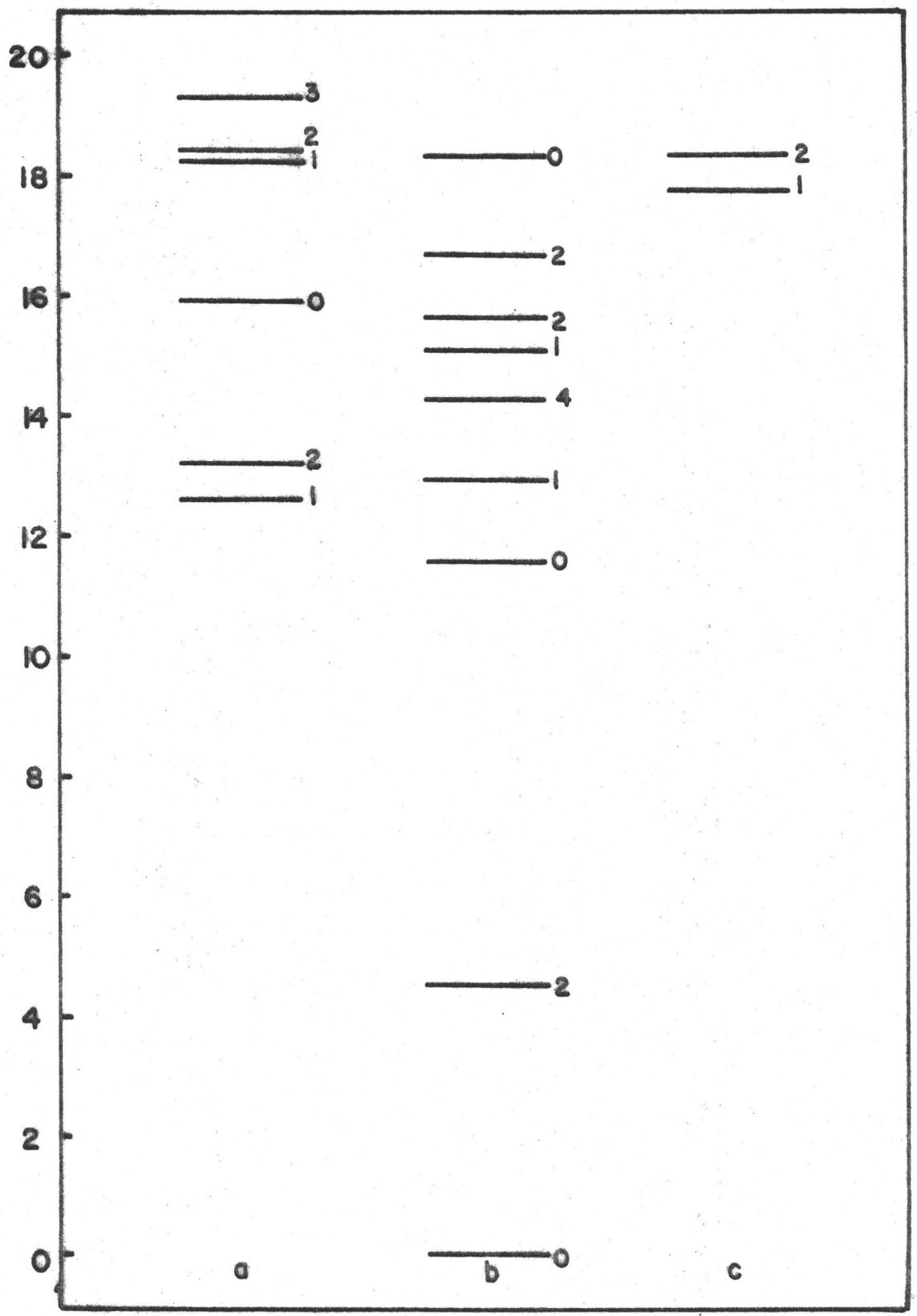

Figure 10.24

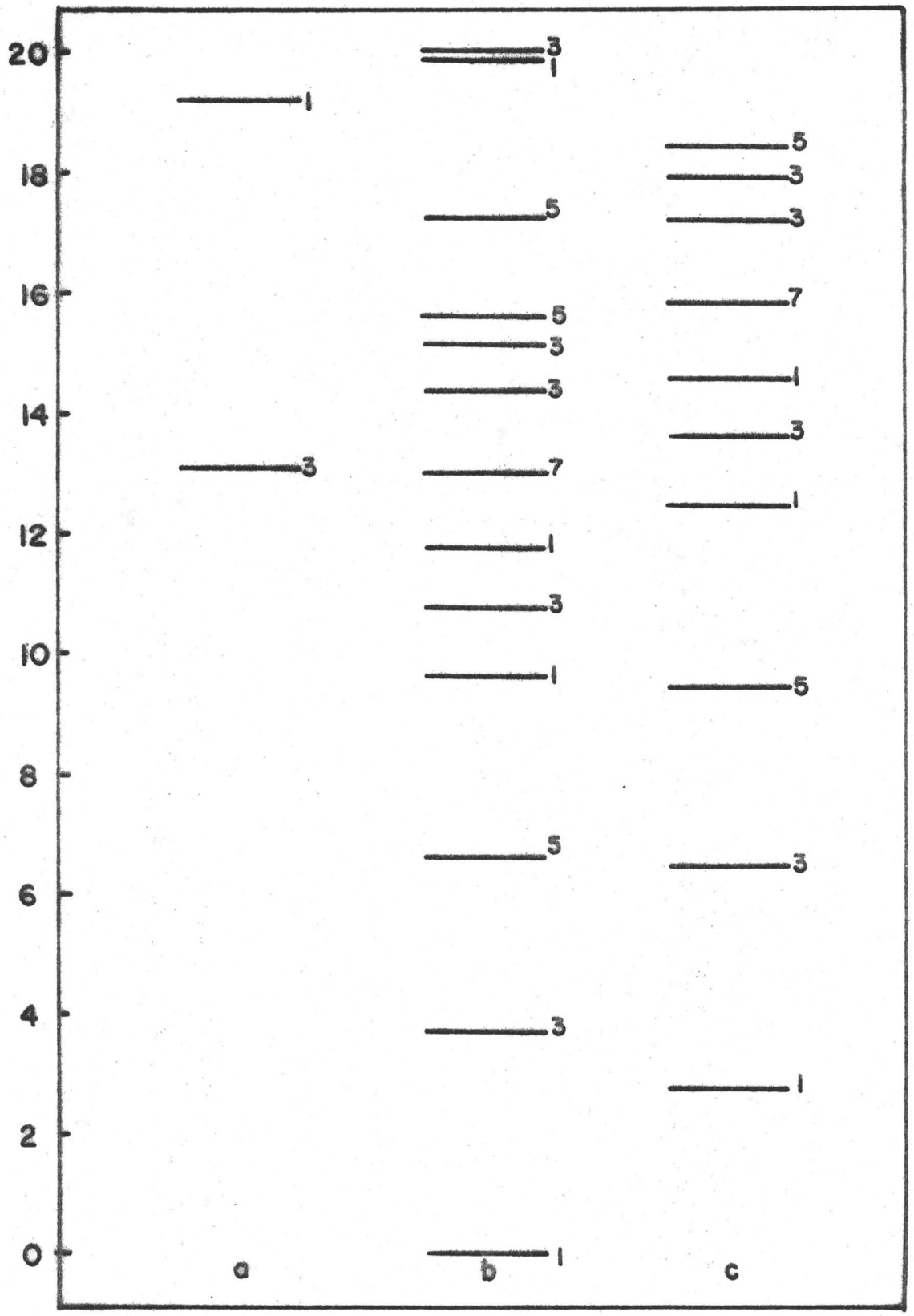

Figure 10.25

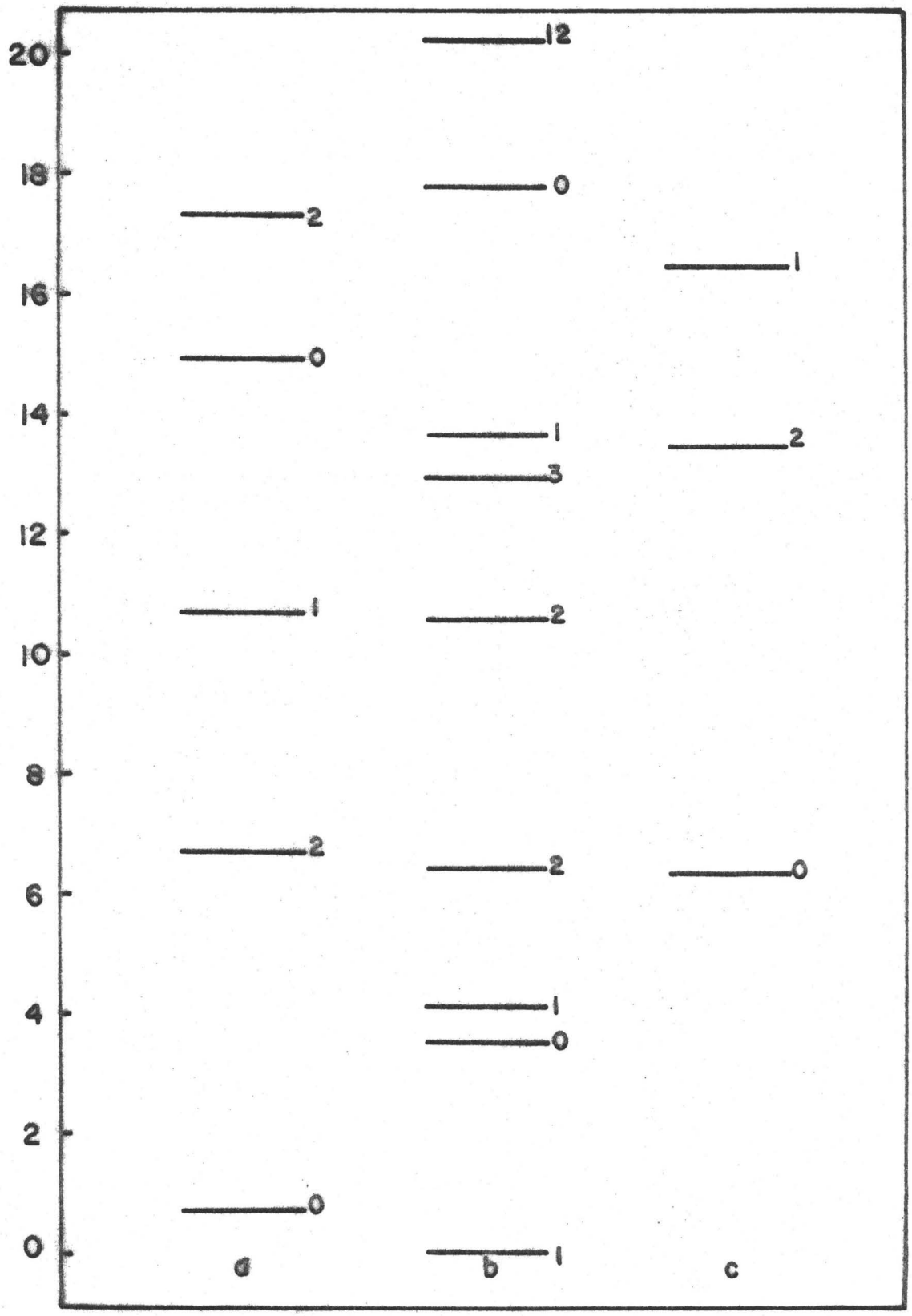

Figure 10.26

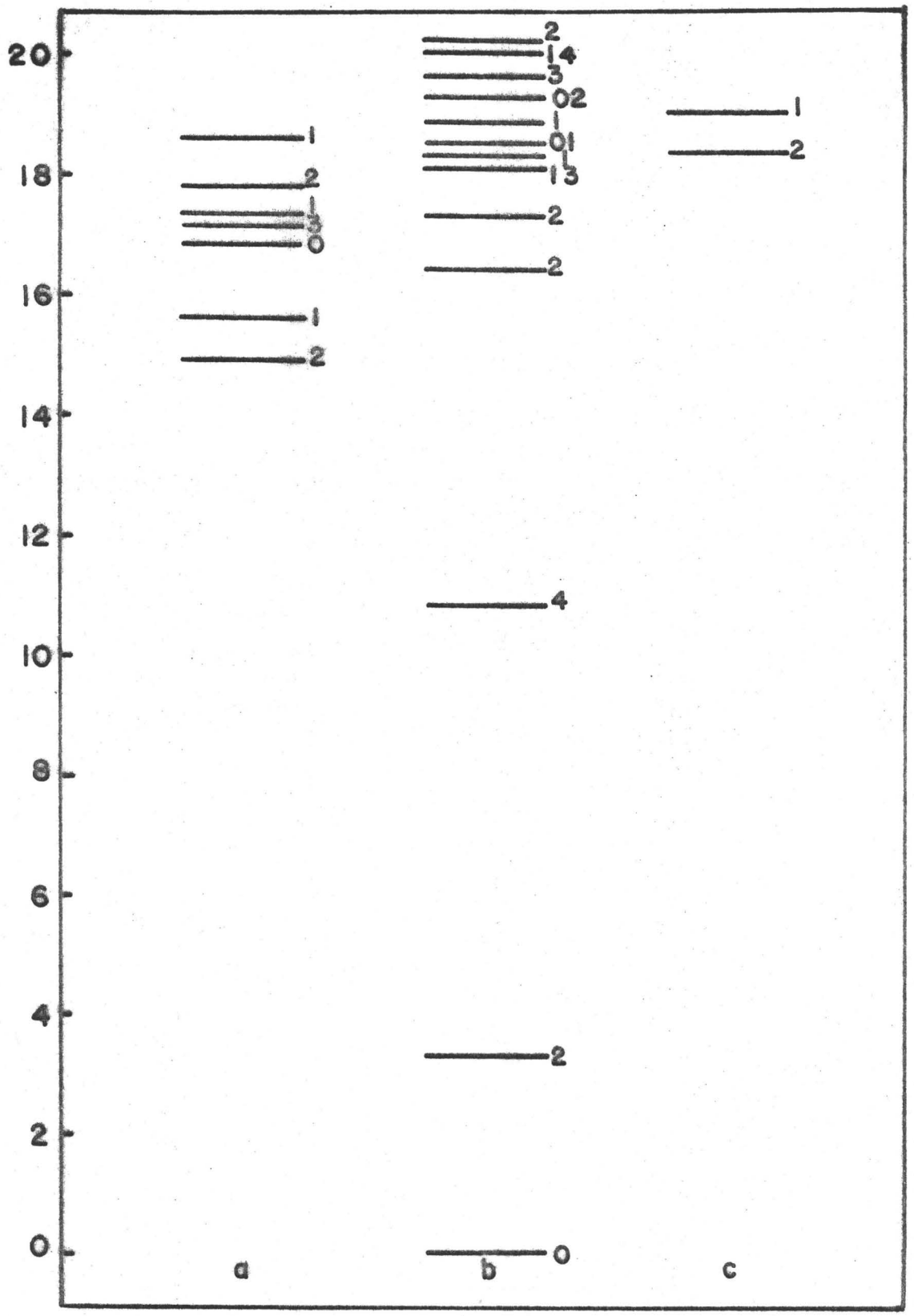

Figure 10.27

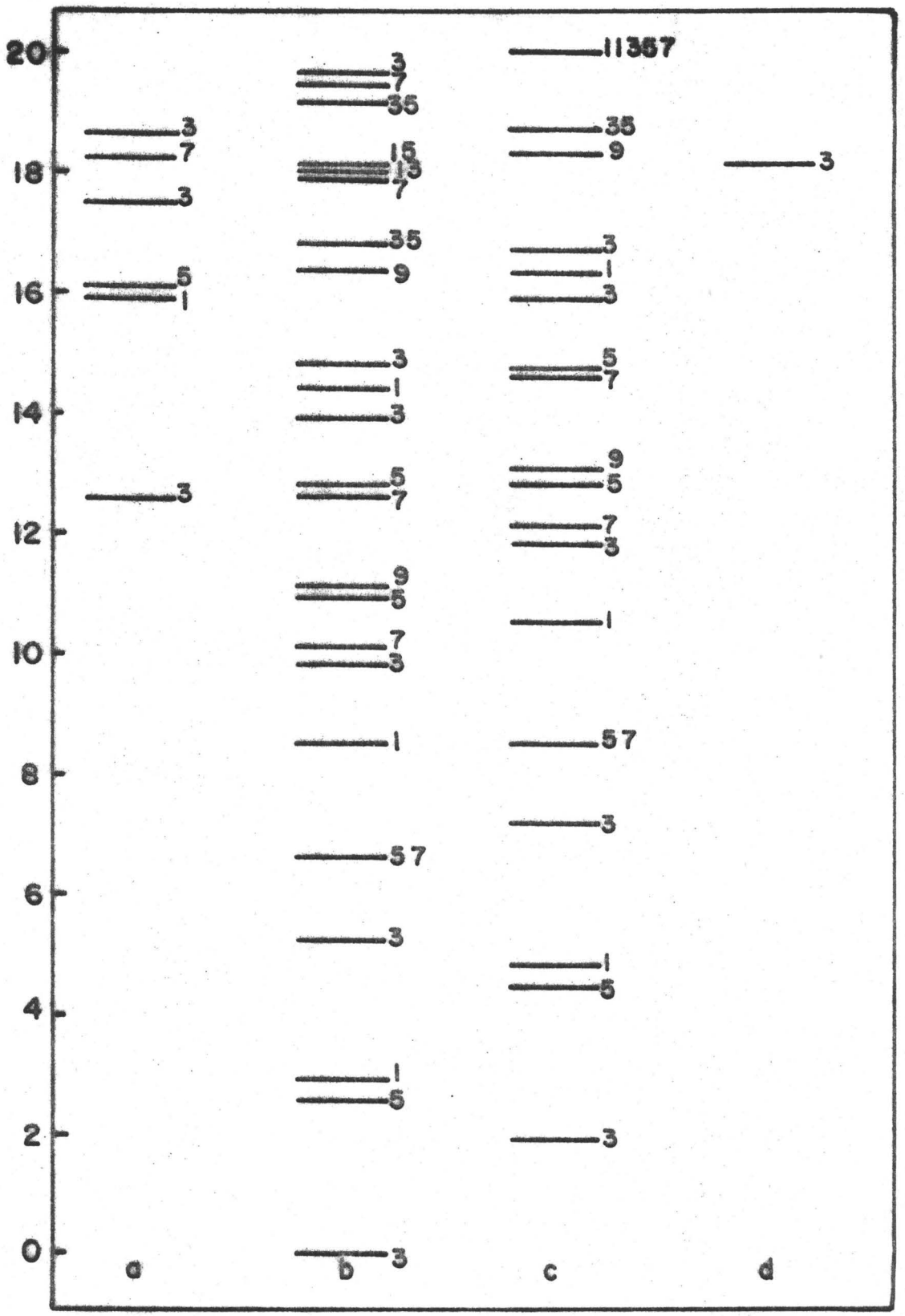

Figure 10.28

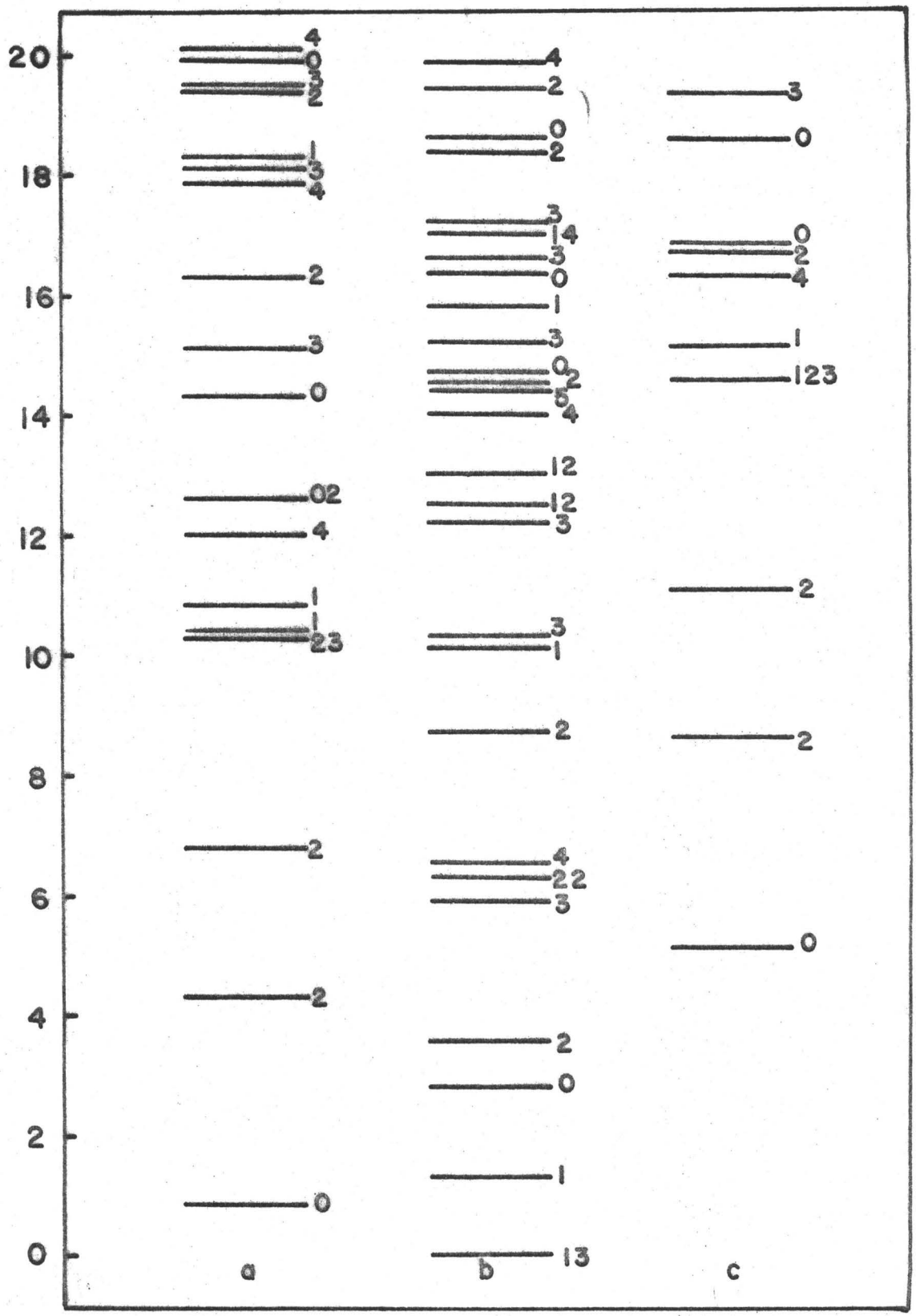
20
18
16
14
12
10
8
6
4
2
0
4
0
3
2
1
3
4
2
3
0
02
4
1
1
23
2
2
0
4
2
0
3
14
3
0
1
3
0
2
5
4
12
12
3
3
1
2
4
22
3
2
0
1
13
2
2
0
a
b
c

Figure 10.29

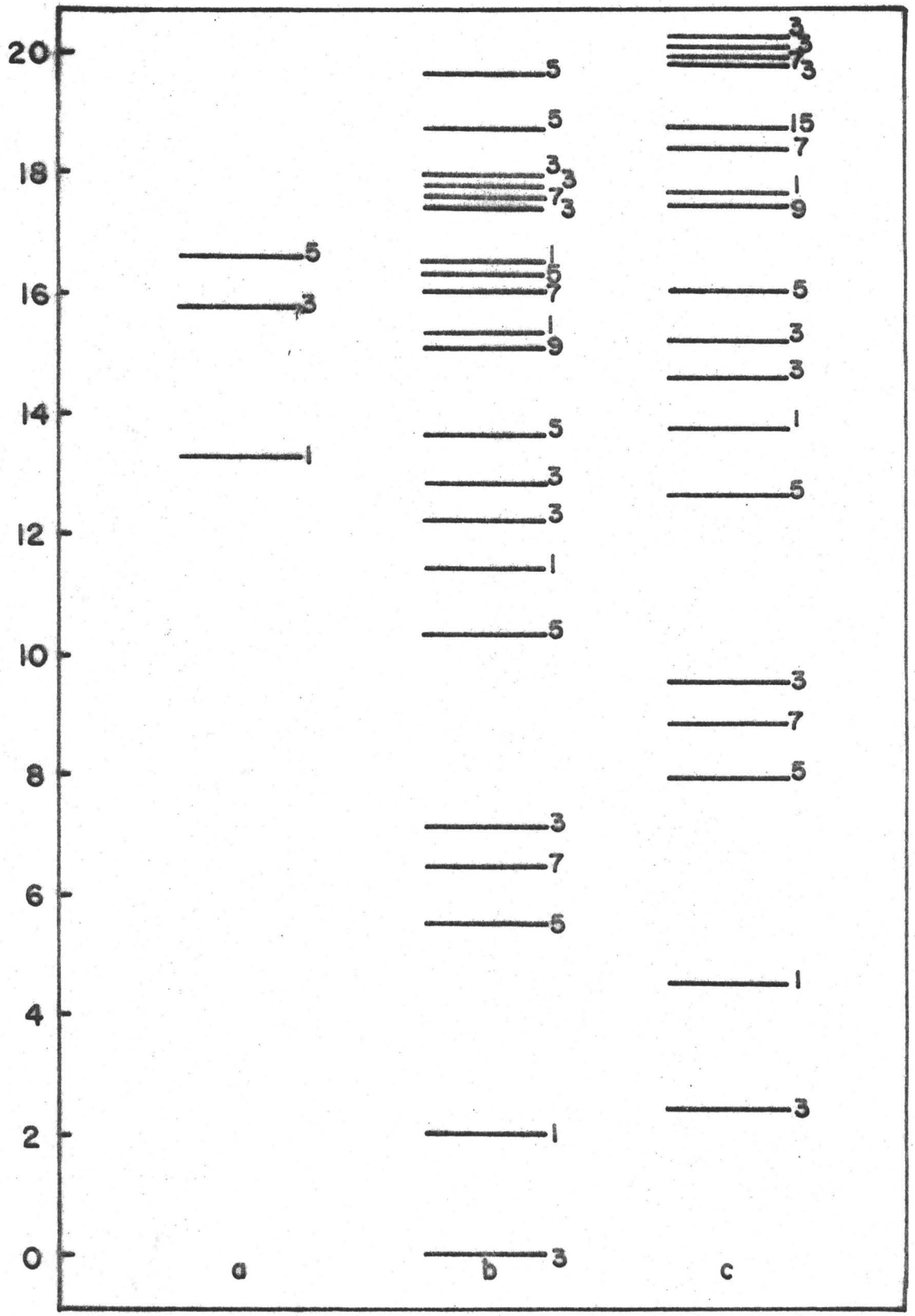

Figure 10.30

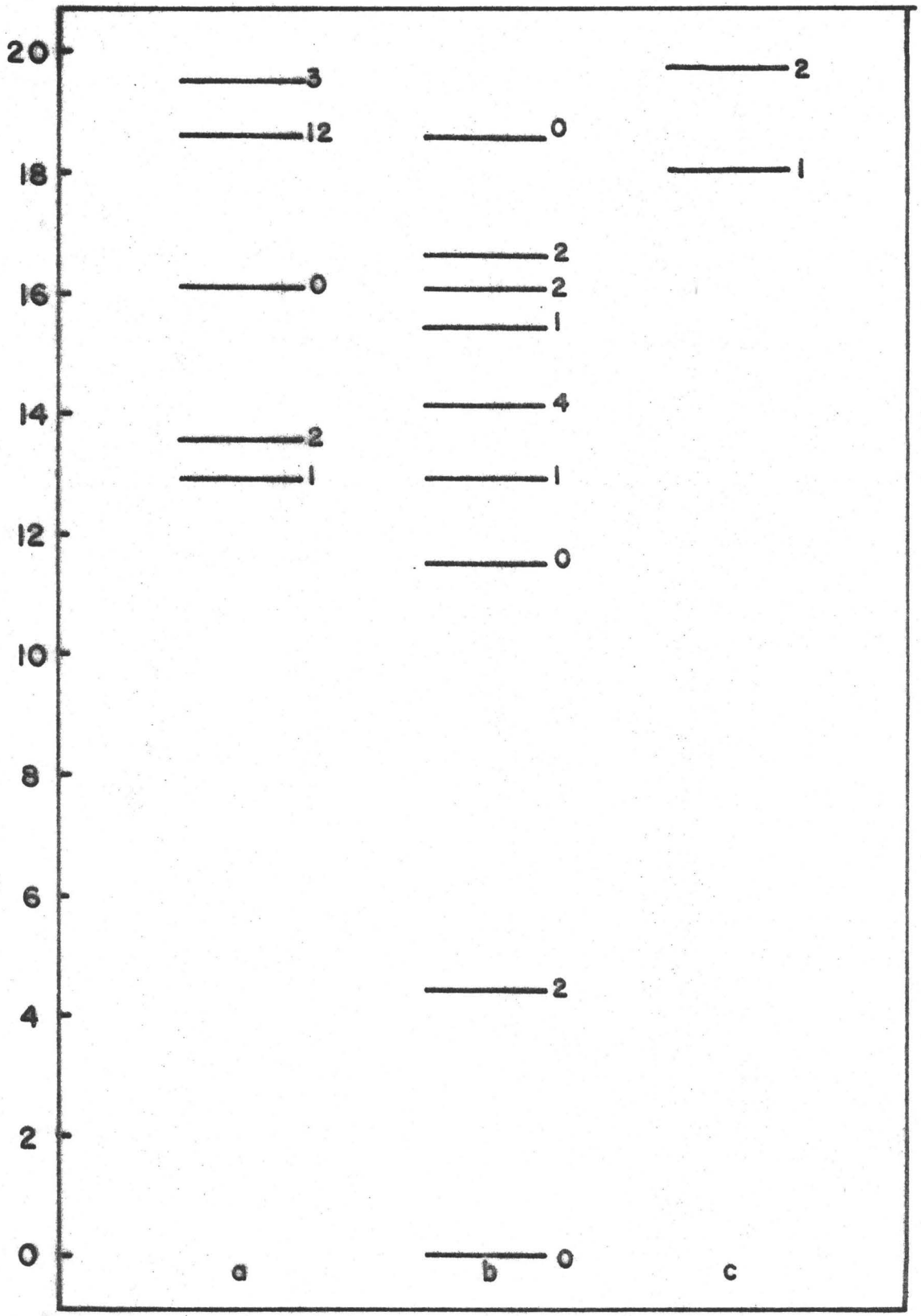

Figure 10.31

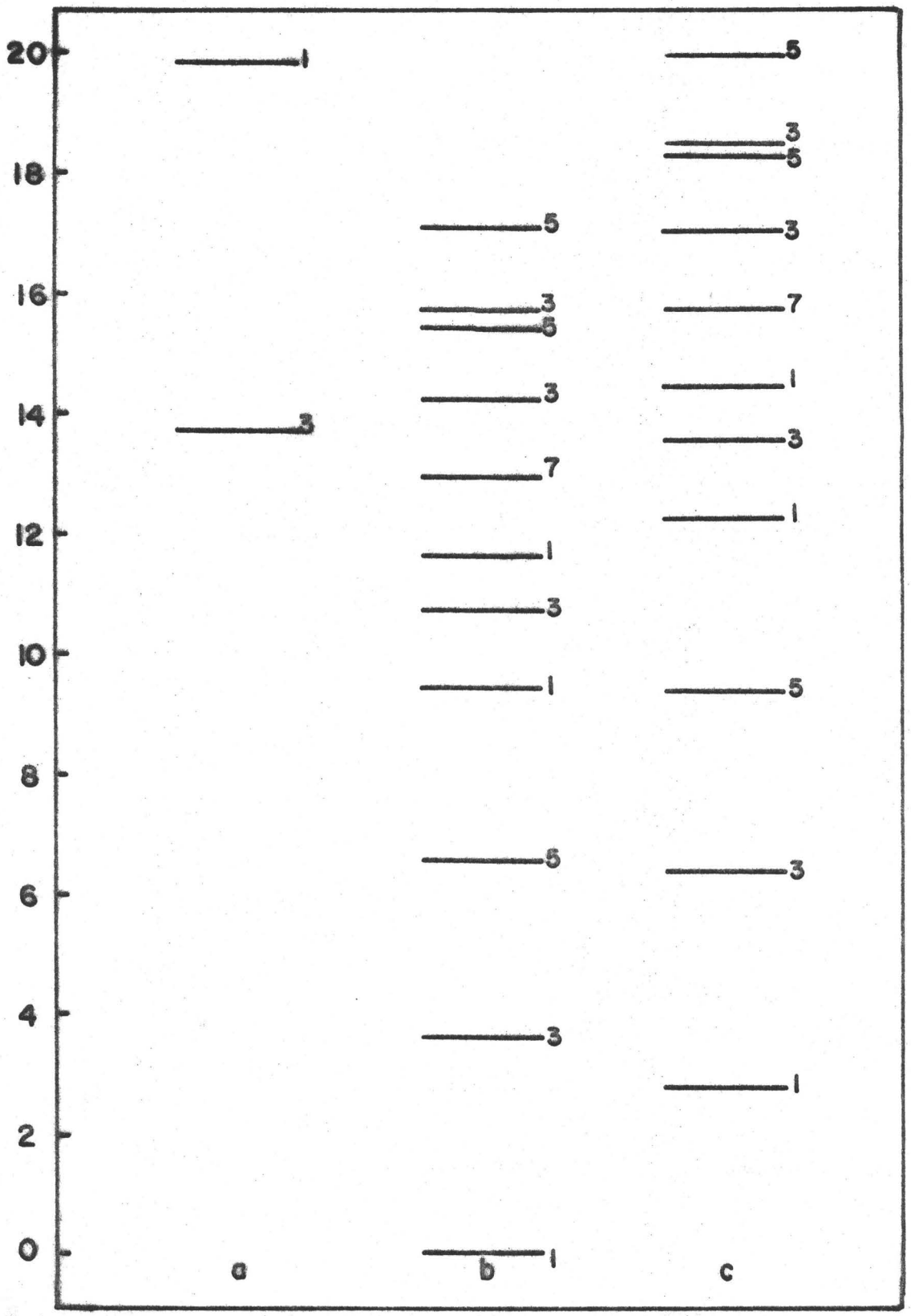

Figure 10.32

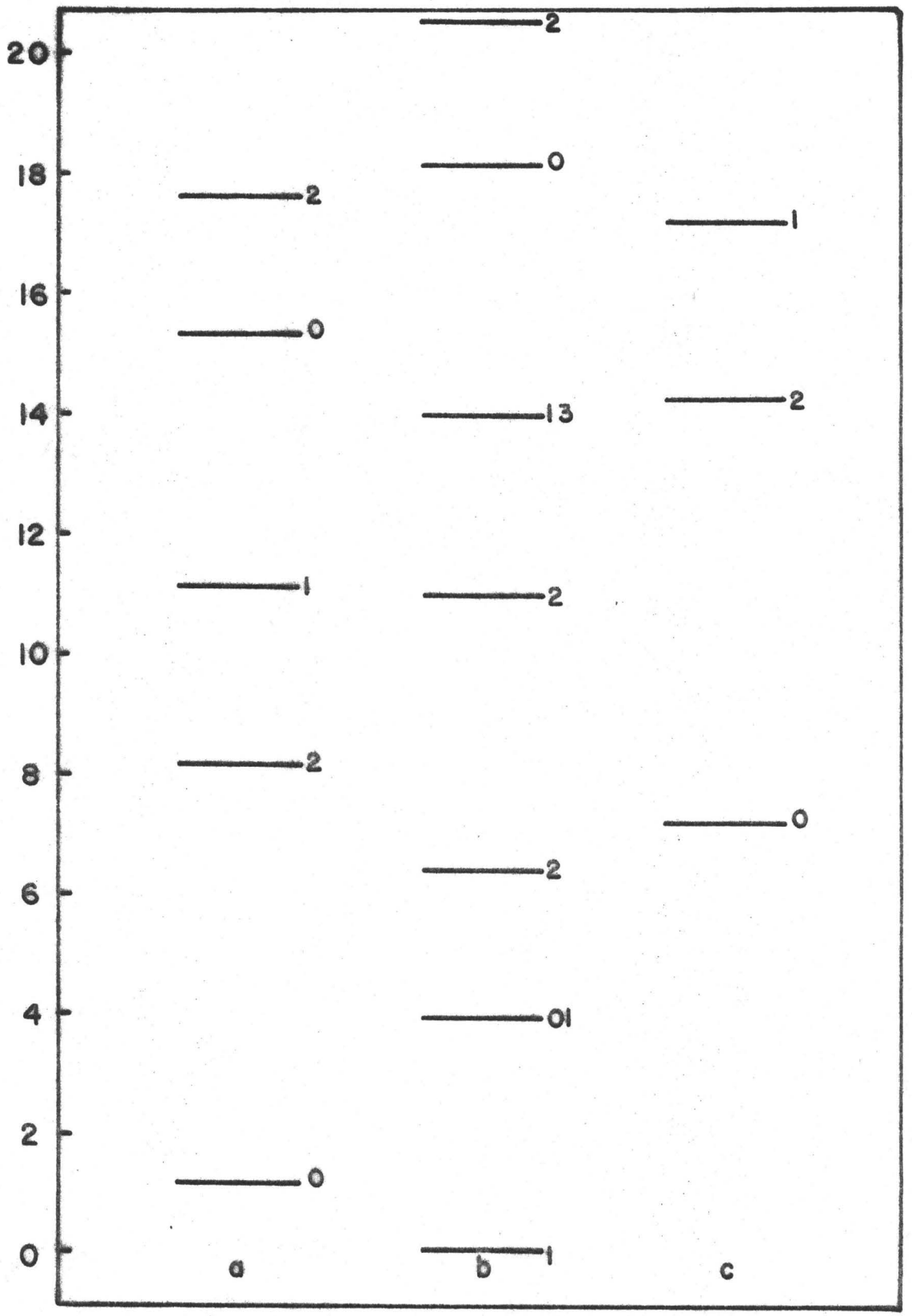

Figure 10.33

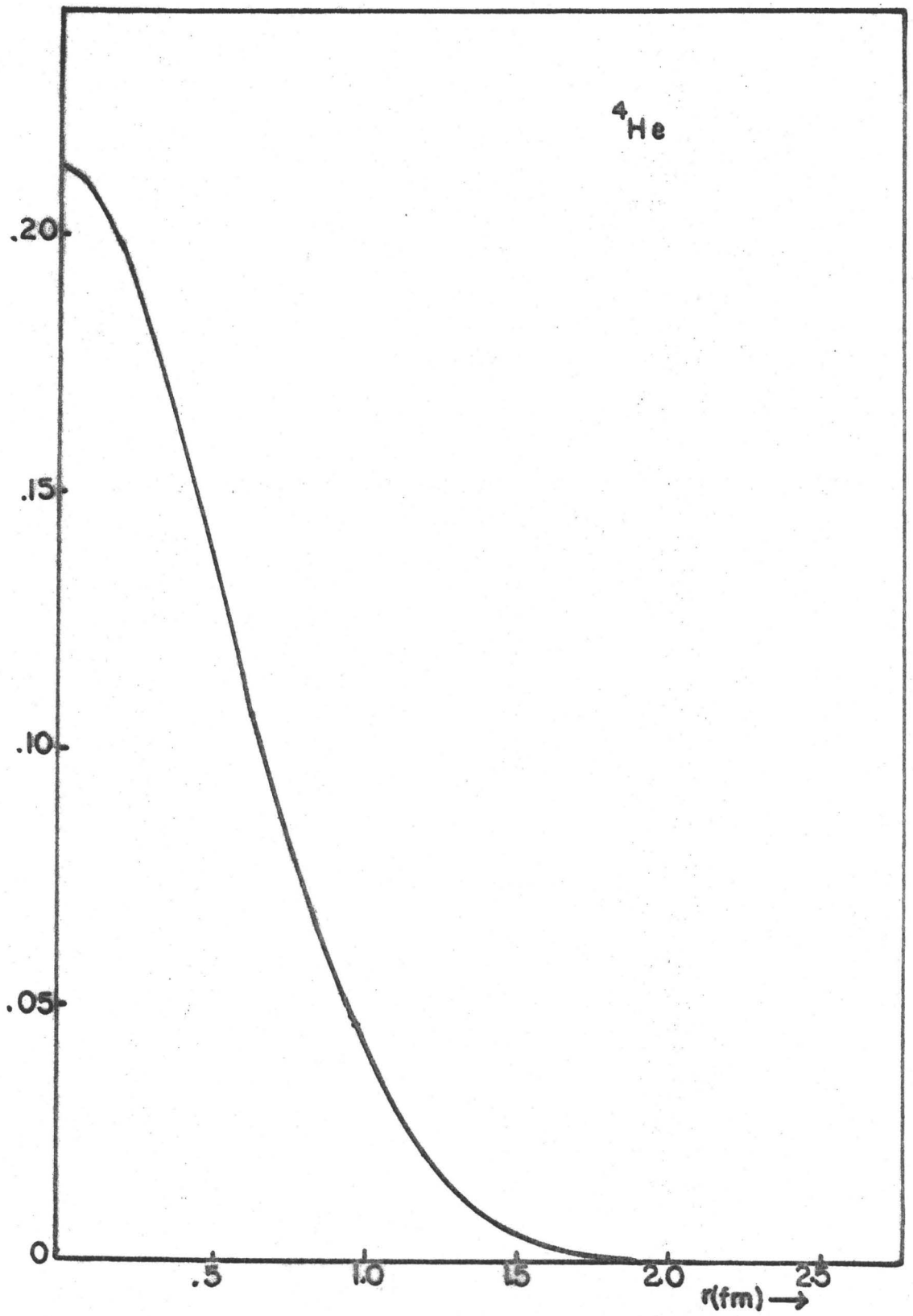

Figure 10.34

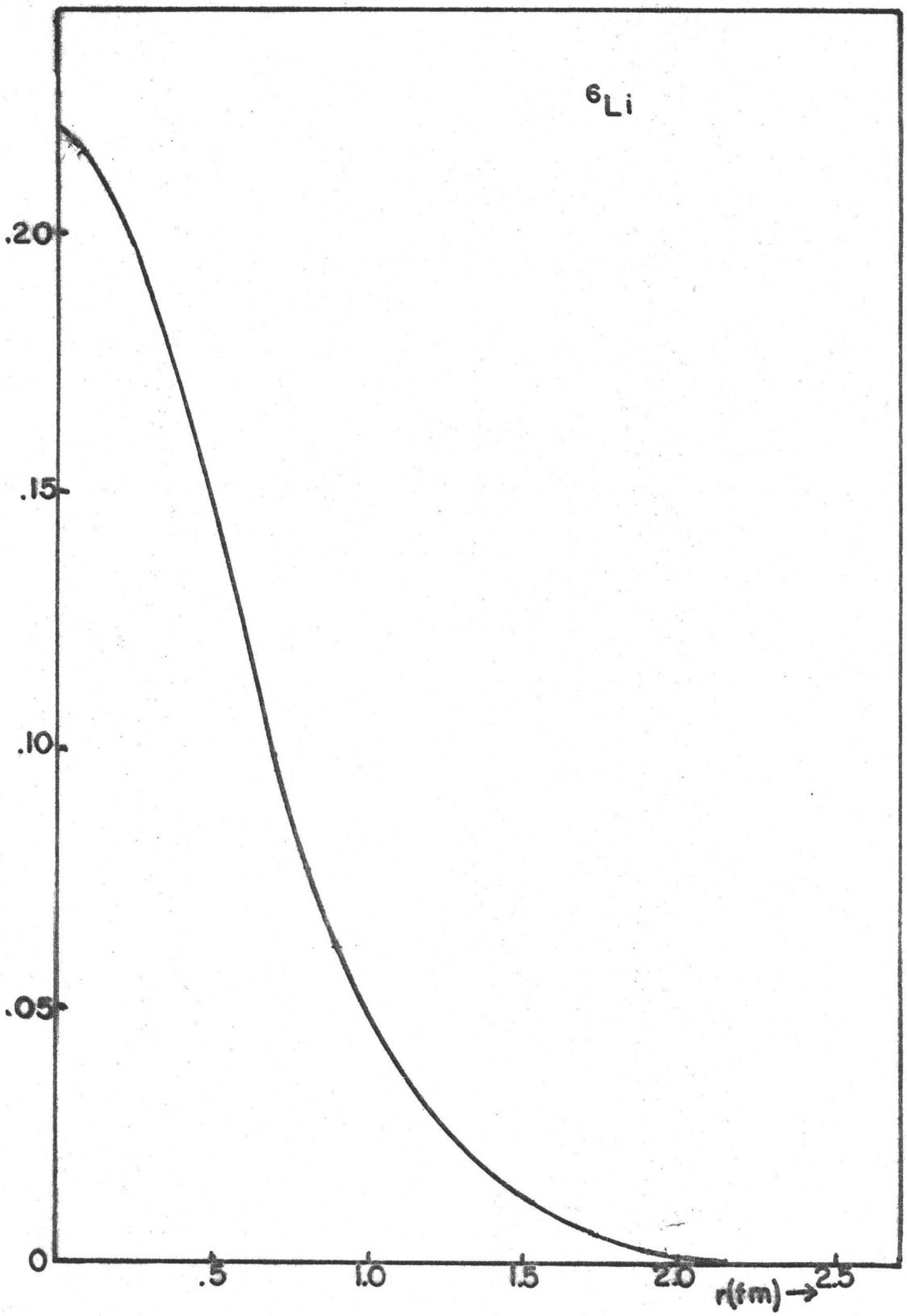

Figure 10.35

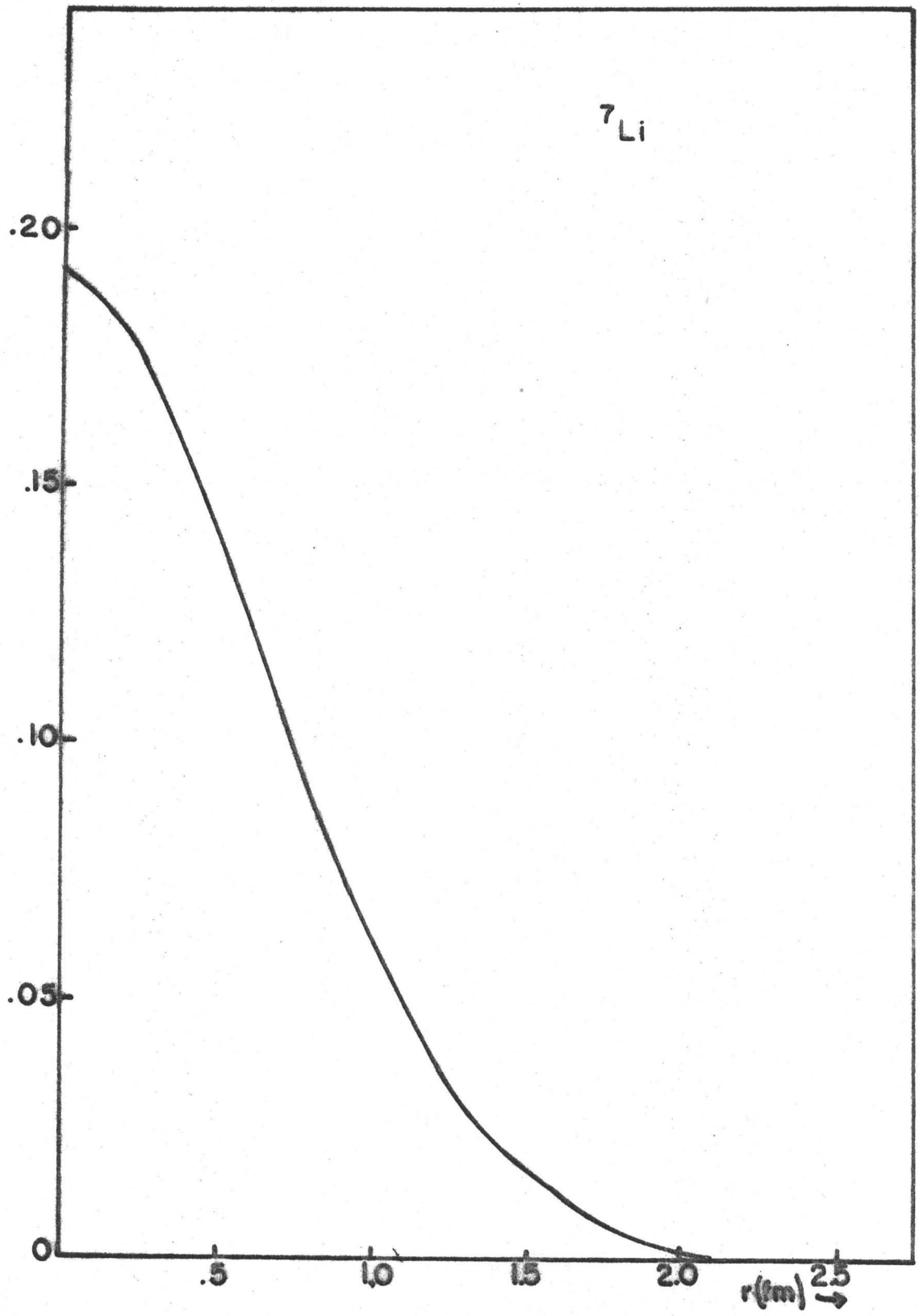

Figure 10.36

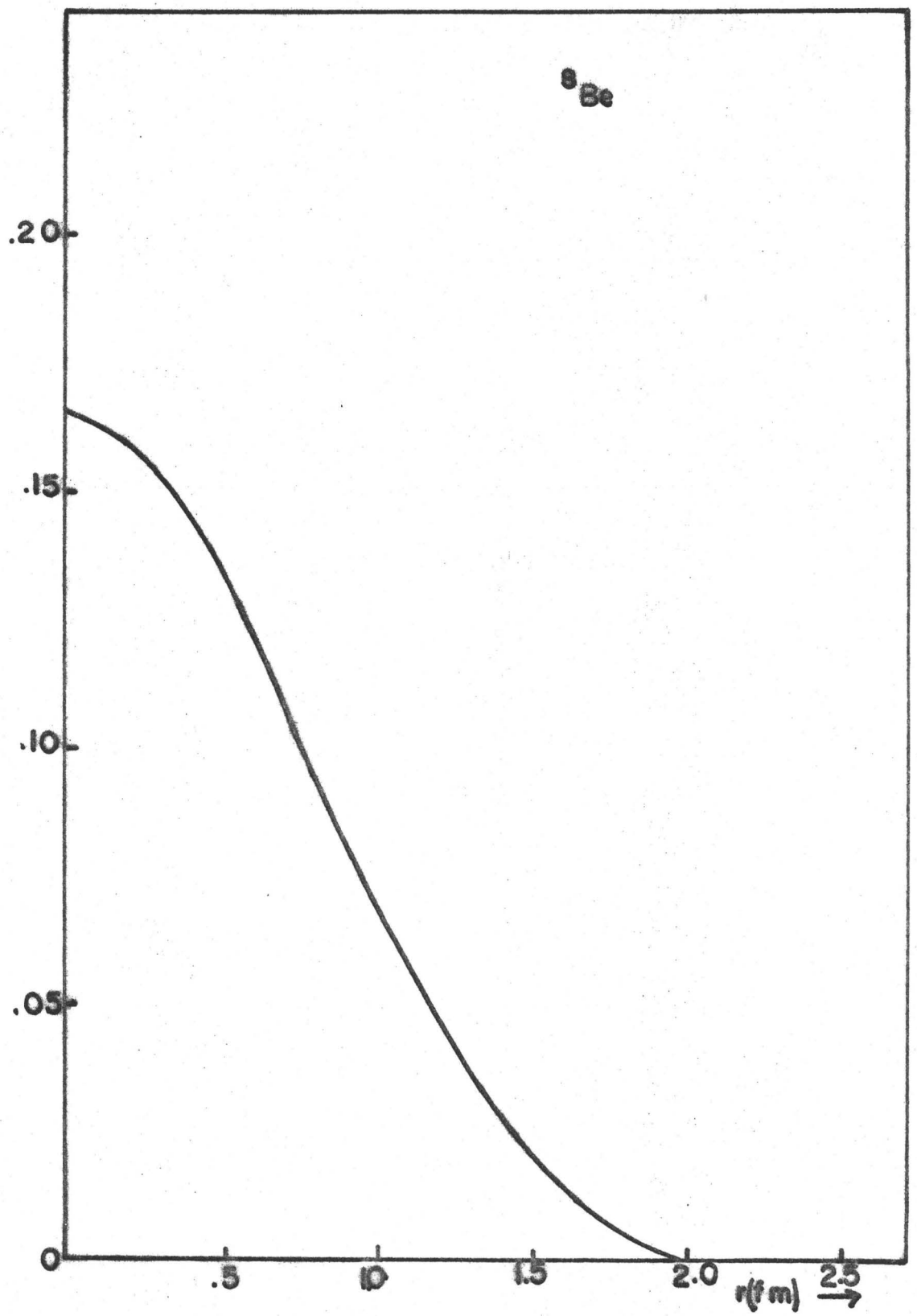

Figure 10.37

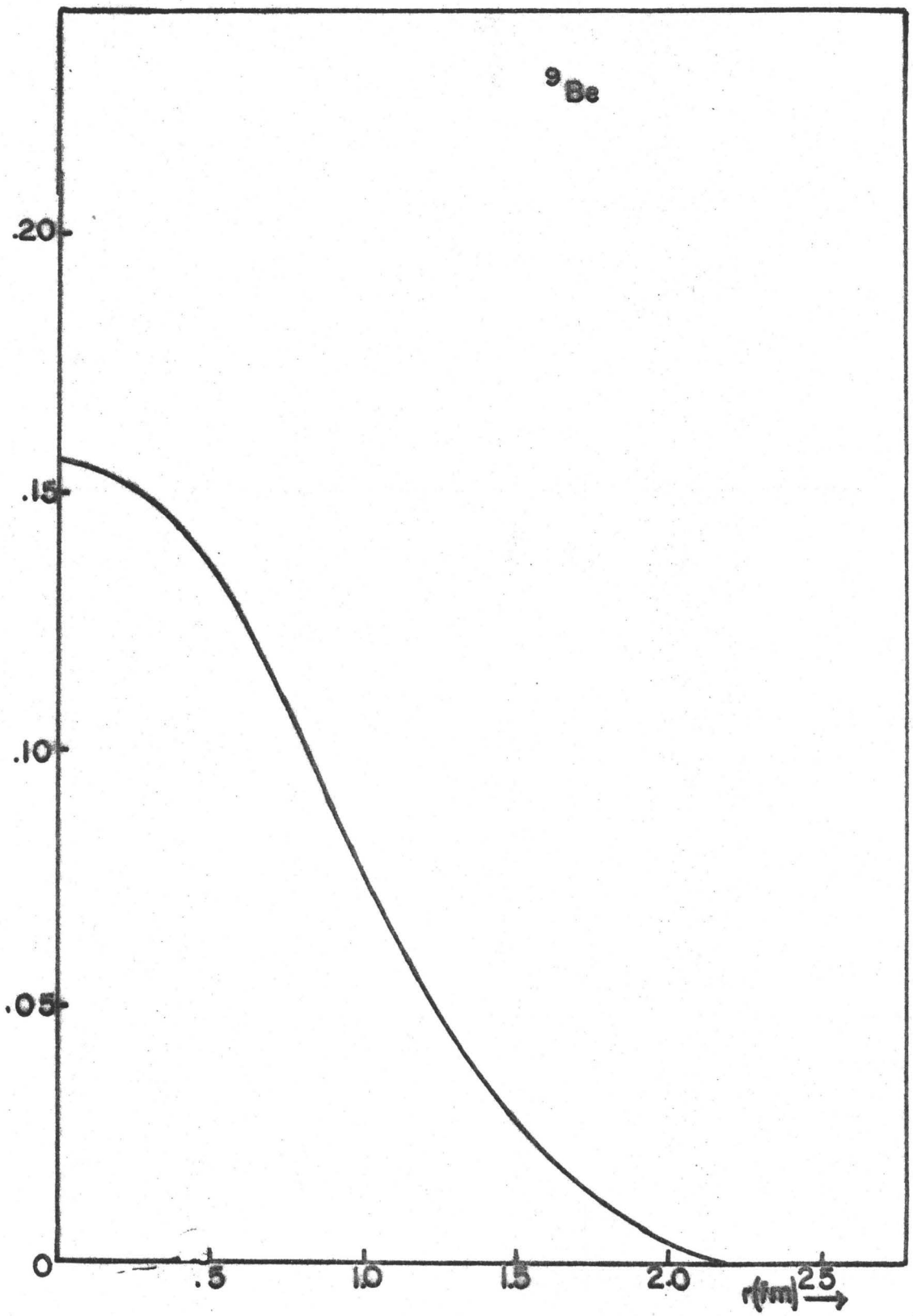

Figure 10.38

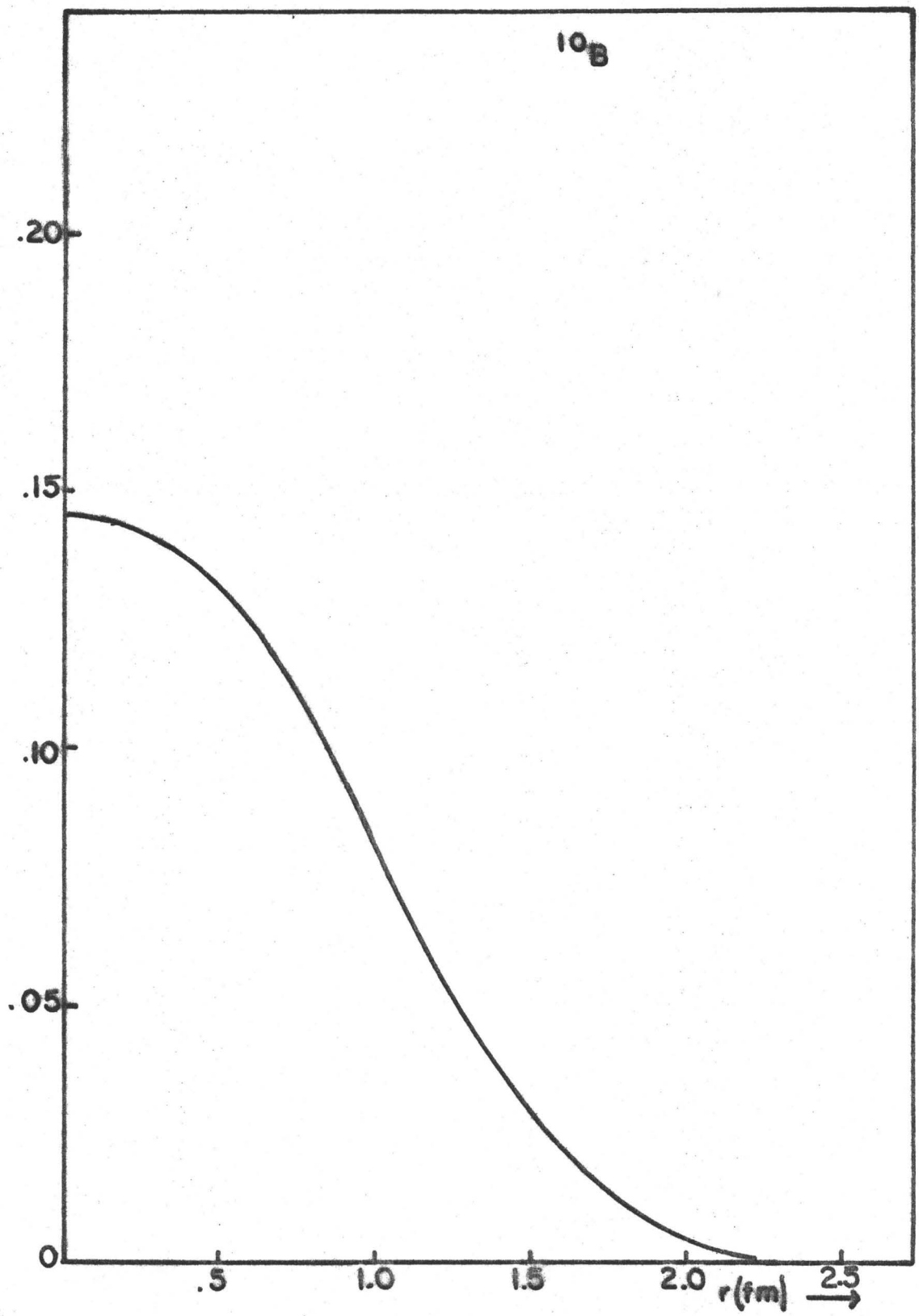

Figure 10.39

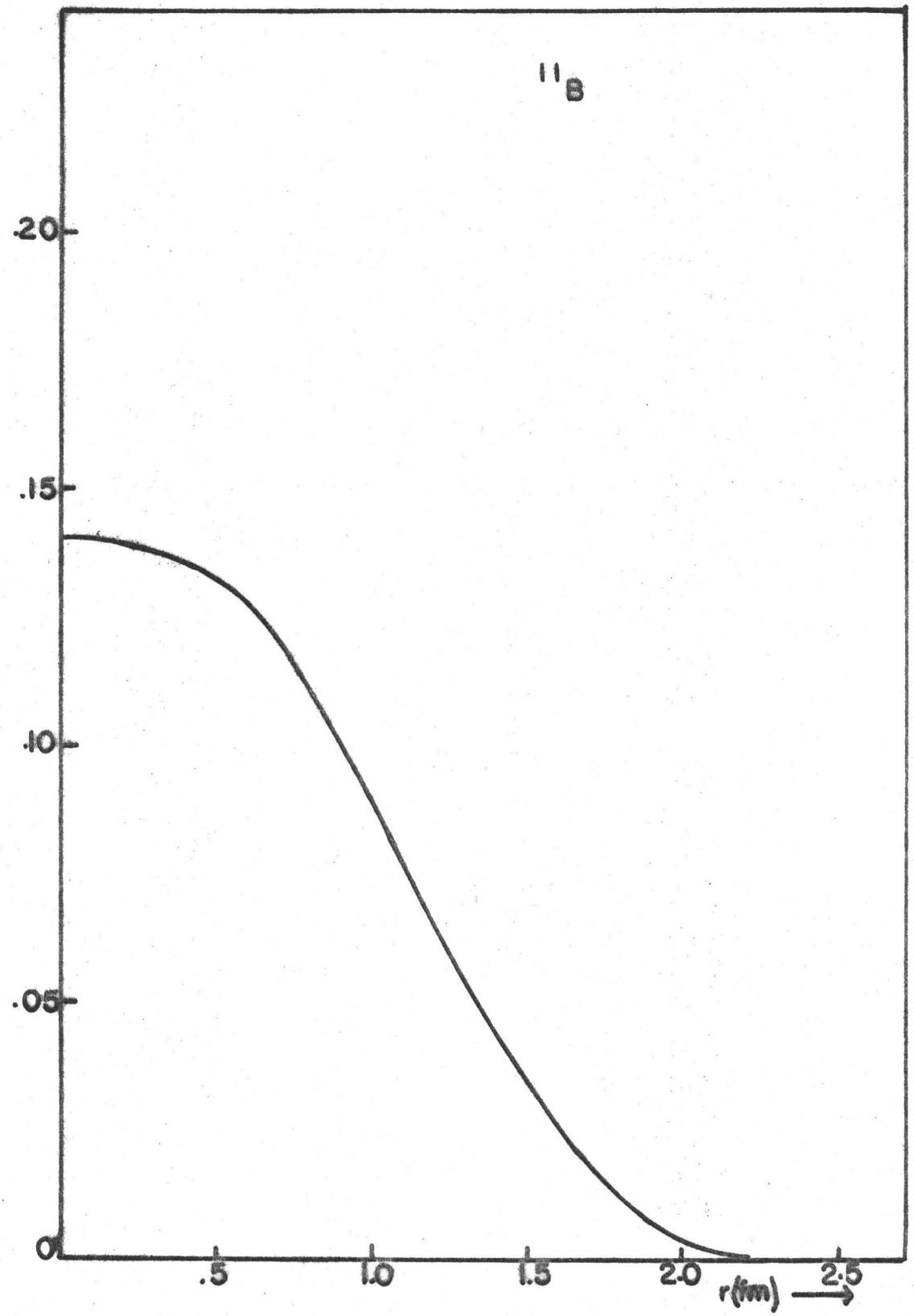

Figure 10.40

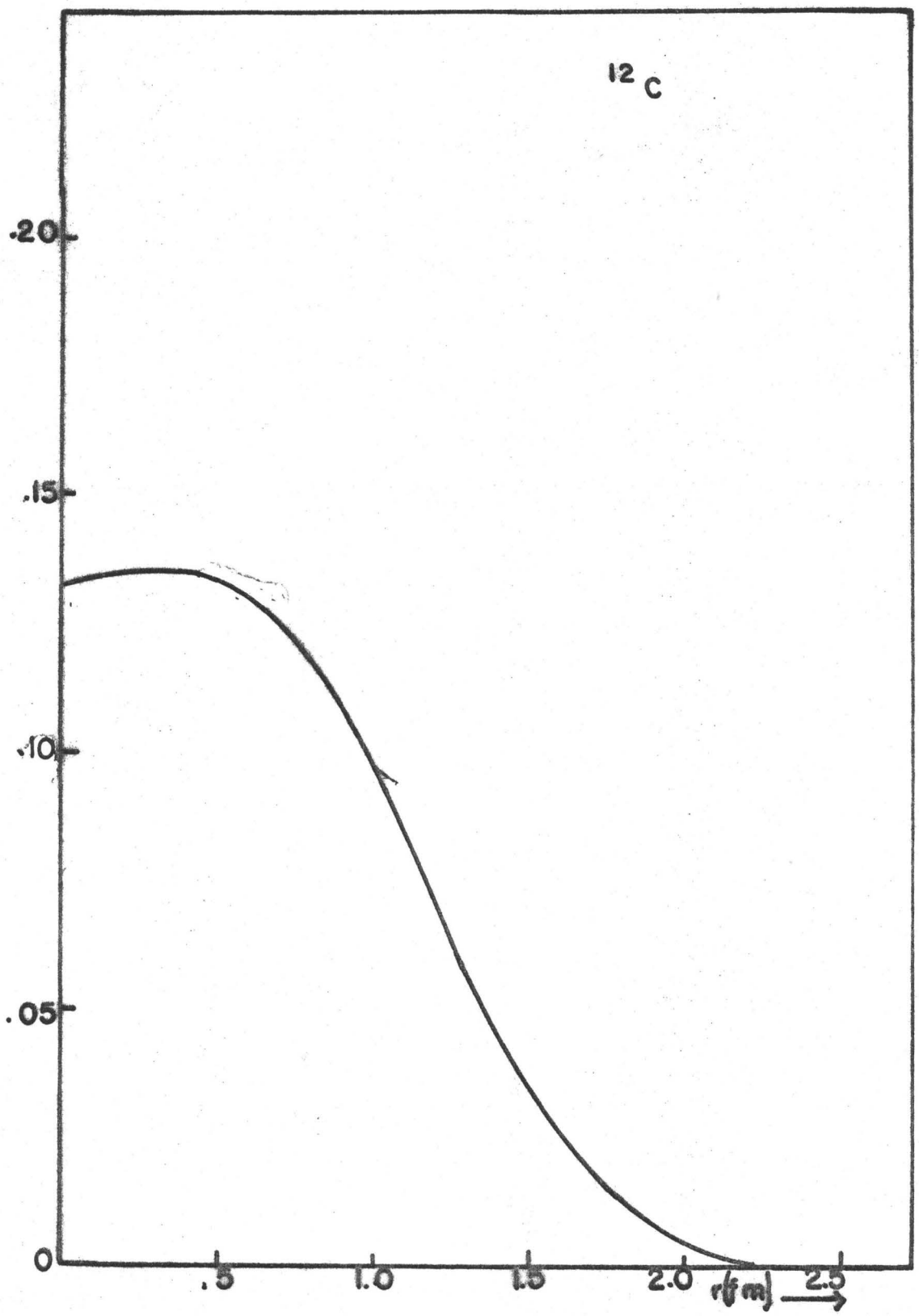

Figure 10.41

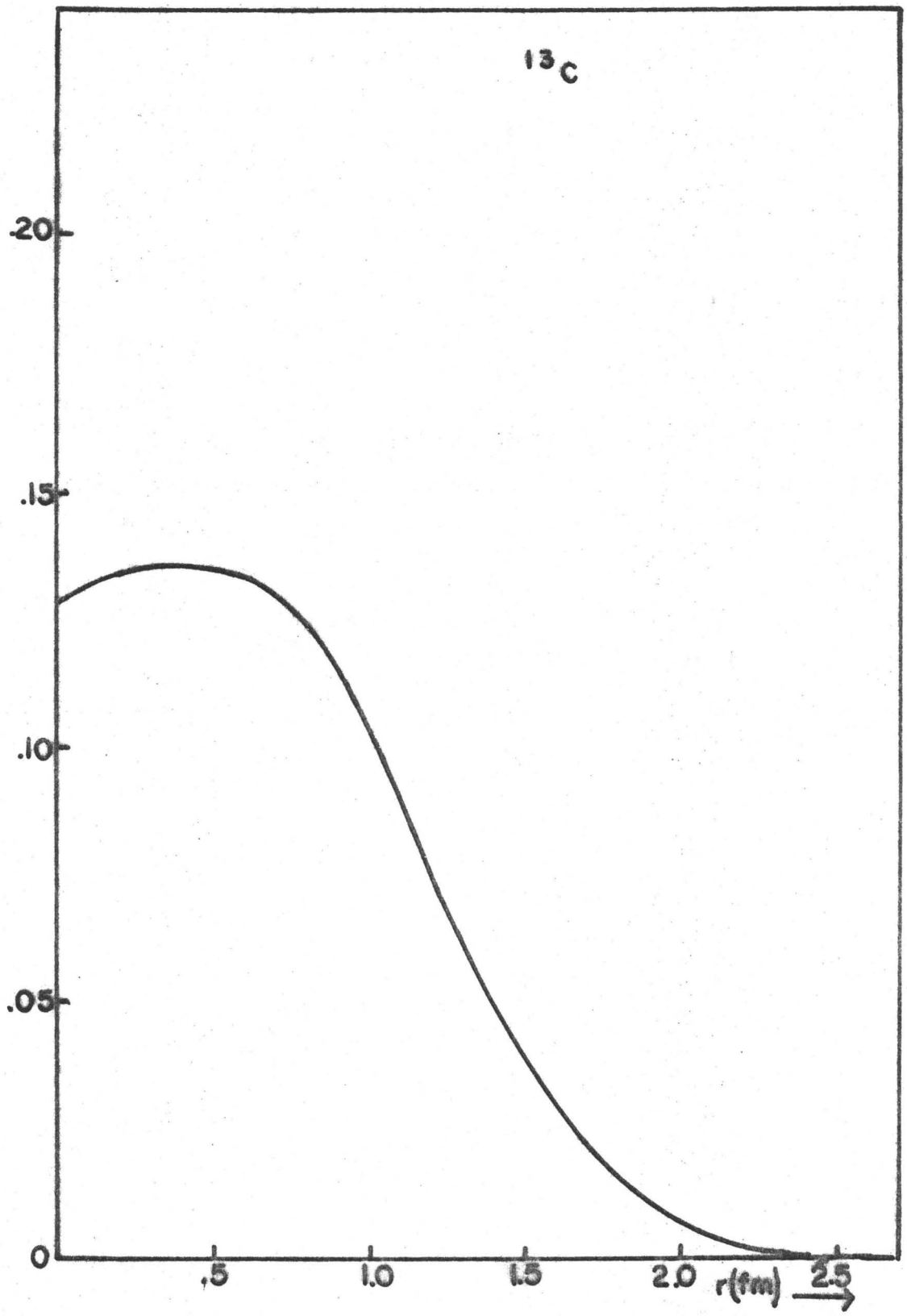

Figure 10.42

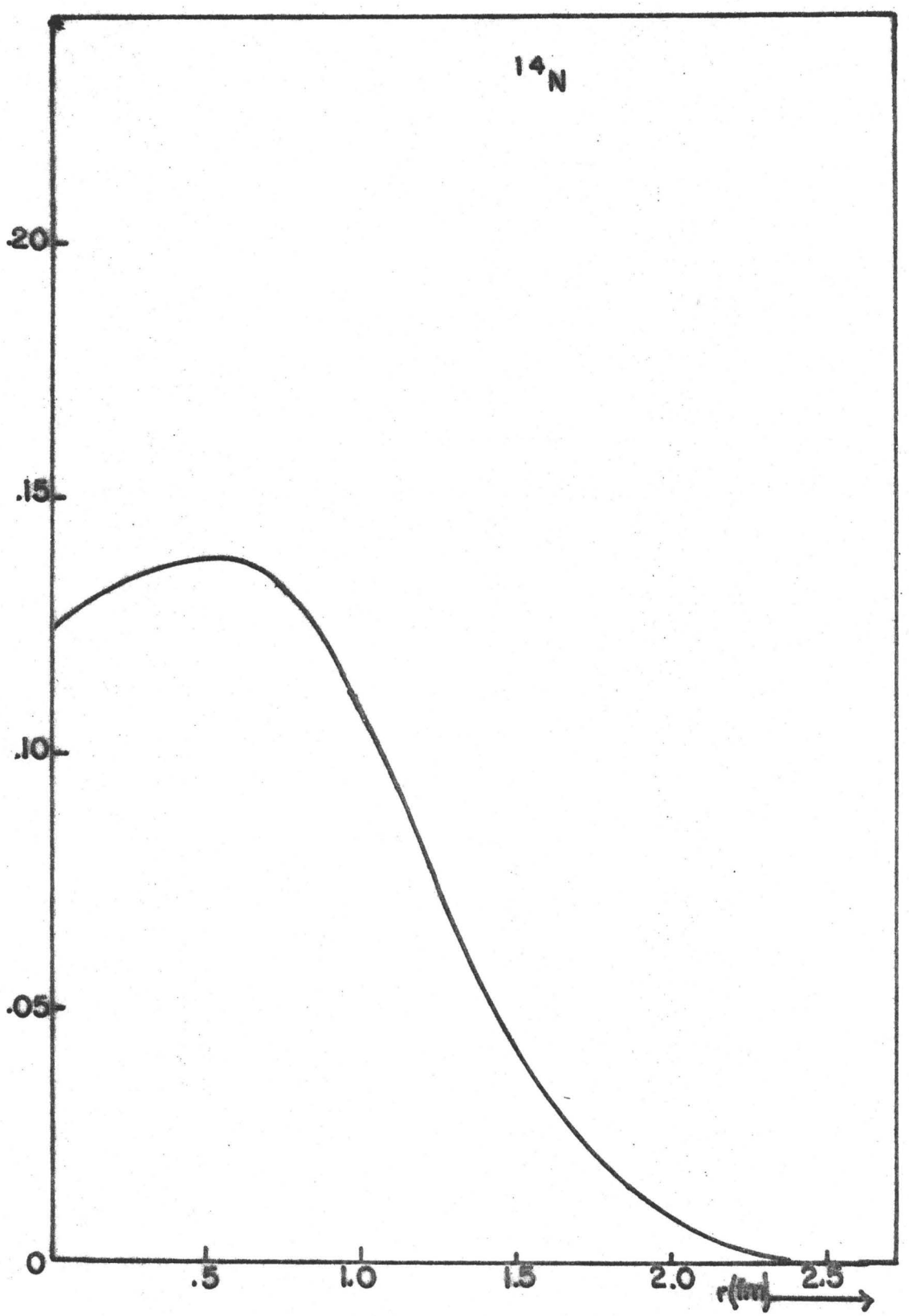

Figure 10.43

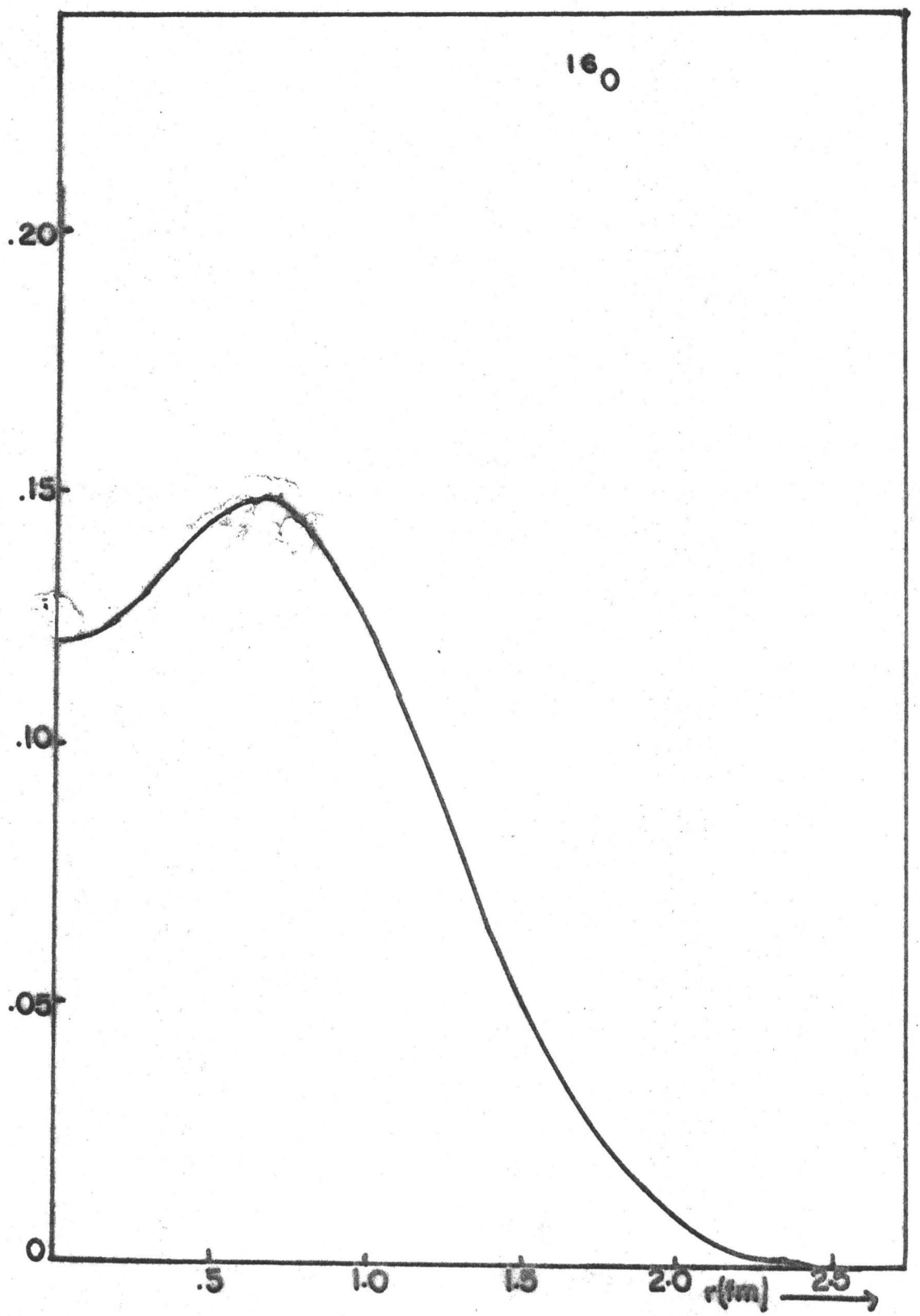

CHAPTER 11

CONCLUSIONS

It has been the purpose of this thesis to develop an "effective" interaction for use in Hartree-Fock and variational calculations. To test the interactions the excitation energies of the excited states and the ground state properties of the 0-p shell nuclei have been calculated and a comparison of the calculated results with the relevant experimental results has been used as a basis in accepting the interaction as a "good" interaction or not.

In Chapter 4 it has been demonstrated that interactions of the local double gaussian type are inadequate because the calculated binding energies of the 0-p shell nuclei are too small for these interactions. A simple modification of the local interaction (making the repulsive range velocity dependent) was also shown to be inadequate on these grounds, although the results for this type of interaction were an improvement on those of the simple local potentials. It was also shown that the admixture of states of the 1s-0d shell had a substantial effect on the excitation energies and binding energies of the 0-p shell nuclei. The idea of an "effective" interaction is to take into account such contributions from the admixture of states from higher

shells. If the wave function basis used in the calculations in this thesis included states of the 0s-1d shell (a near impossibility practically because of the large dimensionality of the wave function basis that would be generated) the best "effective" interaction found would, obviously be very different from Interaction 36 of Chapter 10. It should, however be noted that even with admixtures of 1s-0d states, the predicted binding energies of the open 0-p shell nuclei were still too low. Interactions of the local type lead to the "collapse" of nuclear systems heavier than ^{16}O which was reflected in the small r.m.s. radii for the 0-p shell nuclei.

To prevent this collapse interactions were required to saturate nuclear matter, this being achieved by introducing two density dependent terms into the basic interaction. The idea of adding density dependent terms to the interaction is quite realistic. Bethe (Bet 67), Kuo and Brown (Kuo 65) and Bhaduri and Warke (Bha 68) have all, in realistic calculations, indicated that the internucleon interaction should be density dependent. Although no attempt has been made to link the effective interactions developed in this thesis to realistic interactions in a formal manner, some correspondence with reality has been maintained by insisting that the effective interactions fit some realistic data e.g. the scattering data in zero density limit and the properties of nuclear matter.

Interactions were also required to predict the

experimental binding energy of ^{16}O thus ensuring that the surface energy term is taken into account. The changes in the excitation energies of the O-p shell nuclei which result by fitting the identical basic interaction to different values of the ^{16}O binding energy was examined in Chapter 5 and these changes were shown to be substantial. Fitting the interactions to the scattering data, nuclear matter properties and the ^{16}O binding energy allows one degree of freedom in the choice of the parameters of the interaction; the strength of one of the exchange parameters. It has been indicated in Chapter 5 that the changes in the excitation energies of the excited states of the O-p shell nuclei for different choices of this parameter were not great enough to uniquely define this parameter for any interaction.

It has been demonstrated in Chapter 6 that use of the closed-shell single gaussian density approximation was entirely adequate for the nuclei studied and for the interactions used in this thesis. For "strong" density dependent interactions (where $B.E._{den}$ is large) this may no longer be true and multi-gaussian density approximations may be needed.

It was shown in Chapter 7 that for the family of interactions having fixed λ_a, n_1 and n_2, a λ_r^0 could be found which "fitted" the excitation energies of a large number of excited states and that interactions which predicted the same excitation energy of one of these states

(e.g. the second 2^+ state of ^{8}Be) also predicted the same excitation energies for the other states. The excited states not fitted in this way could be fitted by varying λ_a. It was, thus, demonstrated that for any n_1 and n_2 an "effective" interaction which fitted the binding energies and excited state spectra of the O-p shell nuclei could be found. In this sense, unique values of n_1 and n_2 could not be assigned.

Different density dependencies were studied in Chapter 8 where it was seen that for an interaction having a repulsive range almost equal to the attractive range the excitation energies were virtually the same for any density dependence. The procedure of making the strengths and ranges of the density dependent terms of the interaction identical to the attractive and repulsive non-density parts of the interaction is arbitrary. The results obtained by using different ranges (Chapter 8) and different strengths and ranges (Chapter 9) for the density dependent interaction were not substantially different from those obtained using this assumption. It was further demonstrated in Chapter 9 that (for reasonable repulsive core heights) the scattering data fit is such that "identical" interactions are produced (in the sense that the parameters deduced from the nuclear matter fit and the excitation energies etc. predicted for the O-p shell nuclei were the same for interactions which differ primarily by having different repulsive core heights).

The effect of relaxing the nuclear matter criteria was examined in Chapter 9. The requirement that finite nuclei saturate was also relaxed in Chapter 9 and the importance (for excitation energy studies) of being careful in the minimization of the ground state binding energy of a finite nucleus was clearly seen.

The "best" interaction for n_1=1 and n_2=2 was used in Chapter 10 to calculate all the 0-p shell nuclei. The only properties of the 0-p shell nuclei not adequately predicted by this interaction were the binding energy of ^{4}He and the root-mean-square radii of the lighter nuclei.

In conclusion, the results for Interaction 36 indicate that interactions of the type considered are capable of predicting the qualitative behaviour of the excitation energies of the excited states of, and the binding energies of finite nuclei. The results for the 0-p shell nuclei quoted in Chapter 10 compare favourably with results obtained using the same truncated set of basis wave functions for realistic interactions by Halbert et. al. (Hal 66). Further the j-j coupling matrix elements calculated in Appendix 6 for Interaction 36 compare qualitatively with those of Kuo and Brown (Kuo 67). Thus, since the interactions were also fitted to nuclear matter, calculations of nuclear systems heavier than those considered in this thesis can confidently be undertaken utilizing the interactions developed in this thesis.

APPENDIX 1

EXPERIMENTAL INFORMATION

In this appendix the experimentally determined excitation energies, binding energies and root-mean-square radii of the nuclei ^{4}He, ^{16}O and A=6 to A=14 which can be constructed by limiting the individual nucleons to the O-p shell ($2<Z<8$; $2<N<8$) are tabulated.

Table A1.1 lists the relevant binding energies and are taken from the work of Everling et. al. (Eve 60) with the exception noted (a) which refers to binding energies given by Detraz (Det 65).

The root-mean-square radii (r.m.s.) are tabulated in Table A1.2 where column (a) refers to the work of Wilkinson and Mafethe (Wil 66), column (b) to Elton (Elt 67), column (c) to Backenstoss (Bac 67) and column (d) to Wilkinson and Hay (Wil 66a). The r.m.s. radius of ^{4}He is that of Yearian for the charge distribution (Yea 67).

Figures A1.1 - A1.9 illustrate the excited state spectra. The levels plotted as full lines are those assigned by Lauritsen and Ajzenburg-Selove (Lau 66; Ajz 68; Lau 62). The levels denoted by dashed lines are those found in the following references.

A=6 (a) Man 66; (b) Man 68; (c) Bat 65.

For ^{6}Be Man 66, Ecc 66 and Rog 66 find a level at 1.6 Mev, the latter two authors finding no further levels up to 10 Mev excitation.

A=7 (a) Man 68; (b) Bat 65.

The J^{π}; T assignment for the levels of ^{7}Li at 7.48 Mev and 11.13 Mev excitation is that of Presser et. al. (Pre 69).

A=8 (a) Ker 67; Pau 68.

A=10 (a) Rau 69; (b) Alb 66; (c) Man 66; (d) Ben 67.

The designation of spin for the 6.13 Mev and 6.56 Mev levels of ^{10}B are suggested by Meyer et. al. (Mey 67).

The 2^{+} assignment for the 3.36 Mev level of ^{10}C is suggested by Rousch et. al. (Rou 69) and Benenson et. al. (Ben 67); Benenson et. al. also suggests that the 5.96 Mev level of ^{10}C is a 2^{+} level.

A=11 (a) Pau 67.

A=14 (a) Bel 68; (b) Bla 67; (c) Tow 68.

Blake et. al. (Bla 67) and Cookson (Coo 68) believe that the 7.03 Mev level of ^{14}N is a 2 and a 2^{+} respectively, Blake et. al. further suggests a 1^{+} assignment to the 6.21 Mev level of ^{14}N.

TABLE A1.1

Z	N	A		Binding Energy (MeV)
2	2	4	He	28.30
2	3	5	He	27.34
3	2		Li	26.33
2	4	6	He	29.26
3	3		Li	31.99
2	5	7	He	26.03 (b)
3	4		Li	39.24
4	3		Be	37.60
5	2		B	27.99 (a)
2	6	8	He	31.60<B.E.<32.40 (a)
3	5		Li	41.28
4	4		Be	56.50
5	3		B	37.73
4	5	9	Be	58.16
5	4		B	56.31
4	6	10	Be	64.98
5	5		B	64.75
6	4		C	60.34
5	6	11	B	76.20
6	5		C	73.44
5	7	12	B	79.57
6	6		C	92.16
7	5		N	73.78

TABLE A1.1 - CONTINUED

Z	N	A		Binding Energy (MeV)
5	8	13	B	84.46
6	7		C	97.11
7	6		N	94.10
6	8	14	C	105.28
7	7		N	104.66
8	6		O	98.73
7	8	15	N	115.49
8	7		O	111.95
8	6	16	O	127.62

TABLE A1.2

A	Z	r.m.s.(fm) (a)	r.m.s.(fm) (b) (i)	(ii)	(iii)	r.m.s.(fm) (c)	r.m.s.(fm) (d)
4	2	1.71					
5	2	2.32					
6	3	2.38					
7	3	2.31					
8	4	2.17					
9	4	2.34					2.44
10	5	2.26				2.44	2.31
11	5	2.24				2.26	2.19
12	6	2.32	2.58	2.41 2.51	∿2.4	2.40	2.37
13	6	2.30					2.37
14	7	2.34				2.67	2.37
15	7	2.34					2.45
16	8	2.50		2.71	∿2.9	2.61	2.54

In column (b), (i) are results derived from electron scattering data using wave functions of the Saxon-Woods well; (ii) using wave functions of the harmonic oscillator well; (iii) results derived from μ-mesic x-ray scattering using a Fermi density distribution.

FIGURE CAPTIONS

Figure A1.1 Experimental Level Spectra for (a) ^{6}He, (b) ^{6}Li, (c) ^{6}Be.

Figure A1.2 Experimental Level Spectra for (a) ^{7}Li, (b) ^{7}Be.

Figure A1.3 Experimental Level Spectra for (a) ^{8}Li, (b) ^{8}Be, (c) ^{8}B.

Figure A1.4 Experimental Level Spectra for (a) ^{9}Li, (b) ^{9}Be, (c) ^{9}B.

Figure A1.5 Experimental Level Spectra for (a) ^{10}Be, (b) ^{10}B, (c) ^{10}C.

Figure A1.6 Experimental Level Spectra for (a) ^{11}Be, (b) ^{11}B, (c) ^{11}C.

Figure A1.7 Experimental Level Spectra for (a) ^{12}B, (b) ^{12}C, (c) ^{12}N.

Figure A1.8 Experimental Level Spectra for (a) ^{13}B, (b) ^{13}C, (c) ^{13}N.

Figure A1.9 Experimental Level Spectra for (a) ^{14}C, (b) ^{14}N, (c) ^{14}O.

Figure A1.1

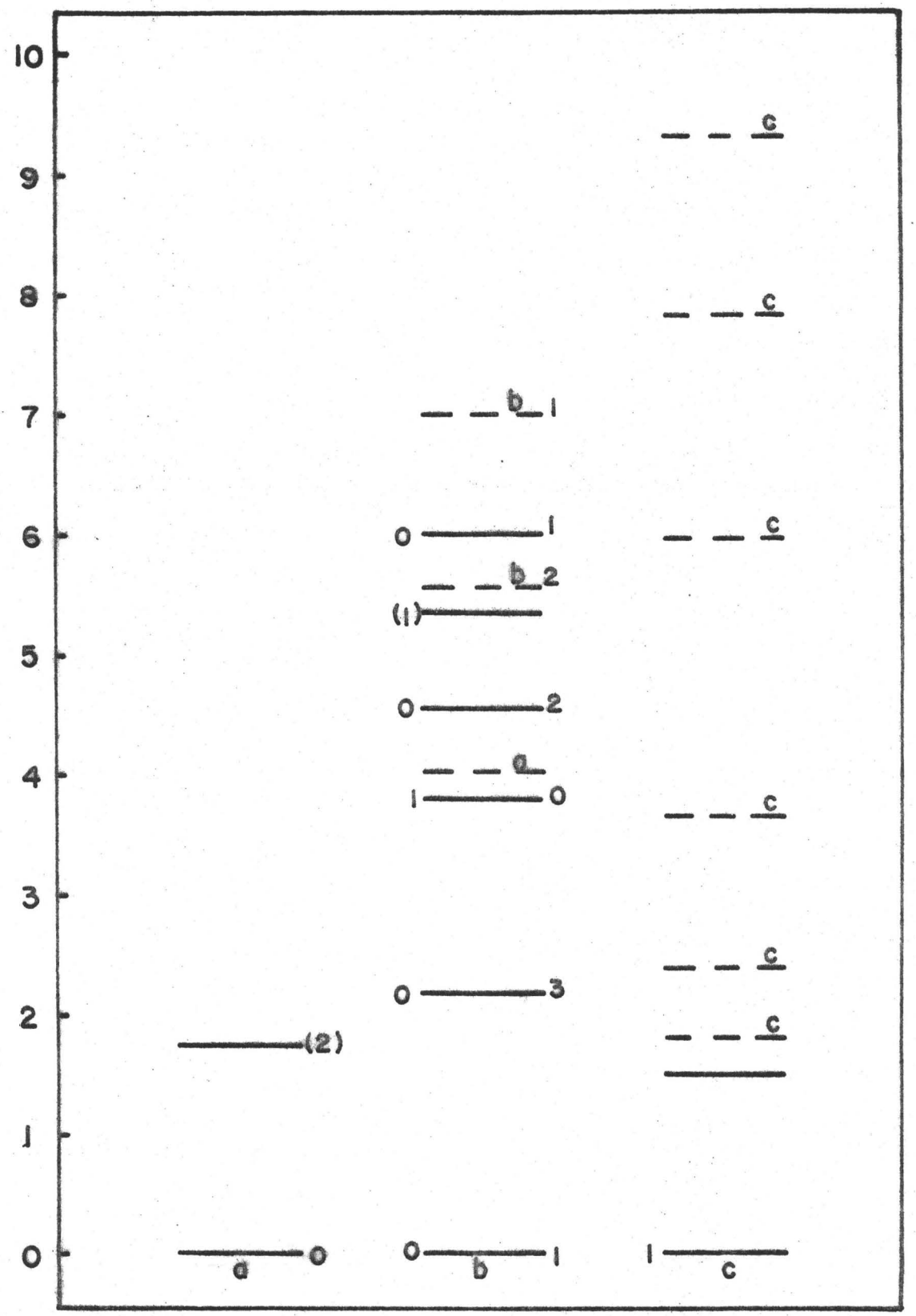

Figure A1.2

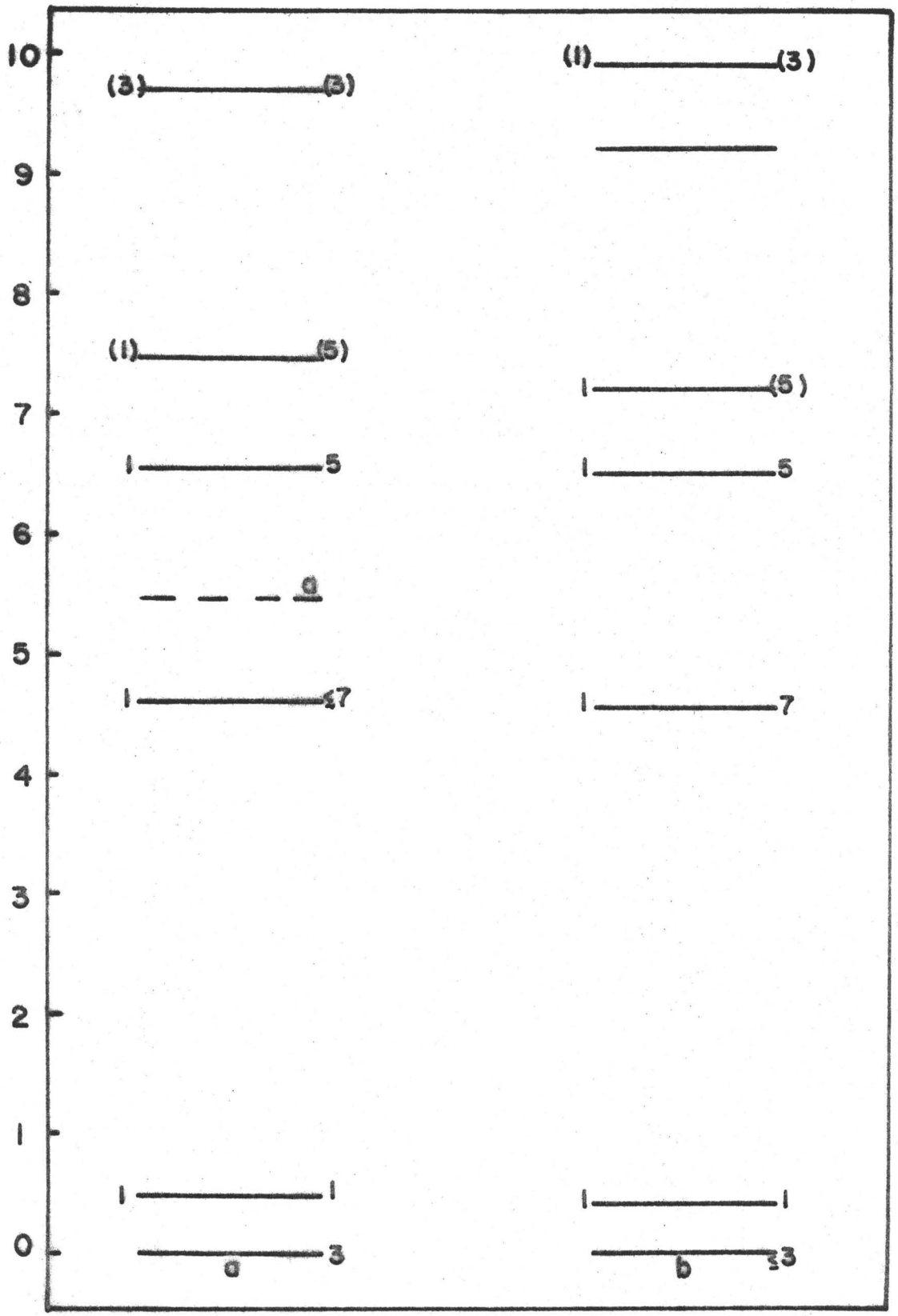

Figure A1.3

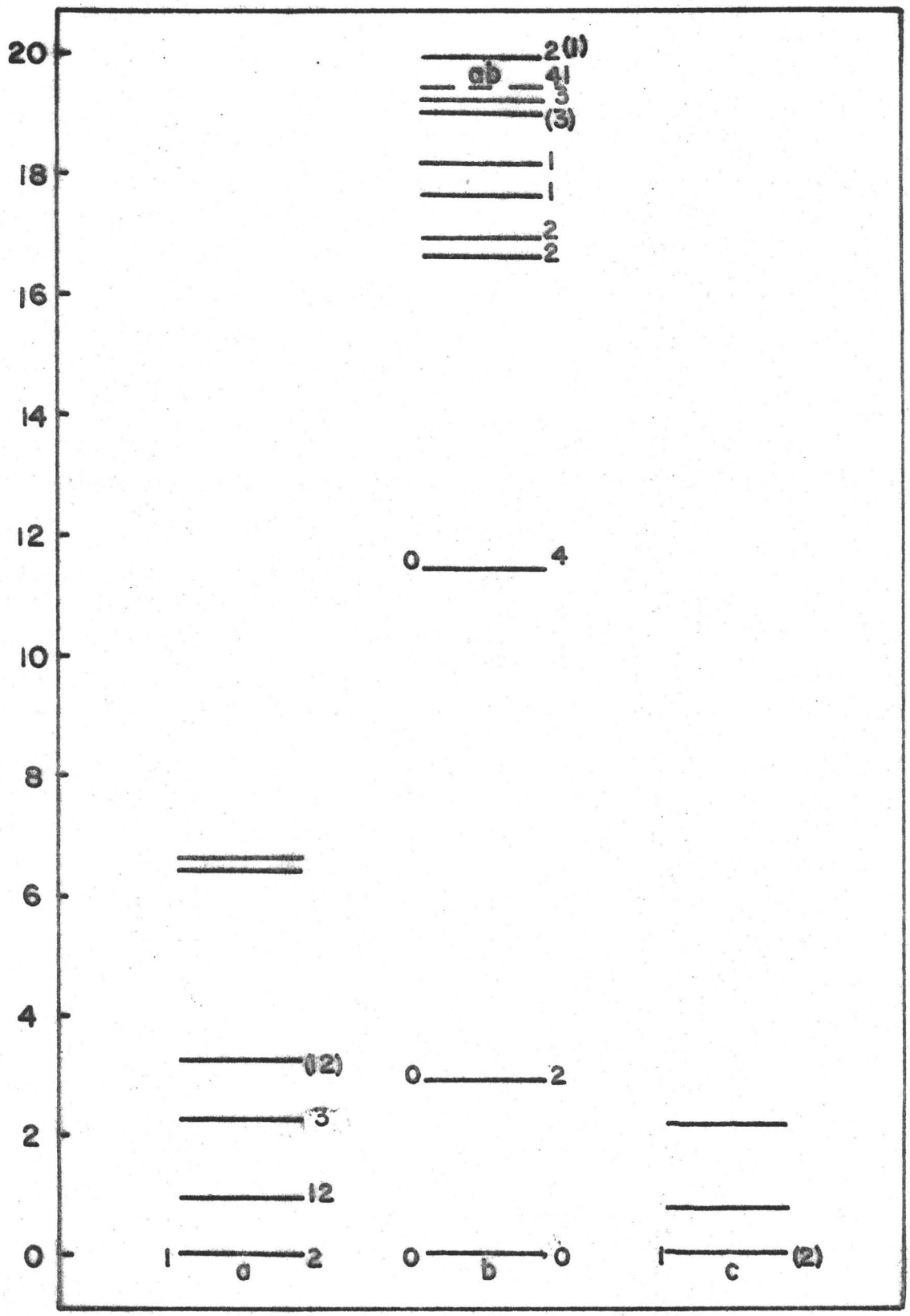

Figure A1.4

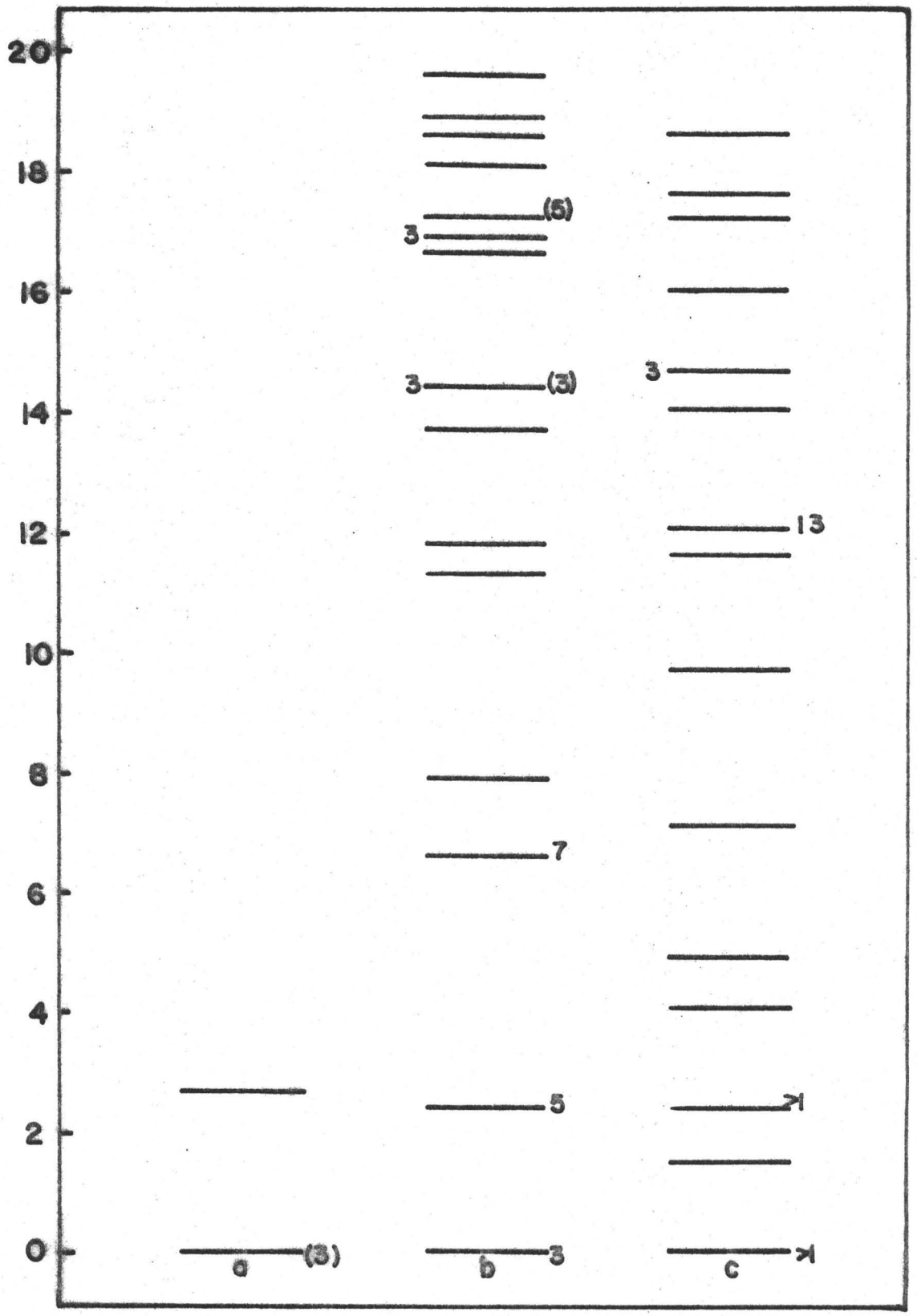

Figure A1.5

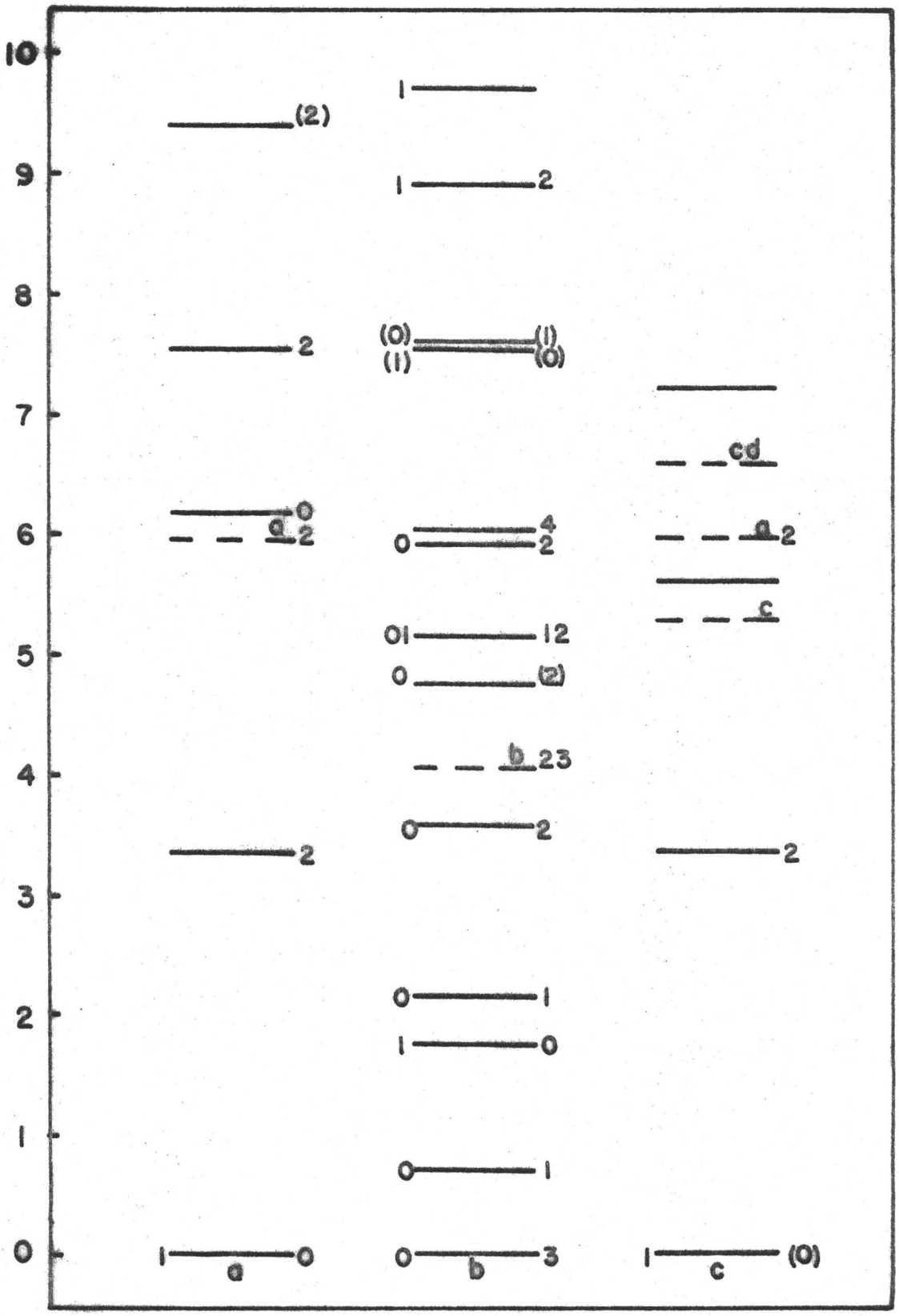
10
9
8
7
6
5
4
3
2
1
0
(2)
2
0
a 2
2
1
2
(0) (1)
(1) (0)
4
0 2
01 12
0 (2)
b 23
0 2
0 1
1 0
0 1
1 0
a
0 3
b
cd
a 2
c
2
1 (0)
c

Figure A1.6

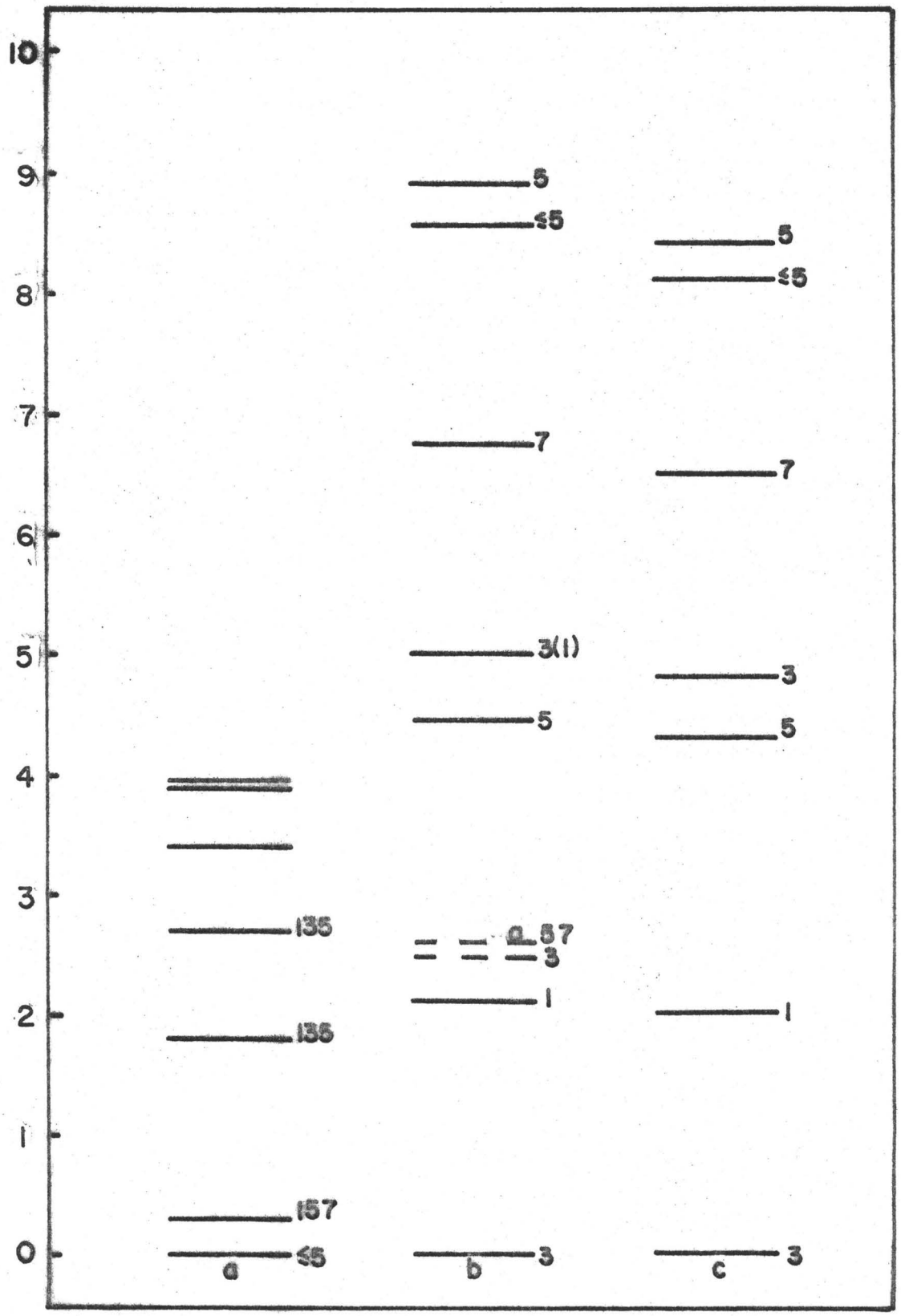

Figure A1.7

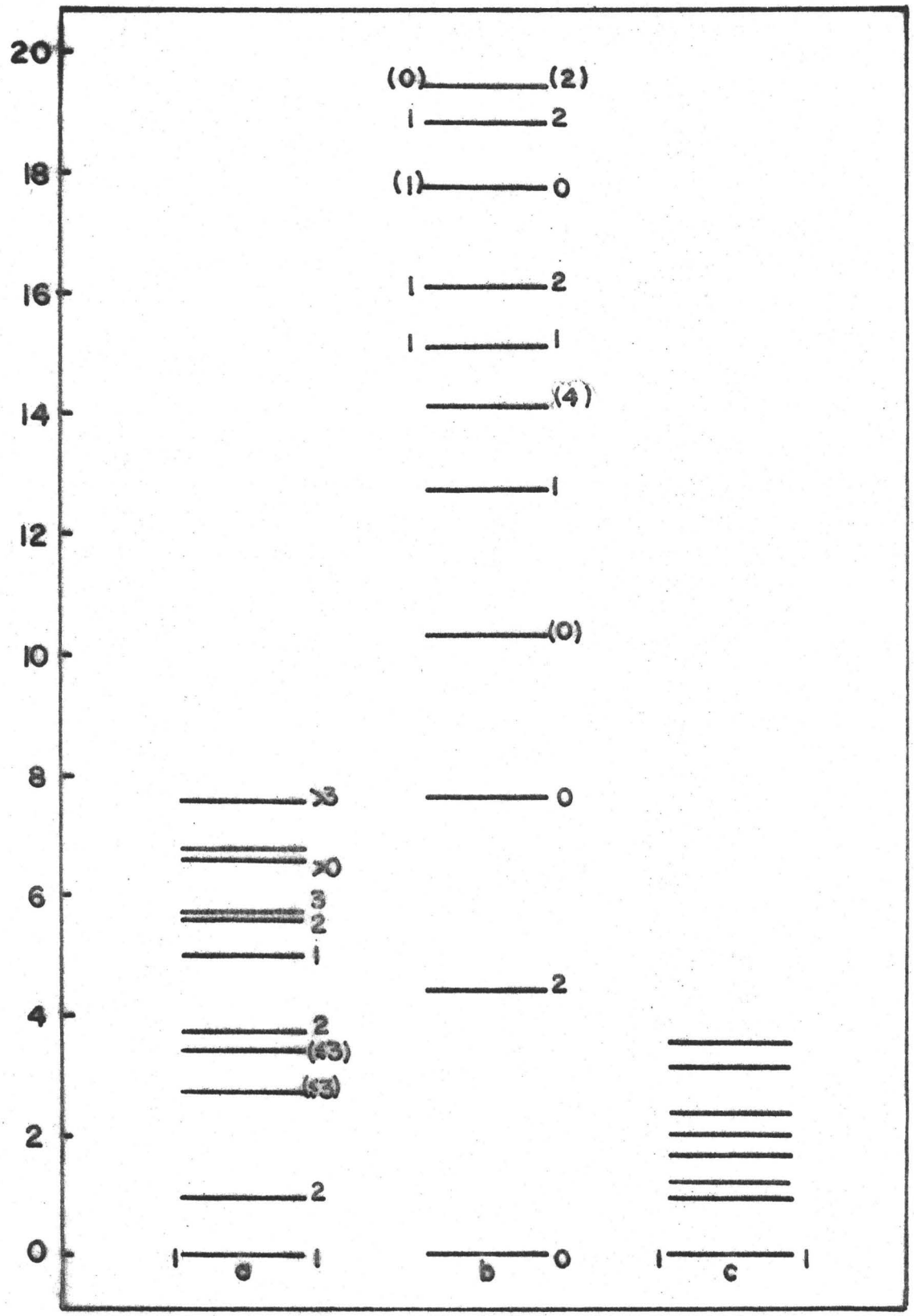

Figure A1.8

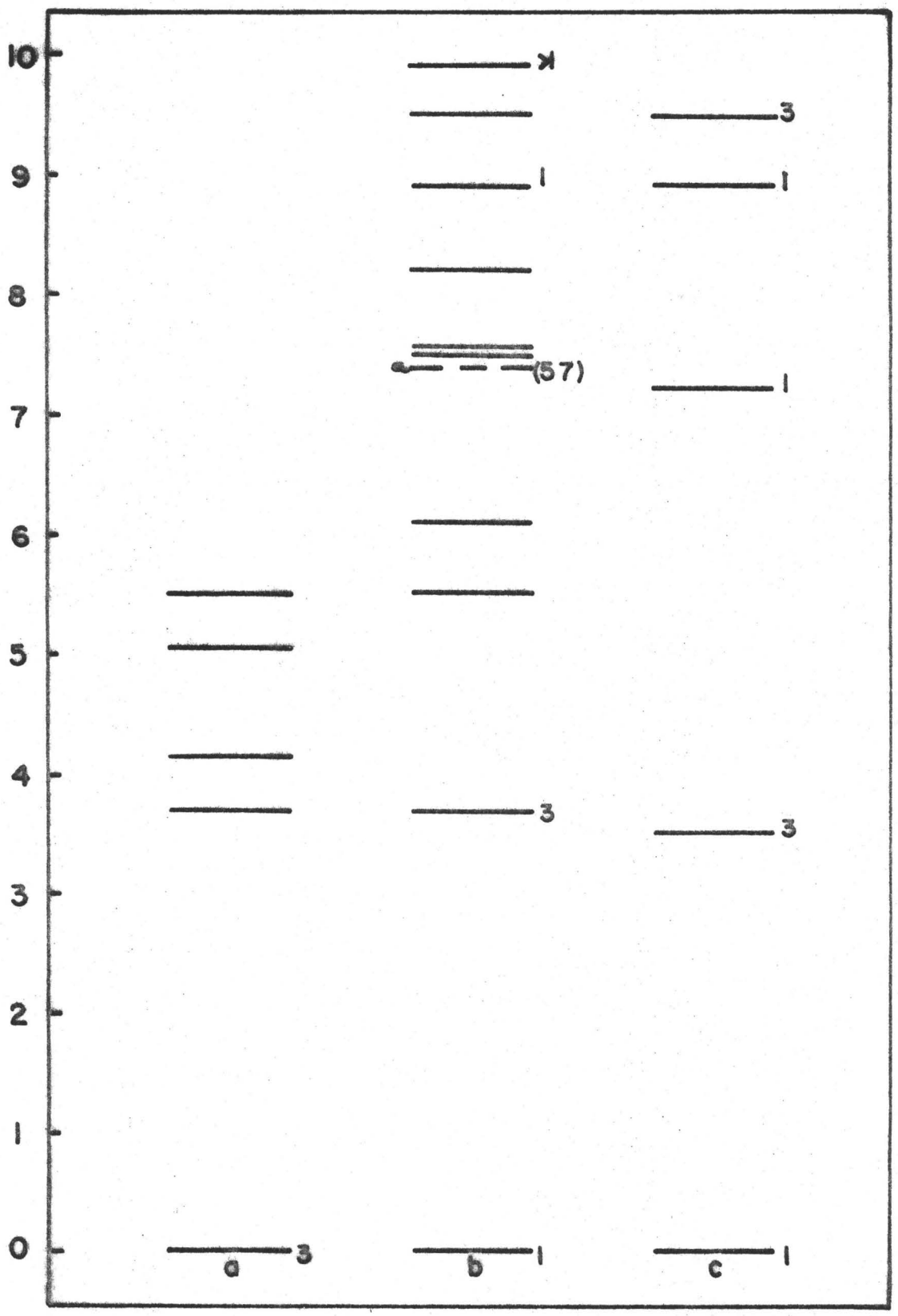

Figure A1.9

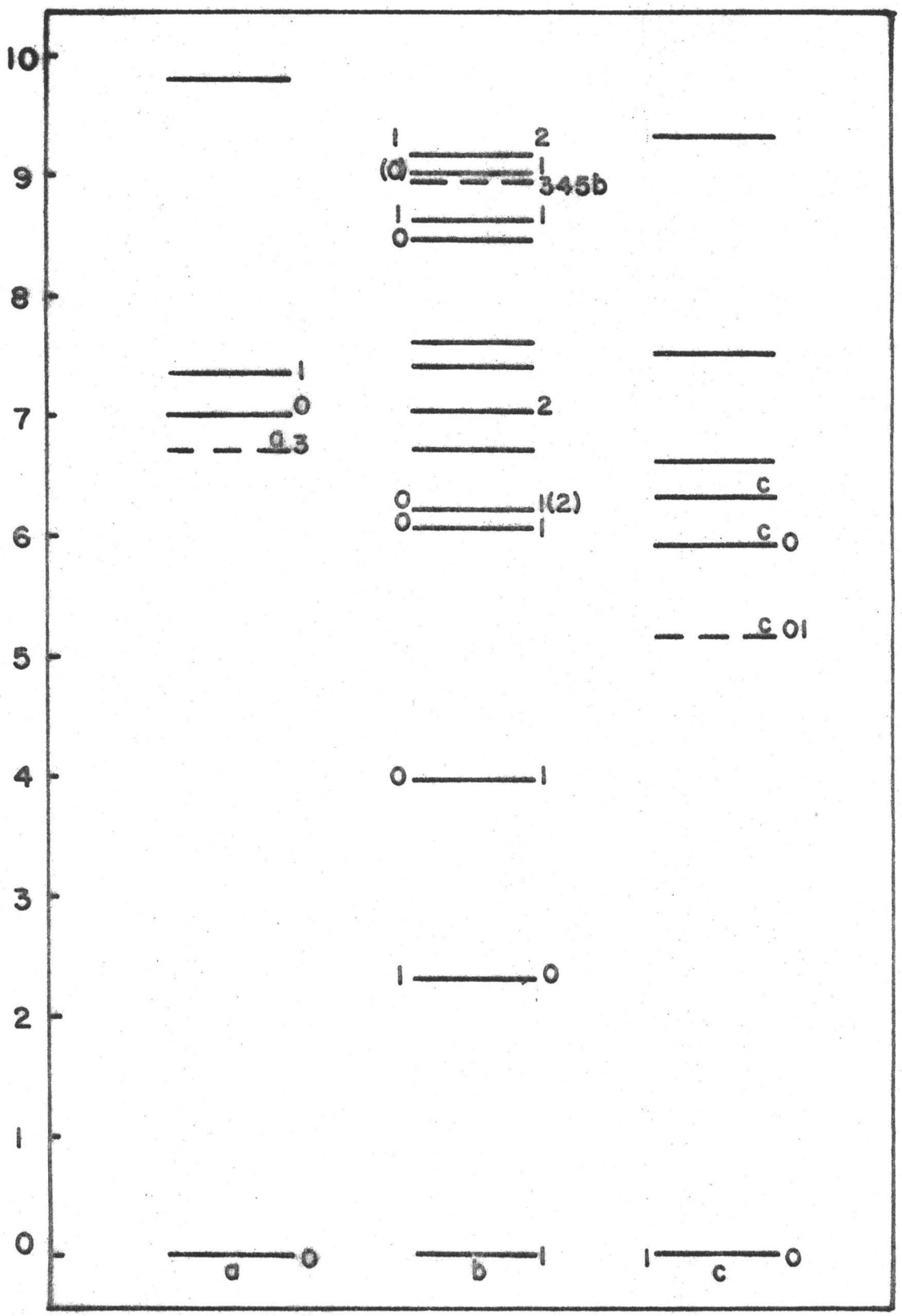

APPENDIX 2

SINGLE PARTICLE WAVE FUNCTIONS

The single particle wave functions used to build up the Slater product determinantal wave function base were those of the harmonic oscillator well having cylindrical symmetry.

They are the solutions of the equation

$$[-\frac{h^2}{2m}\nabla^2 + \frac{m\omega_\rho^2}{2}\rho^2 + \frac{m\omega_z^2}{2}z^2]\psi_{nmn_z} = E_{nmn_z}\psi_{nmn_z}$$

and are the form (Cop 66)

$$\psi_{nmn_z} = N_{nmn_z} e^{im\phi}(\alpha^{\frac{1}{2}}\rho)^{|m|} L_n^{|m|}(\alpha\rho^2) e^{-\frac{1}{2}\alpha\rho^2}$$

$$\times H_{n_z}(\beta^{\frac{1}{2}}z) e^{-\frac{1}{2}\beta z^2}$$

where

$$N_{nmn_z} = \frac{1}{\sqrt{2\pi}}\sqrt{\frac{2\alpha\ n!}{(n+|m|)!}}\left(\frac{\beta}{\pi}\right)^{1/4}\sqrt{\frac{1}{2^{n_z}\ n_z!}}$$

and

$$\alpha = \frac{m\omega_\rho}{\hbar} \quad , \quad \beta = \frac{m\omega_z}{\hbar} \quad .$$

α, β have the dimension $(\text{length})^{-2}$ and are related to the more conventional oscillator well parameters (Gol 63)

by

$$(\alpha,\beta) = (\frac{1}{a^2}, \frac{1}{b^2}) \quad .$$

E_{nmn_z}, the kinetic energy of a single particle state is given by

$$E_{nmn_z} = (2n+|m|+1)\hbar\omega_\rho + (n_z+\tfrac{1}{2})\hbar\omega_z \quad .$$

The specific single particle wave functions used in this thesis were

$$^{O}S \qquad \psi_{000} = \alpha^{1/2}\ \beta^{1/4}\ \pi^{-3/4}\ e^{-\frac{1}{2}\alpha\rho^2}\ e^{-\frac{1}{2}\beta z^2}$$

$$^{O}P_{\pm 1} \qquad \psi_{0\pm 10} = \alpha\ \beta^{1/4}\ \pi^{-3/4}\ \rho\ e^{\pm i\phi}\ e^{-\frac{1}{2}\alpha\rho^2}\ e^{-\frac{1}{2}\beta z^2}$$

$$^{O}P_0 \qquad \psi_{001} = 2^{1/2}\ \alpha^{1/2}\ \beta^{3/4}\ \pi^{-3/4}\ z\ e^{-\frac{1}{2}\alpha\rho^2}\ e^{-\frac{1}{2}\beta z^2} \quad .$$

The mean square radius for a single particle state is the square root of the sum of the expectation values of ρ^2 and z^2

and

$$\langle\rho^2\rangle = (2n+|m|+1)/\alpha$$

$$\langle z^2\rangle = (n_z+\tfrac{1}{2})/\beta \quad .$$

The state ψ_{nmn_z} is prolate, spherical, or oblate as

$$(2n_z+1)\alpha - (2n+|m|+1)\beta \lessgtr 0 \quad .$$

The four single particle states considered in this thesis are orthonormal to each other for any and all values of the oscillator parameters. For higher states this is no longer true and the requirement of orthonormality imposes restrictions on the different oscillator parameters (Man 67).

APPENDIX 3

POTENTIAL MATRIX ELEMENTS

The most general form of the density dependence used in this work is of the kind $\rho^{\alpha}(R)$ where

$$R = \underline{r}_1 + \underline{r}_2 \ .$$

$\rho^{\alpha}(R)$ is approximated by gaussian and thus, essentially for purposes of matrix element evaluation a term $\exp(-k_D(\underline{r}_1+\underline{r}_2)^2/2|$ appears in the integration over all space.

The general matrix element that must be evaluated is (Cop 66)

$$<\psi_{n_1 m_1 n_{z_1}}(\sqrt{\alpha}\ \underline{\rho}_1, \phi_1, \sqrt{a}\ z_1),\ \psi_{n_2 m_2 n_{z_2}}(\sqrt{\beta}\ \underline{\rho}_2, \phi_2, \sqrt{b}\ z_2)$$

$$|\exp(-\tfrac{1}{2}k((\underline{\rho}_1-\underline{\rho}_2)^2 + (z_1-z_2)^2) \ .$$

$$\exp(-\tfrac{1}{2}k_D((\underline{\rho}_1+\underline{\rho}_2)^2 + (z_1+z_2)^2)|$$

$$\psi_{n_3 m_3 n_{z_3}}(\sqrt{\gamma}\ \underline{\rho}_1, \phi_1, \sqrt{c}\ z_1)\ \psi_{n_4 m_4 n_{z_4}}(\sqrt{\delta}\ \underline{\rho}_2, \phi_2, \sqrt{d}\ z_2)$$

$$= M(n_1 m_1 \alpha\ , n_2 m_2 \beta, n_3 m_3 \gamma, n_4 m_4 \delta; k; k_D)$$

$$I(n_{z_1} a; n_{z_2} b; n_{z_3} c; n_{z_4} d)$$

where the radial and angular parts of the matrix element, M, can be separated from I, the z-part of the matrix element.

The Radial and Angular Matrix Element

For, convenience, the normalization constants are ignored for the present and the unnormalized radial and angular matrix element is written as

$$M(n_1 m_1 \alpha, n_2 m_2 \beta, n_3 m_3 \gamma, n_4 m_4 \delta; k; k_D)$$

$$= \int\int\int\int (\sqrt{\alpha}\ \underline{\rho}_1)^{|m_1|} L_{n_1}^{|m_1|}(\alpha \underline{\rho}_1^2) e^{-\frac{1}{2}\alpha \underline{\rho}_1^2} e^{-im_1\phi_1}$$

$$(\sqrt{\beta}\ \underline{\rho}_2)^{|m_2|} L_{n_2}^{|m_2|}(\beta \underline{\rho}_2^2) e^{-\frac{1}{2}\beta \underline{\rho}_2^2} e^{-im_2\phi_2}$$

$$e^{-\frac{1}{2}k(\underline{\rho}_1^2+\underline{\rho}_2^2-2\underline{\rho}_1\underline{\rho}_2 \cos\phi_{12})} e^{-\frac{1}{2}k_D(\rho_1^2+\rho_2^2+2\rho_1\rho_2 \cos\phi_{12})}$$

$$(\sqrt{\gamma}\ \rho_1)^{|m_3|} L_{n_3}^{|m_3|}(\gamma\rho_1^2)\ e^{im_3\phi_1}\ e^{-\frac{1}{2}\gamma\rho_1^2}$$

$$(\sqrt{\delta}\ \rho_2)^{|m_4|} L_{n_4}^{|m_4|}(\delta\rho_2^2)\ e^{im_4\phi_2}\ e^{-\frac{1}{2}\delta\rho_2^2}$$

$$\rho_1\rho_2\ d\rho_1\ d\rho_2\ d\phi_1\ d\phi_2$$

The angular variables are chosen as ϕ_2 and $\chi = \phi_{12} = \phi_1 - \phi_2$. The ϕ_2 integration, which is performed second gives a factor $2\pi\delta_{m_1+m_2-m_3-m_4,0}$ i.e. the selection rule which

conserves the projection of the angular momentum along the z-axis. For the ϕ_{12} integration use is made of the relation (Leb 65)

$$\int_0^{2\pi} e^{i(m_3-m_1)\phi_{12}} e^{(k-k_D)\rho_1\rho_2 \cos\phi_{12}} d\chi$$

$$= 2\pi e^{\frac{1}{2}i(m_3-m_1)\pi}$$

$$J_{(m_3-m_1)}(-i(k-k_D)\rho_1\rho_2)$$

Defining $\rho_1' = \sqrt{\lambda'}\,\rho_1$ where

$$\lambda' = 2(\alpha+\gamma+k+k_D)$$

M now becomes

$$M = 4\pi^2 \int_0^\infty \int_0^\infty J_{(m_3-m_1)}\left(-\frac{i(k-k_D)}{\sqrt{\lambda'}}\rho_1'\rho_2\right)$$

$$e^{\frac{1}{2}i(m_3-m_1)\pi}\, \alpha^{\frac{1}{2}|m_1|}\, \beta^{\frac{1}{2}|m_2|}\, \gamma^{\frac{1}{2}|m_3|}\, \delta^{\frac{1}{2}|m_4|}$$

$$\frac{1}{(\sqrt{\lambda'})^{(|m_1|+|m_3|+2)}}\, \rho_2^{|m_2|+|m_4|}\, \rho_1'^{|m_1|+|m_3|}$$

$$e^{-\frac{1}{2}(\beta+\delta+k+k_D)\rho_2^2}\, e^{-\frac{1}{4}\rho_1'^2}$$

$$L_{n_1}^{|m_1|}\left(\frac{\alpha\,\rho'^2}{\lambda'}\right) L_{n_2}^{|m_2|}(\beta\rho_2^2)\, L_{n_3}^{|m_3|}\left(\frac{\gamma}{\lambda'}\rho_1'^2\right)$$

$$L_{n_4}^{|m_4|}(\delta\rho_2^2)\, \rho_1'\, d\rho_1'\, \rho_2\, d\rho_2$$

But

$$L_p^k(\alpha\rho) = \sum_{s=0}^{p} \mathcal{L}_{ps}^{k}(\alpha)\rho^s$$

where

$$\mathcal{L}_{ps}^{k}(\alpha) = \frac{(p+k)!(-\alpha)^s}{(p-s)!(k+s)!s!}$$

Using this expression for the Laguerre polynomials

$$M = 4\pi^2 \int_0^\infty \int_0^\infty e^{\frac{1}{2}i(m_3-m_1)\pi}\, \alpha^{\frac{1}{2}|m_1|}\beta^{\frac{1}{2}|m_2|}$$

$$\gamma^{\frac{1}{2}|m_3|}\delta^{\frac{1}{2}|m_4|}\lambda'^{-\frac{1}{2}(|m_1|+|m_3|+2)}$$

$$\sum_{r=0}^{n_1} \mathcal{L}_{n_1 r}^{|m_1|}(4\alpha/\lambda')\, \frac{1}{4^r} \sum_{s=0}^{n_2} \mathcal{L}_{n_2 s}^{|m_2|}\left(\frac{\beta\lambda'}{K'^2}\right) \frac{K'^{2s}}{\lambda'^{s}}$$

$$\sum_{t=0}^{n_3} \mathcal{L}_{n_3 t}^{|m_3|}(4\gamma/\lambda')\frac{1}{4^t} \sum_{u=0}^{n_4} \mathcal{L}_{n_4 u}^{|m_4|}\left(\frac{\delta\lambda'}{K'^2}\right) \frac{K'^{2u}}{\lambda'^{u}}$$

$$\rho'^{|m_1|+|m_3|+2r+2t}\, \rho_2^{|m_2|+|m_4|+2s+2u}$$

$$e^{-\frac{1}{4}\rho_1^2} J_{(m_3-m_1)}\left(\frac{-i(k-k_D)}{\sqrt{\lambda'}}\rho_1'\rho_2\right)$$

$$e^{-\frac{1}{2}(\beta+\delta+k+k_D)\rho_2^2}\, \rho_1'\, d\rho_1'\, \rho_2\, d\rho_2$$

The integration over ρ_1' can be performed by making

use of the relation (Leb 65a)

$$\int_0^\infty x^{2n+p+1}\, e^{-\frac{1}{4}x^2}\, Jp(xy)dx$$

$$= 2^{2n+p+1}\, n!\, e^{-y^2} L_n^p(y^2)$$

This expression is valid when p and n are integer for any complex y. Further

$$J_{-p}(x) = (-1)^p\, J_p(x)$$

Thus p can be taken to be

$$p = |m_3-m_1|$$

with

$$y = \frac{-i(k-k_D)}{\sqrt{\lambda'}}\rho_2$$

n is defined as

$$2n = |m_1|+|m_3|+2r+2t-|m_3-m_1|$$

And

$$M = 4\pi^2 \int_0^\infty 2^{|m_1|+|m_3|+1}\, \frac{n!(k-k_D)^{|m_3-m_1|}}{(\lambda')^{\frac{1}{2}|m_3-m_1|}}$$

$$\rho_2^{|m_3-m_1|}\, e^{(k-k_D)^2\rho_2^2/\lambda'}\, L^{|m_3-m_1|}_{(-(k-k_D)^2\rho_2^2/\lambda')}$$

$$\alpha^{\frac{1}{2}|m_1|}\, \beta^{\frac{1}{2}|m_2|}\, \gamma^{\frac{1}{2}|m_3|}\, \delta^{\frac{1}{2}|m_4|}\, \lambda'^{-\frac{1}{2}(|m_1|+|m_3|+2)}$$

$$\sum_{r=0}^{n_1} \mathcal{L}^{|m_1|}_{n_1 r}(4\alpha/\lambda') \sum_{s=0}^{n_2} \mathcal{L}^{|m_2|}_{n_2 s}\left(\frac{\beta\lambda'}{K'^2}\right) \frac{K'^{2s}}{\lambda'^{s}}$$

$$\sum_{t=0}^{n_3} \mathcal{L}^{|m_3|}_{n_3 t}(4\gamma/\lambda') \sum_{u=0}^{n_4} \mathcal{L}^{|m_4|}_{n_4 u}(\delta\lambda'/K'^2) \frac{K'^{2u}}{\lambda'^{u}}$$

$$\rho_2^{|m_2|+|m_4|+2s+2u} e^{-\frac{1}{2}(\beta+\delta+k+k_D)\rho_2^2} \rho_2 d\rho_2$$

where $K'^2 = (\alpha+\gamma+k+k_D)(\beta+\delta+k+k_D)-(k-k_D)^2$.

Expanding the Laguerre polynomial and integrating over $\rho_{2'}$ the unnormalized radial and angular matrix element becomes

$$M = 2^{|m_1|+|m_3|+2} \pi^2 \alpha^{\frac{1}{2}|m_1|} \beta^{\frac{1}{2}|m_2|} \gamma^{\frac{1}{2}|m_3|}$$

$$\delta^{\frac{1}{2}|m_4|} (k-k_D)^{|m_3-m_1|} \lambda'^{\frac{1}{2}(|m_2|+|m_4|-|m_1|-|m_3|)}$$

$$K'^{-(|m_3-m_1|+|m_2|+|m_4|+2)}$$

$$\sum_{r=0}^{n_1} \sum_{s=0}^{n_2} \sum_{t=0}^{n_3} \sum_{u=0}^{n_4} \sum_{v=0}^{n} n!\left(\tfrac{1}{2}(|m_3-m_1|+|m_2|+|m_4|)+s+u+v\right)!$$

$$\mathcal{L}^{|m_1|}_{n_1 r}(4\alpha/\lambda') \mathcal{L}^{|m_2|}_{n_2 s}(\beta\lambda'/K'^2) \mathcal{L}^{|m_3|}_{n_3 t}(4\gamma/\lambda')$$

$$\mathcal{L}^{|m_4|}_{n_4 u}(\delta\lambda'/K'^2) \mathcal{L}^{|m_3-m_1|}_{nv}(-(k-k_D)^2/K'^2)$$

where

$$\lambda' = 2(\alpha+\gamma+k+k_D)$$

$$K'^2 = (\alpha+\gamma+k+k_D)(\beta+\delta+k+k_D)-(k-k_D)^2$$

and

$$2n = |m_1|+|m_3|-|m_3-m_1|+2r+2t$$

The Cartesian Matrix Element

The unnormalized Cartesian matrix element is of the form

$$\mathfrak{J}(n_1a,n_2b,n_3c,n_4d;k,k_D)$$

$$= \int\int H_{n_1}(\sqrt{a}z_1)\, e^{-\frac{1}{2}az_1^2}\, H_{n_2}(\sqrt{b}z_2)\, e^{-\frac{1}{2}bz_2^2}$$

$$e^{-\frac{1}{2}k(z_1-z_2)^2}\, e^{-\frac{1}{2}k_D(z_1+z_2)^2}\, H_{n_3}(\sqrt{c}z_1)$$

$$e^{-\frac{1}{2}cz_1^2}\, H_{n_4}(\sqrt{d}z_2)\, e^{-\frac{1}{2}dz_2^2}\, dz_1dz_2$$

Use can be made of the relation (Bai 48)

$$H_m(\alpha\chi) = \sum_{r=0}^{[m]} h_{mr}(\alpha/\beta)\, H_{m-2r}(\beta\chi)$$

where $[m] = \frac{1}{2}m$ if m is even

$= \frac{1}{2}(m-1)$ if m is odd

and

$$h_{mr}(y) = \frac{m!y^{m-2r}(y^2-1)^r}{r!(m-2r)!}$$

Now

$$\mathcal{I} = \sum_{r=0}^{[n_3]} \int_{-\infty}^{\infty} \int_{-\infty}^{\infty} e^{-\frac{a}{2}z_1^2} e^{-\frac{b}{2}z_2^2} e^{-\frac{c}{2}z_1^2}$$

$$e^{-\frac{d}{2}z_2^2} h_{n_3 r}\left(\left(\frac{c}{a}\right)^{1/2}\right) H_{n_1}(\sqrt{a}z_1) H_{n_3-2r}(\sqrt{a}z_1)$$

$$e^{-\frac{k}{2}(z_1-z_2)^2} e^{-\frac{k_D}{2}(z_1+z_2)^2} H_{n_2}(\sqrt{b}z_2) H_{n_4}(\sqrt{d}z_2)\,dz_1 dz_2$$

Redefining z_1 to be

$$z_1 = \left(\frac{2}{a+c+k+k_D}\right)^{\frac{1}{2}} z_1$$

$$\mathcal{I} = \sum_{r=0}^{[n_3]} \int\int e^{-z_1^2} e^{-\left(\frac{b+d}{2}\right)z_2^2} h_{n_3 r}\left(\left(\frac{c}{a}\right)^{\frac{1}{2}}\right)$$

$$H_{n_1}\left(\left(\frac{2a}{a+c+k+k_D}\right)^{\frac{1}{2}} z_1\right) H_{n_3-2r}\left(\left(\frac{2a}{a+c+k+k_D}\right)^{\frac{1}{2}} z_1\right)$$

$$H_{n_2}(\sqrt{b}z_2)\, e^{kz_1z_2\left(\frac{2}{a+c+k+k_D}\right)^{\frac{1}{2}}} e^{-\frac{k_D}{2}z_2^2}$$

$$e^{-k_D z_1 z_2\left(\frac{2}{a+c+k+k_D}\right)^{\frac{1}{2}}} dz_1 dz_2$$

which reduces to

$$\mathcal{I} = \sum_{r=0}^{[n_3]} \int\int e^{-\left(z_1 - \frac{(k-k_D)}{(2(a+c+k+k_D))^{1/2}} z_2\right)^2}$$

$$e^{-\frac{1}{2}(b+d+k+k_D)z_2^2} \; e^{\frac{(k-k_D)^2}{2(a+c+k+k_D)}z_2^2}$$

$$h_{n_3 r}\left(\left(\frac{c}{a}\right)^{\frac{1}{2}}\right) \; H_{n_1}\left(\left(\frac{2a}{a+c+k+k_D}\right)^{\frac{1}{2}} z_1\right)$$

$$H_{n_3-2r}\left(\left(\frac{2a}{a+c+k+k_D}\right)^{\frac{1}{2}} z_1\right) \; H_{n_2}(\sqrt{b}z_2)$$

$$H_{n_4}(\sqrt{d}z_2)\left(\frac{2}{a+c+k+k_D}\right)^{\frac{1}{2}} dz_1 dz_2$$

Using now the relation (Erd 54)

$$\int_{-\infty}^{\infty} e^{-(x-y)^2} \; H_m(\alpha x) \; H_n(\alpha x)\, dx$$

$$= \sqrt{\pi} \sum_{k=0}^{\min(m,n)} 2^k \; k! \binom{m}{k} \binom{n}{k} (1-\alpha^2)^{\frac{1}{2}(m+n-2k)}$$

$$H_{m+n-2k}\left(\frac{\alpha y}{(1-\alpha^2)^{\frac{1}{2}}}\right)$$

where $\binom{m}{k}$ is the binomial coefficient with

$$y = \frac{(k-k_D)}{(2(a+c+k+k_D))^{\frac{1}{2}}} z_2$$

and

$$\alpha = \left(\frac{2a}{a+c+k+k_D}\right)^{\frac{1}{2}}$$

$$\mathcal{I} = \sqrt{\pi} \sum_{r=0}^{[n_3]} \sum_{s=0}^{\min(n_1, n_3-2r)} 2^s \, s! \binom{n_1}{s} \binom{n_3-2r}{s}$$

$$\left(1 - \frac{2a}{(a+c+k+k_D)}\right)^{\frac{1}{2}(n_1+n_3-2r-2s)}$$

$$H_{n_1+n_3-2r-2s}\left(\left(\frac{a}{(c-a+k+k_D)(a+c+k+k_D)}\right)^{\frac{1}{2}}(k-k_D)z_2\right)$$

$$e^{-\frac{1}{2}(b+d+k+k_D)z_2^2} \; e^{((k-k_D)^2/2(a+c+k+k_D))z_2^2}$$

$$h_{n_3 r}\left(\left(\frac{c}{a}\right)^{\frac{1}{2}}\right) \; H_{n_2}(\sqrt{b}z_2) \; H_{n_4}(\sqrt{d}z_2)$$

$$\left(\frac{2}{a+c+k+k_D}\right)^{\frac{1}{2}} dz_2$$

Expanding the Hermite polynomials further and using (Erd 54a)

$$\int_{-\infty}^{\infty} e^{-y^2} \, H_k(y) \, H_m(y) \, H_n(y) \, dy$$

$$= \frac{\sqrt{\pi} \; k! \; m! \; n! \; 2^s}{(s-k)!\,(s-m)!\,(s-n)!}$$

where $2s = k+m+n$ is even or otherwise the integral vanishes, the integral vanishing also if any of the terms in the denominator becomes negative; the unnormalized matrix element

becomes

$$\mathcal{I} = 2\pi\, K^{-1} \sum_{r=0}^{[n_3]} \sum_{s=0}^{\min(n_1, n_3-2r)} \sum_{t=0}^{[n_1+n_3-2r-2s]} \sum_{u=0}^{[n_2]} \sum_{v=0}^{[n_4]} 2^{s+n}\, s! \binom{n_1}{s} \binom{n_3-2r}{s}$$

$$\frac{(n_1+n_2-2r-2s-2t)!\,(n_2-2u)!\,(n_4-2v)!}{(n-n_1-n_3+2r+2s+2t)!\,(n-n_2+2u)!\,(n-n_4+2v)!}$$

$$\left(\frac{c-a+k+k_D}{a+c+k+k_D}\right)^{\frac{1}{2}(n_1+n_3-2r-2s)}$$

$$h_{(n_1+n_3-2r-2s)}\, t\left(\left(\frac{2a(k-k_D)^2}{(c-a+k+k_D)K'^2}\right)^{\frac{1}{2}}\right)$$

$$h_{n_2 u}\left(\left(\frac{4b\lambda'}{K'^2}\right)^{\frac{1}{2}}\right)\; h_{n_4 v}\left(\left(\frac{4d\lambda'}{K'^2}\right)^{\frac{1}{2}}\right)$$

$$h_{n_3 r}\left(\left(\frac{c}{a}\right)^{\frac{1}{2}}\right)$$

where

$$\lambda' = \tfrac{1}{2}(a+c+k+k_D)$$

$$K'^2 = (a+c)(b+d) + (a+b+c+d)(k+k_D) + 4kk_D$$

and $2n = n_1+n_2+n_3+n_4-2r-2s-2t-2u-2r$. $2n$ must be an even number for this integral to be non-zero. Thus $n_1+n_2+n_3+n_4$ must be even.

The correct normalization constants for the complete matrix element

$$N_{n_1 m_1 n_{z_1}} \; N_{n_2 m_2 n_{z_2}} \; N_{n_3 m_3 n_{z_3}} \; N_{n_4 m_4 n_{z_4}}$$

can be easily evaluated from Appendix 2.

Similarly other expressions for the matrix element can be easily worked out for the other forms of the density function in Chapter 6.

APPENDIX 4

COULOMB MATRIX ELEMENTS

It is desired to evaluate the matrix elements for the Coulomb interaction $e^2/|r_i - r_j|$

i.e. $C(n_1\ m_1\ n_{z_1},\ n_2\ m_2\ n_{z_2},\ n_3\ m_3\ n_{z_3},\ n_4\ m_4\ n_{z_4})$

$$= \int\int\int\int\int\int \psi^*_{n_1 m_1 n_{z_1}}(\underset{\sim}{\rho}_1, z_1)\ \psi^*_{n_2 m_2 n_{z_2}}(\underset{\sim}{\rho}_2, z_2)$$

$$\frac{e^2}{\sqrt{(\underset{\sim}{\rho}_1 - \underset{\sim}{\rho}_2)^2 + (z_1 - z_2)^2}}\ \psi_{n_3 m_3 n_{z_3}}(\underset{\sim}{\rho}_1, z_1)\psi_{n_4 m_4 n_{z_4}}(\underset{\sim}{\rho}_2, z_2)$$

$$\rho_1\ d\rho_1\ d\phi_1\ dz_1\ \rho_2\ d\rho_2\ d\phi_2\ dz_2\ .$$

For the case where the oscillator constants of the single particle states are equal it is comparatively easy to evaluate the coulomb matrix elements needed in this work. For the case of unequal oscillator constants the transformation (Kum 66)

$$(a_1 + a_2)\underset{\sim}{R} = a_1\ \underset{\sim}{\rho}_1 + a_2\ \underset{\sim}{\rho}_2$$

$$\underset{\sim}{\rho} = \underset{\sim}{\rho}_1 - \rho_2$$

$$(b_1 + b_2)Z = b_1 z_1 + b_2 z_2$$

$$z = z_1 - z_2$$

is used.

The inverse transformation is

$$\underset{\sim}{\rho}_1 = \underset{\sim}{R} + \frac{a_2}{a_1+a_2}\,\underset{\sim}{\rho}$$

$$\underset{\sim}{\rho}_2 = \underset{\sim}{R} - \frac{a_1}{a_1+a_2}\,\underset{\sim}{\rho}$$

$$z_1 = Z + \frac{a_2}{a_1+a_2}\,z$$

$$z_2 = Z - \frac{a_1}{a_1+a_2}\,z$$

The volume element $\rho_1\, d\rho_1\, d\phi_1\, dz_1\, \rho_2\, d\rho_2\, d\phi_2\, dz_2$ now becomes $R\, dR\, d\theta dZ \rho d\rho d\phi dz$ and $(\underset{\sim}{\rho}_1-\underset{\sim}{\rho}_2)^2+(z_1-z_2)^2 \rightarrow \underset{\sim}{\rho}^2+z^2$.

The integration over R, θ and Z is easily performed but the integration over ρ and z presents some difficulty.

Considering the integration over ρ first, use can be made of the relation (Rys 63)

$$\int_0^\infty \frac{e^{-\alpha^2\rho^2}}{\sqrt{\rho^2+z^2}}\,\rho\, d\rho = [\,1 - \phi(\alpha z)]\,\frac{\sqrt{\pi}}{2\alpha}\; e^{\alpha^2 z^2}$$

where $$\phi(\alpha z) = \frac{2}{\sqrt{\pi}} \int_0^{\alpha z} e^{-t^2}\, dt\ .$$

Refining, for convenience, a function

$$\mathrm{Erfc}(\alpha z) = 1 - \phi(\alpha z)$$

and noting that

$$\frac{d\phi(\alpha z)}{d\alpha} = \frac{2}{\sqrt{\pi}} e^{-\alpha^2 z^2} z$$

then higher powers of ρ can easily be integrated from this basic relation. Thus

$$\int_0^\infty \rho^2 \frac{e^{-\alpha^2\rho^2}}{\sqrt{\rho^2+z^2}} \rho \, d\rho$$

$$= -\frac{d}{d\alpha} \int_0^\infty \frac{e^{-\alpha^2\rho^2}}{\sqrt{\rho^2+z^2}} \rho \, d\rho$$

$$= -\frac{d}{2\alpha d\alpha} \left[[1 - \phi(\alpha z)] \frac{\sqrt{\pi}}{2\alpha} e^{\alpha^2 z^2} \right]$$

$$= \frac{1}{2\alpha^2} z + \text{Erfc}(\alpha z) \left[\frac{\sqrt{\pi}}{4\alpha^3} - \frac{\sqrt{\pi}}{2\alpha} z^2 \right] e^{\alpha^2 z^2}$$

and

$$\int_0^\infty \rho^4 \frac{e^{-\alpha^2\rho^2}}{\sqrt{\rho^2+z^2}} \rho \, d\rho$$

$$= -\frac{d}{2\alpha d\alpha} \int_0^\infty \rho^2 \frac{e^{-\alpha^2\rho^2}}{\sqrt{\rho^2+z^2}} \rho \, d\rho$$

$$= \frac{1}{2\alpha^4} z + \frac{z}{\sqrt{\pi}\alpha} \left[\frac{\sqrt{\pi}}{4\alpha^3} - \frac{\sqrt{\pi}}{2\alpha} z^2 \right]$$

$$+ \text{Erfc}(\alpha z) \left[\frac{3}{8} \frac{\sqrt{\pi}}{\alpha^5} - \frac{\sqrt{\pi}}{4\alpha^3} z^2 \right] e^{\alpha^2 z^2}$$

$$- \text{Erfc}(\alpha z) \, z^2 \, e^{\alpha^2 z^2} \left[\frac{1}{4} \frac{\sqrt{\pi}}{\alpha^3} - \frac{\sqrt{\pi}}{2\alpha} z^2 \right]$$

$$= \frac{3}{4}\frac{z}{\alpha^4} - \frac{1}{2}\frac{z^3}{\alpha^2} + \frac{\sqrt{\pi}}{\alpha^5} e^{\alpha^2 z^2} \text{ Erfc}(\alpha z)$$

$$[\frac{3}{8} - \frac{1}{2}\alpha^2 z^2 + \frac{1}{2}\alpha^4 z^4]$$

For the further integration over z, use can be made of the integral (Erd 54b)

$$\int_0^\infty z^{\partial-1} \exp(\gamma^2 z^2) \text{ Erfc}(\alpha z) dz$$

$$= \frac{\Gamma(\frac{\partial+1}{2})}{\pi^{\frac{1}{2}} \alpha} \; {}_2F_1(\frac{\partial}{2} ; \frac{\partial+1}{2} ; \frac{\partial}{2} + 1; \gamma^2/\alpha^2)$$

where

$${}_2F_1(a;b;c;x) = \sum_{n=0}^{\infty} \frac{(a)_n (b)_n}{n! (c)_n} x^n \qquad \text{(A4.1)}$$

and $(a)_n = a(a+1)(a+2) \ldots\ldots (a+n-1)$

$(1)_n = n!$

$(a)_0 = 1$

The integrals that are of interest for this work are

$$\int_0^\infty e^{(\alpha^2-\beta^2)z^2} \text{ Erfc}(\alpha z) dz$$

$$= \frac{1}{\pi^{\frac{1}{2}}\alpha} \; {}_2F_1 \; (\frac{1}{2};1;\frac{3}{2};(1 - \frac{\beta^2}{\alpha^2}))$$

$$\int_0^\infty z^2 \; e^{(\alpha^2-\beta^2)z^2} \text{ Erfc}(\alpha z) dz$$

$$= \frac{1}{\pi^{\frac{1}{2}}\alpha^3} \; {}_2F_1\left(\frac{3}{2};2;\frac{5}{2};\left(1 - \frac{\beta^2}{\alpha^2}\right)\right)$$

$$\int_0^\infty z^4 \, e^{(\alpha^2-\beta^2)z^2} \, \mathrm{Erfc}(\alpha z)\,dz$$

$$= \frac{2}{\pi^{\frac{1}{2}}5\;\alpha^5} \; {}_2F_1\left(\frac{5}{2};3;\frac{7}{2};\left(1 - \frac{\beta^2}{\alpha^2}\right)\right)$$

Using the relation (Rys 63a)

$${}_2F_1\left(\frac{\nu}{2};\frac{\nu+1}{2};\frac{\nu}{2}+1;\; 1 - \frac{\beta^2}{\alpha^2}\right)$$

$$= \left(\frac{\alpha}{\beta}\right)^{\nu+1} \; {}_2F_1\left(\frac{\nu+1}{2};1;\frac{\nu}{2} + 1;\; 1 - \frac{\alpha^2}{\beta^2}\right)$$

the above ${}_2F_1$ functions can be expressed as

$${}_2F_1\left(\frac{1}{2};1;\frac{3}{2};1 - \frac{\beta^2}{\alpha^2}\right) = \left(\frac{\alpha}{\beta}\right)^2 \; {}_2F_1\left(1;1;\frac{3}{2};\left(1 - \frac{\alpha^2}{\beta^2}\right)\right)$$

$${}_2F_1\left(\frac{3}{2};2;\frac{5}{2};\; 1 - \frac{\beta^2}{\alpha^2}\right)$$

$$= \left(\frac{\alpha}{\beta}\right)^4 \; {}_2F_1\left(2;1;\frac{5}{2};\left(1 - \frac{\alpha^2}{\beta^2}\right)\right)$$

$${}_2F_1\left(3;1;\frac{7}{2};1 - \frac{\beta^2}{\alpha^2}\right) = \left(\frac{\alpha}{\beta}\right)^6 \; {}_2F_1\left(3;1;\frac{7}{2};\left(1 - \frac{\alpha^2}{\beta^2}\right)\right)$$

Further, using expansion A4.1 it is easily seen that

$${}_2F_1\left(2;1;\frac{5}{2};1 - \frac{\alpha^2}{\beta_2^2}\right) = 1 + \frac{4}{5}\left(1 - \frac{\alpha^2}{\beta^2}\right) {}_2F_1\left(3;1;\frac{7}{2};1 - \frac{\alpha^2}{\beta^2}\right)$$

$$ {}_2F_1(1;1;\tfrac{3}{2};1-\frac{\alpha^2}{\beta^2}) = 1 + \frac{2}{3}(1-\frac{\alpha^2}{\beta^2}) $$

$$ + \frac{8}{15}(1-\frac{\alpha^2}{\beta^2})\ {}_2F_1(3;1;\tfrac{7}{2};1-\frac{\alpha^2}{\beta^2}) $$

Using $$ {}_2F_1\ (a;b;c;x) = \frac{\Gamma(c)}{\Gamma(a)\Gamma(b)} $$

$$ \sum_{n=0}^{\infty} \frac{\Gamma(a+n)\ \Gamma(b+n)}{\Gamma(c+n)}\ \frac{x^n}{n!} $$

$$ {}_2F_1(3;1;\tfrac{7}{2};x) = \frac{\Gamma(\frac{7}{2})}{\Gamma(3)\Gamma(1)} \sum_{n=0}^{\infty} \frac{\Gamma(n+3)}{\Gamma(n+\frac{7}{2})}\ \frac{\Gamma(n+1)}{n!}\ x^n $$

$$ = \frac{\Gamma(\frac{7}{2})}{\Gamma(3)\Gamma(1)} \sum_{n=0}^{\infty} \frac{\Gamma(n+3)}{\Gamma(n+\frac{7}{2})}\ x^n $$

This function can be evaluated numerically to any degree of accuracy required.

Writing $$ Z_0(a,b) = \frac{2}{a}\ {}_2F_1(\tfrac{1}{2};1;\tfrac{3}{2};1-\frac{b}{a}) $$

$$ Z_2(a,b) = \frac{2}{3}\ \frac{1}{a^2}\ {}_2F_1(\tfrac{3}{2};2;\tfrac{5}{2};1-\frac{b}{a}) $$

$$ Z_4(a,b) = \frac{4}{5}\ \frac{1}{a^3}\ {}_2F_1(\tfrac{5}{2};3;\tfrac{7}{2};1-\frac{b}{a}) $$

and

$$ {}_2F_1(3;1;\tfrac{7}{2};1-\frac{a}{b}) = F(\varepsilon) $$

then

$$ Z_4(a,b) = \frac{4}{5}\ \frac{1}{b^3}\ F(\varepsilon) $$

$$ Z_2(a,b) = \frac{2}{3}\ \frac{1}{b^2}\ [1 + \frac{4}{5}(1-\frac{a}{b})F(\varepsilon)] $$

$$ Z_0(a,b) = 2\ \frac{1}{b}[1 + \frac{2}{3}(1-\frac{a}{b}) $$

$$ + \frac{8}{15}(1-\frac{a}{b})^2\ F(\varepsilon)] $$

The basic integrals over ρ, ϕ, and z which have to be evaluated can be expressed as

$$I1 = \int_0^{2\pi} \int_{-\infty}^{\infty} \int_0^{\infty} \frac{e^{-a\rho^2} e^{-bz^2}}{\sqrt{\rho^2 + z^2}} \rho \, d\rho \, dz \, d\phi$$

$$= \pi Z_0(a,b)$$

$$I2 = \int_0^{2\pi} \int_{-\infty}^{\infty} \int_0^{\infty} \frac{z^2 e^{-a\rho^2} e^{-bz^2}}{\sqrt{\rho^2 + z^2}} \rho \, d\rho \, dz \, d\phi$$

$$= \pi Z_2(a,b)$$

$$I3 = \int_0^{2\pi} \int_{-\infty}^{\infty} \int_0^{\infty} \frac{z^4 e^{-a\rho^2} e^{-bz^2}}{\sqrt{\rho^2 + z^2}} \rho \, d\rho \, dz \, d\phi$$

$$= \pi Z_4(a,b)$$

$$I4 = \int_0^{2\pi} \int_{-\infty}^{\infty} \int_0^{\infty} \rho^2 \frac{e^{-a\rho^2} e^{-bz^2}}{\sqrt{\rho^2 + z^2}} \rho \, d\rho \, dz \, d\phi$$

$$= 2 \left[\frac{1}{2ab} + \frac{Z_0(a,b)}{4a} - \frac{Z_2(a,b)}{2}\right]$$

$$I5 = \int_0^{2\pi} \int_{-\infty}^{\infty} \int_0^{\infty} \rho^4 \frac{e^{-a\rho^2} e^{-bz^2}}{\sqrt{\rho^2 + z^2}} \rho \, d\rho \, dz \, d\phi$$

$$= 2\pi \left[\frac{3}{4a^2 b} - \frac{1}{2ab^2} + \frac{3}{8a^2} Z_0(a,b)\right.$$

$$\left. - \frac{1}{2a} Z_2(a,b) + \frac{1}{2} Z_4(a,b)\right]$$

$$I6 = \int_0^{2\pi} \int_{-\infty}^{\infty} \int_0^{\infty} \rho^2 \, z^2 \, \frac{e^{-a\rho^2} \, e^{-bz^2}}{\sqrt{\rho^2 + z^2}} \, \rho \, d\rho \, dz \, d\phi$$

$$= 2\pi \left[\frac{1}{2ab^2} + \frac{1}{4a} \, Z_2(a,b) - \frac{Z_4(a,b)}{2} \right]$$

Writing the oscillator well parameters as

(a_s, b_s) for the 000 state

(a_0, b_0) for the 001 state

and (a_1, b_1) for the 0±1 0 state

the explicit expressions for the coulomb matrix elements used in this thesis are

$$\langle \psi_{000} \, \psi_{000} \left| \frac{e^2}{|r_1 - r_2|} \right| \psi_{000} \, \psi_{000} \rangle = C_{ss}$$

$$= \frac{e^2}{\sqrt{2\pi}} \, a_s \, b_s^{\frac{1}{2}} \, Z_0(a_s, b_s)$$

$$\langle \psi_{000} \, \psi_{001} \left| \frac{e^2}{|r_1 - r_2|} \right| \psi_{000} \, \psi_{001} \rangle = C_{s0}$$

$$= \frac{e^2}{\sqrt{\pi}} \, \frac{a_s \, b_s^{\frac{1}{2}} \, a_0 \, b_0^{\frac{3}{2}}}{(a_s + a_0)(b_s + b_0)^{\frac{1}{2}}} \left[\frac{1}{(b_s + b_0)} \, Z_0 \left(\frac{a_s \, a_0}{a_s + a_0} ; \frac{b_s \, b_0}{b_s + b_0} \right) \right.$$

$$\left. + \frac{2b_s^2}{(b_s + b_0)^2} \, Z_2 \left(\frac{a_s \, a_0}{a_s + a_0} ; \frac{b_s \, b_0}{b_s + b_0} \right) \right]$$

$$\langle \psi_{000}\ \psi_{001} \left| \frac{e^2}{|r_1 - r_2|} \right| \psi_{001}\ \psi_{000} \rangle = C_{s0x}$$

$$= \frac{e^2}{\sqrt{\pi}} \frac{a_s\, b_s^{\frac{1}{2}}\, a_0\, b_0^{\frac{3}{2}}}{(a_s+a_0)(b_s+b_0)^{\frac{1}{2}}} \left[\frac{1}{(b_s+b_0)} Z_0 \left(\frac{a_s+a_0}{4} ; \frac{b_s+b_0}{4} \right) \right.$$

$$\left. - \frac{1}{2} Z_2 \left(\frac{a_s+a_0}{4} ; \frac{b_s+b_0}{4} \right) \right]$$

$$\langle \psi_{000}\ \psi_{0\pm10} \left| \frac{e^2}{|r_1 - r_2|} \right| \psi_{000}\ \psi_{0\pm10} \rangle = C_{s1}$$

$$= \frac{e^2}{\sqrt{\pi}} \frac{a_s\, a_1}{(a_s+a_1)^2} \left[\frac{a_s (b_s+b_1)^{\frac{1}{2}}}{b_s^{\frac{1}{2}}\, b_1^{\frac{1}{2}}} + \frac{b_s^{\frac{1}{2}}\, b_1^{\frac{1}{2}}}{(b_s+b_1)^{\frac{1}{2}}} \left(a_1 + \frac{a_s}{2} \right) \right.$$

$$Z_0 \left(\frac{a_s\, a_1}{a_s+a_1} ; \frac{b_s\, b_1}{b_s+b_1} \right) - \frac{a_s^2\, a_1\, b_s^{\frac{1}{2}}\, b_1^{\frac{1}{2}}}{(a_s+a_1)(b_s+b_1)^{\frac{1}{2}}}$$

$$\left. Z_2 \left(\frac{a_s\, a_1}{a_s+a_1} ; \frac{b_s\, b_1}{b_s+b_1} \right) \right]$$

$$\langle \psi_{000}\ \psi_{0\pm10} \left| \frac{e^2}{|r_1 - r_2|} \right| \psi_{0\pm10}\ \psi_{000} \rangle = C_{s1x}$$

$$= \frac{e^2}{\sqrt{\pi}} \frac{a_s\, b_s^{\frac{1}{2}}\, a_1^2\, b_1^{\frac{1}{2}}}{(a_s+a_1)(b_s+b_1)^{\frac{1}{2}}} \left[\frac{1}{2(a_s+a_1)} Z_0 \left(\frac{a_s+a_1}{4} ; \frac{b_s+b_1}{4} \right) \right.$$

$$\left. - \frac{4}{(a_s+a_1)(b_s+b_1)} + \frac{1}{4} Z_2 \left(\frac{a_s+a_1}{4} ; \frac{b_s+b_1}{4} \right) \right]$$

$$\langle \psi_{001}\ \psi_{001} \left| \frac{e^2}{|r_1 - r_2|} \right| \psi_{001}\ \psi_{001} \rangle = C_{00}$$

$$= \frac{e^2}{\sqrt{\pi}} \frac{a_0 b_0^{1/2}}{2\sqrt{2}} \left[\frac{3}{2} Z_0(a_0;b_0) - 2b_0 Z_2(a_0;b_0) \right.$$

$$\left. + 2\, b_0^2\, Z_4(a_0;b_0) \right]$$

$$\langle \psi_{0\pm10}\ \psi_{001} \left| \frac{e^2}{|r_1 - r_2|} \right| \psi_{0\pm10}\ \psi_{001} \rangle = C_{10}$$

$$= \frac{e^2}{\sqrt{\pi}} \frac{a_1\, a_0\, b_0^{1/2}}{(a_0+a_1)^2 (b_0+b_1)^{1/2}} \left[\frac{b_1^{1/2} b_0}{(b_0+b_1)} \left(a_1 + \frac{a_0}{2}\right) \right.$$

$$Z_0\left(\frac{a_0\, a_1}{a_0+a_1}\ ;\ \frac{b_0\, b_1}{b_0+b_1}\right) + \left(\frac{a_1 b_1^{1/2} b_0}{(b_0+b_1)}\right) \left(\frac{2b_1^2}{(b_0+b_1)} - \frac{a_0^2}{a_0+a_1}\right.$$

$$\left. + \frac{b_1^2\, a_0}{a_1 (b_0+b_1)}\right) Z_2 \left(\frac{a_0\, a_1}{a_0+a_1}\ ;\ \frac{b_0\, b_1}{b_0+b_1}\right)$$

$$- \frac{2\, a_1\, a_0^2\, b_1^{5/2}\, b_0}{(a_0+a_1)(b_0+b_1)^2} Z_4 \left(\frac{a_0\, a_1}{a_0+a_1}\ ;\ \frac{b_0\, b_1}{b_0+b_1}\right)$$

$$\left. + a_0 \left(\frac{1}{b^{1/2}} + \frac{2b_1^{1/2}}{b_0}\right) \right]$$

$$\langle \psi_{0\pm10}\ \psi_{001} \left| \frac{e^2}{|r_1 - r_2|} \right| \psi_{001}\ \psi_{0\pm10} \rangle = C_{10x}$$

$$= \frac{e^2}{\sqrt{\pi}} \frac{a_0\, b_0^{3/2}\, a_1^{\,2}\, b_1^{\frac{1}{2}}}{(a_0+a_1)(b_0+b_1)^{\frac{1}{2}}} \left[\frac{1}{(a_0+a_1)(b_0+b_1)} \frac{1}{2} Z_0\left(\frac{a_0+a_1}{4} ; \frac{b_0+b_1}{4}\right)\right.$$

$$+ \frac{1}{4} \left(\frac{1}{b_0+b_1} - \frac{1}{a_0+a_1}\right) Z_2\left(\frac{a_0+a_1}{4} ; \frac{b_0+b_1}{4}\right)$$

$$\left. - \frac{1}{8} Z_4\left(\frac{a_0+a_1}{4} ; \frac{b_0+b_1}{4}\right) + \frac{4}{(a_0+a_1)(b_0+b_1)^2} \right]$$

$$\langle \psi_{0\pm10}\, \psi_{0\pm10} \left| \frac{e^2}{|r_1-r_2|} \right| \psi_{0\pm10}\, \psi_{0\pm10} \rangle = C_{11}$$

$$= \frac{e^2}{\sqrt{\pi}} \frac{a_1^{\,3}\, b_1^{\frac{1}{2}}}{4\sqrt{2}} \left[\frac{11}{4a_1^{\,2}} Z_0(a_1;b_1) - \frac{1}{a_1} Z_2(a_1;b_1)\right.$$

$$\left. + Z_4(a_1;b_1) + \frac{1}{a_1 b_1} \left(\frac{3}{2a_1} - \frac{1}{b_1}\right)\right]$$

$$\langle \psi_{0\pm10}\, \psi_{0\mp10} \left| \frac{e^2}{|r_1-r_2|} \right| \psi_{0\mp10}\, \psi_{0\pm10} \rangle$$

$$= C_{11x} = \frac{e^2}{\sqrt{\pi}} \frac{a_1^{\,3}\, b_1^{\frac{1}{2}}}{8} \left[\frac{3}{4a_1^{\,2}} Z_0(a_1;b_1) + \right.$$

$$\left. \frac{3}{a_1} Z_2(a_1;b_1) + Z_4(a_1;b_1) - \frac{1}{a_1 b_1} \left(\frac{1}{b_1} + \frac{5}{2a_1}\right)\right]$$

APPENDIX 5

NUCLEAR MATTER

The binding energy of nuclear matter is given in first order by the expression (Bri 67)

$$E/A = \frac{3}{10}\frac{\hbar^2}{m} k_F^2 + \frac{1}{\pi^2}\int_0^{k_F} k^2\, G(\frac{k}{k_F})\, F(k)dk \qquad (A5.1)$$

where k_F is the Fermi wave number and

$$G(x) = 1 - \frac{3}{2}x + \frac{1}{2}x^3$$

$$F(k) = 8\langle k|W_0|k\rangle - 2\langle k|W_0|-k\rangle$$

and

$$\langle k|W_0|k'\rangle = \int e^{-ik.r}\langle r|W_0|r'\rangle \times e^{ik'.r'}\, dr\, dr' \quad .$$

The interactions considered in this thesis are of the form

$$V(r) = (W + MP_M + BP_B + HP_H)f(r)$$

where P_M, P_B, P_H are the usual Mayorana, Bartlett and Isospin exchange operators.

Any potential V can be written in the form

$$V = W_0 + W_1$$

with

$$W_0 = u_0 + \frac{2}{5} u_1 (1-P_M)$$

$$W_1 = u_1 [P_B - \frac{2}{5}(1-P_M)] \quad .$$

W_1 has zero matrix elements between all many particle states which have [444 --- 4] supermultiplet symmetry (Wig 37).

For the interactions considered here

$$W_0 = (W + \frac{2}{5} B + \frac{2}{5} H) f(r)$$

$$+ (M - \frac{2}{5} B - \frac{2}{5} H) P_M f(r)$$

$$\equiv A f(r) + C P_M f(r)$$

with $$A = (W + \frac{2}{5} B + \frac{2}{5} H)$$

and $$C = (M - \frac{2}{5} B - \frac{2}{5} H) \quad .$$

Thus it is required to evaluate

$$\langle k|W_0|k\rangle = A \iiint f(r)\, d^3r + C \iiint f(r)\, e^{-2ik.r}\, d^3r$$

$$\equiv A F + C F_x$$

and

$$\langle k|W_0|-k\rangle = A \iiint f(r)\, e^{-2ik.r}\, d^3r + C \iiint f(r)\, d^3r$$

$$= A F_x + C F \quad .$$

Thus in A5.1

$$F(k) = 8(A\ F + C\ F_x) - 2(A\ F_x + C\ F)$$

$$= (8A - 2C)F + (8C - 2A)F_x$$

f(r) is of the form

$$f(r) = V_a\ e^{-r^2/\alpha^2} + V_r\ e^{-r^2/\beta^2}$$

where V_a and V_r will, in general, contain terms of the kind k_F^n and β will contain terms in powers of k.

Therefore (ignoring the explicit k dependence of β for the moment)

$$F = \iiint (V_a\ e^{-r^2/\alpha^2} + V_r\ e^{-r^2/\beta^2})d^3r$$

$$= 4\pi \int_0^\infty (V_a\ e^{-r^2/\alpha^2} + V_r\ e^{-r^2/\beta^2})r^2dr$$

$$= 4\pi(V_a\ \tfrac{1}{4}\sqrt{\pi}\ \alpha^3 + V_r\ \tfrac{1}{4}\sqrt{\pi}\ \beta^3)$$

$$= \pi^{3/2}(V_a\ \alpha^3 + V_r\ \beta^3) \quad .$$

Now

$$F_x = \iiint (V_a\ e^{-r^2/\alpha^2} + V_r\ e^{-r^2/\beta^2})\ e^{-2ik.r}d^3r \quad .$$

Considering the relation (Erd 55c)

$$g(y) = \int_0^\infty e^{-\beta x^2} \cos xy\ dx$$

$$= \frac{1}{2}\,\pi^{1/2}\,\beta^{-1/2}\,e^{-y^2/4\alpha}$$

$$g(y) = \int_0^\infty e^{-\beta x^2}\left(\frac{e^{iyx} + e^{-iyx}}{2}\right)dx$$

$$= \frac{1}{2}\int_{-\infty}^{\infty} e^{-\beta x^2}\,e^{-iyx}\,dx \quad .$$

Thus

$$\int_{-\infty}^{\infty} e^{-x^2/\alpha^2}\,e^{-2ik_x x}\,dx = \pi^{1/2}\,\alpha\,e^{-\alpha^2 k^2}$$

and

$$\iiint e^{-r^2/\alpha^2}\,e^{-2ik.r}\,d^3r = \pi^{3/2}\,\alpha^3\,e^{-\alpha^2 k^2} \quad .$$

Therefore

$$F_x = \pi^{3/2}(V_a\,\alpha^3\,e^{-\alpha^2 k^2} + V_r\,\beta^3\,e^{-\beta^2 k^2}) \quad .$$

Thus

$$E/A = \frac{3}{10}\,\frac{\hbar^2}{m}\,k_F^{\,2} + \frac{1}{\pi^2}\int_0^{k_F} k^2\left(1 - \frac{3}{2}\,\frac{k}{k_F} + \frac{1}{2}\,\frac{k^3}{k_F^{\,3}}\right)$$

$$x\,[(8A - 2C)F + (8C - 2A)F_x]\,dk \quad .$$

V_a and α are not dependent in any way on k therefore

$$E/A = \frac{3}{10}\,\frac{h^2}{m}\,k_F^{\,2} + \frac{1}{\sqrt{\pi}}\,\frac{1}{24}\,k_F^{\,3}\,\alpha^3\,V_a(8A - 2C)$$

$$+ \frac{1}{\sqrt{\pi}}\int_0^{k_F} k^2\left(1 - \frac{3}{2}\,\frac{k}{k_F} + \frac{1}{2}\,\frac{k^3}{k_F^{\,3}}\right)\,[V_r\,\beta^3(8A - 2C)$$

$$+ (V_a \alpha^3 e^{-\alpha^2 k^2} + V_r \beta^3 e^{-\beta^2 k^2}) (8C - 2A)] \, dk \quad .$$

This integration can easily be evaluated numerically using a gaussian quadrature formula (Spr 65).

In general

$$\beta = \beta_0 (1 + c_1 (k - c_2)^2)$$

$$V_a = (1 + c_3 k_F^n) V_A$$

$$V_r = (1 + c_4 k_F^m) V_R$$

where n, m are not necessarily integer.

V_A, V_R, β_0, c_1 and c_2 are predetermined constants. It is also required that the interactions saturate nuclear matter

i.e. $$\left. \frac{d(E/A)}{dk_F} \right|_{k_{F_0}} = 0$$

where $$k_{F_0} = 1.36 \text{ fm usually.}$$

Now

$$\frac{d(E/A)}{dk_F} = \frac{6}{10} \frac{h^2}{m} k_F + \frac{1}{\sqrt{\pi}} \frac{3}{24} \alpha^3 k_F^2 V_A (8A - 2C)$$

$$+ c_3 \frac{1}{\sqrt{\pi}} \frac{1}{24} (n+3) \alpha^3 k_F^{n+2} V_A (8A - 2C)$$

$$+ \frac{1}{\sqrt{\pi}} \int_0^{k_F} k^2 \left(\frac{3}{2} \frac{k}{k_F^2} - \frac{3}{2} \frac{k^3}{k_F^3}\right) [V_R \beta^3 (8A - 2C)$$

$$+ (V_R \beta^3 e^{-\beta^2 k^2} + V_A \alpha^3 e^{-\alpha^2 k^2}) (8C - 2A)]dk$$

$$+ c_4 \frac{1}{\sqrt{\pi}} \int_0^{k_F} k^2 (m k_F^{m-1} - \frac{3}{2} (m-1) k k_F^{m-2}$$

$$+ \frac{1}{2} (m-3) k^3 k_F^{m-4}) [V_R \beta^3 (8A - 2C) + V_R \beta^3$$

$$x e^{-\beta^2 k^2} (8C - 2A)]dk$$

$$+ c_4 \frac{+}{\sqrt{\pi}} c_3 \int_0^{k_F} \frac{1}{\sqrt{\pi}} [k^2 (n k_F^{n-1} - \frac{3}{2} (n-1) k k_F^{n-2}$$

$$+ \frac{1}{2} (n-3) k^3 k_F^{n-4}) V_A \alpha^3 e^{-\alpha^2 k^2} (8C - 2A)]dk.$$

The integrals in this expression can again easily be evaluated numerically. Thus, for a given ν (where $\nu = 10(W-M) + 8(B+H)$ and ν = constant ensures unique values for $(8A - 2C)$ and $(8C - 2A)$) the two conditions

$$E/A = -16 \text{ Mev} \quad \text{and} \quad \frac{d(E/A)}{dk_F}\Big|_{k_F=1.36} = 0$$

determine values for c_3 and c_4.

Compressibility

The compressibility of nuclear matter at the saturation equilibrium is

$$K = k_F^2 \frac{d^2(E/A)}{dk_F^2} .$$

This again can easily be calculated since

$$\frac{d^2(E/A)}{dk_F^2} = \frac{6}{10}\frac{\hbar^2}{m} + \frac{1}{\sqrt{\pi}}\frac{1}{4}\alpha^3 k_F V_A(8A - 2C)$$

$$+ \frac{1}{\sqrt{\pi}}\int_0^{k_F} k^2\left(6\frac{k^3}{k_F^5} - 3\frac{k}{k_F^3}\right)\left[V_R \beta^3(8A - 2C)\right.$$

$$\left. + (V_R \beta^3 e^{-\beta^2 k^2} + V_A \alpha^3 e^{-\alpha^2 k^2})(8C - 2A)\right]dk$$

$$+ c_4 \frac{1}{\sqrt{\pi}}\int_0^{k_F} \left(m(m-1) k_F^{m-2} - \frac{3}{2}(m-1)(m-2) k k_F^{m-3}\right.$$

$$\left. + \frac{(m-4)}{2}(m-3) k^3 k_F^{m-5}\right)\left[V_R \beta^3(8A - 2C)\right.$$

$$\left. + V_R \beta^3 e^{-\beta^2 k^2}(8C - 2A)\right]dk$$

$$+ c_3\left[\frac{1}{\sqrt{\pi}}\frac{1}{24}(n+3)(n+2)\alpha^3 k_F^{n+1} V_A(8A - 2C)\right.$$

$$+ \frac{1}{\sqrt{\pi}}\int_0^{k_F} k^2\left(n(n-1) k_F^{n-2} - \frac{3}{2}(n-1)(n-2) k k_F^{n-3}\right.$$

$$\left.\left. + \frac{1}{2}(n-3)(n-4) k^3 k_F^{n-5}\right) V_A \alpha^3 e^{-\alpha^2 k^2}(8C - 2A)\, dk\right].$$

The computer code written for a CDC 6400 is capable of determining c_3, c_4 and K in less than $\frac{1}{10}$ sec.

APPENDIX 6

j-j COUPLING MATRIX ELEMENTS

It is desired to evaluate the matrix element

$$A\langle\psi_{n_1\ell_1 j_1}(r_1)\ \psi_{n_2\ell_2 j_2}(r_2)|V_{12}|\psi_{n_3\ell_3 j_3}(r_1)\ \psi_{n_4\ell_4 j_4}(r_2)\rangle_A^{JT}$$

where r_1 and r_2 refer to the spin and isospin coordinates as well as the space coordinates; A indicates that the total wave function is antisymmetrized and the particles couple to given J and T.

This is accomplished by first transforming the wave functions to the L - S coupling scheme in the usual manner i.e.

$$|j_1 j_2;JT\rangle = \sum_{L,S} \begin{Bmatrix} S_1 S_2 S \\ \ell_1 \ell_2 L \\ j_1 j_2 J \end{Bmatrix} \sqrt{(2S+1)(2L+1)(2j_1+1)(2j_2+1)}\ |\ell_1\ell_2;LST\rangle.$$

$|\ell_1\ell_2;LST\rangle$ can be expanded in terms of single particle states which are solutions of the Schroedinger equation of the spherically symmetric harmonic oscillator well which, in turn can be transformed to single particle states of the cylindrically symmetric harmonic oscillator well and the formulae of Appendix 3 can be applied.

It should be noted that in general

$$|j_1 j_2; JT\rangle_A = (-1)^{j_1+j_2-J+1-T} |j_2 j_1; JT\rangle_A$$

so that

$${}_A\langle j_1 j_2; JT|V_{12}|j_3 j_4; JT\rangle_A = (-1)^{j_1+j_2+j_2+j_4} {}_A\langle j_2 j_1; JT|V_{12}|j_4 j_3; JT\rangle_A$$

with like expressions if the order of coupling is only changed in the bra or ket vectors.

Table A6.1 shows a comparison of matrix elements of the 1s-0d shell calculated for Interaction 36 and those calculated by Kuo and Brown (Kuo 67). The oscillator well parameter was the same in both cases ($\hbar\omega$ = 14 Mev). The density used in the calculation of the matrix elements was that of a single determinant forming a closed shell ^{16}O system. The value of both G, the first order G matrix element and the matrix element, Tot, with some higher order terms included is quoted from the results of Kuo and Brown. Some of the matrix elements of the kind $\sum_{i=1}^{4} j_i$, odd calculated for Interaction 36 differed in sign from those of Kuo and Brown. When this occured the sign of the matrix element was changed in Table A6.1 to agree with the Kuo-Brown phase convention. The matrix elements of Interaction 36 are fairly close to the G matrix elements calculated by Kuo and Brown particularly for the more substantial matrix elements.

Tables A6.2, A6.3, A6.4 list further matrix elements

calculated for $\hbar\omega$ = 14 Mev using Interaction 36 with the closed shell density being that of ^{4}He, ^{16}O and ^{40}Ca. The identical matrix elements calculated using Interaction 37 are listed in Tables A6.5, A6.6 and A6.7.

It can be seen that there is no qualitative differences between the matrix elements calculated for the two interactions.

TABLE A6.1

T=1					Matrix Elements		
					This Work	Kuo and Brown	
J	a	b	c	d	(Mev)	G(Mev)	Tot(Mev)
0	4	4	4	4	-2.16	-1.24	-2.44
	4	4	5	5	-0.82	-0.63	-0.97
	4	4	6	6	-2.43	-3.02	-3.79
	5	5	5	5	-1.63	-2.05	-1.95
	5	5	6	6	-0.66	-0.53	-0.74
	6	6	6	6	-1.17	-0.09	-0.81
1	4	6	4	6	0.81	-0.33	-0.13
	4	6	5	6	0.00	-0.17	-0.10
	5	6	5	6	0.50	-0.33	0.22
2	4	4	4	4	-0.52	-1.01	-1.04
	4	4	4	5	-0.68	-0.56	-0.85
	4	4	4	6	-0.98	-0.41	-0.40
	4	4	5	6	-0.55	-0.55	-0.84
	4	4	6	6	-0.90	-0.60	-0.90
	4	5	4	5	-1.31	-1.17	-1.29
	4	5	4	6	-0.48	-0.18	-0.22
	4	5	5	6	-1.48	-1.45	-1.55
	5	5	5	5			
	4	5	6	6	-0.52	-0.75	-0.74
	5	5	5	6			
	4	6	4	6	0.05	-0.36	-0.20
	4	6	5	6	-0.39	-0.66	-0.77
	4	6	6	6	-0.52	-0.78	-1.01

TABLE A6.1 - CONTINUED

	5	6	5	6	-0.71	-0.59	-0.33
	5	6	6	6	-0.42	-0.04	-0.21
	6	6	6	6	-0.24	-0.28	0.08
3	4	5	4	5	0.50	-0.29	0.17
	4	5	4	6	0.00	-0.06	-0.09
	4	6	4	6	0.37	-0.40	0.13
	4	4	4	4	-0.21	-0.43	-0.05
	4	4	4	6	-1.17	-1.05	-1.36
	4	6	4	6	-1.96	-2.02	-1.66
		4	4	6			
T=0							
1	4	4	4	4	-1.04	-0.30	-1.03
	4	4	4	6	3.30	2.60	3.17
	4	4	5	5	-1.08	-0.27	-0.60
	4	4	5	6	-0.98	-0.11	-0.24
	4	4	6	6	3.75	2.10	1.62
	4	6	4	6	-5.91	-4.33	-5.83
	4	6	5	5	1.63	1.61	1.71
	4	6	5	6	-1.30	-1.42	-1.91
	4	6	6	6	0.19	-0.11	0.04
	5	5	5	5	-3.16	-3.01	-3.18
	5	5	5	6	0.00	-0.08	0.31
	5	5	6	6	0.58	-0.42	-0.21
	5	6	5	6	-4.88	-3.02	-3.28
	5	6	6	6	1.84	0.82	0.80

TABLE A6.1 - CONTINUED

	6	6	6	6	-1.56	-0.22	-0.47
2	4	5	4	5	-0.76	-0.53	-0.62
	4	5	4	6	-1.55	-1.30	-1.45
	4	5	5	6	-3.37	-2.51	-2.58
	4	6	4	6	-3.69	-3.59	-4.53
	4	6	5	6	-1.90	-1.59	-1.54
	5	6	5	6	-2.14	-1.57	-1.61
3	4	4	4	4	-1.86	-0.79	-0.86
	4	4	4	5	-1.93	-1.24	-1.57
	4	4	4	6	2.07	1.47	1.87
	4	4	6	6	1.41	0.39	0.50
	4	5	4	5	-4.88	-3.12	-3.69
	4	5	4	6	-1.49	1.01	1.16
	4	5	6	6	0.32	0.12	0.03
	4	6	4	6	-1.40	-1.11	-1.13
	4	6	6	6	1.87	1.72	2.16
	6	6	6	6	-3.89	-2.43	-2.59
4	4	6	4	6	-4.94	-4.16	-4.31
5	4	4	4	4	-4.94	-3.42	-3.66

TABLE A6.2

N1	L1	2J1	N2	L2	2J2	N3	L3	2J3	N4	L4	2J4	J	T	M.E.(MEV)
0	0	1	0	0	1	0	0	1	0	0	1	1	0	-13.75
0	0	1	0	0	1	0	0	1	0	0	1	0	1	-7.08
0	0	1	0	0	1	0	1	1	0	1	1	1	0	-1.54
0	0	1	0	0	1	0	1	1	0	1	1	0	1	2.57
0	0	1	0	0	1	0	1	1	0	1	3	1	0	-6.19
0	0	1	0	0	1	0	1	3	0	1	3	1	0	4.66
0	0	1	0	0	1	0	1	3	0	1	3	0	1	3.36
0	0	1	0	1	1	0	0	1	0	1	1	1	0	-8.18
0	0	1	0	1	1	0	0	1	0	1	1	0	0	-13.74
0	0	1	0	1	1	0	0	1	0	1	1	1	1	-1.87
0	0	1	0	1	1	0	0	1	0	1	1	2	1	.74
0	0	1	0	1	1	0	0	1	0	1	3	1	0	-7.66
0	0	1	0	1	1	0	0	1	0	1	3	1	1	3.69
0	0	1	0	1	3	0	0	1	0	1	1	1	0	-7.66
0	0	1	0	1	3	0	0	1	0	1	1	1	1	3.69
0	0	1	0	1	3	0	0	1	0	1	3	2	0	-13.74
0	0	1	0	1	3	0	0	1	0	1	3	1	0	-2.03
0	0	1	0	1	3	0	0	1	0	1	3	2	1	.74
0	0	1	0	1	3	0	0	1	0	1	3	1	1	-4.47
0	1	1	0	1	1	0	1	1	0	1	1	1	0	-5.20
0	1	1	0	1	1	0	1	1	0	1	1	0	1	-1.56
0	1	1	0	1	1	0	1	1	0	1	3	1	0	1.00
0	1	1	0	1	1	0	1	3	0	1	3	1	0	4.11
0	1	1	0	1	1	0	1	3	0	1	3	0	1	-3.21
0	1	1	0	1	3	0	1	1	0	1	1	1	0	1.00
0	1	1	0	1	3	0	1	1	0	1	3	2	0	-7.57
0	1	1	0	1	3	0	1	1	0	1	3	1	0	-7.75
0	1	1	0	1	3	0	1	1	0	1	3	2	1	-2.29
0	1	1	0	1	3	0	1	1	0	1	3	1	1	.74
0	1	1	0	1	3	0	1	3	0	1	3	1	0	5.69

0	1	1		0	1	3		0	1	3		0	1	3		2		1	-2.13
0	1	3		0	1	3		0	1	3		0	1	3		3		0	-7.37
0	1	3		0	1	3		0	1	3		0	1	3		1		0	-3.56
0	1	3		0	1	3		0	1	3		0	1	3		2		1	-.79
0	1	3		0	1	3		0	1	3		0	1	3		0		1	-3.83

TABLE A6.3

N1	L1	2J1	N2	L2	2J2	N3	L3	2J3	N4	L4	2J4	J	T	M.E.(MEV)
0	1	1	0	1	1	0	1	1	0	1	1	1	0	-4.94
0	1	1	0	1	1	0	1	1	0	1	1	0	1	-1.55
0	1	1	0	1	1	0	1	1	0	1	3	1	0	1.66
0	1	1	0	1	1	0	1	3	0	1	3	1	0	3.94
0	1	1	0	1	1	0	1	3	0	1	3	0	1	-2.96
0	1	1	0	1	1	1	0	1	1	0	1	1	0	-.15
0	1	1	0	1	1	1	0	1	1	0	1	0	1	.20
0	1	1	0	1	1	1	0	1	0	2	3	1	0	1.50
0	1	1	0	1	1	0	2	3	0	2	3	1	0	1.99
0	1	1	0	1	1	0	2	3	0	2	3	0	1	1.00
0	1	1	0	1	1	0	2	3	0	2	5	1	0	-.77
0	1	1	0	1	1	0	2	5	0	2	5	1	0	-2.74
0	1	1	0	1	1	0	2	5	0	2	5	0	1	1.97
0	1	1	0	1	3	0	1	1	0	1	1	1	0	1.66
0	1	1	0	1	3	0	1	1	0	1	3	2	0	-7.02
0	1	1	0	1	3	0	1	1	0	1	3	1	0	-7.01
0	1	1	0	1	3	0	1	1	0	1	3	2	1	-2.16
0	1	1	0	1	3	0	1	1	0	1	3	1	1	.74
0	1	1	0	1	3	0	1	3	0	1	3	1	0	5.25
0	1	1	0	1	3	0	1	3	0	1	3	2	1	-2.09
0	1	1	0	1	3	1	0	1	1	0	1	1	0	-.21
0	1	1	0	1	3	1	0	1	0	2	3	2	0	1.55
0	1	1	0	1	3	1	0	1	0	2	3	1	0	-.75
0	1	1	0	1	3	1	0	1	0	2	3	2	1	-.46
0	1	1	0	1	3	1	0	1	0	2	5	2	0	1.10
0	1	1	0	1	3	1	0	1	0	2	5	2	1	.27
0	1	1	0	1	3	0	2	3	0	2	3	1	0	-.18
0	1	1	0	1	3	0	2	3	0	2	3	2	1	.70
0	1	1	0	1	3	0	2	3	0	2	5	2	0	3.48
0	1	1	0	1	3	0	2	3	0	2	5	1	0	4.95

0	1	1	0	1	3	0	2	3	0	2	5	2	1	.48
0	1	1	0	1	3	0	2	3	0	2	5	1	1	-.57
0	1	1	0	1	3	0	2	5	0	2	5	1	0	-3.16
0	1	1	0	1	3	0	2	5	0	2	5	2	1	1.23
0	1	1	1	0	1	0	1	1	1	0	1	1	0	-2.73
0	1	1	1	0	1	0	1	1	1	0	1	0	0	-5.74
0	1	1	1	0	1	0	1	1	1	0	1	1	1	-.44
0	1	1	1	0	1	0	1	1	1	0	1	0	1	.81
0	1	1	1	0	1	0	1	1	0	2	3	1	0	1.96
0	1	1	1	0	1	0	1	1	0	2	3	1	1	-.67
0	1	1	1	0	1	0	1	3	1	0	1	1	0	4.23
0	1	1	1	0	1	0	1	3	1	0	1	1	1	-1.78
0	1	1	1	0	1	0	1	3	0	2	3	1	0	-2.26
0	1	1	1	0	1	0	1	3	0	2	3	0	0	3.74
0	1	1	1	0	1	0	1	3	0	2	3	1	1	.54
0	1	1	1	0	1	0	1	3	0	2	3	0	1	-.09
0	1	1	1	0	1	0	1	3	0	2	5	1	0	-1.21
0	1	1	1	0	1	0	1	3	0	2	5	1	1	-.82
0	1	1	0	2	3	0	1	1	1	0	1	1	0	1.56
0	1	1	0	2	3	0	1	1	1	0	1	1	1	-.67
0	1	1	0	2	3	0	1	1	0	2	3	2	0	-6.93
0	1	1	0	2	3	0	1	1	0	2	3	1	0	-1.11
0	1	1	0	2	3	0	1	1	0	2	3	2	1	.08
0	1	1	0	2	3	0	1	1	0	2	5	1	1	-1.09
0	1	1	0	2	3	0	1	1	0	2	5	2	0	1.18
0	1	1	0	2	3	0	1	1	0	2	5	2	1	-.14
0	1	1	0	2	3	0	1	3	1	0	1	2	0	.55
0	1	1	0	2	3	0	1	3	1	0	1	1	0	-.71
0	1	1	0	2	3	0	1	3	1	0	1	2	1	-.01
0	1	1	0	2	3	0	1	3	1	0	1	1	1	-.89
0	1	1	0	2	3	0	1	3	0	2	3	2	0	-3.67

0	1	1	0	2	3	0	1	3	0	2	3	1	0	1.72
0	1	1	0	2	3	0	1	3	0	2	3	2	1	.08
0	1	1	0	2	3	0	1	3	0	2	3	1	1	.79
0	1	1	0	2	3	0	1	3	0	2	5	2	0	3.37
0	1	1	0	2	3	0	1	3	0	2	5	1	0	3.78
0	1	1	0	2	3	0	1	3	0	2	5	2	1	-.54
0	1	1	0	2	3	0	1	3	0	2	5	1	1	-2.47
0	1	1	0	2	5	0	1	1	0	2	3	2	0	1.18
0	1	1	0	2	5	0	1	1	0	2	3	2	1	-.14
0	1	1	0	2	5	0	1	1	0	2	5	3	0	-4.32
0	1	1	0	2	5	0	1	1	0	2	5	2	0	-4.80
0	1	1	0	2	5	0	1	1	0	2	5	3	1	-1.41
0	1	1	0	2	5	0	1	1	0	2	5	2	1	.96
0	1	1	0	2	5	0	1	3	1	0	1	2	0	2.59
0	1	1	0	2	5	0	1	3	1	0	1	2	1	-.06
0	1	1	0	2	5	0	1	3	0	2	3	3	0	-4.91
0	1	1	0	2	5	0	1	3	0	2	3	2	0	1.54
0	1	1	0	2	5	0	1	3	0	2	3	3	1	1.69
0	1	1	0	2	5	0	1	3	0	2	3	2	1	.25
0	1	1	0	2	5	0	1	3	0	2	5	3	0	-.21
0	1	1	0	2	5	0	1	3	0	2	5	2	0	4.32
0	1	1	0	2	5	0	1	3	0	2	5	3	1	-1.76
0	1	1	0	2	5	0	1	3	0	2	5	2	1	-.39
0	1	3	0	1	3	0	1	3	0	1	3	3	0	-7.02
0	1	3	0	1	3	0	1	3	0	1	3	1	0	-2.67
0	1	3	0	1	3	0	1	3	0	1	3	2	1	-.71
0	1	3	0	1	3	0	1	3	0	1	3	0	1	-3.74
0	1	3	0	1	3	1	0	1	1	0	1	1	0	.40
0	1	3	0	1	3	1	0	1	1	0	1	0	1	.28
0	1	3	0	1	3	1	0	1	0	2	3	1	0	-.48
0	1	3	0	1	3	1	0	1	0	2	3	2	1	-.33

0	1	3	0	1	3	1	0	1	0	2	5	3	0	1.75
0	1	3	0	1	3	1	0	1	0	2	5	2	1	.40
0	1	3	0	1	3	0	2	3	0	2	3	3	0	-.46
0	1	3	0	1	3	0	2	3	0	2	3	1	0	-2.97
0	1	3	0	1	3	0	2	3	0	2	3	2	1	.65
0	1	3	0	1	3	0	2	3	0	2	3	0	1	2.18
0	1	3	0	1	3	0	2	3	0	2	5	3	0	-2.10
0	1	3	0	1	3	0	2	3	0	2	5	1	0	-3.51
0	1	3	0	1	3	0	2	3	0	2	5	2	1	.84
0	1	3	0	1	3	0	2	5	0	2	5	3	0	2.75
0	1	3	0	1	3	0	2	5	0	2	5	1	0	1.45
0	1	3	0	1	3	0	2	5	0	2	5	2	1	.40
0	1	3	0	1	3	0	2	5	0	2	5	0	1	2.15
0	1	3	1	0	1	0	1	3	1	0	1	2	0	-5.74
0	1	3	1	0	1	0	1	3	1	0	1	1	0	.24
0	1	3	1	0	1	0	1	3	1	0	1	2	1	.01
0	1	3	1	0	1	0	1	3	1	0	1	1	1	-1.70
0	1	3	1	0	1	0	1	3	0	2	5	2	0	-1.06
0	1	3	1	0	1	0	1	3	0	2	3	1	0	1.50
0	1	3	1	0	1	0	1	3	0	2	3	2	1	.09
0	1	3	1	0	1	0	1	3	0	2	3	1	1	.97
0	1	3	1	0	1	0	1	3	0	2	5	2	0	-2.42
0	1	3	1	0	1	0	1	3	0	2	5	1	0	1.41
0	1	3	1	0	1	0	1	3	0	2	5	2	1	.06
0	1	3	1	0	1	0	1	3	0	2	5	1	1	-1.25
0	1	3	0	2	3	0	1	3	1	0	1	2	0	-1.06
0	1	3	0	2	3	0	1	3	1	0	1	1	0	1.50
0	1	3	0	2	3	0	1	3	1	0	1	2	1	.09
0	1	3	0	2	3	0	1	3	1	0	1	1	1	.97
0	1	3	0	2	3	0	1	3	0	2	3	3	0	-4.93
0	1	3	0	2	3	0	1	3	0	2	3	2	0	-2.66

0	1	3	0	2	5	0	1	3	0	2	3	1	0	-5.22
0	1	3	0	2	3	0	1	3	0	2	3	0	0	-9.23
0	1	3	0	2	3	0	1	3	0	2	3	3	1	-1.84
0	1	3	0	2	3	0	1	3	0	2	3	2	1	.56
0	1	3	0	2	3	0	1	3	0	2	3	1	1	.40
0	1	3	0	2	3	0	1	3	0	2	3	0	1	.60
0	1	3	0	2	3	0	1	3	0	2	5	3	0	-1.62
0	1	3	0	2	3	0	1	3	0	2	5	2	0	-2.03
0	1	3	0	2	3	0	1	3	0	2	5	1	0	-4.07
0	1	3	0	2	3	0	1	3	0	2	5	3	1	1.62
0	1	3	0	2	3	0	1	3	0	2	5	2	1	.47
0	1	3	0	2	3	0	1	3	0	2	5	1	1	1.15
0	1	3	0	2	5	0	1	3	1	0	1	2	0	-2.42
0	1	3	0	2	5	0	1	3	1	0	1	1	0	1.41
0	1	3	0	2	5	0	1	3	1	0	1	2	1	.06
0	1	3	0	2	5	0	1	3	1	0	1	1	1	-1.29
0	1	3	0	2	5	0	1	3	0	2	3	3	0	-1.62
0	1	3	0	2	5	0	1	3	0	2	3	2	0	-2.03
0	1	3	0	2	5	0	1	3	0	2	3	1	0	-4.07
0	1	3	0	2	5	0	1	3	0	2	3	3	1	1.62
0	1	3	0	2	5	0	1	3	0	2	3	2	1	.47
0	1	3	0	2	5	0	1	3	0	2	3	1	1	1.15
0	1	3	0	2	5	0	1	3	0	2	5	4	0	-9.74
0	1	3	0	2	5	0	1	3	0	2	5	3	0	-.88
0	1	3	0	2	5	0	1	3	0	2	5	2	0	-2.99
0	1	3	0	2	5	0	1	3	0	2	5	1	0	-1.00
0	1	3	0	2	5	0	1	3	0	2	5	4	1	.22
0	1	3	0	2	5	0	1	3	0	2	5	3	1	-.62
0	1	3	0	2	5	0	1	3	0	2	5	2	1	.10
0	1	3	0	2	5	0	1	3	0	2	5	1	1	-2.54
1	0	1	1	0	1	1	0	1	1	0	1	1	0	-5.18

1	0	1	1	0	1	1	0	1	1	0	1	0	1	-1.03
1	0	1	1	0	1	0	2	3	0	2	3	1	0	.58
1	0	1	1	0	1	0	2	3	0	2	3	0	1	-.66
1	0	1	1	0	1	0	2	3	0	2	5	1	0	1.03
1	0	1	1	0	1	0	2	5	0	2	5	1	0	-1.08
1	0	1	1	0	1	0	2	5	0	2	5	0	1	-.61
1	0	1	0	2	3	1	0	1	0	2	3	2	0	-2.14
1	0	1	0	2	3	1	0	1	0	2	3	1	0	-4.88
1	0	1	0	2	3	1	0	1	0	2	3	2	1	-.71
1	0	1	0	2	3	1	0	1	0	2	3	1	1	.90
1	0	1	0	2	3	1	0	1	0	2	5	2	0	-3.37
1	0	1	0	2	3	1	0	1	0	2	5	2	1	1.46
1	0	1	0	2	3	0	2	3	0	2	3	1	0	-1.84
1	0	1	0	2	3	0	2	3	0	2	3	2	1	.42
1	0	1	0	2	3	0	2	3	0	2	5	2	0	-1.90
1	0	1	0	2	3	0	2	3	0	2	5	1	0	1.30
1	0	1	0	2	3	0	2	3	0	2	5	2	1	.39
1	0	1	0	2	3	0	2	5	0	2	5	1	0	.98
1	0	1	0	2	3	0	2	5	0	2	5	2	1	.99
1	0	1	0	2	5	1	0	1	0	2	3	2	0	-3.37
1	0	1	0	2	5	1	0	1	0	2	3	2	1	1.46
1	0	1	0	2	5	1	0	1	0	2	5	3	0	-4.88
1	0	1	0	2	5	1	0	1	0	2	5	2	0	-.78
1	0	1	0	2	5	1	0	1	0	2	5	3	1	.50
1	0	1	0	2	5	1	0	1	0	2	5	2	1	-1.31
1	0	1	0	2	5	0	2	3	0	2	3	3	0	.32
1	0	1	0	2	5	0	2	3	0	2	3	2	1	-.52
1	0	1	0	2	5	0	2	3	0	2	5	3	0	1.49
1	0	1	0	2	5	0	2	3	0	2	5	2	0	-1.55
1	0	1	0	2	5	0	2	3	0	2	5	2	1	-.48
1	0	1	0	2	5	0	2	5	0	2	5	3	0	-1.93

1	0	1		0	2	5		0	2	5		0	2	5		2		1		-.68
0	2	3		0	2	3		0	2	3		0	2	3		3		0		-3.89
0	2	3		0	2	3		0	2	3		0	2	3		1		0		-1.56
0	2	3		0	2	3		0	2	3		0	2	3		2		1		-.24
0	2	3		0	2	3		0	2	3		0	2	3		0		1		-1.17
0	2	3		0	2	3		0	2	3		0	2	5		3		0		1.88
0	2	3		0	2	3		0	2	3		0	2	5		1		0		.19
0	2	3		0	2	3		0	2	3		0	2	5		2		1		-.52
0	2	3		0	2	3		0	2	5		0	2	5		3		0		1.41
0	2	3		0	2	5		0	2	5		0	2	5		1		0		.75
0	2	3		0	2	3		0	2	5		0	2	5		2		1		-.90
0	2	3		0	2	3		0	2	5		0	2	5		0		1		-2.42
0	2	3		0	2	5		0	2	3		0	2	3		3		0		1.88
0	2	3		0	2	5		0	2	3		0	2	3		1		0		.19
0	2	3		0	2	5		0	2	3		0	2	3		2		1		-.52
0	2	3		0	2	5		0	2	3		0	2	5		4		0		-4.94
0	2	3		0	2	5		0	2	3		0	2	5		3		0		-1.40
0	2	3		0	2	5		0	2	3		0	2	5		2		0		-3.09
0	2	3		0	2	5		0	2	5		0	2	5		1		0		-3.92
0	2	3		0	2	5		0	2	3		0	2	5		4		1		-1.98
0	2	3		0	2	5		0	2	3		0	2	5		3		1		.37
0	2	3		0	2	5		0	2	3		0	2	5		2		1		.05
0	2	3		0	2	5		0	2	3		0	2	5		1		1		.81
0	2	3		0	2	5		0	2	5		0	2	5		5		0		2.08
0	2	3		0	2	5		0	2	5		0	2	5		1		0		3.30
0	2	3		0	2	5		0	2	5		0	2	5		4		1		-1.17
0	2	3		0	2	5		0	2	5		0	2	5		2		1		-.98
0	2	5		0	2	5		0	2	5		0	2	5		5		0		-4.94
0	2	5		0	2	5		0	2	5		0	2	5		5		0		-1.86
0	2	5		0	2	5		0	2	5		0	2	5		1		0		-1.04

0	2	5		0	2	5		0	2	5		0	2	5		4	1	-.21
0	2	5		0	2	5		0	2	5		0	2	5		2	1	-.52
0	2	5		0	2	5		0	2	5		0	2	5		0	1	-2.16

N1	L1	2J1	N2	L2	2J2	N3	L3	2J3	N4	L4	2J4	J	T	M.E.(MEV)
1	0	1	1	0	1	1	0	1	1	0	1	1	0	-1.94
1	0	1	1	0	1	1	0	1	1	0	1	0	1	-.92
0	2	3	0	2	3	0	2	3	0	2	3	3	0	-3.57
0	2	3	0	2	3	0	2	3	0	2	3	1	0	-1.16
0	2	3	0	2	3	0	2	3	0	2	3	2	1	-.16
0	2	3	0	2	3	0	2	3	0	2	3	0	1	-.61
0	2	5	0	2	5	0	2	5	0	2	5	5	0	-4.57
0	2	5	0	2	5	0	2	5	0	2	5	3	0	-1.59
0	2	5	0	2	5	0	2	5	0	2	5	1	0	-.49
0	2	5	0	2	5	0	2	5	0	2	5	4	1	-.16
0	2	5	0	2	5	0	2	5	0	2	5	2	1	-.41
0	2	5	0	2	5	0	2	5	0	2	5	0	1	-1.56
1	1	1	1	1	1	1	1	1	1	1	1	1	0	-1.27
1	1	1	1	1	1	1	1	1	1	1	1	0	1	-.16
1	1	3	1	1	3	1	1	3	1	1	3	3	0	-1.97
1	1	3	1	1	3	1	1	3	1	1	3	1	0	-.50
1	1	3	1	1	3	1	1	3	1	1	3	2	1	-.14
1	1	3	1	1	3	1	1	3	1	1	3	0	1	-.62
0	3	5	0	3	5	0	3	5	0	3	5	5	0	-2.96
0	3	5	0	3	5	0	3	5	0	3	5	3	0	-.67
0	3	5	0	3	5	0	3	5	0	3	5	1	0	-.55
0	3	5	0	3	5	0	3	5	0	3	5	4	1	-.01
0	3	5	0	3	5	0	3	5	0	3	5	2	1	-.24
0	3	5	0	3	5	0	3	5	0	3	5	3	1	-.59
0	3	7	0	3	7	0	3	7	0	3	7	7	0	-3.54
0	3	7	0	3	7	0	3	7	0	3	7	5	0	-1.10
0	3	7	0	3	7	0	3	7	0	3	7	3	0	-.76
0	3	7	0	3	7	0	3	7	0	3	7	1	0	.00
0	3	7	0	3	7	0	3	7	0	3	7	6	1	-.04
0	3	7	0	3	7	0	3	7	0	3	7	4	1	-.12

0	3	7		0	3	7		0	3	7		0	3	7		2		1	-.58
0	3	7		0	3	7		0	3	7		0	3	7		0		1	-1.02

TABLE A6.5

N1	L1	2J1	N2	L2	2J2	N3	L3	2J3	N4	L4	2J4	J	T	M.E.(MEV)
0	0	1	0	0	1	0	0	1	0	0	1	1	0	-14.04
0	0	1	0	0	1	0	0	1	0	0	1	0	1	-8.70
0	0	1	0	0	1	0	1	1	0	1	1	1	0	-1.38
0	0	1	0	0	1	0	1	1	0	1	1	0	1	2.24
0	0	1	0	0	1	0	1	1	0	1	3	1	0	-6.20
0	0	1	0	0	1	0	1	3	0	1	3	1	0	4.95
0	0	1	0	0	1	0	1	3	0	1	3	0	1	3.18
0	0	1	0	1	1	0	0	1	0	1	1	1	0	-8.45
0	0	1	0	1	1	0	0	1	0	1	1	0	0	-14.30
0	0	1	0	1	1	0	0	1	0	1	1	1	1	-1.79
0	0	1	0	1	1	0	0	1	0	1	1	0	1	.74
0	0	1	0	1	1	0	0	1	0	1	3	1	0	-8.29
0	0	1	0	1	1	0	0	1	0	1	3	1	1	3.99
0	0	1	0	1	3	0	0	1	0	1	1	1	0	-8.29
0	0	1	0	1	3	0	0	1	0	1	1	1	1	3.99
0	0	1	0	1	3	0	0	1	0	1	3	2	0	-14.30
0	0	1	0	1	3	0	0	1	0	1	3	1	0	-2.57
0	0	1	0	1	3	0	0	1	0	1	3	2	1	.74
0	0	1	0	1	3	0	0	1	0	1	3	1	1	-4.30
0	1	1	0	1	1	0	1	1	0	1	1	1	0	-5.99
0	1	1	0	1	1	0	1	1	0	1	1	0	1	-1.46
0	1	1	0	1	1	0	1	1	0	1	3	1	0	1.82
0	1	1	0	1	1	0	1	3	0	1	3	1	0	4.44
0	1	1	0	1	1	0	1	3	0	1	3	0	1	-3.11
0	1	1	0	1	3	0	1	1	0	1	1	1	0	1.82
0	1	1	0	1	3	0	1	1	0	1	3	2	0	-7.87
0	1	1	0	1	3	0	1	1	0	1	3	1	0	-8.82
0	1	1	0	1	3	0	1	1	0	1	3	2	1	-2.26
0	1	1	0	1	3	0	1	1	0	1	3	1	1	.74

0	1	1		0	1	3		0	1	3		0	1	3		1	0	6.00
0	1	1		0	1	3		0	1	3		0	1	3		2	1	-2.11
0	1	3		0	1	3		0	1	3		0	1	3		3	0	-7.67
0	1	3		0	1	3		0	1	3		0	1	3		1	0	-3.31
0	1	3		0	1	3		0	1	3		0	1	3		2	1	-.77
0	1	3		0	1	3		0	1	3		0	1	3		3	1	-3.67

TABLE A6.6

N1	L1	2J1	N2	L2	2J2	N3	L3	2J3	N4	L4	2J4	J	T	M.E.(MEV)
0	1	1	0	1	1	0	1	1	0	1	1	1	0	-5.15
0	1	1	0	1	1	0	1	1	0	1	1	0	1	-1.33
0	1	1	0	1	1	0	1	1	0	1	3	1	0	1.72
0	1	1	0	1	1	0	1	3	0	1	3	1	0	4.15
0	1	1	0	1	1	0	1	3	0	1	3	0	1	-2.67
0	1	1	0	1	1	1	0	1	1	0	1	1	0	-.19
0	1	1	0	1	1	1	0	1	1	0	1	0	1	.27
0	1	1	0	1	1	1	0	1	0	2	3	1	0	1.58
0	1	1	0	1	1	0	2	3	0	2	3	1	0	2.11
0	1	1	0	1	1	0	2	3	0	2	3	0	1	1.01
0	1	1	0	1	1	0	2	3	0	2	5	1	0	-.82
0	1	1	0	1	1	0	2	5	0	2	5	1	0	-2.93
0	1	1	0	1	1	0	2	5	0	2	5	0	1	1.93
0	1	1	0	1	3	0	1	1	0	1	1	1	0	1.72
0	1	1	0	1	3	0	1	1	0	1	3	2	0	-7.31
0	1	1	0	1	3	0	1	1	0	1	3	1	0	-7.37
0	1	1	0	1	3	0	1	1	0	1	3	2	1	-2.10
0	1	1	0	1	3	0	1	1	0	1	3	1	1	.68
0	1	1	0	1	3	0	1	3	0	1	3	1	0	5.54
0	1	1	0	1	3	0	1	3	0	1	3	2	1	-1.97
0	1	1	0	1	3	1	0	1	1	0	1	1	0	-.77
0	1	1	0	1	3	1	0	1	0	2	3	2	0	1.42
0	1	1	0	1	3	1	0	1	0	2	3	1	0	-.79
0	1	1	0	1	3	1	0	1	0	2	3	2	1	-.45
0	1	1	0	1	3	1	0	1	0	2	5	2	0	1.16
0	1	1	0	1	3	1	0	1	0	2	5	2	1	.55
0	1	1	0	1	3	0	2	3	0	2	3	1	0	-.20
0	1	1	0	1	3	0	2	3	0	2	3	2	1	.69
0	1	1	0	1	3	0	2	3	0	2	5	2	0	3.70
0	1	1	0	1	3	0	2	3	0	2	5	1	0	5.29

0	1	1	0	1	3	0	2	3	0	2	5	2	1	.48
0	1	1	0	1	3	0	2	3	0	2	5	1	1	-.54
0	1	1	0	1	3	0	2	5	0	2	5	1	0	-3.39
0	1	1	0	1	3	0	2	5	0	2	5	2	1	1.21
0	1	1	1	0	1	0	1	1	1	0	1	1	0	-2.99
0	1	1	1	0	1	0	1	1	1	0	1	0	0	-6.08
0	1	1	1	0	1	0	1	1	1	0	1	1	1	-.48
0	1	1	1	0	1	0	1	1	1	0	1	0	1	.72
0	1	1	1	0	1	0	1	1	0	2	3	1	0	1.30
0	1	1	1	0	1	0	1	1	0	2	3	1	1	-.62
0	1	1	1	0	1	0	1	3	1	0	1	1	0	4.42
0	1	1	1	0	1	0	1	3	1	0	1	1	1	-1.71
0	1	1	1	0	1	0	1	3	0	2	5	1	0	-2.50
0	1	1	1	0	1	0	1	3	0	2	3	0	0	3.78
0	1	1	1	0	1	0	1	3	0	2	3	1	1	.91
0	1	1	1	0	1	0	1	3	0	2	3	0	1	-.06
0	1	1	1	0	1	0	1	3	0	2	5	1	0	-1.96
0	1	1	1	0	1	0	1	3	0	2	5	1	1	-.78
0	1	1	0	2	3	0	1	1	1	0	1	1	0	1.30
0	1	1	0	2	3	0	1	1	1	0	1	1	1	-.62
0	1	1	0	2	3	0	1	1	0	2	5	2	0	-7.54
0	1	1	0	2	3	0	1	1	0	2	3	1	0	-1.19
0	1	1	0	2	3	0	1	1	0	2	3	2	1	.07
0	1	1	0	2	3	0	1	1	0	2	3	1	1	-1.10
0	1	1	0	2	3	0	1	1	0	2	5	2	0	1.27
0	1	1	0	2	3	0	1	1	0	2	5	2	1	-.14
0	1	1	0	2	3	0	1	3	1	0	1	2	0	.55
0	1	1	0	2	3	0	1	3	1	0	1	1	0	-.75
0	1	1	0	2	3	0	1	3	1	0	1	2	1	-.01
0	1	1	0	2	3	0	1	3	1	0	1	1	1	-.85
0	1	1	0	2	3	0	1	3	0	2	3	2	0	-3.91

0	1	1	0	2	3	0	1	3	0	2	3	1	0	1.61
0	1	1	0	2	3	0	1	3	0	2	3	2	1	.09
0	1	1	0	2	3	0	1	3	0	2	3	1	1	.78
0	1	1	0	2	3	0	1	3	0	2	5	2	0	3.61
0	1	1	0	2	5	0	1	3	0	2	5	1	0	4.05
0	1	1	0	2	3	0	1	3	0	2	5	2	1	-.54
0	1	1	0	2	3	0	1	3	0	2	5	1	1	-2.43
0	1	1	0	2	5	0	1	1	0	2	3	2	0	1.27
0	1	1	0	2	5	0	1	1	0	2	3	2	1	-.14
0	1	1	0	2	5	0	1	1	0	2	5	3	0	-4.58
0	1	1	0	2	5	0	1	1	0	2	5	2	0	-5.13
0	1	1	0	2	5	0	1	1	0	2	5	3	1	-1.40
0	1	1	0	2	5	0	1	1	0	2	5	2	1	.52
0	1	1	0	2	5	0	1	3	1	0	1	2	0	2.62
0	1	1	0	2	5	0	1	3	1	0	1	2	1	-.04
0	1	1	0	2	5	0	1	3	0	2	3	3	0	-5.22
0	1	1	0	2	5	0	1	3	0	2	3	2	0	1.61
0	1	1	0	2	5	0	1	3	0	2	3	3	1	1.82
0	1	1	0	2	5	0	1	3	0	2	3	2	1	.24
0	1	1	0	2	5	0	1	3	0	2	5	3	0	-.19
0	1	1	0	2	5	0	1	3	0	2	5	2	0	4.03
0	1	1	0	2	5	0	1	3	0	2	5	3	1	-1.72
0	1	1	0	2	5	0	1	3	0	2	5	2	1	-.30
0	1	3	0	1	3	0	1	3	0	1	3	3	0	-7.31
0	1	3	0	1	3	0	1	3	0	1	3	1	0	-3.01
0	1	3	0	1	3	0	1	3	0	1	3	2	1	-.71
0	1	3	0	1	3	0	1	3	0	1	3	0	1	-3.37
0	1	3	0	1	3	1	0	1	1	0	1	1	0	.61
0	1	3	0	1	3	1	0	1	1	0	1	0	1	.39
0	1	3	0	1	3	1	0	1	0	2	3	1	0	-.30
0	1	3	0	1	3	1	0	1	0	2	3	2	1	-.32

0	1	3	0	1	3	1	0	1	0	2	5	3	0	1.03
0	1	3	0	1	3	1	0	1	0	2	5	2	1	.39
0	1	3	0	1	3	0	2	3	0	2	3	3	0	-.48
0	1	3	0	1	3	0	2	3	0	2	3	1	0	-3.19
0	1	3	0	1	3	0	2	3	0	2	3	2	1	.09
0	1	3	0	1	3	0	2	3	0	2	3	0	1	2.15
0	1	3	0	1	3	0	2	3	0	2	5	3	0	-2.24
0	1	3	0	1	3	0	2	3	0	2	5	1	0	-3.76
0	1	3	0	1	3	0	2	3	0	2	5	2	1	.01
0	1	3	0	1	3	0	2	5	0	2	5	3	0	2.00
0	1	3	0	1	3	0	2	5	0	2	5	1	0	1.52
0	1	3	0	1	3	0	2	5	0	2	5	2	1	.41
0	1	3	0	1	3	0	2	5	0	2	5	0	1	2.14
0	1	3	1	0	1	0	1	3	1	0	1	2	0	-3.08
0	1	3	1	0	1	0	1	3	1	0	1	1	0	.18
0	1	3	1	0	1	0	1	3	1	0	1	2	1	.74
0	1	3	1	0	1	0	1	3	1	0	1	1	1	-1.09
0	1	3	1	0	1	0	1	3	0	2	3	2	0	-1.07
0	1	3	1	0	1	0	1	3	0	2	3	1	0	1.53
0	1	3	1	0	1	0	1	3	0	2	3	2	1	.02
0	1	3	1	0	1	0	1	3	0	2	3	1	1	.33
0	1	3	1	0	1	0	1	3	0	2	5	2	0	-2.43
0	1	3	1	0	1	0	1	3	0	2	5	1	0	1.50
0	1	3	1	0	1	0	1	3	0	2	5	2	1	.04
0	1	3	1	0	1	0	1	3	0	2	5	1	1	-1.16
0	1	3	0	2	3	0	1	3	1	0	1	2	0	-1.07
0	1	3	0	2	3	0	1	3	1	0	1	1	0	1.53
0	1	3	0	2	3	0	1	3	1	0	1	2	1	.02
0	1	3	0	2	3	0	1	3	1	0	1	1	1	.33
0	1	3	0	2	3	0	1	3	0	2	5	3	0	-5.22
0	1	3	0	2	3	0	1	3	0	2	5	2	0	-2.03

0	1	3	0	2	3	0	1	3	0	2	3	1	0	-5.58
0	1	3	0	2	3	0	1	3	0	2	3	0	0	-9.86
0	1	3	0	2	3	0	1	3	0	2	3	3	1	-1.81
0	1	3	0	2	3	0	1	3	0	2	3	2	1	.55
0	1	3	0	2	3	0	1	3	0	2	3	1	1	.56
0	1	3	0	2	3	0	1	3	0	2	3	0	1	.75
0	1	3	0	2	3	0	1	3	0	2	5	3	0	-1.74
0	1	3	0	2	3	0	1	3	0	2	5	2	0	-2.20
0	1	3	0	2	3	0	1	3	0	2	5	1	0	-4.56
0	1	3	0	2	3	0	1	3	0	2	5	3	1	1.78
0	1	3	0	2	3	0	1	3	0	2	5	2	1	.46
0	1	3	0	2	3	0	1	3	0	2	5	1	1	1.11
0	1	3	0	2	5	0	1	3	1	0	1	2	0	-2.45
0	1	3	0	2	5	0	1	3	1	0	1	1	0	1.58
0	1	3	0	2	5	0	1	3	1	0	1	2	1	.04
0	1	3	0	2	5	0	1	3	1	0	1	1	1	-1.16
0	1	3	0	2	5	0	1	3	0	2	3	3	0	-1.74
0	1	3	0	2	5	0	1	3	0	2	5	2	0	-2.20
0	1	3	0	2	5	0	1	3	0	2	5	1	0	-4.56
0	1	3	0	2	5	0	1	3	0	2	3	3	1	1.78
0	1	3	0	2	5	0	1	3	0	2	5	2	1	.40
0	1	3	0	2	5	0	1	3	0	2	3	1	1	1.11
0	1	3	0	2	5	0	1	3	0	2	5	4	0	-1.34
0	1	3	0	2	5	0	1	3	0	2	5	3	0	-.95
0	1	3	0	2	5	0	1	3	0	2	5	2	0	-3.16
0	1	3	0	2	5	0	1	3	0	2	5	1	0	-1.04
0	1	3	0	2	5	0	1	3	0	2	5	4	1	.21
0	1	3	0	2	5	0	1	3	0	2	5	3	1	-.02
0	1	3	0	2	5	0	1	3	0	2	5	2	1	.07
0	1	3	0	2	5	0	1	3	0	2	5	1	1	-2.55
1	0	1	1	0	1	1	0	1	1	0	1	1	0	-3.82

1	0	1	1	0	1	1	0	1	1	0	1	0	1	-1.62
1	0	1	1	0	1	0	2	3	0	2	3	1	0	.65
1	0	1	1	0	1	0	2	3	0	2	3	0	1	-.68
1	0	1	1	0	1	0	2	3	0	2	5	1	0	1.79
1	0	1	1	0	1	0	2	5	0	2	5	1	0	-1.19
1	0	1	1	0	1	0	2	5	0	2	5	0	1	-.63
1	0	1	0	2	3	1	0	1	0	2	3	2	0	-2.26
1	0	1	0	2	3	1	0	1	0	2	3	1	0	-5.19
1	0	1	0	2	3	1	0	1	0	2	3	2	1	-.71
1	0	1	0	2	3	1	0	1	0	2	3	1	1	.47
1	0	1	0	2	3	1	0	1	0	2	5	2	0	-3.56
1	0	1	0	2	5	1	0	1	0	2	5	2	1	1.44
1	0	1	0	2	3	0	2	3	0	2	3	1	0	-1.90
1	0	1	0	2	3	0	2	3	0	2	3	2	1	.40
1	0	1	0	2	3	0	2	3	0	2	5	2	0	-1.96
1	0	1	0	2	3	0	2	3	0	2	5	1	0	1.54
1	0	1	0	2	3	0	2	3	0	2	5	2	1	.97
1	0	1	0	2	5	0	2	5	0	2	5	1	0	1.01
1	0	1	0	2	3	0	2	5	0	2	5	2	1	.55
1	0	1	0	2	5	1	0	1	0	2	3	2	0	-3.56
1	0	1	0	2	5	1	0	1	0	2	3	2	1	1.44
1	0	1	0	2	5	1	0	1	0	2	5	3	0	-5.19
1	0	1	0	2	5	1	0	1	0	2	5	2	0	-.80
1	0	1	0	2	5	1	0	1	0	2	5	3	1	.47
1	0	1	0	2	5	1	0	1	0	2	5	2	1	-1.30
1	0	1	0	2	5	0	2	3	0	2	3	3	0	.55
1	0	1	0	2	5	0	2	3	0	2	3	2	1	-.50
1	0	1	0	2	5	0	2	3	0	2	5	3	0	1.55
1	0	1	0	2	5	0	2	3	0	2	5	2	0	-1.80
1	0	1	0	2	5	0	2	3	0	2	5	2	1	-.46
1	0	1	0	2	5	0	2	5	0	2	5	3	0	-1.99

1	0	1	0	2	5	0	2	5	0	2	5	2	1	-.05
0	2	3	0	2	3	0	2	3	0	2	5	3	0	-4.10
0	2	3	0	2	3	0	2	3	0	2	3	1	0	-1.00
0	2	3	0	2	5	0	2	5	0	2	3	2	1	-.25
0	2	3	0	2	5	0	2	3	0	2	5	0	1	-1.10
0	2	5	0	2	5	0	2	3	0	2	5	3	0	2.04
0	2	3	0	2	3	0	2	3	0	2	5	1	0	.25
0	2	3	0	2	5	0	2	3	0	2	5	2	1	-.55
0	2	3	0	2	5	0	2	5	0	2	5	3	0	1.54
0	2	3	0	2	3	0	2	5	0	2	5	1	0	4.09
0	2	3	0	2	3	0	2	5	0	2	5	2	1	-.90
0	2	5	0	2	5	0	2	5	0	2	5	0	1	-2.40
0	2	5	0	2	5	0	2	5	0	2	5	3	0	2.04
0	2	3	0	2	5	0	2	3	0	2	3	1	0	.25
0	2	3	0	2	5	0	2	3	0	2	3	2	1	-.55
0	2	3	0	2	5	0	2	3	0	2	5	4	0	-5.52
0	2	3	0	2	5	0	2	5	0	2	5	3	0	-1.47
0	2	3	0	2	5	0	2	3	0	2	5	2	0	-4.01
0	2	3	0	2	5	0	2	3	0	2	5	1	0	-8.50
0	2	5	0	2	5	0	2	5	0	2	5	4	1	-1.90
0	2	5	0	2	5	0	2	3	0	2	5	3	1	.37
0	2	3	0	2	5	0	2	3	0	2	5	2	1	.05
0	2	3	0	2	5	0	2	3	0	2	5	1	1	.78
0	2	5	0	2	5	0	2	5	0	2	5	3	0	2.28
0	2	3	0	2	5	0	2	5	0	2	5	1	0	3.57
0	2	5	0	2	5	0	2	5	0	2	5	4	1	-1.10
0	2	5	0	2	5	0	2	5	0	2	5	2	1	-.97
0	2	5	0	2	5	0	2	5	0	2	5	5	0	-5.52
0	2	5	0	2	5	0	2	5	0	2	5	3	0	-2.00
0	2	5	0	2	5	0	2	5	0	2	5	1	0	-1.08
0	2	5	0	2	5	0	2	5	0	2	5	4	1	-.21

0	2	5		0	2	5		0	2	5		0	2	5		2		1	-.54
0	2	5		0	2	5		0	2	5		0.	2	5		0		1	-2.17

TABLE A6.7

N1	L1	2J1	N2	L2	2J2	N3	L3	2J3	N4	L4	2J4	J	T	M.E.(MEV)
1	0	1	1	0	1	1	0	1	1	0	1	1	0	-1.18
1	0	1	1	0	1	1	0	1	1	0	1	0	1	-.56
0	2	3	0	2	3	0	2	3	0	2	3	3	0	-3.75
0	2	3	0	2	3	0	2	3	0	2	3	1	0	-1.44
0	2	3	0	2	3	0	2	3	0	2	3	2	1	-.22
0	2	3	0	2	3	0	2	3	0	2	3	0	1	-1.01
0	2	5	0	2	5	0	2	5	0	2	5	5	0	-4.78
0	2	5	0	2	5	0	2	5	0	2	5	3	0	-1.76
0	2	5	0	2	5	0	2	5	0	2	5	1	0	-.66
0	2	5	0	2	5	0	2	5	0	2	5	4	1	-.19
0	2	5	0	2	5	0	2	5	0	2	5	2	1	-.48
0	2	5	0	2	5	0	2	5	0	2	5	0	1	-1.88
1	1	1	1	1	1	1	1	1	1	1	1	1	0	-1.40
1	1	1	1	1	1	1	1	1	1	1	1	0	1	-.56
1	1	3	1	1	3	1	1	3	1	1	3	3	0	-1.99
1	1	3	1	1	3	1	1	3	1	1	3	1	0	-.61
1	1	3	1	1	3	1	1	3	1	1	3	2	1	-.19
1	1	3	1	1	3	1	1	3	1	1	3	0	1	-.91
0	3	5	0	3	5	0	3	5	0	3	5	5	0	-3.26
0	3	5	0	3	5	0	3	5	0	3	5	3	0	-1.03
0	3	5	0	3	5	0	3	5	0	3	5	1	0	-.60
0	3	5	0	3	5	0	3	5	0	3	5	4	1	-.05
0	3	5	0	3	5	0	3	5	0	3	5	2	1	-.30
0	3	5	0	3	5	0	3	5	0	3	5	0	1	-.61
0	3	7	0	3	7	0	3	7	0	3	7	7	0	-3.69
0	3	7	0	3	7	0	3	7	0	3	7	5	0	-1.27
0	3	7	0	3	7	0	3	7	0	3	7	3	0	-.94
0	3	7	0	3	7	0	3	7	0	3	7	1	0	-.29
0	3	7	0	3	7	0	3	7	0	3	7	6	1	-.06
0	3	7	0	3	7	0	3	7	0	3	7	4	1	-.15

0	3	7		0	3	7		0	3	7		0	3	7		2		1	-.49
0	3	7		0	3	7		0	3	7		0	3	7		0		1	-1.52

BIBLIOGRAPHY

(1) Abr 69 Y. Abragall, G. Baron, E. Courier and G. Monsonego, Nucl. Phys. A131 (1969) 609

(2) Ajz 68 F. Ajzenberg-Selove and T. Lauritsen, Nucl. Phys. A114 (1968) 1

(3) Alb 66 D. E. Alburger, P. B. Parker and D. J. Breelin, Phys. Rev. 143 (1966) 692

(4) Ami 64 D. Amit and A. Katz, Nucl. Phys. 58 (1964) 388

(5) Bac 67 G. Backenstoss, S. Charalambus, H. Daniel, H. Koch, G. Poely, H. Schmitt and L. Tauscher, Phys. Letters 25B (1967) 547

(6) Bai 48 W. N. Bailey, J. London Math. Soc. 23 (1948) 291

(7) Ban 69 I. M. Band, V. N. Guman, L. A. Sliv and Yu. I. Kharitonov, Phys. Letters 28B (1969) 313

(8) Bar 66 F. C. Barker, Nucl. Phys. 83 (1966) 418

(9) Bat 65 C. J. Batty, E. Friedman, P. C. Rowe and J. B. Hunt, Phys. Letters 9 (1965) 35

(10) Bel 68 R. A. I. Bell, R. D. Gill, B. C. Robertson, J. S. Lopes and H. J. Rose, Nucl. Phys. A118 (1968) 481

(11) Ben 67 W. Benenson, G. M. Crawley, J. D. Dreisbach and W. P. Johnson, Nucl. Phys. A97 (1967) 510

(12) Bet 66 H. A. Bethe, invited lecture, 1966, Gatlinberg Conference

(13) Bet 67 H. A. Bethe, Proceedings of the International Nuclear Physics Conference, Gatlinberg, Tennessee (Academic Press 1967) 625

(14) Bet 68 H. A. Bethe, Phys. Rev. 167 (1968) 879

Bet 68a H. A. Bethe and R. Jackiw, Intermediate Quantum Mechanics, (W. A. Benjamin 1968)

(15) Bha 65 R. K. Bhaduri and E. Tomusiak, Proc. Phys. Soc. 86 (1965) 451

(16) Bha 68 R. K. Bhaduri and Chindu S. Warke, Phys. Rev. Letters 20 (1968) 1379

(17) Bha 67 P. Bhargava and D. W. L. Sprung, Ann. of Phys. 42 (1967) 222

(18) Bla 67 R. S. Blake, E. B. Paul, C. H. Sinex and S. T. Emerson, Nucl. Phys. A102 (1967) 305

(19) Boe 67 E. Boeker, Nucl. Phys. A91 (1967) 27

(20) Boe 68 E. Boeker, Nucl. Phys. A119 (1968) 435

(21) Bof 68 S. Boffi, M. Bouten, C. Ciofi Degli Atti and J. Sawicki, preprint (1968)

(22) Bou 67 M. Bouten, P. van Leuven and H. Depuydt, Nucl. Phys. A94 (1967) 687

(23) Bou 68 M. Bouten, M. C. Bouten, H. Depuydt and L. Schotsman, Phys. Letters 27B (1968) 61

(24) Bou 69 M. Bouten, P. van Leuven and H. Depuydt, Nucl. Phys. A94 (1967) 687

(25) Boy 64 A. N. Boyarkina, Izv. Akad. SSSR, Ser. Fiz, 28 (1964) 337;
Bull. Acad. Sci. USSR, Phys. Ser., (U.S.A.) 28 (1965) 255

(26) Bra 65 B. Brandow, "Theory of the Effective Interaction", Varenna Summer School (1965)

(27) Bri 65 D. Brink, Varenna Lectures (1965)

(28) Bri 67 D. M. Brink and E. Boeker, Nucl. Phys. A91 (1967) 1

(29) Bro 67 G. E. Brown, International Nuclear Physics Conference, Paris (1967)

(30) Bru 56 K. Brueckner and W. Wada, Phys. Rev. 103 (1956) 1008

(31) Bru 59 K. A. Brueckner and D. T. Goldman, Phys. Rev. 116 (1959) 424

(32) Bun 65 G. G. Bunatyan and M. A. Mikulinski, Soviet J. Nucl. Phys. 1 (1965) 26

(33) Coh 65 S. Cohen and D. Kurath, Nucl. Phys. 73 (1965) 1

(34) Coo 68 J. A. Cookson, Phys. Letters 27B (1968) 619

(35) Cop 66 L. A. Copley and A. B. Volkov, Nucl. Phys. 84 (1966) 417

(36) Det 65 C. Detraz, J. Cerny and R. H. Pehl, Phys. Rev. Letters 14 (1965) 708

(37) Ecc 66 S. F. Eccles, C. Wong and J. D. Anderson, Phys. Letters 20 (1966) 190

(38) Elt 61 L. R. B. Elton, Nuclear Sizes, (Oxford University Press, 1961)

(39) Elt 67 L. R. B. Elton, Int. Conf. on Electromagnetic Sizes of Nuclei, Ottawa 1967

(40) Erd 54 A. Erdelyi, W. Magnus, E. Overhettinger and F. G. Tricomi, Tables of Integral Transforms, Vol. 11, McGraw Hill Book Co., 1954, Vol. 2, 291

Erd 54a ibid, 290

Erd 54b ibid, 306

Erd 54c ibid, 15

(41) Eve 60 F. Everling, L. A. Konig, J. H. E. Mattauch and A. H. Wapstra, Nucl. Phys. 18 (1960) 529

(42) Fae 68 A. Faessler, P. V. Sauer and M. M. Stingl, Zeitschrift fur Physik, 212 (1968) 1

(43) Gol 63 P. Goldhammer, Rev. of Modern Physics 35 (1963) 40

(44) Gol 68 P. Goldhammer, J. R. Hill and J. Nachamkin, Nucl. Phys. A106 (1968) 62

(45) Gol 57 J. Goldstone, Proc. Roy. Soc. (London) A239 (1957) 267

(46) Gre 62 A. M. Green, Nucl. Phys. 33 (1962) 218

(47) Gre 67 A. M. Green, Phys. Letters 24B (1967) 384

(48) Hal 66 E. C. Halbert, Y. E. Kim and T. T. S. Kuo, Phys. Letters 20 (1966) 657

(49) Hug 66 D. J. Hughes and A. B. Volkov, Phys. Letters 23 (1966) 113

(50) Hug 66a D. J. Hughes, D. W. L. Sprung and A. B. Volkov, Proc. of the International Nuclear Physics Conference, Gatlinberg, Tennessee, Academic Press (1967)

(51) Ing 52 D. R. Inglis, Phys. Rev. 87 (1952) 915

(52) Ing 53 D. R. Inglis, Rev. of Modern Physics 25 (1953) 390

(53) Kal 64 A. Kallio and K. Koltveit, Nucl. Phys. 53 (1964) 87

(54) Kal 65 A. Kallio, Phys. Letters 18 (1965) 51

(55) Ker 69 A. K. Kerman, M.I.T. Report CTP #62, Notes on Lectures given at the Summer School at Cargese (1968)

(56) Ker 67 M. W. Kermode, Phys. Letters 25B (1967) 183

(57) Kre 66 S. J. Kreiger, M. Baranger and K. T. R. Davies, Phys. Letters 22 (1966) 607

(58) Kum 66 K. Kumar, Journal of Math. Phys. 7 (1966) 671

(59) Kuo 65 T. T. S. Kuo and G. E. Brown, Phys. Letters 18 (1965) 54

(60) Kuo 66 T. T. S. Kuo and G. E. Brown, Nucl. Phys. 85 (1966) 40

(61) Kuo 67 T. T. S. Kuo, Nucl. Phys. A103 (1967) 71

(62) Kuo 56 D. Kurath, Phys. Rev. 101 (1956) 216

(63) Lan 67 A. Lande and J. P. Svenne, Phys. Letters 25B (1967) 91

(64) Lan 68 A. Lande, A. Molinari and G. E. Brown, Nucl. Phys. A115 (1968) 241

(65) Lau 62 T. Lauritsen and F. Ajzenberg-Selove, National Academy of Sciences, National Research Council (1962)

(66) Lau 66 T. Lauritsen and F. Ajzenberg-Selove, Nucl. Phys. 78 (1966) 1

(67) Leb 65 N. N. Lebedev, Special Functions and Their Applications (Prentice Hall, 1965) 115

Leb 65a ibid 81

(68) Man 68 G. S. Mani and A. D. B. Dix, Nucl. Phys. A106 (1968) 251

(69) Man 68a G. S. Mani and A. Tarratts, Nucl. Phys. A107 (1968) 624

(70) Man 66 M. Mangelson, F. Ajzenberg-Selove, M. Reed and C. C. Lee, Nucl. Phys. 88 (1966) 137

(71) Man 67 M. Manning, Ph.D. Thesis, (McMaster University), unpublished

(72) Man 67a M. Manning, private communication

(73) Mcf 67 M. Mcfarlane, The Reaction Matrix in Nuclear Shell Theory (Argonne Phys. Division Informal Report, PHY-1967-B)

(74) Mey 67 V. Meyer, R. E. Dixley and P. Truol, Nucl. Phys. A101 (1967) 321

(75) Moi 66 B. L. Moiseiwitsch, Variational Principles (Interscience Publishers, 1966)

(76) Mos 60 S. Moszkowski and B. Scott, Annals of Physics 11 (1960) 65

(77) Nem 68 J. Nemeth and H. A. Bethe, Nucl. Phys. A116 (1968) 241

(78) Nes 68 C. W. Nester, Jr., K. T. R. Davies, S. J. Kreiger and M. Baranger, Nucl. Phys. A113 (1968) 14

(79) Pau 67 P. Paul and N. G. Puttasivamy, Phys. Rev. 164 (1967) 1332

(80) Pau 68 P. Paul, D. Kohler and K. A. Snauer, Phys. Rev. 173 (1968) 919

(81) Pre 69 G. Presser, R. Bass and K. Kruger, Nucl. Phys. A131 (1969) 679

(82) Rog 66 P. C. Rogers and H. E. Wegner, Phys. Rev. Letters 17 (1966) 148

(83) Rou 69 M. L. Roush, F. C. Young, P. D. Forsyth and W. F. Homyak, Nucl. Phys. A128 (1969) 401

(84) Rys 63 I. M. Rysik and I. S. Gradstein, Tables of Series, Products and Integrals (Plenum Press 1963) 295

Rys 63a ibid, 386

(85) Sky 59 T. H. R. Skyrme, Nucl. Phys. 9 (1959) 615

(86) Spe 68 J. Speth, Zeitschrift fur Physik 214 (1968) 457

(87) Spr 65 D. W. L. Sprung and D. J. Hughes, Math. of Computation 89 (1965) 139

(88) Spr 69 D. W. L. Sprung, paper delivered at the International Conference on Atomic Masses, Winnipeg, 1969

(89) Spr 69a D. W. L. Sprung, private communication

(90) Tab 66 F. Tabakin and K. T. R. Davies, Phys. Rev. 150 (1966) 793

(91) Tal 60 I. Talmi and I. Unna, Annual Review of Nuclear Science 10 (1960) 353

(92) Tow 68 J. H. Towle and G. T. Wall, Nucl. Phys. A118 (1968) 500

(93) Vol 64 A. B. Volkov, Phys. Letters 12 (1964) 118

(94) Vol 65 A. B. Volkov, Nucl. Phys. 74 (1965) 33

(95) Vol 70 A. B. Volkov, Nucl. Phys. A141 (1970) 337

(96) Vol 70a A. B. Volkov, private communication

(97) Wig 37 E. P. Wigner, Phys. Rev. 51 (1937 106, 947

(98) Wil 66 D. H. Wilkinson and M. E. Mafethe, Nucl. Phys. 85 (1966) 97

(99) Wil 66a D. H. Wilkinson and W. D. Hay, Phys. Letters 21 (1966) 80

(100) Won 67 C. W. Wong, Nucl. Phys. A91 (1967) 399

(101) Yea 67 M. R. Yearian, Int. Conf. on Electromagnetic Sizes of Nuclei, Ottawa 1967.